THE UNIVERSITY OF CHICAGO

INVESTIGATING THE GENETIC BASIS OF CISPLATIN-INDUCED NEUROTOXICITIES IN ADULT-ONSET CANCER SURVIVORS

A DISSERTATION SUBMITTED TO

THE FACULTY OF THE DIVISION OF THE BIOLOGICAL SCIENCES

AND THE PRITZKER SCHOOL OF MEDICINE

IN CANDIDACY FOR THE DEGREE OF

DOCTOR OF PHILOSOPHY

INTERDISCIPLINARY SCIENTIST TRAINING PROGRAM:

CANCER BIOLOGY

BY

SWETHA NAKSHATRI

CHICAGO, ILLINOIS

DECEMBER 2025

To my parents, Poornima and Harikrishna Nakshatri, and my sister, Sapna Nakshatri, for their unconditional love and support.

Acknowledgments

This milestone would not have been possible without the support of so many people who have acted as mentors, collaborators, and friends.

First and foremost, I would like to thank my advisor, Dr. Eileen Dolan, who is a dedicated mentor and educator. I came into this PhD with no computational experience, but she encouraged my goals and my enthusiasm and supported me in learning the skills needed for my project. She has given me the freedom to take my research in new directions and has always been open to trying anything that I proposed. Working with her has made me a more skilled scientist and more confident in my ability to be an independent researcher. Her investment in the future cancer workforce will benefit us all. Dr. Dolan, thank you so much for allowing me the opportunity to work with you. Despite your busy schedule, you have always made time to meet with me and support my progress. Your kindness and belief in my abilities have motivated me to keep going. You inspire me in so many ways: as a scientist, as a mentor, and as an advocate for health equity. I will remember the lessons I have learned from you during my PhD for the rest of my career and life.

I would also like to thank my thesis committee members, Drs. Alexander Pearson, Brandon Pierce, and Dezheng Huo. This project took Dr. Dolan and I in completely new directions for the lab and the success of this project would not have been possible without their guidance. Thank you for your insights and for always being engaged and ready to answer my questions.

Thank you to the past members of the Dolan Lab, Xindi Zhang and Dr. Mohammad Shahbazi, who were instrumental in teaching me computational basics. Thank you to everyone involved in *The Platinum Study*, especially Drs. Lois Travis and Paul Dinh, who welcomed me

into the fold and have helped me along every step of my project, from accessing data to proofreading manuscripts. It was such an honor to contribute to the important work being conducted by *The Platinum Study* team. Thank you to Dr. Nancy Cox for her guidance on genetic methodology. I would also like to thank all of the clinicians involved in recruiting patients for *The Platinum Study* and all of the participants, without whom this research would not be possible.

My journey to this goal has been guided by so many research mentors. Thank you to Dr. Jian Du, my first research mentor. My positive experience in your lab as a high schooler was what compelled me to pursue a career in science. Thank you to Dr. Raghu Mirmira, for encouraging me to consider an MD/PhD as a path. I would like to give an immense thank you to Dr. Jeffrey Gordon, my undergraduate PI. Working with you gave me the confidence that I could one day be an independent researcher. Thank you for always believing in me and encouraging me to pursue an MD/PhD. I am incredibly lucky to have had so many people teaching me and cheering me on.

I would like to thank all of the members of the MSTP administration, past and present, for their support throughout all phases of this program and their work in making sure that all students have the resources they need for success. I would also like to thank the leadership of the Committee on Cancer Biology.

I am incredibly grateful for the opportunities I have received through the Cancer Health Equity Training Program. Through this program, I have learned so much and have strengthened my resolve to work towards a more equitable future. I would like to thank the CHETP leadership: Dr. Dolan, Dr. Rosie Huggins, and Michelle Domecki, for all that they do to facilitate

this important program. I would particularly like to thank Michelle Domecki for all of help with logistics and scheduling over the last four years.

I would like to thank my friends, who have always been a source of joy and encouragement for me. I am so lucky to have such an amazing group of people in my corner who will be in my life for years to come. In particular, I would like to thank Sarah Tinaphong, Shriya Vinjimoor, Olivia Wang, and Kimaya Raje, who have been there for me for almost 15 years and are like family. I am so lucky to have gotten to grow up with you. I can't wait for many more exciting milestones as we work towards accomplishing our goals. I would also like to thank my friends and peers in the MSTP and from the Pritzker School of Medicine who inspire me as future scientists and clinicians.

Finally, I would like to thank my family, particularly my parents and my sister. My parents have supported me throughout every step of my journey, have always emphasized the importance of education, and have kept me grounded throughout the most exciting and challenging times. They are my biggest inspirations and I am so lucky to have them. My sister is my best friend and is always there with a smile or encouragement whenever I need her. Thank you for everything.

Table of Contents

List of Figures

List of Tables

Abbreviations

ADL Activity of Daily Living

AFR (AFRAFR) African

AHO Adverse Health Outcome

AI Artificial Intelligence

ALL Acute Lymphoblastic Leukemia

ANOVA Analysis of Variance

ASCO American Society of Clinical Oncology

ASN Asian

ASW African ancestry in Southwest USA

AUC Area Under the Curve

AUROC Area Under the Receiver Operating Characteristic Curve

BEPx3 Three Cycles of Bleomycin, Etoposide, and Cisplatin

BioVU Vanderbilt University Biorepository

blup best linear unbiased predictor

BSA Body Surface Area

bslmm Bayesian sparse linear model

C_MEDHBP Blood Pressure Medication

C_MEDHCL Cholesterol Medication

Ca^{2+} Calcium

CBM Cumulative Burden of Morbidity

cDNA complementary DNA

CEU Utah Residents from North and West Europe

CHB Han Chinese in Beijing

CHR Chromosome

CHS Han Chinese, South China

CI Confidence Interval

CIPN Chemotherapy-Induced Peripheral Neuropathy

CMT Charcot-Marie Tooth

CNN Convolutional Neural Networks

CNV Copy Number Variant

COG Children's Oncology Group

CPIC Clinical Pharmacogenomics Implementation Consortium

CRISPR Clustered Regularly Interspersed Palindromic Repeats

CTCAE Common Terminology Criteria for Adverse Events

CV Cross Validation

dbSNP Single Nucleotide Polymorphism Database

DMEM Dulbecco's Modified Eagle Medium

DMSO Dimethyl Sulfoxide

DRG Dorsal Root Ganglion

EFO Experimental Factor Ontology (Monarch)

eGFR estimated Glomerular Filtration Rate

EMEM Eagle's Minimum Essential Medium

enet elastic-net regression with mixing parameter of 0.5

EORTC European Organization for Research and Treatment of Cancer

EORTC-QLQ-C30 European Organization for Research and Treatment of Cancer Quality of Life 30-item Questionnaire

EPx4 four cycles of etoposide and cisplatin

eQTL expression Quantitative Trait Locus

ER Endoplasmic Reticulum

EUR European

EURAMOS European and American Osteosarcoma Studies

FACT-GOG-Ntx Functional Assessment of Cancer Therapy-Gynecologic Oncology Group-Neurotoxicity

FBS Fetal Bovine Serum

FDA Food and Drug Administration

FDR False Discovery Rate

FIN Finnish in England

F_{ST} Fixation Index

GBR British in England and Scotland

GCT Germ Cell Tumor

GM412 Geometric Mean of Hearing Thresholds from 4-12 kilohertz

GO Gene Ontology

GOLD Germ Cell Tumor Outcomes and Late Effects

GSA Global Screening Array

GSH Glutathione

GTEx Genotype-Tissue Expression Project

GWAS Genome-Wide Association Study

HDL High Density Lipoprotein

HDR Homology-Directed Repair

HHIA Hearing Handicap Inventory for Adults

HL Hearing Loss

HPO Human Phenotype Ontology

HR Hazard Ratio

HRC Haplotype Reference Consortium

HSQ Heritability

HWE Hardy-Weinberg Equilibrium

IBD Identity-By-Descent

IBS Iberian population in Spain

IC_{50} Half Maximal Inhibitory Concentration

IPR InterPro

iPSC induced Pluripotent Stem Cell

JPT Japanese in Tokyo, Japan

kD Kilodaltons

KEGG Kyoto Encyclopedia of Genes and Genomes

kHz Kilohertz

LASSO Least Absolute Shrinkage and Selection Operator

LD Linkage Disequilibrium

LDL Low Density Lipoprotein

lncRNA long non-coding RNA

LRT Likelihood Ratio Test

LWK Luhya in Webuye, Kenya

MAF Minor Allele Frequency

mRMR Minimum Redundancy Maximum Relevance

MXL Mexican ancestry in Los Angeles, CA

NCCN National Comprehensive Cancer Network

NCI National Cancer Institute

NSCLC Non-Small Cell Lung Cancer

OR Odds Ratio

PBS Phosphate-Buffered Saline

PC Principal Component

PF Pfam

PNS Peripheral Nervous System

PPI Protein-Protein Interaction

PROMIS Patient-Reported Outcomes Measurement Information System

PRS Polygenic Risk Score

PSN Peripheral Sensory Neuropathy

PUR Puerto Rican in Puerto Rico

QC Quality Control

qPCR quantitative Polymerase Chain Reaction

RET Receptor Tyrosine Kinase

RFE Recursive Feature Elimination

RMSE Root Mean Squared Error

ROC Receiver Operating Characteristic

ROS Reactive Oxygen Species

ROSE Random Over-Sampling Examples

SC Subcutaneous

SCIN Scale for Chemotherapy-Induced Long-Term Neurotoxicity

SD Standard Deviation

SEER Surveillance, Epidemiology, and End Results

SERCA Sarco/Endoplasmic Reticulum Calcium ATPase

SGLT Sodium-Glucose Transporter

SIOP The International Society of Pediatric Oncology

siRNA small interfering RNA

SLC Solute Carrier

SNP Single Nucleotide Polymorphism

sQTL splicing Quantitative Trait Locus

SRT Speech Recognition Threshold

STS Sodium Thiosulfate

susie sum of single effects regression

SVM Support Vector Machines

top1 single best eQTL

TPFQ Tinnitus Primary Function Questionnaire

TPM Transcripts Per Million

TRP Transient Receptor Potential

TSI Toscani in Italia

TWAS Transcriptome-Wide Association Study

VO Visceral Omentum

WP WikiPathways

XGBoost Extreme Gradient Boosting

YRI Yoruba in Ibadan, Nigeria

Abstract

As cancer treatment has advanced, there is an increasing number of cancer survivors. Cancer survivors face unique health challenges due to the long-term effects of aggressive treatments. Cisplatin, a commonly used chemotherapy agent worldwide, can cause peripheral sensory neuropathy and ototoxicities such as tinnitus, hearing loss, and vertigo. Long-term consequences of these neurotoxicities include cognitive decline, decreased quality of life, and increased mortality, with no FDA-approved treatments or preventive therapies for adult-onset cancer survivors. Therefore, it is critically important to understand the risk factors for these toxicities.

Although single nucleotide polymorphisms (SNPs) have been found to be associated with cisplatin-induced neurotoxicities through genome-wide association studies (GWAS), there are major gaps in knowledge that must be addressed before findings are clinically applicable. Individual SNPs, even those significantly associated with toxicities, are not sufficient for predicting risk. Thus, we trained and tested machine learning prediction models for cisplatin-induced peripheral sensory neuropathy, tinnitus, and hearing loss, utilizing a variety of clinical and genetic inputs as predictors. Models for predicting severe cisplatin-induced peripheral sensory neuropathy were particularly effective, with strong sensitivity and specificity. Models with high sensitivity were also trained for predicting overall cisplatin-induced peripheral sensory neuropathy. Models predicting cisplatin-induced hearing loss showed a significant correlation between hearing thresholds predicted by the model and actual hearing thresholds. Analyzing the input features used to train models highlighted the importance of dyslipidemia and altered lipid measurements in the risk for cisplatin-induced peripheral sensory neuropathy.

The second area of interest was to determine whether there were population disparities in cisplatin-induced neurotoxicities. We found that survivors of African ancestry were significantly more likely to have peripheral sensory neuropathy and vertigo than those of European ancestry, with no significant differences in clinical and lifestyle factors (smoking, drinking, and medication use for blood pressure, cholesterol, and diabetes) between these populations. Filtering SNPs to find independent, functional ancestry-informative markers and assessing the association between these variants and toxicities identified expression quantitative trait loci for RNF24 in nerve tissue that were among the SNPs with the strongest p-values of association with neuropathy. SNPs impacting MFSD4B expression in nerve tissue and REV3L expression in brain tissue and SNPs impacting DDX25 expression in nerve tissue were among those with the strongest p-values of association with vertigo. Based on *in silico* validation, MFSD4B and REV3L expression were significantly correlated with cisplatin sensitivity in cancer cell lines.

This project provides important insights into the clinical and genetic risk factors for cisplatin-induced neurotoxicities. In the future, our work will help inform clinical risk prediction of cisplatin-induced neurotoxicities prior to treatment. It can also contribute to more effective dosing and monitoring in adult-onset cancer patients treated with cisplatin as well as the development of targeted interventions.

Chapter 1. Introduction

1.1 Cancer survivorship and chemotherapy-induced toxicities

Cancer survivorship

The number of cancer survivors has increased as the global population ages and advances in early diagnosis and more effective treatment options have become available to cancer patients. Improved treatment strategies, including chemotherapy, radiotherapy, immunotherapy, and targeted therapy, have improved survival rates over time across cancer types[1]. The most recent Surveillance, Epidemiology, and End Results (SEER) Cancer Statistics Review (1975-2017) noted that the five-year relative survival rate for cancers across all sites is 68.9% for White patients and 65.0% for Black patients (2011-2017)[2]. In the earliest available SEER Cancer Statistics Review (1973-1993), for cancers diagnosed between 1974-1976, the five-year relative survival rate was 50.3% for White patients and 38.9% for Black patients, indicating both an increase in survival over time as well as a narrowing of disparities in survival between populations[3]. This increase in five-year survival rate is also seen in the pediatric and adolescent population (diagnosed ages 0-19), as the five-year survival rate is now over 85% with a -75.7% percent change in mortality in the United States for those diagnosed from ages 0-14 from 1950 to 2018[3,4]. As a result, a sizeable portion of the population is now aging cancer survivors who have lived for many years with the effects from both their disease and treatment. As of January 2022, there are over 18 million cancer survivors in the United States, with 53% diagnosed within the past ten years, and 18% diagnosed over 20 years ago[5].

Long-term toxicities of cancer treatment

As the number of cancer survivors increases, there is a heightened awareness of the long-term toxicities caused by therapy and their subsequent impact on quality of life. These toxicities

can be physical, psychological, and financial, among others, and can result from varied treatment strategies including chemotherapy, radiotherapy, and immunotherapy[6–8]. Cancer treatments can impact all organ systems, with different therapies causing neurotoxicity (including ototoxicity), pulmonary toxicity, hepatic toxicity, nephrotoxicity, cardiac toxicity, osteonecrosis, pancreatitis, and myelosuppression[6]. In many cases, treatment-related adverse health outcomes are common. For example, 95% of childhood cancer survivors will develop a serious adverse health outcome by the age of 45 from either the cancer or its treatment, including endocrine disorders, cardiovascular disease, and even secondary cancers[4]. Those receiving cranial irradiation or hematopoietic stem cell transplants are at particularly high risks for adverse health outcomes, with chemotherapy also causing long-term toxicities. Patients receiving only surgical resection for solid tumors with minimal chemotherapy have a risk for toxicity similar to non-survivors[4].

1.2 Chemotherapy-induced neurotoxicities

Chemotherapy-induced neurotoxicities: an overview

A particularly concerning category of toxicities associated with cancer therapy is neurotoxicity. Neurotoxicities can impact both the peripheral nervous system, caused by drugs such as paclitaxel and cisplatin, as well as the central nervous system, caused by chemotherapy drugs that can cross the blood-brain barrier such as methotrexate, which can lead to severe complications such as encephalopathy or intracranial hemorrhage from chemotherapy-induced thrombocytopenia[9]. Chemotherapy-induced cognitive impairment can impact up to 75% of patients during the course of treatment, with 35% experiencing still experiencing symptoms such as impairments to memory, concentration, attention, and executive function as well as increased fatigue for months following the cessation of treatment[10]. Chemotherapy also impacts the

peripheral nervous system, resulting in peripheral sensory neuropathy[9], as well as the inner ear, resulting in ototoxicity, which encompasses hearing loss, tinnitus, and vertigo[11].

Chemotherapy-induced peripheral neuropathy can be caused by a wide variety of mechanistically distinct chemotherapeutics including platinum drugs (cisplatin, oxaliplatin), taxanes (e.g. paclitaxel), bortezomib, vinca alkaloids (e.g. vincristine) and newer targeted agents[9]. Injury, inflammation, or degradation of peripheral nerve fibers causes peripheral neuropathy and symptoms can be acute or chronic, with between 19 and 85% of patients experiencing chemotherapy-induced peripheral sensory neuropathy depending on therapy[12,13], with severity varying across patients. Peripheral sensory neuropathy manifests as abnormal cutaneous sensations such as paresthesia, dysesthesia, numbness, tingling, pressure, and experiencing cold or warmth without an external stimulus[13]. Cisplatin causes peripheral sensory neuropathy in 36-38% of patients, paclitaxel causes peripheral sensory neuropathy in up to 60% of patients, and vincristine-induced paresthesia in hands and feet occurs in up to 57% of patients[11,12].

Ototoxicity is also a common long-term chemotherapy-induced and radiotherapy-induced toxicity, a category that includes hearing loss, tinnitus, and vertigo. In a study of head and neck cancer patients, those treated with cranial radiotherapy were significantly more likely to experience severe hearing loss compared to those not exposed to cranial radiotherapy[14]. Platinating agents can also cause ototoxicity in survivors, with 75-80% of those treated with cisplatin experiencing some degree of sensorineural, bilateral, irreversible hearing loss and 13-18% developing severe hearing loss[11]. Up to 40% of cisplatin-treated patients develop tinnitus, or the perception of sound in the absence of an external stimulus, with 13-22% experiencing

severe tinnitus[11]. A study of cisplatin-treated adult cancer survivors found that 17% reported balance issues, with vertigo being the most common issue (9.7%)[15].

Mechanisms of chemotherapy-induced neurotoxicities

Different therapies have different mechanisms of causing neuropathy[12]. Taxanes such as paclitaxel impact microtubule depolymerization and repolymerization, impairing cell division and leading to cell death, which is involved in both cancer cell death and the development of peripheral sensory neuropathy[13]. Paclitaxel directly damages peripheral nerves, resulting in demyelination and neuronal fiber loss and impacting Ca^{2+} homeostasis[13]. Vinca alkaloids also impact microtubules, promoting their disassembly and preventing their assembly, thus inducing impacts on axonal transport like seen with paclitaxel treatment and leading to neuropathy[13].

Cisplatin commonly causes peripheral sensory neuropathy, ototoxicity, nephrotoxicity, and myelotoxicity[13]. Cisplatin is known to induce apoptosis of cancer cells through numerous mechanisms, including by forming DNA-platinum adducts and preventing DNA replication, altering the respiratory chain in mitochondria, increasing the production of reactive oxygen species (ROS), interfering with mitochondrial DNA replication and transcription, activating the release of pro-inflammatory cytokines, and impacting calcium signaling and protein kinase pathways[13]. Platinum adducts accumulate in dorsal root ganglion (DRG) and trigeminal ganglion neurons and have similar impacts on mitochondrial function, ROS production, and cellular signaling. Altered sodium, potassium, and transient receptor potential (TRP) channel activity, with downstream effects on peripheral neuron excitability, are also potentially implicated in the development of cisplatin-induced peripheral sensory neuropathy[13].

The mechanisms of cisplatin-induced ototoxicity are currently being explored, specifically the impact of cisplatin on hair cells. Cisplatin is retained in the cochlea, particularly

the stria vascularis, for months to years after treatment, impacting the electrochemical potential of endolymph, which mediates the mechanoelectrical transduction of hair cells critical for hearing[16]. Similar to cisplatin-induced peripheral sensory neuropathy, ototoxicity results from an increased concentration of ROS, platination of mitochondrial DNA, and the induction of apoptosis through p53 activation in the hair cells[11,17]. Cisplatin-induced tinnitus may be a result of hyperactivity in the dorsal cochlear nucleus triggered by cisplatin-induced hair cell loss[18]. Animal studies in rats, guinea pigs, and mice have found that cisplatin-induced vestibular/utricular hair cell loss and damage may be caused via mechanisms such as increased inflammatory cytokines, ROS, and apoptosis, leading to vertigo[19].

Long-term consequences of chemotherapy-induced neurotoxicities

Chemotherapy-induced neurotoxicities lead to long-term complications and functional limitations in children and adults, negatively impacting quality of life. When peripheral neuropathy is dose-limiting, toxicity can also impact treatment efficacy and overall survival. The Common Fund's Patient-Reported Outcomes Measurement Information System (PROMIS) survey provides rigorous patient-reported outcome measurements that quantify pain, fatigue, emotional distress, social participation, and physical function[20]. In a study of cisplatin-treated testicular cancer survivors, neuropathic pain was significantly associated with worse global mental health and peripheral neuropathy score was significantly associated with reductions in global physical health score as evaluated by the PROMIS v1.2 survey[21]. Reductions in physical health are likely partially due to difficulty with physical activity and exercise as a result of neuropathic pain. In a group of patients with type 2 diabetes, neuropathy was associated with a reduction in steps per day and decreased muscle strength[22]. A cohort study of participants with peripheral neuropathy (not limited to chemotherapy-induced) found that peripheral neuropathy

was significantly associated with both increased cardiovascular mortality and all-cause mortality in patients with and without diabetes[23].

Ototoxicity also has long-term consequences. Chronic tinnitus interferes with sleeping and concentration and leads to increased anxiety, depression, and insomnia as well as reduced productivity[24]. Both hearing loss and tinnitus can lead to cognitive decline and dementia[24,25], and older adults with moderate to severe hearing loss are more likely to have impairments with activities of daily living (ADLs) and instrumental ADLs (activities beyond basic self-care that allow for independent living)[26].

When longitudinally assessing cisplatin-treated testicular cancer survivors, the cumulative burden of morbidity (CBM), a score including the incidence and severity of adverse health outcomes (AHO), worsened for 23% of patients over time[27]. This worsening was associated with increases in tinnitus, hearing loss, neuropathy, neuropathic pain, and Raynaud's phenomenon over time, indicating the impact of these toxicities on morbidity[27]. In addition to impacts on physical health, testicular cancer survivors with cisplatin-induced neurotoxicities had worsened mental health and cognitive function than those without neurotoxicities. Hearing loss and neuropathic pain were significantly associated with cognitive impairment, which was shown to negatively impact daily activities and quality of life[28]. Survivors were studied for toxicity-specific functional impairment using the Hearing Handicap Inventory for Adults (HHIA)[29] and the Tinnitus Primary Function Questionnaire (TPFQ)[30], with severe hearing loss and tinnitus associated with significant functional impairment[31]. For both cisplatin-induced hearing loss and tinnitus, survivors with severe toxicity were significantly more likely to have cognitive dysfunction, depression, fatigue, and worse overall health. Severe hearing loss-related functional impairment was also significantly associated with cognitive dysfunction, fatigue, and worse

health[31]. Cisplatin-induced tinnitus and peripheral sensory neuropathy were also significantly associated with the use of anxiety and/or depression medication[32]. Survivors with neuropathic pain had significantly higher mortality (hazard ratio (HR) = 3.64), mediated through the impact of neuropathic pain on physical activity[27]. Taken together, these studies of the long-term impacts of chemotherapy-induced neurotoxicities indicate the importance of preventing and treating these toxicities in the future.

Lack of effective treatments for chemotherapy-induced neurotoxicities

The 2020 American Society of Clinical Oncology (ASCO) guidelines noted no standard treatments for the prevention and management of chemotherapy-induced peripheral neuropathy in adult cancer survivors. Duloxetine was the only agent with evidence of providing patients with painful neuropathy limited benefit[33]. Numerous trials have been conducted testing various agents for the prevention and treatment of chemotherapy-induced peripheral neuropathy with limited evidence of benefit and some evidence of negative impacts[33–36]. These include trials of acetyl-L-carnitine, alpha-lipoic acid, intravenous calcium and magnesium, L-carnosine, GM-1, Goshajinkigan, metformin, gabapentin, vitamin B, and vitamin E[33]. A trial studying the use of Calmangafodipir for preventing oxaliplatin-induced peripheral neuropathy in metastatic colorectal cancer patients showed promise in a randomized phase 2 clinical study, but failed in two randomized phase 3 trials[34]. There are mixed results regarding the benefit of cryotherapy, compression therapy, and cryo-compression therapy for neuropathy, with ongoing investigations of the utility of these treatments[33].

There are a few interventions for peripheral neuropathy that show promise. One study noted that both venlafaxine and duloxetine-treated patients showed significant decreases in grades of cranial, sensory, and motor neuropathy as well as neuropathic pain[35]. A 2024 study

similarly saw a reduction in neuropathic pain in patients given venlafaxine or duloxetine[36]. Exercise has shown benefits for reducing peripheral sensory neuropathy symptom severity and acupuncture may also provide pain relief[33]. However, there are no standard, Food and Drug Administration (FDA)-approved drugs for either the prevention or treatment of chemotherapy-induced peripheral neuropathy[37,38].

For cisplatin-induced hearing loss, the FDA approved PEDMARK, a sodium thiosulfate (STS) drug, in 2022, specifically to be used in pediatric patients with non-metastatic solid tumors[39]. In a trial in hepatoblastoma patients, 20 g/m^2 of STS was given to patients six hours after completing cisplatin treatment and these patients were compared to patients who only received cisplatin. In patients receiving cisplatin and STS, there was a 48% decrease in the incidence of grade 1 or higher hearing loss, with no impacts on overall and event-free survival[40]. However, no such trial exists for adult-onset cancer survivors.

There have been a few animal studies to test otoprotective pharmacological strategies, including antioxidants such as apocynin, which prevented hair cell loss in a zebrafish model[41] and alpha-lipoic acid, which protected against cisplatin-induced ototoxicity in mice[42]. Other categories of agents tested include antioxidants and compounds involved in anti-inflammation and anti-apoptosis[43]. Patients with sensorineural hearing loss may also benefit from hearing aids or cochlear implants[44]. However, there are no FDA-approved agents for the treatment or prevention of cisplatin-induced ototoxicity beyond PEDMARK for pediatric populations[39] .

Currently, chemotherapy-induced peripheral neuropathy and ototoxicity are irreversible. Therefore, studying clinical and genetic risk factors could provide insights into avenues for prevention as well as targets for future intervention.

Clinical risk factors for chemotherapy-induced neurotoxicities

Many clinical and modifiable risk factors have been found to be associated with chemotherapy-induced neurotoxicities, with many overlapping risk factors across agents and toxicities. In a study of patients receiving taxane-based and platinum-based chemotherapies, older age, alcohol intake, and statin usage were associated with chemotherapy-induced peripheral neuropathy, with diabetes showing a trend towards neuropathy development[45]. Another cohort study of patients treated with paclitaxel and oxaliplatin found that lower hemoglobin levels prior to treatment, higher body mass index, older age, and female sex were associated with worse neuropathy[46]. In cisplatin-treated testicular cancer survivors, clinical factors such as older age at diagnosis and taking anti-hypertensive medication were associated with peripheral sensory neuropathy, hearing loss, and tinnitus[47]. Additionally in this cohort, body mass index at evaluation was associated with hearing loss, excess drinking was associated with peripheral sensory neuropathy, and taking cholesterol medication was associated with tinnitus, while lifestyle factors such as smoking were associated with both peripheral sensory neuropathy and tinnitus[47].

Genetic risk factors for chemotherapy-induced neurotoxicities

There are also genetic risk factors for chemotherapy-induced neurotoxicities. Understanding genetic risk factors can help physicians determine which patients are at the highest risk of neurotoxicities to facilitate appropriate dosing, monitoring, and post-treatment management as well as contribute to developing genetically-targeted treatment regimens that may help survivors in the future. Genome-wide association studies (GWAS) and candidate gene/variant-specific studies have been conducted across chemotherapy agents, including cisplatin[13,47–53], paclitaxel[13,54–59], and vincristine[13,60,61] to find genes or variants associated with neurotoxicities.

Studies of genetic risk factors for paclitaxel and vincristine-induced neuropathy have encompassed multiple populations and have noted the association of variants impacting numerous genes and pathways with neuropathy. For example, for paclitaxel-induced peripheral neuropathy, single nucleotide polymorphisms (SNPs) associated with drug metabolism (CYP2C8*3)[56], genes in the WNT pathway (FZD3, GPR177)[54,55], and genes associated with congenital neuropathy (FGD4)[54] have been found to be associated with toxicity. Variants related to genes that are chemotherapy targets, such as those in the promoter region of β-tubulin IIα, have also been found to be associated with neuropathy risk[57].

Although chemotherapy agents cause neuropathy by different mechanisms, there may be some shared genetic risk factors between paclitaxel and vincristine-induced peripheral neuropathies. Genetic variants in a Charcot-Marie Tooth (CMT) disease gene ARHGEF10 were significantly associated with paclitaxel-induced polyneuropathy[58], with a gene-based analysis in African American survivors finding SBF2, a gene associated with Type 4B2 CMT disease also to be associated with paclitaxel-induced neuropathy[59]. Similarly, CMT1A patients were particularly susceptible to vincristine-induced neurotoxicity[13,60]. CMT disease is a group of inherited peripheral sensory (and motor) neuropathies[62]. There may be shared genetic architecture between chemotherapy-induced peripheral neuropathies and hereditary neuropathies.

Studies of genetic risk factors for cisplatin-induced neurotoxicities have encompassed multiple cancer types, including those in cohorts of childhood cancer survivors[63], testicular cancer survivors[48–51,64], and head and neck cancer patients[52]. A study of adult nasopharyngeal carcinoma patients noted some shared genetic architecture between hereditary and chemoradiation-induced deafness, with variants for hereditary deafness genes significantly enriched in top GWAS signals[52]. Studies have discovered and replicated an ACYP2 variant

(rs1872328) associated with pediatric cisplatin-induced ototoxicity (including in studies without concurrent cranial irradiation), with the impact of ACYP2 on Ca^{2+} homeostasis potentially being implicated in cisplatin-induced hearing loss[53,65,66]. GWAS have also been conducted in cisplatin-treated testicular cancer survivors, the cohort of interest in our study[48–51,64].

1.3 *The Platinum Study* and cisplatin-induced neurotoxicities

The Platinum Study

Knowing the long-term complications associated with chemotherapy-induced neurotoxicities as well as the lack of treatment options, understanding the risk factors for these toxicities to prevent and target them in the future is imperative. *The Platinum Study* aims to study the clinical and genetic risk factors for cisplatin-induced neurotoxicities to help determine which patients are at the highest risk and to work towards future interventions for prevention and treatment. Cisplatin is a metal-based drug used in the treatment of numerous solid tumors, including testicular, ovarian, and head and neck cancers, treating approximately 50% of cancer patients[67]. Cisplatin forms either intra-strand DNA adducts or inter-strand crosslinks[68], stopping critical cancer cell proliferation and triggering DNA damage pathways as well as signal transduction pathways leading to p53-induced apoptosis[67]. Cisplatin's cytotoxicity is also due to the induction of oxidative stress and the failure of nucleotide excision and mismatch repair[67]. The toxicities associated with cisplatin are vast, including neurotoxicities (ototoxicity, neuropathy), but also nephrotoxicity and myelosuppression[11].

The Platinum Study is a multicenter study of cisplatin-treated testicular cancer survivors recruited from eight institutions across the US, the UK, and Canada[47]. The Dolan Lab has been involved with *The Platinum Study* since its inception in 2013. Despite the importance of cisplatin in decreasing mortality, particularly for those diagnosed with testicular germ cell tumors, some

have described cisplatin-based regimens as a "pyrrhic victory", due to the adverse health outcomes resulting from receiving cisplatin treatment earlier in life[69]. Testicular cancer survivors provide a unique opportunity for studying the long-term impacts of cisplatin-induced neurotoxicities. Most testicular cancer survivors are young men, with many of the observed adverse health outcomes being attributed to the impact of cisplatin treatment rather than other age-related comorbidities[69]. Additionally, treatments for testicular cancer are uniform: patients receive either three or four cycles of cisplatin (three cycles of bleomycin, etoposide, and cisplatin (BEPx3) or four cycles of etoposide and cisplatin (EPx4)), with cisplatin being the only neurotoxic agent[69]. This is in contrast to cisplatin-treated head and neck cancer patients, who also receive cranial radiotherapy, which can contribute to ototoxicity and make it more difficult to study the risk factors for cisplatin-induced neurotoxicities without the confounding effects of other treatments[14]. There are a few other European cohorts studying cisplatin-induced toxicities in testicular cancer survivors[70–74], although none are as extensively phenotyped and genotyped as *The Platinum Study*.

Over the past 12 years, investigators within *The Platinum Study* have recruited over 1800 cisplatin-treated testicular cancer survivors with extensive genotyping and phenotyping information. Eligible patients undergo a physical exam, a cholesterol panel, endocrine studies, and audiometry testing. They also consent to a medical records review and answer an extensive questionnaire that asks about health conditions including toxicities, lifestyle factors, and prescription medications. They also give a blood specimen for genotyping. A subset of survivors have been part of longitudinal studies, including repeated audiometry, questionnaires about adverse health outcomes, the PROMIS questionnaire for physical and mental health, and

assessments of cognitive impairment. Continued follow-up has also provided information about all-cause mortality in this survivor population.

Genetic studies conducted in *The Platinum Study*

Our group has led numerous GWAS of cisplatin-based neurotoxicities conducted in testicular cancer survivors in *The Platinum Study*. These studies have helped to determine SNPs associated with peripheral sensory neuropathy[48], sensorineural hearing loss[49], tinnitus[50], residual serum platinum levels[64], and multiple severe neurotoxicities[51]. PrediXcan analysis found that lower expression of MIDN and RPRD1B and higher expression of THEM5 were associated with cisplatin-induced peripheral neuropathy, with significant replication of the RPRD1B gene in two other datasets: Vanderbilt's electronic health database (BioVU) and the CALGB 90401 trial of docetaxel-induced neuropathy[48]. RPRD1B is involved in DNA repair and is also a co-activator of the β-catenin-TCF complex[48]. Typically, variants associated with toxicities caused by one chemotherapy do not overlap with those associated with another chemotherapy. However, when comparing the results from GWAS for paclitaxel-induced peripheral sensory neuropathy to GWAS for cisplatin-induced peripheral sensory neuropathy, the SNP rs7349683 in EPHA5, which was among the SNPs most strongly associated with paclitaxel-induced neuropathy ($p = 9.6x10^{-7}$)[54], passed replication significance ($5.0x10^{-2}$) and had the same direction of effect in cisplatin-treated testicular cancer survivors[48].

In a study of cisplatin-induced hearing loss, a SNP (rs62283056) that was significantly associated with hearing loss was in the first intron of WFS1 and the association between decreased WFS1 expression and hearing loss was replicated in BioVU[49]. A GWAS for cisplatin-induced tinnitus found that a variant near OTOS (rs7606353) was suggestively significant and OTOS overexpression in a mouse auditory cell line led to resistance to cisplatin-induced

toxicity[50]. For multiple severe neurotoxicities, a gene-based association analysis discovered that RGS17 and FAM20C were nearly genome-wide significant, with *in silico* validation in tumor cell lines showing that decreased FAM20C expression was marginally associated with increased cisplatin sensitivity[51]. In the most recent GWAS for cisplatin-induced neurotoxicities in an expanded cohort of over 1600 testicular cancer survivors in *The Platinum Study*, while there were no SNPs significantly associated with any toxicity, gene-based analyses found a borderline significant association between TXNRD1, a gene in critical in redox regulation, and hearing loss and a significant association between WNT8A and tinnitus[47]. In a replication cohort, the SNP in WFS1 found to be associated with cisplatin-induced hearing loss was marginally significant[47].

Although these GWAS have provided important insights into the SNPs associated with cisplatin-induced neurotoxicities, they did not replicate variants found in other studies, such as SNPs in genes such as GSTP1, TPMT, or COMT[48,49] and have only been conducted in survivors of European ancestry[48–51,64]. Most of these studies also lack *in vitro* functional validation[48,49,51,64]. Results from GWAS have not been utilized to develop clinically applicable risk prediction models[48–51,64], unlike a polygenic risk score (PRS) built for paclitaxel-induced peripheral neuropathy with top GWAS SNPs[75] and a machine learning prediction model for vincristine-induced peripheral neuropathy incorporating variants discovered by GWAS[76]. Therefore, a lot of work is required to move forward so that information from genetic studies of cisplatin-induced neurotoxicities can be applied in a clinical context.

1.4 Machine learning and clinical risk prediction

Expanding GWAS to risk prediction

GWAS and other studies such as gene-based analyses provide important information regarding the SNPs and genes associated with phenotypes. However, variants found to be

significantly associated with disease phenotypes by GWAS often do not have the power, particularly independently, to define druggable targets or serve as determinants of phenotype risk[77,78]. Even after 15 years of published GWAS, diagnosis of common diseases based only on GWAS results remains improbable[79]. There are numerous potential reasons for this. One is that even if a SNP is significantly associated with a phenotype, the effect sizes of individual variants are small[78]. Therefore, risk prediction may benefit from a larger number of SNP predictors, even those that do not achieve genome-wide significance on their own. Q-Q plots of p-values show that there is deviation from the diagonal prior to the threshold for statistical significance, meaning that other, non-significant SNPs are also associated with the phenotype and combining the smaller signals from each SNP may help improve risk prediction[78]. Complex phenotypes also tend to be polygenic, underscoring how a single variant may not provide enough information for prediction[80]. There is a gap between what can be learned from GWAS and how this knowledge can be implemented in a clinical/translational setting.

Machine learning methods such as penalized logistic regression, which combines elements of feature selection and coefficient estimation, may allow us to understand how GWAS summary statistics can be used for risk prediction model building better than simply choosing the most strongly associated SNPs as predictors[78]. Machine learning has the capability to learn complex relationships between features that are impossible to discover without its computational complexity.

Machine learning (a subset of artificial intelligence (AI)) has become a useful tool for better understanding the underlying biology of disease phenotypes as well as for clinical risk prediction. This has been a goal of computation since the conceptualization of AI and implementation in a medicine context has begun to make progress due to advancements in both

technology and data availability. Image processing models in the late 1990s and early 2000s allowed for the reading of images such as electrocardiograms and histology slides among other data types and continue to be used[81]. Now, machine learning and AI models have been used to process immense amounts of clinical, genomic, proteomic, metabolomic, histologic, and radiologic data, and have been used in risk prediction and diagnosis[82,83].

Machine learning in cancer and chemotherapy-induced toxicities

Machine learning models can range from classical techniques such as simple logistic regression, random forests, and support vector machines to deep learning techniques suited to more complex data and larger datasets[84]. In the context of cancer, as new datasets have been collected, the application of machine learning has broadened, including the development of models for understanding cancer risk, identifying biomarkers, and predicting treatment efficacy and toxicity[85]. Cancer prediction and classification models have been trained using various model building techniques and input features such as pathology slides, gene expression microarrays, and radiomics data, with many models achieving great predictive success[85]. These models have been demonstrated to improve clinical outcomes. For example, a study trained machine learning models on head and neck squamous cell carcinoma patients in the National Cancer database using clinical and demographic features to predict which patients might benefit from chemoradiation versus radiation alone. Adherence to model recommendations demonstrated a significant survival benefit[86]. In the context of testicular cancer, models developed by integrating radiomics and deep learning features from ultrasounds with clinical data were able to define testicular tumors versus non-tumorous lesions and benign versus malignant masses, surpassing the assessments of radiologists and models that used clinical

signatures and radiomics alone[87]. These are a few studies out of many that span numerous cancers, input feature modalities, algorithms, and outcomes of interest[85].

Machine learning studies are less common for chemotherapy-induced toxicities. One major reason is that there are fewer large datasets that contain extensive phenotype and genotype information. Nonetheless, there have been some successful studies in smaller cohorts with toxicity information, particularly using clinical and laboratory information as predictors. For predicting anthracycline-based cardiotoxicity, including cardiac dysfunction and reduced ejection fraction, in breast cancer patients, clinical, chemotherapy regimen, and echocardiographic predictors were used to train random forest, support vector clustering, k-nearest neighbors, LightGBM, logistic regression, and multilayer perceptron models[88]. Multilayer perceptron models were relatively successful at predicting cardiac dysfunction (area under the curve (AUC) = 0.66) and better at predicting reduced ejection fraction (AUC = 0.79)[88]. When considering models for chemotherapy-induced toxicities trained on genetic features, a study in a cohort of 72 patients demonstrated the success of using machine learning methods to predict vincristine-induced peripheral neuropathy. Researchers were able to use SNP genotypes from GWAS to achieve a prediction accuracy of 93.8% using a support vector machine model[76].

Researchers have also developed predictive models for platinum-induced toxicities. In a cohort of 118 non-small cell lung cancer (NSCLC) patients, an artificial neural network model trained with a combination of clinical and genomic features was very successful (area under the receiver operating characteristic curve (AUROC) = 0.90) for predicting platinum-induced nephrotoxicity[89] . A Danish group trained machine learning models to predict self-reported hearing loss in a group of cisplatin-treated testicular survivors (n = 424 with hearing loss data), integrating both clinical and genetic features as predictors and utilizing models to understand

which genes were critical for cisplatin-induced hearing loss, allowing for a deeper biological understanding of the underlying mechanisms of this toxicity[90]. Currently, machine learning models for predicting cisplatin-induced peripheral sensory neuropathy and tinnitus have not been published and models published for predicting cisplatin-induced hearing loss in adult-onset cancer survivors have used self-reported hearing loss rather than an audiometry-based phenotype[90]. Additionally, *The Platinum Study* (numbers ranging from ~1000-1500 with genotyping and phenotyping data depending on toxicity) is larger than the cohorts used to train previous models of chemotherapy-induced toxicities. We also have extensive clinical, medication, lifestyle, and genotyping data to use as inputs for machine learning models. Utilizing these advantages, we trained machine learning models to predict cisplatin-induced peripheral neuropathy, hearing loss and tinnitus to fill in gaps in knowledge regarding risk prediction of cisplatin-induced neurotoxicities.

1.5 Diversity in pharmacogenomic studies

Homogeneity of genetic studies

Another gap in knowledge is there have been very few GWAS of chemotherapy-induced toxicities including survivors of non-European ancestry[91]. When considering GWAS across all traits, 78% of participants within the studies were of European descent, as of 2018[92]. This has not improved over time, as 2023 data in the GWAS Diversity Monitor noted that in the discovery stage, 86.6% of participants in GWAS were of European descent and when exploring the count of all associations discovered, 73% were in Europeans[93]. A 2017 review noted a similar lack of diversity in GWAS conducted for chemotherapy-induced neurotoxicities, with 22 out of 28 studies being ancestrally homogenous[91]. In both contexts, individuals of African descent are particularly underrepresented, with only 2% of subjects included in GWAS across phenotypes

and 3.7% of subjects included in GWAS of chemotherapy-induced toxicities being of African ancestry[91,92].

While there are ongoing efforts to improve diversity in genetic studies[94], there is a particular lack of studies examining the genetic risk factors for cisplatin-induced neurotoxicities that include non-European patients. Unlike genetic studies of paclitaxel-induced neuropathy, which studied genetic risk factors in numerous ancestral populations[54,55,58,59,95], published GWAS of cisplatin-induced neurotoxicities in testicular cancer survivors in *The Platinum Study* have focused only on survivors of European ancestry[47–51].

Allele frequency differences between populations

While the vast majority of SNPs are conserved across populations and geographies, some SNPs or copy number variants (CNV) are more common in one population versus others, with significant differences in minor allele frequencies (MAF) between populations[96]. These differences may reflect the possibility that a newer variant has not yet spread to other populations, or more commonly may reflect adaptation to the local environment and selection of adaptive variants, as evidenced by population disparities in hereditary lactase persistence and malaria resistance (as well as resultant sickle cell disease risk)[96].

Minor allele frequency differences are particularly relevant in the context of pharmacogenetics and pharmacogenomics, as genetic variation between populations can contribute to differences in drug efficacy and toxicity. An example of this is G6PD deficiency, the frequency of which varies across populations (higher in those with ancestry from sub-Saharan African) due to adaptation to chronic geographic pressures (protection from malaria)[92,97]. These population differences in enzyme deficiency have major implications for hemolysis risk in response to drugs, including primaquine for malaria treatment[92]. Not

considering population variation in risk allele frequency (or in this case, enzyme deficiency frequency) has led to negative consequences for understudied populations. Chlorproguanil-dapsone was an antimalarial drug combination that was put on the market in 2003, but was withdrawn from the market in 2008 because of a lack of consideration of the high frequency (up to 25%) of G6PD deficiency in patients from sub-Saharan Africa, which increased their risk for drug toxicity[92]. Understanding population variation in pharmacogenomic risk alleles is also actionable, as clinicians have begun utilizing this information for prescribing. For abacavir, an HIV drug, genetically guided prescription is standard, as screening for the HLA-B*5701 allele was found to decrease the incidence of life-threatening abacavir hypersensitivity syndrome[94]. Initially, pre-treatment screening for the HLA-B*5701 allele was only conducted in patients of European descent, as incidence of abacavir hypersensitivity syndrome in this group was 5-8%, thought to be higher than the incidence in other populations. However, after further study of allele frequency distribution across populations, genetic variation was found even within broader racial categories, with the Kenyan Masai population having an allelic prevalence of 13.6% and the Nigerian Yoruba population having an allelic prevalence of 0%[94]. Without genetic research in diverse populations, screening would have remained only available to patients of European ancestry, leaving numerous other patients at risk of this life-threatening toxicity. Therefore, understanding population-level genetic variation in risk alleles associated with cisplatin-induced neurotoxicities can have clinical impact when considering how to mitigate toxicity risk across diverse groups.

Genetic ancestry for disparities research

A number of previous studies of population differences in disease phenotypes, including some studies of disparities in cisplatin-induced nephrotoxicity, have used self-reported race to

define categories[98,99]. The abacavir hypersensitivity example not only illustrates the importance of understanding population allele frequency differences, but also highlights the inadequacy of simply using self-reported race for personalized prescribing, as allele frequencies were more granular when studying genetic ancestry versus broader racial categories[94]. Geography and genetic similarity are strongly correlated, thus illustrating the importance of a metric such as biogeographical/genetic ancestry[100]. As race is a social construct and racial categories and genetic ancestry as defined by ancestry-informative markers sometimes disagree[100], ancestry is a better descriptor for understanding differences in population characteristics attributed to genetic variation while race may be better suited to studying disparities attributed to the societal implications of racism.

Ancestral disparities in chemotherapy-induced toxicities

Therapy-related toxicities across organ systems vary in frequency and severity between populations. Bevacizumab, which blocks VEGF through an anti-angiogenic monoclonal antibody and is used as a targeted therapy in numerous cancer types, causes numerous toxicities including hypertension, proteinuria, and thromboembolism among others[101]. In a study comparing East Asian and non-Asian non-small cell lung cancer (NSCLC) patients, the rates of severe bleeding and thromboembolism were significantly higher in non-Asian versus Asian patients, while the rate of severe proteinuria was significantly higher in Asian versus in non-Asian patients[101]. Multiple studies of bevacizumab-induced toxicities found that hypertension is more common in patients of African ancestry than patients of European ancestry, both in the context of bevacizumab-induced hypertension and the worsening of pre-existing hypertension while receiving treatment[102–104]. In a study of disparities in patient-reported adverse events and

toxicities in early-stage breast cancer patients, for anthracycline-regimens, Black patients were significantly more likely to report lymphedema than White patients[105].

Disparities in chemotherapy-induced peripheral sensory neuropathy

There are numerous studies of disparities in paclitaxel-induced and vincristine-induced peripheral neuropathy that note population differences in peripheral sensory neuropathy risk and severity. It is well established that the overall incidence/prevalence and severity of paclitaxel-induced neuropathy is significantly greater in those of African ancestry/African Americans versus other populations. In the same study of early-stage breast cancer patients described above, in those receiving non-anthracycline regimes (usually combination therapies including a taxane), Black patients were significantly more likely to report moderate, severe, or very severe peripheral neuropathy even after controlling for diabetes, with a significant difference in dose reduction between populations[105]. Another cohort of early-stage breast cancer patients treated with taxane-based chemotherapy also found significantly greater sensory neuropathy symptom severity in Black versus White patients. Disparities in symptom severity were not modified when controlling for age, diabetes, body mass index, cancer stage, time since treatment, taxane type (docetaxel vs. paclitaxel), cumulative dosage, or dose modification[106]. In a randomized phase III trial of breast cancer patients, patients of African ancestry had more grade 2-4 and grade 3-4 taxane-induced peripheral neuropathy versus other ancestries[55,102]. In another study of patients receiving carboplatin and paclitaxel, paclitaxel alone, or oxaliplatin, African ancestry was associated with worse peripheral neuropathy compared to European or Asian ancestry[107]. When studying patients receiving doxorubicin and cyclophosphamide followed by paclitaxel, the percentage of patients with grade 3 or greater taxane-induced peripheral neuropathy was 11.6% in European Americans and 22.3% in African Americans[108].

Interestingly, vincristine-induced neuropathy is significantly more common in White patients than African American patients. In a group of pediatric acute lymphoblastic leukemia (ALL) patients treated with vincristine, 34.8% of White patients experienced symptoms versus only 4.8% of African American patients, with White patients having higher average neurotoxicity grade and significantly more toxicity-related dose reductions[109]. These disparities are thought to be related to genetic variation between populations, specifically in CYP3A5 expression, as CYP3A5 is a much more efficient metabolizer of vincristine than CYP3A4[110] and the *CYP3A5*1* allele required for functional CYP3A5 is more common in African American patients than White patients[61]. Therefore, disparities in chemotherapy-induced neurotoxicities may be attributed to population differences in the frequency of risk alleles.

Disparities in cisplatin-induced toxicities

In a cohort of cisplatin-treated head and neck cancer patients, African American patients were significantly more likely to develop nephrotoxicity compared to White patients[98]. Although this study did not examine the cause for these disparities, the authors hypothesized that genetic variation in enzymes in the pathway that metabolizes cisplatin into a glutathione-cisplatin conjugate and then a nephrotoxin may be implicated[98]. This disparity in cisplatin-induced nephrotoxicity was also seen in a more recent study[99]. However, despite the knowledge of population differences in neuropathy caused by other chemotherapies and in cisplatin-induced nephrotoxicity, there are not studies of disparities in cisplatin-induced neurotoxicities. This is a major gap in knowledge, as cisplatin is used to treat a large number of cancers and cisplatin-induced neurotoxicities are extremely prevalent. This was a major area of interest for us, as *The Platinum Study*, while largely European due to the epidemiology of testicular cancer[111], does

have non-European survivors who were excluded from previous GWAS. This provides us an opportunity to study disparities in cisplatin-induced neurotoxicities.

1.6 Research goals

The overall goal of this project was to investigate the clinical and genetic risk factors for cisplatin-induced neurotoxicities in adult-onset cancer survivors. This project had two major aims. The first aim was to train models to predict cisplatin-induced neurotoxicities using clinical and genetic features and supervised machine learning methods. The second aim was to determine if there are disparities in cisplatin-induced neurotoxicities related to genetic ancestry and if associations between functional ancestry-informative variants and cisplatin-induced neurotoxicity phenotypes could be related to population differences.

In Chapter 2, we utilized both clinical and genetic information to train and test machine learning prediction models for cisplatin-induced peripheral sensory neuropathy (both overall and specifically severe neuropathy), tinnitus, and hearing loss in *The Platinum Study*. Prior to model building, we pre-processed input features through methods such as transcriptome-wide association studies (TWAS) and association analyses between external PRS and cisplatin-induced neurotoxicities, which provided valuable information on the risk factors for cisplatin-induced neurotoxicities. These models provide the groundwork for clinical risk prediction of cisplatin-induced neurotoxicities prior to treatment and further our understanding of the biological pathways involved in cisplatin-induced neurotoxicities, potentially providing targets for prevention and/or treatment.

In Chapter 3, we classified testicular cancer survivors in *The Platinum Study* based on genetic ancestry and determined if there were significant disparities in cisplatin-induced peripheral sensory neuropathy, tinnitus, hearing loss, and vertigo between as well as clinical and

lifestyle factors between ancestral populations. We filtered SNPs to find independent, functional ancestry-informative markers that impacted gene expression and/or splicing in nerve/brain tissue and determined if these variants were associated with toxicities. We also utilized *in silico* and *in vitro* validation methods to assess if differences in gene expression based on expression quantitative trait loci associated with cisplatin-induced neurotoxicities corresponded to differences in cellular cisplatin sensitivity and/or neuronal cell viability. With this work, we are closer to understanding the genetic risk factors for cisplatin-induced neurotoxicities across patient populations.

Our work is significant because of (1) the widespread use of platinum compounds across cancer types[67]; (2) the high incidence of severe neurotoxicities after cisplatin treatment[11,12]; (3) the lack of FDA-approved agents for prevention or treatment of cisplatin-induced neurotoxicities in adult-onset cancer survivors[33]; (4) significant functional impairment due to cisplatin-induced neurotoxicities[31]; (5) hearing loss and tinnitus as risk factors for cognitive decline and dementia[24,25,112]; and (6) the association of cisplatin-induced neuropathic pain with increased mortality[27].

Chapter 2. Building Machine Learning Models for Risk Prediction of Cisplatin-Induced Neurotoxicities in Adult-Onset Cancer Survivors

2.1 Introduction

In patients treated with cisplatin, around 36-38% of patients get peripheral sensory neuropathy, 75-80% experience some degree of sensorineural hearing loss, and up to 42% develop permanent tinnitus[11,113]. Despite over 40 years of cisplatin use and the high incidence of these adverse events, it is difficult to predict who will develop toxicities in response to chemotherapy[113]. Due to the irreversible nature of cisplatin-induced neurotoxicities and their negative impact on physical and mental health[21,32], including cognitive decline[28], it is critical to identify patients at risk for neurotoxicities to guide dosing before treatment, monitoring during treatment, and post-treatment management. This is particularly relevant for testicular cancer patients, who can be treated with multiple standard cisplatin-based regimens. These include either three cycles of bleomycin, etoposide, and cisplatin (BEPx3) or four cycles of etoposide and cisplatin (EPx4) for patients with good prognosis[69]. Being able to predict a patient's risk of developing toxicities can help clinicians choose the appropriate treatment.

As previously described, *The Platinum Study* is a cross-sectional study of cisplatin-treated testicular cancer survivors who have been genotyped, undergone a physical exam and audiometry testing, and completed questionnaires regarding their lifestyle, medication use, and the prevalence/severity of post-treatment toxicities[47]. The data collected in *The Platinum Study* has allowed our group to conduct GWAS to find SNPs associated with cisplatin-induced toxicities, including peripheral sensory neuropathy[48], sensorineural hearing loss[49], tinnitus[50], and multiple severe neurotoxicities[51]. Clinical and lifestyle factors/behaviors such as age at diagnosis, taking blood pressure or cholesterol medication, and smoking and drinking have also

been found to be associated with cisplatin-induced neurotoxicities[47–51]. Although GWAS of testicular cancer survivors have found SNPs associated with permanent and life-altering cisplatin-induced neurotoxicities, clinical utility can only be realized through the creation of comprehensive prediction models, as a single polymorphism cannot adequately explain or predict risk[78,80].

Machine learning has been employed to predict clinical outcomes for individuals across disease types. The advantage of machine learning is its ability to integrate large volumes of information and learn complex relationships between a variety of inputs including clinical and laboratory information, genomic data, and imaging information[114]. In the context of cancer, machine learning techniques are being used to predict the risk of recurrence for breast cancer[115], the benefit of chemoradiation for head and neck cancer patients[86], and to identify radiomic, pathomic, and molecular biomarkers for the efficacy of immune-oncology drugs[116], among other uses.

Machine learning models have also been developed to predict chemotherapy-induced neurotoxicities. Many studies have used non-genetic factors for prediction, including building models to predict infection in chronic lymphocytic leukemia patients[117], severe vasomotor symptoms such as hot flashes and night sweats in breast cancer patients[118], anthracycline therapy-induced cardiotoxicity in breast cancer patients[88], and xerostomia in head and neck cancer patients[119]. However, there are now models using genetic input features as predictors. As briefly described in the introduction, one study successfully trained support vector machine and neural network models to predict vincristine-induced peripheral neuropathy at 93.8% accuracy, using a training set of 56 patients and a test set of 16 patients and two of the top three associated SNPs based on GWAS as predictors[76]. However, this study did not provide the area under the

receiver operating characteristic curve (AUROC), which is a more relevant metric for binary classification, incorporating both sensitivity and specificity information. This model was also trained on an extremely small training data set, leaving much room for improvement when training models to predict chemotherapy-induced neurotoxicities using genetic input features.

Specifically related to cisplatin-induced neurotoxicities, a study in 146 affected and 278 unaffected testicular cancer patients incorporated both clinical and genetic data into models to predict self-reported cisplatin-induced hearing loss, achieving an AUROC = 0.73[90]. A recently published paper by Millstein et al., developed a model to predict hearing loss in a pediatric population treated with cisplatin-containing regimens (n = 1,115 in training set), resulting in an area under the curve (AUC) of 0.76 in an external validation cohort[120]. Although this model was trained on a sizable training set and was validated in an external cohort, it was trained and tested in a pediatric patient population receiving varied treatment regimens and did not incorporate genetic variables. As hearing loss is highly associated with age and treatment regimen, this may preclude the clinical application of this model in adult-onset cancer survivors, such as testicular cancer survivors.

The Platinum Study, with over 1600 testicular cancer survivors with robust clinical and genetic data, including quantitative audiometry data, provided us with an unprecedented opportunity to use machine learning methods to train models to predict survivors at risk for various cisplatin-induced neurotoxicities. We evaluated the contribution of both clinical and genetic input features (derived from various methods, including GWAS, TWAS, and external PRS) and trained and tested the first machine learning prediction models for cisplatin-induced peripheral sensory neuropathy and tinnitus as well as new models for predicting cisplatin-induced hearing loss in adult-onset cancer survivors. In the future, these models can be evaluated

in other datasets of cisplatin-treated patients. These models will have a significant clinical impact, not only by predicting patients at risk for these devastating toxicities, but also by uncovering the most important predictive features for cisplatin-induced neurotoxicities.

2.2 Methods

Recruiting testicular cancer survivors to *The Platinum Study*

Testicular cancer survivors were enrolled in *The Platinum Study*, which is a multi-institutional study that recruited participants across eight cancer centers in the US, UK, and Canada. Eligibility criteria have been described in past publications from *The Platinum Study*[49,50]. Principles of informed written consent were applied to all survivors for participation, access to medical records, and blood genotyping. Each participating institution's Human Subject Review Board approved study procedures. All study procedures were performed in compliance with the US Common Rule.

Defining cisplatin-induced neurotoxicity phenotypes in *The Platinum Study*

Peripheral sensory neuropathy was defined using eight questions in the validated European Organization for Research and Treatment of Cancer-Chemotherapy-Induced Peripheral Neuropathy (EORTC-CIPN)-20 questionnaire[121]: tingling in hands/feet, numbness in hands/feet, shooting or burning pain in hands/feet, problems standing or walking due to difficulty feeling the ground, and difficulty distinguishing between hot/cold water (Appendix Table A1). Each question was answered on a 0-3 scale and the mean of responses was converted to a 0-3 scale using the ceiling function: "none" (category 0), "a little" (category 1), and "quite a bit"/"very much" (categories 2 and 3 combined). There were two neuropathy phenotypes: overall neuropathy (any versus none/yes versus no) and severe neuropathy (severe versus none). Severe neuropathy included those in categories 2 and 3 while any neuropathy (yes) included those in

categories 1, 2, and 3. For the severe versus none category, those with a mean of responses of 1 (“a little”) were excluded, comparing those in categories 2 and 3 (“quite a bit” and “very much”) with those in category 0 (‘none”). For the yes versus no (any versus none) neuropathy phenotype, those with a mean of responses of 0 (“none”) were compared to those with a mean of responses 1, 2, or 3 (“a little”, “quite a bit,” and “very much”).

For hearing loss, audiometry was conducted at 11 frequencies between 0.25-12 kilohertz (kHz). A summary measure was derived by calculating the geometric mean of bilateral hearing thresholds at frequencies 4-12 kHz[49].

Tinnitus was based on the following question from the Scale for Chemotherapy-Induced Long-Term Neurotoxicity (SCIN) questionnaire[122]: “In the last 4 weeks, have you had ringing or buzzing in the ears?”, with those answering “not at all” classified as controls and those answering “quite a bit” or “very much” classified as cases (Appendix Table A2). For quality control, answers to a second question “Do you have ringing or buzzing in the ears?” were considered. Survivors whose answers were not consistent between the two questions were excluded from further analysis.

Defining clinical and lifestyle variables in *The Platinum Study*

In addition to answering questions regarding toxicity, the questionnaires completed by *Platinum Study* participants included questions about lifestyle and behavioral factors, medication use, and other health outcomes. One important question was “excess drinking”, which was classified by how many alcoholic drinks were consumed on average over the last year from a scale of 0 to 8. To be classified as “excessively drinking,” survivors were in categories 6-8 (greater than 2 drinks per day on average). Survivors were also asked about current and past cigarette use and prescription medication use for hypertension and hypercholesterolemia.

Answers available were “never”, “past only”, “yes, current”, and “don’t know/not sure.” Those answering “never” were controls and those answering “yes, current” were cases with other responses excluded.

Continuous clinical and demographic variables were also part of analysis, such as age at diagnosis and age at questionnaire, as well as the difference between these two time points. Other clinical variables included weight at chemotherapy in kilograms, used along with height in centimeters to calculate body surface area (BSA) with the Mosteller formula[123]. The formula is BSA (m^2) = sqrt((height (cm) x weight (kg))/3600).

Genotyping, quality control, and imputation

At the time of questionnaire completion, survivors enrolled in *The Platinum Study* gave peripheral blood samples from which DNA was extracted for genotyping. Testicular cancer survivors were genotyped by the Regeneron Genetic Center in two batches. All initial analyses in *The Platinum Study* were conducted on a batch of 1680 survivors genotyped on the Illumina Global Screening Array (GSA) v1 design. The second batch included 1833 samples processed on the Illumina GSA v2 design. Of these, 153 samples were from patients not included in the original batch who had never had any previous genetic analyses conducted on them. These 1833 samples were processed by Regeneron, with 30 samples failing their genotyping quality control (QC) metrics of gender discordance, call rate < 90%, sample duplications, and exome discordance. This left 1803 survivors with genotyping data available for analysis.

For QC, individuals and variants with missingness > 0.2 followed by > 0.02 were filtered out. X chromosome homozygosity rates were used to check for any sex discrepancies. For variants, SNPs with a minor allele frequency (MAF) < 0.05 and Hardy-Weinberg Equilibrium (HWE) p-value < $1x10^{-6}$ were excluded. Individuals deviating more than three standard

deviations from the mean heterozygosity rate were excluded along with individuals with pairwise identity-by-descent (IBD) > 0.2. The University of Michigan Imputation Server[124] was used to conduct imputation with the reference panel Haplotype Reference Consortium (HRC) r1.1 2016[125], which has 64,940 haplotypes of mostly European ancestry. For QC following imputation, SNPs with imputation $R^2 < 0.8$, MAF < 0.05, and HWE p-value < 1×10^{-6} were excluded. SNPs and individuals with missingness > 0.1 were excluded. The results of QC filtering at each are detailed in Figure 2.1.

Distinction between training and test sets

The Platinum Study survivor cohort was divided into a training and test set based on the two batches of genotyping done by Regeneron. The samples in the second batch of survivors in *The Platinum Study* genotyped by Regeneron that were included in the first genotyped batch were the training set (n = 1485). The samples in the second batch of survivors in *The Platinum Study* genotyped by Regeneron that were not included in the first genotyped batch were an independent test set (n = 128) (Figure 2.1). Survivors in the test set were not part of any previous studies conducted for *The Platinum Study*, including previous GWAS. These survivors in the test set were not included in TWAS, external PRS association analyses, and clinical variable association analyses. Therefore, all genetic and clinical inputs were based solely on analyses conducted in the training set, with the test set serving as an independent set of cisplatin-treated testicular cancer survivors for validation.

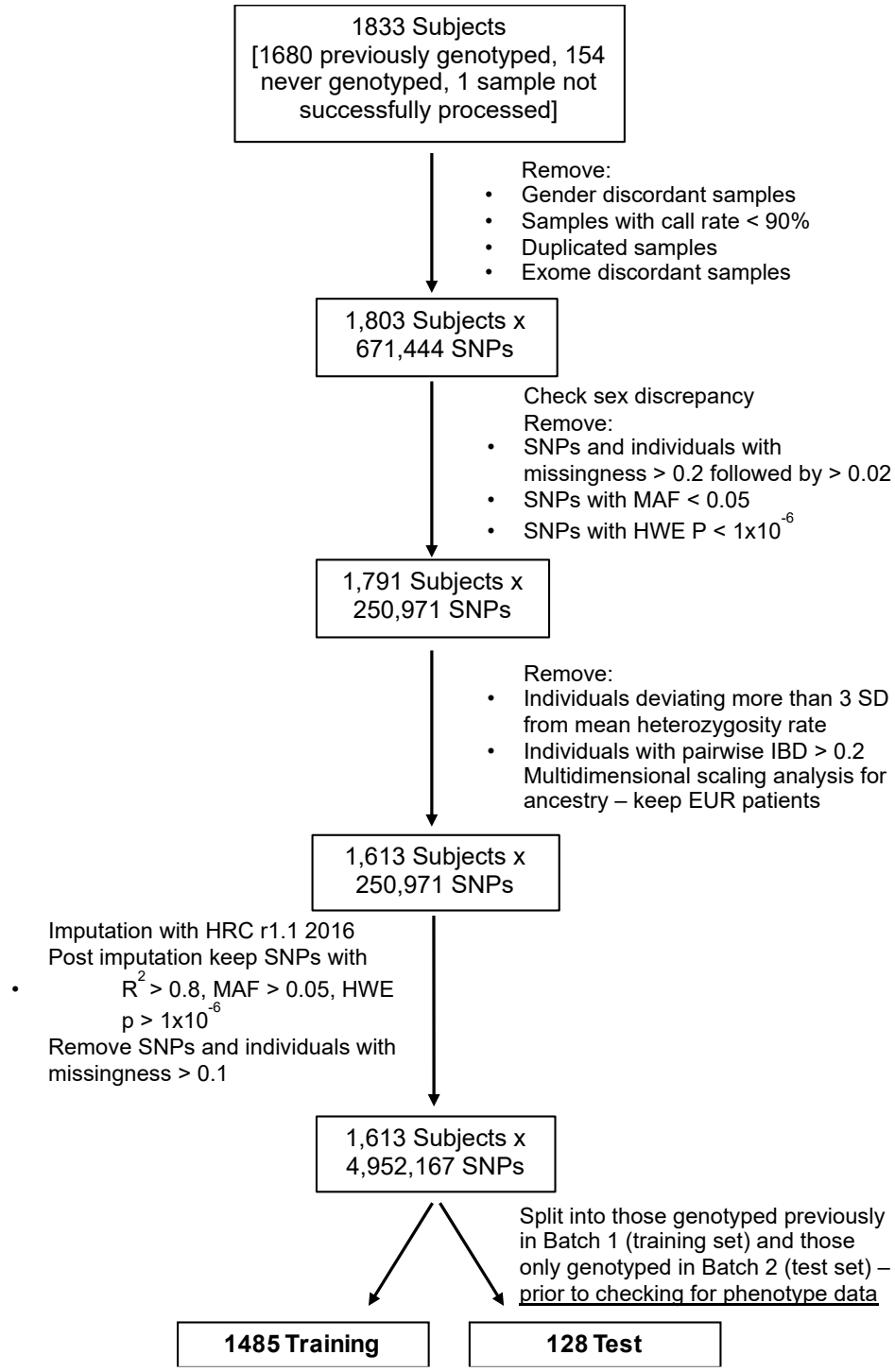

Figure 2.1. Subject and variant genotyping quality control for training and test sets

Figure 2.1. Subject and variant genotyping quality control for training and test sets (cont). Workflow for quality control for subjects prior to genotyping and for subjects and variants post genotyping as well as imputation, post-imputation quality control, and splitting subjects into training and test sets.
MAF = minor allele frequency, HWE = Hardy-Weinberg Equilibrium, IBD = identity-by-descent, SD = standard deviation, HRC = Haplotype Reference Consortium, EUR = European.

Exploration of phenotype distribution for training and test sets

The distribution of cisplatin-induced neurotoxicities in survivors in the test set were compared to the distribution in the training set to ensure no significant differences in proportion of survivors in training/test sets experiencing peripheral sensory neuropathy or tinnitus and no significant differences in hearing thresholds between training and test set survivors. The distribution of the continuous hearing loss phenotype was assessed using a Shapiro-Wilk normality test and a Wilcoxon rank sum test was used to calculate whether there was a significant difference in hearing thresholds between the training and test sets. For peripheral sensory neuropathy, the association between the toxicity and training/test set was calculated using multinomial logistic regression for the categorical phenotype and binomial logistic regression for the binary phenotype (any versus none). For tinnitus, the association between the toxicity and training/test set was calculated using binomial logistic regression.

Genetic inputs for machine learning: GWAS SNPs and TWAS eQTLs

Summary statistics from previous GWAS for cisplatin-induced peripheral sensory neuropathy, tinnitus, and hearing loss in testicular cancer survivors in *The Platinum Study* were utilized to select input SNPs[47]. These GWAS were conducted in testicular cancer survivors that were part of the training set, with no overlap with those in the test set. SNPs were filtered at three p-value thresholds for each toxicity: $p < 1x10^{-5}$, $p < 1x10^{-4}$, and $p < 1x10^{-3}$. The National Cancer Institute's (NCI) LDmatrix tool was used to calculate linkage disequilibrium (LD) between

SNPs[126]. For SNPs in LD, with $R^2 > 0.75$ in the European (CEU (Utah Residents from North and West Europe), TSI (Toscani in Italia), FIN (Finnish in England), GBR (British in England and Scotland), and IBS (Iberian population in Spain)) 1000 Genomes populations[127], the SNP with the smallest p-value of association in GWAS was kept for input, with a few exceptions when that SNP was not genotyped in our training/test sets or was in LD with another SNP not part of the same LD block. In this case, the SNP with the next smallest p-value of association was chosen. In rare cases, two SNPs with $R^2 > 0.75$ were kept as inputs if one SNP had a p-value at a magnitude of 10x lower compared to other SNPs in the LD block that were not in LD with the other input SNP. SNPs that were not biallelic were removed. As the GWAS used to determine the input SNPs assumed additive effects, the genotypes were converted to "0", "1", and "2" based on the number of instances of the minor allele (determined by the Single Nucleotide Polymorphism database (dbSNP)[128] and the Ensembl Genome Browser[129]).

The GWAS previously conducted for tinnitus had a MAF threshold of < 0.01, which was different from the MAF threshold our training and test data were subject to during QC (< 0.05)[47]. Therefore, there were some SNPs with a MAF between 0.01 and 0.05 in GWAS summary statistics that were excluded as input features as they were removed during QC.

TWAS were performed for cisplatin-induced peripheral sensory neuropathy, tinnitus, and hearing loss using FUSION[130], which identifies expression-trait associations using previously conducted GWAS summary statistics[47] and gene expression weights from Genotype-Tissue Expression Project (GTEx) tissues[131]. Previously conducted GWAS summary statistics[47] (e.g., rsID, A1 allele, and Z scores with respect to A1) were utilized as inputs and TWAS was conducted using pre-computed expression weights for tissues potentially related to cisplatin metabolism, platinum retention, body composition, and cisplatin-induced neurotoxicities. These

included tibial nerve, cerebellum (as a representative brain tissue), whole blood, kidney, liver, testis, adipose (both subcutaneous (SC) and visceral omentum (VO)), and skeletal muscle tissues from GTEx v8, using pre-computed .pos files with genes that achieved significant heritability. Brain RNASeq gene expression data from the CommonMind Consortium study was also used as an input for TWAS[132]. The TWAS p-value threshold for significance for each tissue was the Bonferroni adjusted p-value threshold (0.05/number of genes tested for each tissue independently). For potential inputs into machine learning models, three TWAS p-value thresholds were used: $p < 0.0005$, $p < 0.005$, or $p < 0.05$.

Transcriptome-wide associations were further post-processed. At each p-value threshold level, marginally associated and jointly significant genes were selected. The outputs of interest were the gene, the rsID of the best expression quantitative trait locus (eQTL) in the gene locus, the Z score of this eQTL, the GWAS Z score for the best eQTL, the TWAS Z score (which may be for an eQTL or non-eQTL model depending on performance), and the TWAS p-value. For our machine learning models, the genotype of the "best eQTL" in the gene locus served as the input, regardless of whether the top gene expression imputation model was the single best eQTL or another model incorporating more SNPs at the gene locus. Duplicate eQTLs were discarded and LDmatrix was used to determine LD (R^2 cutoff = 0.75). For SNPs in LD, the SNP with the highest absolute eQTL Z score value was kept (or the average of eQTL Z score values in the case of an eQTL across numerous tissues), with a few exceptions when the eQTL with the highest absolute Z score had $R^2 > 0.75$ with the eQTL chosen in another LD block or was not genotyped in which case the eQTL with the next highest absolute Z score was chosen. SNPs that were not biallelic were removed. Duplicates and LD were also compared with GWAS SNPs when GWAS

and TWAS inputs were combined. eQTL genotypes were also converted to “0”, “1”, and “2” based on the number of instances of the minor allele.

The verbiage used by the creators of the FUSION TWAS program for the output of their algorithm was "best eQTL”. This referred to the cis-eQTL in the gene locus that when considered alone, had the highest accuracy of gene expression imputation (adjusted accuracy calculated using the cross validation R^2 between prediction and actual expression and normalized by cis-h^2_g (heritability))[130]. This “best eQTL” was what was selected as the potential input feature for machine learning models. However, in the FUSION method, a non-eQTL model was always used to compute the TWAS statistic regardless of the accuracy of the best eQTL model. The TWAS summary statistics were based on the best performing prediction model, which could be blup best linear unbiased predictor (blup), Bayesian sparse linear model (bslmm), elastic-net regression with mixing parameter of 0.5 (enet), Least Absolute Shrinkage and Selection Operator (LASSO), sum of single effects regression (susie), or single best eQTL (top1). The methods by which GWAS and TWAS for cisplatin-induced neurotoxicities were performed and incorporated as potential inputs into machine learning models are detailed in Figure 2.2.

To understand the functional relevance of the TWAS genes with the strongest p-values of association ($p < 0.0005$, $p < 0.005$, $p<0.05$) with cisplatin-induced neurotoxicities and to find significant functionally enriched pathways, these genes/encoded proteins were input into STRING pathway analysis[133].

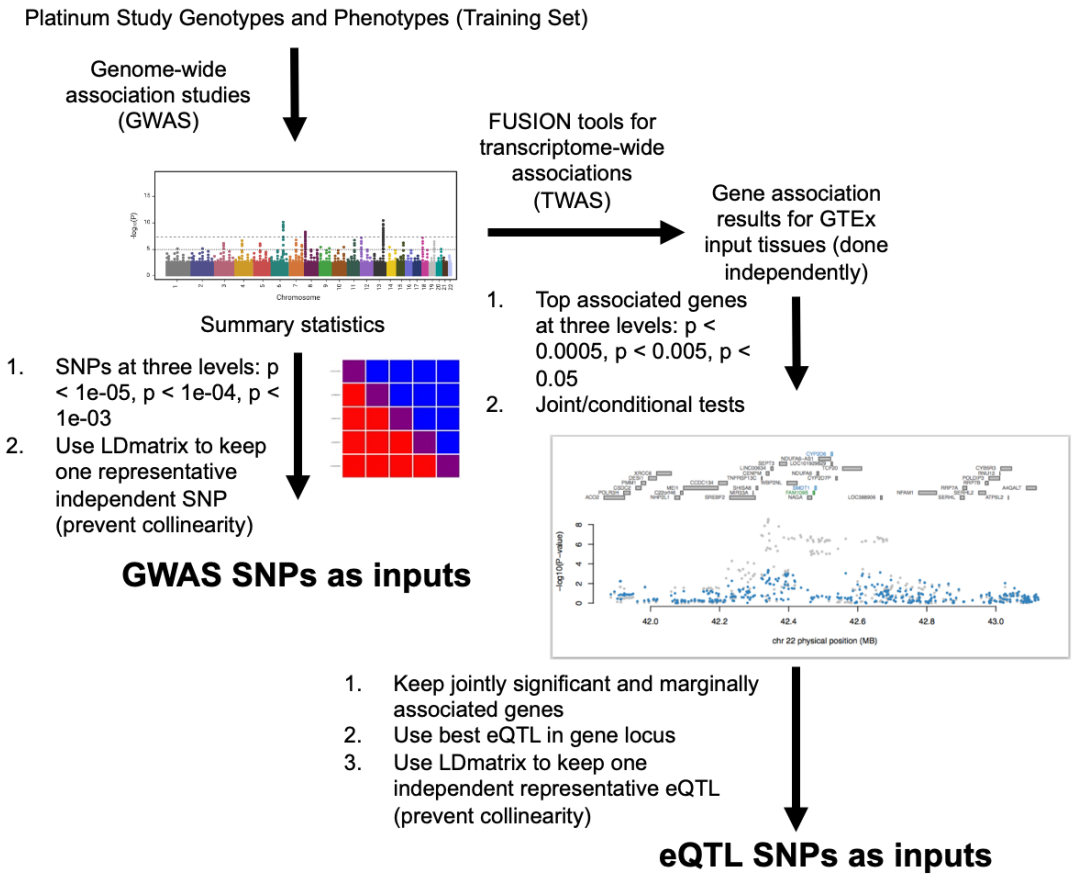

Figure 2.2 Genetic inputs for machine learning: GWAS and TWAS inputs. Workflow for filtering SNPs associated with cisplatin-induced neurotoxicities by GWAS for input into machine learning models at three different p-value thresholds as well as the application of the FUSION method to conduct TWAS and the filtering of TWAS results at three different p-value thresholds for input into machine learning models.
GTEx = Genome-Tissue Expression project. eQTL = expression quantitative trait loci.
GWAS image icon from BioRender.com, heatmap image icon adapted from NCI LDmatrix[126], TWAS image icon from FUSION tool[130] tutorial (Gusev lab website/ https://github.com/gusevlab/fusion_twas?tab=readme-ov-file).

Genetic inputs for machine learning: applying external PRS to cisplatin-treated testicular survivors

PRS incorporate the weight of numerous GWAS SNP effects to calculate quantifiable genetic risk[80]. Published external PRS built in the UK Biobank[134–136] were selected from the PGS Catalog and PRS for these traits were calculated in cisplatin-treated testicular cancer survivors in

The Platinum Study using PRSice 2.3.3[137]. PRS were calculated for several categories of traits: *de novo* toxicities or related phenotypes (peripheral nerve disorders, self-reported hearing loss, dementia, Alzheimer's), kidney function (e.g., creatinine clearance, cystatin C, estimated glomerular filtration rate (eGFR)), lipid profile (e.g., total cholesterol, high density lipoprotein (HDL), low density lipoprotein (LDL), triglycerides), pharmacokinetics/body composition (e.g., weight, body fat percentage) and other potentially related traits (e.g., vitamin D measurement, nonalcoholic liver disease). The associations between PRS and cisplatin-induced toxicities were calculated in the training dataset. For hearing loss, Shapiro-Wilk tests for normality were conducted for each PRS and association between external PRS and hearing loss was calculated using Spearman's rank correlation. For peripheral sensory neuropathy (both any versus none and severe versus none) and tinnitus, the Shapiro-Wilk test for normality was used to assess the distribution of PRS in the training set. Based on distribution, either a Welch's two-sample t-test (for normally distributed PRS) or a Wilcoxon rank sum test (for not normally distributed PRS) were calculated between PRS and the cisplatin-induced neurotoxicity phenotype in the training set in R4.1.2. Following calculation of association between PRS and cisplatin-induced neurotoxicities, PRS were used as machine learning inputs.

Genetic inputs for machine learning: cisplatin-associated SNPs

Another set of potential inputs included SNPs associated with genes related to cisplatin uptake, metabolism, and effect, based on a literature search[138–140]. These included genes in multiple categories, including those related to antioxidant protection, import/export of cisplatin, solute carrier (SLC) transporters, DNA repair, metallothionine, glutathione (GSH) synthesis, apoptosis, and downstream pathways like protein kinase and mitogen-active protein kinases. SNPs of interest were eQTLs, splicing quantitative trait loci (sQTLs), and upstream,

downstream, intronic, and coding variants for the genes listed in Table 2.1. GTEx data[131] (V8 release) was used to determine eQTLs and sQTLs for cisplatin-associated genes across tissues and dbSNP[128] was used to find other variants associated with these genes, with duplicates removed. Similar to GWAS and TWAS variant inputs, LDmatrix[126] was used to find LD blocks of SNPs with $R^2 > 0.75$ in the 1000 Genomes European populations[127] and one representative SNP was retained for input into machine learning analysis. SNPs that were not biallelic were removed. SNP genotypes were also converted to "0", "1", and "2" based on number of instances of the minor allele. Cisplatin-associated genes are listed in Table 2.1.

Table 2.1. Cisplatin-associated genes of interest.

Category	**Gene**
Antioxidant Protection	GSTM1, GSTP1, GSTO1
Import (main)	SLC31A1 (CTR1), SLC7A2 (CTR2)
Export	ATP7B, ABCC2
DNA repair	1. XPA, ERCC1/2/4 2. POLQ, POLN, POLD1, PNKP, BARD1, PARP1 3. FEN1, FAAP24
Metallothionine	MT1A, MT2A, MT3, MT4, MTR1, MTF-1, ZBTB1, USF1, SPI1 (PU.1), SMARCA4 (BRG1), MBD3, CEBPα, XRCC5 (KU80), NFIA (NF1), DNMT3A
Other SLC transporters	SLC22A5/7, SLC22A10-13, SLC2216, SLC22A20, SLC31A2
GSH synthesis	GSS, GCLC, GCLM
Apoptosis	1. BCL2, BCL2L1, TP63 2. CFLAR
Protein Kinase	PRKCA, PRKCB
Mitogen-active protein kinase	MAPK3,MAPK13,MAP3K1
Transcription factors	NFKB1/2, TWIST, SNAI1
Miscellaneous	FOS, CDKN2C, TLR4

Abbreviations: SLC, solute carrier; GSH, glutathione.

Clinical inputs for machine learning

Clinical inputs for machine learning included age at diagnosis, age at questionnaire, time difference between diagnosis and questionnaire, BSA (m^2), weight at chemotherapy (kg), cholesterol medication, blood pressure medication, excess drinking, and current or ever smoking. The first five clinical variables were continuous and the others were categorical. In the training set, associations between cisplatin-induced neurotoxicities and clinical variables were calculated. For hearing loss, Shapiro-Wilk tests for normality were conducted for each continuous clinical variable and association with hearing loss was calculated using Spearman's rank correlation. For categorical clinical variables, a Wilcoxon rank sum test was calculated between hearing thresholds and clinical variables. For peripheral sensory neuropathy (any versus none and severe versus none) and tinnitus, the Shapiro-Wilk test for normality was used to assess distribution of categorical variables in the training set. Based on distribution, Wilcoxon rank sum tests (as continuous variables were not normally distributed) were calculated between continuous clinical variables and the cisplatin-induced neurotoxicity phenotypes in the training set. For categorical variables, binomial logistic regression was calculated between clinical variables and toxicity phenotypes. Association analyses were conducted in in R4.1.2.

Imputation of missing values for clinical variables

For a small number of testicular cancer survivors, some clinical variables had missing for values from physical exam (e.g. weight at chemotherapy) or from questionnaire (e.g. medications). Missing values were imputed so that rows would not have to be disregarded from training and test sets due to NA values. The method utilized was the missForest technique based on random forest, which is a non-parametric method that trained a random forest model for clinical variables with missing values and then used the model that was trained in order to predict

any missing values[141]. The success of imputation was assessed by comparing the distribution of histograms before and after imputation.

Machine learning model building, feature selection, and tuning

Multiple machine learning models were trained for prediction including penalized logistic regression (LASSO and ridge), radial and polynomial kernel support vector machines (SVM), random forests, and extreme gradient boosting[142–144]. Machine learning models were initially trained on only clinical or only genetic inputs. Models were then trained combining clinical and genetic input features to determine if model performance improved compared to models trained on only one type of input feature.

Feature selection is particularly pertinent if the number of features is large in relation to the number of patients in the training data. Application of feature selection is critical for determining which features contribute the most to the model. More parsimonious models are more relevant for implementation. Feature selection methods tested included: recursive feature elimination (RFE) (random forest criteria) and minimum redundancy maximum relevance (mRMR)[145,146].

Recursive feature elimination

Recursive feature elimination operates through an iterative feature selection process. It recursively eliminates features from the dataset and evaluates model performance at each step. Feature elimination occurs by ranking features based on their relevance to the target variable and removing the least important variables until optimal model performance is achieved. It is a particularly robust feature selection method when combined with cross-validation[145].

The “caret” algorithm used for recursive feature elimination was random forest (rfFuncs) in R4.1.2, due to its capacity for determining feature importance. The outer resampling method

was repeated cross-validation with 10-fold cross-validation repeated 5 times. Outputs of interest were accuracy and kappa for binary phenotypes and root mean squared error (RMSE) and Rsquared for hearing loss, with the algorithm selecting the optimal number of features for each set of input features (GWAS/TWAS, clinical variables, external PRS) based on these outputs.

Minimum redundancy maximum relevance

The minimum redundancy maximum relevance (mRMR) feature selection method is based upon the principle of choosing features that are strongly related to the classification output but weakly related to other features. This algorithm calculates the relevance score and redundancy score and calculates an importance score as either the ratio or the difference between the relevance and redundancy scores[146]. mRMR is also iterative, as the relevance of all input variables is first calculated and the feature with the highest relevance is selected, followed by a calculation of redundancy between all other features with this feature as well as a calculation of the importance scores, selecting the feature with the maximum importance scores and adding it to the list of selected features. The number of features to select is pre-defined and the mean redundancy is calculated between all of the remaining features and those selected, generating new importance scores and selecting the feature with the highest score until the previously determined number of features is reached[146].

mRMR was conducted using the ensemble function[147] in R4.1.2, with the feature count set at 50%, 25%, 10% etc. of the total number of features. The ensemble function was set at a solution count of 10, and each feature selected was the most common feature amongst the 10 solutions (or the most common feature that was not a repeat of a previous feature).

Subsampling and metrics for class imbalance

For both severe versus no peripheral sensory neuropathy and tinnitus, there was class imbalance between the cases and controls, with approximately 80% of survivors in both the training and test sets not having the toxicity. Class imbalance between the majority and minority can lead to skewed prediction as it can be more challenging for the model to learn from the minority class, thus biasing the model towards more classification errors for the minority class. This is an issue due to the fact that the minority class is the toxicity of interest that we want to predict. In order to address this, different subsampling/sampling techniques were assessed in the training set using the caret function in R4.1.2, including down-sampling and up-sampling, as well as the hybrid technique random over-sampling examples (ROSE) simulates synthetic data to balance the majority and minority classes. Down-sampling is a technique that randomly takes a subset of the majority class in the training set so that its class frequency will match the minority class. Up-sampling randomly samples the minority class to match the size of the majority class (with replacement).

Preprocessing

When appropriate, i.e. when predictors (such as clinical variables) had different ranges, pre-processing by centering and scaling was applied to data (SVM, tree-based models). This was also important when combining different modalities of input features so that features with large ranges did not overtake the model. This ensured that all feature types contributed equally to the learning process during model building.

Hyperparameter tuning and model building with tree-based models (random forests, extreme gradient boosting)

Random forests is a supervised machine learning algorithm that is a decision tree-based ensemble method[143]. The three main hyperparameters of interest for random forests are mtry

(value that sets the number of features randomly sampled at each split), number of trees (ntree), and node size (controls tree depth and complexity). For our study, the tuning grid for hyperparameter optimization had mtry values of 1, 5, and 10. The number of trees tested were 500 and 1000 and the node sizes were 1 and 5. Hyperparameter tuning was based on 10-fold cross-validation repeated 3 times in the training set and tuning to appropriate outcomes (accuracy for peripheral sensory neuropathy any versus none, AUROC for peripheral sensory neuropathy severe versus none and tinnitus, and root mean squared error (RMSE) for hearing loss). Hyperparameters were chosen based on model performance in the training set. The workflow for training, tuning, and testing random forest models is described in Figure 2.3.

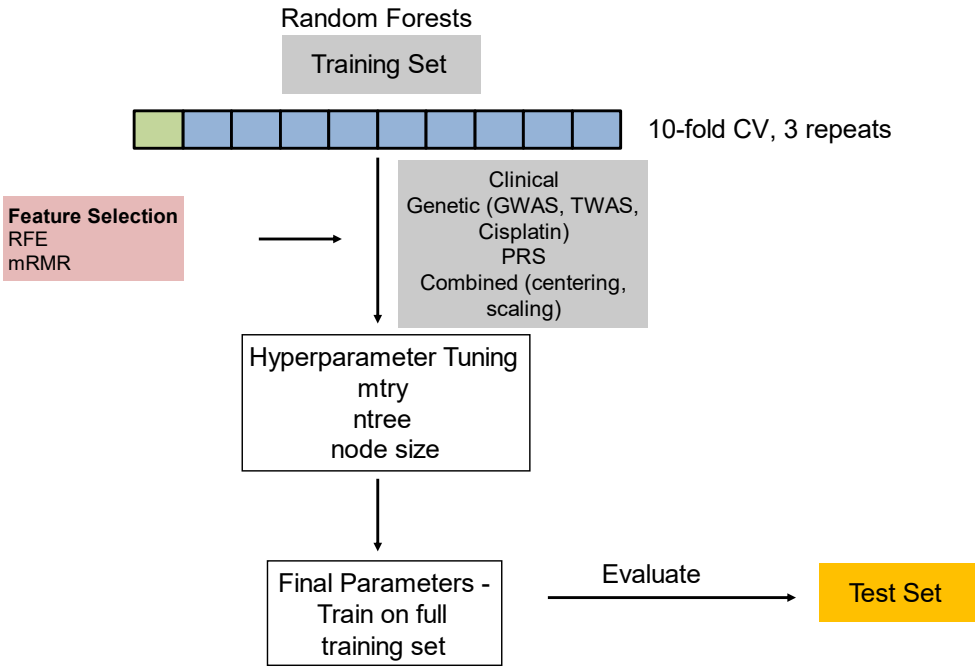

Figure 2.3. Workflow for training and testing random forest models. Workflow for training, hyperparameter tuning, and testing of random forest models.
CV = cross validation. RFE = recursive feature elimination. mRMR = minimum redundancy maximum relevance.

Extreme gradient boosting (XGBoost) is another tree-based supervised learning technique that utilizes a gradient descent algorithm for boosting[144]. Again, hyperparameter

tuning was based on 10-fold cross-validation repeated 3 times in the training set. There were many hyperparameters for XGBoost in our tuning grid, including nrounds (initially 200, 300, 400, 500, 600), eta/learning rate (0.025, 0.05, 0.1, 0.3), maximum depth (initially 4, 5, 6), gamma (initially 0, 1, 2), colsample_by_tree (initially 0.1, 0.25, 0.5, 0.75, 1.0), min_child_weight (initially 1, 3, 5), and subsample (set constant to default at 1). The workflow for training, tuning, and testing XGBoost models is described in Figure 2.4.

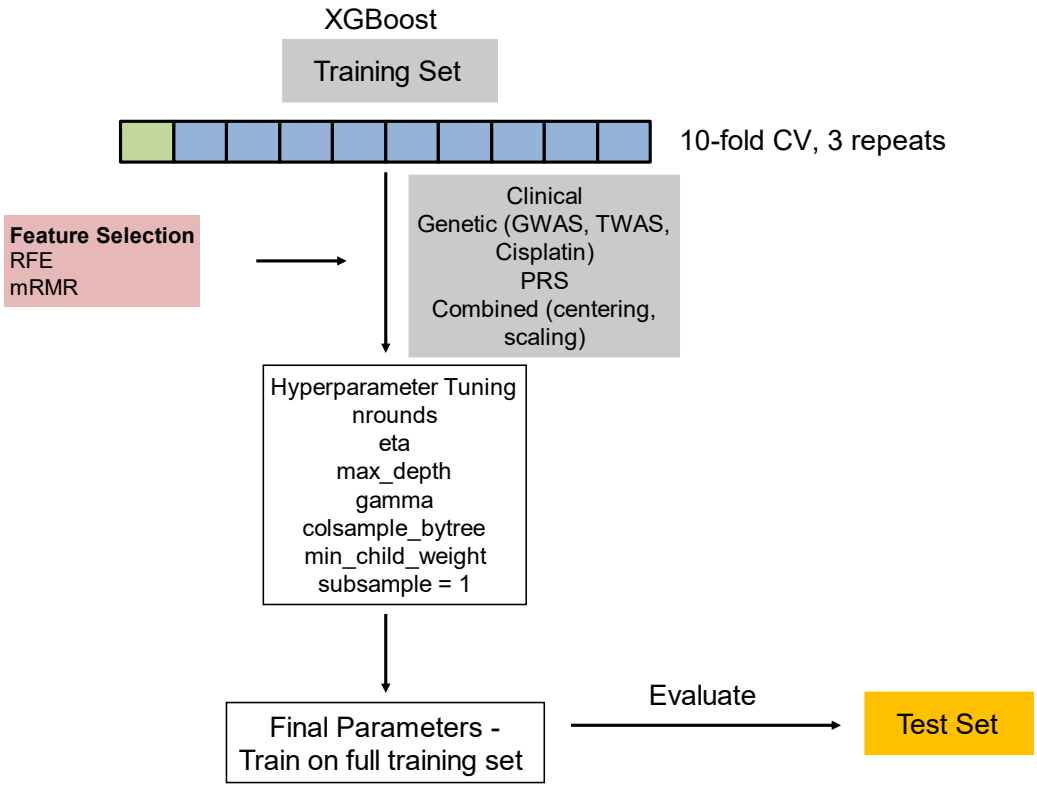

Figure 2.4. Workflow for training and testing extreme gradient boosting models.
Workflow for training, hyperparameter tuning, and testing of extreme gradient boosting models.
XGBoost = extreme gradient boosting. CV = cross validation. RFE = recursive feature elimination. mRMR = minimum redundancy maximum relevance.

Hyperparameter tuning and model building with support vector machines

Support vector machine (SVM) models operate on the principle of finding the optimal hyperplane to separate between classes (or for predicting continuous outputs for regression)[143].

Hyperparameter tuning for SVM models also used 10-fold cross-validation repeated 3 times in the training set. Both the radial and polynomial kernels were tuned with a variety of grid values for cost and gamma (radial) and cost, degree and scale (polynomial). The workflow for training, tuning, and testing SVM models is described in Figure 2.5.

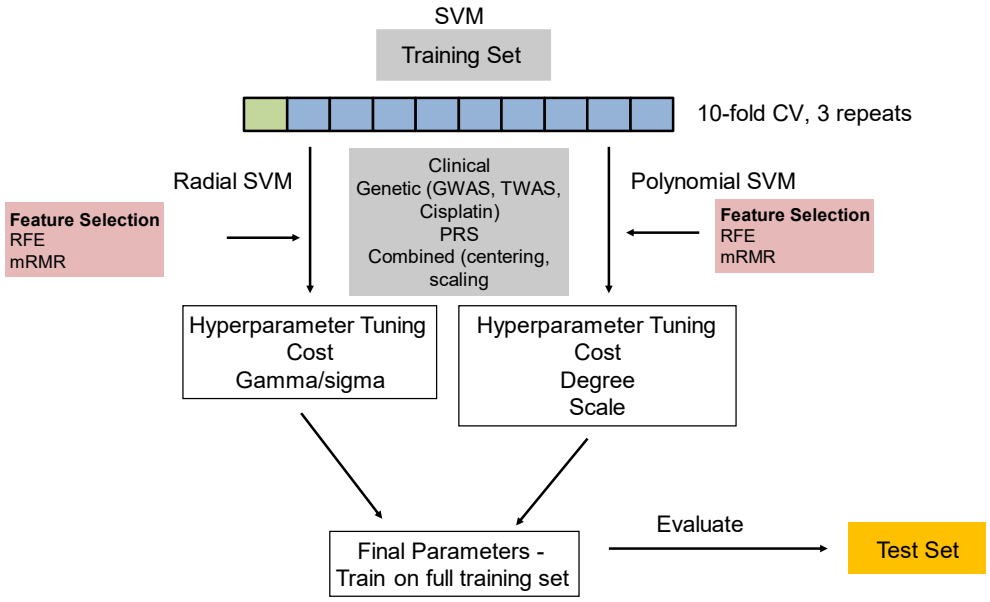

Figure 2.5. Workflow for training and testing support vector machine models. Workflow for training, hyperparameter tuning, and testing of support vector machine models. SVM = support vector machine. CV = cross validation. RFE = recursive feature elimination. mRMR = minimum redundancy maximum relevance.

Penalized regression and L1 and L2 regularization (LASSO, Ridge)

The most basic machine learning models were penalized logistic regression (neuropathy and tinnitus) or linear regression (hearing loss) models. Penalized regression models combine feature selection and model building by shrinking the coefficients of the input variables that contribute the least to the model to zero (LASSO) or towards zero (ridge). The LASSO penalized regression method uses L1 regularization (constant alpha = 1). The ridge penalized regression method uses L2 regularization (constant alpha = 0)[142]. In our models, the penalty parameter

lambda was optimized with 10-fold cross validation in the training data before fitting the final models in the test set with the minimum lambda value.

Assessing success of final models on test set

For all model types, following hyperparameter tuning, models were tested by training the model on the training set with the selected input features and optimized parameters and applying this model to the test set. Models were trained on individual modalities of input features (clinical and genetic (SNP genotypes and external PRS) features) alone and then models were trained on combinations of input features. For final model performance, AUROC, sensitivity, and specificity were the metrics of greatest importance for the models for predicting the binary phenotypes (cisplatin-induced neuropathy and tinnitus) and RMSE and Rsquared were the metrics of greatest importance for the models for predicting cisplatin-induced hearing loss. For hearing loss, in addition to using RMSE and Rsquared as metrics of model performance, the Spearman correlation coefficient was calculated between the actual GM412 values in the test set and the GM412 values predicted by the model to assess if there was a significant correlation between these values. Additionally for AUROC, the 95% confidence intervals (CI) were calculated using DeLong's test.

STRING pathway analysis

For each phenotype, if a successful model (based on AUROC or RMSE) used SNPs as input features, those SNPs were further analyzed. For each SNP, dbSNP[128], GTEx[131] (V10), and the GWAS catalog[148] were used to find genes related to these SNPs, including genes for which these SNPs may be coding variants, may be upstream or downstream of the gene, or may impact gene expression and/or splicing across GTEx tissues. Once a list of genes was created, STRING was used to analyze protein-protein interaction between proteins encoded by those genes[133] and

to conduct functional enrichment analysis to identify networks and biological pathways that may be related to risk for cisplatin-induced neurotoxicities.

2.3 Results

Definition and distribution of toxicities in training and test sets

The number of testicular cancer survivors in *The Platinum Study* in the training and test sets for each cisplatin-induced neurotoxicity are listed in Table 2.2.

Table 2.2. Number of testicular cancer survivors in training and test sets for each cisplatin-induced neurotoxicity

Phenotype	**Number in Training Set**	**Number in Test Set**
Peripheral Sensory Neuropathy (Yes vs. No/Any vs. None)	1441	124
Peripheral Sensory Neuropathy (Severe vs. None)	778	62
Tinnitus	1072	87
Hearing Loss	1087	76

There were no significant differences in the distribution of cases and controls between training and test sets for peripheral sensory neuropathy any versus none ($p = 0.52$), peripheral sensory neuropathy severe versus none ($p = 0.98$), tinnitus ($p = 0.40$), and hearing loss ($p = 0.58$) (Figure 2.6).

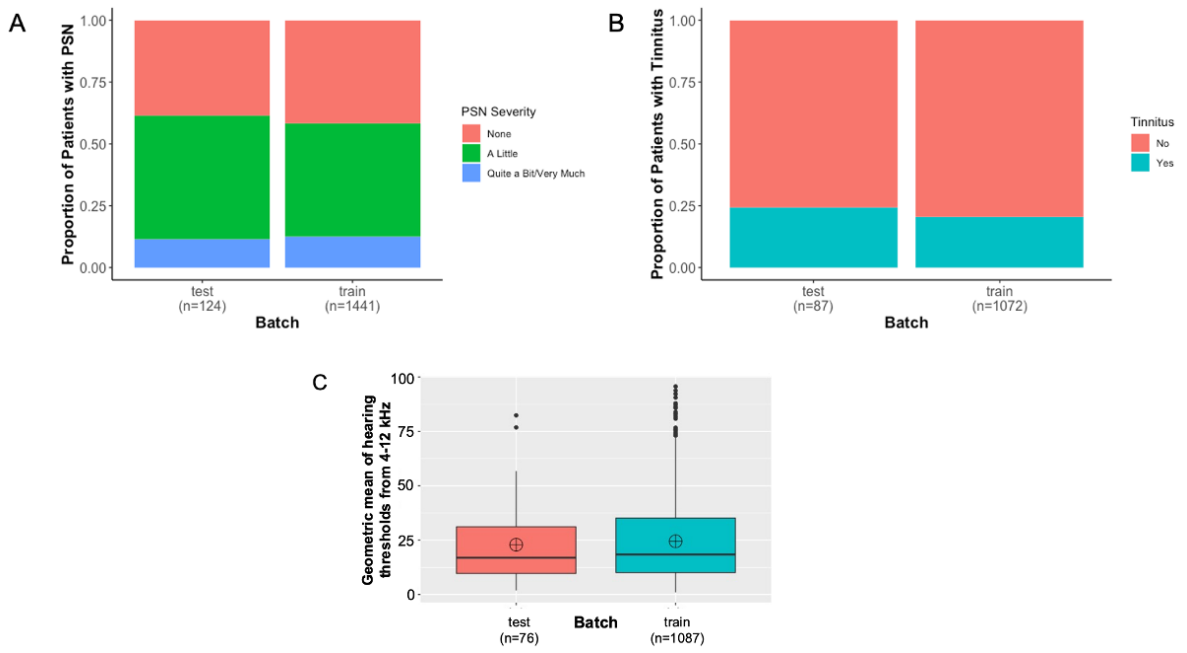

Figure 2.6. Distribution of toxicity phenotypes in training and test sets. A, Distribution of PSN phenotype in training and test sets. **B,** Distribution of tinnitus phenotype in training and test sets. **C,** Distribution of GM412 (kHz) in training and test sets.
GM412 = Geometric mean of hearing thresholds from 4-12 kilohertz.

Association of clinical variables with cisplatin-induced neurotoxicities in training set

Age at diagnosis, age at questionnaire, cholesterol medication, and blood pressure medication were significantly associated ($p < 0.05$) with all toxicities, including overall peripheral sensory neuropathy (any versus none), severe peripheral sensory neuropathy (severe versus none), tinnitus, and hearing loss. Weight at time of chemotherapy (kg), BSA (m^2), and ever smoking were significantly associated with all toxicities except for tinnitus. Excess drinking and currently smoking were significantly associated with overall peripheral sensory neuropathy (any versus none) and severe peripheral sensory neuropathy (severe versus none). The time difference between diagnosis and evaluation was only significantly associated with hearing loss. Tinnitus was only significantly associated with age (at diagnosis and questionnaire) and medication use (both blood pressure and cholesterol) (Table 2.3).

Table 2.3. Associations between clinical variables and cisplatin-induced neurotoxicities in *The Platinum Study* training set

Clinical Variable	PSN (Any vs. None/Yes vs. No)	PSN (Severe vs. None)	Tinnitus	Hearing Loss
Age at Diagnosis	$< 2.2x10^{-16}$	$1.7x10^{-15}$	$6.4x10^{-4}$	$< 2.2x10^{-16}$
Age at Questionnaire	$7.6x10^{-14}$	$7.5x10^{-12}$	$1.1x10^{-4}$	$< 2.2x10^{-16}$
Time Difference	$6.1x10^{-2}$	0.39	0.71	$4.0x10^{-15}$
Weight at Chemotherapy (kg)	$2.0x10^{-2}$	$3.2x10^{-4}$	0.20	$4.3x10^{-5}$
Body Surface Area (m^2) (calculated)	$2.9x10^{-2}$	$7.2x10^{-4}$	0.38	$2.6x10^{-4}$
Cholesterol Medication	$6.5x10^{-3}$	$1.3x10^{-3}$	$1.6x10^{-4}$	$2.2x10^{-14}$
Blood Pressure Medication	$1.2x10^{-6}$	$2.7x10^{-8}$	$5.3x10^{-8}$	$2.4x10^{-16}$
Excess Drinking	$1.4x10^{-2}$	$2.8x10^{-2}$	0.36	0.21
Current Smoker	$2.9x10^{-2}$	$4.3x10^{-3}$	0.31	0.10
Ever Smoked	$5.8x10^{-4}$	$1.2x10^{-4}$	0.14	$3.4x10^{-2}$

Imputation of missing values for clinical variables

Multiple clinical variables had some missing data for patients, including two continuous variables (weight at chemotherapy and body surface area (BSA)) and categorical variables (cholesterol and blood pressure medication, current and ever smoking, excess drinking). Using the missForest method for imputation of missing values for clinical variables did not show major changes in the distribution of values for continuous clinical variables pre- and post-imputation when visually comparing histograms (Appendix Figure A1). Imputed clinical variables were used for input into machine learning models.

Association of external PRS with cisplatin-induced neurotoxicities in the training set

PRS built in the UK Biobank for numerous traits were calculated in cisplatin-treated testicular cancer survivors in *The Platinum Study*. Associations between PRS and cisplatin-induced neurotoxicity phenotypes were calculated in the training set, finding numerous PRS

which were significantly associated with toxicities ($p < 0.05$) (Tables 2.4, 2.5, 2.6, 2.7). PRS significantly associated with overall peripheral sensory neuropathy (any versus none) included PRS for otosclerosis as well as PRS for lipid-related traits such as apolipoprotein A, total cholesterol, LDL, and HDL levels. The other category of PRS associated with cisplatin-induced peripheral sensory neuropathy (any versus none) were related to kidney function, including three PRS for cystatin C measurement, two PRS for serum albumin measurement, and two PRS for urine sodium measurement (Table 2.4). A PRS for dementia and a PRS for serum protein (non-albumin) measurement as well as multiple PRS related to body composition, including lean body mass, two PRS for body fat mass, and two PRS for body fat percentage were significantly associated with severe peripheral sensory neuropathy (severe versus none) along with lipid-related PRS, such as PRS for total cholesterol and LDL levels (Table 2.5).

Table 2.4. Associations between external PRS and cisplatin-induced peripheral sensory neuropathy (yes vs. no) in testicular cancer survivors in *The Platinum Study* training set ($p < 0.05$)

Trait	**Mean in Survivors with No Neuropathy**	**Mean in Survivors with Neuropathy**	**p-value**
Otosclerosis PGS002046	-7.2×10^{-10}	-7.9×10^{-10}	3.8×10^{-2}
Apolipoprotein A PGS000671	4.9×10^{-6}	4.7×10^{-6}	3.8×10^{-2}
Cholesterol PGS000677	6.0×10^{-6}	5.6×10^{-6}	8.8×10^{-4}
LDL PGS000688	5.0×10^{-6}	4.6×10^{-6}	6.7×10^{-3}
HDL PGS000686	9.3×10^{-6}	9.0×10^{-6}	1.6×10^{-2}
Cystatin C PGS002165	6.6×10^{-8}	7.2×10^{-8}	3.9×10^{-3}
Cystatin C PGS001947	6.3×10^{-7}	6.9×10^{-7}	1.3×10^{-3}
Cystatin C PGS000680	8.7×10^{-7}	1.0×10^{-6}	1.7×10^{-2}
Serum Albumin PGS001886	8.6×10^{-6}	8.0×10^{-6}	2.3×10^{-2}
Serum Albumin PGS002099	9.9×10^{-7}	9.3×10^{-7}	1.5×10^{-2}

Continuation of Table 2.4

Urine Sodium PGS002007	$-1.8x10^{-5}$	$-2.7x10^{-5}$	$2.0x10^{-2}$
Urine Sodium PGS002226	$5.2x10^{-7}$	$9.8x10^{-8}$	$1.9x10^{-2}$

Abbreviations: LDL, low-density lipoprotein; HDL, high-density lipoprotein.

Table 2.5. Associations between external PRS and cisplatin-induced peripheral sensory neuropathy (severe vs. none) in testicular cancer survivors in *The Platinum Study* training set ($p < 0.05$)

Trait	**Mean in Survivors with No Neuropathy**	**Mean in Survivors with Severe Neuropathy**	**p-value**
Dementia PGS001827	$4.2x10^{-3}$	$3.2x10^{-3}$	$1.4x10^{-2}$
Lean Body Mass PGS001950	$-1.2x10^{-7}$	$-7.9x10^{-8}$	$1.6x10^{-2}$
Body Fat Mass PGS001951	$7.3x10^{-7}$	$9.2x10^{-7}$	$5.4x10^{-4}$
Body Fat Mass PGS002169	$7.2x10^{-8}$	$9.2x10^{-8}$	$9.3x10^{-4}$
Body Fat Percentage PGS001917	$1.2x10^{-7}$	$1.5x10^{-7}$	$1.1x10^{-3}$
Body Fat Percentage PGS002133	$9.8x10^{-9}$	$1.3x10^{-8}$	$2.2x10^{-3}$
Total Cholesterol PGS002108	$9.3x10^{-7}$	$8.5x10^{-7}$	$4.1x10^{-2}$
Cholesterol PGS000677	$6.0x10^{-6}$	$5.6x10^{-6}$	$3.0x10^{-2}$
LDL PGS002150	$3.7x10^{-7}$	$3.0x10^{-7}$	$2.3x10^{-2}$
Serum Protein Non-Albumin PGS000691	$2.7x10^{-7}$	$6.5x10^{-8}$	$3.5x10^{-2}$

Abbreviations: LDL, low-density lipoprotein.

A PRS for hearing difficulties and three PRS for hypertension were significantly associated with cisplatin-induced tinnitus, along with multiple PRS related to kidney function, including a PRS for urine creatinine measurement, cystatin C measurement, and kidney failure. Like for cisplatin-induced peripheral sensory neuropathy, multiple PRS related to dyslipidemia, including two PRS for apolipoprotein B measurement and one PRS for LDL measurement were

associated with tinnitus. (Table 2.6). The PRS significantly associated with cisplatin-induced hearing loss included PRS for *de novo* neurotoxicity and ototoxicity including a PRS for peripheral nervous system disorders and two for hearing difficulties, showing a significant relationship between increased PRS for these toxicities and increased hearing thresholds (more severe hearing loss) (Table 2.7). Also significantly associated with cisplatin-induced hearing loss, like other cisplatin-induced toxicities were PRS related to body composition (body fat mass and body fat percentage) and kidney function (urine creatinine, cystatin C, and urine potassium measurement) (Table 2.7). All associations between external PRS and cisplatin-induced neurotoxicities in the training set are in Appendix Tables A3-A6.

Table 2.6. Associations between external PRS and cisplatin-induced tinnitus in testicular cancer survivors in *The Platinum Study* training set ($p < 0.05$)

Trait	**Mean in Survivors with No Tinnitus**	**Mean in Survivors with Tinnitus**	**p-value**
Hearing Difficulties PGS002104	$3.6x10^{-9}$	$8.5x10^{-9}$	$7.6x10^{-3}$
Hypertension PGS001838	$6.6x10^{-6}$	$7.4x10^{-6}$	$1.4x10^{-2}$
Hypertension PGS002047	$4.0x10^{-8}$	$4.8x10^{-8}$	$1.7x10^{-2}$
Hypertension PGS000706	$6.6x10^{-6}$	$7.6x10^{-6}$	$1.4x10^{-3}$
Apolipoprotein B PGS001889	$2.2x10^{-6}$	$1.6x10^{-6}$	$1.6x10^{-2}$
Apolipoprotein B PGS002102	$-7.9x10^{-9}$	$-3.0x10^{-8}$	$4.1x10^{-2}$
LDL PGS001933	$8.8x10^{-6}$	$7.8x10^{-6}$	$3.0x10^{-2}$
Urine Creatinine PGS000679	$-3.1x10^{-6}$	$-2.1x10^{-6}$	$3.6x10^{-2}$
Cystatin C PGS000680	$8.9x10^{-7}$	$1.1x10^{-6}$	$4.0x10^{-2}$
Kidney Failure PGS000708	$6.1x10^{-7}$	$9.8x10^{-7}$	$3.0x10^{-2}$

Abbreviations: LDL, low-density lipoprotein.

Table 2.7. Associations between external PRS and cisplatin-induced hearing loss in testicular cancer survivors in *The Platinum Study* training set ($p < 0.05$)

Trait	Correlation Coefficient (rho)	p-value
PNS disorder PGS002039	$8.4x10^{-2}$	$5.7x10^{-3}$
Hearing Difficulties PGS001891	$8.1x10^{-2}$	$7.4x10^{-3}$
Hearing Difficulties PGS002104	$9.8x10^{-2}$	$1.2x10^{-3}$
Body Fat Mass PGS001951	$6.2x10^{-2}$	$4.1x10^{-2}$
Body Fat Percentage PGS002133	$6.2x10^{-2}$	$4.3x10^{-2}$
Urine Creatinine PGS000679	$6.8x10^{-2}$	$2.4x10^{-2}$
Cystatin C PGS001947	$6.8x10^{-2}$	$2.6x10^{-2}$
Urine Potassium PGS000693	$6.5x10^{-2}$	$3.1x10^{-2}$

Abbreviations: PNS, peripheral nervous system, LDL, low-density lipoprotein; HDL, high-density lipoprotein.

Transcriptome-wide association analyses and STRING pathway analysis

As GWAS for cisplatin-induced neurotoxicities conducted in *The Platinum Study* did not find any SNPs reaching genome-wide significance[47], it is not surprising that no genes reached transcriptome-wide significance (based on Bonferroni correction) across GTEx V8 and Common Mind Consortium tissues. However, of interest as potential inputs into machine learning models were genes that passed the p-value thresholds of $p < 0.0005$, $p < 0.005$, and $p < 0.05$, specifically those which were jointly significant or marginally associated following post-processing (and their associated eQTLs as described in the methods). Genes that passed these p-value thresholds and post-processing are listed in Appendix Tables A7 through A15.

At $p < 0.0005$, there were 17 genes associated with cisplatin-induced peripheral sensory neuropathy (protein-protein interaction (PPI) enrichment p-value of 1), 33 associated with tinnitus (PPI enrichment p-value of 0.56), and 22 associated with hearing loss (PPI enrichment p-value of 1). There were no shared genes between those associated with toxicities (Figure 2.7A).

At $p < 0.005$, there were 202 genes associated with peripheral sensory neuropathy (PPI enrichment p-value of 2.9×10^{-2}), 221 associated with tinnitus (PPI enrichment p-value of 4.0×10^{-2}), and 207 associated with hearing loss (PPI enrichment p-value of 3.6×10^{-2}) (Figure 2.7C). The PPI enrichment p-values for all of the cisplatin-induced neurotoxicities were significant, indicating that the networks had significantly more interactions than expected if the proteins were random. However, functional enrichment analysis did not show any significant functionally enriched pathways among these genes. There were some shared genes between those associated with cisplatin-induced neurotoxicities at $p < 0.005$ (Figure 2.7B, Appendix Table A16).

At $p < 0.05$, there were 254 genes associated with peripheral sensory neuropathy (PPI enrichment p-value of 1.1×10^{-4}), 240 associated with tinnitus (PPI enrichment p-value of 1.2×10^{-4}), and 267 associated with hearing loss (PPI enrichment p-value of 7.6×10^{-14}) (Figure 2.7C). For all three toxicities, there were significant functional enrichments in the network of genes. For peripheral sensory neuropathy, the enriched pathway was one based on human phenotype ontology (HPO) from Monarch data, described as cholesteryl ester 16:0 measurement, with false discovery rate (FDR) = 4.7×10^{-2} (Figure 2.7D, Table 2.8). For tinnitus, based on Kyoto Encyclopedia of Genes and Genomes (KEGG) pathways, one enriched pathway was glycolysis/gluconeogenesis (FDR = 8.8×10^{-3}), and the other was metabolic pathways (FDR = 3.3×10^{-2}) (Figure 2.7E, Table 2.8). For hearing loss, numerous pathways, including many for the perception of taste, were enriched, such as the taste transduction pathway in KEGG (FDR = 5.2×10^{-6}) (Table 2.8). There were some shared genes between those associated with cisplatin-induced neurotoxicities at $p < 0.05$. Two genes were associated with all cisplatin-induced neurotoxicities at $p < 0.05$: AMT and NICN1 (Figure 2.7C, Appendix Table A17).

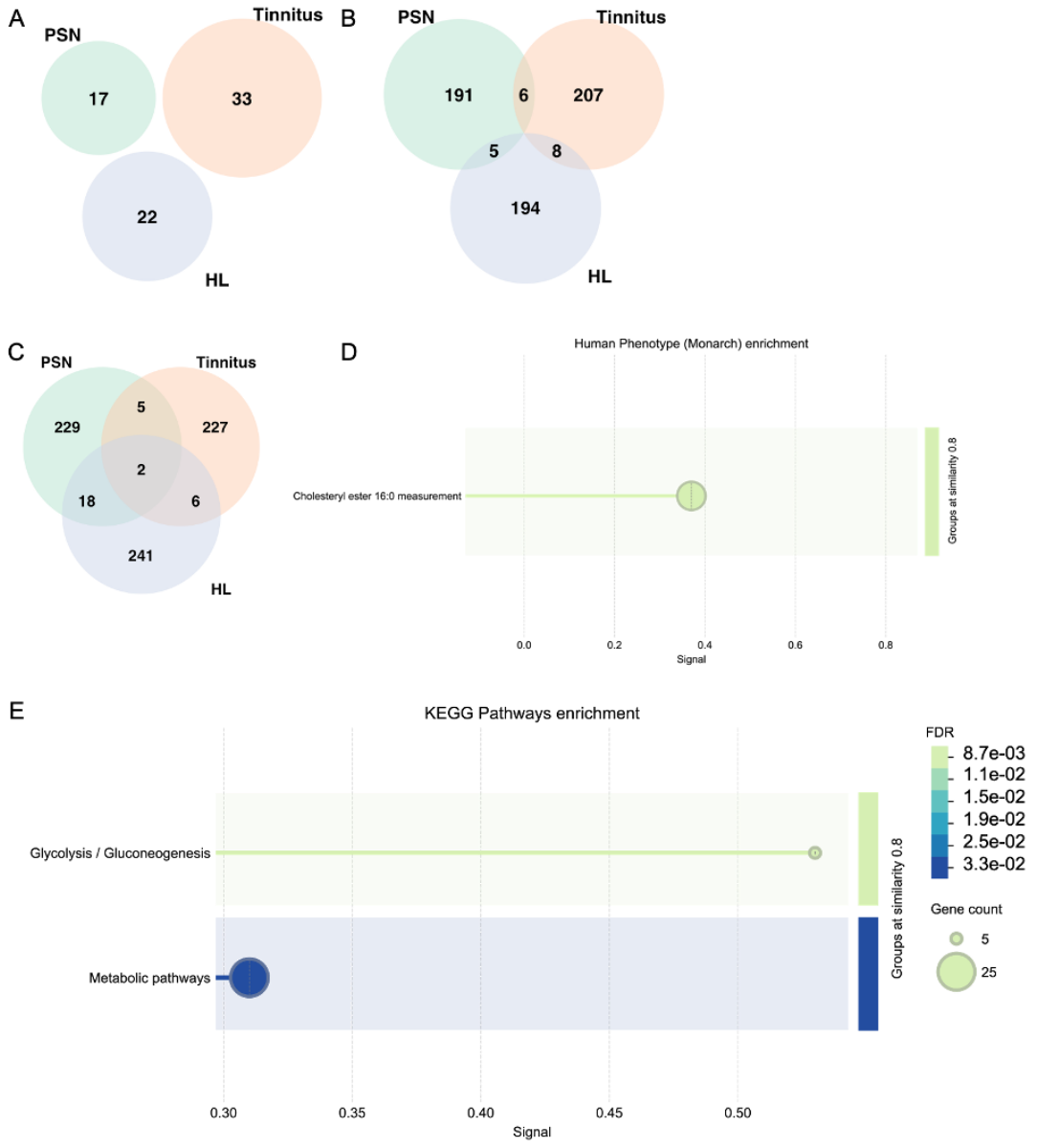

Figure 2.7. Number of TWAS genes associated with cisplatin-induced PSN, tinnitus, and hearing loss at p < 0.0005, p < 0.005, and p < 0.05 and STRING functional enrichment analysis. A, Number of genes associated with cisplatin-induced PSN, tinnitus and hearing loss at p < 0.0005. **B,** Number of genes associated with cisplatin-induced PSN, tinnitus, and hearing loss at p < 0.005. **C,** Number of genes associated with cisplatin-induced PSN, tinnitus, and hearing loss at p < 0.05. **D,** Significant functionally enriched pathway for genes associated with cisplatin-induced PSN at p < 0.05. **E,** Significant functionally enriched pathways for genes associated with cisplatin-induced tinnitus at p < 0.05.
Figure 2.7D and 2.7E were created with STRING[133].

Table 2.8. Functionally enriched pathways in group of genes associated with cisplatin-induced PSN, tinnitus, and hearing loss in TWAS at $p < 0.05$

Phenotype	**Category**	**Pathway/Domain/Phenotype**	**Description**	**Count in Network**	**FDR**	**Matching Proteins in Network**
PSN	Human Phenotype Ontology	EFO:0010341	Cholesteryl ester 16:0 measurement	4/9	$4.7x10^{-2}$	AMT,FADS2,FADS1,GNAL
Tinnitus	KEGG	hsa00010	Glycolysis / Gluconeogenesis	6/64	$8.8x10^{-3}$	ADH1A,PFKL,ADPGK,ENO3,BPGM,ADH1C
Tinnitus	KEGG	hsa01100	Metabolic pathways	26/1435	$3.3x10^{-2}$	ADH1A,ACO2,PYGL,GGT1,LPCAT2,L2HGDH,PFKL,AMT,ETHE1,ATP6V0A4,ADPGK,PANK2,ENO3,AACS,HADHB,GALNT9,PLB1,COMT,CHIA,BPGM,HDDC3,TYMP,DOT1L,CHKB,ADH1C,CEPT1
HL	GO Process	GO:0050909	Sensory perception of taste	10/69	$1.7x10^{-5}$	TAS2R10,TAS2R19,TAS2R31,TAS2R13,TAS2R50,TAS2R43,TAS2R46,TAS2R20,TAS2R14,TAS2R30
HL	GO Function	GO:0033038	Bitter taste receptor activity	9/20	$2.4x10^{-8}$	TAS2R10,TAS2R31,TAS2R13,TAS2R50,TAS2R43,TAS2R46,TAS2R20,TAS2R14,TAS2R30
HL	STRING clusters	CL:38624	Taste receptor type 2, and GPCR, family 3, extracellular calcium-sensing receptor-related	10/37	$9.2x10^{-8}$	TAS2R10,TAS2R19,TAS2R31,TAS2R13,TAS2R50,TAS2R43,TAS2R46,TAS2R20,TAS2R14,TAS2R30
HL	STRING clusters	CL:38627	Taste receptor type 2, and GPCR, family 3, extracellular calcium-sensing receptor-related	8/28	$1.7x10^{-6}$	TAS2R10,TAS2R19,TAS2R31,TAS2R13,TAS2R43,TAS2R46,TAS2R14,TAS2R30
HL	STRING clusters	CL:38629	Taste receptor activity, and PLC-beta C terminal	6/23	$2.2x10^{-4}$	TAS2R10,TAS2R31,TAS2R43,TAS2R46,TAS2R14,TAS2R30

Continuation of Table 2.8

HL	STRING clusters	CL:38632	Taste receptor activity	5/17	1.0×10^{-3}	TAS2R10,TAS2R31,TAS2R43,TAS2R46,TAS2R14
HL	KEGG	hsa04742	Taste transduction	10/80	5.2×10^{-6}	TAS2R10,TAS2R19,TAS2R31,TAS2R13,TAS2R50,TAS2R43,TAS2R46,TAS2R20,TAS2R14,TAS2R30
HL	Reactome	HSA-420499	Class C/3 (Metabotropic glutamate/pheromone receptors)	10/39	7.1×10^{-8}	TAS2R10,TAS2R19,TAS2R31,TAS2R13,TAS2R50,TAS2R43,TAS2R46,TAS2R20,TAS2R14,TAS2R30
HL	Reactome	HSA-9717207	Sensory perception of sweet, bitter, and umami (glutamate) taste	10/41	7.1×10^{-8}	TAS2R10,TRPM4,TAS2R31,TAS2R13,TAS2R50,TAS2R43,TAS2R46,TAS2R20,TAS2R14,TAS2R30
HL	Reactome	HSA-418594	G alpha (i) signaling events	12/309	3.8×10^{-2}	TAS2R10,PRKAR2A,ADORA1,TAS2R19,TAS2R31,TAS2R13,TAS2R50,TAS2R43,TAS2R46,TAS2R20,TAS2R14,TAS2R30
HL	UniProt Keywords	KW-0919	Taste	10/34	6.6×10^{-9}	TAS2R10,TAS2R19,TAS2R31,TAS2R13,TAS2R50,TAS2R43,TAS2R46,TAS2R20,TAS2R14,TAS2R30
HL	Pfam	PF05296	Taste receptor protein (TAS2R)	10/24	1.3×10^{-9}	TAS2R10,TAS2R19,TAS2R31,TAS2R13,TAS2R50,TAS2R43,TAS2R46,TAS2R20,TAS2R14,TAS2R30
HL	InterPro	IPR007960	Taste receptor type 2	10/24	4.1×10^{-9}	TAS2R10,TAS2R19,TAS2R31,TAS2R13,TAS2R50,TAS2R43,TAS2R46,TAS2R20,TAS2R14,TAS2R30

Abbreviations: GO, Gene Ontology; KEGG, Kyoto encyclopedia of genes and genomes, FDR, false discovery rate; PF, Pfam; IPR, InterPro; EFO, experimental factor ontology (Monarch).

Another result of interest was that at the most stringent p-value threshold ($p < 0.0005$), WFS1 gene expression across numerous tissues, including nerve tissue, brain RNASeq data, subcutaneous adipose tissue, and visceral adipose tissue, was consistently associated with cisplatin-induced hearing loss. WFS1 expression in blood, skeletal muscle, testis, and cerebellum

tissue was also associated with toxicity at $p < 0.005$ (Table 2.9). The negative TWAS z-scores indicate that decreased WFS1 expression in these tissues was associated with cisplatin-induced hearing loss.

Table 2.9. TWAS results for WFS1 association with cisplatin-induced hearing loss across tissue types ($p < 0.005$)

Tissue	HSQ	BEST.GWAS.ID	GWAS.Z	EQTL.ID	EQTL.Z	EQTL.GWAS.Z	TWAS.Z	TWAS.P
Adipose (VO)	0.11	rs17718958	4.5	rs4689393	-5.8	4.2	-4.2	$2.9x10^{-5}$
Adipose (SC)	$8.9x10^{-2}$	rs17718958	4.5	rs10010131	-6.7	3.8	-3.8	$1.3x10^{-4}$
Tibial Nerve	0.16	rs17718958	4.5	rs10010131	-8.2	3.8	-3.8	$1.7x10^{-4}$
Brain	0.10	rs17718958	4.5	rs1046314	-4.7	3.8	-3.8	$1.8x10^{-4}$
Whole Blood	$8.3x10^{-2}$	rs17718958	4.5	rs4688982	-4.4	3.5	-3.5	$5.5x10^{-4}$
Testis	0.25	rs17718958	4.5	rs4688982	-7.9	3.5	-3.5	$5.5x10^{-4}$
Muscle	0.17	rs17718958	4.5	rs13107806	-9.1	3.3	-3.4	$6.2x10^{-4}$
Cerebellum	0.74	rs17718958	4.5	rs13107806	-10.0	3.3	-3.4	$7.2x10^{-4}$

Abbreviations: eQTL, expression quantitative trait locus; CHR, chromosome, HSQ, mean heritability estimate; Best.GWAS.ID, most significantly associated variant in the locus; GWAS.Z, z-score of most significantly associated variant in the locus; eQTL.ID, best eQTL in the locus; eQTL.GWAS.Z, GWAS z-score for best eQTL; TWAS.Z, TWAS z-score; TWAS.P, TWAS p-value; VO, visceral omentum; SC, subcutaneous.

Using hyperparameter tuning and cross-validation in training set to optimize models

After preprocessing of input features, the next step was to build machine learning risk prediction models. Based on assessments from hyperparameter tuning and 10-fold cross-validation in the training set, the best set of genetic input features for predicting peripheral sensory neuropathy (any versus none) was GWAS SNPs at $1x10^{-4}$, which performed better for both random forests and radial kernel support vector machine models compared to GWAS SNPs at other p-value thresholds based on accuracy and kappa. Additionally, adding TWAS SNPs as input features to GWAS SNPs at any p-value threshold did not improve prediction for these models in the training set. Using GWAS SNPs at $p < 1x10^{-3}$ as input features also did not lead to

successful prediction of severe peripheral sensory neuropathy and tinnitus in the cross-validated training set based on results for radial kernel support vector machine models (down-sample and ROSE). Models were more successful when using GWAS SNPs at $p < 1x10^{-4}$ or even $p < 1x10^{-5}$ as inputs. Combining GWAS SNPs at any p-value threshold with TWAS SNPs at $p < 0.05$ and $p < 0.005$ either did not improve or decreased AUROC in the cross-validated training set.

As discussed in the methods, subsampling/sampling approaches were tested to deal with class imbalance for the severe neuropathy and tinnitus phenotypes. Up-sampling was not the best method of dealing with class imbalance, as up-sampling seemed to falsely elevate the AUROC, sensitivity, and specificity within the cross-validated training set. The AUROC was high regardless of the input variables, even those that were not predictive when using other subsampling methods such as cisplatin-related SNPs. Therefore, up-sampling resulted in overly optimistic results within cross-validated training set data that would not apply when model performance was assessed in the test set. For models for predicting severe neuropathy and tinnitus, down-sampling in the training set was the best method of subsampling compared to ROSE and up-sampling as well as the compared to using the training set for model building without any subsampling/sampling.

For hearing loss, clinical variables performed much better in the training set than genetic variables based on RMSE and Rsquared. For GWAS input SNPs, the best performance was from GWAS SNPs at $1x10^{-3}$ when using mRMR to select the top 100 GWAS SNPs at this p-value threshold.

Based on poor performance in training set for all phenotypes even after hyperparameter tuning, cisplatin-induced SNPs were not used as predictors to train final models. Hyperparameter tuning for random forests, support vector machine models, and extreme gradient boosting models

selected the optimal parameters that were used to train final models before assessing performance in the test set.

Model building

For models predicting overall peripheral neuropathy (any neuropathy versus no neuropathy), the best input features were a combination of GWAS SNPs at $p < 1x10^{-4}$ (82 SNPs) and clinical variables. For this phenotype, SVM models performed better than tree-based models or penalized logistic regression models based on AUROC. The radial kernel SVM model trained on GWAS SNPs ($p < 1x10^{-4}$) had an AUROC of 0.58 (95% CI, 0.50 to 0.66) and the polynomial kernel SVM models trained on GWAS SNPs ($p < 1x10^{-4}$) had an AUROC of 0.59 (95% CI, 0.51 to 0.67). The radial kernel SVM model trained using clinical variable predictors had an AUROC of 0.61 (95% CI, 0.52 to 0.69) and the polynomial kernel SVM model trained using clinical variable predictors had an AUROC of 0.60 (95% CI, 0.51 to 0.68). When combining the two types of input features, model performance improved, particularly when using the top 3 clinical variables selected by recursive feature elimination, which were age at diagnosis, age at questionnaire, and blood pressure medication use. For models trained using polynomial kernel SVM with GWAS SNPs at $p < 1x10^{-4}$ and clinical variables selected by recursive feature elimination as input features, the AUROC was 0.68 (95% CI, 0.60 to 0.76), with sensitivity of 0.82 and specificity of 0.54 (Figure 2.8A). For the model trained using radial kernel SVM and the same input features, the AUROC was 0.66 (95% CI, 0.57 to 0.74), with sensitivity of 0.75 and specificity of 0.56 (Figure 2.8B).

SVM models were more successful than tree-based models trained using the same combination of input features. The random forest model had an AUROC of 0.56 (95% CI, 0.47-0.64) and the XGBoost model had an AUROC of 0.56 (95% CI, 0.48 to 0.65), which did not

have significantly higher AUROC than 0.5 as determined by 95% confidence intervals calculated by DeLong's test. SVM models were also better than models trained using penalized logistic regression with the same combination of input features, including LASSO (AUROC: 0.63, 95% CI, 0.54 to 0.72) and ridge (AUROC: 0.61, 95% CI, 0.52 to 0.70). LASSO and ridge penalized logistic regression models traded off the high sensitivity of over 80% in SVM models for higher specificity, with the LASSO model having sensitivity of 0.62 and specificity of 0.65 and the ridge model having sensitivity of 0.59 and specificity of 0.63. For clinical prediction of those at risk for neuropathy, high sensitivity is critical.

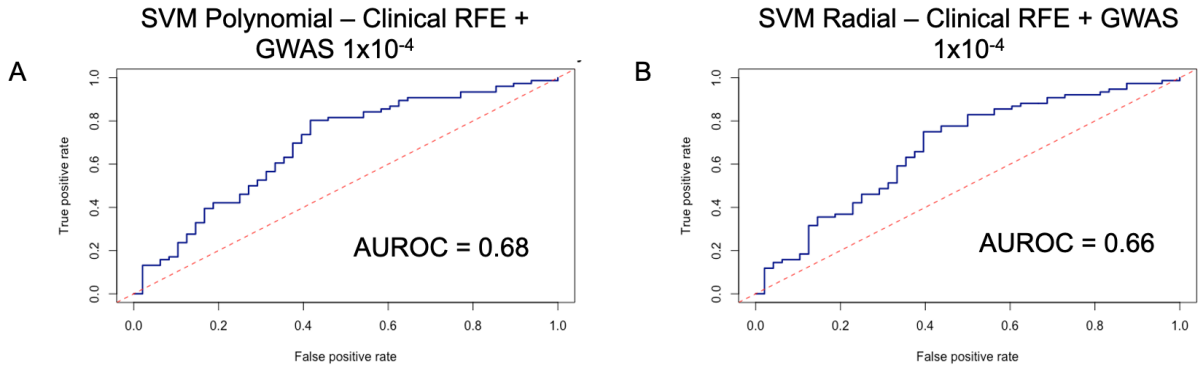

Figure 2.8. Performance of models predicting overall peripheral sensory neuropathy (any versus none) in cisplatin-treated testicular cancer survivors. A, AUROC for polynomial kernel support vector machine model trained on GWAS SNPs at $p < 1x10^{-4}$ and clinical variables after feature selection by recursive feature elimination. **B,** AUROC for radial kernel support vector machine model trained on GWAS SNPs at $p < 1x10^{-4}$ and clinical variables after feature selection by recursive feature elimination.

Based on AUROC, the most successful models we built were those predicting severe peripheral sensory neuropathy. The models discussed below were trained using the randomly down-sampled training set. Tree-based models (random forests and XGBoost) performed better than SVM or penalized logistic regression models. A model trained with XGBoost using only clinical variables as input features had an AUROC of 0.74 (95% CI, 0.61 to 0.87), sensitivity of 0.79 and specificity of 0.69 (Figure 2.9A). This model improved when incorporating genetic

features. The best prediction model for severe peripheral neuropathy was an XGBoost model trained on clinical and external PRS input features, which had an AUROC of 0.80 (95% CI, 0.69 to 0.92), sensitivity of 0.86, and specificity of 0.75 (Figure 2.9B). Using random forests, a model trained using clinical variables alone had an AUROC of 0.71 (95% CI, 0.56 to 0.85), sensitivity of 0.64, and specificity of 0.77 (Figure 2.9C). However, combining clinical variables with GWAS SNPs and/or external PRS improved model performance. The random forest model trained with a combination of clinical variables and GWAS SNPs at $p < 1x10^{-4}$ with feature selection for both using recursive feature elimination had an AUROC of 0.75 (95% CI, 0.62 to 0.89), sensitivity of 0.71, and specificity of 0.79 (Figure 2.9D). The random forest model trained using both clinical variables and external PRS had an AUROC of 0.76 (95% CI, 0.63 to 0.89), sensitivity of 0.79, and specificity of 0.73 (Figure 2.9E). Models trained using GWAS SNPs at $p<1x10^{-4}$ (feature selection of top 75 SNPs by RFE), clinical variables, and external PRS as input features performed better when input features were combined compared to models trained on each of these modalities of features alone. Table 2.10 has the results for the selected tree-based models discussed, while Appendix Table A18 has expanded results for all model types, including SVM and penalized logistic regression models and other combinations of input features with and without feature selection by recursive feature elimination.

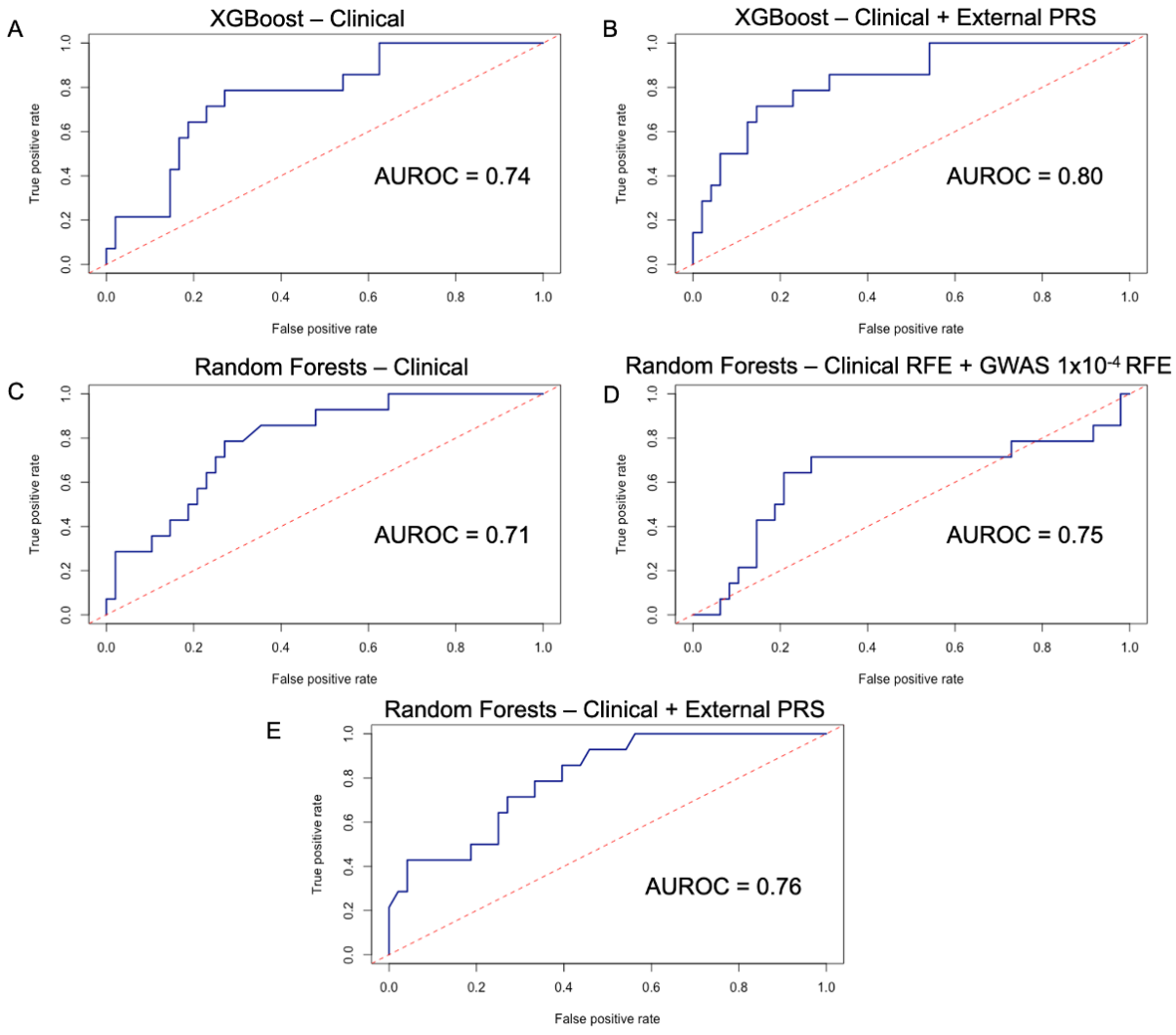

Figure 2.9. Performance of models predicting severe peripheral sensory neuropathy in cisplatin-treated testicular cancer survivors. A, AUROC for extreme gradient boosting model trained on clinical features. **B,** AUROC for extreme gradient boosting model trained on clinical and external PRS features. **C,** AUROC for random forest model trained on clinical features. **D,** AUROC for random forest model trained on GWAS SNP $p<1x10^{-4}$ (RFE) and clinical (RFE) features. **E,** AUROC for random forest model trained on clinical and external PRS features.
RFE = recursive feature elimination.

Table 2.10. Results for selected tree-based models predicting severe cisplatin-induced peripheral sensory neuropathy in the *Platinum Study* test set

Model	Inputs (Down-sampled training set)	AUROC (95% CI)	Sensitivity	Specificity
Random Forest	GWAS $1x10^{-4}$ RFE	0.56 (0.41-0.71)	0.43	0.69
Random Forest	External PRS	0.61 (0.46-0.76)	0.57	0.65
Random Forest	**Clinical**	**0.71 (0.56-0.85)**	**0.64**	**0.77**
Random Forest	GWAS $1x10^{-4}$ RFE + Clinical	0.69 (0.55-0.84)	0.57	0.81
Random Forest	**GWAS $1x10^{-4}$ RFE + Clinical RFE**	**0.75 (0.62-0.89)**	**0.71**	**0.79**
Random Forest	**Clinical + External PRS**	**0.76 (0.63-0.89)**	**0.79**	**0.73**
Random Forest	GWAS $1x10^{-4}$ RFE + Clinical + External PRS	0.69 (0.54-0.83)	0.64	0.73
XGBoost	GWAS $1x10^{-4}$ RFE	0.48 (0.33-0.63)	0.36	0.60
XGBoost	External PRS	0.55 (0.40-0.70)	0.43	0.67
XGBoost	**Clinical**	**0.74 (0.61-0.87)**	**0.79**	**0.69**
XGBoost	GWAS $1x10^{-4}$ RFE + Clinical	0.71 (0.56-0.85)	0.64	0.77
XGBoost	GWAS $1x10^{-4}$ RFE + Clinical RFE	0.65 (0.50-0.78)	0.57	0.73
XGBoost	**Clinical + External PRS**	**0.80 (0.69-0.92)**	**0.86**	**0.75**
XGBoost	GWAS $1x10^{-4}$ RFE + Clinical + External PRS	0.69 (0.54-0.83)	0.64	0.73

Abbreviations: RFE, recursive feature elimination.

A benefit of tree-based models versus SVM models in predicting severe peripheral sensory neuropathy is that for a random forests or XGBoost model, relative variable importance can be calculated using mean decrease in Gini as the importance measure, with the option to scale importance values to a range of 0 to 100. For the random forest model trained only on clinical variables, clinical variables related to age and body proportions (weight and BSA) were relatively more important in models compared to medication and lifestyle factors (Figure 2.10A). This was similar for the extreme gradient boosting model (Figure 2.10B).

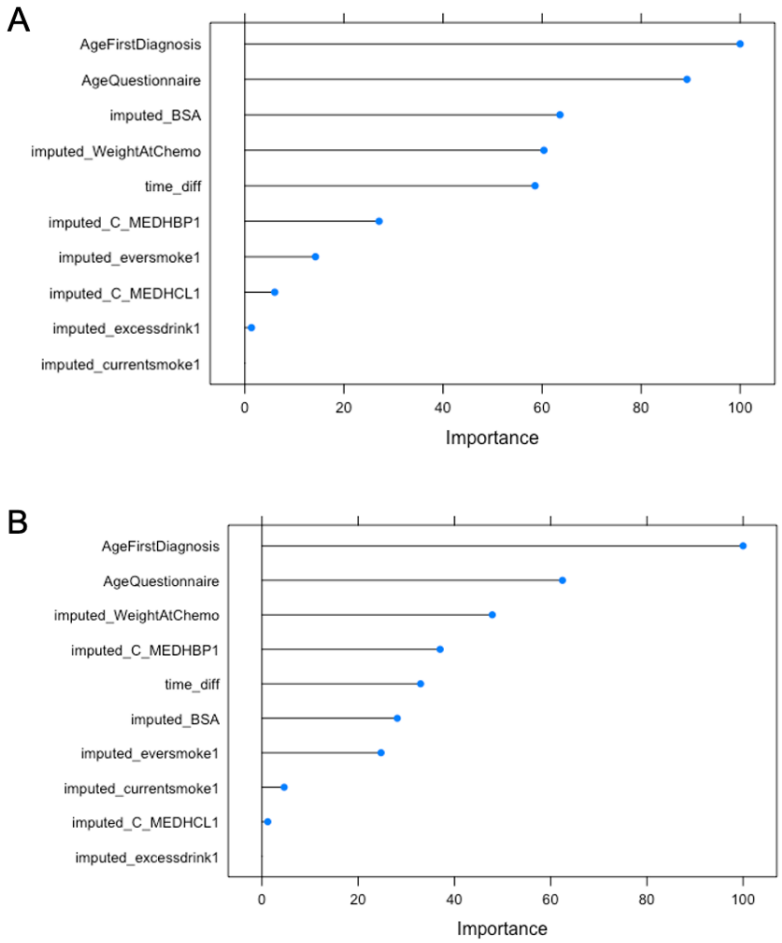

Figure 2.10. Relative variable importance for tree-based models predicting cisplatin-induced severe peripheral sensory neuropathy with clinical features. A, Relative variable importance for random forest model trained on clinical features. **B,** Relative variable importance for extreme gradient boosting model trained on clinical features.
BSA = body surface area. C_MEDHBP = blood pressure medication. C_MEDHCL = cholesterol medication.

When examining the relative importance of input features in the random forest model that was trained using clinical variables and external PRS as predictors, the most important PRS in the model were related to body composition and fat mass followed by PRS related to kidney function (blood protein, serum protein (not albumin), urine microalbumin, urine creatinine, urine

potassium, and urea measurements) (Figure 2.11A). The most important input features were similar, but not the same, for XGBoost models trained with the same inputs (Figure 2.11B).

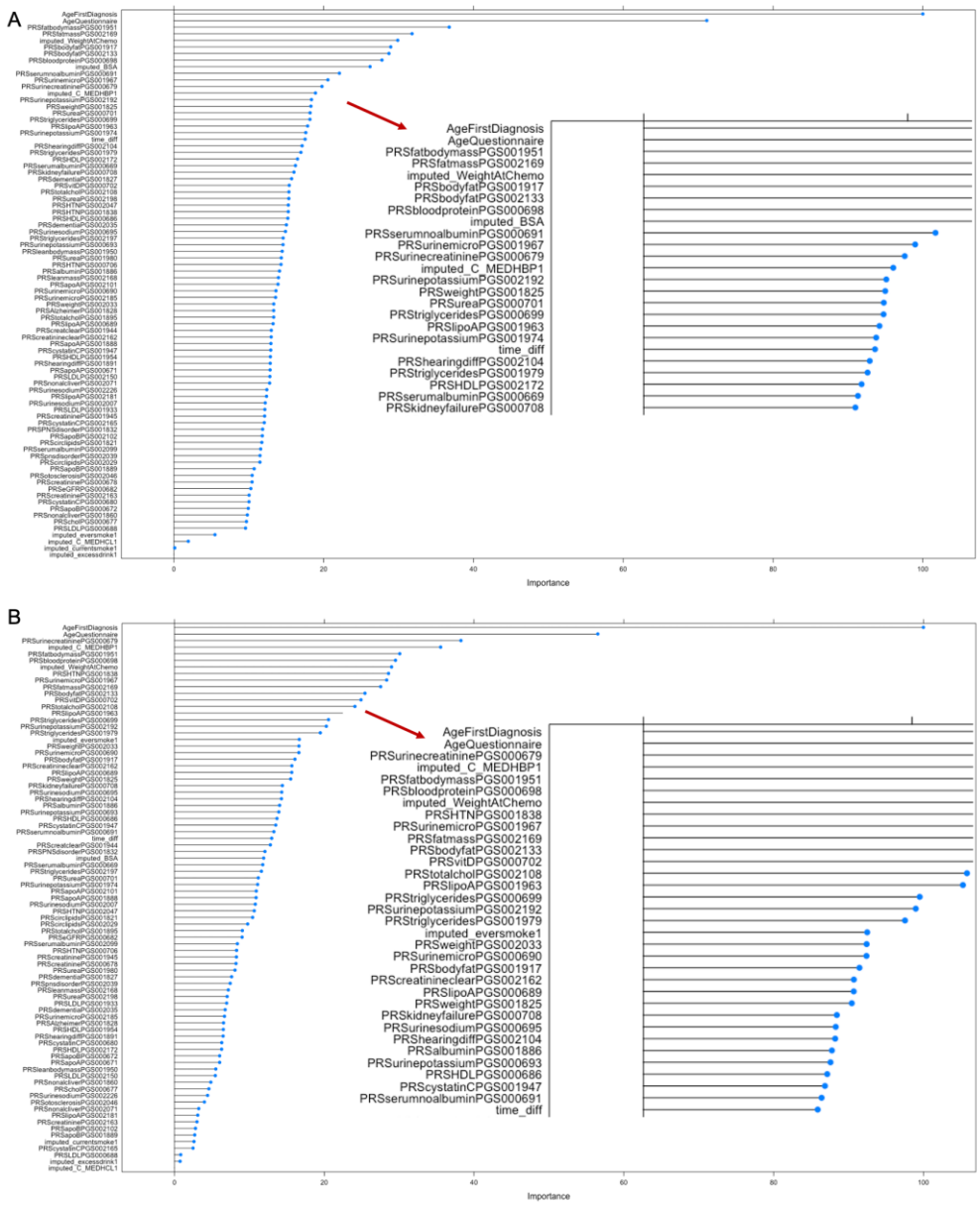

Figure 2.11. Relative variable importance for tree-based models predicting cisplatin-induced severe peripheral sensory neuropathy with clinical features and external PRS. **A,** Relative variable importance for random forest model trained on clinical and external PRS features. **B,** Relative variable importance for extreme gradient boosting model trained on clinical and external PRS features.
C_MEDHBP = blood pressure medication. C_MEDHCL = cholesterol medication. HDL = high density lipoprotein. BSA = body surface area.

Models were not very successful at predicting tinnitus in the test set, even after down-sampling the training data and trying GWAS SNPs at $p < 1x10^{-5}$ as inputs, adding TWAS SNPs at $p < 0.0005$, and combining clinical and genetic inputs. The models presented were trained on randomly down-sampled training data. The best genetic inputs were GWAS SNPs at $p < 1x10^{-5}$ or a combination of GWAS SNPs at $p < 1x10^{-5}$ with TWAS eQTLs at $p < 0.0005$, depending on the model. Tree-based models performed better than either SVM or penalized logistic regression models, which performed very poorly. However, the lower end of the 95% confidence intervals for AUROC were below 0.5 for even the most successful tree-based models for predicting cisplatin-induced tinnitus. Tree-based models for predicting cisplatin-induced tinnitus had AUROC around 0.6, while other models either had AUROC lower than 0.5 or around 0.5 regardless of combination of inputs, with the one exception being a ridge logistic regression model using GWAS SNPs at $p < 1x10^{-5}$ as predictors, which had an AUROC of 0.59 (95% CI, 0.48 to 0.70). However, this model had a very poor sensitivity (0.29), which does not bode well for clinical application. Random forests and XGBoost models had better sensitivity, although the highest sensitivities were still only around 57%, much lower than the sensitivities for models predicting peripheral sensory neuropathy. The best models for tinnitus included a random forest model trained using clinical variables after recursive feature elimination as input features, which included weight at chemotherapy (kg), blood pressure medication use, body surface area (m^2), age at first diagnosis, age at questionnaire, cholesterol medication use, time difference between age at diagnosis and evaluation, and ever smoking. This model had an AUROC of 0.60 (95% CI, 0.47 to 0.72), sensitivity of 0.57, and specificity of 0.62 (Table 2.11). A random forest model trained using a combination of clinical variables with external PRS as predictors performed similarly, with an AUROC of 0.60 (95% CI, 0.48 to 0.72), sensitivity of 0.48, and specificity of

0.73 (Table 2.11). Performing the best out of all models predicting cisplatin-induced tinnitus (based on AUROC) was a random forest model trained using GWAS SNPs at $p < 1x10^{-5}$ and TWAS eQTLs at $p < 0.0005$ combined with external PRS, with an AUC of 0.61 (95% CI, 0.49 to 0.73), sensitivity of 0.48, and specificity of 0.74 (Table 2.11).

For tinnitus models trained with the XGBoost algorithm, models using GWAS SNPs at $p < 1x10^{-5}$ and TWAS eQTLs at $p < 0.0005$, external PRS, and clinical variables as input features performed similarly, with AUROCs of 0.57 (95% CI, 0.45 to 0.70), 0.60 (95% CI, 0.47 to 0.72), and 0.58 (95% CI, 0.46 to 0.70), respectively (Table 2.11). Combining features did not improve model performance. While the best models for predicting tinnitus had AUROC of only around 0.6 in the test set, there are no published risk prediction models for cisplatin-induced tinnitus. Therefore, more work needs to be done to find better predictors so that we can improve risk prediction models for cisplatin-induced tinnitus.

Table 2.11. Results for tree-based models predicting cisplatin-induced tinnitus in the *Platinum Study* test set

Model	**Inputs (Down-sampled training set)**	**AUROC (95% CI)**	**Sensitivity**	**Specificity**
Random Forest	GWAS 1e-05	0.53 (0.42-0.64)	0.29	0.77
Random Forest	GWAS 1e-05 + TWAS 0.0005	0.51 (0.40-0.63)	0.29	0.74
Random Forest	External PRS	0.52 (0.39-0.64)	0.43	0.61
Random Forest	Clinical	0.49 (0.36-0.61)	0.38	0.59
Random Forest	**Clinical RFE**	**0.60 (0.47-0.72)**	**0.57**	**0.62**
Random Forest	**Clinical + External PRS**	**0.60 (0.48-0.72)**	**0.48**	**0.73**
Random Forest	Clinical RFE + External PRS	0.49 (0.37-0.61)	0.33	0.65
Random Forest	GWAS 1e-05 + Clinical	0.55 (0.44-0.66)	0.29	0.82
Random Forest	GWAS 1e-05 + external PRS	0.54 (0.42-0.66)	0.43	0.65
Random Forest	GWAS 1e-05 + TWAS 0.0005 + Clinical	0.55 (0.44-0.67)	0.33	0.77
Random Forest	**GWAS 1e-05 + TWAS 0.0005 + External PRS**	**0.61 (0.49-0.73)**	**0.48**	**0.74**

Continuation of Table 2.11

Random Forest	GWAS 1e-05 + TWAS 0.0005 + External PRS + Clinical	0.54 (0.43-0.65)	0.29	0.80
XGBoost	GWAS 1e-05	0.56 (0.43-0.68)	0.43	0.68
XGBoost	**GWAS 1e-05 + TWAS 0.0005**	**0.57 (0.45-0.70)**	**0.48**	**0.67**
XGBoost	**External PRS**	**0.60 (0.47-0.72)**	**0.57**	**0.62**
XGBoost	**Clinical**	**0.58 (0.46-0.70)**	**0.48**	**0.68**
XGBoost	Clinical RFE	0.52 (0.39-0.64)	0.43	0.61
XGBoost	Clinical + External PRS	0.52 (0.39-0.64)	0.43	0.61
XGBoost	Clinical RFE + External PRS	0.49 (0.37-0.62)	0.38	0.61
XGBoost	GWAS 1e-05 + Clinical	0.54 (0.42-0.65)	0.33	0.74
XGBoost	GWAS 1e-05 + External PRS	0.52 (0.40-0.65)	0.43	0.62
XGBoost	GWAS 1e-05 + TWAS 0.0005 + Clinical	0.54 (0.42-0.66)	0.38	0.70
XGBoost	GWAS 1e-05 + TWAS 0.0005 + External PRS	0.56 (0.43-0.68)	0.52	0.59
XGBoost	GWAS 1e-05 TWAS 0.0005 + External PRS + Clinical	0.53 (0.41-0.65)	0.33	0.73

Abbreviations: RFE, recursive feature elimination.

For hearing loss, regression models were used, as the phenotype is continuous. One metric of importance for assessing the success of models on test data was root mean squared error (RMSE). However, another metric that provided important information was Rsquared, which is a measurement of the proportion of the dependent variable (hearing thresholds (GM412)) that is explained by the independent variables (input features for machine learning models). Models trained on genetic variables did not successfully predict hearing thresholds (GM412) and all model types performed similarly. Based on results in the training set (with cross-validation), prediction was better when applying feature selection to GWAS $p < 1x10^{-3}$, using mRMR to train models on only the top 100 variables in the training set. However, for models trained using the top 100 GWAS SNPs as predictors, the RMSE was still high and less than 5% of variation in GM412 was explained by these SNP genotypes, as shown by the low Rsquared values (Table 2.12). Additionally, when using Spearman's correlation to assess the

relationship between the actual hearing threshold (GM412) values and the predicted hearing threshold values in the test set, the models trained using the top 100 GWAS SNPs ($p < 1x10^{-3}$) as predictors did not show significant correlation between these values, although p-values for Spearman correlation were approaching significance (< 0.1) for LASSO and ridge models (Table 2.12).

In contrast, clinical variables performed much better than genetic variables for prediction of hearing thresholds in test set data based on all performance metrics. When clinical variables were used as predictors, the RMSE values for all models were between 13.1 and 13.5, and Rsquared values were between 0.41 and 0.47, with no major differences in model performance based on model type. Between 40%-50% of the variation in hearing thresholds (GM412) could be explained by clinical variables depending on the model. Spearman's correlation showed significant associations between predicted and actual hearing thresholds in all models trained using clinical variables alone, with correlation coefficients between 0.65 and 0.69 and significant p-values (Table 2.12, Figure 2.12A-F). Therefore, models for predicting cisplatin-induced hearing loss using clinical variables as predictors explained a moderate percentage of variation in hearing thresholds and showed significant correlation between predicted and actual GM412 values in the test set. Combining clinical variables with genetic variables (GWAS $1x10^{-3}$ mRMR 100) did not improve upon models trained on just clinical variables, as while p-values of association were still significant, correlation coefficients were lower than for models trained with clinical variables alone (Table 2.12). RMSE values also increased and Rsquared values decreased for models training on clinical features and GWAS SNPs together compared to those trained only on clinical features. Therefore, of the input features, clinical variables were the most strongly predictive of the continuous hearing loss phenotype.

Table 2.12. Results for models predicting cisplatin-induced hearing loss in the *Platinum Study* test set

Model	Inputs	RMSE	Rsquared	Spearman's Cor Coefficient	Spearman's p-value
Random Forest	GWAS $1x10^{-3}$ mRMR 100	17.4	0.023	0.14	0.24
Random Forest	Clinical	13.4	0.42	0.65	$2.1x10^{-10}$
Random Forest	Clinical + GWAS $1x10^{-3}$ mRMR 100	14.2	0.29	0.60	$7.2x10^{-9}$
SVM Radial	GWAS $1x10^{-3}$ mRMR 100	18.7	0.017	0.17	0.13
SVM Radial	Clinical	13.2	0.47	0.69	$5.0x10^{-12}$
SVM Radial	Clinical + GWAS $1x10^{-3}$ mRMR 100	15.1	0.28	0.56	$1.9x10^{-7}$
SVM Poly	GWAS $1x10^{-3}$ mRMR 100	18.7	0.017	0.17	0.13
SVM Poly	Clinical	13.2	0.47	0.69	$6.3x10^{-12}$
SVM Poly	Clinical + GWAS $1x10^{-3}$ mRMR 100	15.1	0.27	0.56	$1.9x10^{-7}$
XGBoost	GWAS $1x10^{-3}$ mRMR 100	17.7	0.032	0.17	0.14
XGBoost	Clinical	13.5	0.41	0.67	$5.1x10^{-11}$
XGBoost	Clinical + GWAS $1x10^{-3}$ mRMR 100	15.0	0.27	0.56	$1.8x10^{-7}$
LASSO	GWAS $1x10^{-3}$ mRMR 100	18.7	0.028	0.22	$6.1x10^{-2}$
LASSO	Clinical	13.1	0.45	0.69	$7.4x10^{-12}$
LASSO	Clinical + GWAS $1x10^{-3}$ mRMR 100	14.9	0.29	0.57	$7.2x10^{-8}$
Ridge	GWAS $1x10^{-3}$ mRMR 100	18.3	0.024	0.20	$8.9x10^{-2}$
Ridge	Clinical	13.1	0.45	0.69	$4.9x10^{-12}$
Ridge	Clinical + GWAS $1x10^{-3}$ mRMR 100	15.0	0.28	0.57	$7.0x10^{-8}$

Abbreviations: GM412, geometric mean of hearing thresholds from 4-12 kilohertz; mRMR, minimum redundancy maximum relevance.

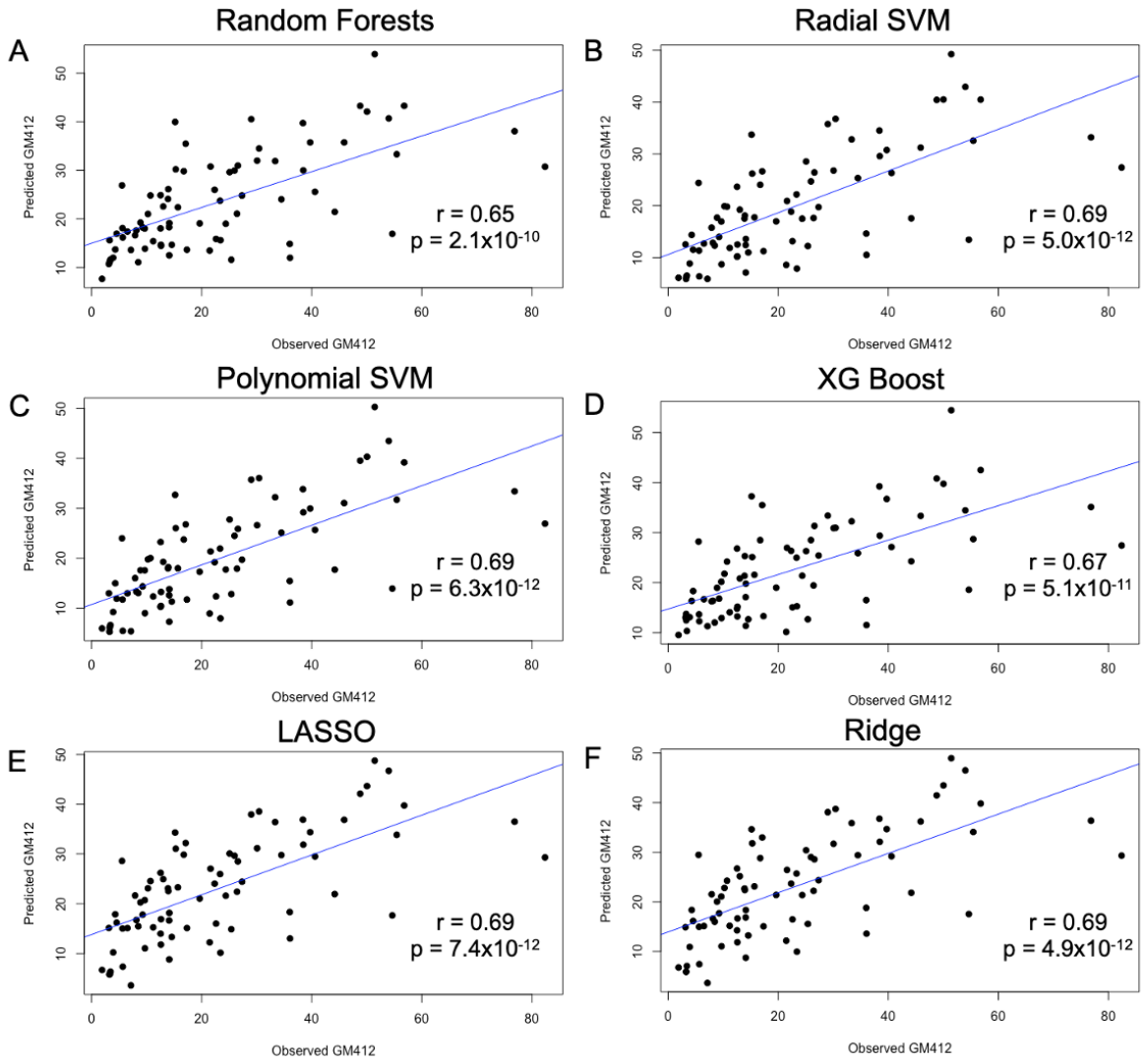

Figure 2.12. Correlation between observed and predicted GM412 for models predicting cisplatin-induced hearing loss with clinical features. A, Correlation between observed and predicted GM412 for random forest model trained on clinical features. **B,** Correlation between observed and predicted GM412 for radial kernel SVM model trained on clinical features. **C,** Correlation between observed and predicted GM412 for polynomial kernel SVM model trained on clinical features. **D,** Correlation between observed and predicted GM412 for XGBoost model trained on clinical features. **E,** Correlation between observed and predicted GM412 for LASSO model trained on clinical features. **F,** Correlation between observed and predicted GM412 for ridge model trained on clinical features.
GM412 = Geometric mean of hearing thresholds from 4-12 kilohertz. r = Spearman correlation coefficient.

A comparison of relative variable importance between random forests and XGBoost models found that for both model types, clinical variables including age at diagnosis and

questionnaire, time difference between diagnosis and evaluation, body surface area, and weight at time of chemotherapy were more important predictors than medication use and lifestyle factors such as smoking and drinking (Figure 2.13A, B). Continuous variables were better at predicting a continuous outcome versus categorical variables. For LASSO models, age at diagnosis and at questionnaire, blood pressure medication use, and ever smoking were the variables that were retained in models after L1 regularization and shrinking the coefficients.

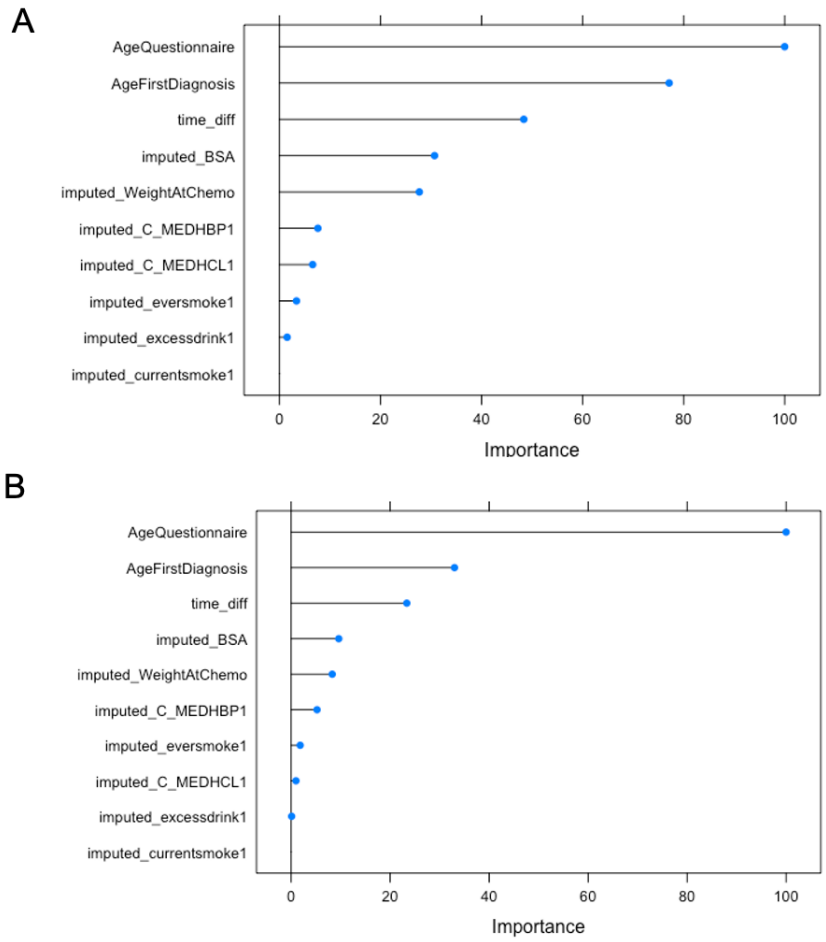

Figure 2.13. Relative variable importance for tree-based models predicting cisplatin-induced hearing loss with clinical features. A, Relative variable importance for random forest model trained on clinical features. **B,** Relative variable importance for extreme gradient boosting model trained on clinical features. BSA = body surface area. C_MEDHCL = cholesterol medication. C_MEDHBP = blood pressure medication.

STRING pathway analysis based on most predictive features

Input features in a machine learning model can provide important information regarding the relevant factors predictive of outcomes. Of particular interest were the genetic inputs (SNPs from GWAS) that were predictive features, as SNPs may impact gene expression, splicing, coding, or activity. These genes may be part of pathways that can be further explored for their relationship to cisplatin-induced neurotoxicities.

For models predicting overall peripheral sensory neuropathy (any versus none), the best set of genetic input features were GWAS SNPs at a p-value threshold of $1x10^{-4}$. After using dbSNP, GTEx v10, and the GWAS catalog to find a list of genes related to these SNPs (Appendix Table A19), this list was input into STRING pathway analysis to study protein-protein interactions and find functionally enriched pathways. For this set of 82 SNPs, the genes associated with those SNPs, and the proteins encoded by those genes, the PPI enrichment p-value was significant ($p = 3.1x10^{-2}$), indicating that the network had significantly more interactions than expected (Figure 2.14). Upon functional enrichment analysis using STRING, the majority of pathways significantly enriched in this network of genes were related to fatty acid metabolism and measurement, including omega-3/omega-6 fatty acid synthesis (FDR = $3.2x10^{-2}$), fatty acid desaturase (FDR = $1.3x10^{-2}$), and docosapentaenoic acid measurement (FDR = $3.6x10^{-7}$), among many others (Table 2.13). Many pathways were also related to the measurement of membrane lipids such as sphingolipid measurement (FDR = $5.3x10^{-6}$), phosphatidylcholine ether measurement (FDR = $4.0x10^{-5}$), and glycerophospholipid measurement (FDR = $1.1x10^{-4}$) (Table 2.13). Multiple functionally enriched pathways were also related to iron, with pathways including total iron binding capacity (FDR = $2.9x10^{-3}$), cytochrome b5-like heme/steroid binding domain (FDR = $2.8x10^{-2}$), and iron biomarker measurement (FDR = $4.2x10^{-2}$) (Table 2.13).

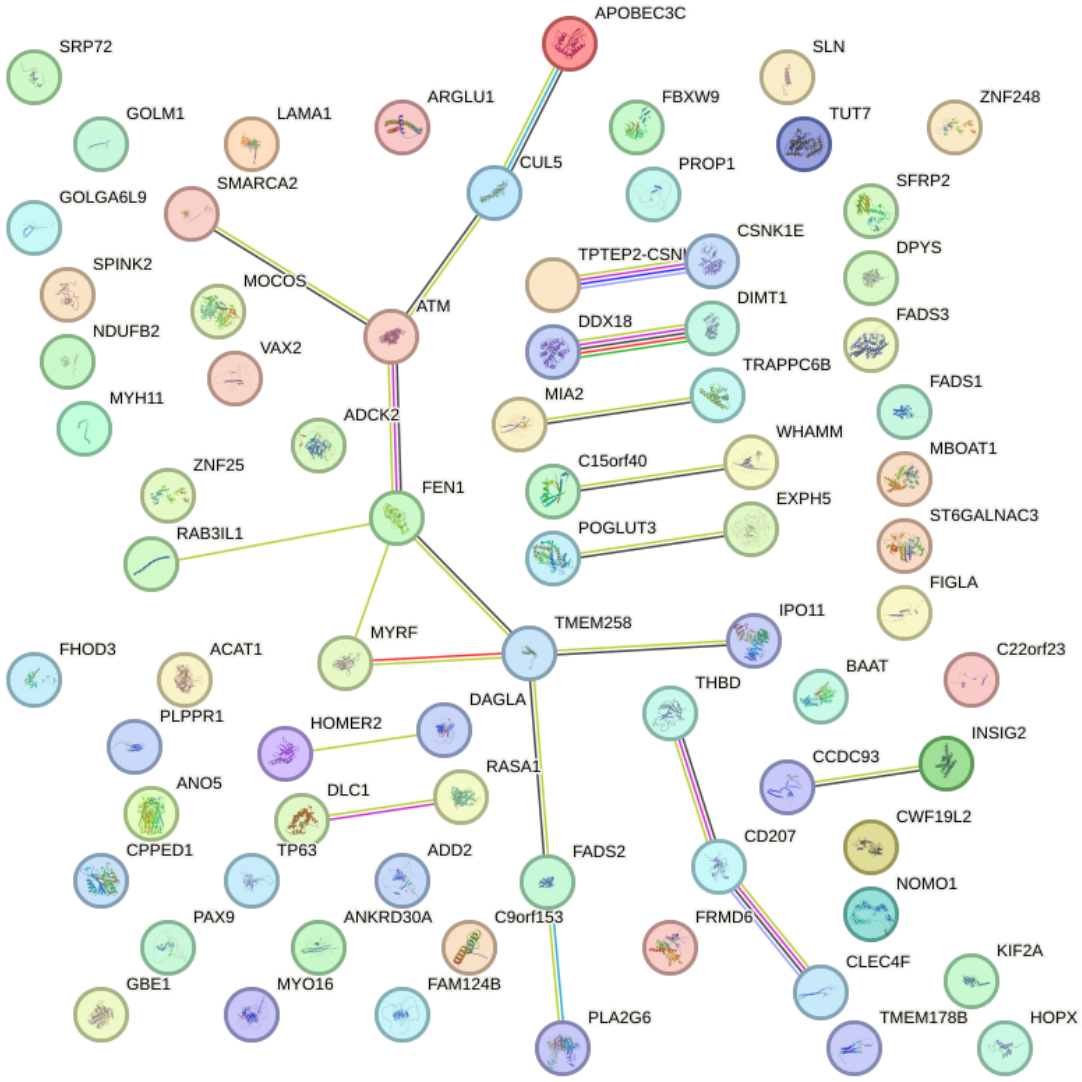

Figure 2.14. Protein-protein interaction network for proteins encoded by genes associated with predictive SNPs in cisplatin-induced peripheral sensory neuropathy prediction models. Protein-protein interaction network for proteins encoded by genes associated with GWAS SNPs at $p < 1x10^{-4}$ (network image produced by STRING[133]).

Table 2.13. Functionally enriched pathways in the group of genes associated with SNPs used as predictors in cisplatin-induced peripheral sensory neuropathy (any vs. none) prediction models

Pathway/Domain/Phenotype	Description	Count in Network	FDR	Matching Proteins in Network
EFO:0006809	Docosapentaenoic acid measurement	6/11	$3.6x10^{-7}$	DAGLA,MYRF,FADS2,FEN1,FADS1,TMEM258

Continuation of Table 2.13

EFO:0006824	Cis/trans-18:2 fatty acid measurement	5/8	$5.3x10^{-6}$	MYRF,FADS2,FEN1,FADS1,TMEM258
EFO:0004622	Sphingolipid measurement	8/76	$5.3x10^{-6}$	FADS3,MYRF,FADS2,FADS1,ANKRD30A,RAB3IL1,IPO11,TMEM258
EFO:0007759	Alpha-linolenic acid measurement	5/10	$6.1x10^{-6}$	MYRF,FADS2,FEN1,FADS1,TMEM258
EFO:0007760	Eicosapentaenoic acid measurement	5/13	$1.4x10^{-5}$	MYRF,FADS2,FEN1,FADS1,TMEM258
EFO:0010227	Phosphatidylcholine ether measurement	4/5	$4.0x10^{-5}$	MYRF,FADS2,FADS1,TMEM258
EFO:0005680	omega-6 polyunsaturated fatty acid measurement	6/41	$4.0x10^{-5}$	DAGLA,MYRF,FADS2,FEN1,FADS1,TMEM258
EFO:0010229	Phosphatidylethanolamine ether measurement	4/6	$5.3x10^{-5}$	MYRF,FADS2,FADS1,TMEM258
EFO:0006808	Arachidonic acid measurement	4/6	$5.3x10^{-5}$	MYRF,FADS2,FADS1,TMEM258
EFO:0010118	Sphingomyelin measurement	6/47	$5.4x10^{-5}$	FADS3,MYRF,FADS2,FADS1,IPO11,TMEM258
EFO:0007762	Gamma-linolenic acid measurement	4/7	$6.3x10^{-5}$	MYRF,FADS2,FADS1,TMEM258
EFO:0007763	Dihomo-gamma-linolenic acid measurement	4/8	$8.1x10^{-5}$	MYRF,FADS2,FADS1,TMEM258
EFO:0007630	Glycerophospholipid measurement	4/9	$1.1x10^{-4}$	MYRF,FADS2,FADS1,TMEM258
EFO:0010119	omega-3 polyunsaturated fatty acid measurement	4/10	$1.4x10^{-4}$	MYRF,FADS2,FADS1,TMEM258
EFO:0008589	Esterified cholesterol measurement	4/11	$1.8x10^{-4}$	MYRF,FADS2,FADS1,TMEM258
EFO:0010226	Phosphatidylcholine measurement	6/65	$1.9x10^{-4}$	FADS3,MYRF,FADS2,FADS1,RAB3IL1,TMEM258
EFO:0010968	Phosphate measurement	8/175	$2.9x10^{-4}$	FADS3,MYRF,FADS2,FEN1,FADS1,RAB3IL1,IPO11,TMEM258
EFO:0004351	Resting heart rate	6/76	$4.1x10^{-4}$	MYRF,FADS2,FADS1,MYH11,TMEM258,FHOD3

Continuation of Table 2.13

EFO:0007975	Gondoic acid measurement	3/3	$6.0x10^{-4}$	MYRF,FADS2,TMEM258
EFO:0006807	Linoleic acid measurement	4/17	$6.0x10^{-4}$	DAGLA,FADS2,FEN1,FADS1
EFO:0010222	Ceramide measurement	4/20	$1.0x10^{-3}$	MYRF,FADS2,FADS1,TMEM258
EFO:0010351	Cholesteryl ester measurement	5/54	$1.5x10^{-3}$	MYRF,FADS2,FADS1,RAB3IL1,TMEM258
EFO:0010387	Phosphatidylcholine 38:5 measurement	3/6	$2.1x10^{-3}$	FADS3,MYRF,TMEM258
EFO:0010386	Phosphatidylcholine 38:4 measurement	3/7	$2.9x10^{-3}$	FADS2,FADS1,RAB3IL1
EFO:0006334	Total iron binding capacity	4/28	$2.9x10^{-3}$	MYRF,FADS2,FADS1,TMEM258
EFO:0010364	Lysophosphatidylcholine 20:5 measurement	3/9	$4.6x10^{-3}$	FADS2,FADS1,RAB3IL1
EFO:0004465	Fasting blood glucose measurement	6/126	$4.6x10^{-3}$	DAGLA,MYRF,FADS2,FADS1,PLA2G6,TMEM258
EFO:0010348	Cholesteryl ester 20:4 measurement	3/12	$9.1x10^{-3}$	FADS2,FADS1,RAB3IL1
EFO:0004469	HOMA-B	4/40	$9.1x10^{-3}$	MYRF,FADS2,FADS1,TMEM258
IPR012171	Fatty acid desaturase	3/4	$1.3x10^{-2}$	FADS3,FADS2,FADS1
PF00487	Fatty acid desaturase	3/7	$1.4x10^{-2}$	FADS3,FADS2,FADS1
EFO:0010437	Triacylglycerol 58:10 measurement	3/15	$1.4x10^{-2}$	FADS2,FADS1,RAB3IL1
HP:0025487	Abnormality of bladder morphology	4/46	$1.4x10^{-2}$	TP63,MYRF,SMARCA2,MYH11
IPR005804	Fatty acid desaturase domain	3/7	$2.2x10^{-2}$	FADS3,FADS2,FADS1
SM01117	Cytochrome b5-like Heme/Steroid binding domain	3/14	$2.8x10^{-2}$	FADS3,FADS2,FADS1
EFO:0004979	Comprehensive strength index	2/2	$2.9x10^{-2}$	FADS2,FADS1
WP4723	Omega-3/omega-6 fatty acid synthesis	3/15	$3.2x10^{-2}$	FADS2,FADS1,PLA2G6

Continuation of Table 2.13

EFO:0004557	Population measurement	10/607	$3.6x10^{-2}$	TP63,DLC1,DPYS,FADS2,FADS1,FRMD6,C9orf153,PLPPR1,SMARCA2,TMEM178B
EFO:0004461	Iron biomarker measurement	5/124	$4.2x10^{-2}$	MYRF,FADS2,FADS1,MYO16,TMEM258
EFO:0010434	Triacylglycerol 56:7 measurement	2/3	$4.3x10^{-2}$	MYRF,TMEM258
EFO:0007974	Vaccenic acid measurement	2/3	$4.3x10^{-2}$	MYRF,TMEM258

Abbreviations: FDR, false discovery rate; WP, WikiPathways; PF, Pfam; SM, SMART; IPR, InterPro; EFO, experimental factor ontology (Monarch).

When predicting severe peripheral sensory neuropathy, the best set of SNP input features was GWAS SNPs at a p-value threshold < $1x10^{-4}$ with recursive feature elimination selecting the top 75 SNPs. For this set of 75 SNPs and the subsequent genes/proteins associated with those SNPs, the PPI enrichment p-value was $2.2x10^{-2}$. The functional enrichments in this subset of 75 SNPs were the same as those for all 82 SNPs, with the majority of pathways being related to fatty acid metabolism, fatty acid measurement, and phospholipid membrane component measurement.

2.4 Discussion

The goal of this study was to train and test machine learning prediction models for cisplatin-induced neurotoxicities that can be used in the future to guide cisplatin dosing and monitoring of at-risk patients. The most effective models were those predicting overall peripheral sensory neuropathy (any versus none/yes versus no) and severe peripheral sensory neuropathy (severe versus none) using clinical and genetic factors, with high sensitivity (>75%) and strong AUROC in the independent test set. The best model for overall peripheral sensory neuropathy used clinical variables and GWAS SNPs ($p < 1.0x10^{-4}$) as inputs and had an AUROC of 0.68 and the best model for severe peripheral sensory neuropathy used clinical variables and

external PRS as inputs and had an AUROC of 0.8. We also developed reasonable models for predicting cisplatin-induced hearing loss using clinical features, with over 40% of variation in hearing thresholds (GM412) explained by clinical features and significant associations between predicted and actual hearing thresholds in the test set. Additionally, much was learned about the risk factors for cisplatin-induced neurotoxicities from the pre-processing of input features prior to model training and from analyzing features used to build successful models after testing.

Model building and external validation

The prediction models trained for peripheral sensory neuropathy, both for predicting overall neuropathy and specifically severe neuropathy, are the first of their kind for cisplatin-treated adult-onset cancer survivors. A few models have been developed for diabetic peripheral neuropathy utilizing clinical features as inputs[149–151], with some overlap between the clinical input features for these models and the clinical input features in models of cisplatin-induced peripheral sensory neuropathy such as age[150], hypertension and smoking status[149], and body composition measurements[151]. *The Platinum Study* data was used to successfully train and test models that can not only predict any future neuropathy, but specifically predict severe neuropathy with high sensitivity and AUROC. The size of *The Platinum Study* data and the extensive genotyping and phenotyping information provided an opportunity to develop models using sizable internal training and test sets and allowed us to explore model building with a variety of types of input features.

The previously published model for self-reported hearing loss in cisplatin-treated testicular cancer survivors had only 424 survivors across training and test sets versus 1163 survivors in *The Platinum Study* (combined across training and test sets)[90]. Additionally, our continuous hearing loss phenotype based on audiometry is more objective than self-reported

hearing loss and can be used in the future to dichotomize this phenotype based on numerous hearing loss criteria such as Brock, Chang, SIOP, or ASHA standards[152]. Another published model for cisplatin-induced hearing loss was trained and tested in a pediatric population[120], which may not be generalizable to adult-onset cancer survivors. Our models for predicting cisplatin-induced hearing loss in adult-onset cancer survivors successfully showed a significant correlation (correlation coefficient between 0.65-0.69) between actual hearing thresholds (GM412) in the test set and hearing thresholds predicted by the model.

Although models for both overall peripheral sensory neuropathy and severe peripheral sensory neuropathy performed better when using a combination clinical and genetic input features (GWAS SNPs and/or external PRS), the utility of models trained on only clinical or genetic input features is that they may be more generalizable for external validation. While clinical variables in datasets may differ based on questionnaires or physician discretion, standard genotyping data can be used to find SNP genotypes or calculate external PRS. Conversely, not all clinical settings have the resources for genotyping and so models trained on only clinical predictors may be more applicable in these scenarios. Therefore, even though models improve when including both clinical and genetic predictors, it is important to note what can be gleaned from each modality of input data individually and how models can be used in situations with limited clinical and/or genetic data.

What was most critical for successful prediction was the selection of appropriate input features. Therefore, patterns learned from analyzing the most successful predictors can inform risk factors for cisplatin-induced neurotoxicities. For the less successful tinnitus models, similarities between those in the test set who were misclassified should be studied to further understand the limitations of input features for risk prediction and determine if other input

features may be more appropriate for future models. Future work can try other input features to see if models for classifying cisplatin-induced tinnitus improve.

Although neuropathy and hearing loss models are promising, evaluating the models in externally validated test sets of cisplatin-treated cancer survivors outside of *The Platinum Study* would be of value. To determine the generalizability of models across patient populations, models should be tested in other cancer types treated with cisplatin, such as head and neck cancer, ovarian cancer or lung cancer[67]. Limitations may exist in external datasets which were not considerations when training and testing models in cisplatin-treated testicular cancer survivors, such as concurrent treatment with other chemotherapy agents or radiotherapy which may also cause neurotoxicities[14]. Another limitation of this study is that these models were only trained and tested in survivors of European ancestry. In the future, models should be tested in diverse populations to assess if they are generalizable. If these models are not generalizable across populations, genetic ancestry should be incorporated as a predictor or models should be trained and tested in different populations to inform risk prediction for all patients.

Lipid metabolism and cisplatin-induced neurotoxicities

In addition to the clinical relevance of risk prediction for peripheral sensory neuropathy and hearing loss, machine learning models are a research tool that can provide information about the SNPs used as features in prediction models. Models predicting overall and severe peripheral sensory neuropathy showed that the best set of SNP inputs were SNPs that were associated with neuropathy at $p < 1x10^{-4}$ in GWAS. When exploring the genes which were related to these SNPs and the interactions between these genes and the proteins encoded by these genes, there were significant protein-protein interactions and significant functional enrichments in the gene network. The majority of these significant functional enrichments were related to fatty acid

metabolism and measurement of numerous fatty acids, including omega-3 and omega-6 polyunsaturated fatty acid synthesis and measurement. The other common pathways were related to the measurement of phospholipid membrane components such as sphingolipids and glycerophospholipids. Additionally, external PRS for apolipoprotein A, total cholesterol, LDL, and HDL were significantly associated with cisplatin-induced neuropathy (any versus none) and external PRS for total cholesterol and LDL were significantly associated with severe cisplatin-induced neuropathy (severe versus none). Taking cholesterol medication was significantly associated with both overall and severe cisplatin-induced peripheral sensory neuropathy as well as with cisplatin-induced hearing loss and tinnitus. When examining relative feature importance for tree-based models for predicting severe peripheral neuropathy, among the most important external PRS in the models were those related to body fat composition and fat mass.

Lipids are an important component of nerves, as the dry weight of the soma is about 37% lipid-based, including phospholipids (phosphatidylethanolamine, phosphatidylcholine), cholesterol, ceramide, and triglycerides, with neurites also having a similar relative percentage of phospholipids[153]. Thus, disruptions to lipid metabolism can lead to impairments in neurons that can potentially be linked to neuropathy. Alterations to sphingolipid metabolism have been shown to be involved in hereditary peripheral neuropathies, including Charcot-Marie-Tooth disease (mutations in sphingolipid degrading enzyme S1P-lyase) and hereditary sensory and autonomic neuropathy 1, which is caused by missense mutations in genes encoding for subunits of serine-palmitoyl transferase (SPT), which catalyzes the first step in sphingolipid synthesis[153]. Dyslipidemia such as elevated LDL, cholesterol, and triglycerides have been shown to be associated with diabetic peripheral neuropathy[154]. Therefore, disruptions to lipid metabolism and abnormal lipid levels are associated with neuropathy unrelated to cisplatin treatment. Deletion of

fatty acid synthase in satellite glial cells impaired axon regeneration in peripheral sensory neurons, which illustrates how disruptions in fatty acid metabolism may impact response to cisplatin-induced neuronal injury[155]. Lipidomic analysis on patients receiving taxane treatment also noted an association between elevated baseline lipid levels and high-grade taxane-induced peripheral neuropathy[156].

Based on our results and the literature, there is increasing evidence that focusing on mitigating lipid abnormalities may be the way forward to find treatments and/or preventions for cisplatin-induced peripheral sensory neuropathy. This may be through pharmacological or even behavioral interventions. There is evidence that elevated levels of omega-6 polyunsaturated fatty acids characteristic of a Western diet can lead mice to develop peripheral nerve damage that can be attenuated with pharmacological inhibition of PLA2g7 or adjustment to a diet with high omega-3 polyunsaturated fatty acids[157]. Further validation of the association between dyslipidemia and disrupted fatty acid metabolism and cisplatin-induced peripheral sensory neuropathy should be conducted *in vitro* and *in vivo* before moving forward with intervention trials.

Age and age-related comorbidities as risk factors for cisplatin-induced neurotoxicities

Clinical variables tested for association with cisplatin-induced neurotoxicities and incorporated into machine learning models fell into multiple categories, including age (age at diagnosis, age at questionnaire, time difference), medication use (blood pressure and cholesterol), body composition (weight at chemotherapy and body surface area), and lifestyle/behaviors (currently or ever smoking and excess drinking). When assessing relative variable importance for tree-based models predicting severe peripheral sensory neuropathy and hearing loss, age at diagnosis and age at questionnaire were the two most important variables

across models for both toxicities. This remained valid when also incorporating genetic predictors (external PRS or GWAS) into models for severe peripheral sensory neuropathy. Age at diagnosis and questionnaire and taking medications for age-related morbidities like high blood pressure and cholesterol were also significantly associated with all cisplatin-induced neurotoxicities in an association analysis. Therefore, when assessing toxicity risk prior to cisplatin treatment, age and age-related comorbidities should be considered, even more than modifiable risk factors such as smoking or drinking.

Kidney function as a risk factor for cisplatin-induced neurotoxicities

When assessing relative variable importance for tree-based models predicting severe peripheral sensory neuropathy, among the most important external PRS contributing to models, after those related to body composition, were those related to kidney function. These included PRS for measurements of total blood protein, serum protein (no albumin), urine microalbumin, urine creatinine, urine potassium, and urea, as well as a PRS for kidney failure. The relationship between kidney function and cisplatin-induced neurotoxicities was also shown when studying the association between external PRS and toxicity phenotypes in the training set. PRS for cystatin C measurement were significantly associated with peripheral sensory neuropathy, tinnitus, and hearing loss. Higher cystatin C PRS values (worse kidney function) were associated with increased overall neuropathy (any versus none), tinnitus, and hearing loss (positive correlation between cystatin C PRS and GM412). Cystatin C is a protein present across nucleated cells that is both freely filtered and reabsorbed. Cystatin C eGFR is a great estimator of kidney function, particularly because it is not impacted by body composition unlike serum creatinine[158]. In the kidney, cisplatin accumulates in and injures the cells of the proximal tubule, where cystatin C is filtered and reabsorbed[158,159]. Other PRS related to kidney function were also

significantly associated with cisplatin-induced neurotoxicities. Cisplatin is excreted by the kidneys after binding to plasma proteins and forming conjugates with glutathione[160]. Inability to excrete cisplatin properly may be related to downstream neurotoxicities, as in a study of residual serum platinum levels in cisplatin-treated testicular cancer survivors, survivors with high residual serum platinum levels (versus medium or low) had significantly greater Raynaud's phenomenon ($p = 4.0x10^{-2}$) and were more likely to have tinnitus ($p = 7.0x10^{-2}$)[64]. Results from our studies provide further evidence that healthy kidney function is important for preventing cisplatin-induced neurotoxicities.

WFS1 and cisplatin-induced hearing loss

The WFS1 gene expression across four tissues was associated with cisplatin-induced hearing loss at suggestively significant $p < 0.0005$, as well as at the less stringent p-value threshold of $p < 0.005$ (eight tissues). This finding is consistent with results from multiple GWAS of cisplatin-induced hearing loss, including in *The Platinum Study*, which in a smaller dataset of 511 individuals found that rs62283056, a SNP in the first intron of WFS1 and an eQTL for WFS1, was significantly associated with hearing loss ($p = 1.4x10^{-8}$) and that decreased WFS1 expression was associated with hearing loss in the BioVU cohort[49]. In a cohort of 229 cisplatin-treated testicular cancer patients with a binary hearing loss phenotype, rs62283056 was not significantly associated with cisplatin-induced ototoxicity but was significantly associated with general hearing loss ($p = 5.7x10^{-3}$), with the authors of this study highlighting that patients with a variant in WFS1 may be more susceptible to hearing loss that could potentially be worsened by cisplatin treatment[161]. Our results also suggested that decreased WFS1 expression is associated with cisplatin-induced hearing loss.

WFS1 encodes Wolframin transmembrane glycoprotein and mutations in WFS1 cause autosomal dominant sensorineural hearing loss and Wolfram syndrome, which causes autosomal recessive hearing loss, among other symptoms[162]. In the same study of 511 testicular cancer survivors, SNPs in and near 84 Mendelian deafness genes were significantly enriched ($p = 4.8x10^{-2}$) for stronger associations (lower p-values) in the GWAS for cisplatin-induced hearing loss[49], indicating some shared genetic architecture between hereditary and cisplatin-induced hearing loss.

WFS1 is also critical for maintaining calcium (Ca^{2+}) homeostasis, especially in the endoplasmic reticulum (ER). WFS1 deficient-neurons have shown lower calcium transfer from the ER to the mitochondria, inhibiting mitochondrial ATP production and negatively impacting neuronal health[163]. Overall, calcium levels have been shown to be very important in the context of cisplatin-induced ototoxicity, as the rs1872328 variant on ACYP2, which encodes a protein with a role in calcium homeostasis, has been found to be significantly associated with cisplatin-induced hearing loss across multiple studies, as well as in a meta-analysis[53,65,164]. Our results provide further evidence of the importance of WFS1 expression, hereditary deafness genes, and perturbations to calcium homeostasis in the risk for cisplatin-induced hearing loss.

Relationship between *de novo* phenotypes and cisplatin-induced neurotoxicities

Based on association analysis between PRS and toxicities in the training set, the PRS for *de novo* hearing difficulties as built in the UK Biobank data was significantly associated with both cisplatin-associated tinnitus (one PRS) and cisplatin-associated hearing loss (two PRS). For general tinnitus, hearing loss is a major risk factor[165]. This may indicate that in addition to potentially shared genetic architecture between cisplatin-induced hearing loss and hereditary hearing loss, there may also be shared genetic architecture between cisplatin-induced hearing

loss and tinnitus and *de novo* hearing difficulties. However, a recent study published comparing GWAS between *de novo* tinnitus in the UK Biobank and cisplatin-induced tinnitus in *The Platinum Study* showed no replicated lead variants between studies[166]. Additionally, a soon to be published study testing if variants associated with hearing loss in the overall population were also associated with cisplatin-induced hearing loss in *The Platinum Study* found no significant associations, with one variant reaching significance at a less stringent p-value cutoff of 10^{-4}. Therefore, the evidence for shared genetic architecture between cisplatin-induced ototoxicity and *de novo* ototoxicity is limited and requires further investigation. Our results may highlight the relevance of utilizing a polygenic risk score that incorporates multiple variants versus focusing on single SNPs that meet significance when exploring genetic risk factors for cisplatin-induced neurotoxicities.

2.5 Conclusion

To further extend our knowledge regarding the clinical and genetic risk factors for cisplatin-induced neurotoxicities, we developed machine learning prediction models for these toxicities. The goal was to train models that could successfully predict toxicities in cisplatin-treated testicular cancer survivors with the hope that these models may be tested in other datasets of cisplatin-treated patients in the future. We were able to successfully predict cisplatin-induced overall and severe peripheral sensory neuropathy, with the model developed for predicting overall neuropathy (any versus none/yes versus no) having an AUROC of 0.68 and high sensitivity (over 80%) and the best model for predicting severe peripheral neuropathy having an AUROC of 0.8 and high sensitivity of 86%. Clinical variables were successful in predicting the continuous hearing loss phenotype and showed significant associations between observed and expected GM412 values. While models for predicting cisplatin-induced were not as successful,

there may be other predictors that can be tested to improve models. These models were also used to assess which features were the most important predictors. In the context of genetic predictors, we explored biological pathways that may be associated with the risk of cisplatin-induced peripheral sensory neuropathy such as fatty acid metabolism. In the future, these models could be used in a clinical setting to predict the risk of neurotoxicities prior to cisplatin treatment. This is particularly important in a landscape where no treatments or preventions exist for adult-onset cancer survivors.

Chapter 3. Impact of Population Pharmacogenomics on Cisplatin-Induced Neurotoxicities in Adult-Onset Cancer Survivors

3.1 Introduction

Although studies have described population disparities in the prevalence/severity of chemotherapy-induced neuropathy in patients treated with paclitaxel and vincristine[55,102,107–109], data on disparities in cisplatin-induced neurotoxicities is scarce. Breast cancer survivors of African ancestry have significantly greater incidence/prevalence of and more severe paclitaxel-induced sensory neuropathy compared to survivors of European ancestry[55,102,107,108]. In contrast, African American survivors of childhood acute lymphoblastic leukemia treated with vincristine have less neurotoxicity than their European American counterparts[109]. Many pharmacogenomic variants impacting drug response have varied allele frequency across ancestral populations[167,168], suggesting the potential contribution of allele frequency differences to disparities in drug toxicity between populations. As discussed in Chapter 1, allele frequency differences between populations are often due to the selection of alleles in response to environmental pressures[96]. For example, cisplatin-induced vascular toxicities are similar to the cardiovascular toxicities associated with environmental heavy metals, the metabolism of which may vary due to genetic variation related to adaptation to different exposures across geographies[169,170].

Given the lack of data regarding disparities in cisplatin-induced neurotoxicities unlike other chemotherapy agents, we evaluated our cohort of cisplatin-treated testicular cancer survivors in *The Platinum Study* to assess if genetic ancestry was associated with cisplatin-induced peripheral sensory neuropathy, hearing loss, tinnitus, and vertigo. As discussed in Chapter 1, since race is a social construct rather than biological and racial categories may disagree with classification based on ancestry-informative markers[100], we used genetic ancestry

to study disparities. We focused on finding functional, ancestry-informative SNPs that impact gene expression and/or splicing and testing their associations with cisplatin-induced neurotoxicities. We also evaluated whether population differences in cisplatin-induced neurotoxicities could be explained by disparities in clinical or modifiable risk factors for adverse health outcomes. Based on the results of genotype-phenotype association analyses, we studied the impact of gene expression differences on cisplatin sensitivity and neuronal cell viability.

3.2 Methods

Study Population

As described in the previous chapter, all survivors that were part of this analysis were enrolled in *The Platinum Study*. Eligible survivors[49,50] underwent physical examination, phlebotomy, audiometry, genotyping, and completed extensive questionnaires. Medical records were used for diagnosis and treatment data. Informed written consent was obtained from all participants and the study protocol was approved by Human Subject Review Boards at each participating institution. Procedures were conducted in accordance with U.S. Common Rule.

Toxicity phenotypes

Peripheral sensory neuropathy was again defined using eight relevant items in the validated EORTC-CIPN20 questionnaire[121] (Appendix Table A1). The mean of responses was converted to a 0-3 numeric scale with the ceiling function: 0: “none”, 1: “a little” 2: “quite a bit”, 3: “very much.” Categories 2 and 3 were combined for a severe peripheral sensory neuropathy phenotype and responses were also converted to a binary (any neuropathy (1, 2, 3) versus no neuropathy (0)) to study overall peripheral sensory neuropathy.

The cisplatin-induced sensorineural hearing loss phenotype was defined by calculating the geometric mean of quantitative bilateral hearing thresholds from 4 to 12 kHz.

Cisplatin-induced tinnitus was based on the question: "In the last 4 weeks, have you had ringing or buzzing in the ears?" in the SCIN questionnaire[122] (Appendix Table A2). Answers were converted to cases and controls, with those responding, "not at all" being classified as controls and "quite a bit" or "very much" being classified as cases, excluding those who answered "a little", with a second question asking the same to check for consistency. The cisplatin-induced vertigo phenotype was based on a question asking if survivors experienced persistent dizziness or vertigo with options "yes", "no", and "don't know/not sure". Those who answered "don't know/not sure" were excluded from analyses.

Additional survivor data for analysis

Testicular cancer survivors enrolled in *The Platinum Study* completed extensive questionnaires covering numerous topics, including lifestyle behaviors and prescription medication use. Of interest for this study were excess drinking (described as greater than 2 drinks per day) and current and past cigarette use. Additionally, questionnaires asked if survivors were taking prescription medications for hypertension and/or hypercholesterolemia, and if they had diabetes and took insulin and/or tablets/prescription medication. The answer choices were "never", "past only", "yes, current", and "don't know/not sure." Controls were those who answered "never" and cases were those who answered "yes, current," with other survivors excluded. Self-reported health was evaluated with the question: "would you rate your health as: 1) excellent, 2) very good, 3) good, 4) fair, or 5) poor?" "Fair" and "poor" categories were combined, due to low numbers in the latter.

Additional data of relevance were age at diagnosis, age at questionnaire completion, and cumulative cisplatin dose in mg/m^2.

Genotyping and imputation

DNA was extracted from the peripheral blood of survivors enrolled in *The Platinum Study* at the time of questionnaire completion. The Infinium Global Screening Array-24 chip (GSA-24v1-0_A1; Illumina) at Regeneron Pharmaceuticals was used for genotyping. Quality control (QC) removed individuals and SNPs with missingness > 0.2 followed by > 0.02. Sample QC included removing individuals with pairwise IBD > 0.2 and individuals deviating more than 3 standard deviations from the mean heterozygosity rate. SNP QC excluded SNPs with a minor allele frequency (MAF) < 0.05 and Hardy-Weinberg Equilibrium (HWE) $p < 1x10^{-6}$. Sex discrepancy was assessed with X chromosome homozygosity rates. Imputation was conducted using the University of Michigan Imputation Server[124] with the 1000 Genomes Phase 3 Reference Panel[127], which has 5,008 haplotypes from 26 global populations. Post-imputation QC excluded SNPs with imputation $R^2 < 0.8$, MAF < 0.05 and HWE $p < 1x10^{-6}$ as well as SNPs and individuals with missingness > 0.1 (Figure 3.1A, B).

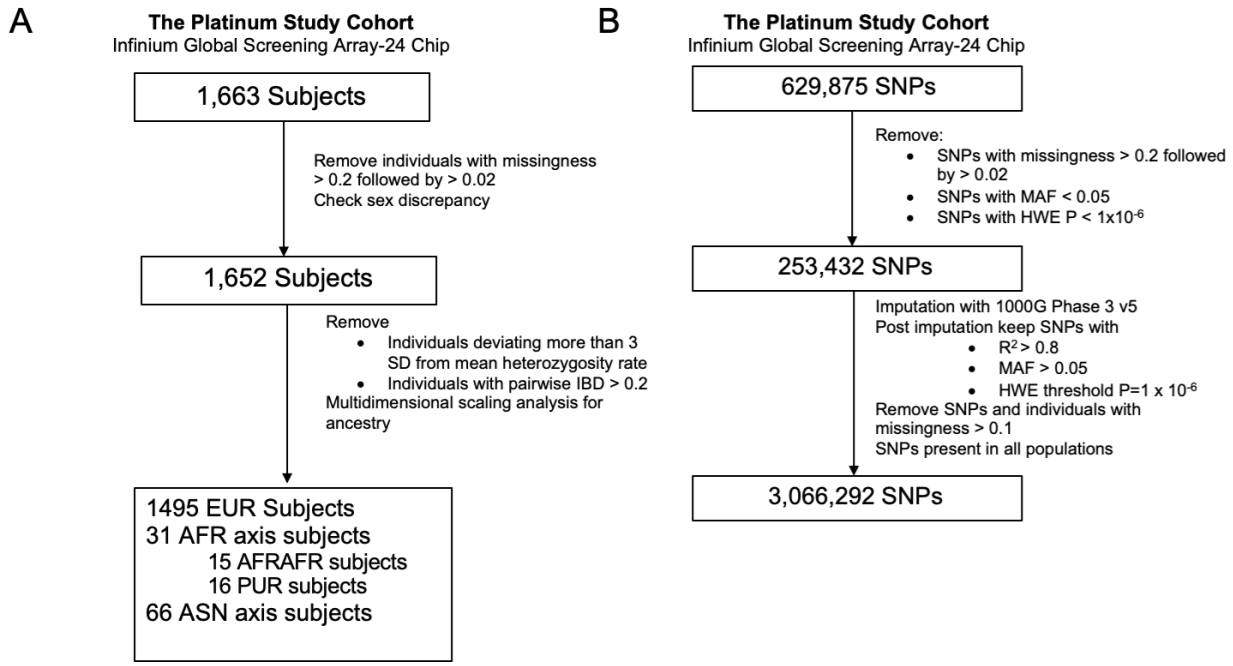

Figure 3.1 Subject and variant quality control for population pharmacogenomic analysis.

Figure 3.1. Subject and variant quality control for population pharmacogenomic analysis (cont). A, Quality control for survivors and population stratification using multidimensional scaling. **B,** Quality control and imputation for SNPs.
MAF = minor allele frequency. HWE = Hardy-Weinberg equilibrium. IBD = identity-by-descent. SD = standard deviation. EUR = European. AFR/AFRAFR = African. PUR = Puerto Rican. ASN = Asian.

Defining genetic ancestry

Ancestry was determined using multidimensional scaling, which generates scores of genetic variation for each sample by calculating the genome-wide average proportion of alleles shared between each sample pair in the population. Scores were plotted and anchored by reference data from the 1000 Genomes population[127]. Based on visual cutoffs from the resulting plot, survivors were divided into categories of European (EUR) (British from England and Scotland (GBR), Finnish in Finland (FIN), Toscani in Italy (TSI), and Utah Residents with Northern and Western European ancestry (CEU)), along the axis towards African ancestry (AFR) (Puerto Rican from Puerto Rico (PUR), Yoruba in Nigeria (YRI), Luhya in Kenya (LWK), and Americans of African Ancestry (ASW)), and along the axis towards East Asian ancestry (ASN) (Mexican in Los Angeles (MXL), Southern Han Chinese (CHS), Han Chinese in Beijing (CHB), and Japanese in Tokyo (JPT)) (Figure 3.2). Survivors along the axis towards AFR ancestry were further divided into those closer to EUR ancestry (PUR) and those closer to AFR ancestry (AFRAFR), including the YRI, LWK, and ASW populations.

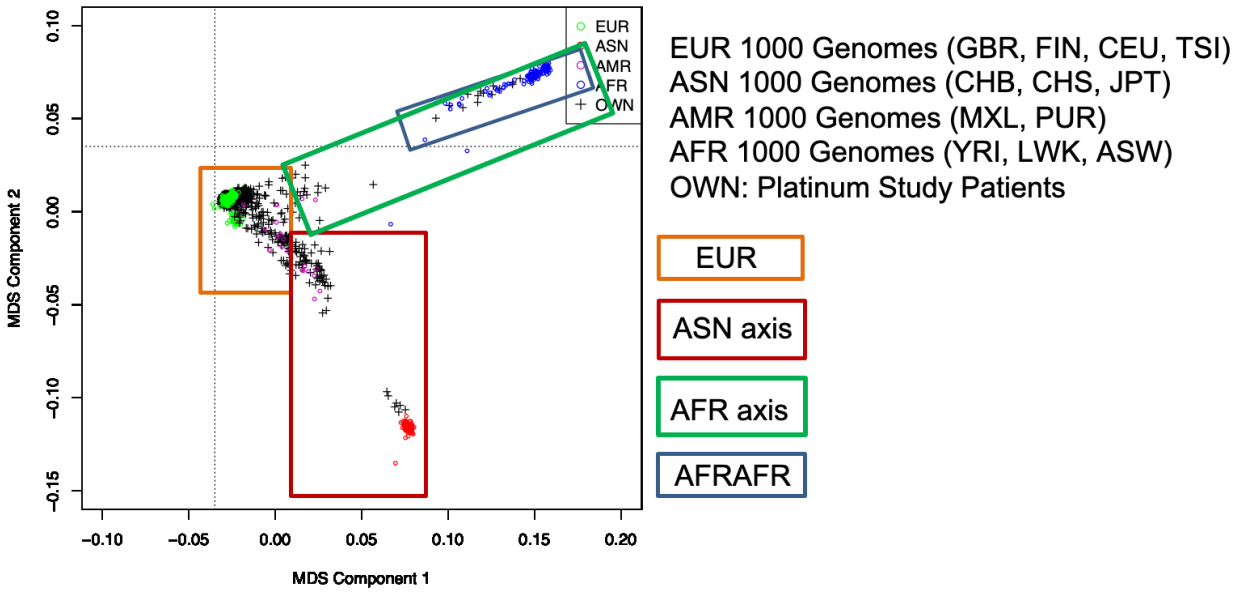

Figure 3.2. Multidimensional scaling analysis to assign genetic ancestry to testicular cancer survivors. Multidimensional scaling scores were calculated for testicular cancer survivors and the 1000 Genomes reference population and were plotted. Overlap between MDS scores was used to classify testicular cancer survivors into genetic ancestral populations based on 1000 Genomes reference. EUR included EUR 1000 Genomes populations (GBR, FIN, CEU, TSI). ASN axis included ASN 1000 Genomes populations (CHB, CHS, JPT) and MXL population and AFR axis included AFR 1000 Genomes populations (YRI, LWK, ASW) and PUR population. AFR axis population was further split into those with just AFR ancestry (AFRAFR).
MDS = multidimensional scaling, EUR = European, AFR = African, ASN = Asian, AMR = American, GBR = British from England and Scotland, FIN = Finnish in Finland, CEU = Northern Europeans from Utah, TSI = Tuscans from Italy, CHB = Han Chinese in Beijing, China, CHS = Han Chinese, South China, JPT = Japanese in Tokyo, Japan, MXL = Mexican Ancestry in Los Angeles, CA, USA, PUR = Puerto Rican in Puerto Rico, YRI = Yoruba in Ibadan, Nigeria, LWK = Luhya in Webuye, Kenya, ASW = African Ancestry in southwest USA.

Ancestry-phenotype association analysis

For categorical phenotypes (peripheral sensory neuropathy, tinnitus, vertigo, lifestyle behaviors, medications, self-reported health), logistic regression (multinomial (neuropathy – "none", "a little", "quite a bit/very much") or binary (other phenotypes)) was used to evaluate the association between genetic ancestry and cisplatin-induced neurotoxicities, with a particular emphasis on the AFRAFR population based on past studies in paclitaxel and vincristine focusing

on disparities in this population. For association analyses between cisplatin-induced neurotoxicities and genetic ancestry, subset analysis of survivors receiving 400-450 mg/m^2 of cisplatin was conducted, as 13/15 survivors with AFRAFR ancestry received this dose, hypothesized to be due to their treatment center. All patients in this subset received four cycles of cisplatin-based chemotherapy, with dosage extrapolated by study staff using medical records and BSA. Across ancestries, over 97% of patients in this subset receiving four cycles received 400 mg/m^2, including all patients of AFRAFR ancestry (Table 3.1). A few patients in the EUR and ASN axis populations received between 400 and 450 mg/mg^2, with the mean cisplatin doses in these populations being 400.36 mg/m^2 and 400.20 mg/m^2, respectively (Table 3.1). Association analyses between lifestyle and medications were conducted in testicular cancer survivors receiving all doses of cisplatin, without subset analysis, as these phenotypes were not impacted by cisplatin dose. Association analyses between genetic ancestry and neurotoxicities for patients receiving four cycles of cisplatin were conducted using logistic regression.

Table 3.1. Cisplatin dose across genetic ancestries for testicular cancer survivors in *The Platinum Study* receiving four cycles of cisplatin

Characteristic	**AFRAFR (n=13)**	**EUR (n=701)**	**ASN axis (n=45)**
Cisplatin Dose (mg/m^2)			
Mean	400	400.36	400.20
400	13	684	44
>400-410	0	8	1
≥410-420	0	2	0
≥420-430	0	5	0
≥430-450	0	2	0

Abbreviations: ASN, Asian axis ancestry; EUR, European ancestry; AFRAFR, African ancestry.

For the continuous audiometrically-defined phenotype of hearing loss, the non-parametric Kruskal-Wallis rank sum test determined if there were statistically significant differences between geometric means of bilateral hearing thresholds between ancestral groups in the subset of survivors who received four cycles of cisplatin chemotherapy. This same statistical analysis was used to compare age at diagnosis and age at questionnaire between populations (also subset

analysis). Multiple pairwise comparisons between groups were conducted with pairwise Wilcoxon tests, with the Benjamini-Hochberg p-value adjustment. Statistical analyses were conducted in R4.1.2.

Identification of SNPs with allele frequency differences between populations

A list of SNPs genotyped in all survivors after QC, regardless of genetic ancestry, was compiled. To filter variants with differentiation in allele frequencies between populations, F_{ST}DB, a database with each SNP's fixation index (F_{ST}), a metric for calculating population differentiation, was used. F_{ST}DB was built at Vanderbilt University by calculating the F_{ST} for each SNP in the 1000 Genomes reference population using the unbiased estimator as described by Weir and Cockerham for all population pairings[171]. SNPs in *The Platinum Study* survivors were filtered for those with $F_{ST} > 0.25$ in the 1000 Genomes reference population[127].

Identification of SNPs associated with gene expression or splicing

Following F_{ST} filtering, GTEx data[131] (V8 release) in the GTEx portal was used to identify SNPs that were eQTLs or sQTLs in tibial nerve or brain tissue. SNPs that were not eQTLs/sQTLs in nerve/brain tissue and those associated only with long non-coding RNAs (lncRNA), open reading frames, antisense transcripts, and reverse strands were excluded. GTEx data was used to evaluate how the SNP genotype of eQTLs/sQTLs impacted the normalized expression (eQTL) or intron-excision ratio (sQTL) of SNP-associated genes.

Identification of candidate gene SNPs

SNPs that were eQTLs and sQTLs for genes involved in cisplatin uptake, metabolism, and effect based on the literature were also included[138–140] (Table 2.1). These were the same genes described in Chapter 2 and listed in Table 2.1. SNPs that were eQTLs and sQTLs for these

genes across tissues (not just in nerve/brain tissue) were determined using GTEx data. These SNPs were subject to the same F_{ST} cutoff of 0.25.

After genome-wide and cisplatin-associated SNP filtering for eQTLs and sQTLs, the NCI's LDmatrix tool[126] was used to calculate the R^2 between pairs of SNP across all 1000 Genomes populations to determine LD between SNPs[127]. For SNPs with $R^2 > 0.75$, one independent SNP was kept for association analysis. For cisplatin-associated SNPs, variants were kept that were not duplicates/in LD with variants retained by nerve/brain eQTL/sQTL filtering (unless the SNP in LD was not an eQTL/sQTL for a cisplatin-associated gene of interest).

Association analysis between genotypes and cisplatin-induced neurotoxicities

To determine if SNPs with population differentiation in allele frequencies were associated with toxicity phenotype, SNPs passing the above filters were evaluated. Logistic regression analyses for association between genotype and phenotype were conducted, with covariates including age at questionnaire and 10 genetic principal components (PCs). Analyses were conducted in R 4.1.2. Genetic PCs were added as covariates to adjust for population structure (critical due to the absence of sufficiently large populations to independently evaluate genotype-phenotype associations in each population). For SNPs with p-value of association with toxicity $< 1.0 \times 10^{-4}$ (suggestively significant), the ancestral allele was determined using the Ensembl Genome Browser[129].

The workflow for determining disparities in cisplatin-induced neurotoxicities between ancestral populations as well as filtering for independent, functional SNPs with population allele frequency differences and association analysis is outlined in Figure 3.3.

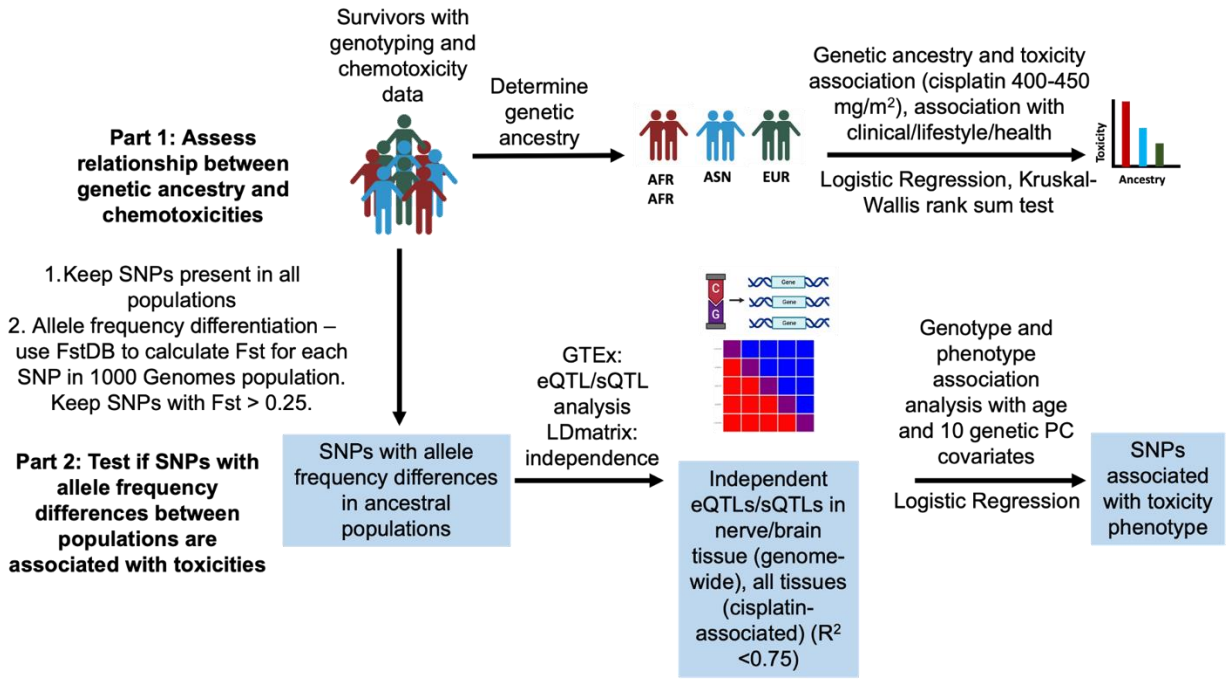

Figure 3.3. Population pharmacogenomics workflow. Workflow for assessing disparities between populations and testing if independent, functional SNPs with population allele frequency differences were associated with toxicities.
Fst = fixation index. GTEx = Genotype-tissue expression project. eQTL = expression quantitative trait loci. sQTL = splicing quantitative trait loci. PC = principal component. Some image icons created with BioRender.com and heatmap icon adapted from NCI LDmatrix[126].

In silico analysis of gene expression and cisplatin toxicity in cell lines

For eQTLs/sQTLs and their associated genes found to be associated with cisplatin-induced neurotoxicities, gene expression across cancer cell lines was obtained from DepMap's Batch corrected Expression Public 24Q2 data[172] (https://depmap.org/portal). Data on cancer cell line sensitivity to cisplatin was obtained from The Genomics of Drug Sensitivity in Cancer Project[173]. The association between gene expression (log2(transcripts per million (TPM)+1)) in cancer cell lines and the sensitivity of cancer cell lines to cisplatin (AUC) (n = 575 cell lines) was plotted. Spearman correlation was calculated in R4.1.2.

Expression/dependency of genes of interest in SH-SY5Y cells

The expression of the RNF24 gene in the SH-SY5Y cell line was assessed in DepMap[172] (https://depmap.org/portal) to ensure that it served as a viable gene candidate for knockdown. Gene dependency was also assessed based on the Chronos score to determine whether the SH-SY5Y cell line's survival was dependent on RNF24.

SH-SY5Y cell culture

SH-SY5Y, a cloned subline derived from the SK-N-SH neuroblastoma cell line from a metastatic bone tumor (ATCC CRL-2266) was cultured in Eagle's Minimum Essential Medium (EMEM) (ATCC 30-2003) (contains non-essential amino acids, L-glutamine, sodium pyruvate, and sodium bicarbonate) with 10% fetal bovine serum (FBS) (Gibco) and 1% penicillin/streptomycin (Gibco 15140-122). With a doubling time of approximately 67 hours, cells were split/passaged approximately every three days, plated in 60 mm cell culture dishes, and incubated at 37°C in a humidified chamber.

Cisplatin cytotoxicity assay

To assess cellular sensitivity to cisplatin in SH-SY5Y cells without any small interfering RNA (siRNA) transfection and ensure sensitivity of this cell line to cisplatin, SH-SY5Y cells were counted and plated at 5000 cells per well in 96 well plates (Corning 3603) in 50 μL of media. Cisplatin (Sigma-Aldrich) was dissolved in the dark in dimethyl sulfoxide (DMSO) and solution was vortexed for one minute to obtain a 20 mM stock solution. Working stock solutions of 1, 2.5. 5, and 10 mM were prepared in DMSO by serial dilution. Prior to adding to incubated cells, 20 μL of DMSO or each working stock solution were added to 10 mL of media. After 24 hours of incubating cells at 37°C, cells were treated with 50 μL of cisplatin at concentrations of 1, 2.5. 5, 10, or 20 μM or DMSO vehicle in complete media for a total volume of 100 μL. At 48 hours post drug treatment, 100 μL of CellTiter-Glo (Promega) was added to each well in a

darkened hood, as per manufacturer's instructions. Luminescence was measured on a Cytation 5 plate reader (BioTek) with a gain setting of 115. Each concentration was evaluated in 8 replicates on the plate. Any outliers were identified and removed using the ROUT method (Q = 1%). Half maximal inhibitory concentration (IC_{50}) values were calculated using Prism 10 software with the nonlinear regression of the cisplatin concentration versus response with a variable slope (four parameters). This was a test of cisplatin cytotoxicity in this cell line and not duplicated like other experiments.

RNF24 siRNA preparation and treatment

Three different Dharmacon human RNF24 siRNAs (catalog no. J-006943-05-0005, J-006943-06-0005, J-006943-08-0005) and one ON-TARGETplus Non-targeting Control Pool (catalog no. D-001810-10-05) were purchased from Horizon Discovery at 5 nmol and were diluted in sterile RNAase free water to make 20 μmol/L stock. In two 60 mm cell culture dishes per treatment (control, RNF24 siRNA1, 2, 3), media was changed from EMEM to serum free media (Dulbecco's Modified Eagle Medium (DMEM) without FBS or penicillin/streptomycin added). Cells were transfected using Lipofectamine 3000 (Invitrogen – L3000015) with slight adjustments to manufacturer's protocol following troubleshooting. To achieve increased transfection of this difficult-to-transfect cell line, 15 μL of Lipofectamine 3000 was added to 125 μL of serum-free media and 15 μL (rather than 10 μL) of siRNA (or non-targeting control) was added to 125 μL of serum-free media in two separate tubes to incubate at room temperature for 3 minutes. The two mixtures were combined and incubated at room temperature for 10 minutes before being added to 60 mm plates containing cells and serum free media. Cells were incubated at 37°C in a humidified chamber for 24 hours before serum free media was exchanged for EMEM + 10% FBS and 1% penicillin/streptomycin. Cells were incubated at 37°C in a

humidified chamber for 48 hours prior to being harvested for RNA extraction and plating for cisplatin sensitivity and cell viability assays. Two independent experiments were conducted.

Quantitative PCR for RNF24 gene knockdown

72 hours after siRNA treatment (and 48 hours after media was changed from serum free media back to complete media), cells were pelleted by centrifugation following trypsinization. After two washes with phosphate-buffered saline (PBS), cells were stored at -80°C in lysis buffer RLT (Qiagen) with 10 μL of beta-mercaptoethanol for every mL of buffer. RNA was isolated using Qiashredder (Qiagen) and the RNeasy Mini Kit (Qiagen). Following measurement of RNA concentration with the NanoDrop 2000 Spectrophotometer, complementary DNA (cDNA) was synthesized using 1 μg (experiment 1) or 0.5 μg (experiment 2) of RNA, based on overall RNA concentration. cDNA was synthesized using the iScript^{TM} cDNA synthesis kit (Bio-Rad) in the T100 Thermal Cycler (Bio-Rad). Expression of human RNF24 was determined using quantitative polymerase chain reaction (qPCR) with TaqMan primer RNF24 (Hs00939203) with human *Actβ* (Hs01060665) as the endogenous control. The comparative $\Delta\Delta C_T$ method was used to determine the percent change of RNF24 expression upon siRNA treatment compared to the non-targeting control siRNA. Two independent experiments were conducted and each sample was run in duplicate with an RNAase free H_2O no template control. qPCR was run on the StepOnePlus^{TM} Real-Time PCR System Thermal Cycling Block (Applied Biosystems).

SH-SY5Y cisplatin sensitivity assay

To determine cellular sensitivity to cisplatin, cells were washed with PBS, trypsinized, and resuspended in complete media before being counted in the Cell Drop FL Cell Counter (DeNovix) 72 hours after siRNA treatment (and 48 hours after serum free media replaced was with complete media). Cells were diluted in complete media and plated at 2000 cells per well in

50 μL of media in 96 well plates (Corning). Each treatment (non-targeting control and RNF24 siRNAs) was plated in a separate plate. Plates were incubated at 37°C for 24 hours before being treated with cisplatin at concentrations of 1, 2.5. 5, 10, or 20 μmol/L or DMSO vehicle in 50 μL with preparation as described above. After 48 hours of cisplatin treatment, 100 μL of CellTiter-Glo (Promega) was added to each well in a darkened hood and luminescence was measured on the Cytation 5 plate reader (BioTek) with a gain setting of 115 for signal amplification. Each concentration was evaluated in 8 replicates on the plate, except for DMSO, which was evaluated in 16 replicates on the plate. Two independent experiments were conducted. Outliers in technical replicates were removed using the ROUT method (Q = 1%) prior to further analysis. The mean of luminescence was calculated for each concentration with percent inhibition calculated with respect to the mean of the DMSO control in order to assess relative cell viability at each cisplatin dose. IC_{50} values were calculated using Prism 10 software with the nonlinear regression of the cisplatin concentration versus response with a variable slope (four parameters). To determine if IC_{50} values were significantly different after RNF24 gene expression knockdown, the IC_{50} was calculated for each duplicate experiment and the mean IC_{50} values for RNF24 siRNA 1 and RNF24 siRNA 2 were compared to the mean IC_{50} for the non-targeting control siRNA in Prism 10 using a one-way analysis of variance (ANOVA) test with the Holm-Šídák's multiple comparisons test (as recommended by Prism software).

SH-SY5Y cell viability assay

72 hours after siRNA treatment (and 48 hours after serum free media was replaced with complete media), cells were harvested and plated at 2000 cells per well in 50 μL of media in 96 well plates (Corning) as described above. Each plate contained a column with media, the cells treated with the non-targeting control, and cells treated with each RNF24 siRNA treatment.

Plates were incubated for 72 hours at 37°C. At 72 hours, 50 μL of CellTiter-Glo (Promega) was added to each well in a darkened hood, based on manufacturer's instructions. Luminescence was measured on the Cytation 5 plate reader (BioTek) with a gain 115. Each treatment (control and siRNA) was evaluated in 8 replicates and two independent experiments were conducted. Using Prism 10, outliers were removed with the ROUT method (Q = 1%). Average relative luminescence units, a metric for cell viability, was calculated across replicates and then standardized to the control siRNA, which was standardized at 1. Standardized mean cell viability was compared between RNF24 siRNA treatment with control siRNA using the one-way ANOVA test with Dunnett's multiple comparisons test.

3.3 Results

Population differences in cisplatin-induced neurotoxicities

Using genetic ancestry demarcations of *The Platinum Study's* testicular cancer survivors based on the 1000 Genomes reference population (Figure 3.2), we evaluated each population for the proportion of survivors with peripheral sensory neuropathy, tinnitus, vertigo, and hearing loss. As previously stated, we noted that 13/15 survivors with African ancestry received four cycles of cisplatin, and therefore evaluated population differences in toxicity for survivors receiving this dose to ensure that disparities were not due to increased cisplatin dosage. Survivors with AFRAFR ancestry had significantly increased prevalence of cisplatin-induced peripheral sensory neuropathy (Figure 3.4A) and vertigo (Figure 3.4B), but not tinnitus (Figure 3.4C) compared to survivors with European ancestry or those along the axis towards East Asian ancestry (Table 3.2). Survivors with AFRAFR ancestry were more likely to have severe neuropathy compared to those of EUR ancestry, although this was approaching significance ($p < 0.1$) (Table 3.2).

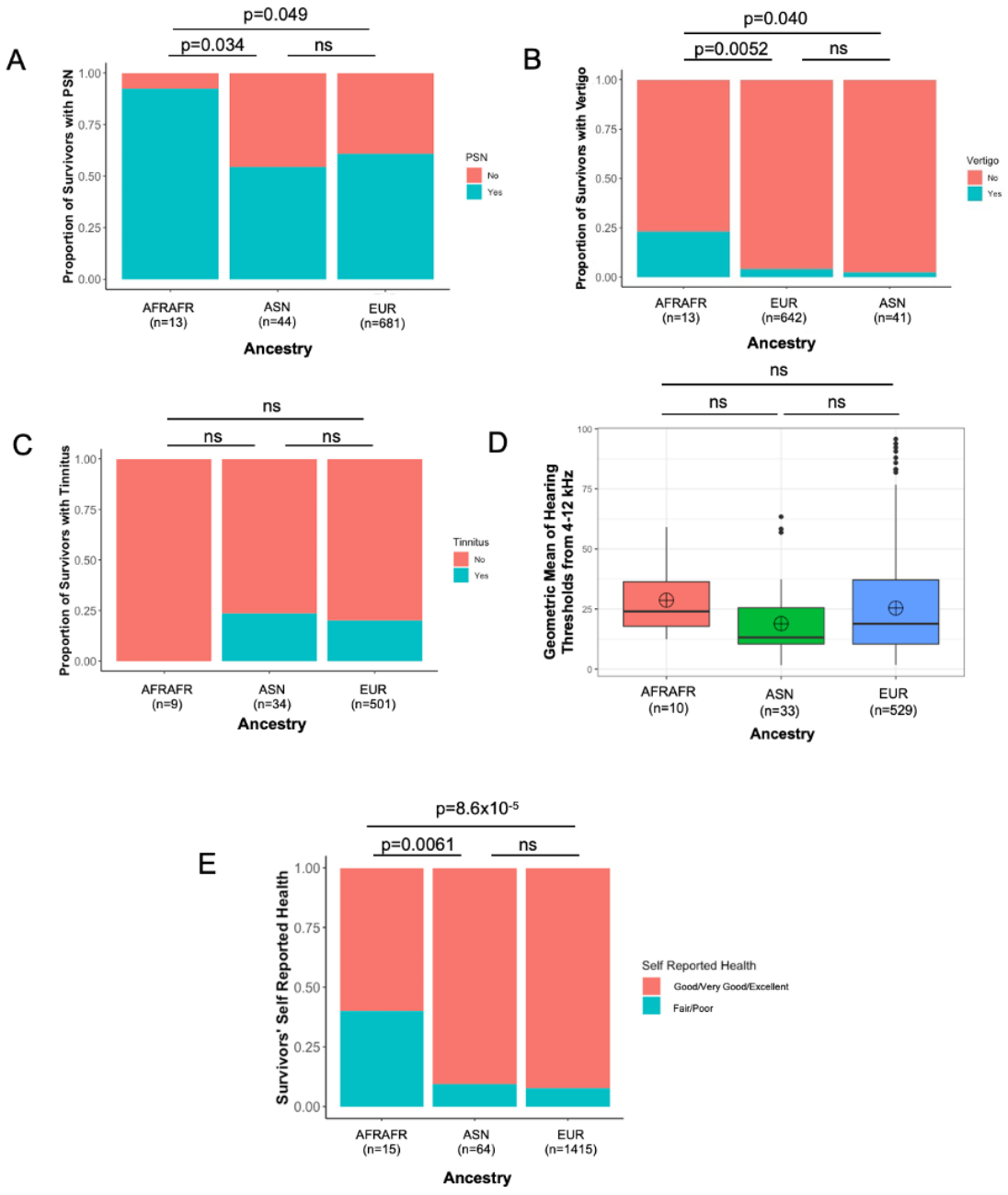

Figure 3.4. Association between genetic ancestry and cisplatin-induced neurotoxicities and self-reported health . A, Association between PSN and ancestry for survivors receiving 4 cycles of cisplatin. **B,** Association between vertigo and ancestry for survivors receiving 4 cycles of cisplatin. **C,** Association between tinnitus and ancestry for survivors receiving 4 cycles of cisplatin. **D,** Association between hearing loss and ancestry for survivors receiving 4 cycles of cisplatin. **E,** Association between self-reported health and ancestry for all survivors across cisplatin doses (3 and 4 cycles).
ASN = Asian-axis ancestry. EUR = European ancestry. AFRAFR = African ancestry.

For peripheral sensory neuropathy (any versus none), the odds ratio (OR) was 10.0 for the AFRAFR versus the ASN axis population ($p = 3.4x10^{-2}$) and was 7.8 for the AFRAFR versus the EUR population ($p = 4.9x10^{-2}$). For vertigo, the OR was 12 for the AFRAFR versus the ASN axis population ($p = 4.0x10^{-2}$) and 6.8 for the AFRAFR versus the EUR population ($p = 5.2x10^{-3}$) (Table 3.2). The ASN axis population had a lower hearing threshold (less hearing loss) than the EUR and AFRAFR populations (Figure 3.4D). However, the Kruskal-Wallis rank sum test demonstrated no significant difference between ancestral groups ($p = 0.09$) for hearing loss. Multiple pairwise comparisons (with Benjamini-Hochberg correction) between groups showed a p-value of 0.072 between AFRAFR and ASN axis survivors and a p-value of 0.12 between EUR and ASN axis survivors. There were no disparities in tinnitus. Survivors of African ancestry were significantly more likely to classify their self-reported health as "fair/poor" versus "very good", "good", or "excellent" compared to other populations with an OR = 6.4 for the AFRAFR versus ASN axis ($p = 6.1x10^{-3}$) and an OR = 8.2 for AFRAFR versus EUR ($p = 8.6x10^{-5}$) (Figure 3.4E).

Table 3.2. Association between genetic ancestry and cisplatin-induced neurotoxicities in testicular cancer survivors in *The Platinum Study* receiving cisplatin dose 400-450 mg/m^2

	ASN axis vs. EUR		**AFRAFR vs. ASN axis**		**AFRAFR vs. EUR**	
	OR (95% CI)	**p-value**	**OR (95% CI)**	**p-value**	**OR (95% CI)**	**p-value**
PSN (Quite a Bit/Very Much vs. No)	1.2 (0.53, 2.7)	0.67	6.7 (0.61, 73)	0.12	8.0 (0.82, 77)	$7.4x10^{-2}$
PSN (Yes vs. No/Any vs. None)	0.78 (0.42, 1.5)	0.42	10.0 (1.7, 190)	$3.4x10^{-2}$	7.8 (1.5, 142)	$4.9x10^{-2}$
Vertigo	0.57 (0.032, 2.8)	0.59	12 (1.4, 260)	$4.0x10^{-2}$	6.8 (1.5, 24)	$5.2x10^{-3}$
Tinnitus	1.2 (0.51, 2.7)	0.62	-	0.99	-	0.99

Abbreviations: ASN, Asian axis ancestry; EUR, European ancestry; AFRAFR, African ancestry; OR, odds ratio; CI: Confidence Interval

Since age is associated with cisplatin-induced neurotoxicities[11], age at diagnosis and questionnaire were compared between ancestral populations in survivors receiving four cycles of cisplatin (Table 3.3). Multiple pairwise comparisons demonstrated that the ASN axis population had a significantly lower age at diagnosis than the EUR ($p = 1.6x10^{-5}$) and AFRAFR ($p = 8.2x10^{-3}$) populations, with no significant difference in age at diagnosis between the EUR and AFRAFR populations ($p = 0.34$). Similarly, multiple pairwise comparisons showed that the ASN axis population had significantly lower age at questionnaire than the EUR ($p = 1.2x10^{-5}$) and AFRAFR ($p = 4.0x10^{-3}$) populations, with no significant difference between EUR and AFRAFR populations ($p = 0.38$), perhaps explaining less hearing loss in the ASN axis population.

Table 3.3. Age at diagnosis and questionnaire across genetic ancestries for testicular cancer survivors in *The Platinum Study* receiving four cycles of cisplatin

Characteristic	AFRAFR (n=13)	EUR (n=701)	ASN axis (n=45)
Age at Diagnosis (years)			
Mean	35.7	32.7	26.2
<20	0	50	6
≥20-30	4	271	26
≥30-40	4	214	13
≥40	5	166	0
Age at Questionnaire (years)			
Mean	42.4	39.5	31.5
<20	0	5	1
≥20-30	2	157	18
≥30-40	4	229	23
≥40	7	300	3
Not available	0	10	0

Abbreviations: ASN, Asian axis ancestry; EUR, European ancestry; AFRAFR, African ancestry.

To assess whether clinical and lifestyle factors contributed to population disparities in cisplatin-induced neurotoxicities (neuropathy and vertigo), we evaluated differences in medication use for cholesterol, blood pressure, and diabetes as well as lifestyle factors such as smoking and drinking between populations. Across all cisplatin doses, clinical and lifestyle factors were not significantly different between populations, except the ASN axis population had

significantly lower anti-hypertensive medication use versus other populations (ASN axis versus EUR (OR = 0.11; p = $3.2x10^{-2}$); AFRAFR versus ASN axis (OR = 24; p = $6.3x10^{-3}$)) (Table 3.4), and lower cholesterol medication use versus the EUR population (OR = 0.14; p = $5.0x10^{-2}$) (Table 3.4) perhaps reflecting their younger age at time of diagnosis/questionnaire.

Table 3.4. Association between genetic ancestry and medication use and lifestyle behaviors in testicular cancer survivors in *The Platinum Study* (all doses)

	ASN axis vs. EUR		**AFRAFR vs. ASN axis**		**AFRAFR vs. EUR**	
	OR (95% CI)	**p-value**	**OR (95% CI)**	**p-value**	**OR (95% CI)**	**p-value**
Cholesterol Medication (Y vs. N)	0.14 (0.0078, 0.63)	$5.0x10^{-2}$	9.8 (0.88, 220)	$7.1x10^{-2}$	1.4 (0.21, 5.0)	0.69
Blood Pressure Medication (Y vs. N)	0.11 (0.0065, 0.52)	$3.2x10^{-2}$	24 (3.22, 505)	$6.3x10^{-3}$	2.8 (0.76, 8.5)	$8.5x10^{-2}$
Diabetes Requiring Insulin (Y vs. N)	-	0.99	-	1	-	0.99
Diabetes Requiring Tablets/Pills (Y vs. N)	0.65 (0.036, 3.1)	0.67	-	1.0	-	0.98
Ever Smoked (Y vs. N)	1.4 (0.85, 2.3)	0.18	0.50 (0.14, 1.6)	0.25	0.70 (0.22, 2.0)	0.52
Current Smoker (Y vs. N)	0.66 (0.20, 1.6)	0.42	-	1.0	-	0.98
Excess Drinking (Y vs. N)	0.33 (0.079, 0.89)	$6.0x10^{-2}$	5.1 (0.85, 31)	$6.3x10^{-2}$	1.7 (0.37, 5.3)	0.44

Abbreviations: ASN, Asian axis ancestry; EUR, European ancestry; AFRAFR, African ancestry; OR, odds ratio; CI, confidence interval; Y, Yes; N, No.

Filtering SNPs for population pharmacogenomic association analysis

To identify a subgroup of functional SNPs with population allele frequency differences using a genome-wide approach, we filtered 3,066,292 SNPs shared across all survivors for those with $F_{ST} > 0.25$ in 1000 Genomes, after which 364,278 SNPs remained. This was expected, as the majority of SNPs do not show allele frequency differentiation between populations and most SNPs have an $F_{ST} < 0.05$, as illustrated by the F_{ST} distribution for SNPs in chromosome 20 (Figure 3.5A). We used GTEx to filter for eQTLs/sQTLs in nerve and/or brain tissue followed by determination of SNPs in linkage disequilibrium ($R^2 > 0.75$), leaving 19,874 independent, functional SNPs for genotype-phenotype association analysis (Figure 3.5B). We also used a candidate gene approach, identifying 30,813 SNPs that were eQTLs/sQTLs for cisplatin-associated genes across all tissues according to GTEx data. From those, 13,210 SNPs were genotyped across all *Platinum Study* testicular cancer survivors after removing duplicate SNPs between genes. Upon removing SNPs with $F_{ST} < 0.25$, 2,013 SNPs remained, with 416 SNPs remaining following LDmatrix filtering. We ensured no duplication of SNPs from the genome-wide approach and no variants in LD with SNPs from the genome-wide approach, leaving us with 118 candidate SNPs for genotype-phenotype association analysis (Figure 3.5C). In total, 19,992 SNPs were included for genotype-phenotype association analyses across genome-wide and cisplatin candidate gene approaches.

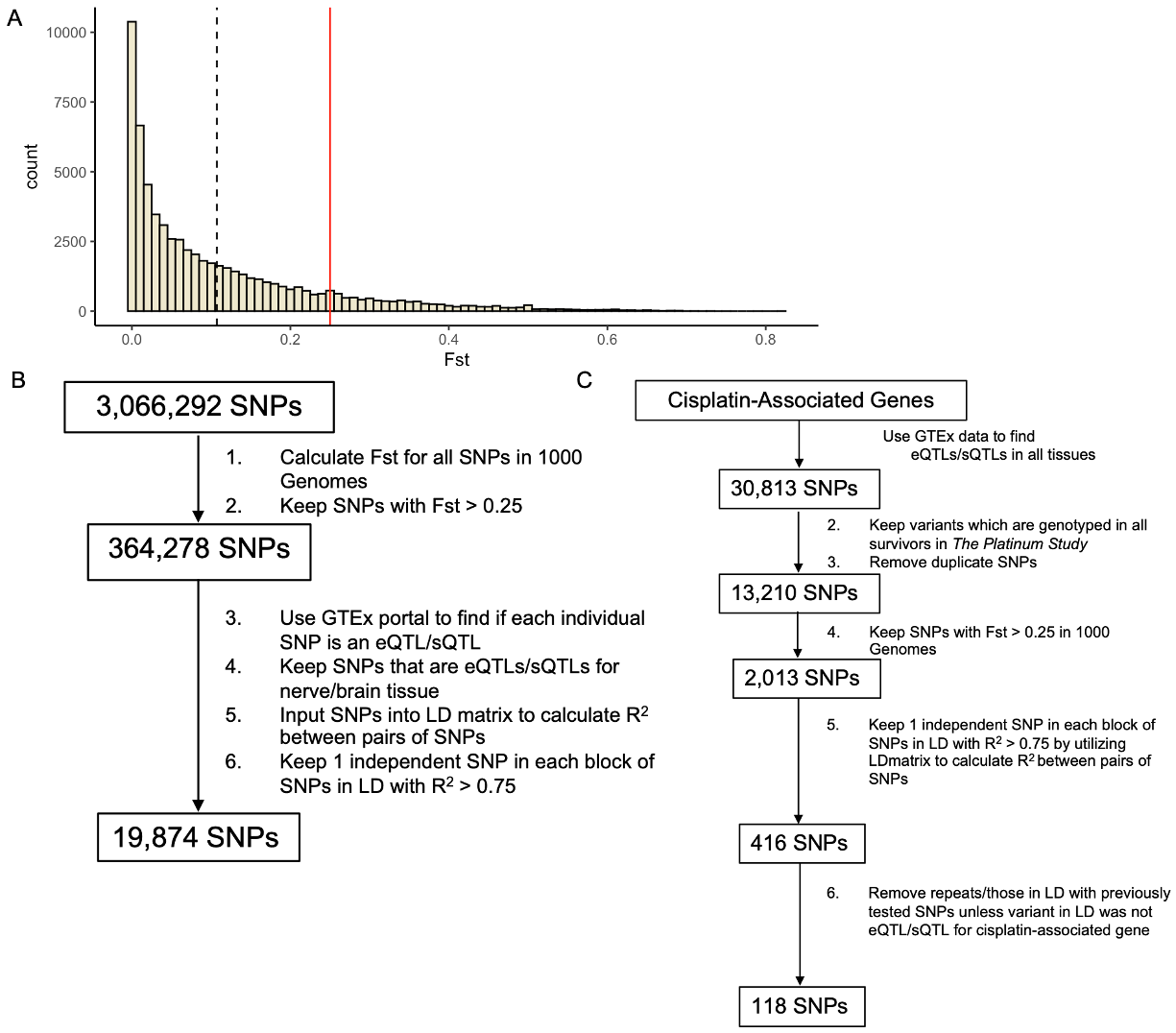

Figure 3.5. Filtering SNPs for population pharmacogenomic analysis. A, Distribution of F_{ST} values for SNPs located on chromosome 20, with dotted line illustrating average F_{ST} and red line illustrating F_{ST} cutoff of 0.25. **B,** Genome-wide approach to select SNPs for genotype-phenotype analysis between independent, functional ancestry-informative SNPs and neurotoxicity phenotype. **C,** Candidate gene approach to select cisplatin-associated SNPs for genotype-phenotype analysis between independent, functional ancestry-informative, cisplatin-associated SNPs and neurotoxicity phenotype.
F_{ST} = fixation index, GTEx = Genotype-tissue expression project, LD = linkage disequilibrium.

Genotype-phenotype association analysis and *in silico* validation

We evaluated the association between the SNP genotype and the overall peripheral sensory neuropathy (any/none; n = 1,513) and vertigo (yes/no; n = 1,427) phenotypes. Although

no SNPs passed the Bonferroni threshold for multiple testing corrections ($p = 2.5x10^{-6}$), 2 SNPs for peripheral sensory neuropathy and 4 SNPs for vertigo passed a suggestively significant p-value threshold ($p < 1.0x10^{-4}$) (Table 3.5).

Table 3.5. SNPs with association between genotype and cisplatin-induced neurotoxicity phenotypes with p-value < $1.0x10^{-4}$

Neurotoxicity	SNP	chr	F_{ST}	Genotype	Category Yes vs. No		Allele more frequent in AFRAFR population	Ancestral Allele	eQTL/sQTL gene	eQTL/sQTL tissue
					OR	p-value				
PSN	rs2063249	5	0.31	CC	ref.	ref.	C	C	eQTL - COMMD10	Brain
				CT	1.6	$5.3x10^{-3}$				
				TT	2.0	$2.8x10^{-5}$				
	rs34904346	20	0.26	AA	ref.	ref.	T	T	eQTL - RNF24	Nerve (tibial)
				AT	1.7	$1.7x10^{-4}$				
				TT	1.9	$2.0x10^{-5}$				
Vertigo	rs28516482	5	0.26	AA	ref.	ref.	A	A	sQTL - PRELID	Nerve (tibial)
				AG	0.13	$1.4x10^{-3}$				
				GG	0.091	$5.0x10^{-5}$				
	rs3777909	6	0.27	AA	ref.	ref.	A	G	eQTL - MFSD4B	Nerve (tibial)
				AG	0.14	$6.6x10^{-6}$			eQTL - REV3L	Brain
				GG	0.21	$3.1x10^{-5}$				
	rs2297771	9	0.38	AA	ref.	ref.	A	A	eQTL – ODF2, SPTAN1	Brain
				AG	0.057	$6.4x10^{-6}$			sQTL – WDR34, SPTAN1	Nerve (tibial)
				GG	0.098	$3.0x10^{-5}$			sQTL – WDR34, CERCAM	Brain
	rs56819906	11	0.34	AA	ref.	ref.	A	G	eQTL- DDX25, CDON	Nerve (tibial)
				AG	0.19	$1.5x10^{-3}$				
				GG	0.14	$7.6x10^{-5}$				

Abbreviations: AFRAFR, African ancestry; EUR, European ancestry; ASN, Asian axis ancestry; OR, odds ratio; eQTL, expression quantitative trait loci; sQTL, splicing quantitative trait loci.

The risk allele for rs2063349 associated with increased peripheral sensory neuropathy prevalence had a decreased frequency in the AFRAFR population compared to other populations, while for rs34904346, the risk allele associated with increased peripheral sensory

neuropathy had an increased frequency in the AFRAFR population compared to other populations. For vertigo, all 4 SNPs showed increased frequency of the risk allele associated with increased vertigo in the AFRAFR population versus other populations. We evaluated whether the risk allele was also the ancestral allele. For both SNPs associated with peripheral sensory neuropathy (rs2063249, rs34904346) and 2 SNPs associated with vertigo (rs28516482, rs2297771), the ancestral allele was the same as the allele most frequent in the AFRAFR population, indicating a shift in allele frequencies in the ASN axis and EUR populations over time, associated with decreased cisplatin-induced toxicity for 3 out of 4 SNPs. For 2 SNPs associated with vertigo (rs3777909, rs56819906), the ancestral allele was not the allele most frequent in the AFRAFR population, indicating a shift in allele frequencies in this population, associated with increased cisplatin-induced vertigo (Table 3.5). Results for genotype-phenotype association analyses for SNPs associated with cisplatin-induced peripheral sensory neuropathy and vertigo at $p < 5.0x10^{-2}$ are in Appendix Table A20 and A21, respectively.

For the peripheral sensory neuropathy phenotype (any versus none), the SNP associated with this toxicity with the strongest p-value ($p = 2.0x10^{-5}$) was rs34904346, with an $F_{ST} = 0.26$ (Table 3.5). In testicular cancer survivors in *The Platinum Study*, the T allele frequency was 90%, 69%, 61% and 58% in the AFRAFR, AFR axis, ASN axis and EUR populations, respectively (Figure 3.6A). Those with the AT genotype had an OR = 1.7 ($p = 1.7x10^{-4}$) and those with the TT genotype had an OR = 1.9 ($p = 2.0x10^{-5}$) for overall peripheral sensory neuropathy compared to those with the AA genotype, demonstrating increased peripheral sensory neuropathy prevalence associated with the T allele (Table 3.5). This SNP was an eQTL in tibial nerve tissue for the RNF24 gene, with the TT genotype associated with increased RNF24 expression (Figure 3.6B). Three other SNPs in chromosome 20 (rs6084530, rs6084557,

rs149150396) with $F_{ST} > 0.25$ and which had at least a nominally significant association ($p < 0.01$) between SNP genotype and cisplatin-induced peripheral sensory neuropathy were also eQTLs for RNF24 in nerve/brain tissue (cortex results shown) (Figure 3.6B, C, Appendix Table A20). None of these three SNPs were in LD with rs34904346 (Figure 3.6D). These results provide evidence for the role of differential RNF24 gene expression in contributing to disparities in cisplatin-induced peripheral sensory neuropathy incidence/prevalence across populations. Only 194 SNPs out of the 19,992 SNPs tested in the genotype-phenotype association analysis with peripheral sensory neuropathy had a $p < 0.01$. Multiple eQTLs for RNF24 in nerve/brain tissue were within the top 1% of the SNPs tested with the strongest p-values of association with cisplatin-induced peripheral sensory neuropathy.

The T allele of rs34904346 was more frequent in the AFRAFR population and was associated with an increased risk of cisplatin-induced peripheral sensory neuropathy and increased RNF24 expression in tibial nerve tissue in GTEx data (Figure 3.6A, B). Other SNPs not in LD with rs34904346 that were eQTLs for RNF24 in nerve/brain tissue and nominally associated with peripheral sensory neuropathy showed the same direction of effect for the risk allele/genotype and normalized effect size in GTEx v8 (Figure 3.6B, C, Table 3.6). Therefore, it was expected that increased RNF24 expression would be associated with increased sensitivity to cisplatin. The association between RNF24 expression (log2(TPM+1)) and cisplatin sensitivity (AUC) in cancer cell lines ($n = 575$) was not significant ($p = 0.21$), although the direction of association was as expected ($R = -0.052$) (Figure 3.6E). Therefore, *in silico* data does not support the hypothesis that RNF24 expression impacts cell sensitivity to cisplatin. It is possible that the relationship between this gene and the risk of cisplatin-induced peripheral sensory neuropathy may be mediated through other impacts on neuronal cell survival.

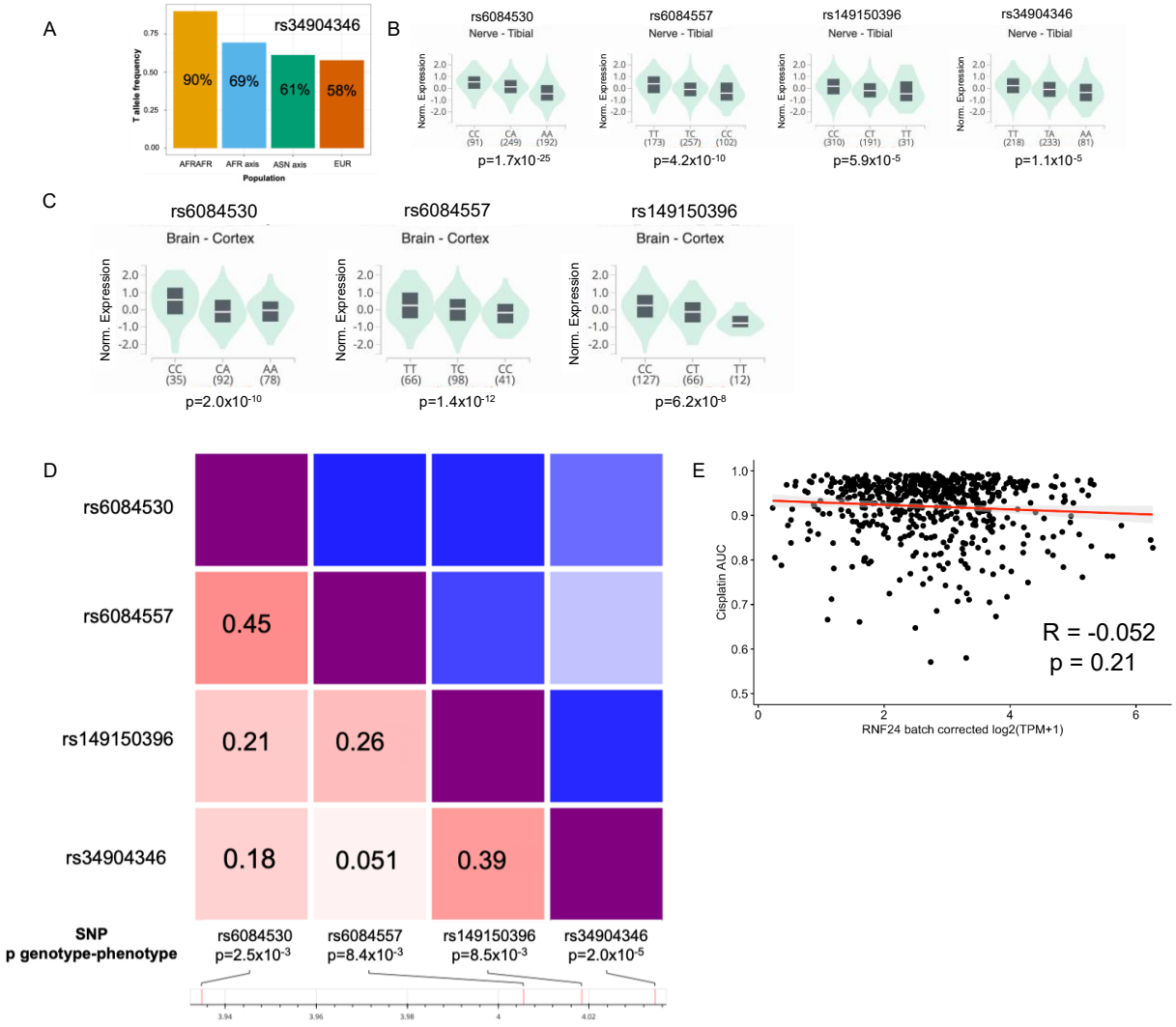

Figure 3.6. eQTLs for RNF24 in nerve/brain tissue associated with cisplatin-induced peripheral sensory neuropathy. A, T allele frequency for rs34904346 in testicular cancer survivors in *The Platinum Study* across populations. **B,** Normalized gene expression data and p-values for eQTLs for RNF24 in nerve tissue (GTEx V8). **C,** Normalized gene expression data and p-value for eQTLs for RNF24 in cortex tissue (GTEx V8). **D,** Heatmap matrix of pairwise LD statistics (R^2 labeled) for RNF24 eQTLs with association between genotype and peripheral sensory neuropathy ($p < 0.01$). **E,** Correlation between RNF24 expression in cancer cell lines and cisplatin AUC.
AFRAFR = African ancestry. AFR axis = along the axis towards African ancestry. ASN axis = along the axis towards Asian ancestry. EUR = European ancestry. GTEx = Genotype-Tissue expression project. AUC = area under the curve.
Figures 3.6B and 3.6C were created using GTEx V8 data obtained from the GTEx Portal[131] between 10/2023 and 12/2023, with visualizations created in 05/2024. Figure 3.6D was adapted from NCI LDmatrix[126].

Table 3.6. Association between genotype and RNF24 expression in nerve/brain tissue in GTEx V8 data for RNF24 eQTLs associated with cisplatin-induced peripheral sensory neuropathy ($p < 0.01$)

SNP	p-value for ref. vs. opposite genotype (yes vs. no peripheral neuropathy)	Normalized Effect Size (nerve tissue)	p-value (RNF24 gene expression in nerve tissue)	Normalized Effect Size (brain tissue)	p-value (RNF24 gene expression in cortex tissue)
rs34904346	$2.0x10^{-5}$	-0.16	$1.1x10^{-5}$	-	-
rs6084530	$2.5x10^{-3}$	-0.38	$1.7x10^{-25}$	-0.34	$2.0x10^{-10}$
rs6084557	$8.4x10^{-3}$	-0.23	$4.2x10^{-10}$	-0.38	$1.4x10^{-12}$
rs149150396	$8.5x10^{-3}$	-0.17	$5.9x10^{-5}$	-0.35	$6.2x10^{-8}$

For vertigo, the SNP of interest, with a strong association between genotype and phenotype, was rs3777909 ($F_{ST} = 0.27$) (Table 3.5). For this SNP, the A allele had a frequency of 57%, 42%, 30% and 17% in the AFRAFR, AFR axis, ASN axis and EUR populations in *The Platinum Study*, respectively (Figure 3.7A). In evaluating survivors with or without vertigo, those with the GG genotype had an OR = 0.21 ($p = 3.1x10^{-5}$) for vertigo compared to those with the AA genotype, indicating an increased risk of vertigo associated with the A allele (Table 3.5). This SNP was an eQTL in tibial nerve tissue for MFSD4B (Figure 3.7B) and in brain tissue for REV3L (Figure 3.7C). Additional SNPs not in LD with rs3777909 were nominally significantly associated with vertigo ($p < 0.05$) (Figure 3.7D, Appendix Table A21) and were also eQTLs/sQTLs for MFSD4B and REV3L in nerve/brain tissue (Figure 3.7B, C). For MFSD4B, rs7742724, rs9374263, and rs174373 were also eQTLs in tibial nerve tissue and these SNPs as well as rs9487668 were also eQTLs for REV3L in brain tissue, with the same direction of effect between the risk allele/genotype and normalized effect size in GTEx v8 (Table 3.7). 786 SNPs out of the 19,992 SNPs tested for genotype-phenotype association analysis with vertigo had a $p < 0.05$, meaning that multiple eQTLs for MFSD4B and REV3L in nerve/brain tissue were within

the SNPs tested with top 5% of strongest p-values of association with cisplatin-induced vertigo. For rs3777909, the A allele was more frequently expressed in the AFRAFR population and was associated with increased vertigo in cisplatin-treated testicular cancer survivors.

Consistent with the association of the A allele of rs3777909 with increased MFSD4B and REV3L expression as well as increased vertigo, there was an inverse relationship (negative correlation coefficient) between MFSD4B expression and cisplatin AUC in cancer cell lines (n = 575) ($R = -0.12$; $p = 5.8 \times 10^{-3}$) (Figure 3.7E) and between REV3L expression and cisplatin AUC in cancer cell lines (n = 575) ($R = -0.17$; $p = 5.1 \times 10^{-5}$) (Figure 3.7F). This indicates that higher MFSD4B and REV3L expression were significantly associated with greater sensitivity to cisplatin in these cell lines.

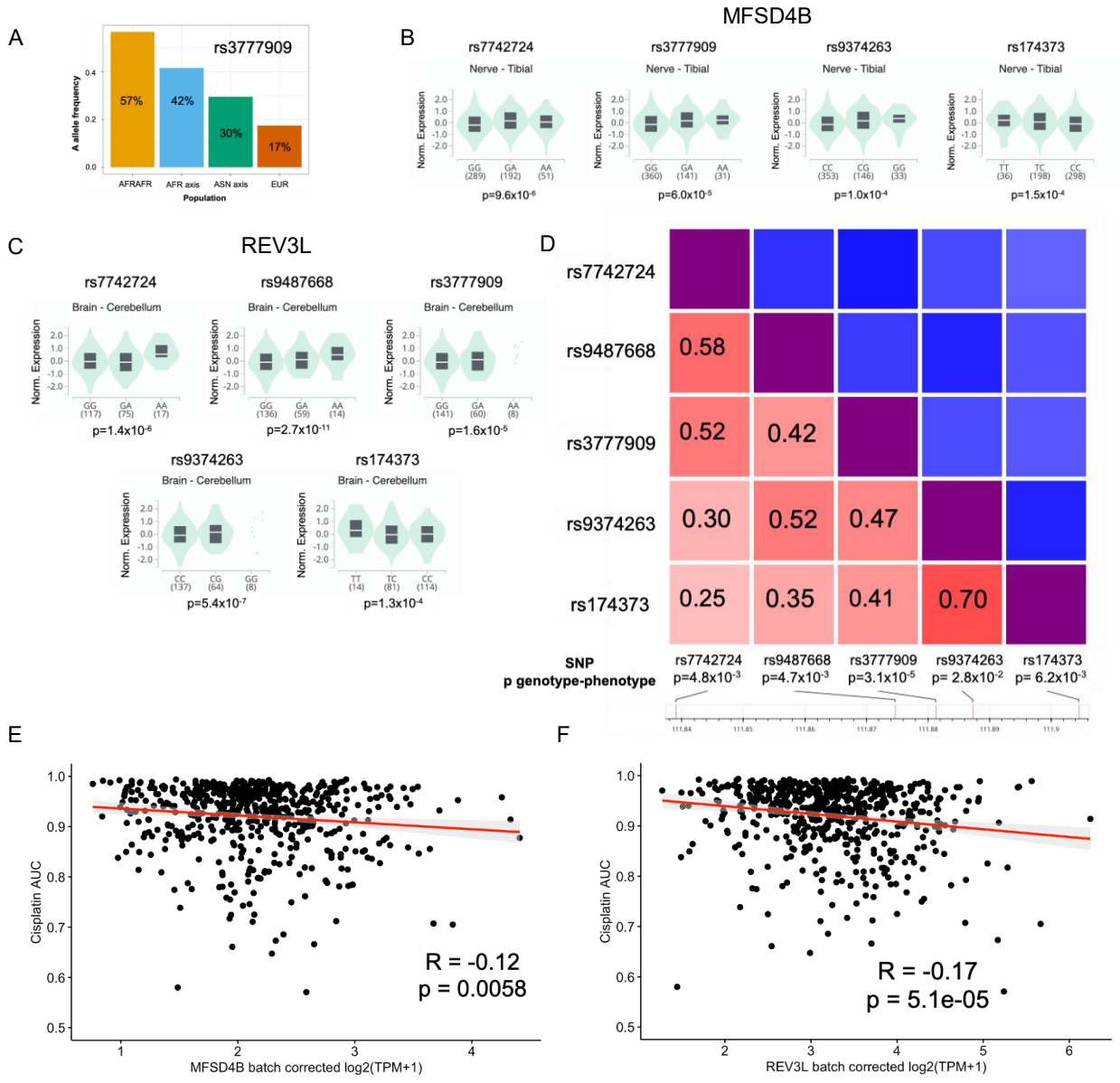

Figure 3.7. eQTLs for MFSD4B and REV3L in nerve/brain tissue associated with cisplatin-induced vertigo.

Figure 3.7. eQTLs for MFSD4B and REV3L in nerve/brain tissue associated with cisplatin-induced vertigo (cont). A, A allele frequency for rs3777909 in testicular cancer survivors in *The Platinum Study* across populations. **B,** Normalized gene expression data and p-values for eQTLs for MFSD4B in nerve tissue (GTEx V8). **C,** Normalized gene expression data and p-values for eQTLs for REV3L in cerebellum tissue (GTEx V8). **D,** Heatmap matrix of pairwise LD statistics (R^2 labeled) for eQTLs for MFSD4B/REV3L with association between genotype and vertigo ($p < 0.05$). **E,** Correlation between MFSD4B expression in cancer cell lines and cisplatin AUC. **F,** Correlation between REV3L expression in cancer cell lines and cisplatin AUC.
AFRAFR = African ancestry. AFR axis = along the axis towards African ancestry. ASN axis = along the axis towards Asian ancestry. EUR = European ancestry. GTEx = Genotype-tissue expression project. AUC = area under the curve.
Figures 3.7B and 3.7C were created using GTEx V8 data accessed from the GTEx Portal[131] between 10/2023 and 12/2023, with visualizations generated in 05/2024. Figure 3.7D was adapted from NCI LDmatrix[126].

Table 3.7. Association between genotype and MFSD4B/REV3L expression in nerve/brain tissue in GTEx V8 data for MFSD4B/REV3L eQTLs associated with vertigo ($p < 0.05$)

SNP	p-value for ref. vs. opposite genotype (Yes vs. No Vertigo)	Normalized Effect Size (MSFD4B)	p-value (MFSD4B gene expression in nerve tissue)	Normalized Effect Size (REV3L)	p-value (REV3L gene expression in cerebellum tissue)
rs3777909	$3.1x10^{-5}$	0.18	$6.0x10^{-5}$	0.27	$1.6x10^{-5}$
rs9487668	$4.7x10^{-3}$	-	-	0.38	$2.7x10^{-11}$
rs7742724	$4.8x10^{-3}$	0.19	$9.6x10^{-6}$	0.28	$1.4x10^{-6}$
rs174373	$6.2x10^{-3}$	-0.16	$1.5x10^{-4}$	-0.23	$1.3x10^{-4}$
rs9374263	$2.8x10^{-2}$	0.17	$1.0x10^{-4}$	0.31	$5.4x10^{-7}$

Abbreviations: GTEx, genotype-tissue expression.

Similarly, rs56819906 and rs73626678, with allele frequency differences between ancestral populations, and which were not in strong LD ($R^2 = 0.52$), were both eQTLs for DDX25 in nerve tissue and were associated with vertigo (Figure 3.8A-D). Those with the GG vs. AA genotype for rs56819906 had an OR = 0.14 and a p-value of $7.6x10^{-5}$ and those with TT vs. CC genotype for rs73626678 had an OR = 0.21 and a p-value of $1.8x10^{-4}$ for cisplatin-induced vertigo (Table 3.5, Appendix Table A21). These two SNPs were within the top 10 SNPs tested

with the strongest p-values of association with cisplatin-induced vertigo. The alleles associated with increased risk of vertigo (A and C alleles, respectively) were associated with decreased DDX25 expression in nerve tissue (Figure 3.8C). However, there was no significant association between DDX25 expression and cisplatin AUC in cancer cell lines (R = -0.049, p = 0.24).

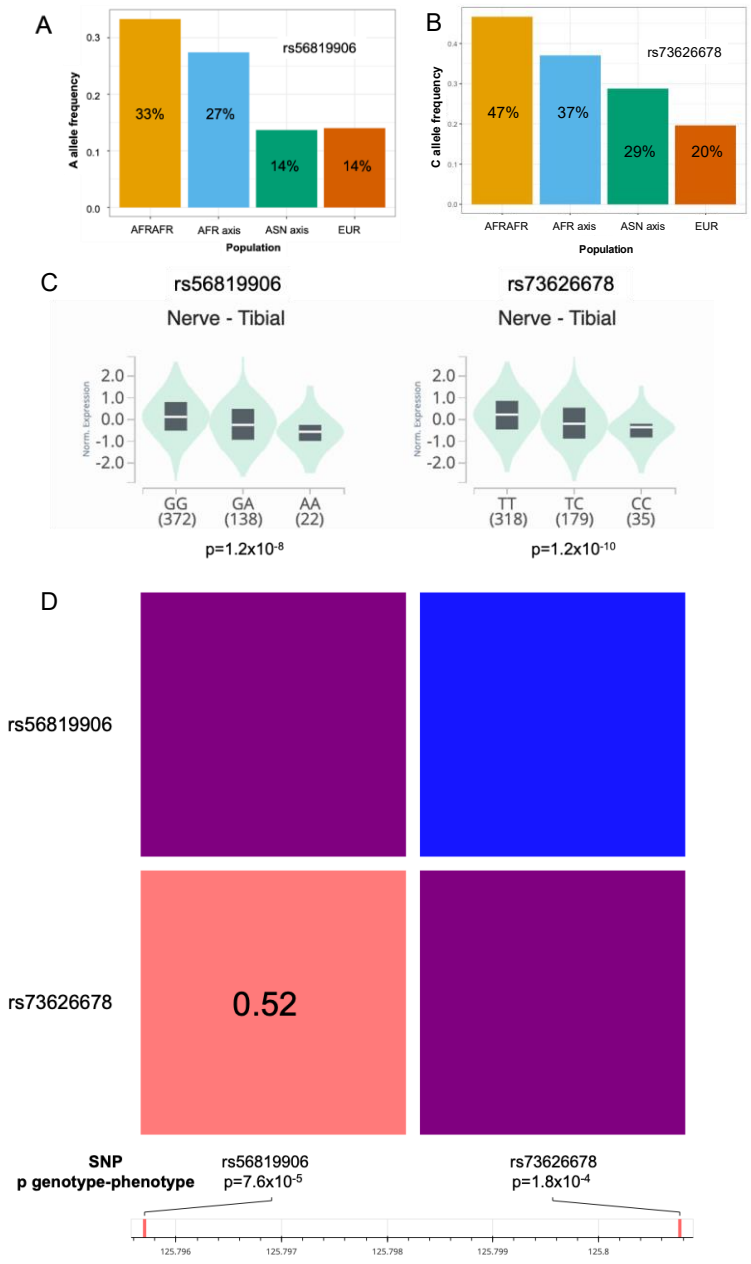

Figure 3.8. eQTLs for DDX25 in nerve tissue associated with cisplatin-induced vertigo.

Figure 3.8. eQTLs for DDX25 in nerve tissue associated with cisplatin-induced vertigo (cont). A, A allele frequency for rs56819906 in testicular cancer survivors in *The Platinum Study* across populations. **B,** C allele frequency for rs73626678 in testicular cancer survivors in *The Platinum Study* across populations. **C,** Normalized gene expression data and p-values for eQTLs for DDX25 in nerve tissue (GTEx V8). **D,** Heatmap matrix of pairwise LD statistics (R^2 labeled) for eQTLs for DDX25 with association between SNP genotype and vertigo phenotype ($p < 1x10^{-3}$).
AFRAFR = African ancestry. AFR axis = along the axis towards African ancestry. ASN axis = along the axis towards Asian ancestry. EUR = European ancestry. GTEx = Genotype-tissue expression project. AUC = area under the curve.
Figure 3.8C was generated using GTEx V8 data obtained from the GTEx Portal[131] between 10/2023 and 12/2023, with visualization created in 05/2024. Figure 3.8D was adapted from NCI LDmatrix[126].

Interestingly, rs3777909 (MFSD4B/REV3L eQTL), rs56819906 (DDX25 eQTL), and rs73626678 (DDX25 eQTL), also had nominally significant associations with cisplatin-induced peripheral sensory neuropathy (p-value of association with severe and/or overall peripheral sensory neuropathy < 0.05) (Table 3.8).

Table 3.8. Association between genotype and cisplatin-induced peripheral sensory neuropathy phenotype for MFSD4B/REV3L and DDX25 eQTLs with strong associations between genotype and cisplatin-induced vertigo

SNP		**Severe vs. No PSN**		**Yes vs. No PSN**		**Yes vs. No Vertigo**	
rs3777909		**OR**	**p-value**	**OR**	**p-value**	**OR**	**p-value**
	AA	ref.	ref.	ref.	ref.	ref.	ref.
	AG	0.38	$2.3x10^{-2}$	0.35	$9.4 x 10^{-4}$	0.14	$6.6x10^{-6}$
	GG	0.35	$1.2x10^{-2}$	0.36	$9.0 x10^{-4}$	0.21	$3.1x10^{-5}$
rs56819906		**OR**	**p-value**	**OR**	**p-value**	**OR**	**p-value**
	AA	ref.	ref.	ref.	ref.	ref.	ref.
	AG	0.22	$4.3x10^{-3}$	0.42	$4.7x10^{-2}$	0.19	$1.5x10^{-3}$
	GG	0.26	$8.9x10^{-3}$	0.44	$5.2x10^{-2}$	0.14	$7.6x10^{-5}$
rs73626678		**OR**	**p-value**	**OR**	**p-value**	**OR**	**p-value**
	CC	ref.	ref.	ref.	ref.	ref.	ref.
	CT	0.41	$2.6x10^{-2}$	0.53	$2.7x10^{-2}$	0.24	$1.1x10^{-3}$
	TT	0.47	$4.9x10^{-2}$	0.54	$2.7x10^{-2}$	0.21	$1.8x10^{-4}$

DepMap analysis of RNF24 dependency in the SH-SY5Y cell line

The RNF24 gene was moderately expressed in the SH-SY5Y (ACH-001188) cell line with a batch corrected log2(TPM+1) of 3.1 in the Batch corrected Expression Public 24Q4 data, making it a viable candidate for siRNA knockdown in this cell line (Figure 3.9A). In an

assessment of perturbation effects in DepMap, in the context of clustered regularly interspersed palindromic repeats (CRISPR) experiments, the Chronos score for RNF24 in the SH-SY5Y cell line was 0.16, indicating that RNF24 is a non-essential gene in this cell line (Figure 3.9B). While this value was relatively close to zero, it was positive, indicating that perhaps gene knockout could lead to the enhanced survival of SH-SY5Y cells.

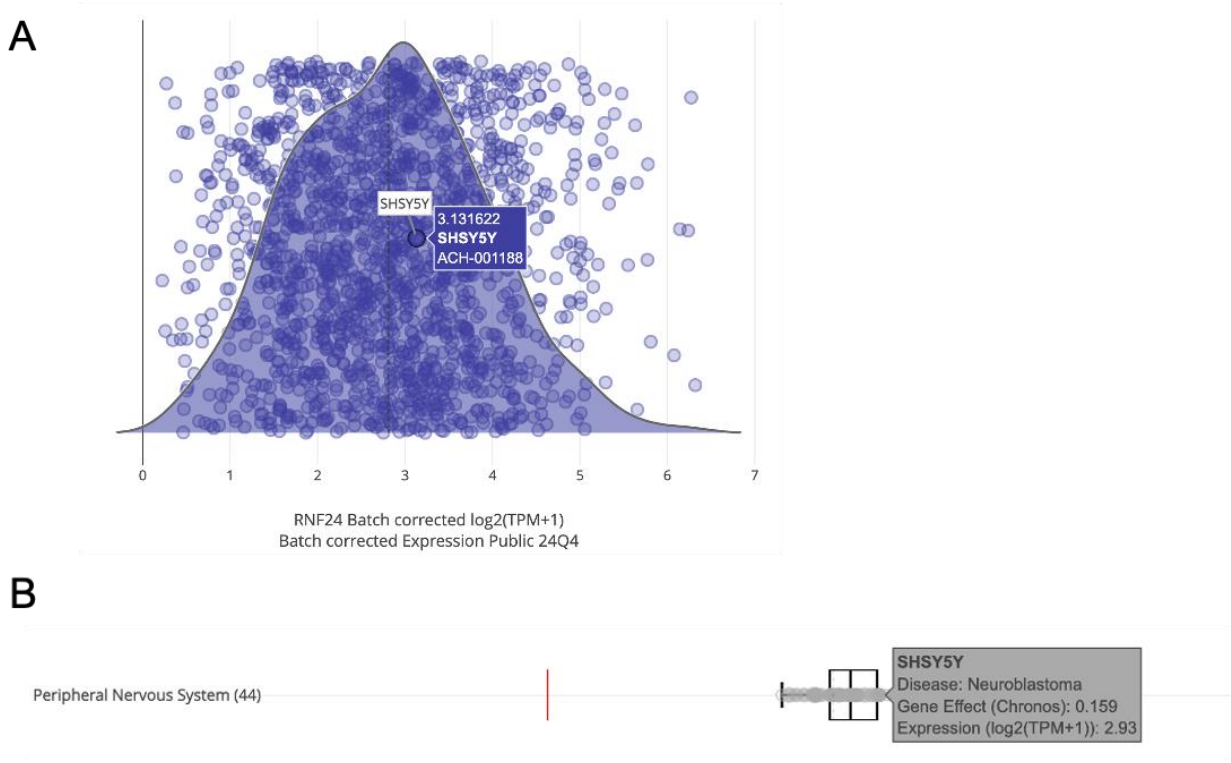

Figure 3.9. RNF24 expression and dependency in SH-SY5Y neuroblastoma cell line. A, Gene expression level of RNF24 in SH-SY5Y cells compared to other cell lines in DepMap's batch corrected expression public 24Q4 data. **B,** Gene effect (Chronos) score for RNF24 in SH-SY5Y cells and gene expression level in DepMap's expression data.
Figures 3.9A and 3.9B were produced using DepMap portal[172] (https://depmap.org/portal).

In vitro analysis

The cisplatin sensitivity assay on SH-SY5Y cells without siRNA treatment confirmed that SH-SY5Y cells are sensitive to cisplatin between the given range of zero to 20 μM of treatment, thus justifying this range for further assays to study the effect of gene knockdown on

cisplatin sensitivity in this cell line (Figure 3.10). In this assay, the IC_{50} for cisplatin treatment of SH-SY5Y cells was 3.86 μM.

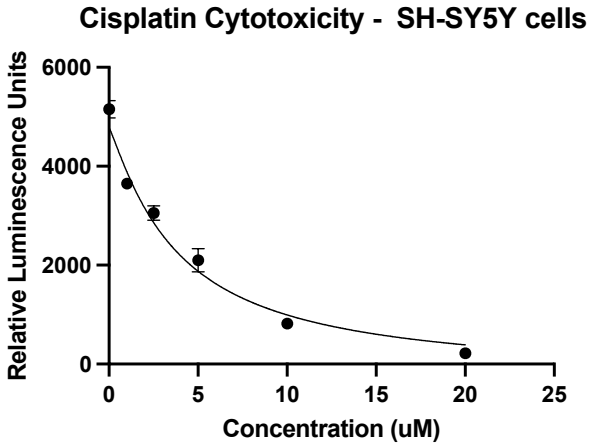

Figure 3.10. Cisplatin cytotoxicity in SH-SY5Y cells at a range of 0 to 20 μM.

Transfection of SH-SY5Y cells with siRNA was a challenge, and the manufacturer's protocol for Lipofectamine 3000 indicated a transfection efficiency of less than 30% in this cell type, much lower than other cell lines. Therefore, some necessary changes were made to the manufacturer's protocol for Lipofectamine 3000 siRNA transfection of non-targeting control as well as three separate RNF24 siRNAs into SH-SY5Y cells. Following troubleshooting, a 20-30% knockdown of RNF24 gene expression was achieved as compared to the control siRNA consistently in both duplicate experiments for RNF24 siRNA 1 (J-006943-05-0005) and RNF24 siRNA 2 (J-006943-06-0005), but not consistently for RNF24 siRNA 3 (J-006943-08-0005) (Figure 3.11). When the relative abundance of RNF24 transcript was standardized to 1 for the control siRNA, the mean relative abundance for RNF24 siRNA 1 was 0.72 and the mean relative abundance for RNF24 siRNA 2 was 0.75, compared to a mean relative abundance for RNF24 siRNA 3 of 0.84, with a major difference in knockdown between the duplicate experiments. Therefore, cisplatin sensitivity and cell viability assays will be discussed for the RNF24 siRNA1

and RNF24 siRNA2 treatments compared to the non-targeting control siRNA. Western blots were conducted for protein knockdown, however, there was non-specific binding of the RNF24 primary antibody, with protein bands between 35 and 55 kilodaltons (kD), but the RNF24 protein being only 17kD. Therefore, only qPCR was used as a reference for gene expression knockdown with RNF24 siRNA treatment.

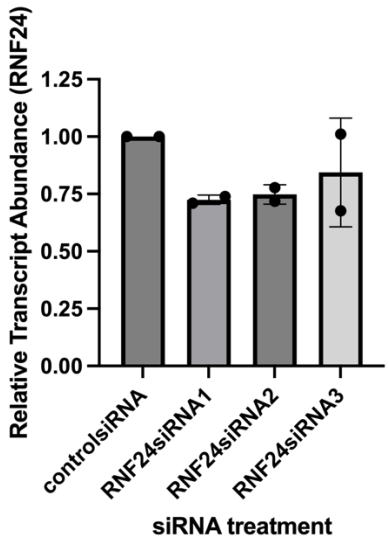

Figure 3.11. RNF24 siRNA knockdown in SH-SY5Y cells. Comparison of RNF24 knockdown with an adjusted Lipofectamine 300 protocol using three different RNF24 siRNAs compared to a non-targeting control siRNA in two separate replicate experiments.

There were no significant differences in cisplatin sensitivity between SH-SY5Y cells treated with non-targeting control siRNA versus RNF24 siRNA1 and RNF24 siRNA2 (Figure 3.12). The mean IC_{50} values were 6.72 μM for control siRNA, 5.70 μM for RNF24 siRNA1, and 6.66 μM for RNF24 siRNA2. There were no significant differences in cisplatin IC_{50} values between control siRNA and RNF24 siRNA, with an overall ANOVA p-value of 0.89, a control siRNA versus RNF24 siRNA1 adjusted p-value of 0.91, and a control siRNA versus RNF24 siRNA adjusted p-value of 0.98.

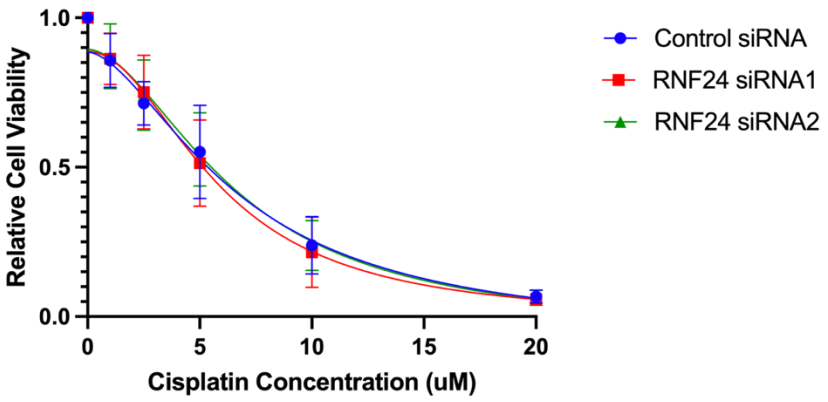

Figure 3.12. Impact of RNF24 knockdown on cisplatin sensitivity. Relative cell viability across multiple cisplatin doses from 0-20 μM for SH-SY5Y cells treated with control siRNA, RNF24 siRNA 1, and RNF24 siRNA 2.

In addition to determining if RNF24 gene expression knockdown impacted the sensitivity of SH-SY5Y cells to cisplatin, we also wanted to determine if RNF24 gene expression knockdown impacted SH-SY5Y cell viability. Upon knockdown of RNF24, SH-SY5Y cell viability was greater in cells with RNF24 siRNA knockdown compared to cells treated with the non-targeting control at 72 hours post-plating (approaching significance, $p < 0.1$). After the mean cell viability for SH-SY5Y cells treated with non-targeting control siRNA was standardized to 1, the standardized mean cell viability for SH-SY5Y cells treated with RNF24 siRNA1 was 1.31 and the standardized mean cell viability for SH-SY5Y cells treated with RNF24 siRNA2 was 1.35. When comparing these mean cell viability between siRNA treatment arms, the overall ANOVA p-value was 0.069, with a control siRNA versus RNF24 siRNA1 adjusted p-value of 0.084 and a control siRNA versus RNF24 siRNA2 adjusted p-value of 0.064 (Table 3.9).

Table 3.9. Comparison of relative SH-SY5Y cell viability between control siRNA and RNF24 siRNA treated cells 72 hours after plating

Overall ANOVA p-value	RNF24 siRNA1 Mean Relative Cell Viability	Control siRNA vs. RNF24 siRNA1 mean difference (95% CI)	Control siRNA vs. RNF24 siRNA1 adjusted p-value	RNF24 siRNA2 Mean Relative Cell Viability	Control siRNA vs. RNF24 siRNA1 mean difference (95% CI)	Control siRNA vs. RNF24 siRNA1 adjusted p-value
0.069	1.31	-0.31 (-0.69 to 0.072)	0.084	1.35	-0.35 (-0.73 to 0.036)	0.064

Abbreviations: ANOVA, analysis of variance; CI, confidence interval

The relative increase in SH-SY5Y cell viability corresponded to the relative knockdown of RNF24 expression. For both RNF24 siRNA1 and RNF24 siRNA, the relative RNF24 transcript abundance was about 20-30% lower than control siRNA and the mean relative cell viability for both RNF24 siRNA1 and RNF24 siRNA2 was about 30% greater than for control siRNA (Figure 3.13). This indicates that knockdown of RNF24 may be associated with increased SH-SY5Y cell viability, but does not impact cellular sensitivity to cisplatin. Genetic analyses indicated that eQTL genotypes associated with increased RNF24 expression were associated with an increased risk of peripheral sensory neuropathy, which could be due to decreased neuronal viability.

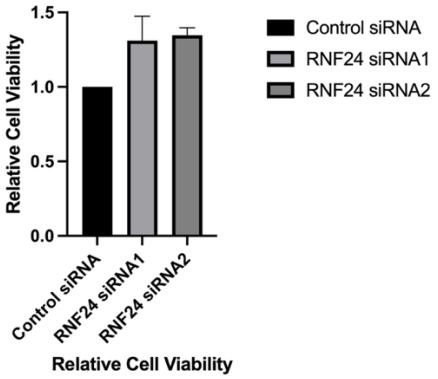

Figure 3.13. Impact of RNF24 knockdown on SH-SY5Y neuronal cell viability (cont). Comparison of relative SH-SY5Y cell viability 72 hours after plating between cells treated with control siRNA, RNF24 siRNA1, or RNF24 siRNA2.

3.4 Discussion

This study is the first, to our knowledge, to identify disparities in cisplatin-induced neurotoxicities. Testicular cancer survivors of African ancestry showed significantly increased peripheral sensory neuropathy and vertigo compared to survivors of European ancestry, reflected in poorer self-reported health in this population. Clinical/lifestyle variables were not significantly different in survivors of African ancestry survivors versus those of European ancestry, underscoring the potential contribution of genetic variation to observed differences in neurotoxicity. After filtering for independent, functional ancestry-informative variants and conducting association analyses between these SNPs and cisplatin-induced peripheral sensory neuropathy and vertigo, six SNPs were associated with these neurotoxicities at suggestively significant $p < 1.0x10^{-4}$, with five out of six of those SNPs showing a higher frequency of the risk allele in the African ancestry population versus other populations.

A SNP suggestively significantly associated with neuropathy, rs34904346, was an eQTL for RNF24 in nerve tissue, with 3 other independent RNF24 eQTLs in nerve/brain tissue also associated with neuropathy at $p < 0.01$. rs3777909, an eQTL for MFSD4B in nerve tissue and for REV3L in brain tissue, was suggestively significantly associated with vertigo, with several other independent eQTLs for these genes in nerve/brain tissue also associated with vertigo at $p<0.05$. MFSD4B and REV3L expression in cancer cell lines were significantly correlated with cisplatin sensitivity *in silico*, and while RNF24 knockdown in SH-SY5Y neuroblastoma cells did not impact cisplatin sensitivity, knockdown did increase cell viability at a similar level to the percentage of gene expression knockdown. These disparities were associated, to some extent, with allele frequency differences in variants concomitant with gene expression differences in

neurons. Understanding the extent to which disparities impact the long-term health of survivors is critical so that all survivors may be appropriately dosed, treated, and monitored.

Ancestral differences in chemotherapy-induced neurotoxicities

As discussed briefly in the introduction, several studies have demonstrated an increased risk of paclitaxel-induced neuropathy in breast cancer survivors of African versus European ancestry[55,102,107,108]. In a phase III breast cancer clinical trial of 3431 survivors, the frequency of Grade 2-4 peripheral neuropathy was 43.3% in survivors of African ancestry versus 24.6% in all other groups (HR = 2.1, $p = 5.6 \times 10^{-16}$)[55] . In a separate study, breast cancer survivors of African ancestry had significantly more grade 3-4 taxane-induced peripheral neuropathy (OR = 2.9, $p = 2.4 \times 10^{-11}$) and more dose reductions ($p = 6.6 \times 10^{-6}$) than those of European ancestry[102]. The North American Breast Cancer Intergroup clinical trial found that the percentage of severe neuropathies was 22.3% in African Americans and 11.6% in European Americans[108].

In a cohort of pediatric ALL patients, White patients were more likely to have symptoms of vincristine-induced peripheral neuropathy than African American patients ($p = 7.0 \times 10^{-3}$) and more neurotoxicity-related dose reductions ($p < 1.0 \times 10^{-4}$)[109]. This difference in neuropathy may be due to the impact of CYP3A5 expression levels on vincristine metabolism[110]. Between CYP3A5 expressers and non-expressors, there was a significant difference in the risk of neurotoxicity and the proportion of months during treatment with neurotoxicity[61]. Functional CYP3A5 enzymes depend on the *CYP3A5*1* allele, which has a higher frequency in patients of African ancestry (70% have at least one allele) versus European ancestry, as the most common allelic variants in European populations are *CYP3A5*3, CYP3A5*6*, and *CYP3A5*7*[61]. This study was the motivation for studying how population risk allele frequency differences may be implicated in disparities in cisplatin-induced neurotoxicities. Due to the opposite directions of

disparities in chemotherapy-induced neuropathy for paclitaxel and vincristine, we did not know what to expect regarding population differences in cisplatin-induced neuropathy.

Using self-reported race, African American head and neck cancer patients had increased risk of cisplatin-induced kidney injury compared to White patients, measured by assessing renal dysfunction using Kidney Disease Improving Global Outcomes criteria ($p = 1.0x10^{-2}$)[174] and increased relative percentage change in eGFR at 1 year of evaluation compared to White patients ($p = 3.0x10^{-2}$)[99]. Our work adds to information on disparities in cisplatin-induced toxicities, as we found that survivors with African ancestry were significantly more likely to have cisplatin-induced peripheral sensory neuropathy and vertigo versus survivors with European ancestry. Therefore, cisplatin-treated testicular cancer patients with African ancestry may have to receive appropriate dosing (BEPx3 versus EPx4) or be more closely monitored for adverse events during treatment to prevent long-term nephrotoxicity and neurotoxicity.

Pharmacogenomic alleles evolve based on population environmental pressures

For four out of six of SNPs with the greatest association with toxicity ($p < 1.0x10^{-4}$), the ancestral allele is the same as the allele most frequent in the AFRAFR population, while for two, the AFRAFR population has evolved away from the ancestral allele. Allele frequency differences between populations may reflect adaptations to different environments and may be a response to unique selective pressures in each environment. Many pharmacogenomic alleles have differing allele frequencies across populations[175]. Studies have identified SNPs associated with resistance to heavy metals[170]. One study found allele frequency differences in SNPs associated with heavy metal burden between Korean, European, and African populations[176]. These differences may contribute to disparities in cisplatin-induced toxicities between populations, as vascular toxicities associated with platinum therapy may have shared risk

mechanisms with cardiovascular events associated with exposure to heavy metals like arsenic and lead[169]. Research has characterized how alleles respond to environmental changes via directional and stabilizing selection[177,178]. Therefore, the evolution of allele frequencies in SNPs related to metal metabolism/resistance across different geographies due to unique selective pressures from the environment may be reflected in population disparities in cisplatin-induced toxicities.

Role of RNF24 in cisplatin-induced neurotoxicity

We identified multiple independent eQTLs for RNF24 in the top 1% of SNPs associated with cisplatin-induced peripheral sensory neuropathy, including one eQTL that was associated with this toxicity at $p = 2.0x10^{-5}$, providing evidence for a role of RNF24 gene expression in cisplatin-induced peripheral sensory neuropathy. RNF24 regulates the intracellular trafficking of transient receptor potential cation channel subfamily C proteins (TRPC), especially TRPC6, and their cell surface expression, with pulldown experiments showing that RNF24 interacts with all TPRC proteins[179]. TRPCs are calcium (Ca^{2+}) permeable channels involved in neurite growth repression, and intracellular Ca^{2+} levels are critical for the balance between neuronal survival and death[180,181]. Changes in RNF24 gene expression may be associated with changes in TRPC cell surface expression, thus potentially disrupting neuronal Ca^{2+} entry via proteins such as TRPC3[182]. As discussed in Chapter 2 in the context of WFS1, calcium levels are known to be related to cisplatin-induced injury, as a variant in ACYP2, involved in Ca^{2+} homeostasis, was found to be associated with risk of cisplatin-induced ototoxicity[164] and changes in Ca^{2+} entry and efflux impact oxidative stress and cisplatin-induced death across cell types[183,184]. TRPCs may also be involved in protection from neuronal injury by mediating apoptosis[181]. Thus,

differences in RNF24 expression and the subsequent impact on TRPC levels and cell surface expression may be involved in the balance between neuronal cell survival and death.

Role of MFSD4B and REV3L in cisplatin-induced neurotoxicity

Similarly, for vertigo, rs3777909 ($p = 3.1x10^{-5}$) was an eQTL for MFSD4B in nerve tissue and REV3L in brain tissue, with additional SNPs not in linkage disequilibrium also being eQTLs for these genes and associated with vertigo at $p < 0.05$. MFSD4B (SLC60A2) is a sodium-dependent glucose transporter[185]. Solute carrier (SLC) transporters have an important role in neurodegenerative disorders through mediating ion and neurotransmitter transport[186], although little is known regarding MFSD4B's effect on the biology/physiology of inner ear cells. Evidence indicates the importance of glucose and glucose metabolism for neuronal function[187]. A variant in SLC16A5, which transports monocarboxylate intermediates and products of glucose metabolism such as lactate and pyruvate across membranes, was associated with cisplatin-induced ototoxicity in testicular cancer survivors[188]. REV3L may have a more direct role in cellular response to cisplatin and cisplatin sensitivity, as it encodes the catalytic subunit of DNA polymerase zeta and is important for translesion DNA synthesis and DNA repair[189].

Choosing an *in vitro* model for studying peripheral sensory neuropathy

In vitro cell culture approaches have commonly been used to study the impact of altering specific genes on cellular sensitivity to drugs. While *in vitro* models of the peripheral nervous system do not replicate the complex interactions between various neuronal subpopulations without co-culture and cannot be used to study pharmacokinetics and pharmacodynamics, they do allow for fast and reproducible preliminary validation experiments[190].

There are a few *in vitro* model systems appropriate for the functional validation of genes associated with peripheral sensory neuropathy. Previous studies have utilized induced pluripotent

stem cell (iPSC)-derived neurons to confirm results from genetic association analyses and study the impact of gene expression on chemotherapy-induced neurotoxicity by analyzing neuronal measurements such as outgrowth, process number and length, branch number, and cell body area[95,191,192]. For example, after a SNP in the promoter region of CEP72 was found to be significantly associated with vincristine-induced neuropathy in ALL patients, the effect of lower CEP72 expression on increased neuronal sensitivity to vincristine was validated in iPSC-derived neurons[191]. Another study noted that siRNA knockdown of VAC14 in iPSC-derived neurons increased their docetaxel sensitivity, validating the effect of a significant SNP in this gene that was associated with docetaxel-induced neuropathy in prostate cancer patients in a GWAS[193]. However, iPSC-derived neurons are a relatively expensive model system that are difficult to work with and iPSCs may demonstrate genomic instability and have mediocre reprogramming efficiency[190]. Therefore, for a preliminary analysis of how gene expression differences impact neuronal viability and drug sensitivity, we decided that other model systems were more appropriate.

We decided to use the SH-SY5Y neuroblastoma cell line to model peripheral sensory neurons. SH-SY5Y cells express the genes and ion channels that are traditionally expressed in peripheral sensory neurons such as the sodium voltage-gated channel alpha subunit 9 (Na1.7) and genes like RET, PRPH, and TH[194,195]. When studying the transcriptome of SH-SY5Y cells, SH-SY5Y cells were found to express peripheral sensory neuronal markers GDNF receptor tyrosine kinase (RET) and TrkA (NTRK1)[194]. While SH-SY5Y cells lack the nociceptive neuron marker TPRV1, along with some itch receptors, mechanoreceptors, and proprioceptor markers, and cannot be used to directly model neuropathic pain[194], they have been used as a tool for studying neurotoxicology in numerous contexts such as pollutants[190,196] and drug toxicity[197].

SH-SY5Y cells show reductions in neurite length after exposure to cisplatin and paclitaxel, illustrating their sensitivity to chemotherapy agents[198,199]. SH-SY5Y cells have been used to study the intracellular mechanisms of peripheral sensory neuropathy and apoptosis upon treatment with platinum compounds[200,201]. For example, a study demonstrated that cisplatin caused apoptosis in SH-SY5Y cells based on increased activated caspase-3 expression upon treatment[201]. Another study used this cell line to show how altering treatment of SH-SY5Y cells to increase VEGF-A expression in sensory neurons attenuated cisplatin-induced neurodegeneration[198]. SH-SY5Y cells are an established *in vitro* method to assess the impact of altering gene expression on neuronal sensitivity to cisplatin and neuronal viability as a model for peripheral sensory neuropathy. Therefore, based on a comparison of the advantages and disadvantages of the model systems, we decided that the SH-SY5Y neuroblastoma cell line was an appropriate *in vitro* model system with which to validate the impact of RNF24 expression on neuronal cell viability and cisplatin sensitivity.

RNF24 expression and neuronal cell viability

The expression of RNF24 impacted SH-SY5Y cell viability, but not sensitivity to cisplatin. Decreased RNF24 expression via siRNA knockdown was associated with increased cell viability after 72 hours of incubation, with a 20-30% knockdown in RNF24 expression leading to an approximately 30% increase in neuronal cell viability, approaching significance. However, there were no differences in cisplatin cytotoxicity between SH-SY5Y cells with RNF24 siRNA knockdown and those treated with the non-targeting control. This is aligned with the *in silico* results, which did not find a significant association between RNF24 expression in cancer cell lines and cisplatin sensitivity. These results insinuate that the relationship between RNF24 expression and cisplatin-induced peripheral sensory neuropathy may be a function of

how RNF24 expression impacts neuronal cell health and viability independently of cisplatin-induced stress. However, these findings are preliminary and need to be verified.

Strengths and limitations

Major strengths of this study include its novelty and conduct in a well-characterized cohort of testicular cancer survivors treated with homogeneous cisplatin-based chemotherapy. Testicular cancer survivors in *The Platinum Study* were rigorously phenotyped and received uniform, standard treatment, with cisplatin being the only neurotoxic agent administered to all patients. Furthermore, age-related comorbidities such as age-related hearing loss are not likely to be confounders when studying the risk factors for cisplatin-induced neurotoxicities in *The Platinum Study* because our cohort of testicular cancer survivors is relatively young. Additionally, the percentage of patients with other potential causes of neuropathy such as diabetes is very low (less than 3% taking insulin or tablets for diabetes management). Testicular cancer survivors provide a unique opportunity to study disparities in cisplatin-induced neurotoxicities.

The Platinum Study cohort allowed us to evaluate population differences in cisplatin-induced neurotoxicities, in contrast to other datasets of testicular cancer survivors studying cisplatin-induced neurotoxicities, many of which were based in Europe (Denmark, Netherlands, Norway, Germany) and did not include non-European populations[70–74]. Although we had a low number of survivors of non-European ancestry, the composition of our cohort reflects the epidemiology of testicular cancer, which has a two to five-fold increased incidence in non-Hispanic white males versus other racial/ethnic groups[111] . Our investigation represents an important first step in improving diversity in genetic studies of risk factors for cisplatin-induced neurotoxicities. Our findings of disparities in cisplatin-induced neurotoxicities between

populations are also relevant in light of the increasing rates of testicular cancer in non-White individuals[202]. In the future, it will be important to validate our findings in larger, more racially diverse cohorts of cisplatin-treated patients (e.g., those with gynecologic cancers). With larger numbers of non-European cisplatin-treated cancer survivors, genotype-phenotype association analyses could be conducted in each population independently in addition to association analyses that adjust for population structure using genetic principal components. These steps are important to eventually ensure personalized precision medicine, the importance of which was reviewed in the American Association for Cancer Research's Cancer Disparities Progress Report 2024[203].

For *in vitro* validation, the major limitation was the limited (20-30%) knockdown of RNF24 expression. Therefore, the lack of impact of siRNA knockdown on cisplatin sensitivity in this cell line may either be because there is no relationship between RNF24 expression and cisplatin sensitivity in neurons or because there was not enough gene knockdown to see an effect. Additionally, while this knockdown showed an effect on overall SH-SY5Y cell viability to the extent of the knockdown, the results were approaching significance and there may be a greater impact if the RNF24 knockdown was greater. This level of gene knockdown was likely due to the limitations of the siRNA system in this cell line, as the manufacturer's protocol for Lipofectamine 3000 noted that transfection efficiency in SH-SY5Y cells was < 30% compared to other cell lines such as HEK 293 or HeLa with an efficiency > 80%. We explored other transfection reagents through a literature search, however, in a study that compared transfection reagents in SH-SY5Y cells, including lipofectin, RNAiMax, Fugene, and Lipofectamine 2000, Lipofectamine 3000 was shown to be the best siRNA transfection reagent based on relative transfection efficiency, without a major impact in cell viability[204]. Therefore, if greater

knockdown is to be achieved in the future, another technique for gene knockdown should be tested, such as CRISPR. Another *in vitro* model system can also be tested, such as iPSC-derived neurons, which can be manipulated to carry a specific allele at a variant by using a CRISPR-induced double stranded break and homology-directed repair (HDR)[205,206].

Comment

Moving forward, it must be recognized that in many cases, disparities are also influenced by social determinants of health. For example, African American breast cancer survivors face acute survivorship challenges that are exacerbated by differences in care[207]. We conducted association analyses between genetic ancestry and several clinical factors (blood pressure, cholesterol, and diabetes medication) and lifestyle factors (smoking and drinking). However, we did not identify significant differences between the African ancestry population and European ancestry population for these clinical and lifestyle factors. There may be other factors that may contribute to disparities in cisplatin-induced neurotoxicities that are not explicitly part of *The Platinum Study*. For this reason, we do not attribute causality of disparities to genetics, but rather highlight how differences in the frequency of risk alleles in certain variants between population groups and the subsequent impact on gene expression levels may be a contributing factor. This study provides rationale and a building block for future studies in this area.

3.5 Conclusion

We aimed to determine if there were disparities in cisplatin-induced neurotoxicities and if differences in risk allele frequencies between populations contributed to these disparities. We found that survivors with African ancestry were significantly more likely to have peripheral sensory neuropathy and vertigo versus survivors of European ancestry. These differences could not be attributed to disparities in several clinical and lifestyle factors. Ancestry-informative SNPs

that impact the expression of RNF24 in nerve tissue were suggestively significantly or nominally associated with cisplatin-induced peripheral sensory neuropathy. Ancestry-informative SNPs that impact the expression of MFSD4B in nerve tissue and REV3L in brain tissue were suggestively significantly or nominally associated with cisplatin-induced vertigo as well as ancestry-informative SNPs that impact DDX25 expression in nerve tissue. Higher MFSD4B and REV3L expression were significantly associated with greater cisplatin sensitivity in cancer cell lines *in silico*. Knocking down RNF24 expression in SH-SY5Y cell lines led to increased neuronal cell viability in preliminary validation studies. Understanding the genetic risk factors for cisplatin-induced neurotoxicities across populations can improve the safety and efficacy of cisplatin treatment and help mitigate adverse events across all patients in the future.

Chapter 4. Discussion

4.1 Summary

The work presented fills critical gaps in knowledge regarding the risk factors for cisplatin-induced neurotoxicities in adult-onset cancer survivors. We built machine learning models that incorporated multiple types of input data to predict cisplatin-induced neurotoxicities and used the information about predictors to explore the biological pathways associated with cisplatin-induced neuropathy risk. We also furthered our understanding of the disparities in cisplatin-induced neurotoxicities across ancestral populations and assessed the impact of population pharmacogenomics on disparities.

The focus of Chapter 2 was to develop machine learning models that could predict cisplatin-induced neurotoxicities in testicular cancer survivors. The prediction models we trained and tested in *The Platinum Study* data included well-genotyped and phenotyped testicular cancer survivors treated with standard cisplatin-based therapy regimens in the training set. We incorporated numerous types of input data, including variants from GWAS and TWAS, external PRS built in the UK Biobank and applied to testicular cancer survivors in *The Platinum Study*, and clinical variables. Successful models were able to predict cisplatin-induced neuropathy as well as hearing loss in the test set, with the most successful model for predicting overall peripheral sensory neuropathy being a polynomial kernel support vector machine model having an AUROC of 0.68 and 82% sensitivity, incorporating both clinical variables and GWAS SNPs ($p < 1x10^{-4}$) as predictors. Models were even more successful at predicting severe neuropathy, with the best model being an extreme gradient boosting model with an AUROC of 0.80 and 86% sensitivity, utilizing clinical variables and external PRS as predictors. Clinical variables explained about 40-50% of the variation in continuous hearing thresholds (GM412) depending

on the model and there was a significant correlation between actual GM412 values and those predicted by machine learning models using clinical variables as predictors. These models were the first of their kind for cisplatin-induced peripheral sensory neuropathy. Additionally, the previously published prediction models for cisplatin-induced hearing loss either utilized self-reported hearing loss as a phenotype[90] or were trained and tested in a pediatric population[120], for which generalizability to adult survivors may be limited. Therefore, our models for predicting a continuous audiometry-based cisplatin-induced hearing loss phenotype in adult-onset cancer survivors are important contributions to the field of clinical risk prediction. We also learned important information from pre-processing the input features, such as significant associations between clinical and lifestyle factors and toxicities, TWAS genes and pathways of interest such as the relationship between cisplatin-induced hearing loss and WFS1 expression, and significant associations between PRS for various traits, such as those related to kidney function and dyslipidemia, and cisplatin-induced neurotoxicities. Focusing on the SNPs that were predictors in successful peripheral sensory neuropathy prediction models and exploring functionally enriched pathways among the genes associated with these SNPs found that pathways related to fatty acid metabolism and fatty acid and membrane lipid levels were among those potentially related to cisplatin-induced peripheral neuropathy risk.

In Chapter 3, we studied disparities in cisplatin-induced neurotoxicities and found that survivors of African ancestry were significantly more likely to have cisplatin-induced peripheral neuropathy and vertigo than European ancestry survivors, with no significant differences between populations in cisplatin-induced tinnitus and hearing loss. Survivors along the axis towards Asian ancestry had less hearing loss than other populations (marginally significant p-values), but this could be driven by their significantly lower age at diagnosis and evaluation

compared to other ancestries. There were no significant disparities in clinical/lifestyle factors such as medication use or behaviors (smoking, drinking) between the European and African ancestry populations.

We tested if independent, functional ancestry-informative markers that impacted gene expression and/or splicing in nerve/brain tissue were associated with cisplatin-induced neuropathy and vertigo. Among the suggestively significant SNPs ($p < 1x10^{-4}$), two SNPs were associated with neuropathy and four with vertigo, with five out of six SNPs showing higher frequency of the risk allele in African ancestry populations compared to other populations. Further analysis of genes whose expression were impacted by these SNPs revealed that in addition to rs34904346, which had a p-value of association with neuropathy of $2.0x10^{-5}$, there were three other eQTLs for the RNF24 gene in nerve/brain tissue that were associated with neuropathy at $p < 0.01$, within the top 1% of lowest p-values of association among the SNPs tested. A similar result was seen when studying vertigo, which found that in addition to rs3777909 ($p = 3.1x10^{-5}$), three additional eQTLs for MFSD4B in the nerve tissue and four additional eQTLs for REV3L in the brain tissue were associated with vertigo at $p < 0.05$, within the top 5% of lowest p-values of association among the SNPs tested. Additionally, there was a significant association between MFSD4B and REV3L expression in cancer cell lines and their sensitivity to cisplatin *in silico*. Two SNPs associated with DDX25 expression in the nerve tissue were also strongly associated with cisplatin-induced vertigo.

We studied whether manipulating RNF24 gene expression in the SH-SY5Y neuroblastoma cell line impacted cellular sensitivity to cisplatin or neuronal cell viability. While RNF24 knockdown did not impact cisplatin sensitivity in this cell line, siRNA knockdown increased SH-SY5Y cell viability compared to SH-SY5Y cells treated with control siRNA. A 20-

30% knockdown of RNF24 expression corresponded to a 30% increase in SH-SY5Y cell viability. This is consistent with our results from association analyses, which indicated that the genotypes associated with increased RNF24 expression were associated with increased peripheral sensory neuropathy. This result indicates that the impact of RNF24 gene expression on the incidence/prevalence of peripheral sensory neuropathy may be related to the impact of this gene on neuronal health rather than cisplatin sensitivity.

4.2 Biological implications of insights on risk factors for cisplatin-induced neurotoxicities

When analyzing the results from both studies, there were patterns that provided some biological insights into the potential risk factors for cisplatin-induced neurotoxicities and the genes/pathways that may be involved.

One such observation was the importance of disruptions in cellular Ca^{2+} homeostasis in contributing to toxicities. In Chapter 2, a TWAS found that decreased WFS1 gene expression in multiple tissues, including nerve and brain tissue, was associated with cisplatin-induced hearing loss ($p < 0.0005$). WFS1 is a gene for which the intronic SNP rs62283056 was previously found to be associated with hearing loss in a subset of 511 cisplatin-treated testicular cancer survivors[49]. As discussed, mutations in WFS1 are associated with Wolfram syndrome and sensorineural hearing loss[162]. Wolfram syndrome is also associated with dysfunctional Ca^{2+} handling, as WFS1 maintains cellular Ca^{2+} homeostasis in neurons and is important for Ca^{2+} transfer from the ER to the mitochondria, with impairments negatively impacting neuronal health[163]. In Chapter 3, eQTLs for RNF24 in nerve/brain tissue were found to be associated with cisplatin-induced peripheral sensory neuropathy. RNF24 interacts with Ca^{2+} permeable TRPC channels and impacts their expression at the cell surface[179,182]. TRPC channels initiate Ca^{2+} entry and maintain Ca^{2+} levels in the cytosol, ER, and the mitochondria, with silencing of TPRC1 and

TRPC3 inhibiting neuronal proliferation[180]. Increased Ca^{2+} levels in neurons can over activate intracellular processes that rely on Ca^{2+}, causing "metabolic derangement," and Ca^{2+} levels, modulated by release from ER stores and influx through the plasma membrane, are involved in regulating numerous critical neuronal functions, including exocytosis, transcription, differentiation, and proliferation[180]. Disruptions in calcium homeostasis have been implicated in numerous neurodegenerative diseases, including Alzheimer's and Parkinson's, and diverging from the Ca^{2+} set point can contribute to ER stress and apoptosis[180]. Dysregulation of Ca^{2+} levels in the cell, whether through differences in WFS1 or RNF24 expression, may impact neuronal response to cellular stressors and overall neuronal health, contributing to neurotoxicities.

The importance of changes in calcium homeostasis in the risk for cisplatin-induced neurotoxicities has previously been studied. Multiple studies found an association between the rs1872328 variant on ACYP2 and cisplatin-induced hearing loss in adult[161] and pediatric[53,65] cancer patients. Another SNP in ACYP2, rs843748, was discovered to be associated with severe oxaliplatin-induced peripheral neuropathy in patients with colorectal cancer[208,209]. In SH-SY5Y neuroblastoma cells, acylphosphatase enzymes impact calcium homeostasis by hydrolyzing the phosphorylated intermediate of sarco/endoplasmic reticulum calcium ATPase (SERCA), which increases Ca^{2+} transport across the ER[210]. Dysregulation of calcium homeostasis may also impact cisplatin transport into the hair cell body. One study proposed that calcium influx into cells via the mechanoelectrical transduction channel may activate calmodulin-dependent endocytosis and the transport of cisplatin from stereocilia into the hair cell, causing cisplatin-induced damage[211]. Disruptions of calcium homeostasis are also hypothesized to be involved in the pathophysiology of chemotherapy-induced peripheral neuropathy for numerous therapies including cisplatin, oxaliplatin, vincristine, and paclitaxel[212]. Therefore, based on both the results from our studies

and support from the literature, there is substantial evidence that regulating cellular calcium homeostasis is critical for mitigating cisplatin-induced neurotoxicities.

Our studies found that metabolic pathways, specifically glucose-related pathways and fatty acid metabolism, were associated with cisplatin-induced neurotoxicities. When studying the association between functional ancestry-informative variants and cisplatin-induced vertigo in Chapter 3, an eQTL for MFSD4B, a membrane sodium/glucose transporter, in nerve tissue was associated with this toxicity at $p < 1.0x10^{-4}$ along with other eQTLs for this gene at $p < 0.05$. Our work found that genotypes associated with increased MFSD4B expression were associated with increased cisplatin-induced vertigo. In Chapter 2, TWAS followed by STRING pathway analysis showed that two pathways, glycolysis/gluconeogenesis and general metabolic pathways, were significantly enriched among the network of genes associated with cisplatin-induced tinnitus at $p < 0.05$. Glucose levels are important for neuronal health, as neurons require a large amount of energy for maintenance and require glycolysis for functioning, as demonstrated by neuronal deficits in mice with a deletion of a neuronal glucose transporter or a pyruvate-kinase isoform[187]. However, much like calcium levels, a balance in glucose levels may be required for maintaining neuronal health. Another study showed that in the cerebellum, increased sodium-glucose transporter (SGLT)-1 expression in response to stress (in this case, ischemic stress) was associated with increased neuronal damage and that suppressing the elevation of SGLT-1 decreased neuronal cell death[213]. Therefore, the regulation of glucose transport, maintenance of cellular glucose levels, and the downstream impact on glucose metabolism should be further studied to determine their relationship with cisplatin-induced neurotoxicities (specifically ototoxicity). More work should be done to examine the impact of manipulating the expression of glucose transporters such as MFSD4B on the risk of developing cisplatin-induced ototoxicity.

Several analyses in Chapter 2 point to the relationship between fatty acid metabolism pathways, as well as general lipid levels and body fat composition, and the risk for cisplatin-induced peripheral sensory neurotoxicities. In an analysis of clinical risk factors, taking cholesterol medication was significantly associated with cisplatin-induced hearing loss, tinnitus and neuropathy. Additionally, PRS for total cholesterol, LDL, and HDL levels were significantly associated with overall cisplatin-induced peripheral sensory neuropathy and PRS for body fat composition (body fat mass and body fat percentage) were associated with severe cisplatin-induced neuropathy and hearing loss. The pathway enriched among the network of genes associated with cisplatin-induced peripheral sensory neuropathy by TWAS ($p < 0.05$) was cholesteryl ester 16:0 measurement. Additionally, STRING pathway analysis showed that among the network of genes associated with the SNPs that were input features in successful prediction models for cisplatin-induced peripheral sensory neuropathy, there was significant functional enrichment of fatty acid metabolism and lipid measurement pathways. Finally, when assessing variable importance in the tree-based models that successfully predicted severe peripheral neuropathy using clinical and external PRS as predictors, the among the most important PRS in the models were those related to body fat composition. Chapter 2 discusses the importance of lipids, particularly fatty acids and membrane lipids, for neuronal composition[153], as well as how alterations to lipid metabolism and dyslipidemia have been found to be related to hereditary[153], diabetic[154], and chemotherapy-induced peripheral neuropathy[156]. Our work provides even more evidence of how perturbations in fatty acid metabolism pathways may contribute to the risk for cisplatin-induced peripheral sensory neuropathy.

4.3 Clinical implications of insights on risk factors for cisplatin-induced neurotoxicities

Predicting a patient's risk of cisplatin-induced neurotoxicities before they receive treatment will be clinically impactful, as patients at higher risk can be dosed accordingly. This is particularly relevant in the context of cisplatin-treated testicular cancer, as effective treatment regimens can include either three cycles of cisplatin (BEPx3) or four cycles of cisplatin (EPx4)[69]. Assessing risk prior to treatment may also be applicable in the context of other cancers that may have alternate therapy regimens that do not involve cisplatin. This work can also allow providers to make lifestyle recommendations to high-risk patients, such as limiting noise-related exposures if they are at increased risk of hearing loss. An understanding of the most important risk factors for cisplatin-induced neurotoxicities can also lead to the development of targeted interventions, as there are no standard strategies for prevention and treatment of these toxicities in adult-onset cancer survivors[33].

Some risk factors are more actionable than others. Disruptions to Ca^{2+} homeostasis may increase the risk of cisplatin-induced neurotoxicities. However, pharmacological interventions targeting Ca^{2+} homeostasis by regulating Ca^{2+} influx/efflux or intracellular transport may be difficult to target to only neuronal or inner hair cells or to specific organelles such as the ER or the mitochondria. As so many cellular processes are dependent on calcium, and calmodulin, a calcium sensor protein responsible for many downstream impacts of calcium signaling, is expressed across all eukaryotic cells[214], many interventions lack specificity for calcium channels[215], have off-target effects[216], or show poor cell targeting when tested *in vivo*[215]. Additionally, while a mitochondrial Ca^{2+} uptake inhibitor, Ru360, has been successful in reducing ROS and preventing amyloid-beta-induced apoptosis in microglia[217] and blocking excitotoxicity in cortical neurons[218], there are still concerns about the low cell permeability of this compound[215,216]. There is still a lot of work to be done before we can pharmacological

interventions to help maintain Ca^{2+} homeostasis in neurons or inner ear cells to combat cisplatin-induced neurotoxicities.

In contrast, metabolic risk factors for cisplatin-induced peripheral sensory neuropathy, particularly related to cholesterol and lipid levels, body fat composition, and the downstream impacts on fatty acid metabolism, may be easier to target for immediate interventions. Interventions can include controlling cholesterol levels through medications, but also preventing or reducing symptoms of neuropathic pain through specific diets or exercise. For patients treated with a variety of chemotherapies, a randomized control trial of an at-home walking and resistance training exercise program significantly improved peripheral neuropathy symptoms, with even more of an effect in older patients, who are at increased risk of neuropathy[219]. The promise of exercise-based interventions has been supported by the NCI, which recently approved a cooperative oncology group trial to study the effectiveness of exercise on reducing neuropathy symptoms[33]. Exercise can also help control comorbidities that were shown to be associated with neurotoxicities, such as blood pressure and cholesterol. While exercise may improve symptoms and improve strength and balance in cancer survivors who already have neuropathy[220], using exercise interventions to prevent or reduce dyslipidemia may also help decrease the development of cisplatin-induced neuropathy.

Dietary interventions may also help regulate lipid levels. As mentioned in Chapter 2, an *in vivo* mouse study showed that an omega-6 fatty acid-rich Western diet led to neuropathy-like peripheral nerve damage that could be mitigated with an omega-3 fatty acid rich diet[157]. There are studies over 20 years old on the impact of adjusting dietary fatty acids on diabetic neuropathy, including a study finding that oral administration of an ethyl esterification product from eicosapentaenoic acid improved neuropathy symptoms in type II diabetes patients[221].

Eicosapentaenoic acid measurement was one of the enriched pathways highlighted in Chapter 2 (Table 2.13). Another study found that docosahexaenoic acid-enriched phospholipids were protective against decreases in nerve conduction velocity and nerve blood flow in diabetic neuropathy[222]. While further study is required in the context of cisplatin-induced peripheral neuropathy, dietary interventions targeting specific fatty acid levels and combating dyslipidemia may be a future direction for symptom management and treatment of neuropathy. In the long term, pharmacological interventions targeting fatty acid metabolism may become options. Short-term solutions are important for symptom relief and can be implemented as recommendations for clinicians in the National Comprehensive Cancer Network (NCCN)'s Task Force's report on the management of neuropathy in cancer or the ASCO guidelines for prevention and management of chemotherapy-induced peripheral neuropathy in adults[33,223]. Neither set of guidelines currently indicate support for dietary interventions to prevent or treat neuropathy, although they mention that people have studied the use of omega-3 and -6 fatty acids among a list of varied dietary supplements for symptom management[33,223]. Functional studies assessing the impact of perturbing fatty acid metabolism and changing fatty acid levels on cisplatin-induced neuropathy should be considered. Additionally, randomized clinical trials of fatty acid-targeted dietary interventions in cisplatin-treated patients should be conducted prior to making clinical recommendations.

4.4 Disparities research and clinical implementation

Disparities research should continue to be prioritized, particularly in the context of pharmacogenomics, as there are important downstream impacts of understanding risk alleles across diverse populations. The Clinical Pharmacogenetics Implementation Consortium (CPIC) has different levels of actionable recommendations for variants related to current drugs, however

many of these variants critical for drug metabolism show allele frequency differences between populations[224]. Changes to established guidelines should be considered upon more research in diverse populations. For example, while CYP2C9 metabolizes over 20% of drugs on the market, different polymorphisms are common in various populations, with *CYP2C9 *2* and *CYP2C9 *3* being more common in European ancestry populations and the *CYP2C9 *8* and *CYP2C9 *11* alleles being found only in patients of African ancestry[224]. The use of genotyping panels that included *CYP2C9 *8* and *CYP2C9 *11* improved warfarin dosing in a cohort of African American patients compared to the International Warfarin Pharmacogenomics Consortium's standard dosing algorithms[225]. Incorporation of these relevant SNPs into genotyping panels could not have been implemented if pharmacogenomic studies of drug metabolism and toxicity were only conducted in European ancestry populations. In the context of our study, if associations between ancestry-informative markers and cisplatin-induced peripheral sensory neuropathy and vertigo are validated in other cohorts, all patients, but particularly those in populations with increased risk allele frequencies, should be genotyped prior to treatment to determine risk and mitigate disparities through appropriate dosing and monitoring. Preventing cisplatin-induced neurotoxicities in all patients should be a priority.

4.5 The burden of chemotherapy-induced neurotoxicities

As discussed in Chapter 1, cisplatin-induced neurotoxicities have numerous long-term consequences, including functional impairment[31], cognitive impairment and decreased mental and physical health[28], and increased mortality[27]. There are also direct and indirect financial costs of these toxicities. 68% of responders to a web-based questionnaire on the impact of chemotherapy-induced neurotoxicity said that they had difficulty performing their normal work duties and a number of responders noted modifying work due to symptoms[226]. Toxicity is also a

direct financial burden to patients and the healthcare system. Patients with chemotherapy-induced peripheral neuropathy have average healthcare costs that are $17,344 higher than those without neuropathy and also use more resources in the healthcare system, including more outpatient visits and hospitalizations than their counterparts without neuropathy[227]. These diverse and devastating consequences of chemotherapy-induced neurotoxicities highlight the clinical relevance of our work and support the need for a continued focus on cancer survivorship research.

Chapter 5. Future Directions

5.1 External validation of machine learning models

While the machine learning models we developed in this study have provided us with significant information about the clinical and genetic risk factors for cisplatin-induced neurotoxicities and can successfully predict peripheral sensory neuropathy and hearing thresholds in *The Platinum Study* test set, there is still more to be done before clinical implementation. Models should be prospectively validated in a cohort of recently diagnosed testicular cancer patients receiving long-term follow up for neurotoxicities to assess their utility as tools for risk prediction and clinical decision making prior to treatment. Additionally, models should be externally validated in other cohorts of cisplatin-treated cancer patients outside of *The Platinum Study*. External validation can help assess whether these models can be applicable in cohorts other than cisplatin-treated testicular cancer survivors. *The Platinum Study* has data from survivors who have received one of two standard cisplatin-based chemotherapy regimens without other neurotoxic or ototoxic treatments. This is in contrast to other cohorts, which may have survivors with confounding exposures such as radiation therapy or combination chemotherapy regimens. It is important to study if models developed to predict cisplatin-induced neurotoxicities in testicular cancer survivors can to predict toxicity in other clinical contexts, such as in head and neck cancer or childhood cancer patients treated with cisplatin-based regimens. Therefore, models trained and tested in *The Platinum Study* data should be evaluated on external datasets.

The plans for external validation of models in other datasets have been initiated through contacting principal investigators of other studies of cisplatin-induced neurotoxicities. Three validation data sets have been confirmed for testing (Table 5.1). One of these is the GCT (germ

cell tumor) Outcomes and Late effects (GOLD) Study, which is an ongoing genetic epidemiology study of pediatric germ cell tumor survivors recruited from the Children's Oncology Group (COG) registry protocols[228]. This study includes individuals diagnosed with a germ cell tumor at any location prior to the age of 19. As of February 2025, 600 patients have consented and 383 have completed surveys with information about toxicities, including tinnitus and neuropathy. The cisplatin-induced peripheral neuropathy phenotype is based on the Functional Assessment of Cancer Therapy/Gynecologic Oncology Group-Neurotoxicity (FACT-GOG-Ntx) scale[229]. In this data set, hearing loss is defined through numerous metrics, including surveys, audiograms, and the SHOEBOX test. For this study, target enrollment is 600, with approximately 75% of survivors enrolled having being treated with cisplatin-based chemotherapy. Another cohort is osteosarcoma patients from the European and American Osteosarcoma Studies (EURAMOS) clinical trial[230] with annotated treatment and toxicity (including hearing loss, and likely neuropathy and tinnitus) information. The process of acquiring genomic data from COG is currently ongoing, along with determining the exact numbers of patients in this cohort treated with cisplatin. The last external validation dataset is from a European cohort of pediatric cancer survivors treated with cisplatin (osteosarcoma, brain, other) with hearing loss information using Common Terminology Criteria for Adverse Events (CTCAE)[231] criteria and The International Society of Pediatric Oncology (SIOP) scales[152].

Table 5.1. Overview of phenotypes, training and test Sets for internal and external validation

Phenotype	**Number in Internal Training Set/Test Set in *The Platinum Study***	**External data set**
Neuropathy – Any vs. None	1,441/124	• GOLD study – FACT-GOG-Ntx neuropathy • EURAMOS osteosarcoma pediatric cohort
Neuropathy – Severe vs. None	778/62	• GOLD study – FACT-GOG-Ntx neuropathy • EURAMOS osteosarcoma pediatric cohort
Tinnitus	1,072/87	• GOLD study – tinnitus survey • EURAMOS osteosarcoma pediatric cohort
Hearing Loss	1,087/76	• GOLD study – audiograms, SHOEBOX hearing, surveys • "Osteosarcoma/Brain/Other" pediatric cohort – CTCAE/SIOP • EURAMOS osteosarcoma pediatric cohort

Abbreviations: GOLD Study, Germ Cell tumor Outcomes and Late effects study; FACT-GOG-Ntx, Functional Assessment of Cancer Therapy-Gynecologic Oncology Group-Neurotoxicity; EURAMOS, European and American Osteosarcoma studies, CTCAE, Common Terminology Criteria for Adverse Events; SIOP, The International Society of Pediatric Oncology

A limitation is that all of the confirmed external validation cohorts are from pediatric studies, which may impact generalizability of our models trained and tested in adult-onset cancer survivors. As models trained on clinical variables provided the best prediction of cisplatin-induced hearing loss within *The Platinum Study* test set, it must be considered that certain variables used for prediction may not be applicable to a pediatric population, including lifestyle factors such as smoking, drinking, and medication use. Separate models may need to be developed for different age groups. However, models for neuropathy include genetic predictors, which do not change over the course of lifespan and therefore may be more generalizable predictors across demographics. There are a few studies of adult cisplatin-treated cancer survivors that can also potentially be explored as external validation sets in the future[90,232]. One is the PGxLung Study, which is a multicenter prospective study of NSCLC patients treated with

first line platinum-based chemotherapy regimens, with neuropathy, ototoxicity, nephrotoxicity, and gastrointestinal toxicity data and blood samples collected for DNA isolation and genotyping[232,233]. In this cohort, while all patients received at least one cycle of a platinum-agent, treatment regimens were not consistent, as the platinum agent was combined with a another chemotherapy agent, targeted therapy, and/or immunotherapy with concurrent or post-platinum radiotherapy based on tumor and patient characteristics and physician discretion[232]. However, it is unrealistic to find external datasets that align exactly with the conditions utilized in *The Platinum Study* and it is important to test if our models can still predict cisplatin-induced neurotoxicities in patients treated with variable cisplatin-based regimens. If possible, models should also be tested in non-European validation cohorts to assess applicability across populations.

Another ongoing direction is standardizing and dichotomizing the hearing loss phenotype so that models trained in *The Platinum Study* data can be more easily tested on external datasets. A binary phenotype for hearing loss may also be more clinically interpretable. The cisplatin-induced hearing loss prediction models described in Chapter 2 define hearing loss as a continuous phenotype based on quantitative audiometry, which is a more objective metric than self-reported hearing loss. However, many published studies on cisplatin-induced hearing loss define hearing loss as a binary or ordinal phenotype, whether through a questionnaire[90] or by categorizing audiometry data[120]. Therefore, we plan to train and test models for a binary cisplatin-induced hearing loss phenotype in the future. Numerous metrics exist for categorizing hearing loss. In an analysis of multiple severe neurotoxicities in *The Platinum Study*, hearing loss was dichotomized based on the American Speech-Language-Hearing Association (ASHA) criteria, classifying survivors with moderate, moderately severe, severe, or profound hearing loss

(geometric mean of hearing thresholds greater than 40 dB at 4-12 kHz) as cases and those with no or mild hearing loss (geometric mean of hearing thresholds less than 40 dB at 4-12 kHz) as controls[51]. This criteria may be applied to training and test sets to categorize hearing loss. Other scales such as the CTCAE and SIOP grading scales may also be applied to our audiometry data[152].

Another consideration is that thus far, studies of cisplatin-induced hearing loss in testicular cancer survivors in *The Platinum Study* have focused on high frequency hearing loss (frequencies between 4 to 12 kHz)[47,49,51], as this is the most common form of hearing loss caused by cisplatin[17]. However, the frequency of speech is lower than this range[234]. A study of speech recognition threshold (computed at 0.5, 1, and 2 kHz) in testicular cancer survivors in *The Platinum Study* found significant associations between this metric and both self-reported hearing loss and problems hearing in crowds[235]. Therefore, future models may consider including this frequency range when defining hearing loss, particularly if external validation sets include these ranges in their definitions of hearing loss. Models trained for predicting a cisplatin-induced hearing loss phenotype that includes a lower range of frequencies may also be more applicable to external validation cohorts that define hearing loss through self-report.

5.2 Improving prediction of cisplatin-induced tinnitus

Future work should also focus on improving models for cisplatin-induced tinnitus. There may be other predictors that could be explored to improve the classification of tinnitus. In particular, because some of the better prediction models included external PRS as input features, there may be other external PRS that could be included as predictors beyond those selected for this study. When thinking about the shared genetic architecture between cisplatin-induced tinnitus and disorders affecting the nervous system, our focus was on neurodegenerative

diseases, including peripheral nervous system disorders, Alzheimer's, and dementia. However, there is evidence that there may be shared genetic architecture between *de novo* tinnitus and neuropsychiatric disorders[236]. A GWAS using UK Biobank data followed by gene-set enrichment analyses found significant associations between tinnitus and gene sets related to psychiatric and psychological phenotypes, including bipolar disorder, cognitive ability, and fast beta encephalogram as well as behaviors such as feeling worried and sensation seeking. Other gene sets that showed significant association with tinnitus included those for cardiovascular traits such as hypertension (accounted for in our PRS association analyses), ischemic stroke, blood pressure (systolic and diastolic), plateletcrit, and mean arterial pressure as well as medication-related phenotypes such as those related to diuretics, metformin, fenofibrate, and TNF inhibitor for rheumatoid arthritis[236]. There may be significant associations between cisplatin-induced tinnitus and PRS for these traits. While some of these PRS have already been built, such PRS for bipolar disorder[237], others still need to be built. Adding PRS for these traits to input features may improve machine learning prediction models for tinnitus. Also, for cisplatin-induced tinnitus and hearing loss, for which genetic inputs from GWAS and TWAS were not highly predictive or did not explain much of the variation in hearing thresholds, models may benefit incorporating more targeted SNPs of interest as predictors, such as honing in on SNPs associated with Mendelian deafness or calcium homeostasis, such as SNPs impacting WFS1 expression.

5.3 Studying the impact of population pharmacogenomics on disparities in cisplatin-induced neurotoxicities in additional cohorts

As mentioned in Chapter 3, our study of disparities in cisplatin-induced neurotoxicities and how risk allele frequency differences between populations may be associated with observed disparities is preliminary. This is largely due to the fact that because of the epidemiology of

testicular cancer[111], the vast majority of the cisplatin-treated testicular cancer survivors in this study were of European ancestry, with much fewer of African ancestry. Despite this imbalance, we found significant disparities between the European and African populations in the prevalence of cisplatin-induced peripheral sensory neuropathy and vertigo and were able to study the association between these toxicities and ancestry-informative eQTLs. In order to expand our knowledge of disparities in cisplatin-induced neurotoxicities and see if eQTLs/genes associated with toxicities can be replicated, we should to apply these methods to datasets of cisplatin-induced neuropathy that may have more survivors of non-European ancestry, including cohorts of head and neck and gynecologic cancer patients. Both of these cancers have a substantial number of patients of non-European ancestry, with ovarian cancer incidence in the United States in non-Hispanic white women being 12.0 per 100000 and 9.4 per 100000 for African American women[238] and increasing head and neck incidence rates across races[239].

A few cohorts exist that study cisplatin-induced neuropathy in gynecological cancer patients, including a multi-center international trial PORTEC-3, which includes high-risk endometrial cancer patients randomly assigned to either radiotherapy or a chemoradiotherapy regimen that includes cisplatin, carboplatin, and paclitaxel with neuropathy as measured by the ovarian cancer module of EORTC-QLQ-C30[240,241]. However, it is unclear if this dataset has genotyping information and what the demographic characteristics are with regards to ancestry. Another potential replication dataset may be the previously described PGxLung study. A drawback of this cohort is that of the 350 NSCLC patients included, 173 did not receive cisplatin and of those who did, only 17 were of non-European ancestry, meaning that it is not much more diverse than *The Platinum Study* cohort[242]. However, it is still worth assessing whether disparities in cisplatin-induced peripheral sensory neuropathy persist in other cohorts. A group of

104 cisplatin-treated epithelial ovarian cancer patients with genotyping data and information about neuropathy and ototoxicity phenotypes may be another potential dataset of interest, although demographic information is not published[243]. If we are not able to find validation cohorts of cisplatin-treated cancer patients with larger numbers of non-European survivors, the priority should be recruiting more non-European testicular cancer survivors to *The Platinum Study* to expand the scope of our analyses.

With greater numbers of non-European survivors, and in particular, survivors of African ancestry, the association analyses between genotypes and phenotypes can be conducted not only in the overall population, with genetic principal components as covariates to account for population structure, but can also be conducted in each population independently to assess the strength of association between SNP genotypes and toxicity phenotypes. Expanded analyses in more diverse cohorts will make results more conclusive and move us closer to our goal of understanding the genetic risk factors for cisplatin-induced neurotoxicity across all survivors.

6. Appendix. Additional Figures and Tables

Table A1. Questions for defining the peripheral sensory neuropathy phenotype in *The Platinum Study* questionnaire from the EORTC-CIPN20 questionnaire

During the past 4 weeks did you have:		Not at all	A little	Quite a bit	Very much
A.	Tingling fingers or hands?	0	1	2	3
B.	Tingling toes or feet?	0	1	2	3
C.	Numbness in your fingers or hands?	0	1	2	3
D.	Numbness in your toes or feet?	0	1	2	3
E.	Shooting or burning pain in your fingers or hands?	0	1	2	3
F.	Shooting or burning pain in your toes or feet?	0	1	2	3
I.	Problems standing or walking because of difficulty feeling the ground under your feet?	0	1	2	3
J.	Difficulty in distinguishing between hot and cold water?	0	1	2	3

Abbreviations: EORTC-CIPN20, European Organization for Research and Treatment of Cancer-Chemotherapy-Induced Peripheral Neuropathy Questionnaire

Table A2. Questions from the SCIN questionnaire in *The Platinum Study* questionnaire

Have you suffered in the last 4 weeks from:		Not at all	A little	Quite a bit	Very much
A.	Pain and tingling in your feet/toes?	0	1	2	3
B.	Pain and tingling in your hands/fingers?	0	1	2	3
C.	White/cold hands/fingers when it is cold?	0	1	2	3
D.	White/cold feet/toes when it is cold?	0	1	2	3
E.	**Ringing in your ears?**	**0**	**1**	**2**	**3**
F.	Reduced hearing?	0	1	2	3

Abbreviations: SCIN, scale for chemotherapy-induced long-term neurotoxicity

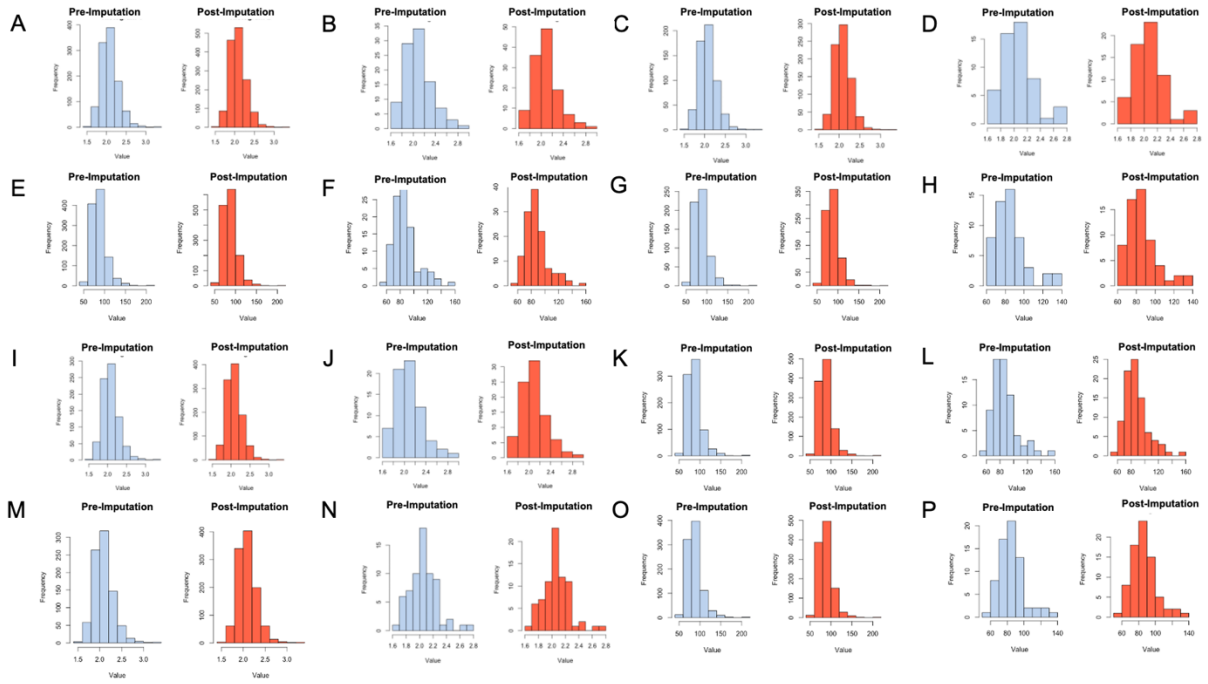

Figure A1. Distribution of BSA and weight at chemotherapy pre- and post-imputation. **A,** Overall PSN (any versus none) training set BSA. **B,** Overall PSN (any versus none) test set BSA. **C,** Severe PSN (severe versus none) training set BSA. **D,** Severe PSN (severe versus none) test set BSA. **E,** Overall PSN (any versus none) training set weight at chemotherapy. **F,** Overall PSN (any versus none) test set weight at chemotherapy. **G,** Severe PSN (severe versus none) training set weight at chemotherapy. **H,** Severe PSN (severe versus none) test set weight at chemotherapy. **I,** Tinnitus training set BSA. **J,** Tinnitus test set BSA. **K,** Tinnitus training set weight at chemotherapy. **L,** Tinnitus test set weight at chemotherapy. **M,** HL training set BSA. **N,** HL test set BSA. **O,** HL training set weight at chemotherapy. **P,** HL test set weight at chemotherapy.

Table A3. Associations between external PRS and cisplatin-induced peripheral sensory neuropathy (yes vs. no) in testicular cancer survivors in *The Platinum Study* training set

Trait	Mean in Survivors with No Neuropathy	Mean in Survivors with Neuropathy	p-value
PNS disorder PGS002039	$1.4x10^{-8}$	$1.4x10^{-8}$	0.31
PNS disorder PGS001832	$1.9x10^{-5}$	$1.9x10^{-5}$	0.70
Hearing Difficulties PGS001891	$4.5x10^{-6}$	$4.2x10^{-6}$	0.17
Hearing Difficulties PGS002104	$5.1x10^{-9}$	$4.6x10^{-9}$	0.70
Otosclerosis PGS002046	$-7.2x10^{-10}$	$-7.9x10^{-10}$	**$3.9x10^{-2}$**
Dementia PGS001827	$4.2x10^{-3}$	$4.2x10^{-3}$	0.55
Dementia PGS002035	$2.5x10^{-8}$	$2.5x10^{-8}$	0.86
Alzheimer's PGS001828	$5.5x10^{-3}$	$5.5x10^{-3}$	0.62
Weight PGS001825	$1.3x10^{-5}$	$1.3x10^{-5}$	0.61
Weight PGS002033	$-7.6x10^{-9}$	$-7.5x10^{-9}$	0.75
Lean Body Mass PGS001950	$-1.2x10^{-7}$	$-1.1x10^{-7}$	0.26
Lean Body Mass PGS002168	$5.2x10^{-9}$	$6.9x10^{-9}$	0.29
Body Fat Mass PGS001951	$7.3x10^{-7}$	$7.8x10^{-7}$	0.15
Body Fat Mass PGS002169	$7.2x10^{-8}$	$7.7x10^{-8}$	0.17
Body Fat Percentage PGS001917	$1.2x10^{-7}$	$1.3x10^{-7}$	0.19
Body Fat Percentage PGS002133	$9.8x10^{-9}$	$1.1x10^{-8}$	0.26
Hypertension PGS001838	$7.0x10^{-6}$	$6.7x10^{-6}$	0.31
Hypertension PGS002047	$4.4x10^{-8}$	$4.2x10^{-8}$	0.36
Hypertension PGS000706	$6.9x10^{-6}$	$6.9x10^{-6}$	0.99
Triglycerides PGS001979	$-2.9x10^{-6}$	$-3.0x10^{-6}$	0.16
Triglycerides PGS002197	$-2.4x10^{-7}$	$-2.5x10^{-7}$	0.12
Triglycerides PGS000699	$-6.3x10^{-6}$	$-6.2x10^{-6}$	0.76
Abnormal Circulating Lipids PGS002029	$4.0x10^{-8}$	$3.8x10^{-8}$	0.13

Continuation of Table A3

Abnormal Circulating Lipids PGS001821	$1.0x10^{-5}$	$9.9x10^{-6}$	0.31
Lipoprotein A PGS001963	$-7.4x10^{-5}$	$-7.7x10^{-5}$	0.62
Lipoprotein A PGS002181	$-2.3x10^{-5}$	$-2.3x10^{-5}$	0.66
Lipoprotein A PGS000689	$-7.5x10^{-6}$	$-8.1x10^{-6}$	0.99
Apolipoprotein A PGS001888	$2.0x10^{-6}$	$1.9x10^{-6}$	0.12
Apolipoprotein A PGS002101	$2.5x10^{-7}$	$2.4x10^{-7}$	0.29
Apolipoprotein A PGS000671	$4.9x10^{-6}$	$4.7x10^{-6}$	**$3.8x10^{-2}$**
Apolipoprotein B PGS001889	$2.2x10^{-6}$	$2.0x10^{-6}$	0.30
Apolipoprotein B PGS002102	$-3.6x10^{-9}$	$-1.4x10^{-8}$	0.20
Apolipoprotein B PGS000672	$2.2x10^{-6}$	$1.8x10^{-6}$	*$5.8x10^{-2}$*
Total Cholesterol PGS001895	$2.3x10^{-5}$	$2.2x10^{-5}$	0.18
Total Cholesterol PGS002108	$9.3x10^{-7}$	$8.8x10^{-7}$	*$6.0x10^{-2}$*
Cholesterol PGS000677	$6.0x10^{-6}$	$5.6x10^{-6}$	**$8.8x10^{-4}$**
LDL PGS001933	$8.8x10^{-6}$	$8.4x10^{-6}$	0.21
LDL PGS002150	$3.7x10^{-7}$	$3.3x10^{-7}$	*$7.9x10^{-2}$*
LDL PGS000688	$5.0x10^{-6}$	$4.6x10^{-6}$	**$6.7x10^{-3}$**
HDL PGS001954	$2.4x10^{-6}$	$2.4x10^{-6}$	0.17
HDL PGS002172	$2.8x10^{-7}$	$2.8x10^{-7}$	0.40
HDL PGS000686	$9.3x10^{-6}$	$9.0x10^{-6}$	**$1.6x10^{-2}$**
Creatinine Clearance PGS001944	$-1.9x10^{-7}$	$-2.8x10^{-7}$	0.11
Creatinine Clearance PGS002162	$5.0x10^{-8}$	$4.5x10^{-8}$	*$9.5x10^{-2}$*
Creatinine PGS001945	$2.4x10^{-7}$	$2.6x10^{-7}$	0.28
Creatinine PGS002163	$2.8x10^{-8}$	$3.0x10^{-8}$	0.34
Creatinine PGS000678	$6.4x10^{-7}$	$7.7x10^{-7}$	0.11

Continuation of Table A3

Urine Creatinine PGS000679	$-3.0x10^{-6}$	$-2.9x10^{-6}$	0.72
Cystatin C PGS002165	$6.6x10^{-8}$	$7.2x10^{-8}$	**$3.9x10^{-3}$**
Cystatin C PGS001947	$6.3x10^{-7}$	$6.9x10^{-7}$	**$1.3x10^{-3}$**
Cystatin C PGS000680	$8.7x10^{-7}$	$1.1x10^{-6}$	**$1.7x10^{-2}$**
eGFR PGS000682	$-5.2x10^{-7}$	$-6.3x10^{-7}$	*$7.3x10^{-2}$*
Serum Albumin PGS001886	$8.6x10^{-6}$	$8.0x10^{-6}$	**$2.3x10^{-2}$**
Serum Albumin PGS002099	$9.9x10^{-7}$	$9.3x10^{-7}$	**$1.5x10^{-2}$**
Serum Albumin PGS000669	$1.6x10^{-6}$	$1.5x10^{-6}$	0.27
Serum Protein Non-Albumin PGS000691	$2.7x10^{-7}$	$2.0x10^{-7}$	0.37
Total Blood Protein PGS000698	$3.0x10^{-7}$	$2.8x10^{-7}$	0.38
Urine Microalbumin PGS001967	$-4.8x10^{-6}$	$-4.9x10^{-6}$	0.80
Urine Microalbumin PGS002185	$1.9x10^{-8}$	$1.9x10^{-8}$	0.79
Urine Microalbumin PGS000690	$2.1x10^{-5}$	$1.2x10^{-5}$	*$7.0x10^{-2}$*
Urine Potassium PGS001974	$1.6x10^{-7}$	$1.1x10^{-7}$	0.32
Urine Potassium PGS002192	$3.5x10^{-9}$	$1.1x10^{-9}$	0.15
Urine Potassium PGS000693	$-8.1x10^{-6}$	$-8.0x10^{-6}$	0.81
Urine Sodium PGS002007	$-1.8x10^{-5}$	$-2.7x10^{-5}$	**$2.0x10^{-2}$**
Urine Sodium PGS002226	$5.2x10^{-7}$	$9.8x10^{-8}$	**$1.9x10^{-2}$**
Urine Sodium PGS000695	$2.5x10^{-6}$	$2.1x10^{-6}$	0.20
Urea PGS001980	$-3.1x10^{-7}$	$-3.3x10^{-7}$	0.39
Urea PGS002198	$-1.9x10^{-9}$	$-3.1x10^{-9}$	0.57
Urea PGS000701	$-3.2x10^{-6}$	$-3.4x10^{-6}$	0.17
Kidney Failure PGS000708	$6.5x10^{-7}$	$8.5x10^{-7}$	*$9.6x10^{-2}$*
Non Alcoholic Liver Disease PGS002071	$-7.3x10^{-10}$	$-7.6x10^{-10}$	0.80

Continuation of Table A3

Non Alcoholic Liver Disease PGS001860	$1.1x10^{-4}$	$1.0x10^{-4}$	0.57
Vitamin D PGS000702	$-1.2x10^{-5}$	$-1.2x10^{-5}$	0.96

Abbreviations: PNS, peripheral nervous system, LDL, low-density lipoprotein; HDL, high-density lipoprotein, eGFR, estimated glomerular filtration rate.

Table A4. Associations between external PRS and cisplatin-induced peripheral sensory neuropathy (severe vs. none) in testicular cancer survivors in *The Platinum Study* training set

Trait	Mean in Survivors with No Neuropathy	Mean in Survivors with Severe Neuropathy	p-value
PNS disorder PGS002039	$1.4x10^{-8}$	$1.5x10^{-8}$	0.13
PNS disorder PGS001832	$1.9x10^{-5}$	$2.0x10^{-5}$	0.31
Hearing Difficulties PGS001891	$4.5x10^{-6}$	$4.3x10^{-6}$	0.48
Hearing Difficulties PGS002104	$5.1x10^{-9}$	$5.6x10^{-9}$	0.84
Otosclerosis PGS002046	$-7.2x10^{-10}$	$-7.4x10^{-10}$	0.79
Dementia PGS001827	$4.2x10^{-3}$	$3.2x10^{-3}$	**$1.4x10^{-2}$**
Dementia PGS002035	$2.5x10^{-8}$	$2.1x10^{-8}$	0.18
Alzheimer's PGS001828	$5.5x10^{-3}$	$4.4x10^{-3}$	0.10
Weight PGS001825	$1.3x10^{-5}$	$1.4x10^{-5}$	0.77
Weight PGS002033	$-7.6x10^{-9}$	$-7.0x10^{-9}$	0.38
Lean Body Mass PGS001950	$-1.2x10^{-7}$	$-7.9x10^{-8}$	**$1.6x10^{-2}$**
Lean Body Mass PGS002168	$5.2x10^{-9}$	$9.9x10^{-9}$	*$5.8x10^{-2}$*
Body Fat Mass PGS001951	$7.3x10^{-7}$	$9.2x10^{-7}$	**$5.4x10^{-4}$**
Body Fat Mass PGS002169	$7.2x10^{-8}$	$9.2x10^{-8}$	**$9.3x10^{-4}$**
Body Fat Percentage PGS001917	$1.2x10^{-7}$	$1.5x10^{-7}$	**$1.1x10^{-3}$**
Body Fat Percentage PGS002133	$9.8x10^{-9}$	$1.3x10^{-8}$	**$2.2x10^{-3}$**
Hypertension PGS001838	$7.0x10^{-6}$	$6.8x10^{-6}$	0.58
Hypertension PGS002047	$4.4x10^{-8}$	$4.1x10^{-8}$	0.39
Hypertension PGS000706	$6.9x10^{-6}$	$7.0x10^{-6}$	0.80
Triglycerides PGS001979	$-2.9x10^{-6}$	$-3.0x10^{-6}$	0.17
Triglycerides PGS002197	$-2.4x10^{-7}$	$-2.5x10^{-7}$	0.16
Triglycerides PGS000699	$-6.3x10^{-6}$	$-6.6x10^{-6}$	0.63
Abnormal Circulating Lipids PGS002029	$4.0x10^{-8}$	$3.7x10^{-8}$	*$7.1x10^{-2}$*

Continuation of Table A4

Abnormal Circulating Lipids PGS001821	$1.0x10^{-5}$	$9.5x10^{-6}$	0.15
Lipoprotein A PGS001963	$-7.4x10^{-5}$	$-7.9x10^{-5}$	0.28
Lipoprotein A PGS002181	$-2.3x10^{-5}$	$-2.4x10^{-5}$	0.26
Lipoprotein A PGS000689	$-7.5x10^{-6}$	$-7.9x10^{-6}$	0.47
Apolipoprotein A PGS001888	$2.0x10^{-6}$	$1.9x10^{-6}$	0.36
Apolipoprotein A PGS002101	$2.5x10^{-7}$	$2.4x10^{-7}$	0.43
Apolipoprotein A PGS000671	$4.9x10^{-6}$	$4.8x10^{-6}$	0.30
Apolipoprotein B PGS001889	$2.2x10^{-6}$	$1.8x10^{-6}$	0.11
Apolipoprotein B PGS002102	$-3.6x10^{-9}$	$-2.6x10^{-8}$	*0.050*
Apolipoprotein B PGS000672	$2.2x10^{-6}$	$1.8x10^{-6}$	0.15
Total Cholesterol PGS001895	$2.3x10^{-5}$	$2.1x10^{-5}$	0.13
Total Cholesterol PGS002108	$9.3x10^{-7}$	$8.5x10^{-7}$	**$4.1x10^{-2}$**
Cholesterol PGS000677	$6.0x10^{-6}$	$5.6x10^{-6}$	**$3.0x10^{-2}$**
LDL PGS001933	$8.8x10^{-6}$	$8.2x10^{-6}$	0.15
LDL PGS002150	$3.7x10^{-7}$	$3.0x10^{-7}$	**$2.3x10^{-2}$**
LDL PGS000688	$5.0x10^{-6}$	$4.5x10^{-6}$	*$5.3x10^{-2}$*
HDL PGS001954	$2.4x10^{-6}$	$2.4x10^{-6}$	0.33
HDL PGS002172	$2.8x10^{-7}$	$2.8x10^{-7}$	0.45
HDL PGS000686	$9.3x10^{-6}$	$9.0x10^{-6}$	0.18
Creatinine Clearance PGS001944	$-1.9x10^{-7}$	$-1.8x10^{-7}$	0.94
Creatinine Clearance PGS002162	$5.0x10^{-8}$	$5.0x10^{-8}$	0.86
Creatinine PGS001945	$2.4x10^{-7}$	$2.2x10^{-7}$	0.47
Creatinine PGS002163	$2.8x10^{-8}$	$2.6x10^{-8}$	0.56
Creatinine PGS000678	$6.4x10^{-7}$	$7.4x10^{-7}$	0.44

Continuation of Table A4

Urine Creatinine PGS000679	$-3.0x10^{-6}$	$-1.9x10^{-6}$	*$7.0x10^{-2}$*
Cystatin C PGS002165	$6.6x10^{-8}$	$6.6x10^{-8}$	0.96
Cystatin C PGS001947	$6.3x10^{-7}$	$6.3x10^{-7}$	0.83
Cystatin C PGS000680	$8.7x10^{-7}$	$8.4x10^{-7}$	0.77
eGFR PGS000682	$-5.2x10^{-7}$	$-6.3x10^{-7}$	0.32
Serum Albumin PGS001886	$8.6x10^{-6}$	$8.1x10^{-6}$	0.26
Serum Albumin PGS002099	$9.9x10^{-7}$	$9.6x10^{-7}$	0.52
Serum Albumin PGS000669	$1.6x10^{-6}$	$1.5x10^{-6}$	0.19
Serum Protein Non-Albumin PGS000691	$2.7x10^{-7}$	$6.5x10^{-8}$	**$3.5x10^{-2}$**
Total Blood Protein PGS000698	$3.0x10^{-7}$	$2.2x10^{-7}$	*$5.3x10^{-2}$*
Urine Microalbumin PGS001967	$-4.8x10^{-6}$	$-4.9x10^{-6}$	0.94
Urine Microalbumin PGS002185	$1.9x10^{-8}$	$2.1x10^{-8}$	0.60
Urine Microalbumin PGS000690	$2.1x10^{-5}$	$2.7x10^{-5}$	0.43
Urine Potassium PGS001974	$1.6x10^{-7}$	$1.7x10^{-7}$	0.92
Urine Potassium PGS002192	$3.5x10^{-9}$	$3.4x10^{-9}$	0.98
Urine Potassium PGS000693	$-8.1x10^{-6}$	$-7.2x10^{-6}$	0.16
Urine Sodium PGS002007	$-1.8x10^{-5}$	$-2.4x10^{-5}$	0.33
Urine Sodium PGS002226	$5.2x10^{-7}$	$2.7x10^{-7}$	0.41
Urine Sodium PGS000695	$2.5x10^{-6}$	$2.7x10^{-6}$	0.74
Urea PGS001980	$-3.1x10^{-7}$	$-3.5x10^{-7}$	0.22
Urea PGS002198	$-1.9x10^{-9}$	$-4.6x10^{-9}$	0.40
Urea PGS000701	$-3.2x10^{-6}$	$-3.5x10^{-6}$	*$8.5x10^{-2}$*
Kidney Failure PGS000708	$6.5x10^{-7}$	$7.8x10^{-7}$	0.49
Non Alcoholic Liver Disease PGS002071	$-7.3x10^{-10}$	$-6.7x10^{-10}$	0.99

Continuation of Table A4

Non Alcoholic Liver Disease PGS001860	$1.1x10^{-4}$	$1.2x10^{-4}$	0.91
Vitamin D PGS000702	$-1.2x10^{-5}$	$-1.2x10^{-5}$	0.48

Abbreviations: PNS, peripheral nervous system, LDL, low-density lipoprotein; HDL, high-density lipoprotein, eGFR, estimated glomerular filtration rate.

Table A5. Associations between external PRS and cisplatin-induced tinnitus in testicular cancer survivors in *The Platinum Study* training set

Trait	Mean in Survivors with No Tinnitus	Mean in Survivors with Tinnitus	p-value
PNS disorder PGS002039	$1.4x10^{-8}$	$1.5x10^{-8}$	*$9.8x10^{-2}$*
PNS disorder PGS001832	$1.9x10^{-5}$	$2.0x10^{-5}$	0.21
Hearing Difficulties PGS001891	$4.2x10^{-6}$	$4.7x10^{-6}$	0.14
Hearing Difficulties PGS002104	$3.6x10^{-9}$	$8.5x10^{-9}$	**$7.6x10^{-3}$**
Otosclerosis PGS002046	$-7.8x10^{-10}$	$-7.5x10^{-10}$	0.31
Dementia PGS001827	$4.2x10^{-3}$	$3.7x10^{-3}$	0.16
Dementia PGS002035	$2.5x10^{-8}$	$2.3x10^{-8}$	0.83
Alzheimer's PGS001828	$5.4x10^{-3}$	$4.9x10^{-3}$	0.12
Weight PGS001825	$1.3x10^{-5}$	$1.4x10^{-5}$	0.40
Weight PGS002033	$-7.7x10^{-9}$	$-7.7x10^{-9}$	0.93
Lean Body Mass PGS001950	$-1.2x10^{-7}$	$-1.2x10^{-7}$	0.77
Lean Body Mass PGS002168	$5.9x10^{-9}$	$5.8x10^{-9}$	0.97
Body Fat Mass PGS001951	$7.4x10^{-7}$	$7.6x10^{-7}$	0.56
Body Fat Mass PGS002169	$7.2x10^{-8}$	$7.7x10^{-8}$	0.32
Body Fat Percentage PGS001917	$1.2x10^{-7}$	$1.3x10^{-7}$	0.32
Body Fat Percentage PGS002133	$9.7x10^{-9}$	$1.1x10^{-8}$	0.12
Hypertension PGS001838	$6.6x10^{-6}$	$7.4x10^{-6}$	**$1.4x10^{-2}$**
Hypertension PGS002047	$4.1x10^{-8}$	$4.8x10^{-8}$	**$1.7x10^{-2}$**
Hypertension PGS000706	$6.7x10^{-6}$	$7.6x10^{-6}$	**$1.4x10^{-3}$**
Triglycerides PGS001979	$-2.9x10^{-6}$	$-2.8x10^{-6}$	0.40
Triglycerides PGS002197	$-2.5x10^{-7}$	$-2.3x10^{-7}$	0.35
Triglycerides PGS000699	$-6.4x10^{-6}$	$-5.7x10^{-6}$	0.12
Abnormal Circulating Lipids PGS002029	$3.9x10^{-8}$	$3.7x10^{-8}$	0.18

Continuation of Table A5

Abnormal Circulating Lipids PGS001821	$1.0x10^{-5}$	$9.7x10^{-6}$	0.32
Lipoprotein A PGS001963	$-7.4x10^{-5}$	$-8.3x10^{-5}$	*$8.4x10^{-2}$*
Lipoprotein A PGS002181	$-2.2x10^{-5}$	$-2.4x10^{-5}$	0.24
Lipoprotein A PGS000689	$-7.3x10^{-6}$	$-8.9x10^{-6}$	0.94
Apolipoprotein A PGS001888	$2.0x10^{-6}$	$2.0x10^{-6}$	0.80
Apolipoprotein A PGS002101	$2.5x10^{-7}$	$2.5x10^{-7}$	0.87
Apolipoprotein A PGS000671	$4.8x10^{-6}$	$4.9x10^{-6}$	0.91
Apolipoprotein B PGS001889	$2.2x10^{-6}$	$1.6x10^{-6}$	**$1.6x10^{-2}$**
Apolipoprotein B PGS002102	$-7.9x10^{-9}$	$-3.0x10^{-8}$	**$4.1x10^{-2}$**
Apolipoprotein B PGS000672	$2.1x10^{-6}$	$1.7x1^{0-6}$	*$8.9x10^{-2}$*
Total Cholesterol PGS001895	$2.2x10^{-5}$	$2.1x10^{-5}$	0.12
Total Cholesterol PGS002108	$9.1x10^{-7}$	$8.7x10^{-7}$	0.23
Cholesterol PGS000677	$5.9x10^{-6}$	$5.7x10^{-6}$	0.26
LDL PGS001933	$8.8x10^{-6}$	$7.8x10^{-6}$	**$3.0x10^{-2}$**
LDL PGS002150	$3.5x10^{-7}$	$3.0x10^{-7}$	*$7.4x10^{-2}$*
LDL PGS000688	$4.9x10^{-6}$	$4.5x10^{-6}$	*$7.9x10^{-2}$*
HDL PGS001954	$2.4x10^{-6}$	$2.4x10^{-6}$	0.71
HDL PGS002172	$2.8x10^{-7}$	$2.8x10^{-7}$	0.72
HDL PGS000686	$9.2x10^{-6}$	$9.0x10^{-6}$	0.23
Creatinine Clearance PGS001944	$-2.5x10^{-7}$	$-2.4x10^{-7}$	0.87
Creatinine Clearance PGS002162	$4.6x10^{-8}$	$4.6x10^{-8}$	0.99
Creatinine PGS001945	$2.3x10^{-7}$	$2.5x10^{-7}$	0.50
Creatinine PGS002163	$2.7x10^{-8}$	$2.9x10^{-8}$	0.49
Creatinine PGS000678	$6.2x10^{-7}$	$7.9x10^{-7}$	0.16

Continuation of Table A5

Urine Creatinine PGS000679	$-3.2x10^{-6}$	$-2.1x10^{-6}$	**$3.6x10^{-2}$**
Cystatin C PGS002165	$6.8x10^{-8}$	$7.2x10^{-8}$	0.27
Cystatin C PGS001947	$6.4x10^{-7}$	$6.9x10^{-7}$	0.22
Cystatin C PGS000680	$8.9x10^{-7}$	$1.1x10^{-6}$	**$4.0x10^{-2}$**
eGFR PGS000682	$-4.9x10^{-7}$	$-6.6x10^{-7}$	0.13
Serum Albumin PGS001886	$8.4x10^{-6}$	$8.4x10^{-6}$	0.94
Serum Albumin PGS002099	$9.7x10^{-7}$	$9.5x10^{-7}$	0.62
Serum Albumin PGS000669	$1.6x10^{-6}$	$1.6x10^{-6}$	0.58
Serum Protein Non-Albumin PGS000691	$2.3x10^{-7}$	$1.7x10^{-7}$	0.56
Total Blood Protein PGS000698	$3.0x10^{-7}$	$2.8x10^{-7}$	0.66
Urine Microalbumin PGS001967	$-4.8x10^{-6}$	$-7.3x10^{-6}$	*$6.4x10^{-2}$*
Urine Microalbumin PGS002185	$1.9x10^{-8}$	$1.4x10^{-8}$	*$8.3x10^{-2}$*
Urine Microalbumin PGS000690	$1.4x10^{-5}$	$1.5x10^{-5}$	0.88
Urine Potassium PGS001974	$9.7x10^{-8}$	$1.5x10^{-7}$	0.53
Urine Potassium PGS002192	$8.8x10^{-10}$	$2.6x10^{-9}$	0.49
Urine Potassium PGS000693	$-8.2x10^{-6}$	$-7.1x10^{-6}$	*$7.6x10^{-2}$*
Urine Sodium PGS002007	$-2.4x10^{-5}$	$-2.4x10^{-5}$	0.95
Urine Sodium PGS002226	$2.3x10^{-7}$	$1.9x10^{-7}$	0.88
Urine Sodium PGS000695	$2.2x10^{-6}$	$2.7x10^{-6}$	0.20
Urea PGS001980	$-3.2x10^{-7}$	$-3.3x10^{-7}$	0.83
Urea PGS002198	$-3.1x10^{-9}$	$-2.0x10^{-9}$	0.71
Urea PGS000701	$-3.4x10^{-6}$	$-3.2x10^{-6}$	0.20
Kidney Failure PGS000708	$6.1x10^{-7}$	$9.8x10^{-7}$	**$3.0x10^{-2}$**
Non Alcoholic Liver Disease PGS002071	$-6.8x10^{-10}$	$-9.0x10^{-10}$	0.54

Continuation of Table A5

Non Alcoholic Liver Disease PGS001860	$1.1x10^{-4}$	$9.8x10^{-5}$	0.64
Vitamin D PGS000702	$-1.2x10^{-5}$	$-1.2x10^{-5}$	0.83

Abbreviations: PNS, peripheral nervous system, LDL, low-density lipoprotein; HDL, high-density lipoprotein, eGFR, estimated glomerular filtration rate.

Table A6. Associations between external PRS and cisplatin-induced hearing loss in testicular cancer survivors in *The Platinum Study* training set

Trait	Correlation Coefficient (rho)	p-value
PNS disorder PGS002039	$8.4x10^{-2}$	**$5.7x10^{-3}$**
PNS disorder PGS001832	$1.8x10^{-2}$	0.54
Hearing Difficulties PGS001891	$8.1x10^{-2}$	**$7.5x10^{-3}$**
Hearing Difficulties PGS002104	$9.8x10^{-2}$	**$1.2x10^{-3}$**
Otosclerosis PGS002046	$-1.4x10^{-2}$	0.64
Dementia PGS001827	$-1.2x10^{-2}$	0.70
Dementia PGS002035	$-2.6x10^{-2}$	0.40
Alzheimer's PGS001828	$-1.8x10^{-2}$	0.56
Weight PGS001825	$3.6x10^{-3}$	0.91
Weight PGS002033	$6.1x10^{-3}$	0.84
Lean Body Mass PGS001950	$1.2x10^{-2}$	0.70
Lean Body Mass PGS002168	$-1.0x10^{-2}$	0.74
Body Fat Mass PGS001951	$6.2x10^{-2}$	**$4.1x10^{-2}$**
Body Fat Mass PGS002169	$5.4x10^{-2}$	*$7.8x10^{-2}$*
Body Fat Percentage PGS001917	$5.6x10^{-2}$	*$6.7x10^{-2}$*
Body Fat Percentage PGS002133	$6.2x10^{-2}$	**$4.3x10^{-2}$**
Hypertension PGS001838	$1.6x10^{-2}$	0.60
Hypertension PGS002047	$1.1x10^{-2}$	0.72
Hypertension PGS000706	$2.1x10^{-2}$	0.49
Triglycerides PGS001979	$2.8x10^{-2}$	0.36
Triglycerides PGS002197	$2.0x10^{-2}$	0.50
Triglycerides PGS000699	$2.9x10^{-2}$	0.34
Abnormal Circulating Lipids PGS002029	$-2.8x10^{-2}$	0.35

Continuation of Table A6

Abnormal Circulating Lipids PGS001821	$-1.3x10^{-2}$	0.66
Lipoprotein A PGS001963	$-4.2x10^{-2}$	0.17
Lipoprotein A PGS002181	$-1.9x10^{-2}$	0.54
Lipoprotein A PGS000689	$5.3x10^{-3}$	0.86
Apolipoprotein A PGS001888	$-3.7x10^{-2}$	0.22
Apolipoprotein A PGS002101	$-2.6x10^{-2}$	0.40
Apolipoprotein A PGS000671	$-2.2x10^{-2}$	0.46
Apolipoprotein B PGS001889	$2.4x10^{-2}$	0.42
Apolipoprotein B PGS002102	$2.0x10^{-2}$	0.50
Apolipoprotein B PGS000672	$1.7x10^{-2}$	0.57
Total Cholesterol PGS001895	$-9.1x10^{-3}$	0.77
Total Cholesterol PGS002108	$-1.7x10^{-3}$	0.96
Cholesterol PGS000677	$-2.6x10^{-3}$	0.93
LDL PGS001933	$-4.3x10^{-3}$	0.89
LDL PGS002150	$-1.3x10^{-3}$	0.96
LDL PGS000688	$3.4x10^{-3}$	0.91
HDL PGS001954	$-4.2x10^{-2}$	0.17
HDL PGS002172	$-3.8x10^{-2}$	0.21
HDL PGS000686	$-3.0x10^{-2}$	0.33
Creatinine Clearance PGS001944	$1.7x10^{-2}$	0.58
Creatinine Clearance PGS002162	$-1.5x10^{-3}$	0.96
Creatinine PGS001945	$1.4x10^{-2}$	0.64
Creatinine PGS002163	$5.3x10^{-3}$	0.86
Creatinine PGS000678	$-4.7x10^{-4}$	0.99

Continuation of Table A6

Urine Creatinine PGS000679	$6.8x10^{-2}$	**$2.4x10^{-2}$**
Cystatin C PGS002165	$5.5x10^{-2}$	*$6.8x10^{-2}$*
Cystatin C PGS001947	$6.8x10^{-2}$	**$2.6x10^{-2}$**
Cystatin C PGS000680	$5.4x10^{-2}$	*$7.4x10^{-2}$*
eGFR PGS000682	$-9.4x10^{-3}$	0.76
Serum Albumin PGS001886	$2.4x10^{-2}$	0.44
Serum Albumin PGS002099	$2.1x10^{-2}$	0.49
Serum Albumin PGS000669	$-2.2x10^{-4}$	0.99
Serum Protein Non-Albumin PGS000691	$-5.6x10^{-2}$	*$6.4x10^{-2}$*
Total Blood Protein PGS000698	$-4.4x10^{-2}$	0.14
Urine Microalbumin PGS001967	$-9.9x10^{-3}$	0.74
Urine Microalbumin PGS002185	$-3.1x10^{-2}$	0.30
Urine Microalbumin PGS000690	$4.7x10^{-2}$	0.12
Urine Potassium PGS001974	$3.6x10^{-2}$	0.23
Urine Potassium PGS002192	$1.4x10^{-2}$	0.64
Urine Potassium PGS000693	$6.5x10^{-2}$	**$3.1x10^{-2}$**
Urine Sodium PGS002007	$-4.3x10^{-2}$	0.15
Urine Sodium PGS002226	$-3.0x10^{-2}$	0.33
Urine Sodium PGS000695	$3.7x10^{-2}$	0.22
Urea PGS001980	$-8.2x10^{-3}$	0.79
Urea PGS002198	$-7.8x10^{-3}$	0.80
Urea PGS000701	$-4.6x10^{-3}$	0.88
Kidney Failure PGS000708	$5.0x10^{-2}$	*$9.6x10^{-2}$*
Non Alcoholic Liver Disease PGS002071	$1.9x10^{-3}$	0.95

Continuation of Table A6

Non Alcoholic Liver Disease PGS001860	$-2.7x10^{-2}$	0.38
Vitamin D PGS000702	$6.3x10^{-3}$	0.84

Abbreviations: PNS, peripheral nervous system, LDL, low-density lipoprotein; HDL, high-density lipoprotein, eGFR, estimated glomerular filtration rate.

Table A7. Genes associated with cisplatin-induced peripheral sensory neuropathy by TWAS ($p < 0.0005$)

Tissue	Gene	CHR	HSQ	BEST.GWAS.ID	BEST.GWAS.Z	EQTL.ID	EQTL.Z	EQTL.GWAS.Z	NSNP	MODEL	TWAS.Z	TWAS.P
Nerve	SEC61A2	10	0.24	rs10906086	3.7	rs2399786	-11.2	3.7	523	enet	-3.7	$1.8x10^{-4}$
Nerve	RP11-413H22.3	16	0.42	rs9933064	-3.6	rs10438565	12.6	-3.4	455	lasso	-3.8	$1.8x10^{-4}$
Cerebellum	SEC61A2	10	0.67	rs10906086	3.7	rs1053403	-10.4	3.5	527	top1	-3.5	$4.5x10^{-4}$
Brain	FAM124B	2	0.044	rs11674099	3.9	rs12613725	5.3	-3.5	444	top1	-3.5	$4.5x10^{-4}$
Brain	TTC26	7	0.059	rs11525873	3.6	rs11525873	4.6	3.6	430	top1	3.6	$3.9x10^{-4}$
Brain	ZNF770	15	0.14	rs16960222	3.5	rs16960222	-8.7	3.5	404	top1	-3.5	$4.2x10^{-4}$
Brain	LOC100505812	19	0.10	rs8108419	-3.3	rs1421674	-3.8	-2.9	514	lasso	3.6	$3.9x10^{-4}$
Kidney	BICDL1	12	0.46	rs7959743	-3.3	rs2859287	3.7	-2.2	380	lasso	-3.5	$4.9x10^{-4}$
Kidney	RP11-413H22.3	16	0.69	rs9933064	-3.6	rs7188330	4.5	-3.6	463	top1	-3.6	$3.8x10^{-4}$
Adipose (SC)	CASQ2	1	0.082	rs10923418	-3.8	rs10923418	4.5	-3.8	488	top1	-3.8	$1.4x10^{-4}$
Adipose (SC)	KIAA1549L	11	0.20	rs2615919	3.5	rs7943651	-6.3	2.7	435	enet	-3.5	$4.3x10^{-4}$
Adipose (SC)	RP11-413H22.3	16	0.37	rs9933064	-3.6	rs10438565	12.0	-3.4	461	lasso	-3.6	$3.6x10^{-4}$
Adipose (SC)	Antisense to SUN2	22	0.083	rs7284708	-3.6	rs2235135	-3.4	-2.2	380	susie	3.5	$4.6x10^{-4}$
Adipose (VO)	SEC61A2	10	0.12	rs10906086	3.7	rs10906086	-5.0	3.7	526	susie	-3.8	$1.7x10^{-4}$
Adipose (VO)	POGLUT3	11	0.18	rs11212509	-4.0	rs10890858	-8.4	-3.7	319	susie	3.6	$2.8x10^{-4}$
Adipose (VO)	RP11-413H22.3	16	0.32	rs9933064	-3.6	rs10438565	10.2	-3.4	460	enet	-3.9	$8.6x10^{-5}$
Blood	NXT1	20	0.07	rs844828	-4.8	rs6137832	-4.7	-3.5	563	top1	3.5	$4.6x10^{-4}$
Muscle	SEC61A2	10	0.082	rs10906086	3.7	rs10906086	-6.4	3.7	521	susie	-3.6	$3.3x10^{-4}$
Liver	GOLGA8N	15	0.43	rs1258791	3.6	rs28457217	-5.7	-1.7	394	enet	3.5	$4.8x10^{-4}$

Continuation of Table A7

Liver	RP11-413H22.3	16	0.36	rs9933064	-3.6	rs7188330	7.4	-3.6	464	top1	-3.6	$3.8x10^{-4}$
Testis	KRT8P43	6	0.21	rs761100	3.3	rs2038135	5.7	3.1	626	enet	3.7	$2.4x10^{-4}$
Testis	ACAT1	11	0.17	rs11212509	-4.0	rs12807544	-6.6	3.0	365	enet	-3.6	$3.5x10^{-4}$
Testis	POGLUT3	11	0.14	rs11212509	-4.0	rs4533001	-5.7	-3.4	320	susie	3.7	$2.5x10^{-4}$
Testis	RP11-413H22.3	16	0.35	rs9933064	-3.6	rs7188330	8.7	-3.6	463	susie	-3.6	$3.5x10^{-4}$
Testis	ZNF875	19	0.11	rs860386	3.5	rs10422527	4.5	3.0	284	enet	3.5	$4.1x10^{-4}$
Testis	Antisense to ZNF582	19	0.51	rs10775569	-3.0	rs2904015	9.7	2.7	526	susie	3.5	$4.0x10^{-4}$

Abbreviations: eQTL, expression quantitative trait locus; CHR, chromosome, HSQ, mean heritability estimate; Best.GWAS.ID, most significantly associated variant in the locus; Best.GWAS.Z, z-score of most significantly associated variant in the locus; eQTL ID, best eQTL in the locus; eQTL.GWAS.Z, GWAS z-score for best eQTL; NSNP, number of SNPs in the locus; Model, best performing TWAS model; TWAS.Z, TWAS z-score; TWAS.P, TWAS p-value, enet, elastic-net regression (mixing parameter = 0.5); blup, best linear unbiased predictor from all variants; bslmm, Bayesian sparse linear model; lasso, least absolute shrinkage and selection operator; top1, single best eQTL, susie, sum of single effects regression, VO, visceral omentum; SC, subcutaneous.

Table A8. Genes associated with cisplatin-induced peripheral sensory neuropathy by TWAS ($p < 0.005$)

Tissue	Gene	CHR	HSQ	BEST.GWAS.ID	BEST.GWAS.Z	EQTL.ID	EQTL.Z	EQTL.GWAS.Z	NSNP	MODEL	TWAS.Z	TWAS.P
Nerve	LINC01376	2	0.13	rs851338	3.2	rs6707044	6.4	2.8	555	top1	2.8	$4.5x10^{-3}$
Nerve	CLEC4F	2	0.60	rs3755342	-4.4	rs7594319	9.9	3.2	551	susie	2.8	$4.6x10^{-3}$
Nerve	CD207	2	0.32	rs3755342	-4.4	rs7594319	8.5	3.2	547	enet	2.9	$3.4x10^{-3}$
Nerve	VAX2	2	0.10	rs3755342	-4.4	rs4852727	5.5	3.3	530	top1	3.3	$1.0x10^{-3}$
Nerve	ATP6V1B1	2	0.13	rs3755342	-4.4	rs7594319	6.9	3.2	526	top1	3.2	$1.3x10^{-3}$
Nerve	EAF1-AS1	3	0.073	rs4395387	3.2	rs2344675	-5.2	-2.0	373	enet	2.8	$4.5x10^{-3}$
Nerve	TMA7	3	0.11	rs2362452	-3.5	rs3214041	-5.1	-3.3	245	top1	3.3	$1.1x10^{-3}$
Nerve	TREX1	3	0.16	rs2362452	-3.5	rs11797	-9.2	-3.1	245	top1	3.1	$1.8x10^{-3}$
Nerve	SHISA5	3	0.063	rs2362452	-3.5	rs11720151	-4.3	-0.65	242	enet	3.2	$1.5x10^{-3}$
Nerve	NICN1	3	0.19	rs3197999	-3.1	rs3448	-11.3	2.5	288	susie	-3.1	$2.0x10^{-3}$
Nerve	TMEM128	4	0.48	rs2916457	3.2	rs2916457	-8.6	3.2	362	enet	-3.0	$2.7x10^{-3}$
Nerve	AIG1	6	0.24	rs3804527	-3.2	rs3804527	8.3	-3.2	472	susie	-3.1	$1.8x10^{-3}$
Nerve	RAET1E	6	0.36	rs6933642	-3.2	rs9383583	-11.2	-3.1	489	susie	3.3	$9.2x10^{-4}$
Nerve	SUN1	7	0.19	rs13171	-2.6	rs4721949	-7.4	-2.6	315	susie	2.8	$4.5x10^{-3}$
Nerve	OPN1SW	7	0.23	rs2228075	3.1	rs1044226	7.9	-2.6	342	enet	-2.9	$3.7x10^{-3}$
Nerve	DOK2	8	0.14	rs899425	-3.3	rs11135701	-6.5	-3.2	477	top1	3.2	$1.6x10^{-3}$
Nerve	SEC61A2	10	0.24	rs10906086	3.7	rs2399786	-11.2	3.7	523	enet	-3.7	$1.8x10^{-4}$
Nerve	NUDT5	10	0.16	rs10906086	3.7	rs10466280	-8.2	3.4	520	susie	-3.4	$7.5x10^{-4}$
Nerve	PARD3-AS1	10	0.16	rs7897283	2.6	rs2492456	7.7	-2.4	319	enet	-2.8	$5.0x10^{-3}$
Nerve	TMEM258	11	0.090	rs174579	-4.0	rs174538	6.7	-3.2	374	top1	-3.2	$1.3x10^{-3}$
Nerve	FADS2	11	0.34	rs174579	-4.0	rs968567	11.3	-3.3	388	top1	-3.3	$1.1x10^{-3}$
Nerve	POGLUT3	11	0.39	rs11212509	-4.0	rs3741060	-11.6	-3.3	318	lasso	3.4	$7.0x10^{-4}$
Nerve	NCAM1	11	0.15	rs7940211	-3.2	rs10789901	-6.0	-2.2	548	enet	2.8	$4.9x10^{-3}$

Continuation of Table A8

Nerve	GRAMD1B	11	0.15	rs12362253	-3.1	rs12362253	-4.9	-3.1	568	susie	3.0	$2.5x10^{-3}$
Nerve	BCAT1	12	0.45	rs12579869	3.3	rs976436	11.1	3.1	552	susie	2.9	$3.4x10^{-3}$
Nerve	CBLN3	14	0.75	rs10134603	2.9	rs2273629	-17.5	-2.7	530	enet	3.0	$2.5x10^{-3}$
Nerve	LRFN5	14	0.20	rs2166751	2.7	rs17112218	-5.2	2.6	351	lasso	-3.0	$2.5x10^{-3}$
Nerve	ACTC1	15	0.11	rs16960222	3.5	rs639735	-6.4	-2.6	395	lasso	3.3	$9.4x10^{-4}$
Nerve	EFL1	15	0.23	rs17269323	4.7	rs3914699	5.7	-0.58	322	lasso	-2.9	$3.8x10^{-3}$
Nerve	SAXO2	15	0.51	rs17269323	4.7	rs9972386	13.9	3.7	322	susie	3.0	$2.8x10^{-3}$
Nerve	RP11-413H22.3	16	0.42	rs9933064	-3.6	rs10438565	12.6	-3.4	455	lasso	-3.8	$1.8x10^{-4}$
Nerve	PRELID3A	18	0.58	rs17615525	-3.3	rs919	16.8	-2.7	400	enet	-2.9	$4.1x10^{-3}$
Nerve	PGLYRP1	19	0.060	rs749818	3.4	rs4803929	3.0	-0.51	411	susie	3.1	$2.3x10^{-3}$
Nerve	CARD8-AS1	19	0.088	rs8108419	-3.3	rs16981882	-4.5	-3.0	514	lasso	3.5	$5.2x10^{-4}$
Nerve	CYTH2	19	0.37	rs8108419	-3.3	rs1799270	-8.4	2.0	523	enet	-2.9	$3.4x10^{-3}$
Cerebellum	PEX13	2	0.17	rs1182688	-3.3	rs1182688	-5.2	-3.3	325	top1	3.3	$1.0x10^{-3}$
Cerebellum	TMA7	3	0.31	rs2362452	-3.5	rs9815103	-8.2	-3.3	255	top1	3.3	$9.4x10^{-4}$
Cerebellum	TREX1	3	0.37	rs2362452	-3.5	rs11797	-8.1	-3.1	255	top1	3.1	$1.8x10^{-3}$
Cerebellum	SHISA5	3	0.21	rs2362452	-3.5	rs3214041	-4.5	-3.3	252	susie	3.0	$3.0x10^{-3}$
Cerebellum	MST1	3	0.39	rs3197999	-3.1	rs9858542	5.5	-3.0	316	enet	-3.0	$3.1x10^{-3}$
Cerebellum	MGLL	3	0.21	rs555183	3.3	rs6439081	5.2	-2.5	393	enet	-2.8	$4.7x10^{-3}$
Cerebellum	N4BP3	5	0.27	rs6883364	-4.0	rs7721220	-6.4	-3.1	397	susie	3.1	$1.7x10^{-3}$
Cerebellum	DHTKD1	10	0.15	rs10906086	3.7	rs3758376	-3.9	3.3	497	top1	-3.3	$9.7x10^{-4}$
Cerebellum	SEC61A2	10	0.67	rs10906086	3.7	rs1053403	-10.4	3.5	527	top1	-3.5	$4.5x10^{-4}$
Cerebellum	ACAT1	11	0.11	rs11212509	-4.0	rs4430476	-4.4	-2.9	365	enet	2.9	$3.9x10^{-3}$
Cerebellum	RP5-1063M23.2	12	0.64	rs887303	3.3	rs1465264	7.7	-3.2	647	enet	-2.8	$4.8x10^{-3}$
Cerebellum	SCFD1	14	0.38	rs229227	-3.2	rs12434151	8.3	-3.2	386	susie	-3.1	$1.7x10^{-3}$

Continuation of Table A8

Cerebellum	DMAC2L	14	0.19	rs1950514	3.5	rs1890978	3.7	2.0	393	susie	3.4	$7.9x10^{-4}$
Cerebellum	LRRC49	15	0.30	rs7180149	-3.3	rs11633699	4.2	2.9	394	lasso	3.1	$2.2x10^{-3}$
Cerebellum	SAXO2	15	0.69	rs17269323	4.7	rs12439679	9.7	3.6	322	enet	2.8	$4.8x10^{-3}$
Cerebellum	PRC1-AS1	15	0.39	rs2301826	-3.0	rs2290203	-7.7	-3.0	487	lasso	3.0	$3.1x10^{-3}$
Cerebellum	NPIPP1	16	0.34	rs3893231	-2.8	rs9923527	4.8	1.3	102	enet	3.0	$2.5x10^{-3}$
Cerebellum	RP11-413H22.3	16	0.42	rs9933064	-3.6	rs7188330	6.1	-3.6	463	susie	-3.3	$1.1x10^{-3}$
Cerebellum	ZNF529	19	0.24	rs826278	3.3	rs1673087	-5.7	2.9	303	Susie	-3.0	$2.6x10^{-3}$
Cerebellum	ZNF793-AS1	19	0.13	rs860386	3.5	rs11673344	4.4	-3.0	275	lasso	-3.0	$2.5x10^{-3}$
Cerebellum	CYTH2	19	0.50	rs8108419	-3.3	rs8108419	5.6	-3.3	528	enet	-3.0	$3.2x10^{-3}$
Cerebellum	SMARCB1	22	0.45	rs6003909	-3.4	rs9612481	-7.1	-2.8	463	susie	3.0	$2.4x10^{-3}$
Brain	PINK1	1	0.068	rs12403580	-3.2	rs1573132	-5.1	-3.1	476	top1	3.1	$2.2x10^{-3}$
Brain	LOC100132111	1	0.19	rs6587622	3.0	rs6587622	-6.1	3.0	334	top1	-3.0	$2.4x10^{-3}$
Brain	LY75	2	0.089	rs6432570	3.0	rs3828323	-6.4	3.0	492	top1	-3.0	$2.5x10^{-3}$
Brain	FAM124B	2	0.044	rs11674099	3.9	rs12613725	5.3	-3.5	444	top1	-3.5	$4.5x10^{-4}$
Brain	TREX1	3	0.16	rs2362452	-3.5	rs6794875	-10.4	-3.5	257	bslmm	3.4	$7.3x10^{-4}$
Brain	SHISA5	3	0.060	rs2362452	-3.5	rs11797	-5.9	-3.1	263	top1	3.1	$1.8x10^{-3}$
Brain	NPHP3-ACAD11	3	0.071	rs16839895	3.5	rs7620792	-3.6	0.16	455	blup	2.9	$4.2x10^{-3}$
Brain	RSRC1	3	0.040	rs1845138	-3.2	rs7613824	-3.6	-3.2	536	top1	3.2	$1.3x10^{-3}$
Brain	CCDC50	3	0.13	rs293809	-3.1	rs9868286	-6.3	-2.8	481	top1	2.8	$4.6x10^{-3}$
Brain	IGFBP7	4	0.38	rs12651664	4.3	rs1718858	-12.6	-3.2	576	enet	3.1	$1.9x10^{-3}$
Brain	SNX25	4	0.12	rs3112911	2.9	rs3112911	4.8	2.9	628	top1	2.9	$3.4x10^{-3}$
Brain	CENPK	5	0.25	rs16894099	3.1	rs11740053	10.7	3.1	436	top1	3.1	$2.1x10^{-3}$
Brain	RASA1	5	0.054	rs4133446	-4.2	rs6879021	3.5	-1.2	307	bslmm	-3.3	$1.0x10^{-3}$
Brain	TTC26	7	0.059	rs11525873	3.6	rs11525873	4.6	3.6	430	top1	3.6	$3.9x10^{-4}$

Continuation of Table A8

Brain	SEC61A2	10	0.13	rs10906086	3.7	rs12569964	6.8	-3.4	552	top1	-3.4	$5.8x10^{-4}$
Brain	PYROXD2	10	0.42	rs2147896	3.2	rs2147896	14.8	3.2	502	lasso	2.9	$3.4x10^{-3}$
Brain	KDELC2	11	0.22	rs11212509	-4.0	rs4533001	-9.7	-3.4	325	top1	3.4	$7.1x10^{-4}$
Brain	CBLN3	14	0.43	rs10134603	2.9	rs4982912	-10.2	-2.7	556	enet	2.9	$3.5x10^{-3}$
Brain	KHNYN	14	0.34	rs10134603	2.9	rs4982912	-9.7	-2.7	562	enet	3.0	$2.9x10^{-3}$
Brain	SCFD1	14	0.16	rs229227	-3.2	rs448175	9.2	-3.2	411	top1	-3.2	$1.6x10^{-3}$
Brain	ZNF770	15	0.14	rs16960222	3.5	rs16960222	-8.7	3.5	404	top1	-3.5	$4.2x10^{-4}$
Brain	COPS2	15	0.066	rs11853754	-2.6	rs1048975	-5.0	-2.4	328	blup	3.0	$2.7x10^{-3}$
Brain	FLCN	17	0.17	rs4985696	-2.6	rs1736204	-5.2	-2.3	396	enet	3.0	$2.7x10^{-3}$
Brain	ABCA5	17	0.11	rs11653085	3.7	rs12949267	-6.6	2.9	432	top1	-2.9	$3.8x10^{-3}$
Brain	TNFRSF11A	18	0.16	rs7243765	-3.5	rs6567263	-7.3	-2.9	502	bslmm	3.1	$1.8x10^{-3}$
Brain	LOC100505812	19	0.10	rs8108419	-3.3	rs1421674	-3.8	-2.9	514	lasso	3.6	$3.9x10^{-4}$
Brain	ZNF765	19	0.15	rs7255193	3.0	rs4803113	-7.4	-2.2	495	bslmm	2.9	$4.1x10^{-3}$
Brain	RPRD1B	20	0.044	rs6013504	-3.4	rs6022259	3.7	-2.5	499	bslmm	-2.9	$4.4x10^{-3}$
Kidney	BICDL1	12	0.46	rs7959743	-3.3	rs2859287	3.7	-2.2	380	lasso	-3.5	$4.9x10^{-4}$
Kidney	RP11-413H22.3	16	0.69	rs9933064	-3.6	rs7188330	4.5	-3.6	463	top1	-3.6	$3.8x10^{-4}$
Adipose (SC)	CASQ2	1	0.082	rs10923418	-3.8	rs10923418	4.5	-3.8	488	top1	-3.8	$1.4x10^{-4}$
Adipose (SC)	IGF2BP2 pseudogene	1	0.12	rs11240099	-3.7	rs671205	-5.0	3.5	310	lasso	-3.3	$9.3x10^{-4}$
Adipose (SC)	PDE4DIP pseudogene	1	0.14	rs11240099	-3.6	rs4950361	5.2	-0.86	314	enet	-2.9	$3.7x10^{-3}$
Adipose (SC)	CLEC4F	2	0.26	rs3755342	-4.4	rs7594319	9.2	3.2	553	enet	3.2	$1.6x10^{-3}$
Adipose (SC)	CD207	2	0.17	rs3755342	-4.4	rs7594319	8.5	3.2	549	susie	3.2	$1.5x10^{-3}$
Adipose (SC)	TREX1	3	0.13	rs2362452	-3.5	rs11797	-8.6	-3.1	244	top1	3.1	$1.8x10^{-3}$

Continuation of Table A8

Adipose (SC)	SHISA5	3	0.025	rs2362452	-3.5	rs13314659	-4.1	-3.3	241	top1	3.3	$1.1x10^{-3}$
Adipose (SC)	NICN1	3	0.196	rs3197999	-3.1	rs3448	-11.0	2.5	288	susie	-2.9	$3.4x10^{-3}$
Adipose (SC)	APEH	3	0.15	rs3197999	-3.1	rs9822268	7.5	-3.0	319	lasso	-2.9	$3.3x10^{-3}$
Adipose (SC)	LRRC77P	3	0.22	rs9818496	2.4	rs11928048	6.3	-2.0	333	enet	-3.2	$1.3x10^{-3}$
Adipose (SC)	CCDC50	3	0.30	rs293809	-3.1	rs9827142	-10.7	-2.8	472	enet	2.9	$3.7x10^{-3}$
Adipose (SC)	TMEM128	4	0.24	rs2916457	3.2	rs2980092	-6.0	2.9	361	enet	-2.9	$4.3x10^{-3}$
Adipose (SC)	SOBP	6	0.058	rs3734677	3.4	rs10457162	3.5	3.4	441	lasso	3.2	$1.3x10^{-3}$
Adipose (SC)	RP1-45I4.3	6	0.17	rs3804527	-3.2	rs7750571	-6.8	-2.5	468	enet	3.1	$1.8x10^{-3}$
Adipose (SC)	AIG1	6	0.13	rs3804527	-3.2	rs3804527	6.0	-3.2	471	lasso	-3.1	$1.9x10^{-3}$
Adipose (SC)	PPIA	7	0.13	rs17134462	2.8	rs17134462	-5.6	2.8	418	lasso	-2.9	$4.4x10^{-3}$
Adipose (SC)	RP11-274B21.9	7	0.15	rs2228075	3.1	rs6467202	6.9	2.0	361	enet	2.9	$3.5x10^{-3}$
Adipose (SC)	OPN1SW	7	0.28	rs2228075	3.1	rs1006023	9.5	-2.5	342	enet	-3.0	$3.0x10^{-3}$
Adipose (SC)	SEC61A2	10	0.16	rs10906086	3.7	rs11257552	6.6	-3.4	524	enet	-2.8	$4.6x10^{-3}$
Adipose (SC)	RP11-326C3.7	11	0.3819	rs909098	3.0	rs909098	9.8	3.0	325	lasso	3.1	$2.0x10^{-3}$
Adipose (SC)	STK33	11	0.20	rs2311390	-3.2	rs1992756	-7.3	-3.1	514	enet	2.9	$4.1x10^{-3}$
Adipose (SC)	KIAA1549L	11	0.20	rs2615919	3.5	rs7943651	-6.3	2.7	435	enet	-3.5	$4.3x10^{-4}$
Adipose (SC)	TMEM258	11	0.074	rs174579	-4.0	rs174538	6.8	-3.2	377	top1	-3.2	$1.3x10^{-3}$
Adipose (SC)	FADS2	11	0.14	rs174579	-4.0	rs968567	8.4	-3.3	391	susie	-3.3	$9.9x10^{-4}$

Continuation of Table A8

Adipose (SC)	POGLUT3	11	0.29	rs11212509	-4.0	rs10890853	-11.7	-3.2	320	lasso	3.5	$5.4x10^{-4}$
Adipose (SC)	RP11-598F7.4	12	0.17	rs1106984	2.7	rs2368834	-6.8	2.2	292	enet	-3.1	$2.1x10^{-3}$
Adipose (SC)	RNF34	12	0.045	rs12300459	-3.2	rs15876	-4.6	-2.8	389	susie	2.8	$4.9x10^{-3}$
Adipose (SC)	PGAM5	12	0.053	rs957800	3.1	rs12282	-4.0	3.0	254	lasso	-3.0	$2.5x10^{-3}$
Adipose (SC)	SCFD1	14	0.13	rs229227	-3.2	rs7154847	-8.3	-3.2	386	enet	3.2	$1.5x10^{-3}$
Adipose (SC)	SNAP23	15	0.14	rs645953	2.5	rs2277533	-4.6	1.7	362	enet	-2.8	$5.0x10^{-3}$
Adipose (SC)	RAB27A	15	0.067	rs1690370	-3.8	rs1915202	4.1	-0.86	437	enet	-2.8	$4.7x10^{-3}$
Adipose (SC)	SAXO2	15	0.55	rs17269323	4.7	rs9972386	15.0	3.7	322	susie	3.1	$1.7x10^{-3}$
Adipose (SC)	PKD1P6	16	0.57	rs12919246	2.7	rs9927842	7.5	1.3	110	enet	2.9	$3.5x10^{-3}$
Adipose (SC)	TMC5	16	0.17	rs226881	-3.3	rs4499218	-6.7	2.3	436	enet	-3.0	$2.8x10^{-3}$
Adipose (SC)	RP11-413H22.3	16	0.37	rs9933064	-3.6	rs10438565	12.0	-3.4	461	lasso	-3.6	$3.6x10^{-4}$
Adipose (SC)	RP11-861E21.1	18	0.43	rs17615525	-3.3	rs919	13.9	-2.7	406	enet	-3.0	$2.6x10^{-3}$
Adipose (SC)	ZNF829	19	0.052	rs860386	3.5	rs4805190	-3.8	2.2	283	enet	-3.0	$2.5x10^{-3}$
Adipose (SC)	CYTH2	19	0.24	rs8108419	-3.3	rs1799270	-6.3	2.0	528	enet	-3.0	$2.6x10^{-3}$
Adipose (SC)	ZNF525	19	0.19	rs7255193	3.0	rs7255193	6.7	3.0	476	enet	3.2	$1.4x10^{-3}$
Adipose (SC)	SMARCB1	22	0.37	rs6003909	-3.4	rs9612481	-12.1	-2.8	465	lasso	2.9	$4.4x10^{-3}$
Adipose (SC)	Antisense to SUN2	22	0.083	rs7284708	-3.6	rs2235135	-3.4	-2.2	380	susie	3.5	$4.6x10^{-4}$
Adipose (VO)	ABCB10	1	0.045	rs10916540	2.8	rs1931331	-3.3	2.3	404	susie	-2.9	$4.2x10^{-3}$

Continuation of Table A8

Adipose (VO)	Sense intronic to BIRC6	2	0.12	rs6723154	3.0	rs2710628	6.2	-2.8	376	susie	-2.8	$4.7x10^{-3}$
Adipose (VO)	HK2	2	0.11	rs3732300	3.8	rs2306805	6.2	3.4	418	susie	3.5	$5.3x10^{-4}$
Adipose (VO)	MYRIP	3	0.14	rs3108335	-2.7	rs4676525	-3.2	-0.20	415	enet	3.5	$5.6x10^{-4}$
Adipose (VO)	TREX1	3	0.28	rs2362452	-3.5	rs11797	-12.4	-3.1	254	top1	3.1	$1.8x10^{-3}$
Adipose (VO)	SHISA5	3	0.061	rs2362452	-3.5	rs6442120	-4.7	-3.4	251	lasso	3.35	$8.1x10^{-4}$
Adipose (VO)	PRKAR2A	3	0.027	rs2362452	-3.5	rs990211	4.3	3.1	272	top1	3.1	$1.9x10^{-3}$
Adipose (VO)	NICN1	3	0.20	rs3197999	-3.1	rs9834003	-9.8	2.4	289	susie	-2.9	$3.6x10^{-3}$
Adipose (VO)	TPRA1	3	0.17	rs555183	3.3	rs782456	-7.7	-3.0	465	susie	2.9	$3.4x10^{-3}$
Adipose (VO)	CCDC50	3	0.23	rs293809	-3.1	rs9868286	-9.2	-2.8	471	enet	3.2	$1.2x10^{-3}$
Adipose (VO)	AIG1	6	0.12	rs3804527	-3.2	rs9321887	5.2	-2.9	473	lasso	-3.1	$2.0x10^{-3}$
Adipose (VO)	OPN1SW	7	0.22	rs2228075	3.1	rs1044226	8.0	-2.6	340	enet	-3.1	$2.3x10^{-3}$
Adipose (VO)	TMEM178B	7	0.055	rs4725500	-3.4	rs534348	-3.3	3.0	383	susie	-2.90	$3.7x10^{-3}$
Adipose (VO)	SEC61A2	10	0.12	rs10906086	3.7	rs10906086	-5.0	3.7	526	susie	-3.8	$1.7x10^{-4}$
Adipose (VO)	IFITM2	11	0.20	rs909098	3.0	rs909098	-6.1	3.0	323	lasso	-3.2	$1.3x10^{-3}$
Adipose (VO)	CTD-2507G9.1	11	0.089	rs10834805	-3.3	rs328486	3.9	1.4	552	enet	2.9	$3.5x10^{-3}$
Adipose (VO)	FADS2	11	0.19	rs174579	-4.0	rs968567	7.4	-3.3	399	susie	-3.3	$1.1x10^{-3}$
Adipose (VO)	POGLUT3	11	0.18	rs11212509	-4.0	rs10890858	-8.4	-3.7	319	susie	3.6	$2.8x10^{-4}$

Continuation of Table A8

Adipose (VO)	SCFD1	14	0.10	rs229227	-3.2	rs229227	-6.2	-3.2	388	top1	3.2	$1.2x10^{-3}$
Adipose (VO)	DMAC2L	14	0.045	rs1950514	3.5	rs12433794	5.1	2.4	393	enet	2.9	$4.0x10^{-3}$
Adipose (VO)	ALDH6A1	14	0.060	rs12587607	-3.0	rs8021337	4.1	2.0	409	lasso	2.8	$4.6x10^{-3}$
Adipose (VO)	FAH	15	0.11	rs11072888	-2.9	rs3974512	4.2	-2.8	525	lasso	-2.9	$3.9x10^{-2}$
Adipose (VO)	SAXO2	15	0.57	rs17269323	4.7	rs9972386	13.3	3.7	322	susie	3.2	$1.2x10^{-3}$
Adipose (VO)	RP11-413H22.3	16	0.32	rs9933064	-3.6	rs10438565	10.2	-3.4	460	enet	-3.9	$8.6x10^{-5}$
Adipose (VO)	RP11-861E21.1	18	0.29	rs17615525	-3.3	rs919	10.4	-2.7	406	lasso	-2.8	$4.8x10^{-3}$
Adipose (VO)	ZNF850	19	0.071	rs860386	3.5	rs1726703	-4.8	-3.1	276	top1	3.1	$2.3x10^{-3}$
Adipose (VO)	LOC728485	19	0.050	rs860386	3.5	rs1726703	-4.7	-3.1	276	lasso	3.1	$2.3x10^{-3}$
Adipose (VO)	ZFP30	19	0.11	rs860386	3.5	rs16958863	-6.7	2.6	292	enet	-3.1	$1.7x10^{-3}$
Adipose (VO)	CYTH2	19	0.18	rs8108419	-3.3	rs8108419	5.4	-3.3	528	susie	-3.4	$7.2x10^{-4}$
Adipose (VO)	SMARCB1	22	0.37	rs6003909	-3.4	rs9612481	-12.1	-2.8	466	enet	2.9	$4.3x10^{-3}$
Blood	CD52	1	0.25	rs4659415	-2.6	rs3795684	-13.9	2.4	392	enet	-2.9	$3.6x10^{-3}$
Blood	TMA7	3	0.033	rs2362452	-3.5	rs9815103	-5.3	-3.3	243	top1	3.3	$9.4x10^{-4}$
Blood	TREX1	3	0.25	rs2362452	-3.5	rs11797	-8.6	-3.1	243	enet	3.1	$1.7x10^{-3}$
Blood	KRT8P43	6	0.059	rs761100	3.3	rs761100	-6.2	3.3	618	top1	-3.3	$9.3x10^{-4}$
Blood	KIAA0319	6	0.26	rs761100	3.3	rs761100	-9.5	3.3	614	enet	-3.1	$2.2x10^{-3}$
Blood	ZMIZ2	7	0.069	rs17134462	2.8	rs17134462	-5.5	2.8	401	top1	-2.8	$4.8x10^{-3}$
Blood	PMS2P1	7	0.092	rs34989573	2.4	rs34989573	-7.3	2.4	291	enet	-2.9	$3.6x10^{-3}$
Blood	TRBV4-2	7	0.38	rs361489	3.1	rs361489	12.8	3.1	417	enet	3.3	$1.2x10^{-3}$
Blood	TRBV6-2	7	0.34	rs361489	3.1	rs361489	11.5	3.1	415	enet	2.8	$4.7x10^{-3}$

Continuation of Table A8

Blood	GFRA2	8	0.13	rs899425	-3.3	rs1479057	-8.0	-3.2	527	top1	3.2	$1.6x10^{-3}$
Blood	DOK2	8	0.092	rs899425	-3.3	rs11135701	-7.3	-3.2	475	top1	3.2	$1.6x10^{-3}$
Blood	UPF2	10	0.040	rs10906086	3.7	rs6602563	-4.1	3.3	464	susie	-3.3	$1.1x10^{-3}$
Blood	SERGEF	11	0.045	rs7112749	3.6	rs7115183	-3.9	-1.6	487	susie	2.9	$3.5x10^{-3}$
Blood	OR52B3P	11	0.29	rs6578490	-3.3	rs6578490	-10.9	-3.3	594	enet	3.3	$1.0x10^{-3}$
Blood	EXT2	11	0.41	rs7126447	-3.0	rs7951555	12.6	-2.6	551	lasso	-2.9	$4.2x10^{-3}$
Blood	TMEM258	11	0.048	rs174579	-4.0	rs968567	6.0	-3.3	376	lasso	-3.3	$8.9x10^{-4}$
Blood	FADS2	11	0.64	rs174579	-4.0	rs968567	19.8	-3.3	390	susie	-3.3	$9.6x10^{-4}$
Blood	FADS1	11	0.039	rs174579	-4.0	rs968567	5.5	-3.3	398	enet	-3.2	$1.6x10^{-3}$
Blood	AP001189.4	11	0.53	rs3197153	-3.5	rs1320645	15.0	-2.6	469	enet	-2.9	$3.5x10^{-3}$
Blood	POGLUT3	11	0.19	rs11212509	-4.0	rs3741060	-10.0	-3.3	318	susie	3.3	$8.9x10^{-4}$
Blood	SCFD1	14	0.21	rs229227	-3.2	rs448175	-13.4	-3.2	385	susie	3.2	$1.4x10^{-3}$
Blood	TEC (RNA gene)	15	0.072	rs1690370	-3.8	rs16976149	4.6	3.1	432	top1	3.1	$2.2x10^{-3}$
Blood	ADAMTS7P1	15	0.040	rs17269323	4.7	rs4778672	5.4	0.80	320	enet	2.8	$5.0x10^{-3}$
Blood	ANKRD11	16	0.10	rs2277908	3.3	rs2965939	-7.6	2.8	421	enet	-3.1	$2.0x10^{-3}$
Blood	PRELID3A	18	0.046	rs17615525	-3.3	rs17524639	5.2	-3.2	399	top1	-3.2	$1.4x10^{-3}$
Blood	CARD8-AS1	19	0.11	rs8108419	-3.3	rs12984288	-8.2	-2.9	514	top1	2.9	$3.9x10^{-3}$
Blood	NXT1	20	0.070	rs844828	-4.8	rs6137832	-4.7	-3.5	563	top1	3.5	$4.6x10^{-4}$
Blood	SMARCB1	22	0.22	rs6003909	-3.4	rs9612480	-11.3	-2.7	463	susie	2.9	$3.9x10^{-3}$
Blood	PDGFB	22	0.12	rs5757573	-3.4	rs5757573	-7.2	-3.4	405	enet	3.3	$1.1x10^{-3}$
Blood	MIRLET7BHG	22	0.082	rs16994265	3.0	rs7510754	-5.4	-2.5	430	lasso	3.1	$1.8x10^{-3}$
Muscle	LRRC47	1	0.12	rs3765731	3.1	rs8520	-6.2	-2.3	529	lasso	2.9	$4.0x10^{-3}$
Muscle	SBF1P2	1	0.082	rs4304595	-3.1	rs4304595	-5.3	-3.1	464	susie	3.0	$2.7x10^{-3}$
Muscle	URB2	1	0.034	rs10916540	2.8	rs16850132	-3.5	2.4	398	susie	-3.1	$2.1x10^{-3}$
Muscle	ADD2	2	0.056	rs3755342	-4.4	rs4852727	4.7	3.3	553	lasso	3.3	$9.6x10^{-4}$
Muscle	CLEC4F	2	0.13	rs3755342	-4.4	rs4852727	9.1	3.3	550	susie	3.3	$1.1x10^{-3}$

Continuation of Table A8

Muscle	CD207	2	0.10	rs3755342	-4.4	rs4852727	6.3	3.3	546	enet	2.9	$3.8x10^{-3}$
Muscle	LRRN1	3	0.28	rs711540	3.4	rs716296	13.4	2.97	651	enet	2.9	$4.0x10^{-3}$
Muscle	TMA7	3	0.54	rs2362452	-3.5	rs6442120	19.5	-3.4	248	lasso	-3.4	$6.1x10^{-4}$
Muscle	RP11-24C3.2	3	0.033	rs2362452	-3.5	rs13076076	3.7	-3.3	247	top1	-3.3	$9.0x10^{-4}$
Muscle	TREX1	3	0.38	rs2362452	-3.5	rs11797	-17.4	-3.1	248	enet	3.0	$2.5x10^{-3}$
Muscle	SHISA5	3	0.083	rs2362452	-3.5	rs2242150	-4.3	-3.4	245	lasso	3.1	$1.9x10^{-3}$
Muscle	KLHDC8B	3	0.043	rs990211	3.1	rs34890793	3.9	2.3	262	enet	3.0	$2.8x10^{-3}$
Muscle	INKA1	3	0.16	rs3197999	-3.1	rs9812791	-11.5	-3.0	316	susie	3.2	$1.6x10^{-3}$
Muscle	TMEM128	4	0.17	rs2916457	3.2	rs2916457	-6.5	3.2	361	susie	-3.0	$2.5x10^{-3}$
Muscle	MRFAP1L1	4	0.084	rs4645287	-3.8	rs4493618	-5.3	3.0	537	susie	-3.0	$2.4x10^{-3}$
Muscle	PTTG1	5	0.23	rs2431099	3.5	rs2910199	-11.3	2.7	468	lasso	-3.0	$3.2x10^{-3}$
Muscle	AIG1	6	0.10	rs3804527	-3.2	rs3804527	5.1	-3.2	471	top1	-3.2	$1.6x10^{-3}$
Muscle	RAET1E	6	0.16	rs6933642	-3.2	rs9383583	-7.1	-3.1	483	top1	3.1	$1.9x10^{-3}$
Muscle	CALU	7	0.13	rs2228075	3.1	rs2290228	-8.5	2.5	352	lasso	-3.1	$2.0x10^{-3}$
Muscle	SEC61A2	10	0.082	rs10906086	3.7	rs10906086	-6.4	3.7	521	susie	-3.6	$3.3x10^{-4}$
Muscle	NUDT5	10	0.080	rs10906086	3.7	rs10906090	-5.7	3.3	517	top1	-3.3	$8.6x10^{-4}$
Muscle	FADS2	11	0.11	rs174579	-4.0	rs968567	7.4	-3.3	389	enet	-2.9	$3.6x10^{-3}$
Muscle	CUL5	11	0.067	rs11212509	-4.0	rs7926222	-5.9	3.0	371	enet	-2.9	$3.7x10^{-3}$
Muscle	POGLUT3	11	0.20	rs11212509	-4.0	rs3741060	-11.7	-3.3	318	top1	3.3	$8.9x10^{-4}$
Muscle	FDX1	11	0.12	rs2358323	-3.5	rs2585800	9.4	-2.7	428	susie	-2.9	$4.2x10^{-3}$
Muscle	TMEM233	12	0.10	rs6490262	-2.9	rs4767835	-8.3	-2.8	480	susie	2.8	$4.9x10^{-3}$
Muscle	GCN1	12	0.048	rs4766965	-3.3	rs3932409	4.2	-1.5	374	enet	-2.8	$4.5x10^{-3}$
Muscle	CBLN3	14	0.45	rs10134603	2.9	rs2273629	-14.8	-2.7	539	enet	2.9	$4.4x10^{-3}$
Muscle	G2E3	14	0.053	rs12434151	-3.2	rs17097024	-4.8	-1.7	382	enet	3.1	$2.3x10^{-3}$
Muscle	SCFD1	14	0.077	rs229227	-3.2	rs11626600	-8.2	-2.8	384	enet	3.2	$1.4x10^{-3}$
Muscle	RP11-413H22.3	16	0.16	rs9933064	-3.6	rs10438565	8.2	-3.4	461	susie	-3.3	$8.2x10^{-4}$

Continuation of Table A8

Muscle	RP11-346C20.3	16	0.056	rs16972035	-2.7	rs6564272	-3.2	-2.5	463	susie	3.1	$2.3x10^{-3}$
Muscle	CARD8-AS1	19	0.28	rs8108419	-3.3	rs12984288	-13.7	-2.9	512	susie	2.9	$4.4x10^{-3}$
Muscle	MMP11	22	0.058	rs6003909	-3.3	rs738791	-4.6	-2.5	474	susie	2.9	$3.8x10^{-3}$
Muscle	SMARCB1	22	0.25	rs6003909	-3.3	rs9612481	-11.5	-2.8	461	lasso	2.8	$4.9x10^{-3}$
Muscle	RP3-333H23.9	22	0.027	rs5757573	-3.4	rs5757680	3.7	-2.3	385	susie	-3.5	$5.2x10^{-4}$
Liver	OXCT2P1	1	0.16	rs2254542	-3.2	rs3916164	4.1	-1.8	375	enet	-3.0	$2.6x10^{-3}$
Liver	HAO2-IT1	1	0.19	rs347910	3.4	rs6667203	7.0	2.9	443	susie	2.9	$4.4x10^{-3}$
Liver	TREX1	3	0.26	rs2362452	-3.48	rs922075	-5.3	-3.5	254	susie	3.5	$5.6x10^{-4}$
Liver	DNAH1	3	0.21	rs3774367	3.1	rs731831	3.7	-1.8	353	enet	-3.0	$2.9x10^{-3}$
Liver	AC004012.1	7	0.41	rs11977715	3.1	rs6973126	7.2	2.4	471	enet	2.9	$4.2x10^{-3}$
Liver	SOX7	8	0.46	rs11249992	3.9	rs6601505	5.2	-2.7	681	enet	-3.2	$1.3x10^{-3}$
Liver	FBRSL1	12	0.30	rs957800	3.1	rs12423664	3.63	0.87	323	susie	3.1	$2.1x10^{-3}$
Liver	TUBA3C	13	0.13	rs9507531	-3.0	rs9507531	5.0	-3.0	336	lasso	-3.2	$1.5x10^{-3}$
Liver	GOLGA8N	15	0.43	rs1258791	3.6	rs28457217	-5.7	-1.7	394	enet	3.5	$4.8x10^{-4}$
Liver	SAXO2	15	0.52	rs17269323	4.7	rs9972386	7.7	3.7	322	enet	2.8	$4.5x10^{-3}$
Liver	RP11-44F14.6	16	0.18	rs8050297	3.1	rs3095634	3.7	-2.1	387	enet	-2.8	$4.7x10^{-3}$
Liver	RP11-413H22.3	16	0.36	rs9933064	-3.6	rs7188330	7.4	-3.6	464	top1	-3.6	$3.8x10^{-4}$
Liver	RP11-676J12.7	17	0.66	rs9328722	3.49	rs8069566	10.3	3.4	423	susie	3.5	$5.3x10^{-4}$
Liver	NXN	17	0.24	rs9328722	3.5	rs8069566	5.6	3.4	435	top1	3.4	$6.2x10^{-4}$
Testis	RP11-147C23.1	1	0.20	rs6663724	-3.5	rs10783028	-5.5	-3.2	429	enet	2.8	$4.6x10^{-3}$
Testis	LY9	1	0.10	rs549103	-3.5	rs512645	3.7	3.1	465	top1	3.1	$2.1x10^{-3}$
Testis	RP11-278H7.3	1	0.15	rs1981226	3.6	rs10803175	5.0	3.5	450	susie	3.2	$1.5x10^{-3}$
Testis	FAM98A	2	0.12	rs11687252	-3.2	rs11695597	5.6	2.9	652	top1	2.9	$4.2x10^{-3}$
Testis	AC012358.7	2	0.17	rs10496038	-2.9	rs1437391	-4.5	-2.3	505	enet	3.1	$2.0x10^{-3}$

Continuation of Table A8

Testis	HK2	2	0.25	rs3732300	3.8	rs10153634	6.1	3.6	428	susie	3.0	$3.2x10^{-3}$
Testis	FBXW12	3	0.16	rs2362452	-3.5	rs13314659	7.7	-3.3	260	top1	-3.3	$1.1x10^{-3}$
Testis	CCDC51	3	0.084	rs2362452	-3.5	rs1459242	5.2	-3.4	256	susie	-3.4	$7.6x10^{-4}$
Testis	TMA7	3	0.10	rs2362452	-3.5	rs9815103	-6.3	-3.3	255	top1	3.3	$9.4x10^{-4}$
Testis	RP11-24C3.2	3	0.098	rs2362452	-3.5	rs9883927	5.7	-3.3	254	susie	-3.4	$8.0x10^{-4}$
Testis	TREX1	3	0.26	rs2362452	-3.5	rs11797	-9.0	-3.1	255	top1	3.1	$1.8x10^{-3}$
Testis	RP11-153F10.2	3	0.21	rs555183	3.3	rs12489937	6.1	-2.1	470	enet	-3.3	$1.1x10^{-3}$
Testis	Overlapping to PLOD2	3	0.36	rs7628805	-3.3	rs6710	-10.9	-2.7	430	enet	2.9	$3.2x10^{-3}$
Testis	MLF1-DT	3	0.089	rs1845138	-3.2	rs7613824	4.7	-3.2	391	enet	-2.9	$3.4x10^{-3}$
Testis	PDCD6 pseudogene	3	0.28	rs2290063	3.4	rs2290064	-6.7	3.4	284	lasso	-3.1	$1.7x10^{-3}$
Testis	TMEM128	4	0.28	rs2916457	3.2	rs2916457	-5.9	3.2	370	enet	-3.2	$1.4x10^{-3}$
Testis	WWC1	5	0.14	rs1897558	2.9	rs12655262	6.1	-2.7	566	susie	-2.9	$3.8x10^{-3}$
Testis	KIAA1191	5	0.11	rs342014	3.1	rs3815898	3.9	2.3	311	enet	3.5	$5.7x10^{-4}$
Testis	Antisense to FAM153A	5	0.32	rs6883364	-4.0	rs7708878	-7.6	3.0	296	enet	-2.9	$3.4x10^{-3}$
Testis	FAM153C	5	0.45	rs6883364	-4.0	rs7708878	-6.7	3.0	367	enet	-3.0	$2.5x10^{-3}$
Testis	RPL19P9	5	0.42	rs6883364	-4.0	rs7708878	-5.9	3.0	389	enet	-2.9	$3.2x10^{-3}$
Testis	KRT8P43	6	0.21	rs761100	3.3	rs2038135	5.7	3.1	626	enet	3.67	$2.4x10^{-4}$
Testis	LRFN2	6	0.68	rs454023	2.7	rs403319	-13.2	2.6	606	susie	-2.9	$4.0x10^{-3}$
Testis	SOGA3	6	0.20	rs2221878	3.0	rs2036966	-7.4	2.9	344	susie	-2.9	$4.1x10^{-3}$
Testis	TCP10L3 pseudogene	6	0.60	rs559097	2.9	rs1831591	-8.9	1.4	389	enet	-2.9	$3.5x10^{-3}$
Testis	LINC02889	7	0.20	rs13223444	-3.4	rs9986681	-6.2	-2.4	530	enet	3.0	$3.2x10^{-3}$
Testis	AC011290.1	7	0.15	rs4720328	3.0	rs6462932	-6.8	2.8	383	susie	-2.9	$4.3x10^{-3}$
Testis	VN1R37P	7	0.25	rs11770305	-2.7	rs11770305	-7.9	-2.7	266	enet	2.9	$3.7x10^{-3}$

Continuation of Table A8

Testis	RP11-981G7.3	8	0.22	rs11249992	3.9	rs4531010	7.3	-2.8	718	enet	-3.3	9.0×10^{-4}
Testis	LINC00208	8	0.17	rs17779791	-3.7	rs2898290	-6.6	2.9	598	susie	-2.9	4.4×10^{-3}
Testis	IFITM2	11	0.50	rs909098	3.0	rs909098	-7.6	3.0	324	susie	-2.8	4.9×10^{-3}
Testis	CAPN1-AS1	11	0.25	rs602922	-3.3	rs3953797	-7.5	2.7	321	enet	-3.2	1.1×10^{-3}
Testis	CWF19L2	11	0.27	rs7924700	4.2	rs12224337	8.6	-2.5	469	enet	-2.9	4.0×10^{-3}
Testis	ACAT1	11	0.17	rs11212509	-4.0	rs12807544	-6.6	3.0	365	enet	-3.6	3.5×10^{-4}
Testis	POGLUT3	11	0.14	rs11212509	-4.0	rs4533001	-5.7	-3.4	320	susie	3.7	2.5×10^{-4}
Testis	LINC02827	12	0.11	rs887303	3.3	rs1465264	4.2	-3.2	643	top1	-3.2	1.4×10^{-3}
Testis	MRPL42	12	0.43	rs6538411	-3.0	rs11107049	9.7	-2.5	453	lasso	-2.9	3.6×10^{-3}
Testis	ALG5	13	0.15	rs4509889	3.5	rs2997190	-5.3	2.0	528	susie	-2.8	4.7×10^{-3}
Testis	RP11-148E17.1	14	0.0081	rs12896524	3.6	rs1570130	-3.3	1.8	291	susie	-3.4	5.8×10^{-4}
Testis	Antisense to FOXN3	14	0.18	rs10484021	3.3	rs3825664	5.5	3.3	541	susie	3.0	3.2×10^{-3}
Testis	RPL18AP1	14	0.11	rs1612612	-2.9	rs3742709	3.8	-2.1	379	enet	-3.3	9.8×10^{-4}
Testis	AQR	15	0.18	rs16960222	3.5	rs2060809	6.5	2.9	399	susie	2.9	3.8×10^{-3}
Testis	DDX11L9	15	0.18	rs2121212	-3.6	rs1513981	5.3	3.1	172	lasso	2.9	3.7×10^{-3}
Testis	PRSS21	16	0.13	rs4786325	3.0	rs4785908	-5.5	2.8	307	susie	-2.8	4.6×10^{-3}
Testis	BMERB1	16	0.60	rs11647019	4.0	rs12929694	-11.5	2.7	253	susie	-3.1	2.3×10^{-3}
Testis	RP11-413H22.3	16	0.35	rs9933064	-3.6	rs7188330	8.7	-3.6	463	susie	-3.6	3.5×10^{-4}
Testis	GINS2	16	0.35	rs11649337	-3.6	rs392863	9.0	-3.3	610	lasso	-2.9	3.8×10^{-3}
Testis	LOC728485	19	0.23	rs860386	3.5	rs1726703	-8.0	-3.1	276	top1	3.1	2.3×10^{-3}
Testis	ZNF875	19	0.11	rs860386	3.5	rs10422527	4.5	3.0	284	enet	3.5	4.1×10^{-4}
Testis	NUP62	19	0.19	rs1290754	2.9	rs1044167	-3.3	-1.8	338	susie	3.0	2.8×10^{-3}
Testis	Antisense to ZNF582	19	0.51	rs10775569	-3.0	rs2904015	9.7	2.7	526	susie	3.5	4.0×10^{-4}
Testis	CD93	20	0.15	rs844828	-4.8	rs2896939	-3.1	-0.71	575	susie	3.2	1.5×10^{-3}
Testis	LINC00656	20	0.16	rs844828	-4.8	rs6083009	-4.3	-4.6	588	lasso	3.0	2.4×10^{-3}

Continuation of Table A8

Testis	SMARCB1	22	0.44	rs6003909	-3.4	rs9612481	-11.6	-2.8	465	lasso	2.9	$3.8x10^{-3}$

Abbreviations: eQTL, expression quantitative trait locus; CHR, chromosome, HSQ, mean heritability estimate; Best.GWAS.ID, most significantly associated variant in the locus; Best.GWAS.Z, z-score of most significantly associated variant in the locus; eQTL ID, best eQTL in the locus; eQTL.GWAS.Z, GWAS z-score for best eQTL; NSNP, number of SNPs in the locus; Model, best performing TWAS model; TWAS.Z, TWAS z-score; TWAS.P, TWAS p-value, enet, elastic-net regression (mixing parameter = 0.5); blup, best linear unbiased predictor from all variants; bslmm, Bayesian sparse linear model; lasso, least absolute shrinkage and selection operator; top1, single best eQTL, susie, sum of single effects regression, VO, visceral omentum; SC, subcutaneous.

Table A9. Genes associated with cisplatin-induced peripheral sensory neuropathy by TWAS ($p < 0.05$)

Tissue	Gene	CHR	HSQ	BEST.GWAS.ID	BEST.GWAS.Z	EQTL.ID	EQTL.Z	EQTL.GWAS.Z	NSNP	MODEL	TWAS.Z	TWAS.P
Nerve	CLEC4F	2	0.60	rs3755342	-4.4	rs7594319	9.9	3.2	551	susie	2.8	$4.6x10^{-3}$
Nerve	CD207	2	0.32	rs3755342	-4.4	rs7594319	8.5	3.2	547	enet	2.9	$3.4x10^{-3}$
Nerve	VAX2	2	0.10	rs3755342	-4.4	rs4852727	5.5	3.3	530	top1	3.3	$1.0x10^{-3}$
Nerve	ATP6V1B1	2	0.13	rs3755342	-4.4	rs7594319	6.9	3.2	526	top1	3.2	$1.3x10^{-3}$
Nerve	AIG1	6	0.24	rs3804527	-3.2	rs3804527	8.3	-3.2	472	susie	-3.1	$1.8x10^{-3}$
Nerve	LRP11	6	0.19	rs6933642	-3.2	rs9371544	-7.6	-2.4	474	susie	2.6	$1.0x10^{-2}$
Nerve	RAET1E-AS1	6	0.077	rs6933642	-3.2	rs6557133	7.6	-2.4	474	susie	-2.3	$2.0x10^{-2}$
Nerve	RAET1E	6	0.36	rs6933642	-3.2	rs9383583	-11.2	-3.1	489	susie	3.3	$9.2x10^{-4}$
Nerve	DOK2	8	0.14	rs899425	-3.3	rs11135701	-6.5	-3.2	477	top1	3.2	$1.6x10^{-3}$
Nerve	NUDT18	8	0.14	rs899425	-3.3	rs1973254	7.6	1.6	430	lasso	2.0	$5.0x10^{-2}$
Nerve	SEC61A2	10	0.24	rs10906086	3.7	rs2399786	-11.2	3.7	523	enet	-3.7	$1.8x10^{-4}$
Nerve	NUDT5	10	0.16	rs10906086	3.7	rs10466280	-8.2	3.4	520	susie	-3.4	$7.5x10^{-4}$
Nerve	OPTN	10	0.086	rs1630635	2.3	rs1561570	4.4	2.0	642	top1	2.0	$4.6x10^{-2}$
Nerve	TMEM258	11	0.090	rs174579	-4.0	rs174538	6.7	-3.2	374	top1	-3.2	$1.3x10^{-3}$
Nerve	FADS2	11	0.34	rs174579	-4.0	rs968567	11.3	-3.3	388	top1	-3.3	$1.1x10^{-3}$
Nerve	FADS1	11	0.20	rs174579	-4.0	rs174555	-9.2	-2.0	396	top1	2.0	$4.1x10^{-2}$
Nerve	POGLUT3	11	0.39	rs11212509	-4.0	rs3741060	-11.6	-3.3	318	lasso	3.4	$7.0x10^{-4}$
Nerve	ACTC1	15	0.11	rs16960222	3.5	rs639735	-6.4	-2.6	395	lasso	3.3	$9.4x10^{-4}$
Nerve	RP11-413H22.3	16	0.42	rs9933064	-3.6	rs10438565	12.6	-3.4	455	lasso	-3.8	$1.8x10^{-4}$
Nerve	CARD8-AS1	19	0.088	rs8108419	-3.3	rs16981882	-4.5	-3.0	514	lasso	3.5	$5.2x10^{-4}$
Nerve	CYTH2	19	0.37	rs8108419	-3.3	rs1799270	-8.4	2.0	523	enet	-2.9	$3.4x10^{-3}$
Nerve	HSD17B14	19	0.30	rs8108419	-3.3	rs16982311	-11.3	2.2	408	top1	-2.2	$3.1x10^{-2}$
Nerve	ALDH16A1	19	0.53	rs1290754	2.9	rs17206882	-13.8	-2.0	369	enet	2.1	$3.8x10^{-2}$

Continuation of Table A9

Nerve	MYH14	19	0.25	rs1290754	2.9	rs627491	5.4	0.96	360	enet	2.0	$4.4x10^{-2}$
Cerebellum	PEX13	2	0.17	rs1182688	-3.3	rs1182688	-5.2	-3.3	325	top1	3.2	$1.0x10^{-3}$
Cerebellum	KIAA1841	2	0.075	rs1182688	-3.3	rs1665278	5.0	2.9	322	susie	2.1	$4.1x10^{-2}$
Cerebellum	ZNF589	3	0.55	rs2362452	-3.5	rs9311421	9.6	-1.9	245	enet	-2.2	$2.8x10^{-2}$
Cerebellum	MRPS18AP1	3	0.52	rs2362452	-3.5	rs936427	9.0	-2.1	249	enet	-2.3	$2.3x10^{-2}$
Cerebellum	FCF1P2	3	0.13	rs2362452	-3.5	rs9311421	-4.9	-1.9	253	susie	2.1	$3.9x10^{-2}$
Cerebellum	TMA7	3	0.31	rs2362452	-3.5	rs9815103	-8.2	-3.3	255	top1	3.3	$9.4x10^{-4}$
Cerebellum	TREX1	3	0.37	rs2362452	-3.5	rs11797	-8.1	-3.1	255	top1	3.1	$1.8x10^{-3}$
Cerebellum	SHISA5	3	0.21	rs2362452	-3.5	rs3214041	-4.5	-3.3	252	susie	3.0	$3.0x10^{-3}$
Cerebellum	P4HTM	3	0.11	rs990211	3.1	rs6769821	-6.3	2.4	260	susie	-2.4	$1.6x10^{-2}$
Cerebellum	LAMB2P1	3	0.11	rs990211	3.1	rs6769821	-4.8	2.4	258	susie	-2.4	$1.8x10^{-2}$
Cerebellum	C3orf62	3	0.065	rs3197999	-3.1	rs13074318	-3.5	-1.6	277	susie	2.0	$5.0x10^{-2}$
Cerebellum	USP4	3	0.047	rs3197999	-3.1	rs6809851	4.3	2.5	278	top1	2.5	$1.4x10^{-2}$
Cerebellum	GPX1	3	0.16	rs3197999	-3.1	rs11710434	5.8	2.5	277	enet	2.6	$8.5x10^{-3}$
Cerebellum	AMT	3	0.43	rs3197999	-3.1	rs3448	-10.3	2.5	288	enet	-2.1	$3.8x10^{-2}$
Cerebellum	NICN1	3	0.10	rs3197999	-3.1	rs7429661	-4.3	2.4	288	lasso	-2.3	$2.1x10^{-2}$
Cerebellum	MST1	3	0.39	rs3197999	-3.1	rs9858542	5.5	-3.0	316	enet	-3.0	$3.1x10^{-3}$
Cerebellum	GMPPB	3	0.47	rs3197999	-3.1	rs4855885	10.4	2.1	318	susie	2.1	$3.3x10^{-2}$
Cerebellum	INKA1	3	0.49	rs3197999	-3.1	rs2352974	9.5	2.2	327	top1	2.2	$3.1x10^{-2}$
Cerebellum	RP11-1252I4.2	5	0.18	rs6883364	-4.0	rs4308500	3.8	2.7	346	top1	2.7	$7.0x10^{-3}$
Cerebellum	RPL19P9	5	0.36	rs6883364	-4.0	rs1800197	-6.8	2.5	389	susie	-2.1	$3.5x10^{-2}$
Cerebellum	N4BP3	5	0.27	rs6883364	-4.0	rs7721220	-6.4	-3.1	397	susie	3.1	$1.7x10^{-3}$
Cerebellum	DHTKD1	10	0.15	rs10906086	3.7	rs3758376	-3.9	3.3	497	top1	-3.3	$9.7x10^{-4}$
Cerebellum	SEC61A2	10	0.67	rs10906086	3.7	rs1053403	-10.4	3.5	527	top1	-3.5	$4.5x10^{-4}$
Cerebellum	GPR12	13	0.41	rs2479505	-2.8	rs943721	-8.4	-2.6	574	top1	2.6	$1.1x10^{-2}$
Cerebellum	RASL11A	13	0.19	rs12870355	-2.8	rs9512603	-4.0	-2.0	597	lasso	2.6	$8.9x10^{-3}$

Continuation of Table A9

Cerebellum	KHNYN	14	0.43	rs10134603	2.9	rs4982912	7.2	-2.7	555	susie	-2.8	$5.4x10^{-3}$
Cerebellum	SCFD1	14	0.38	rs229227	-3.2	rs12434151	8.3	-3.2	386	susie	-3.1	$1.7x10^{-3}$
Cerebellum	VCPKMT	14	0.27	rs1950514	3.5	rs2227276	-6.0	-2.0	351	susie	2.1	$3.8x10^{-2}$
Cerebellum	L2HGDH	14	0.26	rs1950514	3.5	rs11157734	-6.6	2.2	393	top1	-2.2	$2.6x10^{-2}$
Cerebellum	DMAC2L	14	0.19	rs1950514	3.5	rs1890978	3.7	2.0	393	susie	3.4	$7.9x10^{-4}$
Cerebellum	TRIM9	14	0.22	rs11844864	2.4	rs1959534	-3.9	-1.6	611	lasso	2.3	$1.9x10^{-2}$
Cerebellum	LRRC49	15	0.30	rs7180149	-3.3	rs11633699	4.2	2.9	394	lasso	3.1	$2.2x10^{-3}$
Cerebellum	LARP6	15	0.44	rs7180149	-3.3	rs11072220	-10.1	-2.7	394	susie	2.7	$6.5x10^{-3}$
Cerebellum	CT62	15	0.15	rs7180149	-3.3	rs667900	3.7	0.19	447	susie	2.2	$3.2x10^{-2}$
Cerebellum	UNC45A	15	0.28	rs2301826	-3.0	rs734252	-5.5	-1.3	491	lasso	2.3	$2.0x10^{-2}$
Cerebellum	PRC1-AS1	15	0.39	rs2301826	-3.0	rs2290203	-7.7	-3.0	487	lasso	3.0	$3.1x10^{-3}$
Cerebellum	CES1	16	0.15	rs2587878	-3.4	rs11076122	4.6	2.0	516	top1	2.0	$4.5x10^{-2}$
Cerebellum	RP11-413H22.3	16	0.42	rs9933064	-3.6	rs7188330	6.1	-3.6	463	susie	-3.3	$1.1x10^{-3}$
Cerebellum	VPREB3	22	0.30	rs6003909	-3.4	rs131442	5.9	-2.5	478	top1	-2.5	$1.4x10^{-2}$
Cerebellum	MMP11	22	0.33	rs6003909	-3.4	rs2070464	-6.0	-1.5	476	lasso	2.7	$6.8x10^{-3}$
Cerebellum	SMARCB1	22	0.45	rs6003909	-3.4	rs9612481	-7.1	-2.8	463	susie	3.0	$2.4x10^{-3}$
Cerebellum	Antisense to SLC2A11	22	0.24	rs6003909	-3.4	rs5759997	-3.4	-2.6	443	enet	2.0	$4.3x10^{-2}$
Brain	LY75	2	0.089	rs6432570	3.0	rs3828323	-6.4	3.0	492	top1	-3.0	$2.5x10^{-3}$
Brain	FAM124B	2	0.044	rs11674099	3.9	rs12613725	5.3	-3.5	444	top1	-3.5	$4.5x10^{-4}$
Brain	CDC25A	3	0.034	rs2362452	-3.5	rs745116	5.2	-2.0	228	top1	-2.0	$4.4x10^{-2}$
Brain	NME6	3	0.056	rs2362452	-3.5	rs3197223	-6.2	-2.0	256	enet	2.1	$3.5x10^{-2}$
Brain	FBXW12	3	0.064	rs2362452	-3.5	rs936426	3.7	-1.9	264	bslmm	-2.6	$1.0x10^{-2}$
Brain	TREX1	3	0.16	rs2362452	-3.5	rs6794875	-10.4	-3.5	257	bslmm	3.4	$7.3x10^{-4}$
Brain	SHISA5	3	0.060	rs2362452	-3.5	rs11797	-5.9	-3.1	263	top1	3.1	$1.8x10^{-3}$
Brain	GPX1	3	0.12	rs3197999	-3.1	rs4955430	9.6	2.5	275	blup	2.7	$8.1x10^{-3}$

Continuation of Table A9

Brain	MST1	3	0.16	rs3197999	-3.1	rs4855852	5.8	-0.64	314	blup	-2.1	$3.3x10^{-2}$
Brain	MST1R	3	0.027	rs3197999	-3.1	rs2526388	4.8	2.4	312	top1	2.4	$1.5x10^{-2}$
Brain	C3orf18	3	0.034	rs2526388	2.4	rs13076850	4.2	-1.6	265	blup	-2.4	$1.5x10^{-2}$
Brain	SSR3	3	0.085	rs13092077	-2.9	rs13092077	-4.1	-2.9	403	bslmm	2.0	$4.4x10^{-2}$
Brain	LEKR1	3	0.22	rs13092077	-2.9	rs491423	-7.2	1.1	556	lasso	-2.0	$4.8x10^{-2}$
Brain	RSRC1	3	0.040	rs1845138	-3.2	rs7613824	-3.6	-3.2	536	top1	3.2	$1.3x10^{-3}$
Brain	GFM1	3	0.063	rs1845138	-3.2	rs2307064	-4.8	-2.1	405	lasso	2.3	$2.1x10^{-2}$
Brain	RARRES1	3	0.14	rs1845138	-3.2	rs4680460	-8.2	2.2	408	lasso	-2.6	$1.1x10^{-2}$
Brain	IGFBP7	4	0.38	rs12651664	4.3	rs1718858	-12.6	-3.2	576	enet	3.1	$1.9x10^{-3}$
Brain	CENPK	5	0.25	rs16894099	3.1	rs11740053	10.7	3.1	436	top1	3.1	$2.1x10^{-3}$
Brain	RASA1	5	0.054	rs4133446	-4.2	rs6879021	3.5	-1.2	307	bslmm	-3.3	$1.0x10^{-3}$
Brain	TTC26	7	0.059	rs11525873	3.6	rs11525873	4.6	3.6	430	top1	3.6	$3.9x10^{-4}$
Brain	SEC61A2	10	0.13	rs10906086	3.7	rs12569964	6.8	-3.4	552	top1	-3.4	$5.8x10^{-4}$
Brain	PYROXD2	10	0.42	rs2147896	3.2	rs2147896	14.8	3.2	502	lasso	2.9	$3.4x10^{-3}$
Brain	HPS1	10	0.080	rs2147896	3.2	rs6584193	-4.7	-3.0	497	lasso	2.0	$4.3x10^{-2}$
Brain	CWF19L2	11	0.091	rs7924700	4.2	rs17663749	4.8	-0.25	524	blup	-2.8	$5.6x10^{-3}$
Brain	C11orf65	11	0.071	rs11212509	-4.0	rs4753840	4.2	1.6	371	blup	2.1	$3.8x10^{-2}$
Brain	KDELC2	11	0.22	rs11212509	-4.0	rs4533001	-9.7	-3.4	325	top1	3.4	$7.1x10^{-4}$
Brain	EFS	14	0.19	rs2284652	2.9	rs7142405	9.2	2.8	455	bslmm	2.8	$5.8x10^{-3}$
Brain	CBLN3	14	0.43	rs10134603	2.9	rs4982912	-10.2	-2.7	556	enet	2.9	$3.5x10^{-3}$
Brain	KHNYN	14	0.34	rs10134603	2.9	rs4982912	-9.7	-2.7	562	enet	3.0	$2.9x10^{-3}$
Brain	PRKD1	14	0.13	rs1956228	-3.1	rs11850756	4.5	0.64	461	enet	2.2	$3.2x10^{-2}$
Brain	G2E3	14	0.065	rs12434151	-3.2	rs2070340	-5.5	-2.0	397	blup	2.6	$8.2x10^{-3}$
Brain	SCFD1	14	0.16	rs229227	-3.2	rs448175	9.2	-3.2	411	top1	-3.2	$1.6x10^{-3}$
Brain	ZNF770	15	0.14	rs16960222	3.5	rs16960222	-8.7	3.5	404	top1	-3.5	$4.2x10^{-4}$
Brain	COPS2	15	0.066	rs11853754	-2.6	rs1048975	-5.0	-2.4	328	blup	3.0	$2.7x10^{-3}$

Continuation of Table A9

Brain	FLCN	17	0.17	rs4985696	-2.6	rs1736204	-5.2	-2.3	396	enet	3.0	$2.7x10^{-3}$
Brain	LLGL1	17	0.087	rs4633769	-2.4	rs2290507	4.8	2.0	270	enet	2.1	$4.0x10^{-2}$
Brain	TNFRSF11A	18	0.16	rs7243765	-3.5	rs6567263	-7.3	-2.9	502	bslmm	3.1	$1.8x10^{-3}$
Brain	LOC100505812	19	0.10	rs8108419	-3.3	rs1421674	-3.8	-2.9	514	lasso	3.6	$3.9x10^{-4}$
Brain	KCNJ14	19	0.15	rs8108419	-3.3	rs1799257	7.6	2.0	530	top1	2.0	$4.8x10^{-2}$
Brain	CYTH2	19	0.12	rs8108419	-3.3	rs1799270	-4.3	2.0	530	enet	-2.5	$1.3x10^{-2}$
Brain	HSD17B14	19	0.086	rs8108419	-3.3	rs8110220	-6.0	2.0	429	top1	-2.0	$4.4x10^{-2}$
Brain	LIN7B	19	0.077	rs281408	-2.6	rs4802561	6.3	-2.4	396	top1	-2.4	$1.5x10^{-2}$
Brain	RPRD1B	20	0.044	rs6013504	-3.4	rs6022259	3.7	-2.5	499	bslmm	-2.9	$4.4x10^{-3}$
Kidney	LNCSRLR	3	0.59	rs7628805	-3.3	rs3804664	3.7	2.5	425	susie	2.6	$9.4x10^{-3}$
Kidney	TFAP2B	6	0.43	rs7753410	3.4	rs579544	-3.2	-0.73	314	enet	2.8	$5.8x10^{-3}$
Kidney	CAPN1-AS1	11	0.66	rs602922	-3.3	rs3953797	-6.0	2.7	324	susie	-2.6	$1.0x10^{-2}$
Kidney	PPFIA2	12	0.31	rs10746190	2.7	rs1987116	4.3	2.6	384	susie	2.7	$7.5x10^{-3}$
Kidney	BICDL1	12	0.46	rs7959743	-3.3	rs2859287	3.7	-2.2	380	lasso	-3.5	$4.9x10^{-4}$
Kidney	SAXO2	15	0.69	rs17269323	4.7	rs9972386	4.5	3.7	322	lasso	2.8	$5.8x10^{-3}$
Kidney	RP11-413H22.3	16	0.69	rs9933064	-3.6	rs7188330	4.5	-3.6	463	top1	-3.6	$3.8x10^{-4}$
Kidney	RP11-861E21.1	18	0.73	rs17615525	-3.3	rs919	4.9	-2.7	408	top1	-2.7	$7.6x10^{-3}$
Kidney	MTDHP4	19	0.54	rs10417916	2.6	rs2457798	4.4	-1.7	302	enet	-2.6	$9.4x10^{-3}$
Kidney	LINC01535	19	0.82	rs860386	3.5	rs256744	5.2	-2.0	282	top1	-2.0	$4.4x10^{-2}$
Kidney	Antisense to HKR1	19	0.23	rs860386	3.5	rs2909088	3.8	2.8	286	top1	2.8	$5.9x10^{-3}$
Kidney	ZNF571-AS1	19	0.29	rs860386	3.5	rs2161520	3.3	1.5	282	susie	2.0	$4.3x10^{-2}$
Kidney	CTA-212A2.1	22	0.52	rs6000120	2.4	rs6000005	-3.5	-1.8	500	lasso	2.4	$1.7x10^{-2}$
Adipose (SC)	CASQ2	1	0.082	rs10923418	-3.8	rs10923418	4.5	-3.8	488	top1	-3.8	$1.4x10^{-4}$
Adipose (SC)	IGF2BP2 pseudogene	1	0.12	rs11240099	-3.7	rs671205	-5.0	3.5	310	lasso	-3.3	$9.3x10^{-4}$

Continuation of Table A9

Adipose (SC)	PDE4DIP pseudogene	1	0.14	rs11240099	-3.6	rs4950361	5.2	-0.86	314	enet	-2.9	$3.7x10^{-3}$
Adipose (SC)	CLEC4F	2	0.26	rs3755342	-4.4	rs7594319	9.2	3.2	553	enet	3.2	$1.6x10^{-3}$
Adipose (SC)	CD207	2	0.17	rs3755342	-4.4	rs7594319	8.5	3.2	549	susie	3.2	$1.5x10^{-3}$
Adipose (SC)	ZNF638-IT1	2	0.18	rs3755342	-4.4	rs2670740	5.1	-2.0	473	susie	-2.0	$4.1x10^{-2}$
Adipose (SC)	SOBP	6	0.058	rs3734677	3.4	rs10457162	3.5	3.4	441	lasso	3.2	$1.3x10^{-3}$
Adipose (SC)	RP1-45I4.3	6	0.17	rs3804527	-3.2	rs7750571	-6.8	-2.5	468	enet	3.1	$1.8x10^{-3}$
Adipose (SC)	AIG1	6	0.13	rs3804527	-3.2	rs3804527	6.0	-3.2	471	lasso	-3.1	$1.9x10^{-3}$
Adipose (SC)	ALAD	9	0.37	rs6478012	3.4	rs818708	9.2	-2.6	572	enet	-3.0	$3.0x10^{-3}$
Adipose (SC)	LINC00294	11	0.23	rs7933529	-3.0	rs1033716	-10.7	-2.1	302	lasso	2.1	$4.0x10^{-2}$
Adipose (SC)	KIAA1549L	11	0.20	rs2615919	3.5	rs7943651	-6.3	2.7	435	enet	-3.5	$4.3x10^{-4}$
Adipose (SC)	C11orf91	11	0.062	rs2615919	3.3	rs831611	6.6	2.0	421	top1	2.0	$4.5x10^{-2}$
Adipose (SC)	TMEM258	11	0.074	rs174579	-4.0	rs174538	6.8	-3.2	377	top1	-3.2	$1.3x10^{-3}$
Adipose (SC)	FADS2	11	0.14	rs174579	-4.0	rs968567	8.4	-3.3	391	susie	-3.3	$9.9x10^{-4}$
Adipose (SC)	POGLUT3	11	0.29	rs11212509	-4.0	rs10890853	-11.7	-3.2	320	lasso	3.5	$5.4x10^{-4}$
Adipose (SC)	FRY-AS1	13	0.056	rs798978	-3.5	rs11571809	3.7	2.5	484	susie	2.8	$5.3x10^{-3}$
Adipose (SC)	SCFD1	14	0.13	rs229227	-3.2	rs7154847	-8.3	-3.2	386	enet	3.2	$1.5x10^{-3}$
Adipose (SC)	RP11-829H16.3	14	0.043	rs229227	-3.2	rs229244	3.5	-2.7	340	susie	-2.0	$4.1x10^{-2}$

Continuation of Table A9

Adipose (SC)	EFL1	15	0.074	rs17269323	4.7	rs1503068	-4.2	1.9	322	susie	-2.1	$3.8x10^{-2}$
Adipose (SC)	SAXO2	15	0.55	rs17269323	4.7	rs9972386	15.0	3.7	322	susie	3.1	$1.7x10^{-3}$
Adipose (SC)	OGFOD1	16	0.10	rs9933064	-3.6	rs11373	-7.1	-2.5	457	lasso	2.5	$1.4x10^{-2}$
Adipose (SC)	RP11-413H22.3	16	0.37	rs9933064	-3.6	rs10438565	12.0	-3.4	461	lasso	-3.6	$3.6x10^{-4}$
Adipose (SC)	GNAL	18	0.19	rs8090294	2.7	rs8087266	7.4	2.4	445	lasso	2.4	$1.8x10^{-2}$
Adipose (SC)	PRELID3A	18	0.42	rs17615525	-3.3	rs919	15.3	-2.7	400	susie	-2.7	$7.7x10^{-3}$
Adipose (SC)	RP11-861E21.1	18	0.43	rs17615525	-3.3	rs919	13.9	-2.7	406	enet	-3.0	$2.6x10^{-3}$
Adipose (SC)	ZNF525	19	0.19	rs7255193	3.0	rs7255193	6.7	3.0	476	enet	3.2	$1.4x10^{-3}$
Adipose (SC)	ZNF765	19	0.17	rs7255193	3.0	rs4803113	4.6	-2.3	479	enet	-2.5	$1.4x10^{-2}$
Adipose (SC)	ZNF761	19	0.32	rs7255193	3.0	rs4803113	6.8	-2.3	486	enet	-2.6	$8.3x10^{-3}$
Adipose (SC)	CDC42EP1	22	0.22	rs12167035	-2.6	rs5995463	9.1	-2.5	506	top1	-2.5	$1.3x10^{-2}$
Adipose (SC)	Antisense to SUN2	22	0.083	rs7284708	-3.6	rs2235135	-3.4	-2.2	380	susie	3.5	$4.6x10^{-4}$
Adipose (SC)	APOBEC3A	22	0.049	rs5757573	-3.4	rs4821843	-3.9	-0.10	387	enet	-2.2	$3.1x10^{-2}$
Adipose (SC)	RP3-333H23.9	22	0.035	rs5757573	-3.4	rs5750818	4.3	-2.2	386	top1	-2.2	$2.5x10^{-2}$
Adipose (SC)	MGAT3	22	0.090	rs5757573	-3.4	rs5757678	-7.5	-2.4	386	lasso	2.3	$2.1x10^{-2}$
Adipose (VO)	HK2	2	0.11	rs3732300	3.8	rs2306805	6.2	3.4	418	susie	3.5	$5.3x10^{-4}$
Adipose (VO)	MYRIP	3	0.14	rs3108335	-2.7	rs4676525	-3.2	-0.20	415	enet	3.5	$5.6x10^{-4}$
Adipose (VO)	CDC25A	3	0.19	rs2362452	-3.5	rs17647717	10.2	-2.1	226	susie	-2.2	$3.2x10^{-2}$

Continuation of Table A9

Adipose (VO)	ZNF589	3	0.45	rs2362452	-3.5	rs936427	14.1	-2.1	244	susie	-2.0	$4.2x10^{-2}$
Adipose (VO)	MRPS18AP1	3	0.31	rs2362452	-3.5	rs936427	11.9	-2.1	248	enet	-2.0	$4.7x10^{-2}$
Adipose (VO)	FCF1P2	3	0.14	rs2362452	-3.5	rs7619865	-8.7	-2.1	252	susie	2.1	$3.4x10^{-2}$
Adipose (VO)	NME6	3	0.19	rs2362452	-3.5	rs17647717	-10.3	-2.1	255	lasso	2.1	$3.6x10^{-2}$
Adipose (VO)	TREX1	3	0.28	rs2362452	-3.5	rs11797	-12.4	-3.1	254	top1	3.1	$1.8x10^{-3}$
Adipose (VO)	SHISA5	3	0.061	rs2362452	-3.5	rs6442120	-4.7	-3.4	251	lasso	3.4	$8.1x10^{-4}$
Adipose (VO)	PRKAR2A	3	0.027	rs2362452	-3.5	rs990211	4.3	3.1	272	top1	3.1	$1.9x10^{-3}$
Adipose (VO)	AMT	3	0.35	rs3197999	-3.1	rs3448	-14.4	2.5	289	enet	-2.5	$1.1x10^{-2}$
Adipose (VO)	NICN1	3	0.20	rs3197999	-3.1	rs9834003	-9.8	2.4	289	susie	-2.9	$3.6x10^{-3}$
Adipose (VO)	APEH	3	0.099	rs3197999	-3.1	rs3811699	5.0	-2.7	321	susie	-2.7	$6.5x10^{-3}$
Adipose (VO)	RNF123	3	0.20	rs3197999	-3.1	rs11130218	8.6	2.4	318	susie	2.6	$8.5x10^{-3}$
Adipose (VO)	GMPPB	3	0.25	rs3197999	-3.1	rs4855882	10.7	2.2	319	susie	2.3	$2.4x10^{-2}$
Adipose (VO)	IP6K1	3	0.046	rs3197999	-3.1	rs1352889	4.5	2.2	319	top1	2.2	$2.8x10^{-2}$
Adipose (VO)	AIG1	6	0.12	rs3804527	-3.2	rs9321887	5.2	-2.9	473	lasso	-3.1	$2.0x10^{-3}$
Adipose (VO)	SEC61A2	10	0.12	rs10906086	3.7	rs10906086	-5.0	3.7	526	susie	-3.8	$1.7x10^{-4}$
Adipose (VO)	IFITM2	11	0.20	rs909098	3.0	rs909098	-6.1	3.0	323	lasso	-3.2	$1.3x10^{-3}$
Adipose (VO)	RP11.326C3.7	11	0.28	rs909098	3.0	rs909098	7.4	3.0	324	lasso	2.6	$1.1x10^{-2}$
Adipose (VO)	CD151	11	0.33	rs10794284	-3.0	rs7924806	-9.6	-1.6	419	enet	12.0	$4.7x10^{-2}$

Continuation of Table A9

Adipose (VO)	TMEM258	11	0.064	rs174579	-4.0	rs968567	4.5	-3.3	386	enet	-2.7	$8.1x10^{-3}$
Adipose (VO)	FADS2	11	0.19	rs174579	-4.0	rs968567	7.4	-3.3	399	susie	-3.3	$1.1x10^{-3}$
Adipose (VO)	POGLUT3	11	0.18	rs11212509	-4.0	rs10890858	-8.4	-3.7	319	susie	3.6	$2.8x10^{-4}$
Adipose (VO)	SCFD1	14	0.10	rs229227	-3.2	rs229227	-6.2	-3.2	388	top1	3.2	$1.2x10^{-3}$
Adipose (VO)	SAXO2	15	0.57	rs17269323	4.7	rs9972386	13.3	3.7	322	susie	3.2	$1.2x10^{-3}$
Adipose (VO)	RP11-413H22.3	16	0.32	rs9933064	-3.6	rs10438565	10.2	-3.4	460	enet	-3.9	$8.6x10^{-5}$
Adipose (VO)	ZNF850	19	0.071	rs860386	3.5	rs1726703	-4.8	-3.1	276	top1	3.1	$2.3x10^{-3}$
Adipose (VO)	LOC728485	19	0.050	rs860386	3.5	rs1726703	-4.7	-3.1	276	lasso	3.0	$2.3x10^{-3}$
Adipose (VO)	ZNF875	19	0.046	rs860386	3.5	rs10417503	4.3	2.0	284	susie	2.0	$4.9x10^{-2}$
Adipose (VO)	ZNF793	19	0.10	rs860386	3.5	rs2291004	6.8	1.8	275	lasso	2.4	$1.8x10^{-2}$
Adipose (VO)	ZNF781	19	0.31	rs860386	3.5	rs7259272	-11.8	-2.0	296	enet	2.2	$2.8x10^{-2}$
Adipose (VO)	ZFP30	19	0.11	rs860386	3.5	rs16958863	-6.7	2.6	292	enet	-3.1	$1.7x10^{-3}$
Adipose (VO)	CYTH2	19	0.18	rs8108419	-3.3	rs8108419	5.4	-3.3	528	susie	-3.4	$7.2x10^{-4}$
Adipose (VO)	HSD17B14	19	0.23	rs8108419	-3.3	rs16982311	-10.5	2.2	412	susie	-2.2	$3.1x10^{-2}$
Adipose (VO)	NUP62	19	0.14	rs1290754	2.9	rs7246342	-7.8	-2.1	338	top1	2.1	$3.3x10^{-2}$
Adipose (VO)	KLK8	19	0.18	rs8105944	3.0	rs6509509	-7.4	-2.8	565	top1	2.8	$5.7x10^{-3}$
Adipose (VO)	PTTG1IP	21	0.28	rs453176	-3.3	rs2838711	-8.3	2.3	563	susie	-2.2	$2.8x10^{-2}$
Adipose (VO)	AP001505.10	21	0.35	rs453176	-3.3	rs1985483	10.8	-2.1	593	susie	-2.0	$4.3x10^{-2}$

Continuation of Table A9

Adipose (VO)	BNAT1	21	0.17	rs2032253	-3.4	rs13048444	-6.5	-2.1	478	top1	2.1	$3.2x10^{-2}$
Adipose (VO)	COL18A1	21	0.18	rs2032253	-3.4	rs13048444	-6.0	-2.1	478	lasso	2.7	$6.2x10^{-3}$
Blood	ZNF589	3	0.59	rs2362452	-3.5	rs6787500	14.2	-2.1	233	enet	-2.3	$2.3x10^{-2}$
Blood	MRPS18AP1	3	0.22	rs2362452	-3.5	rs6787500	11.1	-2.1	237	enet	-2.1	$3.9x10^{-2}$
Blood	FCF1P2	3	0.10	rs2362452	-3.5	rs9311421	-9.3	-1.9	241	lasso	2.0	$4.8x10^{-2}$
Blood	NME6	3	0.17	rs2362452	-3.5	rs7621785	-11.0	-2.1	244	enet	2.1	$3.5x10^{-2}$
Blood	TMA7	3	0.033	rs2362452	-3.5	rs9815103	-5.3	-3.3	243	top1	3.3	$9.4x10^{-4}$
Blood	TREX1	3	0.25	rs2362452	-3.5	rs11797	-8.6	-3.1	243	enet	3.1	$1.7x10^{-3}$
Blood	AMT	3	0.16	rs3197999	-3.1	rs3448	-13.3	2.5	288	lasso	-2.6	$1.0x10^{-2}$
Blood	APEH	3	0.049	rs3197999	-3.1	rs13100791	3.8	-1.6	319	enet	-2.7	$7.1x10^{-3}$
Blood	MST1	3	0.11	rs3197999	-3.1	rs13100791	4.9	-1.6	316	enet	-2.0	$4.8x10^{-2}$
Blood	GMPPB	3	0.062	rs3197999	-3.1	rs11720705	7.2	2.3	317	enet	2.6	$9.4x10^{-3}$
Blood	UBA7	3	0.24	rs3197999	-3.1	rs7372966	-14.4	2.3	317	susie	-2.1	$3.8x10^{-2}$
Blood	KRT8P43	6	0.059	rs761100	3.3	rs761100	-6.2	3.3	618	top1	-3.3	$9.3x10^{-4}$
Blood	KIAA0319	6	0.27	rs761100	3.3	rs761100	-9.5	3.3	614	enet	-3.1	$2.2x10^{-3}$
Blood	TAS2R5	7	0.094	rs7790976	3.4	rs2301924	-6.1	1.5	477	enet	-2.1	$3.9x10^{-2}$
Blood	TRBV5-1	7	0.088	rs361489	3.2	rs361489	-5.4	3.2	428	enet	-2.8	$5.5x10^{-3}$
Blood	TRBV6-1	7	0.15	rs361489	3.2	rs361489	-5.7	3.2	430	susie	-2.2	$2.9x10^{-2}$
Blood	TRBV4-2	7	0.38	rs361489	3.1	rs361489	12.8	3.1	417	enet	3.3	$1.2x10^{-3}$
Blood	TRBV6-2	7	0.34	rs361489	3.1	rs361489	11.5	3.1	415	enet	2.8	$4.7x10^{-3}$
Blood	TRBV10-1	7	0.29	rs361489	3.3	rs2367191	-12.2	2.2	435	susie	-2.3	$2.4x10^{-2}$
Blood	GFRA2	8	0.13	rs899425	-3.3	rs1479057	-8.0	-3.2	527	top1	3.2	$1.6x10^{-3}$
Blood	DOK2	8	0.092	rs899425	-3.3	rs11135701	-7.3	-3.2	475	top1	3.2	$1.6x10^{-3}$
Blood	UPF2	10	0.040	rs10906086	3.7	rs6602563	-4.1	3.3	464	susie	-3.3	$1.1x10^{-3}$
Blood	DHTKD1	10	0.083	rs10906086	3.7	rs6602563	-5.1	3.3	492	enet	-2.3	$2.2x10^{-2}$

Continuation of Table A9

Blood	SEC61A2	10	0.16	rs10906086	3.7	rs12267387	-8.1	3.3	521	susie	-2.5	$1.2x10^{-2}$
Blood	OR52B3P	11	0.29	rs6578490	-3.3	rs6578490	-10.9	-3.3	594	enet	3.3	$1.0x10^{-3}$
Blood	TRIM68	11	0.074	rs6578490	-3.3	rs7128702	-5.6	2.2	692	susie	-2.1	$3.7x10^{-2}$
Blood	UBQLNL	11	0.11	rs4354673	2.7	rs7939159	7.3	-2.1	877	top1	-2.1	$3.8x10^{-2}$
Blood	VDAC1 pseudogene	11	0.11	rs7924553	3.2	rs11826421	-6.6	-2.0	643	susie	2.1	$4.0x10^{-2}$
Blood	TMEM258	11	0.048	rs174579	-4.0	rs968567	6.0	-3.3	376	lasso	-3.3	$8.9x10^{-4}$
Blood	FADS2	11	0.64	rs174579	-4.0	rs968567	19.8	-3.3	390	susie	-3.3	$9.6x10^{-4}$
Blood	FADS1	11	0.039	rs174579	-4.0	rs968567	5.5	-3.3	398	enet	-3.2	$1.6x10^{-3}$
Blood	CWF19L2	11	0.14	rs7924700	4.2	rs12224337	8.6	-2.5	462	susie	-2.7	$6.2x10^{-3}$
Blood	POGLUT3	11	0.19	rs11212509	-4.0	rs3741060	-10.0	-3.3	318	susie	3.3	$8.9x10^{-4}$
Blood	SCFD1	14	0.21	rs229227	-3.2	rs448175	-13.4	-3.2	385	susie	3.2	0.0014
Blood	TEC (RNA gene)	15	0.072	rs1690370	-3.8	rs16976149	4.6	3.1	432	top1	3.1	$2.2x10^{-3}$
Blood	RSL24D1	15	0.050	rs1690370	-3.8	rs9300	4.7	2.2	432	top1	2.2	$2.5x10^{-2}$
Blood	RAB27A	15	0.049	rs1690370	-3.8	rs28589384	-5.1	2.0	437	lasso	-2.3	$2.2x10^{-2}$
Blood	Antisense to FAM38A	16	0.15	rs7405095	-3.2	rs4238685	-7.3	2.2	392	top1	-2.2	$2.8x10^{-2}$
Blood	ACSF3	16	0.18	rs2277908	3.3	rs7188200	6.1	1.6	434	enet	2.4	$1.5x10^{-2}$
Blood	ANKRD11	16	0.10	rs2277908	3.3	rs2965939	-7.6	2.8	421	enet	-3.1	$2.0x10^{-3}$
Blood	PRELID3A	18	0.046	rs17615525	-3.3	rs17524639	5.2	-3.2	399	top1	-3.2	$1.4x10^{-3}$
Blood	NXT1	20	0.07	rs844828	-4.8	rs6137832	-4.7	-3.5	563	top1	3.5	$4.6x10^{-4}$
Blood	APOBEC3A	22	0.44	rs5757573	-3.4	rs17370615	6.8	-0.68	389	enet	-2.5	$1.2x10^{-2}$
Blood	PDGFB	22	0.12	rs5757573	-3.4	rs5757573	-7.2	-3.4	405	enet	3.3	$1.1x10^{-3}$
Blood	MGAT3	22	0.043	rs5757573	-3.4	rs5757678	4.9	-2.4	388	susie	-2.4	$1.7x10^{-2}$
Blood	CACNA1I	22	0.047	rs5757573	-3.4	rs5757762	3.9	0.86	390	enet	2.6	$9.6x10^{-3}$
Blood	FAM118A	22	0.75	rs16994265	3.0	rs104664	21.2	2.0	605	susie	2.2	$2.9x10^{-2}$

Continuation of Table A9

Blood	MIRLET7BHG	22	0.082	rs16994265	3.0	rs7510754	-5.4	-2.5	430	lasso	3.1	$1.8x10^{-3}$
Blood	TBC1D22A	22	0.069	rs86559	-3.2	rs4437	4.7	-0.89	555	enet	-2.0	$4.5x10^{-2}$
Muscle	ADD2	2	0.056	rs3755342	-4.4	rs4852727	4.7	3.3	553	lasso	3.3	$9.6x10^{-4}$
Muscle	CLEC4F	2	0.13	rs3755342	-4.4	rs4852727	9.1	3.3	550	susie	3.3	$1.1x10^{-3}$
Muscle	CD207	2	0.10	rs3755342	-4.4	rs4852727	6.3	3.3	546	enet	2.9	$3.8x10^{-3}$
Muscle	CDC25A	3	0.27	rs2362452	-3.5	rs936427	16.8	-2.1	220	susie	-2.1	$4.0x10^{-2}$
Muscle	CAMP	3	0.029	rs2362452	-3.5	rs11710257	4.7	-2.0	237	susie	-2.0	$4.7x10^{-2}$
Muscle	ZNF589	3	0.20	rs2362452	-3.5	rs6787500	9.7	-2.1	238	lasso	-2.0	$4.4x10^{-2}$
Muscle	MRPS18AP1	3	0.29	rs2362452	-3.5	rs6787500	14.1	-2.1	242	enet	-2.2	$2.8x10^{-2}$
Muscle	FCF1P2	3	0.075	rs2362452	-3.5	rs3197223	-8.3	-2.0	246	top1	2.0	$4.3x10^{-2}$
Muscle	NME6	3	0.18	rs2362452	-3.5	rs11710257	-13.7	-2.0	249	enet	2.4	$1.8x10^{-2}$
Muscle	TMA7	3	0.54	rs2362452	-3.5	rs6442120	19.5	-3.4	248	lasso	-3.4	$6.1x10^{-4}$
Muscle	Antisense to TMA7	3	0.033	rs2362452	-3.5	rs13076076	3.7	-3.3	247	top1	-3.3	$9.0x10^{-4}$
Muscle	TREX1	3	0.38	rs2362452	-3.5	rs11797	-17.4	-3.1	248	enet	3.0	$2.5x10^{-3}$
Muscle	SHISA5	3	0.083	rs2362452	-3.5	rs2242150	-4.3	-3.4	245	lasso	3.1	$1.9x10^{-3}$
Muscle	PRKAR2A	3	0.029	rs2362452	-3.5	rs4974083	4.6	1.7	265	susie	2.0	$4.9x10^{-2}$
Muscle	PRKAR2A-AS1	3	0.038	rs2362452	-3.5	rs9818758	-3.5	-2.1	265	susie	2.1	$3.7x10^{-2}$
Muscle	NDUFAF3	3	0.090	rs990211	3.1	rs6806356	-5.5	2.5	257	lasso	-2.2	$3.1x10^{-2}$
Muscle	QRICH1	3	0.023	rs990211	3.1	rs4955416	4.7	1.6	252	susie	2.0	$4.4x10^{-2}$
Muscle	KLHDC8B	3	0.043	rs990211	3.1	rs34890793	3.9	2.3	262	enet	3.0	$2.8x10^{-3}$
Muscle	USP4	3	0.048	rs3197999	-3.1	rs9860055	4.4	2.5	278	enet	2.1	$3.6x10^{-2}$
Muscle	RHOA-IT1	3	0.020	rs3197999	-3.1	rs3811699	3.6	-2.7	281	susie	-2.2	$2.6x10^{-2}$
Muscle	RHOA	3	0.065	rs3197999	-3.1	rs6809851	8.2	2.5	288	susie	2.6	$8.6x10^{-3}$
Muscle	AMT	3	0.19	rs3197999	-3.1	rs9860055	-14.9	2.5	288	susie	-2.6	$8.5x10^{-3}$
Muscle	NICN1	3	0.063	rs3197999	-3.1	rs4955417	-8.6	2.4	288	susie	-2.5	$1.3x10^{-2}$
Muscle	RNF123	3	0.042	rs3197999	-3.1	rs2234391	4.6	2.2	316	susie	2.6	$9.4x10^{-3}$

Continuation of Table A9

Muscle	GMPPB	3	0.23	rs3197999	-3.1	rs4855882	11.9	2.2	317	top1	2.2	$3.2x10^{-2}$
Muscle	INKA1	3	0.16	rs3197999	-3.1	rs9812791	-11.5	-3.0	316	susie	3.2	$1.6x10^{-3}$
Muscle	UBA7	3	0.085	rs3197999	-3.1	rs3197999	-5.0	-3.1	317	enet	2.7	$8.0x10^{-3}$
Muscle	SEMA3B-AS1	3	0.078	rs2526388	2.4	rs2236953	4.0	-1.8	311	susie	-2.1	$3.3x10^{-2}$
Muscle	TMEM128	4	0.17	rs2916457	3.2	rs2916457	-6.5	3.2	361	susie	-3.0	$2.5x10^{-3}$
Muscle	MRFAP1L2	4	0.16	rs4645287	-3.8	rs11946525	8.0	2.2	535	top1	2.2	$2.7x10^{-2}$
Muscle	MRFAP1L1	4	0.084	rs4645287	-3.8	rs4493618	-5.3	3.0	537	susie	-3.0	$2.4x10^{-3}$
Muscle	RP1-45I4.3	6	0.070	rs3804527	-3.2	rs1334478	-5.1	-3.1	468	susie	2.8	$5.4x10^{-3}$
Muscle	AIG1	6	0.10	rs3804527	-3.2	rs3804527	5.1	-3.2	471	top1	-3.2	$1.6x10^{-3}$
Muscle	RAET1E-AS1	6	0.018	rs6933642	-3.2	rs9371533	4.7	-2.4	469	top1	-2.4	$1.7x10^{-2}$
Muscle	RAET1E	6	0.16	rs6933642	-3.2	rs9383583	-7.1	-3.1	483	top1	3.1	$1.9x10^{-3}$
Muscle	MMRN2pseudogene	6	0.14	rs6933642	-3.2	rs7742993	12.5	-2.4	499	top1	-2.4	$1.8x10^{-2}$
Muscle	SEC61A2	10	0.082	rs10906086	3.7	rs10906086	-6.4	3.7	521	susie	-3.6	$3.3x10^{-4}$
Muscle	NUDT5	10	0.080	rs10906086	3.7	rs10906090	-5.7	3.3	517	top1	-3.3	$8.6x10^{-4}$
Muscle	OPTN	10	0.074	rs1630635	2.3	rs7095146	-5.4	-2.1	631	susie	2.1	$4.0x10^{-2}$
Muscle	RP11-819C21.1	11	0.14	rs7924700	4.2	rs4754204	-9.3	2.5	467	top1	-2.5	$1.4x10^{-2}$
Muscle	CWF19L2	11	0.17	rs7924700	4.2	rs12224337	10.8	-2.5	463	lasso	-2.0	$4.6x10^{-2}$
Muscle	CUL5	11	0.067	rs11212509	-4.0	rs7926222	-5.9	3.0	371	enet	-2.9	$3.7x10^{-3}$
Muscle	ACAT1	11	0.33	rs11212509	-4.0	rs7931681	13.7	-1.6	360	susie	-2.3	$2.0x10^{-2}$
Muscle	POGLUT3	11	0.20	rs11212509	-4.0	rs3741060	-11.7	-3.3	318	top1	3.3	$8.9x10^{-4}$
Muscle	NBEA	13	0.043	rs9542430	-2.8	rs1416200	4.8	-1.2	280	enet	-2.7	$7.8x10^{-3}$
Muscle	G2E3	14	0.053	rs12434151	-3.2	rs17097024	-4.8	-1.7	382	enet	3.1	$2.3x10^{-3}$
Muscle	SCFD1	14	0.077	rs229227	-3.2	rs11626600	-8.2	-2.8	384	enet	3.2	$1.4x10^{-3}$
Muscle	NUBPL	14	0.28	rs1034233	-3.4	rs1129622	11.8	1.8	320	lasso	2.2	$3.2x10^{-2}$
Muscle	GNAO1	16	0.070	rs9933064	-3.5	rs9923469	-5.8	1.3	479	enet	-2.2	$2.8x10^{-2}$

Continuation of Table A9

Muscle	AMFR	16	0.10	rs9933064	-3.6	rs4924	-6.8	-0.49	452	susie	2.7	$6.4x10^{-3}$
Muscle	RP11-413H22.3	16	0.16	rs9933064	-3.6	rs10438565	8.2	-3.4	461	susie	-3.3	$8.2x10^{-4}$
Muscle	VPREB3	22	0.26	rs6003909	-3.3	rs131442	12.0	-2.5	476	enet	-2.0	$4.6x10^{-2}$
Muscle	MMP11	22	0.058	rs6003909	-3.3	rs738791	-4.6	-2.5	474	susie	2.9	$3.8x10^{-3}$
Muscle	SMARCB1	22	0.25	rs6003909	-3.3	rs9612481	-11.5	-2.8	461	lasso	2.8	$4.9x10^{-3}$
Muscle	RP3-333H23.9	22	0.027	rs5757573	-3.4	rs5757680	3.7	-2.3	385	susie	-3.5	$5.2x10^{-4}$
Muscle	TAB1	22	0.056	rs5757573	-3.4	rs739141	5.2	-2.3	386	susie	-2.4	$1.8x10^{-2}$
Muscle	MGAT3	22	0.077	rs5757573	-3.4	rs5757678	-7.3	-2.4	385	enet	2.1	$3.6x10^{-2}$
Liver	AKIRIN1	1	0.22	rs2254542	-3.2	rs12036597	-3.4	-1.6	396	susie	2.7	$7.8x10^{-3}$
Liver	OXCT2P1	1	0.16	rs2254542	-3.2	rs3916164	4.1	-1.8	375	enet	-3.0	$2.6x10^{-3}$
Liver	PLEK	2	0.19	rs7563924	3.2	rs3816281	3.9	-1.8	509	enet	-2.7	$6.5x10^{-3}$
Liver	CDC25A	3	0.060	rs2362452	-3.5	rs13059037	4.0	-2.2	226	susie	-2.1	$4.1x10^{-2}$
Liver	ZNF589	3	0.28	rs2362452	-3.5	rs6787500	7.3	-2.1	244	lasso	-2.1	$4.1x10^{-2}$
Liver	MRPS18AP1	3	0.15	rs2362452	-3.5	rs7619865	4.4	-2.1	248	top1	-2.1	$3.4x10^{-2}$
Liver	FCF1P2	3	0.095	rs2362452	-3.5	rs3197223	-3.6	-2.0	252	top1	2.0	$4.3x10^{-2}$
Liver	NME6	3	0.21	rs2362452	-3.5	rs3197223	-6.3	-2.0	255	susie	2.1	$4.0x10^{-2}$
Liver	TREX1	3	0.26	rs2362452	-3.5	rs922075	-5.3	-3.5	254	susie	3.5	$5.6x10^{-4}$
Liver	P4HTM	3	0.071	rs990211	3.1	rs4955417	-3.7	2.4	256	susie	-2.2	$2.9x10^{-2}$
Liver	GMPPB	3	0.31	rs3197999	-3.1	rs9824435	7.9	2.2	316	top1	2.2	$3.1x10^{-2}$
Liver	UBA7	3	0.11	rs3197999	-3.1	rs2271961	-5.0	2.2	327	lasso	-2.2	$2.7x10^{-2}$
Liver	SOX7	8	0.46	rs11249992	3.9	rs6601505	5.2	-2.7	681	enet	-3.2	$1.3x10^{-3}$
Liver	AF131215.9	8	0.078	rs17779791	-3.7	rs7004362	3.9	1.9	629	susie	2.2	$2.9x10^{-2}$
Liver	AF131216.4	8	0.10	rs17779791	-3.7	rs2099456	4.3	2.2	647	susie	2.3	$2.3x10^{-2}$
Liver	AC145124.1	8	0.10	rs12541318	-3.4	rs2409836	-5.1	-2.0	202	top1	2.0	$4.2x10^{-2}$
Liver	FBRSL1	12	0.30	rs957800	3.1	rs12423664	3.6	0.87	323	susie	3.1	$2.1x10^{-3}$

Continuation of Table A9

Liver	ZNF268	12	0.15	rs957800	3.1	rs6560927	-4.5	-0.71	129	enet	2.3	$2.2x10^{-2}$
Liver	TUBA3C	13	0.13	rs9507531	-3.0	rs9507531	5.0	-3.0	336	lasso	-3.2	$1.5x10^{-3}$
Liver	USP12	13	0.19	rs12870355	-3.0	rs1327305	4.2	1.2	619	enet	2.8	$5.7x10^{-3}$
Liver	GOLGA8N	15	0.43	rs1258791	3.6	rs28457217	-5.7	-1.7	394	enet	3.5	$4.8x10^{-4}$
Liver	SAXO2	15	0.52	rs17269323	4.7	rs9972386	7.7	3.7	322	enet	2.8	$4.5x10^{-3}$
Liver	RP11-413H22.3	16	0.36	rs9933064	-3.6	rs7188330	7.4	-3.6	464	top1	-3.6	$3.8x10^{-4}$
Liver	RP11-676J12.7	17	0.66	rs9328722	3.5	rs8069566	10.3	3.4	423	susie	3.5	$5.3x10^{-4}$
Liver	NXN	17	0.24	rs9328722	3.5	rs8069566	5.6	3.4	435	top1	3.4	$6.2x10^{-4}$
Liver	PRELID3A	18	0.15	rs17615525	-3.3	rs919	5.4	-2.7	402	top1	-2.7	$7.6x10^{-3}$
Testis	ZNF589	3	0.49	rs2362452	-3.5	rs17647717	13.6	-2.1	245	enet	-2.1	$3.6x10^{-2}$
Testis	MRPS18AP1	3	0.57	rs2362452	-3.5	rs6787500	13.1	-2.1	249	enet	-2.1	$3.3x10^{-2}$
Testis	FCF1P2	3	0.14	rs2362452	-3.5	rs13059037	-7.2	-2.2	253	susie	2.1	$3.8x10^{-2}$
Testis	NME6	3	0.16	rs2362452	-3.5	rs7619865	-7.5	-2.1	256	enet	2.1	$3.6x10^{-2}$
Testis	FBXW12	3	0.16	rs2362452	-3.5	rs13314659	7.7	-3.3	260	top1	-3.3	$1.1x10^{-3}$
Testis	CCDC51	3	0.084	rs2362452	-3.5	rs1459242	5.2	-3.4	256	susie	-3.4	$7.6x10^{-4}$
Testis	TMA7	3	0.10	rs2362452	-3.5	rs9815103	-6.3	-3.3	255	top1	3.3	$9.4x10^{-4}$
Testis	Antisense to TMA7	3	0.098	rs2362452	-3.5	rs9883927	5.7	-3.34	254	susie	-3.4	$8.0x10^{-4}$
Testis	TREX1	3	0.26	rs2362452	-3.5	rs11797	-9.0	-3.1	255	top1	3.1	$1.8x10^{-3}$
Testis	AMT	3	0.41	rs3197999	-3.1	rs11710434	-11.6	2.5	285	enet	-2.1	$3.2x10^{-2}$
Testis	GMPPB	3	0.12	rs3197999	-3.1	rs1491983	5.6	2.3	317	top1	2.3	$2.0x10^{-2}$
Testis	LSMEM2	3	0.32	rs2526388	2.4	rs6776145	-8.2	-2.1	329	susie	2.1	$4.0x10^{-2}$
Testis	TMEM128	4	0.28	rs2916457	3.2	rs2916457	-5.9	3.2	370	enet	-3.2	$1.4x10^{-3}$
Testis	MSX2	5	0.19	rs10463040	-3.4	rs7733337	-3.6	-2.8	603	susie	2.6	$9.7x10^{-3}$
Testis	SFXN1	5	0.18	rs267399	-3.6	rs198039	-4.0	-3.1	569	enet	2.2	$3.0x10^{-2}$
Testis	KIAA1191	5	0.11	rs342014	3.1	rs3815898	3.9	2.3	311	enet	3.5	$5.7x10^{-4}$

Continuation of Table A9

Testis	ARL10	5	0.14	rs342014	3.1	rs342010	6.5	2.2	309	top1	2.2	$2.9x10^{-2}$
Testis	KRT8P43	6	0.21	rs761100	3.3	rs2038135	5.7	3.1	626	enet	3.7	$2.4x10^{-4}$
Testis	RP11-115J16.2	8	0.53	rs17729883	-3.5	rs4520167	-9.0	-2.5	603	susie	2.4	$1.7x10^{-2}$
Testis	MSRA	8	0.16	rs11249992	3.9	rs6985267	-6.3	1.3	627	enet	-2.0	$4.9x10^{-2}$
Testis	RP11-981G7.1	8	0.14	rs11249992	3.9	rs6984615	5.1	2.0	715	top1	2.0	$4.1x10^{-2}$
Testis	LINC03022	8	0.22	rs11249992	3.9	rs4531010	7.0	-2.8	715	susie	-2.7	$6.8x10^{-3}$
Testis	RP11-981G7.3	8	0.22	rs11249992	3.9	rs4531010	7.3	-2.8	718	enet	-3.3	$9.0x10^{-4}$
Testis	AF131215.9	8	0.29	rs17779791	-3.7	rs6601563	-8.5	-2.5	630	susie	2.5	$1.3x10^{-2}$
Testis	AF131215.2	8	0.28	rs17779791	-3.7	rs6601563	-9.2	-2.5	629	susie	2.5	$1.2x10^{-2}$
Testis	FAM167A-AS1	8	0.071	rs17779791	-3.7	rs2618443	-4.7	2.9	635	susie	-2.1	$4.0x10^{-2}$
Testis	LINC00208	8	0.17	rs17779791	-3.7	rs2898290	-6.6	2.9	598	susie	-2.9	$4.4x10^{-3}$
Testis	DEFB134	8	0.059	rs12541318	-3.4	rs2264306	-3.8	-1.7	321	enet	2.0	$4.5x10^{-2}$
Testis	USP17L2 pseudogene	8	0.13	rs4831763	2.4	rs4469501	5.0	1.7	180	enet	2.0	$4.4x10^{-2}$
Testis	AP005273.1	11	0.24	rs7104900	2.9	rs4930402	-8.0	2.0	346	top1	-2.0	$4.4x10^{-2}$
Testis	CAPN1-AS1	11	0.25	rs602922	-3.3	rs3953797	-7.5	2.7	321	enet	-3.3	$1.1x10^{-3}$
Testis	RP11-770G2.2	11	0.086	rs619586	-3.5	rs12146493	4.1	2.5	329	top1	2.5	$1.1x10^{-2}$
Testis	MSANTD4	11	0.14	rs11226845	-2.8	rs10895892	4.9	-1.9	371	susie	-2.0	$4.4x10^{-2}$
Testis	ASS1P13	11	0.34	rs7924700	4.2	rs3758911	-8.8	-1.3	457	susie	2.4	$1.5x10^{-2}$
Testis	CWF19L2	11	0.27	rs7924700	4.2	rs12224337	8.6	-2.5	469	enet	-2.9	$4.0x10^{-3}$
Testis	ACAT1	11	0.17	rs11212509	-4.0	rs12807544	-6.6	3.0	365	enet	-3.6	$3.5x10^{-4}$
Testis	POGLUT3	11	0.14	rs11212509	-4.0	rs4533001	-5.7	-3.4	320	susie	3.7	$2.5x10^{-4}$
Testis	RP11-148E17.1	14	0.081	rs12896524	3.6	rs1570130	-3.3	1.8	291	susie	-3.4	$5.8x10^{-4}$
Testis	RPL18AP1	14	0.11	rs1612612	-2.9	rs3742709	3.8	-2.1	379	enet	-3.3	$9.8x10^{-4}$
Testis	AC040168.2	16	0.082	rs9933064	-3.4	rs1510192	-5.3	-2.1	481	susie	2.2	$3.0x10^{-2}$
Testis	RP11-355E10.1	16	0.27	rs35395489	-3.5	rs1382362	-8.9	-2.2	483	susie	2.1	$4.0x10^{-2}$

Continuation of Table A9

Testis	GNAO1-AS1	16	0.079	rs9933064	-3.5	rs16956086	-4.3	-0.19	479	susie	2.1	$3.8x10^{-2}$
Testis	RP11-413H22.3	16	0.35	rs9933064	-3.6	rs7188330	8.7	-3.6	463	susie	-3.6	$3.5x10^{-4}$
Testis	CTD-2162K18.4	19	0.23	rs860386	3.5	rs1726703	-8.0	-3.1	276	top1	3.1	$2.3x10^{-3}$
Testis	HKR1	19	0.11	rs860386	3.5	rs10422527	4.5	3.0	284	enet	3.5	$4.1x10^{-4}$
Testis	CTD-2086O20.1	19	0.17	rs860386	3.5	rs12984458	-4.5	-1.2	286	enet	2.4	$1.8x10^{-2}$
Testis	ZNF793-AS1	19	0.26	rs860386	3.5	rs2279149	-10.0	2.1	275	top1	-2.1	$3.4x10^{-2}$
Testis	ZNF793	19	0.044	rs860386	3.5	rs10424574	-3.8	2.0	275	susie	-2.2	$2.6x10^{-2}$
Testis	ZNF540	19	0.048	rs860386	3.5	rs10409402	4.1	2.7	290	top1	2.7	$6.6x10^{-3}$
Testis	ZNF781	19	0.24	rs860386	3.5	rs7259272	-9.4	-2.0	296	top1	2.0	$4.7x10^{-2}$
Testis	Antisense to ZNF582	19	0.51	rs10775569	-3.0	rs2904015	9.7	2.7	526	susie	3.5	$4.0x10^{-4}$
Testis	CD93	20	0.15	rs844828	-4.8	rs2896939	-3.1	-0.71	575	susie	3.2	$1.5x10^{-3}$
Testis	LINC00656	20	0.16	rs844828	-4.8	rs6083009	-4.3	-4.6	588	lasso	3.0	$2.4x10^{-3}$
Testis	RP5-851M4.1	20	0.17	rs844828	-4.8	rs6048704	-4.8	-0.035	554	enet	-2.2	$3.1x10^{-2}$
Testis	LINC01431	20	0.19	rs844828	-4.8	rs6083085	6.1	2.5	564	lasso	2.0	$4.6x10^{-2}$
Testis	CST8	20	0.33	rs844828	-4.8	rs2073300	7.7	-1.0	576	susie	-2.1	$4.0x10^{-2}$
Testis	MAD1L1 pseudogene	22	0.42	rs6003909	-3.5	rs2000463	10.1	-2.1	506	top1	-2.1	$3.8x10^{-2}$
Testis	SMARCB1	22	0.44	rs6003909	-3.4	rs9612481	-11.6	-2.8	465	lasso	2.9	$3.8x10^{-3}$
Testis	DERL3	22	0.23	rs6003909	-3.4	rs9612481	5.2	-2.8	447	enet	-2.3	$1.9x10^{-2}$

Abbreviations: eQTL, expression quantitative trait locus; CHR, chromosome, HSQ, mean heritability estimate; Best.GWAS.ID, most significantly associated variant in the locus; Best.GWAS.Z, z-score of most significantly associated variant in the locus; eQTL ID, best eQTL in the locus; eQTL.GWAS.Z, GWAS z-score for best eQTL; NSNP, number of SNPs in the locus; Model, best performing TWAS model; TWAS.Z, TWAS z-score; TWAS.P, TWAS p-value, enet, elastic-net regression (mixing parameter = 0.5); blup, best linear unbiased predictor from all variants; bslmm, Bayesian sparse linear model; lasso, least absolute shrinkage and selection operator; top1, single best eQTL, susie, sum of single effects regression, VO, visceral omentum; SC, subcutaneous.

Table A10. Genes associated with cisplatin-induced tinnitus by TWAS ($p < 0.0005$)

Tissue	Gene	CHR	HSQ	BEST.GWAS.ID	BEST.GWAS.Z	EQTL.ID	EQTL.Z	EQTL.GWAS.Z	NSNP	MODEL	TWAS.Z	TWAS.P
Nerve	TMEM45A	3	0.11	rs4928110	3.7	rs12636452	-6.3	3.6	395	enet	-3.5	$5.0x10^{-4}$
Nerve	PARP14	3	0.41	rs6764971	-3.3	rs6770902	11.1	-3.1	537	enet	-4.0	$6.0x10^{-5}$
Nerve	GAS2	11	0.19	rs10734321	-3.6	rs10766971	-5.3	1.4	393	enet	-3.6	$3.5x10^{-4}$
Nerve	LCMT-1 pseudogene	16	0.055	rs4787667	3.2	rs4787667	-4.6	3.2	394	enet	-3.6	$3.4x10^{-4}$
Nerve	TXNL4B	16	0.80	rs952160	-2.3	rs4788614	7.0	-1.1	346	susie	-3.6	$3.8x10^{-4}$
Nerve	RP11-899L11.1	16	0.19	rs1110338	3.9	rs1110338	7.7	3.9	595	susie	3.7	$2.6x10^{-4}$
Cerebellum	THAP3P1	1	0.15	rs7527726	-4.0	rs7518872	4.2	-3.9	310	lasso	-3.6	$2.7x10^{-4}$
Cerebellum	RP11-164P12.5	4	0.60	rs11726420	3.8	rs1443088	10.7	-3.6	381	top1	-3.6	$3.8x10^{-4}$
Cerebellum	RP11-164P12.3	4	0.48	rs11726420	3.8	rs4235219	8.7	-3.5	381	top1	-3.5	$4.0x10^{-4}$
Cerebellum	KLHL3	5	0.20	rs10515497	4.4	rs2967797	-5.3	3.2	378	enet	-3.8	$1.7x10^{-4}$
Cerebellum	GALNT9	12	0.29	rs34708049	-4.2	rs34708049	4.4	-4.2	331	susie	-4.3	$1.8x10^{-5}$
Cerebellum	L2HGDH	14	0.26	rs2297995	3.8	rs11157734	-6.6	3.7	393	top1	-3.7	$1.8x10^{-4}$
Cerebellum	DNAJA4	15	0.21	rs3813576	2.8	rs8025691	-4.2	2.7	406	lasso	-3.6	$2.9x10^{-4}$
Brain	PROS1	3	0.11	rs36017106	-3.0	rs9289536	-6.4	2.3	165	bslmm	-3.6	$3.2x10^{-4}$
Kidney	RP11-51J9.6	8	0.71	rs11985437	3.8	rs6987718	3.4	-1.3	349	enet	-3.8	$1.7x10^{-4}$
Adipose (SC)	CD1C	1	0.083	rs7514610	3.2	rs6699757	-3.8	2.6	508	susie	-3.5	$4.1x10^{-4}$
Adipose (SC)	CENPA	2	0.21	rs3806517	3.6	rs12992046	-8.4	3.5	380	top1	-3.5	$4.8x10^{-4}$
Adipose (SC)	TMEM45A	3	0.059	rs4928110	3.7	rs4928097	-5.4	2.9	394	lasso	-3.6	$3.5x10^{-4}$
Adipose (SC)	PARP14	3	0.45	rs6764971	-3.3	rs6770902	14.0	-3.1	536	lasso	-3.6	$3.0x10^{-4}$
Adipose (SC)	CHRNA7	15	0.092	rs4779969	4.2	rs16956738	-6.0	2.5	300	enet	-3.6	$3.8x10^{-4}$
Adipose (VO)	CYP1B1	2	0.10	rs41383748	-3.2	rs13398184	-4.8	2.1	575	enet	-3.9	$9.1x10^{-5}$
Adipose (VO)	PARP14	3	0.30	rs6764971	-3.3	rs6770902	9.2	-3.1	541	susie	-3.7	$1.9x10^{-4}$

Continuation of Table A10

Adipose (VO)	DMAC2L	14	0.045	rs2297995	3.8	rs12433794	5.1	3.7	393	enet	3.6	$3.7x10^{-4}$
Blood	CDKL1	14	0.17	rs2297995	3.8	rs1465160	10.8	-2.9	429	enet	-3.5	$4.1x10^{-4}$
Blood	AQP9	15	0.084	rs2280197	-3.5	rs2899619	5.5	-3.2	662	susie	-3.5	$4.5x10^{-4}$
Blood	CHKB	22	0.23	rs28513473	2.9	rs131750	8.0	2.6	284	enet	3.6	$3.2x10^{-4}$
Muscle	L2HGDH	14	0.12	rs2297995	3.8	rs2297995	9.3	3.8	379	enet	3.8	$1.3x10^{-4}$
Muscle	DMAC2L	14	0.22	rs2297995	3.8	rs2275592	11.8	3.7	379	top1	3.7	$2.4x10^{-4}$
Liver	RP4-781K5.6	1	0.26	rs541021	4.7	rs476875	6.2	-3.5	551	susie	-3.9	$1.2x10^{-4}$
Liver	MCPH1-DT	8	0.20	rs2916749	3.1	rs12546419	3.5	1.9	982	susie	3.5	$4.9x10^{-4}$
Testis	RP4-781K5.6	1	0.19	rs541021	4.7	rs605957	7.0	-4.0	550	enet	-4.2	$2.4x10^{-5}$
Testis	CCDC13	3	0.21	rs6768356	-3.3	rs13072026	6.5	2.0	450	enet	3.8	$1.5x10^{-4}$
Testis	PARP14	3	0.47	rs6764971	-3.3	rs6770902	9.8	-3.1	542	enet	-3.7	$2.5x10^{-4}$
Testis	TMEM212-IT1	3	0.13	rs4618247	3.0	rs4618247	-4.8	3.0	446	enet	-3.5	$4.3x10^{-4}$
Testis	ATP6V0A4	7	0.41	rs999228	3.7	rs999228	8.1	3.7	406	enet	4.2	$3.0x10^{-5}$
Testis	ELOBP2	11	0.34	rs7113818	3.0	rs12805829	7.0	-2.4	468	enet	-3.6	$3.6x10^{-4}$
Testis	PSPC1	13	0.18	rs7984806	-2.8	rs2290810	-5.8	-2.5	309	susie	3.6	$3.5x10^{-4}$
Testis	ANKRD20A19P	13	0.38	rs2765107	4.6	rs17071064	-9.6	3.2	737	lasso	-4.2	$3.2x10^{-5}$
Testis	HCN2 pseudogene	15	0.11	rs4779969	4.2	rs6494165	-4.9	4.1	293	top1	-4.1	$3.8x10^{-5}$
Testis	GOLGA8K	15	0.25	rs4779969	4.2	rs6494165	-6.0	4.1	336	top1	-4.1	$3.8x10^{-5}$

Abbreviations: eQTL, expression quantitative trait locus; CHR, chromosome, HSQ, mean heritability estimate; Best.GWAS.ID, most significantly associated variant in the locus; Best.GWAS.Z, z-score of most significantly associated variant in the locus; eQTL ID, best eQTL in the locus; eQTL.GWAS.Z, GWAS z-score for best eQTL; NSNP, number of SNPs in the locus; Model, best performing TWAS model; TWAS.Z, TWAS z-score; TWAS.P, TWAS p-value, enet, elastic-net regression (mixing parameter = 0.5); blup, best linear unbiased predictor from all variants; bslmm, Bayesian sparse linear model; lasso, least absolute shrinkage and selection operator; top1, single best eQTL, susie, sum of single effects regression, VO, visceral omentum; SC, subcutaneous.

Table A11. Genes associated with cisplatin-induced tinnitus by TWAS ($p < 0.005$)

Tissue	Gene	CHR	HSQ	BEST.GWAS.ID	BEST.GWAS.Z	EQTL.ID	EQTL.Z	EQTL.GWAS.Z	NSNP	MODEL	TWAS.Z	TWAS.P
Nerve	NKAIN1	1	0.057	rs2050815	2.9	rs12087046	-3.5	2.9	425	top1	-2.9	$3.8x10^{-3}$
Nerve	ZMPSTE24-DT	1	0.099	rs4660156	3.1	rs12757549	-6.5	-3.0	408	susie	2.9	$3.3x10^{-3}$
Nerve	CD1E	1	0.11	rs7514610	3.2	rs1065457	3.8	-0.26	512	enet	-3.1	$1.9x10^{-3}$
Nerve	SMYD2	1	0.16	rs2919490	2.4	rs1472444	-5.8	-2.1	541	enet	2.9	$3.3x10^{-3}$
Nerve	LINC01376	2	0.13	rs4233765	3.7	rs6707044	6.4	3.4	555	top1	3.4	$6.4x10^{-4}$
Nerve	CENPA	2	0.43	rs3806517	3.6	rs12992046	-12.0	3.5	381	enet	-2.9	$4.2x10^{-3}$
Nerve	Antisense to IMPDH2 and QRICH1	3	0.037	rs7619016	2.9	rs7429661	3.6	2.9	253	top1	2.9	$4.1x10^{-3}$
Nerve	TMEM45A	3	0.11	rs4928110	3.7	rs12636452	-6.3	3.6	395	enet	-3.5	$5.0x10^{-4}$
Nerve	PARP14	3	0.41	rs6764971	-3.3	rs6770902	11.1	-3.1	537	enet	-4.0	$6.0x10^{-5}$
Nerve	ABCF3	3	0.34	rs2230570	2.9	rs2230570	8.2	2.9	483	susie	3.0	$2.5x10^{-3}$
Nerve	RP11-121C2.2	4	0.093	rs1440221	3.5	rs9997555	-6.0	2.8	424	susie	-3.0	$2.9x10^{-3}$
Nerve	PLCXD3	5	0.13	rs380649	-2.7	rs380649	5.6	-2.7	378	susie	-3.0	$3.1x10^{-3}$
Nerve	CCT7P2	5	0.12	rs11958890	3.4	rs2644790	6.4	3.2	291	top1	3.2	$1.3x10^{-3}$
Nerve	KLHL3	5	0.058	rs10515497	4.4	rs4371746	4.7	3.1	376	susie	3.4	$6.6x10^{-4}$
Nerve	SYNJ2	6	0.30	rs3003561	3.4	rs751873	6.9	-1.6	564	susie	-3.0	$2.6x10^{-3}$
Nerve	MCPH1	8	0.21	rs2916749	3.1	rs2083914	8.7	3.1	959	top1	3.1	$2.2x10^{-3}$
Nerve	RP11-722E23.2	8	0.098	rs1829189	3.3	rs10097936	7.7	3.0	240	top1	3.0	$2.6x10^{-3}$
Nerve	SFTA1P	10	0.081	rs11256835	3.3	rs11256835	5.4	3.3	637	top1	3.3	$9.0x10^{-4}$
Nerve	GAS2	11	0.19	rs10734321	-3.6	rs10766971	-5.3	1.4	393	enet	-3.6	$3.5x10^{-4}$
Nerve	PTPRJ	11	0.12	rs10838805	3.6	rs1039481	7.4	3.4	231	top1	3.4	$7.1x10^{-4}$
Nerve	RAB35-AS1	12	0.15	rs3742039	2.9	rs3852587	6.8	-2.0	352	enet	-3.1	$2.0x10^{-3}$

Continuation of Table A11

Nerve	RP11-158L12.4	12	0.31	rs10846834	-3.4	rs12581512	13.7	-3.0	529	lasso	-3.1	$1.7x10^{-3}$
Nerve	AC138466.5	12	0.079	rs34708049	-4.2	rs6598199	5.5	2.9	310	top1	2.9	$3.4x10^{-3}$
Nerve	RGCC	13	0.21	rs9532718	-3.5	rs12429256	10.3	2.8	342	lasso	3.0	$3.0x10^{-3}$
Nerve	LINC01588	14	0.058	rs2297995	3.8	rs11157718	3.8	1.2	350	susie	3.4	$7.6x10^{-4}$
Nerve	GCATP1	14	0.051	rs8012691	-2.9	rs8012691	5.0	-2.9	363	susie	-2.9	$4.3x10^{-3}$
Nerve	ADAM21	14	0.043	rs2182973	3.4	rs10145919	-3.9	3.2	526	top1	-3.2	$1.5x10^{-3}$
Nerve	ZFYVE1	14	0.041	rs6574091	2.7	rs4514602	-4.3	2.3	440	lasso	-2.9	$4.1x10^{-3}$
Nerve	CHRNA7	15	0.080	rs4779969	4.2	rs6494165	-6.3	4.1	300	enet	-3.3	$9.2x10^{-4}$
Nerve	CERS3	15	0.31	rs1972053	-2.8	rs4578625	-7.7	-2.7	588	enet	3.0	$2.8x10^{-3}$
Nerve	LCMT-1 pseudogene	16	0.055	rs4787667	3.2	rs4787667	-4.6	3.2	394	enet	-3.6	$3.4x10^{-4}$
Nerve	SCML2P2	16	0.21	rs4787667	3.2	rs7498149	-8.3	2.8	391	enet	-2.9	$4.2x10^{-3}$
Nerve	TXNL4B	16	0.8	rs952160	-2.3	rs4788614	7.0	-1.1	346	susie	-3.6	$3.8x10^{-4}$
Nerve	LINC02188	16	0.28	rs1110338	3.9	rs1559451	-5.9	-2.5	864	enet	3.1	$1.8x10^{-3}$
Nerve	RP11-899L11.1	16	0.19	rs1110338	3.9	rs1110338	7.7	3.9	595	susie	3.7	$2.6x10^{-4}$
Nerve	TMEM220-AS1	17	0.074	rs9907053	-3.1	rs16943983	-3.3	0.60	489	susie	-2.9	$3.7x10^{-3}$
Nerve	TIMM13	19	0.19	rs7248779	-2.8	rs7248779	5.6	-2.8	417	top1	-2.8	$4.7x10^{-3}$
Nerve	GIPC3	19	0.41	rs122691	-2.8	rs8113232	-8.9	2.3	369	enet	-3.1	$1.8x10^{-3}$
Nerve	BRME1	19	0.082	rs2112464	3.0	rs6511898	4.3	2.8	301	top1	2.8	$4.6x10^{-3}$
Nerve	CHCHD10	22	0.11	rs2070457	3.6	rs2070457	-5.2	3.6	479	lasso	-3.2	$1.4x10^{-3}$
Cerebellum	CASP9	1	0.28	rs4233532	-2.8	rs10927797	-7.0	-2.6	505	enet	3.2	$1.4x10^{-3}$
Cerebellum	THAP3P1	1	0.15	rs7527726	-4.0	rs7518872	4.2	-3.9	310	lasso	-3.6	$2.7x10^{-4}$
Cerebellum	CYP1B1-AS1	2	0.19	rs41383748	-3.2	rs17490310	4.7	-3.1	592	top1	-3.1	$2.1x10^{-3}$
Cerebellum	OXTR	3	0.16	rs884237	2.8	rs237852	-3.9	2.0	737	susie	-2.8	$4.7x10^{-3}$
Cerebellum	P4HTM	3	0.11	rs7619016	2.9	rs6769821	-6.3	2.8	260	susie	-2.8	$4.7x10^{-3}$

Continuation of Table A11

Cerebellum	USP4	3	0.047	rs7619016	2.9	rs6809851	4.3	2.9	278	top1	2.9	$4.0x10^{-3}$
Cerebellum	PARP14	3	0.16	rs6764971	-3.3	rs10934611	4.9	-3.1	547	susie	-3.4	$6.8x10^{-4}$
Cerebellum	RP11-164P12.5	4	0.60	rs11726420	3.8	rs1443088	10.7	-3.6	381	top1	-3.6	$3.8x10^{-4}$
Cerebellum	Antisense to PET112L	4	0.48	rs11726420	3.8	rs4235219	8.7	-3.5	381	top1	-3.5	$4.0x10^{-4}$
Cerebellum	KLHL3	5	0.20	rs10515497	4.4	rs2967797	-5.3	3.2	378	enet	-3.8	$1.7x10^{-4}$
Cerebellum	WNT8A	5	0.090	rs10515497	4.4	rs4835768	4.2	-4.3	313	top1	-4.3	$1.4x10^{-5}$
Cerebellum	MCPH1	8	0.19	rs2916749	3.1	rs2083914	5.5	3.1	977	lasso	3.0	$2.5x10^{-3}$
Cerebellum	PHYHIP	8	0.48	rs4872429	3.2	rs4872429	8.0	3.2	463	top1	3.2	$1.2x10^{-3}$
Cerebellum	STMN4	8	0.17	rs7834529	2.9	rs12056620	3.7	1.2	631	susie	3.2	$1.6x10^{-3}$
Cerebellum	FUT10	8	0.16	rs1829189	3.3	rs2676403	5.9	2.8	251	susie	2.8	$4.5x10^{-3}$
Cerebellum	LETMD1	12	0.22	rs12582592	3.2	rs12582592	5.5	3.2	390	susie	3.1	$1.8x10^{-3}$
Cerebellum	HECTD4	12	0.077	rs4767293	-2.9	rs4767293	-3.9	-2.9	263	top1	2.9	$4.1x10^{-3}$
Cerebellum	AACS	12	0.33	rs10846834	-3.4	rs1080910	6.5	-3.1	545	susie	-3.1	$2.0x10^{-3}$
Cerebellum	RP11-158L12.4	12	0.64	rs10846834	-3.4	rs12581512	10.5	-3.0	540	top1	-3.0	$2.9x10^{-3}$
Cerebellum	GALNT9	12	0.29	rs34708049	-4.2	rs34708049	4.4	-4.2	331	susie	-4.3	$1.8x10^{-5}$
Cerebellum	L2HGDH	14	0.26	rs2297995	3.8	rs11157734	-6.6	3.7	393	top1	-3.7	$1.8x10^{-4}$
Cerebellum	KTN1	14	0.22	rs1188080	3.6	rs12432887	-6.2	3.1	502	top1	-3.1	$2.1x10^{-3}$
Cerebellum	SCG5	15	0.28	rs17228887	3.3	rs345761	3.1	1.4	419	susie	3.0	$2.6x10^{-3}$
Cerebellum	SEMA6D	15	0.23	rs7176161	3.1	rs7176161	5.6	3.1	424	lasso	3.2	$1.5x10^{-3}$
Cerebellum	DNAJA4	15	0.21	rs3813576	2.8	rs8025691	-4.2	2.7	406	lasso	-3.6	$2.9x10^{-4}$
Cerebellum	CTD-3037G24.5	16	0.20	rs7203886	4.5	rs8063664	-4.8	-2.2	666	susie	2.8	$4.7x10^{-3}$
Cerebellum	TRIP11 pseudogene	16	0.25	rs4787667	3.2	rs7498149	-5.3	2.8	394	susie	-2.9	$3.7x10^{-3}$
Cerebellum	MINK1	17	0.32	rs12450045	-3.5	rs12450045	6.0	-3.5	428	top1	-3.5	$5.2x10^{-4}$
Cerebellum	TRAPPC5	19	0.52	rs4804802	3.4	rs4804802	-7.2	3.4	437	top1	-3.4	$5.9x10^{-4}$

Continuation of Table A11

Cerebellum	CD209	19	0.51	rs4804802	3.4	rs4804802	-7.7	3.4	414	susie	-3.1	$2.2x10^{-3}$
Cerebellum	ZNF221	19	0.16	rs400591	3.1	rs377931	5.2	3.0	462	top1	3.0	$3.2x10^{-3}$
Brain	QSOX1	1	0.091	rs3767183	-3.2	rs3842888	-4.6	-3.0	480	top1	3.0	$2.6x10^{-3}$
Brain	DPYSL5	2	0.24	rs3806517	3.6	rs12991828	-10.6	-2.7	409	enet	2.8	$4.8x10^{-3}$
Brain	GALNT13	2	0.089	rs16836088	3.7	rs16834756	4.5	2.3	672	blup	3.3	$9.1x10^{-4}$
Brain	ITGA4	2	0.067	rs4077924	3.6	rs10205700	-4.3	3.0	387	enet	-3.3	$8.3x10^{-4}$
Brain	VIPR1	3	0.11	rs6768356	-3.3	rs6768356	5.6	-3.3	480	top1	-3.3	$1.1x10^{-3}$
Brain	ABHD14B	3	0.056	rs745618	3.4	rs929533	-3.7	3.0	242	top1	-3.0	$2.6x10^{-3}$
Brain	HTR1F	3	0.089	rs7648805	3.8	rs2046796	-6.7	2.9	312	top1	-2.9	$3.3x10^{-3}$
Brain	PROS1	3	0.11	rs36017106	-3.0	rs9289536	-6.4	2.3	165	bslmm	-3.6	$3.2x10^{-4}$
Brain	CENPE	4	0.098	rs3796974	2.9	rs11734396	7.2	-2.6	361	lasso	-2.9	$4.4x10^{-3}$
Brain	METTL14	4	0.057	rs298981	3.7	rs960738	-5.2	3.2	357	top1	-3.2	$1.2x10^{-3}$
Brain	GFM2	5	0.38	rs2218517	3.5	rs2218517	-12.0	3.5	517	lasso	-3.4	$6.4x10^{-4}$
Brain	ELOVL5	6	0.092	rs209500	-3.3	rs209500	-6.9	-3.3	583	top1	3.3	$1.1x10^{-3}$
Brain	SENP6	6	0.067	rs6453843	2.8	rs2647404	-4.2	2.4	364	enet	-3.0	$2.3x10^{-3}$
Brain	HSF2	6	0.14	rs7740530	2.9	rs9375131	-8.3	-2.4	446	bslmm	2.8	$5.0x10^{-3}$
Brain	EPDR1	7	0.24	rs2722309	-3.0	rs1349394	7.4	2.7	597	lasso	3.0	$3.0x10^{-3}$
Brain	KRBA1	7	0.053	rs1636367	-3.0	rs6965416	-3.4	-0.67	315	bslmm	3.0	$2.5x10^{-3}$
Brain	PENK	8	0.14	rs10108774	3.2	rs1440757	4.7	2.1	422	bslmm	3.3	$8.5x10^{-4}$
Brain	INTS4	11	0.10	rs1793343	-3.9	rs3824865	5.3	1.7	385	enet	2.9	$4.1x10^{-3}$
Brain	LETMD1	12	0.11	rs12582592	3.2	rs3759406	5.2	2.9	398	top1	2.9	$3.9x10^{-3}$
Brain	TMEM132B	12	0.11	rs10846834	-3.4	rs12580291	5.1	-2.6	762	bslmm	-2.9	$4.0x10^{-3}$
Brain	EP400NL	12	0.15	rs34708049	-4.2	rs6598199	7.3	2.9	323	lasso	3.0	$2.7x10^{-3}$
Brain	ATP2C2	16	0.073	rs11649239	-3.4	rs12445007	5.2	-2.7	940	lasso	-3.2	$1.2x10^{-3}$
Brain	DOT1L	19	0.049	rs8108653	3.0	rs878439	-3.5	0.14	431	blup	3.0	$2.3x10^{-3}$
Brain	ZNF417	19	0.065	rs10415313	-2.6	rs1529329	-4.3	-0.029	477	enet	-2.9	$4.2x10^{-3}$

Continuation of Table A11

Brain	HNF4A	20	0.22	rs6017227	3.3	rs6031598	-9.7	2.9	528	top1	-2.9	$4.0x10^{-3}$
Brain	RRP1	21	0.055	rs3761385	-3.2	rs3761385	-4.4	-3.2	457	top1	3.2	$1.3x10^{-3}$
Brain	RFPL2	22	0.058	rs9621453	2.7	rs16990001	5.4	-2.6	547	lasso	-2.9	$4.4x10^{-3}$
Kidney	RP1-136B1.1	6	0.77	rs12216224	3.4	rs17608626	3.9	-1.3	549	lasso	-3.1	$1.7x10^{-3}$
Kidney	RP11-51J9.6	8	0.71	rs11985437	3.8	rs6987718	3.4	-1.3	349	enet	-3.8	$1.7x10^{-4}$
Kidney	FUT10	8	0.39	rs1829189	3.3	rs2676403	3.8	2.8	251	susie	3.0	$2.6x10^{-3}$
Kidney	DMAC2L	14	0.31	rs2297995	3.8	rs1955926	3.5	3.2	394	top1	3.2	$1.4x10^{-3}$
Adipose (SC)	CLIC4	1	0.074	rs3120842	-3.2	rs11249167	-5.2	-3.0	455	top1	3.0	$3.0x10^{-3}$
Adipose (SC)	ZMPSTE24-DT	1	0.11	rs4660156	3.1	rs12757549	-8.1	-3.0	407	susie	3.0	$3.2x10^{-3}$
Adipose (SC)	FGGY	1	0.16	rs12752499	2.9	rs591512	4.6	2.0	392	susie	2.9	$3.6x10^{-3}$
Adipose (SC)	DRAM2	1	0.57	rs11584291	3.5	rs3818797	16.9	2.6	572	enet	2.8	$4.8x10^{-3}$
Adipose (SC)	CHI3L2	1	0.19	rs11584291	3.5	rs7515361	7.8	2.6	557	susie	3.3	$9.3x10^{-4}$
Adipose (SC)	CHIA	1	0.30	rs11584291	3.5	rs7515361	11.9	2.6	553	lasso	2.9	$4.0x10^{-3}$
Adipose (SC)	CD1A	1	0.057	rs7514610	3.2	rs17679007	-4.3	2.6	470	enet	-2.9	$4.0x10^{-3}$
Adipose (SC)	CD1C	1	0.083	rs7514610	3.2	rs6699757	-3.8	2.6	508	susie	-3.5	$4.1x10^{-4}$
Adipose (SC)	EPHX1	1	0.061	rs14868	-3.2	rs2740168	4.2	3.0	407	lasso	3.1	$1.9x10^{-3}$
Adipose (SC)	SLC35F6	2	0.080	rs3806517	3.6	rs3845684	-6.3	-3.0	380	susie	2.9	$4.2x10^{-3}$
Adipose (SC)	CENPA	2	0.21	rs3806517	3.6	rs12992046	-8.4	3.5	380	top1	-3.5	$4.8x10^{-4}$
Adipose (SC)	TIMP4	3	0.10	rs7627256	-3.2	rs34206487	-5.3	2.0	507	susie	-2.8	$5.0x10^{-3}$
Adipose (SC)	HTR1F	3	0.082	rs7648805	3.8	rs959132	5.1	-2.2	295	lasso	-2.9	$4.4x10^{-3}$
Adipose (SC)	TMEM45A	3	0.059	rs4928110	3.7	rs4928097	-5.4	2.9	394	lasso	-3.6	$3.5x10^{-4}$
Adipose (SC)	PARP14	3	0.45	rs6764971	-3.3	rs6770902	14.0	-3.1	536	lasso	-3.6	$3.0x10^{-4}$
Adipose (SC)	NFXL1	4	0.14	rs1440221	3.5	rs4695317	-8.1	-2.9	412	top1	2.9	$3.7x10^{-3}$
Adipose (SC)	EPDR1	7	0.22	rs2722309	-3.0	rs2044831	8.5	1.1	577	enet	2.8	$4.5x10^{-3}$
Adipose (SC)	RP11-91J19.2	8	0.069	rs12676364	3.6	rs2034355	4.3	2.7	431	enet	3.0	$3.0x10^{-3}$

Continuation of Table A11

Adipose (SC)	RP11-722E23.2	8	0.096	rs1829189	3.3	rs10097936	8.0	3.0	240	top1	3.0	$2.6x10^{-3}$
Adipose (SC)	FUT10	8	0.30	rs1829189	3.3	rs10097936	13.5	3.0	251	lasso	3.0	$3.0x10^{-3}$
Adipose (SC)	MAK16	8	0.051	rs1829189	3.3	rs2037213	5.7	3.2	254	susie	3.1	$2.1x10^{-3}$
Adipose (SC)	CAT	11	0.20	rs7121766	3.2	rs2420388	-9.6	-2.4	606	enet	2.8	$4.9x10^{-3}$
Adipose (SC)	PTPRJ	11	0.082	rs10838805	3.6	rs10769317	6.9	3.5	225	susie	3.5	$5.5x10^{-4}$
Adipose (SC)	AQP11	11	0.044	rs1793343	-3.9	rs1630344	-4.7	-3.8	364	enet	2.9	$3.3x10^{-3}$
Adipose (SC)	RECQL	12	0.16	rs12810446	2.8	rs7965230	-6.2	2.0	542	enet	-2.8	$4.6x10^{-3}$
Adipose (SC)	RP11-158L12.4	12	0.25	rs10846834	-3.4	rs12581512	11.3	-3.0	531	top1	-3.0	$2.9x10^{-3}$
Adipose (SC)	AC138466.5	12	0.095	rs34708049	-4.2	rs7976069	6.1	2.9	314	top1	2.9	$3.4x10^{-3}$
Adipose (SC)	C1QTNF9B	13	0.13	rs2765107	4.6	rs11551114	-7.1	2.6	750	lasso	-3.1	$2.0x10^{-3}$
Adipose (SC)	CHRNA7	15	0.092	rs4779969	4.2	rs16956738	-6.0	2.5	300	enet	-3.6	$3.8x10^{-4}$
Adipose (SC)	LINC02256	15	0.25	rs4779969	4.2	rs28457217	-8.3	1.6	379	enet	-3.2	$1.3x10^{-3}$
Adipose (SC)	Antisense to SPTBN5	15	0.11	rs1704394	3.3	rs1618332	-5.0	-1.0	416	enet	2.9	$3.6x10^{-3}$
Adipose (SC)	DUT	15	0.13	rs12909189	3.2	rs3784618	-4.5	-2.2	300	susie	3.0	$2.4x10^{-3}$
Adipose (SC)	RAB27A	15	0.067	rs8040756	-3.0	rs1915202	4.1	-2.5	437	enet	-2.9	$4.1x10^{-3}$
Adipose (SC)	MFGE8	15	0.14	rs6496536	2.6	rs1961839	-4.7	2.5	452	enet	-3.5	$5.1x10^{-4}$
Adipose (SC)	MFSD13B	16	0.065	rs715462	-2.7	rs10521117	3.1	-2.1	200	susie	-3.0	$2.9x10^{-3}$
Adipose (SC)	AC009093.6	16	0.26	rs11646140	-3.0	rs9929469	-10.5	-2.3	159	enet	2.8	$4.8x10^{-3}$
Adipose (SC)	AC007336.1	16	0.077	rs3785152	-3.1	rs13339550	5.4	-2.8	654	enet	-2.8	$4.6x10^{-3}$
Adipose (SC)	GP1BA	17	0.12	rs12450045	-3.5	rs9905341	6.4	-2.8	446	susie	-2.8	$4.9x10^{-3}$
Adipose (SC)	DHPS	19	0.18	rs1017180	-2.9	rs8110078	-4.1	-1.5	295	enet	2.8	$4.5x10^{-3}$
Adipose (SC)	SLC1A5	19	0.15	rs4804030	-2.6	rs8105903	7.2	2.3	334	susie	3.2	$1.3x10^{-3}$
Adipose (SC)	PANK2	20	0.092	rs12480318	3.2	rs12480318	5.4	3.2	556	enet	3.1	$2.3x10^{-3}$
Adipose (SC)	ARHGAP8	22	0.10	rs8138173	3.1	rs3761481	4.9	-1.4	707	enet	-3.1	$2.0x10^{-3}$
Adipose (SC)	CHKB	22	0.43	rs28513473	2.9	rs131760	-10.9	-2.6	284	enet	3.4	$6.4x10^{-4}$

Continuation of Table A11

Adipose (VO)	SLC35F6	2	0.071	rs3806517	3.6	rs11126681	-5.3	-2.9	382	top1	2.9	$3.4x10^{-3}$
Adipose (VO)	CYP1B1	2	0.10	rs41383748	-3.2	rs13398184	-4.8	2.1	575	enet	-3.9	$9.1x10^{-5}$
Adipose (VO)	NICN1	3	0.20	rs7619016	2.9	rs9834003	-9.8	2.8	289	susie	-2.8	$4.6x10^{-3}$
Adipose (VO)	TMEM45A	3	0.11	rs4928110	3.7	rs12636452	-5.9	3.6	395	enet	-3.1	$1.7x10^{-3}$
Adipose (VO)	PARP14	3	0.30	rs6764971	-3.3	rs6770902	9.2	-3.1	541	susie	-3.7	$1.9x10^{-4}$
Adipose (VO)	TTC33	5	0.054	rs2459465	-3.2	rs13355305	3.9	2.9	427	top1	2.9	$4.2x10^{-3}$
Adipose (VO)	HDDC2	6	0.18	rs987168	-2.8	rs2243390	-6.7	-2.8	417	top1	2.8	$4.6x10^{-3}$
Adipose (VO)	CCDC28A-AS1	6	0.45	rs12527125	2.9	rs9403000	7.8	1.4	436	susie	3.0	$3.1x10^{-3}$
Adipose (VO)	FAM85B	8	0.061	rs2177254	-4.0	rs2976876	-6.0	-2.8	321	top1	2.8	$4.7x10^{-3}$
Adipose (VO)	FUT10	8	0.25	rs1829189	3.3	rs10097936	11.3	3.0	251	lasso	3.1	$2.1x10^{-3}$
Adipose (VO)	INTS4	11	0.13	rs1793343	-3.9	rs672460	-6.5	-3.8	350	enet	2.9	$3.7x10^{-3}$
Adipose (VO)	RP11-158L12.4	12	0.18	rs10846834	-3.4	rs12581512	9.2	-3.0	537	top1	-3.0	$2.9x10^{-3}$
Adipose (VO)	AC138466.5	12	0.18	rs34708049	-4.2	rs7976069	5.6	2.9	310	lasso	3.0	$3.1x10^{-3}$
Adipose (VO)	CTD-2298J14.2	14	0.075	rs7154122	3.8	rs12884090	3.7	3.5	351	susie	2.9	$4.1x10^{-3}$
Adipose (VO)	DMAC2L	14	0.045	rs2297995	3.8	rs12433794	5.1	3.7	393	enet	3.6	$3.7x10^{-4}$
Adipose (VO)	ADPGK	15	0.036	rs11072383	3.0	rs12594320	4.9	3.0	247	top1	3.0	$3.1x10^{-3}$
Adipose (VO)	SYNM	15	0.33	rs12915090	3.0	rs2602021	11.2	2.3	546	enet	3.0	$2.9x10^{-3}$
Adipose (VO)	ZFP30	19	0.11	rs1725482	-3.2	rs16958863	-6.7	-2.6	292	enet	2.9	$4.0x10^{-3}$
Adipose (VO)	CHKB	22	0.25	rs28513473	2.9	rs131760	-8.8	-2.6	284	susie	2.8	$4.9x10^{-3}$
Blood	UBXN11	1	0.090	rs6676527	3.1	rs6676630	7.3	2.8	391	lasso	3.0	$3.1x10^{-3}$
Blood	SLC35F6	2	0.029	rs3806517	3.6	rs12992046	-3.9	3.5	378	susie	-3.4	$8.1x10^{-4}$
Blood	CORIN	4	0.27	rs1440221	3.5	rs6823698	14.1	2.9	425	top1	2.9	$4.4x10^{-3}$
Blood	NFXL1	4	0.51	rs1440221	3.5	rs6858440	18.6	2.8	412	enet	3.0	$2.9x10^{-3}$
Blood	SYNJ2	6	0.23	rs3003561	3.4	rs1744177	11.4	2.9	564	top1	2.9	$3.5x10^{-3}$
Blood	EPDR1	7	0.19	rs2722309	-3.0	rs4720265	-7.8	-2.6	575	enet	3.0	$2.8x10^{-3}$

Continuation of Table A11

Blood	THAP5	7	0.16	rs1043615	3.0	rs17426315	-7.7	-3.0	442	enet	2.9	$3.5x10^{-3}$
Blood	RP5-855D21.1	8	0.044	rs12676364	3.6	rs11774528	4.5	2.7	318	enet	2.9	$3.9x10^{-3}$
Blood	RP11-722E23.2	8	0.21	rs1829189	3.3	rs2676403	11.3	2.8	240	top1	2.8	$5.0x10^{-3}$
Blood	FUT10	8	0.41	rs1829189	3.3	rs2676403	17.0	2.8	251	susie	2.8	$5.0x10^{-3}$
Blood	TTI2	8	0.076	rs1829189	3.3	rs6982159	-6.7	2.9	253	susie	-3.0	$2.7x10^{-3}$
Blood	OR52L2P	11	0.058	rs12292207	3.1	rs4758406	3.8	1.3	653	susie	2.9	$3.8x10^{-3}$
Blood	LINC02446	12	0.12	rs7305642	3.3	rs4076336	-4.6	3.2	460	enet	-3.2	$1.2x10^{-3}$
Blood	CENPUP2	12	0.037	rs12423443	3.4	rs12810577	-3.9	3.2	563	susie	-3.0	$3.0x10^{-3}$
Blood	Antisense to OR10AD1	12	0.062	rs7485057	-3.3	rs901964	-6.0	-3.1	516	top1	3.1	$2.3x10^{-3}$
Blood	ZNF641	12	0.54	rs7485057	-3.3	rs2634663	-17.9	-3.1	471	susie	3.1	$1.8x10^{-3}$
Blood	AACS	12	0.076	rs10846834	-3.4	rs12581512	3.7	-3.0	532	susie	-2.9	$4.4x10^{-3}$
Blood	RP11-158L12.4	12	0.099	rs10846834	-3.4	rs12581512	8.9	-3.0	527	top1	-3.0	$2.9x10^{-3}$
Blood	SOS2	14	0.057	rs2297995	3.8	rs1955926	5.5	3.2	348	top1	3.2	$1.4x10^{-3}$
Blood	CDKL1	14	0.17	rs2297995	3.8	rs1465160	10.8	-2.9	429	enet	-3.5	$4.1x10^{-4}$
Blood	AQP9	15	0.084	rs2280197	-3.5	rs2899619	5.5	-3.2	662	susie	-3.5	$4.5x10^{-4}$
Blood	ADPGK	15	0.043	rs11072383	3.0	rs12594320	4.9	3.0	229	top1	3.0	$3.1x10^{-3}$
Blood	TBC1D24	16	0.18	rs4786320	3.1	rs4786320	5.9	3.1	308	top1	3.1	$1.9x10^{-3}$
Blood	LOC400499	16	0.29	rs436838	3.2	rs8052665	7.7	-2.0	480	susie	-2.8	$4.5x10^{-3}$
Blood	LPCAT2	16	0.096	rs3785152	-3.1	rs4402561	6.2	2.4	660	enet	3.3	$9.0x10^{-4}$
Blood	CYB5D2	17	0.14	rs938626	-2.5	rs12947597	-3.9	1.9	468	susie	-2.9	$4.0x10^{-3}$
Blood	ETHE1	19	0.067	rs400591	3.1	rs7259375	4.1	2.6	372	enet	3.3	$1.1x10^{-3}$
Blood	PTOV1-AS2	19	0.20	rs16981464	3.6	rs16981492	-7.9	2.7	350	enet	-2.9	$3.7x10^{-3}$
Blood	ARVCF	22	0.11	rs9332316	3.0	rs165849	-6.1	-2.9	550	susie	3.3	$1.1x10^{-3}$
Blood	MMP11	22	0.063	rs2070457	3.6	rs2070464	-4.0	2.2	476	lasso	-2.9	$3.9x10^{-3}$

Continuation of Table A11

Blood	CBX6	22	0.24	rs5750781	-3.2	rs7292074	-6.2	-1.8	393	susie	3.2	$1.3x10^{-3}$
Blood	CHKB	22	0.23	rs28513473	2.9	rs131750	8.0	2.6	284	enet	3.6	$3.2x10^{-4}$
Muscle	ZMPSTE24-DT	1	0.077	rs4660156	3.1	rs6600322	-6.6	-3.0	406	enet	2.9	$3.5x10^{-3}$
Muscle	UHMK1	1	0.23	rs7539281	3.0	rs10919548	-10.9	2.9	637	enet	-2.9	$3.9x10^{-3}$
Muscle	DPYSL5	2	0.089	rs3806517	3.6	rs12991828	-7.9	-2.7	364	enet	3.0	$2.7x10^{-3}$
Muscle	RMDN2	2	0.080	rs41383748	-3.2	rs6544086	3.7	2.1	579	enet	3.1	$1.9x10^{-3}$
Muscle	DUSP7	3	0.063	rs745618	3.4	rs12632423	-5.4	2.9	265	top1	-2.9	$3.4x10^{-3}$
Muscle	HTR1F	3	0.057	rs7648805	3.8	rs4362744	-5.2	3.2	298	susie	-3.1	$1.8x10^{-3}$
Muscle	TMEM45A	3	0.075	rs4928110	3.7	rs12636452	-6.2	3.6	395	enet	-3.0	$2.6x10^{-3}$
Muscle	PARP14	3	0.19	rs6764971	-3.3	rs6770902	11.0	-3.1	534	enet	-3.1	$2.3x10^{-3}$
Muscle	SKIL	3	0.13	rs7616830	2.9	rs6444925	-8.0	2.8	387	enet	-2.8	$4.6x10^{-3}$
Muscle	CDC23	5	0.027	rs10515497	4.4	rs9327809	4.0	-2.7	282	susie	-3.1	$2.0x10^{-3}$
Muscle	BPGM	7	0.068	rs7783456	3.4	rs4732047	5.4	3.0	513	susie	3.1	$2.1x10^{-3}$
Muscle	FUT10	8	0.11	rs1829189	3.3	rs7848	8.8	2.8	251	top1	2.8	$4.5x10^{-3}$
Muscle	TTI2	8	0.049	rs1829189	3.3	rs1829189	-4.8	3.3	253	top1	-3.3	$1.1x10^{-3}$
Muscle	UEVLD	11	0.041	rs11024717	-3.3	rs10832941	4.9	-2.9	458	lasso	-3.2	$1.6x10^{-3}$
Muscle	PTPRJ	11	0.083	rs10838805	3.6	rs1039481	4.9	3.4	231	lasso	3.2	$1.4x10^{-3}$
Muscle	INTS4	11	0.39	rs1793343	-3.9	rs672460	-13.6	-3.8	349	susie	3.2	$1.6x10^{-3}$
Muscle	METTL7A	12	0.058	rs12582592	3.2	rs11514118	4.0	1.3	342	lasso	2.9	$3.9x10^{-3}$
Muscle	RP11-158L12.4	12	0.18	rs10846834	-3.4	rs12581512	12.2	-3.0	527	lasso	-3.2	$1.3x10^{-3}$
Muscle	AC138466.5	12	0.048	rs34708049	-4.2	rs7976069	5.0	2.9	303	susie	3.1	$1.8x10^{-3}$
Muscle	WBP4	13	0.43	rs9532718	-3.5	rs17532490	12.2	1.5	301	susie	2.9	$3.3x10^{-3}$
Muscle	L2HGDH	14	0.12	rs2297995	3.8	rs2297995	9.3	3.8	379	enet	3.8	$1.3x10^{-4}$
Muscle	DMAC2L	14	0.22	rs2297995	3.8	rs2275592	11.8	3.7	379	top1	3.7	$2.4x10^{-4}$
Muscle	GCATP1	14	0.078	rs8012691	-2.9	rs8012691	5.3	-2.9	356	top1	-2.9	$3.4x10^{-3}$
Muscle	LINC02256	15	0.19	rs4779969	4.2	rs8037818	7.5	-1.5	379	enet	-2.9	$3.4x10^{-3}$

Continuation of Table A11

Muscle	ADPGK	15	0.16	rs11072383	3.0	rs12594320	6.2	3.0	225	susie	3.0	$2.9x10^{-3}$
Muscle	AC021739.4	15	0.056	rs4530079	3.2	rs2946365	-4.7	-2.4	557	enet	3.1	$2.0x10^{-3}$
Muscle	LINC02175	16	0.088	rs4787667	3.2	rs7498149	-5.1	2.8	390	susie	-3.0	$3.2x10^{-3}$
Muscle	SLC1A5	19	0.095	rs4804030	-2.6	rs8105903	5.5	2.3	333	lasso	3.0	$2.7x10^{-3}$
Muscle	LILRB3	19	0.14	rs6509825	2.8	rs16985475	6.1	-2.4	485	susie	-2.8	$4.9x10^{-3}$
Muscle	SLC7A4	22	0.44	rs5752500	-2.9	rs2075277	13.9	-2.5	357	enet	-3.0	$3.2x10^{-3}$
Muscle	SREBF2	22	0.08	rs7364180	-3.1	rs7364180	4.3	-3.1	318	top1	-3.1	$2.0x10^{-3}$
Liver	DRAM2	1	0.57	rs11584291	3.5	rs3762374	8.8	2.4	570	susie	3.0	$2.9x10^{-3}$
Liver	CEPT1	1	0.31	rs11584291	3.5	rs657801	-5.5	-2.7	570	susie	2.8	$4.9x10^{-3}$
Liver	RP4-781K5.6	1	0.26	rs541021	4.7	rs476875	6.2	-3.5	551	susie	-3.9	$1.2x10^{-4}$
Liver	DNASE1L3	3	0.17	rs7627013	3.7	rs6787425	3.8	2.0	448	enet	3.3	$1.0x10^{-3}$
Liver	LINC00525	7	0.39	rs6463441	3.5	rs5004318	8.3	3.3	514	susie	3.4	$8.1x10^{-4}$
Liver	MCPH1-DT	8	0.2	rs2916749	3.1	rs12546419	3.5	1.9	982	susie	3.5	$4.9x10^{-4}$
Liver	RP11-722E23.2	8	0.096	rs1829189	3.3	rs10097936	5.0	3.0	240	susie	2.9	$4.0x10^{-3}$
Liver	SFRP1	8	0.26	rs7814391	2.9	rs968427	-4.6	1.8	467	enet	-2.9	$4.3x10^{-3}$
Liver	RP11-158L12.4	12	0.2	rs10846834	-3.4	rs12581512	5.4	-3.0	540	susie	-3.2	$1.2x10^{-3}$
Liver	EXOC5	14	0.33	rs268805	2.4	rs1396512	-3.6	-1.8	403	lasso	3.1	$1.8x10^{-3}$
Liver	GOLGA8B	15	0.25	rs12915800	2.9	rs11629815	-4.7	2.8	402	enet	-2.9	$4.0x10^{-3}$
Liver	Sense Intronic To LIPC	15	0.27	rs2280197	-3.5	rs12900410	-3.7	1.5	527	susie	-3.0	$2.4x10^{-3}$
Liver	CD276	15	0.55	rs568760	4.0	rs8038465	8.8	-3.0	362	enet	-2.9	$4.0x10^{-3}$
Liver	LINC00667	18	0.67	rs12162179	3.2	rs11872923	8.8	2.4	498	enet	2.9	$3.4x10^{-3}$
Liver	TYMP	22	0.18	rs28513473	2.9	rs140521	-4.8	-2.6	318	susie	2.9	$4.3x10^{-3}$
Testis	ZMPSTE24-DT	1	0.056	rs4660156	3.1	rs12744808	-4.5	-2.8	409	susie	2.9	$4.3x10^{-3}$
Testis	FCRL2	1	0.097	rs2778003	3.9	rs869536	-3.2	-2.0	523	susie	-2.9	$3.7x10^{-3}$

Continuation of Table A11

Testis	RP4-781K5.4	1	0.23	rs541021	4.7	rs624329	-6.9	3.4	564	top1	-3.4	$6.7x10^{-4}$
Testis	RP4-781K5.6	1	0.19	rs541021	4.7	rs605957	7.0	-4.0	550	enet	-4.2	$2.4x10^{-5}$
Testis	PLB1	2	0.25	rs12623911	3.0	rs1581035	-5.3	2.7	427	enet	-3.2	$1.4x10^{-3}$
Testis	MOBP	3	0.11	rs11706951	-3.3	rs1768254	3.4	-2.7	437	susie	-2.9	$3.3x10^{-3}$
Testis	CCDC13	3	0.21	rs6768356	-3.3	rs13072026	6.5	2.0	450	enet	3.8	$1.5x10^{-4}$
Testis	PARP14	3	0.47	rs6764971	-3.3	rs6770902	9.8	-3.0	542	enet	-3.7	$2.5x10^{-4}$
Testis	LINC01997	3	0.096	rs17679760	3.7	rs17462666	3.2	-0.15	413	lasso	3.2	$1.4x10^{-3}$
Testis	TMEM212-IT1	3	0.13	rs4618247	3.0	rs4618247	-4.8	3.0	446	enet	-3.5	$4.3x10^{-4}$
Testis	RP11-22A3.2	4	0.096	rs2110898	-3.4	rs2540841	-3.9	2.8	487	top1	-2.8	$4.9x10^{-3}$
Testis	LINC00504	4	0.16	rs4358395	-3.3	rs2604573	-4.3	2.2	484	enet	-3.3	$1.1x10^{-3}$
Testis	SLC10A4	4	0.080	rs12645951	-2.9	rs6844211	-4.9	-2.9	326	susie	2.9	$4.4x10^{-3}$
Testis	FAM13B	5	0.067	rs10515497	4.4	rs4835748	-5.0	4.1	317	susie	-4.3	$2.1x10^{-5}$
Testis	WNT8A	5	0.10	rs10515497	4.4	rs1042124	4.3	3.5	312	lasso	3.2	$1.4x10^{-3}$
Testis	KIF20A	5	0.17	rs10515497	4.4	rs17171767	7.9	-3.0	292	top1	-3.0	$3.0x10^{-3}$
Testis	LYRM4	6	0.26	rs9504259	2.9	rs1983982	-6.1	2.8	627	susie	-2.8	$4.6x10^{-3}$
Testis	RSPH4A	6	0.33	rs11754507	2.6	rs784136	7.4	2.4	356	lasso	3.0	$2.9x10^{-3}$
Testis	C7orf50	7	0.23	rs10081255	-3.2	rs10224368	5.1	-2.9	402	lasso	-2.8	$4.8x10^{-3}$
Testis	CCDC136	7	0.19	rs109829	-2.6	rs7799186	6.0	2.4	340	susie	3.2	$1.3x10^{-3}$
Testis	BPGM	7	0.22	rs7783456	3.4	rs1160049	7.4	3.1	518	enet	3.1	$2.0x10^{-3}$
Testis	ATP6V0A4	7	0.41	rs999228	3.7	rs999228	8.1	3.7	406	enet	4.2	$3.0x10^{-5}$
Testis	GALNTL5	7	0.24	rs6979879	-2.9	rs12539593	-7.1	-2.8	388	susie	2.8	$4.8x10^{-3}$
Testis	MAK16	8	0.13	rs1829189	3.3	rs2043967	3.6	2.0	254	susie	3.3	$9.2x10^{-4}$
Testis	TTI2	8	0.13	rs1829189	3.3	rs3098657	-6.9	2.9	253	lasso	-2.9	$3.7x10^{-3}$
Testis	NDUFC2	11	0.21	rs1793343	-3.9	rs589472	-6.1	-2.9	361	top1	2.9	$3.6x10^{-3}$
Testis	ELOBP2	11	0.34	rs7113818	3.0	rs12805829	7.0	-2.4	468	enet	-3.6	$3.6x10^{-4}$

Continuation of Table A11

Testis	LINC02446	12	0.47	rs7305642	3.3	rs7305642	9.4	3.3	467	enet	3.0	$2.5x10^{-3}$
Testis	ETFRF1	12	0.14	rs12423443	3.4	rs12810577	6.1	3.2	569	lasso	2.8	$4.6x10^{-3}$
Testis	OR8T1P	12	0.44	rs7485057	-3.3	rs10875815	-8.3	-3.2	459	susie	3.1	$2.1x10^{-3}$
Testis	TSPAN8	12	0.13	rs7305768	3.2	rs5010616	-5.0	2.9	433	top1	-2.9	$3.3x10^{-3}$
Testis	RAB35	12	0.15	rs3742039	2.9	rs2240311	3.3	2.4	354	susie	3.2	$1.4x10^{-3}$
Testis	RP11-158L12.4	12	0.61	rs10846834	-3.4	rs12581512	12.2	-3.0	538	top1	-3.0	$2.9x10^{-3}$
Testis	PSPC1	13	0.18	rs7984806	-2.8	rs2290810	-5.8	-2.5	309	susie	3.6	$3.5x10^{-4}$
Testis	C1QTNF9B	13	0.68	rs2765107	4.6	rs9551026	10.7	4.2	751	enet	3.1	$2.0x10^{-3}$
Testis	ANKRD20A19P	13	0.38	rs2765107	4.6	rs17071064	-9.6	3.2	737	lasso	-4.2	$3.2x10^{-5}$
Testis	WASF3	13	0.17	rs1108755	-3.1	rs4769507	-5.0	-2.8	629	lasso	2.9	$4.2x10^{-3}$
Testis	DMAC2L	14	0.14	rs2297995	3.8	rs4901009	6.1	2.5	394	enet	2.9	$4.3x10^{-3}$
Testis	GCATP1	14	0.12	rs8012691	-2.9	rs8012691	5.1	-2.9	377	top1	-2.9	$3.4x10^{-3}$
Testis	RP11-718G2.5	14	0.23	rs2182973	3.4	rs4899342	-8.0	3.3	540	top1	-3.3	$1.1x10^{-3}$
Testis	TTC9	14	0.25	rs2182973	3.4	rs7147575	4.4	-1.9	431	lasso	-2.8	$4.8x10^{-3}$
Testis	HCN2 pseudogene	15	0.11	rs4779969	4.2	rs6494165	-4.9	4.1	293	top1	-4.1	$3.8x10^{-5}$
Testis	GOLGA8K	15	0.25	rs4779969	4.2	rs6494165	-6.0	4.1	336	top1	-4.1	$3.8x10^{-5}$
Testis	DNAJA4	15	0.23	rs3813576	2.8	rs4887025	-7.2	2.8	405	susie	-2.8	$4.9x10^{-3}$
Testis	LCMT-1 pseudogene	16	0.13	rs4787667	3.2	rs7498149	-5.7	2.8	399	lasso	-2.9	$4.2x10^{-3}$
Testis	DPH1	17	0.31	rs3752962	-3.7	rs11871926	7.3	0.93	464	susie	2.9	$3.9x10^{-3}$
Testis	ZNF540	19	0.048	rs1725482	-3.2	rs10409402	4.1	-2.8	290	top1	-2.8	$4.8x10^{-3}$
Testis	Sense Intronic to ZNF155	19	0.16	rs400591	3.1	rs453932	5.7	2.0	478	enet	2.9	$4.1x10^{-3}$

Continuation of Table A11

Testis	Ig lambda chain V region pseudogene	22	0.16	rs1076851	3.2	rs743517	5.0	3.0	408	top1	3.0	$3.2x10^{-3}$
Testis	BMP6P1	22	0.32	rs1076851	3.2	rs928894	5.9	2.8	399	susie	2.9	$4.1x10^{-3}$

Abbreviations: eQTL, expression quantitative trait locus; CHR, chromosome, HSQ, mean heritability estimate; Best.GWAS.ID, most significantly associated variant in the locus; Best.GWAS.Z, z-score of most significantly associated variant in the locus; eQTL ID, best eQTL in the locus; eQTL.GWAS.Z, GWAS z-score for best eQTL; NSNP, number of SNPs in the locus; Model, best performing TWAS model; TWAS.Z, TWAS z-score; TWAS.P, TWAS p-value, enet, elastic-net regression (mixing parameter = 0.5); blup, best linear unbiased predictor from all variants; bslmm, Bayesian sparse linear model; lasso, least absolute shrinkage and selection operator; top1, single best eQTL, susie, sum of single effects regression, VO, visceral omentum; SC, subcutaneous.

Table A12. Genes associated with cisplatin-induced tinnitus by TWAS ($p < 0.05$)

Tissue	Gene	CHR	HSQ	BEST.GWAS.ID	BEST.GWAS.Z	EQTL.ID	EQTL.Z	EQTL.GWAS.Z	NSNP	MODEL	TWAS.Z	TWAS.P
Nerve	LINC01376	2	0.13	rs4233765	3.7	rs6707044	6.4	3.4	555	top1	3.4	$6.4x10^{-4}$
Nerve	TMEM45A	3	0.11	rs4928110	3.7	rs12636452	-6.3	3.6	395	enet	-3.5	$5.0x10^{-4}$
Nerve	PARP14	3	0.41	rs6764971	-3.3	rs6770902	11.1	-3.1	537	enet	-4.0	$6.0x10^{-5}$
Nerve	HSPBAP1	3	0.16	rs6764971	-3.3	rs7650313	5.0	0.88	498	enet	2.1	$4.0x10^{-2}$
Nerve	ADH1A	4	0.15	rs283413	3.4	rs904092	-7.2	2.2	484	top1	-2.2	$3.1x10^{-2}$
Nerve	ADH1C	4	0.13	rs283413	3.4	rs283415	-7.0	2.1	503	susie	-3.6	$3.4x10^{-4}$
Nerve	CCT7P2	5	0.12	rs11958890	3.4	rs2644790	6.4	3.2	291	top1	3.2	$1.3x10^{-3}$
Nerve	CTD-2091N23.1	5	0.072	rs11958890	3.4	rs6868414	5.7	2.3	283	enet	3.1	$1.9x10^{-3}$
Nerve	KLHL3	5	0.058	rs10515497	4.4	rs4371746	4.7	3.1	376	susie	3.4	$6.6x10^{-4}$
Nerve	FAM53C	5	0.11	rs10515497	4.4	rs10900851	4.5	-1.7	292	enet	-3.5	$4.2x10^{-4}$
Nerve	CTNNA1	5	0.048	rs11750814	3.9	rs700618	-6.2	-2.6	312	top1	2.6	$1.0x10^{-2}$
Nerve	CTNNA1-AS1	5	0.39	rs7703938	3.6	rs825762	16.3	-2.6	306	enet	-2.4	$1.6x10^{-2}$
Nerve	SFTA1P	10	0.081	rs11256835	3.3	rs11256835	5.4	3.3	637	top1	3.3	$9.0x10^{-4}$
Nerve	GAS2	11	0.19	rs10734321	-3.6	rs10766971	-5.3	1.4	393	enet	-3.6	$3.5x10^{-4}$
Nerve	PTPRJ	11	0.12	rs10838805	3.6	rs1039481	7.4	3.4	231	top1	3.4	$7.1x10^{-4}$
Nerve	LINC01588	14	0.058	rs2297995	3.8	rs11157718	3.8	1.2	350	susie	3.4	$7.6x10^{-4}$
Nerve	L2HGDH	14	0.079	rs2297995	3.8	rs7148089	-5.1	3.6	390	enet	-2.7	$7.3x10^{-3}$
Nerve	ADAM21	14	0.043	rs2182973	3.4	rs10145919	-3.9	3.2	526	top1	-3.2	$1.5x10^{-3}$
Nerve	OTUD7A	15	0.11	rs4779969	4.2	rs1503002	-5.3	-2.2	320	susie	2.4	$1.9x10^{-2}$
Nerve	CHRNA7	15	0.080	rs4779969	4.2	rs6494165	-6.3	4.1	300	enet	-3.3	$9.2x10^{-4}$

Continuation of Table A12

Nerve	LINC02256	15	0.46	rs4779969	4.2	rs28457217	-9.3	1.6	380	lasso	-2.0	$4.3x10^{-2}$
Nerve	LCMT1 pseudogene	16	0.055	rs4787667	3.2	rs4787667	-4.6	3.2	394	enet	-3.6	$3.4x10^{-4}$
Nerve	LINC02175	16	0.18	rs4787667	3.2	rs7498149	-7.4	2.8	392	top1	-2.8	$5.0x10^{-3}$
Nerve	SCML2P2	16	0.21	rs4787667	3.2	rs7498149	-8.3	2.8	391	enet	-2.9	$4.2x10^{-3}$
Nerve	TRIP11 pseudogene	16	0.15	rs4787667	3.2	rs7498149	-6.8	2.8	390	top1	-2.8	$5.0x10^{-3}$
Nerve	TXNL4B	16	0.80	rs952160	-2.3	rs4788614	7.0	-1.1	346	susie	-3.6	$3.8x10^{-4}$
Nerve	RP11-58A18.1	16	0.16	rs2059285	-3.0	rs300029	-7.6	2.9	875	enet	-2.6	$9.8x10^{-3}$
Nerve	LINC02188	16	0.28	rs1110338	3.9	rs1559451	-5.9	-2.5	864	enet	3.1	$1.8x10^{-3}$
Nerve	RP11-899L11.1	16	0.19	rs1110338	3.9	rs1110338	7.7	3.9	595	susie	3.7	$2.6x10^{-4}$
Nerve	RGL4	22	0.18	rs2070457	3.6	rs17629631	-8.0	-1.4	477	susie	2.0	$4.4x10^{-2}$
Nerve	CHCHD10	22	0.11	rs2070457	3.6	rs2070457	-5.2	3.6	479	lasso	-3.2	$1.4x10^{-3}$
Nerve	SPECC1L	22	0.18	rs2070457	3.6	rs17651189	8.3	2.6	382	top1	2.6	$8.3x10^{-3}$
Nerve	GGT1	22	0.096	rs17651189	2.6	rs5760492	-4.3	-2.1	390	top1	2.1	$3.4x10^{-2}$
Cerebellum	CASP9	1	0.28	rs4233532	-2.8	rs10927797	-7.0	-2.6	505	enet	3.2	$1.4x10^{-3}$
Cerebellum	DNAJC16	1	0.13	rs4233532	-2.8	rs3766160	4.8	2.1	505	susie	2.7	$7.1x10^{-3}$
Cerebellum	SLC25A34	1	0.75	rs4233532	-2.8	rs35352784	-10.5	-1.8	443	lasso	2.0	$4.9x10^{-2}$
Cerebellum	THAP3P1	1	0.15	rs7527726	-4.0	rs7518872	4.2	-3.9	310	lasso	-3.6	$2.7x10^{-4}$
Cerebellum	CYP1B1-AS1	2	0.19	rs41383748	-3.2	rs17490310	4.7	-3.1	592	top1	-3.1	$2.1x10^{-3}$
Cerebellum	PARP14	3	0.16	rs6764971	-3.3	rs10934611	4.9	-3.1	547	susie	-3.4	$6.8x10^{-4}$
Cerebellum	RP11-164P12.5	4	0.60	rs11726420	3.8	rs1443088	10.7	-3.6	381	top1	-3.6	$3.8x10^{-4}$
Cerebellum	Antisense to PET112L	4	0.48	rs11726420	3.8	rs4235219	8.7	-3.5	381	top1	-3.5	$4.0x10^{-4}$
Cerebellum	KLHL3	5	0.20	rs10515497	4.4	rs2967797	-5.3	3.2	378	enet	-3.8	$1.7x10^{-4}$
Cerebellum	WNT8A	5	0.09	rs10515497	4.4	rs4835768	4.2	-4.3	313	top1	-4.3	$1.4x10^{-5}$

Continuation of Table A12

Cerebellum	CTNNA1	5	0.47	rs11750814	3.9	rs1725335	-4.9	-2.6	313	susie	2.9	$3.7x10^{-3}$
Cerebellum	MCPH1	8	0.19	rs2916749	3.1	rs2083914	5.5	3.1	977	lasso	3.0	$2.5x10^{-3}$
Cerebellum	PHYHIP	8	0.48	rs4872429	3.2	rs4872429	8.0	3.2	463	top1	3.2	$1.2x10^{-3}$
Cerebellum	STMN4	8	0.17	rs7834529	2.9	rs12056620	3.7	1.2	631	susie	3.2	$1.6x10^{-3}$
Cerebellum	PTK2B	8	0.20	rs7834529	2.9	rs2292974	-5.5	-2.6	626	top1	2.6	$8.5x10^{-3}$
Cerebellum	SLC11A2	12	0.10	rs12582592	3.2	rs7972608	-4.6	-2.0	385	top1	2.0	$4.9x10^{-2}$
Cerebellum	LETMD1	12	0.22	rs12582592	3.2	rs12582592	5.5	3.2	390	susie	3.1	$1.8x10^{-3}$
Cerebellum	AACS	12	0.33	rs10846834	-3.4	rs1080910	6.5	-3.1	545	susie	-3.1	$2.0x10^{-3}$
Cerebellum	RP11-158L12.4	12	0.64	rs10846834	-3.4	rs12581512	10.5	-3.0	540	top1	-3.0	$2.9x10^{-3}$
Cerebellum	TMEM132B	12	0.32	rs10846834	-3.4	rs4559740	6.6	-2.5	531	enet	-2.3	$2.1x10^{-2}$
Cerebellum	AC138466.5	12	0.20	rs34708049	-4.2	rs12309945	4.5	2.8	314	lasso	2.8	$5.7x10^{-3}$
Cerebellum	GALNT9	12	0.29	rs34708049	-4.2	rs34708049	4.4	-4.2	331	susie	-4.3	$1.8x10^{-5}$
Cerebellum	P2RX2	12	0.18	rs34708049	-4.2	rs14302	4.8	-2.0	277	top1	-2.0	$4.9x10^{-2}$
Cerebellum	MIPEP	13	0.53	rs2765107	4.6	rs11617019	9.3	2.7	764	susie	2.7	$7.5x10^{-3}$
Cerebellum	L2HGDH	14	0.26	rs2297995	3.8	rs11157734	-6.6	3.7	393	top1	-3.7	$1.8x10^{-4}$
Cerebellum	TRIM9	14	0.22	rs1890706	-3.3	rs1959534	-3.9	-1.3	611	lasso	2.0	$4.9x10^{-2}$
Cerebellum	KTN1	14	0.22	rs1188080	3.6	rs12432887	-6.2	3.1	502	top1	-3.1	$2.1x10^{-3}$
Cerebellum	SEMA6D	15	0.23	rs7176161	3.1	rs7176161	5.6	3.1	424	lasso	3.2	$1.5x10^{-3}$
Cerebellum	LINGO1	15	0.28	rs3813576	2.8	rs12441652	5.1	-1.3	408	enet	-2.4	$1.6x10^{-2}$
Cerebellum	GOLGA6AFP	15	0.76	rs3813576	2.8	rs8025691	-10.3	2.7	430	susie	-2.3	$2.0x10^{-2}$
Cerebellum	DNAJA4	15	0.21	rs3813576	2.8	rs8025691	-4.2	2.7	406	lasso	-3.6	$2.9x10^{-4}$
Cerebellum	AC233723.2	17	0.39	rs12450045	-3.5	rs6502823	-5.8	-1.4	436	enet	2.0	$4.5x10^{-2}$
Cerebellum	C17orf114	17	0.52	rs12450045	-3.5	rs11654690	-8.7	-2.3	438	susie	2.4	$1.7x10^{-2}$
Cerebellum	MINK1	17	0.32	rs12450045	-3.5	rs12450045	6.0	-3.5	428	top1	-3.5	$5.2x10^{-4}$
Cerebellum	ENO3	17	0.38	rs12450045	-3.5	rs238247	7.2	-2.6	444	enet	-2.3	$2.0x10^{-2}$

Continuation of Table A12

Cerebellum	INCA1	17	0.24	rs12450045	-3.5	rs418305	4.7	-1.7	438	susie	-2.1	$3.9x10^{-2}$
Cerebellum	RABEP1	17	0.22	rs12450045	-3.5	rs1806261	6.3	-1.9	462	susie	-2.0	$4.4x10^{-2}$
Cerebellum	NUP88	17	0.33	rs1362765	-4.1	rs9908179	6.9	-2.1	528	top1	-2.1	$4.0x10^{-2}$
Cerebellum	TRAPPC5	19	0.52	rs4804802	3.4	rs4804802	-7.2	3.4	437	top1	-3.4	$5.9x10^{-4}$
Cerebellum	CD209	19	0.51	rs4804802	3.4	rs4804802	-7.7	3.4	414	susie	-3.1	$2.2x10^{-3}$
Cerebellum	CLEC4M	19	0.41	rs4804802	3.4	rs868875	-6.5	0.33	428	susie	-2.3	$2.1x10^{-2}$
Brain	GALNT13	2	0.089	rs16836088	3.7	rs16834756	4.5	2.3	672	blup	3.3	$9.1x10^{-4}$
Brain	ITGA4	2	0.067	rs4077924	3.6	rs10205700	-4.3	3.0	387	enet	-3.3	$8.3x10^{-4}$
Brain	VIPR1	3	0.11	rs6768356	-3.3	rs6768356	5.6	-3.3	480	top1	-3.3	$1.1x10^{-3}$
Brain	ABHD14B	3	0.056	rs745618	3.4	rs929533	-3.7	3.0	242	top1	-3.0	$2.6x10^{-3}$
Brain	PROS1	3	0.11	rs36017106	-3.0	rs9289536	-6.4	2.3	165	bslmm	-3.6	$3.2x10^{-4}$
Brain	PRSS12	4	0.084	rs298981	3.7	rs11728902	-4.9	-2.3	304	enet	2.6	$1.0x10^{-2}$
Brain	METTL14	4	0.057	rs298981	3.7	rs960738	-5.2	3.2	357	top1	-3.2	$1.2x10^{-3}$
Brain	GFM2	5	0.38	rs2218517	3.5	rs2218517	-12.0	3.5	517	lasso	-3.4	$6.4x10^{-4}$
Brain	ELOVL5	6	0.092	rs209500	-3.3	rs209500	-6.9	-3.3	583	top1	3.3	$1.1x10^{-3}$
Brain	LRRC1	6	0.11	rs209500	-3.3	rs4715429	-8.1	-1.7	606	enet	2.0	$4.2x10^{-2}$
Brain	FILIP1	6	0.031	rs6453843	2.8	rs2250989	3.7	0.85	344	Bslmm	2.5	$1.2x10^{-2}$
Brain	SENP6	6	0.067	rs6453843	2.8	rs2647404	-4.2	2.4	364	enet	-3.0	$2.3x10^{-3}$
Brain	EPDR1	7	0.24	rs2722309	-3.0	rs1349394	7.4	2.7	597	lasso	3.0	$3.0x10^{-3}$
Brain	KRBA1	7	0.053	rs1636367	-3.0	rs6965416	-3.4	-0.67	315	bslmm	3.0	$2.5x10^{-3}$
Brain	PENK	8	0.14	rs10108774	3.2	rs1440757	4.7	2.1	422	bslmm	3.3	$8.5x10^{-4}$
Brain	LETMD1	12	0.11	rs12582592	3.2	rs3759406	5.2	2.9	398	top1	2.9	$3.9x10^{-3}$

Continuation of Table A12

Brain	TMEM132B	12	0.11	rs10846834	-3.4	rs12580291	5.1	-2.6	762	bslmm	-2.9	$4.0x10^{-3}$
Brain	EP400NL	12	0.15	rs34708049	-4.2	rs6598199	7.3	2.9	323	lasso	3.0	$2.7x10^{-3}$
Brain	N6AMT2	13	0.081	rs9579932	-2.9	rs9579937	4.8	-2.5	524	top1	-2.5	$1.2x10^{-2}$
Brain	OLFM4	13	0.040	rs9536317	-3.0	rs1535576	-3.9	2.8	507	top1	-2.8	$5.2x10^{-3}$
Brain	ATP2C2	16	0.073	rs11649239	-3.4	rs12445007	5.2	-2.7	940	lasso	-3.2	$1.2x10^{-3}$
Brain	CCBE1	18	0.20	rs9966425	3.2	rs3114275	-5.3	2.1	790	enet	-2.8	$5.3x10^{-3}$
Brain	DOT1L	19	0.049	rs8108653	3.0	rs878439	-3.5	0.14	431	blup	3.0	$2.3x10^{-3}$
Brain	TIMM13	19	0.31	rs7248779	-2.8	rs4807260	12.0	-2.6	424	enet	-2.4	$1.7x10^{-2}$
Brain	HNF4A	20	0.22	rs6017227	3.3	rs6031598	-9.7	2.9	528	top1	-2.9	$4.0x10^{-3}$
Brain	RRP1	21	0.055	rs3761385	-3.2	rs3761385	-4.4	-3.2	457	top1	3.2	$1.3x10^{-3}$
Brain	C21orf67	21	0.29	rs2838644	-3.2	rs7278544	-9.2	-1.7	598	enet	2.3	$1.9x10^{-2}$
Brain	RFPL2	22	0.058	rs9621453	2.7	rs16990001	5.4	-2.6	547	lasso	-2.9	$4.4x10^{-3}$
Brain	APOBEC3G	22	0.15	rs5750781	-3.2	rs2011869	8.3	-2.8	398	top1	-2.8	$5.4x10^{-3}$
Kidney	CASP9	1	0.51	rs4233532	-2.8	rs4646047	-4.3	-2.5	505	susie	2.5	$1.1x10^{-2}$
Kidney	FNBP1P1	2	0.55	rs17009396	2.7	rs828844	5.1	-2.5	361	top1	-2.5	$1.1x10^{-2}$
Kidney	WDR6	3	0.24	rs7619016	2.9	rs6446205	4.2	2.1	261	susie	2.2	$2.5x10^{-2}$
Kidney	AMT	3	0.22	rs7619016	2.9	rs12637576	-4.2	2.5	289	top1	-2.5	$1.2x10^{-2}$
Kidney	NICN1	3	0.15	rs7619016	2.9	rs6778080	-3.4	2.9	289	susie	-2.6	$9.2x10^{-3}$
Kidney	LINC02121	5	0.61	rs16875084	-3.2	rs3733787	5.2	-2.5	618	top1	-2.5	$1.3x10^{-2}$
Kidney	RP1-136B1.1	6	0.77	rs12216224	3.4	rs17608626	3.9	-1.3	549	lasso	-3.1	$1.7x10^{-3}$
Kidney	HDDC2	6	0.55	rs987168	-2.8	rs987168	-3.8	-2.8	424	susie	2.6	$8.3x10^{-3}$
Kidney	Zinc finger protein pseudogene	7	0.36	rs1636367	-3.0	rs17630156	-4.2	2.4	386	top1	-2.4	$1.8x10^{-2}$

Continuation of Table A12

Kidney	RP11-51J9.6	8	0.71	rs11985437	3.8	rs6987718	3.4	-1.3	349	enet	-3.8	$1.7x10^{-4}$
Kidney	FUT10	8	0.39	rs1829189	3.3	rs2676403	3.8	2.8	251	susie	3.0	$2.6x10^{-3}$
Kidney	SVIL-AS1	10	0.75	rs10508742	-3.2	rs7089591	3.7	-1.2	719	susie	-2.4	$1.9x10^{-2}$
Kidney	DMAC2L	14	0.31	rs2297995	3.8	rs1955926	3.5	3.2	394	top1	3.2	$1.4x10^{-3}$
Kidney	PRKXP1	15	0.83	rs1972053	-2.8	rs4965320	-4.6	-2.4	593	top1	2.4	$1.7x10^{-2}$
Kidney	RBBP9	20	0.45	rs2104196	2.8	rs2300811	-3.5	-2.0	473	enet	2.1	$4.1x10^{-2}$
Adipose (SC)	DRAM2	1	0.57	rs11584291	3.5	rs3818797	16.9	2.6	572	enet	2.8	$4.8x10^{-3}$
Adipose (SC)	CEPT1	1	0.11	rs11584291	3.5	rs9970286	7.8	2.3	572	top1	2.3	$2.1x10^{-2}$
Adipose (SC)	CHI3L2	1	0.19	rs11584291	3.5	rs7515361	7.8	2.6	557	susie	3.3	$9.3x10^{-4}$
Adipose (SC)	CHIAP2	1	0.30	rs11584291	3.5	rs7515361	12.0	2.6	555	enet	2.5	$1.3x10^{-2}$
Adipose (SC)	CHIA	1	0.30	rs11584291	3.5	rs7515361	11.9	2.6	553	lasso	2.9	$4.0x10^{-3}$
Adipose (SC)	FCRL3	1	0.065	rs2778003	3.9	rs3761959	7.0	-2.2	534	top1	-2.2	$2.5x10^{-2}$
Adipose (SC)	CD1A	1	0.057	rs7514610	3.2	rs17679007	-4.3	2.6	470	enet	-2.9	$4.0x10^{-3}$
Adipose (SC)	CD1C	1	0.083	rs7514610	3.2	rs6699757	-3.8	2.6	508	susie	-3.5	$4.1x10^{-4}$
Adipose (SC)	CD1E	1	0.11	rs7514610	3.2	rs6699757	-4.9	2.6	512	top1	-2.6	$8.6x10^{-3}$
Adipose (SC)	FCER1A	1	0.15	rs2794510	2.9	rs2251746	6.1	-1.9	423	enet	-2.1	$4.0x10^{-2}$
Adipose (SC)	HADHB	2	0.050	rs1275935	-3.0	rs6546899	4.5	2.1	343	top1	2.1	$3.9x10^{-2}$
Adipose (SC)	SLC35F6	2	0.080	rs3806517	3.6	rs3845684	-6.3	-3.0	380	susie	2.9	$4.2x10^{-3}$
Adipose (SC)	CENPA	2	0.21	rs3806517	3.6	rs12992046	-8.4	3.5	380	top1	-3.5	$4.8x10^{-4}$
Adipose (SC)	TMEM45A	3	0.059	rs4928110	3.7	rs4928097	-5.4	2.9	394	lasso	-3.6	$3.5x10^{-4}$
Adipose (SC)	PARP14	3	0.45	rs6764971	-3.3	rs6770902	14.0	-3.1	536	lasso	-3.6	$3.0x10^{-4}$
Adipose (SC)	HSPBAP1	3	0.23	rs6764971	-3.3	rs9830096	8.1	2.5	497	enet	2.4	$1.5x10^{-2}$
Adipose (SC)	PTPRJ	11	0.082	rs10838805	3.6	rs10769317	6.9	3.5	225	susie	3.5	$5.5x10^{-4}$

Continuation of Table A12

Adipose (SC)	MIPEP	13	0.17	rs2765107	4.6	rs17079485	7.6	2.7	763	susie	2.6	$9.0x10^{-3}$
Adipose (SC)	C1QTNF9B	13	0.13	rs2765107	4.6	rs11551114	-7.1	2.6	750	lasso	-3.1	$2.0x10^{-3}$
Adipose (SC)	SPATA13	13	0.17	rs2765107	4.6	rs11619017	5.2	-2.0	737	lasso	-2.1	$3.7x10^{-2}$
Adipose (SC)	LINC02352	15	0.051	rs1075232	3.1	rs3964705	3.8	0.84	447	lasso	2.1	$3.3x10^{-2}$
Adipose (SC)	CHRNA7	15	0.092	rs4779969	4.2	rs16956738	-6.0	2.5	300	enet	-3.6	$3.8x10^{-4}$
Adipose (SC)	LINC02256	15	0.25	rs4779969	4.2	rs28457217	-8.3	1.6	379	enet	-3.2	$1.3x10^{-3}$
Adipose (SC)	GOLGA8N	15	0.55	rs17228887	3.3	rs28457217	-12.0	1.6	393	enet	-2.0	$4.5x10^{-2}$
Adipose (SC)	MFGE8	15	0.14	rs6496536	2.6	rs1961839	-4.7	2.5	452	enet	-3.5	$5.1x10^{-4}$
Adipose (SC)	ZNF710	15	0.082	rs12905387	2.9	rs2939850	5.8	2.0	402	top1	2.0	$4.2x10^{-2}$
Adipose (SC)	HDDC3	15	0.067	rs7178220	3.1	rs1052532	-5.8	2.0	483	top1	-2.0	$4.2x10^{-2}$
Adipose (SC)	STRN4	19	0.18	rs4804030	-2.6	rs314671	-10.1	-1.9	335	lasso	2.1	$3.4x10^{-2}$
Adipose (SC)	SLC1A5	19	0.15	rs4804030	-2.6	rs8105903	7.2	2.3	334	susie	3.2	$1.3x10^{-3}$
Adipose (SC)	C20orf194	20	0.062	rs6052141	2.9	rs1207	4.3	1.5	438	lasso	2.0	$4.3x10^{-2}$
Adipose (SC)	PANK2	20	0.092	rs12480318	3.2	rs12480318	5.4	3.2	556	enet	3.1	$2.3x10^{-3}$
Adipose (SC)	SDC4	20	0.19	rs11698812	3.1	rs6073718	-5.5	-1.5	488	enet	3.4	$6.6x10^{-4}$
Adipose (SC)	ARHGAP8	22	0.10	rs8138173	3.1	rs3761481	4.9	-1.4	707	enet	-3.1	$2.0x10^{-3}$
Adipose (SC)	TYMP	22	0.34	rs28513473	2.9	rs3091397	-9.9	-1.6	318	enet	2.4	$1.6x10^{-2}$
Adipose (SC)	ODF3B	22	0.15	rs28513473	2.9	rs140521	-7.0	-2.6	316	lasso	2.4	$1.5x10^{-2}$
Adipose (SC)	CPT1B	22	0.32	rs28513473	2.9	rs131750	10.6	2.6	295	susie	2.3	$2.2x10^{-2}$
Adipose (SC)	CHKB-DT	22	0.15	rs28513473	2.9	rs131748	8.3	-2.3	293	top1	-2.3	$2.0x10^{-2}$
Adipose (SC)	CHKB	22	0.43	rs28513473	2.9	rs131760	-10.9	-2.6	284	enet	3.4	$6.4x10^{-4}$
Adipose (VO)	CYP1B1	2	0.10	rs41383748	-3.2	rs13398184	-4.8	2.1	575	enet	-3.9	$9.1x10^{-5}$
Adipose (VO)	ATL2	2	0.14	rs41383748	-3.2	rs7606376	6.0	-1.4	473	susie	-2.2	$3.0x10^{-2}$
Adipose (VO)	PARP14	3	0.30	rs6764971	-3.3	rs6770902	9.2	-3.1	541	susie	-3.7	$1.9x10^{-4}$

Continuation of Table A12

Adipose (VO)	HSPBAP1	3	0.12	rs6764971	-3.3	rs3806643	5.8	2.6	502	susie	2.7	$6.8x10^{-3}$
Adipose (VO)	DMAC2L	14	0.045	rs2297995	3.8	rs12433794	5.1	3.7	393	enet	3.6	$3.7x10^{-4}$
Adipose (VO)	SYNM	15	0.33	rs12915090	3.0	rs2602021	11.2	2.3	546	enet	3.0	$2.9x10^{-3}$
Adipose (VO)	SYNM-AS2	15	0.072	rs12915090	3.0	rs2602021	4.6	2.3	541	susie	2.3	$2.1x10^{-2}$
Adipose (VO)	LINC00667	18	0.68	rs12162179	3.2	rs11877315	14.4	2.6	488	lasso	2.7	$6.1x10^{-3}$
Blood	SLC35F6	2	0.029	rs3806517	3.6	rs12992046	-3.9	3.5	378	susie	-3.4	$8.1x10^{-4}$
Blood	EMILIN1	2	0.039	rs3806517	3.6	rs1866561	-4.9	-1.2	306	enet	2.2	$3.1x10^{-2}$
Blood	RP11-164P12.5	4	0.13	rs11726420	3.8	rs4235219	9.8	-3.5	364	lasso	-3.6	$3.5x10^{-4}$
Blood	EPDR1	7	0.19	rs2722309	-3.0	rs4720265	-7.8	-2.6	575	enet	3.0	$2.8x10^{-3}$
Blood	LINC02446	12	0.12	rs7305642	3.3	rs4076336	-4.6	3.2	460	enet	-3.2	$1.2x10^{-3}$
Blood	RPL36AL	14	0.22	rs941604	3.5	rs2985697	-11.3	-1.8	379	susie	2.1	$3.8x10^{-2}$
Blood	LINC01588	14	0.21	rs2297995	3.8	rs8012757	-7.1	-2.5	343	enet	2.3	$2.0x10^{-2}$
Blood	SOS2	14	0.057	rs2297995	3.8	rs1955926	5.5	3.2	348	top1	3.2	$1.4x10^{-3}$
Blood	CDKL1	14	0.17	rs2297995	3.8	rs1465160	10.8	-2.9	429	enet	-3.5	$4.1x10^{-4}$
Blood	PYGL	14	0.10	rs1890706	-3.3	rs10149867	6.2	-2.4	509	top1	-2.4	$1.8x10^{-2}$
Blood	AQP9	15	0.084	rs2280197	-3.5	rs2899619	5.5	-3.2	662	susie	-3.5	$4.5x10^{-4}$
Blood	LPCAT2	16	0.096	rs3785152	-3.1	rs4402561	6.2	2.4	660	enet	3.3	$9.0x10^{-4}$
Blood	AC007336.1	16	0.070	rs3785152	-3.1	rs16955364	5.4	-2.6	656	lasso	-2.7	$8.1x10^{-3}$
Blood	RP11-686D22.5	17	0.17	rs4796089	2.9	rs997655	6.4	-2.3	366	susie	-2.4	$1.7x10^{-2}$
Blood	RP11-686D22.4	17	0.37	rs4796089	2.9	rs1545283	10.2	-2.5	366	enet	-2.6	$1.1x10^{-2}$

Continuation of Table A12

Blood	DTWD2 pseudogene	17	0.26	rs4796089	2.9	rs1545283	8.5	-2.5	367	enet	-3.3	$1.1x10^{-3}$
Blood	RAB32 pseudogene	17	0.14	rs4796089	2.9	rs997655	7.1	-2.3	374	enet	-2.4	$1.6x10^{-2}$
Blood	SLFN12	17	0.35	rs4796089	2.9	rs997655	10.1	-2.3	376	lasso	-2.6	$1.1x10^{-2}$
Blood	SLFN13	17	0.098	rs4796089	2.9	rs17549947	-5.7	-2.7	376	lasso	3.0	$3.1x10^{-3}$
Blood	LINC03078	19	0.64	rs8109124	2.7	rs12461712	11.9	1.5	294	enet	2.7	$8.0x10^{-3}$
Blood	Antisense to CD177	19	0.16	rs8109124	2.7	rs12609638	5.7	1.7	305	lasso	2.4	$1.7x10^{-2}$
Blood	CD177P1	19	0.47	rs8109124	2.7	rs7257560	-11.4	-1.8	309	enet	2.6	$9.4x10^{-3}$
Blood	ETHE1	19	0.067	rs400591	3.1	rs7259375	4.1	2.6	372	enet	3.3	$1.1x10^{-3}$
Blood	CSTB	21	0.37	rs3761385	-3.2	rs2838367	-14.8	-1.9	282	enet	2.8	$5.6x10^{-3}$
Blood	RRP1	21	0.070	rs3761385	-3.2	rs6518323	-5.1	-2.6	289	top1	2.6	$8.8x10^{-3}$
Blood	AATBC	21	0.038	rs3761385	-3.2	rs9985006	-3.8	-2.2	285	top1	2.2	$2.6x10^{-2}$
Blood	PFKL	21	0.20	rs2838644	-3.2	rs8133730	7.0	1.8	394	susie	2.5	$1.3x10^{-2}$
Blood	COMT	22	0.070	rs9332316	3.0	rs933271	5.9	1.3	564	susie	2.1	$3.3x10^{-2}$
Blood	ARVCF	22	0.11	rs9332316	3.0	rs165849	-6.1	-2.9	550	susie	3.3	$1.1x10^{-3}$
Blood	DGCR8	22	0.11	rs9332316	3.0	rs7285397	7.5	-2.6	556	top1	-2.6	$1.0x10^{-2}$
Blood	DGCR6L	22	0.28	rs9332316	3.0	rs4425183	-10.9	-2.6	567	lasso	2.5	$1.3x10^{-2}$
Blood	CBX6	22	0.24	rs5750781	-3.2	rs7292074	-6.2	-1.8	393	susie	3.2	$1.3x10^{-3}$
Blood	PDGFB	22	0.12	rs5750781	-3.2	rs5757573	-7.2	-2.8	405	enet	2.3	$1.9x10^{-2}$
Blood	CPT1B	22	0.54	rs28513473	2.9	rs1557503	-14.2	-0.73	295	enet	2.5	$1.4x10^{-2}$
Blood	CHKB-DT	22	0.081	rs28513473	2.9	rs131748	6.5	-2.3	293	susie	-2.5	$1.2x10^{-2}$
Blood	CHKB	22	0.23	rs28513473	2.9	rs131750	8.0	2.6	284	enet	3.6	$3.2x10^{-4}$

Continuation of Table A12

Muscle	CDC23	5	0.027	rs10515497	4.4	rs9327809	4.0	-2.7	282	susie	-3.1	$2.0x10^{-3}$
Muscle	KDM3B	5	0.056	rs12188779	-4.4	rs10072318	5.7	-2.0	294	susie	-2.2	$2.7x10^{-2}$
Muscle	BPGM	7	0.068	rs7783456	3.4	rs4732047	5.4	3.0	513	susie	3.1	$2.1x10^{-3}$
Muscle	FUT10	8	0.11	rs1829189	3.3	rs7848	8.8	2.8	251	top1	2.8	$4.5x10^{-3}$
Muscle	MAK16	8	0.080	rs1829189	3.3	rs8685	6.2	3.2	254	Enet	2.5	$1.3x10^{-2}$
Muscle	TTI2	8	0.049	rs1829189	3.3	rs1829189	-4.8	3.3	253	top1	-3.3	$1.1x10^{-3}$
Muscle	UEVLD	11	0.041	rs11024717	-3.3	rs10832941	4.9	-2.9	458	lasso	-3.2	$1.6x10^{-3}$
Muscle	MISFA	11	0.11	rs11024717	-3.3	rs12418726	-5.9	2.4	458	Enet	-2.7	$6.7x10^{-3}$
Muscle	PTPRJ	11	0.083	rs10838805	3.6	rs1039481	4.9	3.4	231	lasso	3.2	$1.4x10^{-3}$
Muscle	INTS4	11	0.39	rs1793343	-3.9	rs672460	-13.6	-3.8	349	susie	3.2	$1.6x10^{-3}$
Muscle	THRSP	11	0.12	rs1793343	-3.9	rs589472	6.7	-2.9	345	Enet	-2.0	$4.1x10^{-2}$
Muscle	AACS	12	0.20	rs10846834	-3.4	rs12581512	9.8	-3.0	532	Enet	-2.7	$6.2x10^{-3}$
Muscle	RP11-158L12.4	12	0.18	rs10846834	-3.4	rs12581512	12.2	-3.0	527	lasso	-3.2	$1.3x10^{-3}$
Muscle	AC138466.5	12	0.048	rs34708049	-4.2	rs7976069	5.0	2.9	303	susie	3.1	$1.8x10^{-3}$
Muscle	CYCSP34	13	0.078	rs9532718	-3.5	rs9532657	-5.8	1.8	344	susie	-2.1	$3.3x10^{-2}$
Muscle	WBP4	13	0.43	rs9532718	-3.5	rs17532490	12.2	1.5	301	susie	2.9	$3.3x10^{-3}$
Muscle	RGCC	13	0.091	rs9532718	-3.5	rs12865815	6.5	2.7	341	susie	2.5	$1.1x10^{-2}$
Muscle	L2HGDH	14	0.12	rs2297995	3.8	rs2297995	9.3	3.8	379	Enet	3.8	$1.3x10^{-4}$
Muscle	DMAC2L	14	0.22	rs2297995	3.8	rs2275592	11.8	3.7	379	top1	3.7	$2.4x10^{-4}$
Muscle	GCATP1	14	0.078	rs8012691	-2.9	rs8012691	5.3	-2.9	356	top1	-2.9	$3.4x10^{-3}$

Continuation of Table A12

Muscle	Antisense to MTHFD1	14	0.069	rs2057130	2.5	rs1542313	6.1	1.7	481	susie	2.0	$4.2x10^{-2}$
Muscle	LINC02256	15	0.19	rs4779969	4.2	rs8037818	7.5	-1.5	379	Enet	-2.9	$3.4x10^{-3}$
Muscle	ADPGK	15	0.16	rs11072383	3.0	rs12594320	6.2	3.0	225	susie	3.0	$2.9x10^{-3}$
Muscle	AKAP13	15	0.16	rs4530079	3.2	rs16943484	9.6	2.0	577	top1	2.0	$4.9x10^{-2}$
Muscle	RP11-158M2.3	15	0.075	rs4530079	3.2	rs2542606	6.0	2.6	556	top1	2.6	$1.0x10^{-2}$
Muscle	AC021739.4	15	0.056	rs4530079	3.2	rs2946365	-4.7	-2.4	557	enet	3.1	$2.0x10^{-3}$
Muscle	LINC02883	15	0.072	rs4530079	3.2	rs3169119	-7.1	-2.1	559	top1	2.1	$3.5x10^{-2}$
Muscle	CSTB	21	0.23	rs3761385	-3.2	rs2838367	-11.8	-1.9	276	enet	2.8	$4.7x10^{-3}$
Muscle	ACO2	22	0.062	rs7364180	-3.1	rs2073167	5.7	-2.0	279	enet	-2.1	$3.6x10^{-2}$
Muscle	POLR3H	22	0.37	rs7364180	-3.1	rs738499	8.6	1.8	292	enet	2.1	$3.5x10^{-2}$
Muscle	SREBF2	22	0.08	rs7364180	-3.1	rs7364180	4.3	-3.1	318	top1	-3.1	$2.0x10^{-3}$
Liver	DRAM2	1	0.57	rs11584291	3.5	rs3762374	8.8	2.4	570	susie	3.0	$2.9x10^{-3}$
Liver	CEPT1	1	0.31	rs11584291	3.5	rs657801	-5.5	-2.7	570	susie	2.8	$4.9x10^{-3}$
Liver	DENND2D	1	0.36	rs11584291	3.5	rs629608	-6.4	-2.6	558	susie	2.4	$1.9x10^{-2}$
Liver	OVGP1	1	0.21	rs11584291	3.5	rs1264894	-4.9	-2.0	602	top1	2.0	$4.3x10^{-2}$
Liver	RP4-781K5.6	1	0.26	rs541021	4.7	rs476875	6.2	-3.5	551	susie	-3.9	$1.2x10^{-4}$
Liver	DNASE1L3	3	0.17	rs7627013	3.7	rs6787425	3.8	2.0	448	enet	3.3	$1.0x10^{-3}$
Liver	LINC00525	7	0.39	rs6463441	3.5	rs5004318	8.3	3.3	514	susie	3.4	$8.1x10^{-4}$
Liver	MCPH1-DT	8	0.20	rs2916749	3.1	rs12546419	3.5	1.9	982	susie	3.5	$4.9x10^{-4}$
Liver	RP11-722E23.2	8	0.096	rs1829189	3.3	rs10097936	5.0	3.0	240	susie	2.9	$4.0x10^{-3}$
Liver	FUT10	8	0.22	rs1829189	3.3	rs3098657	7.6	2.9	251	susie	2.8	$5.4x10^{-3}$
Liver	SFRP1	8	0.26	rs7814391	2.9	rs968427	-4.6	1.8	467	enet	-2.9	$4.3x10^{-3}$

Continuation of Table A12

Liver	RP11-158L12.4	12	0.20	rs10846834	-3.4	rs12581512	5.4	-3.0	540	susie	-3.2	$1.2x10^{-3}$
Liver	EXOC5	14	0.33	rs268805	2.4	rs1396512	-3.6	-1.8	403	lasso	3.1	$1.8x10^{-3}$
Liver	GOLGA8B	15	0.25	rs12915800	2.9	rs11629815	-4.7	2.8	402	enet	-2.9	$4.0x10^{-3}$
Liver	Sense Intronic to LIPC	15	0.27	rs2280197	-3.5	rs12900410	-3.7	1.5	527	susie	-3.0	$2.4x10^{-3}$
Liver	CD276	15	0.55	rs568760	4.0	rs8038465	8.8	-3.0	362	enet	-2.9	$4.0x10^{-3}$
Liver	LINC00667	18	0.67	rs12162179	3.2	rs11872923	8.8	2.4	498	enet	2.9	$3.4x10^{-3}$
Liver	APOBEC3G	22	0.32	rs5750781	-3.2	rs2011869	7.4	-2.8	394	susie	-2.8	$5.4x10^{-3}$
Liver	TYMP	22	0.18	rs28513473	2.9	rs140521	-4.8	-2.6	318	susie	2.9	$4.3x10^{-3}$
Liver	CHKB-DT	22	0.39	rs28513473	2.9	rs131748	5.5	-2.3	294	top1	-2.3	$2.0x10^{-2}$
Liver	CHKB	22	0.17	rs28513473	2.9	rs131766	5.0	2.2	285	top1	2.2	$2.6x10^{-2}$
Testis	RP4-781K5.4	1	0.23	rs541021	4.7	rs624329	-6.9	3.4	564	top1	-3.4	$6.7x10^{-4}$
Testis	RP4-781K5.6	1	0.19	rs541021	4.7	rs605957	7.0	-4.0	550	enet	-4.2	$2.4x10^{-5}$
Testis	PLB1	2	0.25	rs12623911	3.0	rs1581035	-5.3	2.7	427	enet	-3.2	$1.4x10^{-3}$
Testis	HHATL	3	0.14	rs6768356	-3.3	rs13072026	-5.3	2.0	466	top1	-2.0	$4.1x10^{-2}$
Testis	CCDC13	3	0.21	rs6768356	-3.3	rs13072026	6.5	2.0	450	enet	3.8	$1.5x10^{-4}$
Testis	EIF4BP8	3	0.20	rs6764971	-3.3	rs1256208	6.2	-2.5	534	susie	-2.7	$7.2x10^{-3}$
Testis	PARP14	3	0.47	rs6764971	-3.3	rs6770902	9.8	-3.1	542	enet	-3.7	$2.5x10^{-4}$
Testis	TMEM212-IT1	3	0.13	rs4618247	3.0	rs4618247	-4.8	3.0	446	enet	-3.5	$4.3x10^{-4}$
Testis	LINC00504	4	0.16	rs4358395	-3.3	rs2604573	-4.3	2.2	484	enet	-3.3	$1.1x10^{-3}$
Testis	FAM13B	5	0.067	rs10515497	4.4	rs4835748	-5.0	4.1	317	susie	-4.3	$2.1x10^{-5}$
Testis	WNT8A	5	0.10	rs10515497	4.4	rs1042124	4.3	3.5	312	lasso	3.2	$1.4x10^{-3}$
Testis	KIF20A	5	0.17	rs10515497	4.4	rs17171767	7.9	-3.0	292	top1	-3.0	$3.0x10^{-3}$
Testis	CDC23	5	0.14	rs10515497	4.4	rs2269954	6.7	-2.9	283	susie	-3.2	$1.6x10^{-3}$
Testis	GFRA3	5	0.071	rs10515497	4.4	rs1468333	-5.4	-2.9	289	top1	2.9	$4.0x10^{-3}$

Continuation of Table A12

Testis	CCDC136	7	0.19	rs109829	-2.6	rs7799186	6.0	2.4	340	susie	3.2	$1.3x10^{-3}$
Testis	LRGUK	7	0.63	rs1160049	3.1	rs892983	6.5	1.6	435	enet	2.1	$3.2x10^{-2}$
Testis	BPGM	7	0.22	rs7783456	3.4	rs1160049	7.4	3.1	518	enet	3.1	$2.0x10^{-3}$
Testis	ATP6V0A4	7	0.41	rs999228	3.7	rs999228	8.1	3.7	406	enet	4.2	$3.0x10^{-5}$
Testis	FUT10	8	0.33	rs1829189	3.3	rs2732315	7.4	2.5	251	susie	2.6	$1.0x10^{-2}$
Testis	MAK16	8	0.13	rs1829189	3.3	rs2043967	3.6	2.0	254	susie	3.3	$9.2x10^{-4}$
Testis	TTI2	8	0.13	rs1829189	3.3	rs3098657	-6.9	2.9	253	lasso	-2.9	$3.7x10^{-3}$
Testis	ELOBP2	11	0.34	rs7113818	3.0	rs12805829	7.0	-2.4	468	enet	-3.6	$3.6x10^{-4}$
Testis	PSPC1	13	0.18	rs7984806	-2.8	rs2290810	-5.8	-2.5	309	susie	3.6	$3.5x10^{-4}$
Testis	MIPEP	13	0.52	rs2765107	4.6	rs17079485	10.2	2.7	764	top1	2.7	$7.5x10^{-3}$
Testis	PCOTH	13	0.53	rs2765107	4.6	rs17079485	-11.0	2.7	764	enet	-2.2	$2.8x10^{-2}$
Testis	C1QTNF9B	13	0.68	rs2765107	4.6	rs9551026	10.7	4.2	751	enet	3.1	$2.0x10^{-3}$
Testis	ANKRD20A19P	13	0.38	rs2765107	4.6	rs17071064	-9.6	3.2	737	lasso	-4.2	$3.2x10^{-5}$
Testis	C1QTNF9	13	0.44	rs2765107	4.6	rs11617793	8.5	1.6	727	enet	2.7	$7.4x10^{-3}$
Testis	TPTE2P6	13	0.21	rs2765107	4.6	rs9511316	6.2	2.8	711	enet	2.2	$3.0x10^{-2}$
Testis	PSPC1P2	13	0.17	rs9511340	2.9	rs9511316	5.1	2.8	641	enet	2.4	$1.5x10^{-2}$
Testis	EXD2	14	0.077	rs12436823	2.9	rs12433032	-3.7	2.6	507	enet	-2.7	$7.0x10^{-3}$
Testis	Antisense to SLC8A3, ADAM20 pseudogene	14	0.13	rs2182973	3.4	rs8013825	-6.8	-2.3	524	susie	2.3	$2.2x10^{-2}$
Testis	ADAM20 pseudogene	14	0.34	rs2182973	3.4	rs9323533	-9.3	-2.2	535	susie	2.2	$2.6x10^{-2}$
Testis	ADAM21P1	14	0.47	rs2182973	3.4	rs17476399	-11.6	-2.2	544	top1	2.2	$3.1x10^{-2}$
Testis	RP11-718G2.5	14	0.23	rs2182973	3.4	rs4899342	-8.0	3.3	540	top1	-3.3	$1.1x10^{-3}$

Continuation of Table A12

Testis	ADAM 20	14	0.089	rs2182973	3.4	rs17565772	-5.1	-2.2	484	top1	2.2	$3.1x10^{-2}$
Testis	TTC9	14	0.25	rs2182973	3.4	rs7147575	4.4	-1.9	431	lasso	-2.8	$4.8x10^{-3}$
Testis	CHRFAM7A	15	0.60	rs11638069	2.0	rs12904872	6.2	-0.68	136	enet	-2.0	$4.7x10^{-2}$
Testis	GOLGA8UP	15	0.15	rs6493462	-3.1	rs4779777	-4.4	0.60	277	enet	-2.1	$4.1x10^{-2}$
Testis	CHRNA7	15	0.10	rs4779969	4.2	rs16956738	-3.4	2.5	300	susie	-2.1	$3.6x10^{-2}$
Testis	HCN2 pseudogene	15	0.11	rs4779969	4.2	rs6494165	-4.9	4.1	293	top1	-4.1	$3.8x10^{-5}$
Testis	GOLGA8K	15	0.25	rs4779969	4.2	rs6494165	-6.0	4.1	336	top1	-4.1	$3.8x10^{-5}$
Testis	GOLGA8N	15	0.54	rs17228887	3.3	rs28457217	-7.5	1.6	394	enet	-2.3	$2.4x10^{-2}$

Abbreviations: eQTL, expression quantitative trait locus; CHR, chromosome, HSQ, mean heritability estimate; Best.GWAS.ID, most significantly associated variant in the locus; Best.GWAS.Z, z-score of most significantly associated variant in the locus; eQTL ID, best eQTL in the locus; eQTL.GWAS.Z, GWAS z-score for best eQTL; NSNP, number of SNPs in the locus; Model, best performing TWAS model; TWAS.Z, TWAS z-score; TWAS.P, TWAS p-value, enet, elastic-net regression (mixing parameter = 0.5); blup, best linear unbiased predictor from all variants; bslmm, Bayesian sparse linear model; lasso, least absolute shrinkage and selection operator; top1, single best eQTL, susie, sum of single effects regression, VO, visceral omentum; SC, subcutaneous.

Table A13. Genes associated with cisplatin-induced hearing loss by TWAS ($p < 0.0005$)

Tissue	Gene	CHR	HSQ	BEST.GWAS.ID	BEST.GWAS.Z	EQTL.ID	EQTL.Z	EQTL.GWAS.Z	NSNP	MODEL	TWAS.Z	TWAS.P
Nerve	FGGY-DT	1	0.34	rs12739770	3.9	rs12758643	12.8	3.8	397	lasso	3.5	$4.6x10^{-4}$
Nerve	WFS1	4	0.16	rs17718958	4.5	rs10010131	-8.2	3.8	662	susie	-3.8	$1.7x10^{-4}$
Nerve	BZW2	7	0.13	rs864212	-3.9	rs1167578	-7.2	-3.7	635	top1	3.7	$2.4x10^{-4}$
Nerve	FGL1	8	0.068	rs17125822	4.5	rs3850746	4.8	-3.7	861	top1	-3.7	$2.5x10^{-4}$
Cerebellum	LINC00958	11	0.27	rs11022588	-4.1	rs11022589	-5.8	-4.1	550	top1	4.1	$4.8x10^{-5}$
Cerebellum	FAM98C	19	0.27	rs2302226	4.0	rs2286550	4.6	3.8	380	lasso	3.9	$9.1x10^{-5}$
Cerebellum	IZUMO1	19	0.38	rs4021	3.4	rs4021	6.3	3.4	429	susie	3.6	$3.9x10^{-4}$
Brain	WFS1	4	0.10	rs17718958	4.5	rs1046314	-4.7	3.8	671	top1	-3.8	$1.8x10^{-4}$
Brain	ERCC8	5	0.11	rs10077663	-4.1	rs162231	6.4	-3.0	327	lasso	-3.6	$2.7x10^{-4}$
Brain	PDLIM4	5	0.11	rs9791170	3.8	rs3900945	9.3	3.5	411	top1	3.5	$4.2x10^{-4}$
Brain	ANKRD49	11	0.059	rs7950328	3.6	rs6483341	-5.2	-2.6	438	enet	3.6	$3.2x10^{-4}$
Kidney	SLC1A7	1	0.80	rs34418279	3.2	rs12731800	4.1	2.2	475	lasso	3.6	$3.9x10^{-4}$
Kidney	LINC00958	11	0.73	rs11022588	-4.1	rs11022588	-5.6	-4.1	553	top1	4.1	$4.4x10^{-5}$
Adipose (SC)	WFS1	4	0.089	rs17718958	4.5	rs10010131	-6.7	3.8	657	susie	-3.8	$1.3x10^{-4}$
Adipose (SC)	PCM1	8	0.15	rs17125822	4.5	rs2301546	-6.6	3.1	868	susie	-4.2	$2.8x10^{-5}$
Adipose (SC)	DTD2	14	0.18	rs11156667	-3.1	rs17097892	-8.2	3.0	305	enet	-3.5	$4.0x10^{-4}$
Adipose (SC)	IZUMO1	19	0.41	rs4021	3.4	rs838143	10.5	3.0	428	enet	3.6	$3.5x10^{-4}$
Adipose (VO)	ATRIP	3	0.35	rs35452137	-4.0	rs35452137	-7.5	-4.0	253	lasso	3.8	$1.8x10^{-4}$
Adipose (VO)	WFS1	4	0.11	rs17718958	4.5	rs4689393	-5.8	4.2	665	top1	-4.2	$2.9x10^{-5}$
Adipose (VO)	PCM1	8	0.17	rs17125822	4.5	rs2285306	-6.6	3.7	871	susie	-4.4	$1.1x10^{-5}$
Adipose (VO)	ZNF408	11	0.052	rs1352307	-3.4	rs4752927	-4.3	-2.7	237	enet	3.7	$2.4x10^{-4}$
Blood	PCM1	8	0.087	rs17125822	4.5	rs12718385	8.0	-3.7	868	enet	-3.7	$2.5x10^{-4}$
Blood	LINC00958	11	0.50	rs11022588	-4.1	rs11022589	17.8	-4.1	546	lasso	-4.0	$6.9x10^{-5}$

Continuation of Table A13

Blood	Antisense to SERPINA9	14	0.086	rs11628686	-3.7	rs6575433	5.0	-3.6	805	susie	-3.5	$4.6x10^{-4}$
Blood	BAX	19	0.10	rs4021	3.4	rs7259013	-6.4	2.8	424	enet	-3.7	$2.4x10^{-4}$
Blood	ARHGAP8	22	0.13	rs3761481	-4.3	rs3761481	5.8	-4.3	705	top1	-4.3	$1.9x10^{-5}$
Muscle	ATG101	12	0.11	rs12424271	-4.1	rs11521	-6.2	-3.2	615	susie	3.6	$3.8x10^{-4}$
Muscle	RALGAPA2	20	0.057	rs6047273	-3.8	rs6137147	4.6	3.8	405	lasso	3.7	$2.7x10^{-4}$
Testis	RP1-182D15.2	6	0.17	rs9478048	-3.2	rs12196723	-4.2	-2.3	439	susie	3.5	$4.5x10^{-4}$
Testis	LINC02385	12	0.13	rs4406890	4.6	rs4964288	4.1	4.0	793	top1	4.0	$7.2x10^{-5}$

Abbreviations: eQTL, expression quantitative trait locus; CHR, chromosome, HSQ, mean heritability estimate; Best.GWAS.ID, most significantly associated variant in the locus; Best.GWAS.Z, z-score of most significantly associated variant in the locus; eQTL ID, best eQTL in the locus; eQTL.GWAS.Z, GWAS z-score for best eQTL; NSNP, number of SNPs in the locus; Model, best performing TWAS model; TWAS.Z, TWAS z-score; TWAS.P, TWAS p-value, enet, elastic-net regression (mixing parameter = 0.5); blup, best linear unbiased predictor from all variants; bslmm, Bayesian sparse linear model; lasso, least absolute shrinkage and selection operator; top1, single best eQTL, susie, sum of single effects regression, VO, visceral omentum; SC, subcutaneous.

Table A14. Genes associated with cisplatin-induced hearing loss by TWAS ($p < 0.005$)

Tissue	Gene	CHR	HSQ	BEST.GWAS.ID	BEST.GWAS.Z	EQTL.ID	EQTL.Z	EQTL.GWAS.Z	NSNP	MODEL	TWAS.Z	TWAS.P
Nerve	FGGY-DT	1	0.34	rs12739770	3.9	rs12758643	12.8	3.8	397	lasso	3.5	$4.6x10^{-4}$
Nerve	RP5-943J3.1	1	0.29	rs1011702	3.8	rs473412	-14.8	3.4	370	susie	-3.3	$1.0x10^{-3}$
Nerve	TMEM167B-DT	1	0.078	rs12066164	3.3	rs616378	6.1	-2.9	409	top1	-2.9	$4.4x10^{-3}$
Nerve	SERTAD4-AS1	1	0.17	rs654523	3.2	rs654523	8.4	3.2	552	lasso	3.3	$1.1x10^{-3}$
Nerve	SMYD2	1	0.16	rs7543972	-2.8	rs1472444	-5.8	-2.5	541	enet	3.1	$1.7x10^{-3}$
Nerve	SOS1	2	0.034	rs2599074	3.5	rs7577088	4.0	2.9	269	susie	2.9	$3.7x10^{-3}$
Nerve	RN7SL145P	3	0.084	rs2742395	3.0	rs1019129	-6.3	2.9	454	top1	-2.9	$3.3x10^{-3}$
Nerve	ATRIP	3	0.12	rs35452137	-4.0	rs3135941	-5.0	-2.6	244	enet	3.4	$7.8x10^{-4}$
Nerve	NCKIPSD	3	0.32	rs35452137	-4.0	rs12493578	-13.6	2.8	252	enet	-3.0	$3.1x10^{-3}$
Nerve	PRKAR2A	3	0.028	rs35452137	-4.0	rs7626445	4.9	3.2	262	susie	3.2	$1.3x10^{-3}$
Nerve	ARIH2	3	0.055	rs35452137	-4.0	rs3212	-6.5	2.6	254	susie	-3.1	$1.8x10^{-3}$
Nerve	P4HTM	3	0.14	rs35452137	-4.0	rs6772452	-9.5	2.8	250	lasso	-3.0	$2.4x10^{-3}$
Nerve	WDR6	3	0.37	rs35452137	-4.0	rs6446205	16.9	3.3	252	susie	3.1	$2.2x10^{-3}$
Nerve	DALRD3	3	0.083	rs35452137	-4.0	rs6781790	-7.9	3.3	254	lasso	-3.3	$8.9x10^{-4}$
Nerve	LAMB2P1	3	0.051	rs7628719	3.4	rs4955416	-4.8	2.9	258	top1	-2.9	$4.3x10^{-3}$
Nerve	CCDC71	3	0.039	rs7628719	3.4	rs4974082	5.0	3.4	259	enet	3.2	$1.3x10^{-3}$
Nerve	RBP1	3	0.19	rs3821546	3.4	rs211587	-5.1	-1.9	493	enet	2.9	$3.8x10^{-3}$
Nerve	ZNF639	3	0.15	rs6443599	-3.5	rs7610174	-7.1	2.7	365	susie	-3.0	$2.6x10^{-3}$
Nerve	XXYLT1	3	0.26	rs7627043	3.6	rs6794037	7.9	3.1	380	susie	3.1	$1.9x10^{-3}$
Nerve	WFS1	4	0.16	rs17718958	4.5	rs10010131	-8.2	3.8	662	susie	-3.8	$1.7x10^{-4}$

Continuation of Table A14

Nerve	FAM153C	5	0.25	rs3812080	-3.8	rs4073772	7.5	-2.6	364	enet	-2.9	$4.3x10^{-3}$
Nerve	CARMIL1	6	0.27	rs2690120	3.2	rs1883393	-7.2	1.3	636	susie	-3.1	$1.7x10^{-3}$
Nerve	BZW2	7	0.13	rs864212	-3.9	rs1167578	-7.2	-3.7	635	top1	3.7	$2.4x10^{-4}$
Nerve	RPL12P10	7	0.066	rs2905325	-3.8	rs4719726	-3.5	1.6	480	susie	-3.0	$2.9x10^{-3}$
Nerve	NSUN5P2	7	0.56	rs34014814	-2.7	rs34014814	8.1	-2.7	94	enet	-2.9	$3.8x10^{-3}$
Nerve	LINC00689	7	0.29	rs2602565	-3.2	rs885861	-8.9	2.6	332	enet	-3.1	$2.0x10^{-3}$
Nerve	USP17L2 pseudogene	8	0.071	rs9325786	-3.4	rs4831828	3.9	2.3	177	enet	2.9	$4.2x10^{-3}$
Nerve	FGL1	8	0.068	rs17125822	4.5	rs3850746	4.8	-3.7	861	top1	-3.7	$2.5x10^{-4}$
Nerve	PCM1	8	0.35	rs17125822	4.5	rs12718385	9.0	-3.7	868	enet	-3.5	$5.4x10^{-4}$
Nerve	HACD4	9	0.08	rs10125958	3.3	rs11789272	5.2	3.1	464	top1	3.1	$2.2x10^{-3}$
Nerve	HMGB3P24	9	0.11	rs10738958	3.6	rs12378860	-5.3	-2.1	397	enet	3.0	$2.6x10^{-3}$
Nerve	C1QL3	10	0.78	rs7079565	2.9	rs7909832	-16.6	-2.7	593	enet	2.9	$3.4x10^{-3}$
Nerve	EID3	12	0.30	rs4406890	4.6	rs11111987	-13.1	3.1	798	lasso	-3.1	$2.1x10^{-3}$
Nerve	SPART-AS1	13	0.062	rs1886856	-3.2	rs9547462	5.5	-3.0	512	enet	-3.1	$1.7x10^{-3}$
Nerve	SPART	13	0.17	rs1886856	-3.2	rs3736919	-8.5	2.5	520	enet	-3.0	$2.6x10^{-3}$
Nerve	DTD2	14	0.24	rs11156667	-3.1	rs17097892	-7.9	3.0	307	enet	-3.3	$1.1x10^{-3}$
Nerve	CA5A pseudogene	16	0.11	rs11862806	3.4	rs8051096	-8.1	3.4	209	top1	-3.4	$7.5x10^{-4}$
Nerve	FTO	16	0.13	rs4783826	-3.4	rs741300	-4.6	3.0	459	top1	-3.0	$3.1x10^{-3}$
Nerve	TXNL4B	16	0.80	rs8052152	-2.6	rs4788614	7.0	0.81	346	susie	3.1	$1.8x10^{-3}$
Nerve	CDH15	16	0.43	rs2016979	3.4	rs12598250	-6.1	2.2	419	enet	-3.0	$2.5x10^{-3}$
Nerve	SHPK	17	0.49	rs170313	3.0	rs9897822	10.2	1.2	526	susie	3.0	$2.7x10^{-3}$
Nerve	SLC25A35	17	0.16	rs9889775	-2.7	rs7216400	-5.1	0.98	446	enet	-2.9	$4.0x10^{-3}$
Nerve	GRIK5	19	0.074	rs3826705	-3.0	rs8099939	4.9	-1.4	213	enet	-3.4	$6.0x10^{-4}$

Continuation of Table A14

Nerve	FUT1	19	0.11	rs4021	3.4	rs4021	5.7	3.4	419	top1	3.4	$7.0x10^{-4}$
Cerebellum	H6PD	1	0.70	rs9435151	2.9	rs9435151	-9.4	2.9	430	enet	-2.8	$4.9x10^{-3}$
Cerebellum	ADORA1	1	0.30	rs4950914	-3.4	rs782803	-4.9	-1.8	511	enet	3.1	$2.3x10^{-3}$
Cerebellum	ST3GAL5	2	0.21	rs4480982	-3.2	rs1866245	-3.0	-3.2	459	top1	3.2	$1.6x10^{-3}$
Cerebellum	CHMP3	2	0.16	rs6735014	2.6	rs11678201	-4.4	2.0	332	enet	-3.1	$2.2x10^{-3}$
Cerebellum	RN7SL145P	3	0.24	rs2742395	3.0	rs2742395	-6.8	3.0	467	top1	-3.0	$2.8x10^{-3}$
Cerebellum	NCKIPSD	3	0.29	rs35452137	-4.0	rs4858828	-8.9	2.8	262	susie	-2.9	$3.3x10^{-3}$
Cerebellum	WDR6	3	0.28	rs35452137	-4.0	rs7626445	9.4	3.2	261	top1	3.2	$1.2x10^{-3}$
Cerebellum	QRICH1	3	0.28	rs7628719	3.4	rs7100	7.5	3.0	253	top1	3.0	$3.2x10^{-3}$
Cerebellum	ADCY5	3	0.25	rs1511580	3.6	rs6809407	3.2	-1.0	409	susie	-3.0	$2.7x10^{-3}$
Cerebellum	NMNAT3	3	0.3	rs6769310	-3.5	rs9790066	4.2	2.8	524	enet	2.9	$4.4x10^{-3}$
Cerebellum	XXYLT1	3	0.22	rs7627043	3.6	rs6794037	5.5	3.1	381	susie	3.4	$7.8x10^{-4}$
Cerebellum	WFS1	4	0.74	rs17718958	4.5	rs13107806	-10.0	3.3	672	susie	-3.4	$7.2x10^{-4}$
Cerebellum	PPP2R2C	4	0.39	rs17718958	4.5	rs13107806	-3.4	3.3	529	susie	-3.2	$1.3x10^{-3}$
Cerebellum	ZCCHC4	4	0.18	rs316807	3.0	rs7689775	5.0	3.0	549	lasso	2.9	$3.6x10^{-3}$
Cerebellum	Antisense to PHACTR1	6	0.59	rs1332845	3.6	rs2496132	8.0	-2.4	524	enet	-2.8	$4.9x10^{-3}$
Cerebellum	RPL10A	6	0.41	rs2076170	-3.0	rs2395626	5.2	-2.7	425	enet	-3.0	$2.9x10^{-3}$
Cerebellum	POU3F2	6	0.12	rs9493282	-3.6	rs2294405	5.6	3.1	427	top1	3.1	$1.8x10^{-3}$
Cerebellum	DNAJC30	7	0.38	rs4717850	2.7	rs8891	-3.9	0.69	267	enet	-2.9	$4.3x10^{-3}$
Cerebellum	PPP1R9A	7	0.21	rs10085641	2.9	rs1830245	-3.5	2.6	355	susie	-3.3	$9.1x10^{-4}$
Cerebellum	LINC00689	7	0.17	rs2602565	-3.2	rs2657323	3.0	-1.3	334	susie	-2.9	$3.9x10^{-3}$
Cerebellum	USP17L2 pseudogene	8	0.32	rs9325786	-3.4	rs6601649	-4.9	0.22	180	enet	2.9	$4.3x10^{-3}$
Cerebellum	RFX3-AS1	9	0.31	rs10814233	3.1	rs10814233	4.9	3.1	541	top1	3.1	$1.7x10^{-3}$
Cerebellum	CNTLN	9	0.16	rs16935340	-3.3	rs10962988	3.9	-2.5	546	lasso	-3.0	$2.9x10^{-3}$
Cerebellum	LINC00958	11	0.27	rs11022588	-4.1	rs11022589	-5.8	-4.1	550	top1	4.1	$4.8x10^{-5}$

Continuation of Table A14

Cerebellum	C11orf49	11	0.30	rs4647709	-3.5	rs7928445	-5.3	-2.8	280	lasso	2.9	$4.1x10^{-3}$
Cerebellum	PRR4	12	0.63	rs7294858	-2.7	rs7132674	9.3	-2.6	365	susie	-3.0	$2.9x10^{-3}$
Cerebellum	EID3	12	0.11	rs4406890	4.6	rs4964788	-4.0	3.3	799	susie	-3.3	$8.9x10^{-4}$
Cerebellum	RP11-236L14.2	15	0.16	rs2589227	-3.3	rs2589227	-3.8	-3.3	540	susie	3.0	$3.2x10^{-3}$
Cerebellum	IGFALS	16	0.49	rs28364711	-2.7	rs2437744	-6.4	-2.3	473	enet	3.2	$1.2x10^{-3}$
Cerebellum	SMCHD1	18	0.40	rs7245003	-3.8	rs28377858	-7.7	-3.5	514	susie	2.8	$4.8x10^{-3}$
Cerebellum	DLGAP1-AS3	18	0.39	rs12954964	-4.3	rs9947561	4.3	2.9	566	top1	2.9	$4.3x10^{-3}$
Cerebellum	FAM98C	19	0.27	rs2302226	4.0	rs2286550	4.6	3.8	380	lasso	3.9	$9.1x10^{-5}$
Cerebellum	IZUMO1	19	0.38	rs4021	3.4	rs4021	6.3	3.4	429	susie	3.6	$3.9x10^{-4}$
Brain	LRRC8C	1	0.079	rs1011702	3.8	rs473412	-6.4	3.4	410	top1	-3.4	$7.3x10^{-4}$
Brain	TMEM167B	1	0.072	rs12066164	3.3	rs616378	-6.4	-2.9	412	top1	2.9	$4.4x10^{-3}$
Brain	ALDH9A1	1	0.22	rs369231	3.6	rs4657468	-6.6	-1.3	614	lasso	2.9	$3.5x10^{-3}$
Brain	LOC151009	2	0.11	rs13426054	2.8	rs12474907	-5.3	2.5	144	blup	-3.5	$5.7x10^{-4}$
Brain	RPL23AP7	2	0.45	rs7595282	-3.0	rs4849261	12.2	-1.3	349	bslmm	-3.0	$2.4x10^{-3}$
Brain	P4HTM	3	0.13	rs35452137	-4.0	rs7432989	-8.3	3.3	264	blup	-3.2	$1.2x10^{-3}$
Brain	RBP1	3	0.13	rs3821546	3.4	rs6802598	6.5	2.7	500	lasso	3.2	$1.7x10^{-3}$
Brain	ZNF639	3	0.10	rs6443599	-3.5	rs1362650	5.7	-3.2	365	top1	-3.2	$1.4x10^{-3}$
Brain	WFS1	4	0.10	rs17718958	4.5	rs1046314	-4.7	3.8	671	top1	-3.8	$1.8x10^{-4}$
Brain	SEL1L3	4	0.19	rs316807	3.0	rs17627409	-5.3	-1.7	531	blup	3.1	$1.9x10^{-3}$
Brain	ELOVL7	5	0.037	rs10077663	-4.1	rs7722373	-4.8	3.1	355	top1	-3.1	$1.8x10^{-3}$
Brain	ERCC8	5	0.11	rs10077663	-4.1	rs162231	6.4	-3.0	327	lasso	-3.6	$2.7x10^{-4}$
Brain	PDLIM4	5	0.11	rs9791170	3.8	rs3900945	9.3	3.5	411	top1	3.5	$4.2x10^{-4}$
Brain	SERPINB1	6	0.17	rs17300141	-3.3	rs12525298	6.6	2.5	654	lasso	2.8	$4.6x10^{-3}$
Brain	IQUB	7	0.13	rs7789409	3.3	rs12673749	-7.0	3.3	398	blup	-2.9	$3.7x10^{-3}$
Brain	LOC286186	8	0.29	rs10102473	-2.7	rs11992528	-12.4	-2.5	365	enet	2.9	$3.6x10^{-3}$

Continuation of Table A14

Brain	PRTFDC1	10	0.12	rs7070190	-2.8	rs3789922	-4.5	1.4	481	bslmm	-3.0	$3.1x10^{-3}$
Brain	ANKRD30A	10	0.056	rs11011154	-3.1	rs12784034	-6.4	-3.1	371	top1	3.1	$2.0x10^{-3}$
Brain	RASSF10	11	0.077	rs11022588	-4.1	rs17418644	4.6	2.1	549	lasso	2.9	$4.2x10^{-3}$
Brain	ANKRD49	11	0.059	rs7950328	3.6	rs6483341	-5.2	-2.6	438	enet	3.6	$3.2x10^{-4}$
Brain	FDX1	11	0.088	rs920722	-3.3	rs17111255	6.2	-2.9	455	top1	-2.9	$3.4x10^{-3}$
Brain	PRH1-PRR4	12	0.28	rs7294858	-2.7	rs7310849	-13.5	2.6	513	lasso	-2.9	$4.1x10^{-3}$
Brain	TAS2R13	12	0.054	rs7294858	-2.7	rs6488330	5.2	-2.4	368	blup	-3.1	$1.7x10^{-3}$
Brain	TAS2R14	12	0.092	rs7294858	-2.7	rs10772397	7.1	-2.2	376	bslmm	-2.9	$3.4x10^{-3}$
Brain	TM7SF3	12	0.20	rs4265668	3.2	rs4963675	-6.6	3.0	552	enet	-3.0	$2.9x10^{-3}$
Brain	LOC728084	12	0.10	rs1519956	2.6	rs7968659	-6.6	2.6	322	enet	-2.8	$4.7x10^{-3}$
Brain	RMST	12	0.30	rs10507087	-4.1	rs1582336	11.0	2.2	646	enet	3.1	$2.1x10^{-3}$
Brain	NUP93	16	0.21	rs158619	-3.3	rs6499852	8.8	3.0	571	top1	3.0	$2.9x10^{-3}$
Brain	LOC100505812	19	0.10	rs4021	3.4	rs1421674	-3.8	-1.2	514	lasso	2.9	$4.1x10^{-3}$
Brain	FUT1	19	0.15	rs4021	3.4	rs4021	-8.7	3.4	433	lasso	-3.2	$1.3x10^{-3}$
Brain	PLK1S1	20	0.082	rs6047319	-4.0	rs6047267	5.3	-2.7	417	lasso	-3.0	$2.9x10^{-3}$
Brain	E2F1	20	0.063	rs2752901	2.7	rs7274811	-4.1	1.1	268	bslmm	-3.4	$6.6x10^{-4}$
Kidney	SLC1A7	1	0.80	rs34418279	3.2	rs12731800	4.1	2.2	475	lasso	3.6	$3.9x10^{-4}$
Kidney	WDR6	3	0.24	rs35452137	-4.0	rs6446205	4.2	3.3	261	susie	3.1	$1.7x10^{-3}$
Kidney	LINC02519	6	0.44	rs9478048	-3.2	rs3006184	-4.2	-2.7	604	enet	3.3	$1.0x10^{-3}$
Kidney	LINC00958	11	0.73	rs11022588	-4.1	rs11022588	-5.6	-4.1	553	top1	4.1	$4.4x10^{-5}$
Adipose (SC)	WNT4	1	0.047	rs10917209	3.2	rs2501275	3.7	-2.9	481	susie	-3.0	$2.4x10^{-3}$
Adipose (SC)	EPHB2	1	0.05	rs294219	3.4	rs4600017	-4.0	-2.4	453	susie	2.9	$3.8x10^{-3}$

Continuation of Table A14

Adipose (SC)	PAFAH2	1	0.14	rs933078	-2.9	rs933078	7.2	-2.9	416	top1	-2.9	$4.0x10^{-3}$
Adipose (SC)	ACOT11	1	0.12	rs10888855	-3.0	rs300280	4.4	1.3	566	enet	2.9	$3.4x10^{-3}$
Adipose (SC)	FGGY-DT	1	0.28	rs12739770	3.9	rs12758288	12.3	3.1	396	enet	3.4	$5.8x10^{-4}$
Adipose (SC)	RP5-943J3.1	1	0.31	rs1011702	3.8	rs473412	-15.1	3.4	373	susie	-3.4	$7.3x10^{-4}$
Adipose (SC)	TMEM167B-DT	1	0.19	rs12066164	3.3	rs616378	8.6	-2.9	408	enet	-3.1	$2.1x10^{-3}$
Adipose (SC)	PTGFRN	1	0.063	rs10802189	3.3	rs10801917	3.6	-2.8	396	susie	-3.1	$2.3x10^{-3}$
Adipose (SC)	SERTAD4-AS1	1	0.086	rs654523	3.2	rs654523	6.3	3.2	547	top1	3.2	$1.5x10^{-3}$
Adipose (SC)	SCCPDH	1	0.14	rs6657743	-3.0	rs3935011	-6.4	2.7	440	lasso	-3.0	$2.8x10^{-3}$
Adipose (SC)	RN7SL145P	3	0.053	rs2742395	3.0	rs2742395	-3.7	3.0	452	susie	-2.9	$3.6x10^{-3}$
Adipose (SC)	ATRIP	3	0.14	rs35452137	-4.0	rs2228561	-6.5	-2.9	243	susie	3.0	$3.0x10^{-3}$
Adipose (SC)	PRKAR2A	3	0.073	rs35452137	-4.0	rs9864243	4.9	2.9	261	enet	2.9	$3.5x10^{-3}$
Adipose (SC)	ARIH2	3	0.062	rs35452137	-4.0	rs7626445	-7.7	3.2	253	susie	-3.2	$1.5x10^{-3}$
Adipose (SC)	P4HTM	3	0.12	rs35452137	-4.0	rs6442130	-6.7	3.1	249	enet	-2.9	$3.4x10^{-3}$
Adipose (SC)	WDR6	3	0.51	rs35452137	-4.0	rs6781790	19.3	3.3	251	enet	3.0	$2.7x10^{-3}$
Adipose (SC)	NDUFAF3	3	0.087	rs35452137	-4.0	rs4974083	-4.2	2.9	253	susie	-2.9	$4.2x10^{-3}$
Adipose (SC)	DALRD3	3	0.10	rs35452137	-4.0	rs9850134	-9.4	3.3	253	susie	-3.2	$1.4x10^{-3}$
Adipose (SC)	QRICH1	3	0.085	rs7628719	3.4	rs7100	9.3	3.0	252	enet	2.9	$3.4x10^{-3}$
Adipose (SC)	DIPK2A	3	0.087	rs16855296	-2.6	rs6763060	-3.8	1.4	418	susie	-3.0	$2.4x10^{-3}$
Adipose (SC)	ZNF639	3	0.25	rs6443599	-3.5	rs1362650	8.8	-3.2	365	enet	-3.4	$7.9x10^{-4}$
Adipose (SC)	OSTN	3	0.20	rs1355365	-2.9	rs6444513	4.6	2.7	494	enet	3.0	$2.7x10^{-3}$
Adipose (SC)	WFS1	4	0.089	rs17718958	4.5	rs10010131	-6.7	3.8	657	susie	-3.8	$1.3x10^{-4}$
Adipose (SC)	LINC00603	5	0.13	rs16869470	-3.5	rs626849	7.3	-2.6	461	enet	-3.1	$2.3x10^{-3}$

Continuation of Table A14

Adipose (SC)	CLASP2 pseudogene	5	0.023	rs9791170	3.8	rs17132288	-4.0	-3.0	392	enet	3.5	$5.3x10^{-4}$
Adipose (SC)	PDLIM4	5	0.12	rs9791170	3.8	rs10463891	8.8	3.2	391	lasso	3.3	$1.1x10^{-3}$
Adipose (SC)	LINC01600	6	0.099	rs17300141	-3.9	rs6918808	6.8	-2.8	579	susie	-2.8	$4.9x10^{-3}$
Adipose (SC)	LINC01011	6	0.14	rs17300141	-3.3	rs4389803	6.2	-1.2	666	lasso	-2.8	$4.7x10^{-3}$
Adipose (SC)	SOBP	6	0.058	rs12194751	4.0	rs10457162	3.5	3.9	441	lasso	3.4	$6.0x10^{-4}$
Adipose (SC)	SNHG15	7	0.11	rs2040863	-2.8	rs10274813	4.4	-2.5	419	enet	-2.9	$4.2x10^{-3}$
Adipose (SC)	NSUN5P2	7	0.45	rs34014814	-2.7	rs34014814	8.4	-2.7	94	enet	-3.5	$5.1x10^{-4}$
Adipose (SC)	PCM1	8	0.15	rs17125822	4.5	rs2301546	-6.6	3.1	868	susie	-4.2	$2.8x10^{-5}$
Adipose (SC)	RFX3-AS1	9	0.37	rs10814233	3.1	rs10814233	9.0	3.1	535	enet	3.1	$1.9x10^{-3}$
Adipose (SC)	CNTLN	9	0.14	rs16935340	-3.3	rs4272484	9.6	-2.7	521	enet	-2.9	$3.9x10^{-3}$
Adipose (SC)	ARHGAP1	11	0.11	rs1352307	-3.4	rs3816614	-7.7	-3.1	233	enet	3.4	$8.2x10^{-4}$
Adipose (SC)	C11orf49	11	0.12	rs4647709	-3.5	rs1352307	-6.9	-3.4	280	top1	3.4	$7.7x10^{-4}$
Adipose (SC)	AC005831.1	12	0.097	rs241964	2.9	rs17836356	-4.2	1.1	656	enet	-2.9	$3.8x10^{-3}$
Adipose (SC)	PDE3A	12	0.12	rs10841520	-3.0	rs10841520	-4.7	-3.0	525	top1	3.0	$2.9x10^{-3}$
Adipose (SC)	EID3	12	0.43	rs4406890	4.6	rs11111987	-15.9	3.1	798	susie	-3.1	$2.1x10^{-3}$
Adipose (SC)	SPART-AS1	13	0.053	rs1886856	-3.2	rs1886856	5.3	-3.2	514	top1	-3.2	$1.4x10^{-3}$
Adipose (SC)	DTD2	14	0.18	rs11156667	-3.1	rs17097892	-8.2	3.0	305	enet	-3.5	$4.0x10^{-4}$
Adipose (SC)	CA5A pseudogene	16	0.11	rs11862806	3.4	rs11863150	-6.7	3.2	209	top1	-3.2	$1.5x10^{-3}$
Adipose (SC)	RFLNB	17	0.085	rs6565733	-3.2	rs11869174	-4.3	-1.4	349	enet	3.2	$1.5x10^{-3}$
Adipose (SC)	IZUMO1	19	0.41	rs4021	3.4	rs838143	10.5	3.0	428	enet	3.6	$3.5x10^{-4}$
Adipose (SC)	PANK2	20	0.092	rs12480318	2.9	rs12480318	5.4	2.9	556	enet	3.4	$5.9x10^{-4}$
Adipose (SC)	KIZ	20	0.081	rs6047319	-4.0	rs6082331	7.1	-2.9	391	lasso	-3.0	$2.8x10^{-3}$

Continuation of Table A14

Adipose (SC)	APMAP	20	0.043	rs1411895	3.1	rs6083670	-4.8	2.9	489	top1	-2.9	$3.6x10^{-3}$
Adipose (VO)	RP5-943J3.1	1	0.27	rs1011702	3.8	rs473412	-12.5	3.4	374	susie	-3.4	$8.0x10^{-4}$
Adipose (VO)	MUC1	1	0.12	rs11264247	-3.3	rs4971092	4.0	-1.0	338	enet	-3.1	$1.9x10^{-3}$
Adipose (VO)	SERTAD4-AS1	1	0.18	rs654523	3.2	rs654523	6.1	3.2	547	lasso	3.4	$7.7x10^{-4}$
Adipose (VO)	LIN9	1	0.054	rs1317646	-4.0	rs506128	3.4	1.5	395	susie	3.0	$2.4x10^{-3}$
Adipose (VO)	PPP3R1	2	0.092	rs12463718	-3.1	rs7592177	-5.4	-2.4	491	enet	2.8	$4.9x10^{-3}$
Adipose (VO)	ATRIP	3	0.35	rs35452137	-4.0	rs35452137	-7.5	-4.0	253	lasso	3.8	$1.8x10^{-4}$
Adipose (VO)	PRKAR2A	3	0.027	rs35452137	-4.0	rs990211	4.3	3.0	272	top1	2.97	$3.0x10^{-3}$
Adipose (VO)	ARIH2	3	0.089	rs35452137	-4.0	rs6446196	-4.8	3.3	264	top1	-3.3	$8.5x10^{-4}$
Adipose (VO)	P4HTM	3	0.088	rs35452137	-4.0	rs9311433	-6.1	3.1	260	susie	-3.1	$1.7x10^{-3}$
Adipose (VO)	WDR6	3	0.24	rs35452137	-4.0	rs9846123	13.3	3.3	262	enet	2.9	$3.3x10^{-3}$
Adipose (VO)	DALRD3	3	0.046	rs35452137	-4.0	rs9850134	-5.9	3.3	264	lasso	-3.2	$1.3x10^{-3}$
Adipose (VO)	RP11-3B7.1	3	0.10	rs7628719	3.4	rs4955418	-8.0	2.7	272	susie	-2.9	$3.9x10^{-3}$
Adipose (VO)	C3orf62	3	0.084	rs7628719	3.4	rs12629759	-4.0	2.7	278	enet	-3.1	$2.0x10^{-3}$
Adipose (VO)	TMEM45A	3	0.11	rs1680508	3.2	rs12636452	-5.9	2.2	395	enet	-3.0	$2.5x10^{-3}$
Adipose (VO)	RYK	3	0.065	rs9846898	-3.2	rs9859680	-4.2	2.9	462	top1	-2.9	$3.8x10^{-3}$
Adipose (VO)	ZNF639	3	0.12	rs6443599	-3.5	rs7610174	-5.9	2.7	365	enet	-3.4	$5.8x10^{-4}$
Adipose (VO)	XXYLT1	3	0.15	rs7627043	3.6	rs6794037	5.7	3.1	376	susie	3.4	$7.6x10^{-4}$
Adipose (VO)	WFS1	4	0.11	rs17718958	4.5	rs4689393	-5.8	4.2	665	top1	-4.2	$2.9x10^{-5}$
Adipose (VO)	CLASP2 pseudogene	5	0.045	rs9791170	3.8	rs2089855	-4.0	-3.2	396	top1	3.2	$1.3x10^{-3}$
Adipose (VO)	PDLIM4	5	0.069	rs9791170	3.8	rs6890009	5.8	3.5	396	lasso	3.6	$2.8x10^{-4}$

Continuation of Table A14

Adipose (VO)	KBTBD11	8	0.076	rs6983882	3.1	rs731869	-3.9	1.6	628	enet	-3.0	$2.7x10^{-3}$
Adipose (VO)	PCM1	8	0.17	rs17125822	4.5	rs2285306	-6.6	3.7	871	susie	-4.4	$1.1x10^{-5}$
Adipose (VO)	RFX3-AS1	9	0.31	rs10814233	3.1	rs10814233	8.1	3.1	536	susie	3.2	$1.5x10^{-3}$
Adipose (VO)	HMGB3P24	9	0.085	rs10738958	3.6	rs10814373	-4.5	-3.0	397	susie	2.8	$4.5x10^{-3}$
Adipose (VO)	ARHGAP1	11	0.15	rs1352307	-3.4	rs10769205	-6.7	-2.4	237	enet	3.0	$2.5x10^{-3}$
Adipose (VO)	ZNF408	11	0.052	rs1352307	-3.4	rs4752927	-4.3	-2.7	237	enet	3.7	$2.4x10^{-4}$
Adipose (VO)	LRP6	12	0.069	rs4763797	-3.4	rs4763797	-4.5	-3.4	550	top1	3.4	$8.1x10^{-4}$
Adipose (VO)	Antisense to TM7SF3	12	0.75	rs4265668	3.2	rs6487582	-12.1	2.3	514	lasso	-2.8	$4.9x10^{-3}$
Adipose (VO)	TM7SF3	12	0.28	rs4265668	3.2	rs11048950	7.6	3.0	522	enet	3.3	$8.7x10^{-4}$
Adipose (VO)	SPART-AS1	13	0.069	rs1886856	-3.2	rs11842927	4.2	-2.9	514	susie	-3.3	$8.3x10^{-4}$
Adipose (VO)	CTD-2292M16.8	14	0.22	rs11541061	3.0	rs1953550	-4.9	-2.2	575	lasso	3.4	$7.1x10^{-4}$
Adipose (VO)	DTD2	14	0.20	rs11156667	-3.1	rs17097892	-7.3	3.0	317	enet	-3.4	$7.5x10^{-4}$
Adipose (VO)	GALNT16	14	0.11	rs2268966	-3.0	rs11623840	-4.1	-2.6	453	lasso	3.0	$3.1x10^{-3}$
Adipose (VO)	RP3-449M8.6	14	0.43	rs10450929	2.6	rs7148018	-9.1	1.4	363	enet	-2.9	$4.1x10^{-3}$
Adipose (VO)	Sense Intronic to ZNF280D	15	0.047	rs1631079	-4.1	rs1963831	3.9	-2.8	340	susie	-3.3	$9.9x10^{-4}$
Adipose (VO)	ZNF280D	15	0.047	rs1631079	-4.1	rs28678122	4.6	-2.4	342	susie	-2.9	$3.9x10^{-3}$
Adipose (VO)	CA5A pseudogene	16	0.068	rs11862806	3.4	rs4787643	-5.0	2.6	209	susie	-2.9	$4.4x10^{-3}$
Adipose (VO)	CDR2L	17	0.14	rs11650024	-3.1	rs902726	3.2	-2.7	395	lasso	-3.1	$1.7x10^{-3}$
Adipose (VO)	CBX3P2	18	0.080	rs7245003	-3.8	rs12608077	-3.3	0.89	507	susie	-2.9	$4.3x10^{-3}$

Continuation of Table A14

Adipose (VO)	SRRM5	19	0.081	rs2239372	3.0	rs427115	4.0	0.85	395	enet	3.5	$5.3x10^{-4}$
Adipose (VO)	KIZ	20	0.13	rs6047319	-4.0	rs6082331	6.7	-2.9	394	top1	-2.9	$3.6x10^{-3}$
Blood	H6PD	1	0.21	rs9435151	2.9	rs732950	-9.6	2.9	426	top1	-2.9	$3.4x10^{-3}$
Blood	RP11-131M11.3	1	0.038	rs10914718	-3.1	rs6425819	4.7	2.7	370	enet	2.8	$4.8x10^{-3}$
Blood	Antisense to NRD1	1	0.051	rs1770791	2.5	rs1770791	-4.6	2.5	191	enet	-3.3	$9.2x10^{-4}$
Blood	RP5-943J3.1	1	0.17	rs1011702	3.8	rs473412	-12.3	3.4	373	susie	-3.4	$7.8x10^{-4}$
Blood	MUC1	1	0.20	rs11264247	-3.3	rs4971059	6.4	-1.7	336	enet	-3.0	$2.4x10^{-3}$
Blood	ARIH2	3	0.016	rs35452137	-4.0	rs4279134	-4.1	2.6	252	susie	-3.1	$2.2x10^{-3}$
Blood	P4HTM	3	0.033	rs35452137	-4.0	rs6796790	-5.5	2.4	248	susie	-3.0	$2.8x10^{-3}$
Blood	WDR6	3	0.23	rs35452137	-4.0	rs9846123	16.3	3.3	250	susie	3.1	$2.2x10^{-3}$
Blood	QRICH1	3	0.051	rs7628719	3.4	rs7100	7.7	3.0	252	top1	3.0	$3.2x10^{-3}$
Blood	CCDC71	3	0.038	rs7628719	3.4	rs4279134	6.0	2.6	259	susie	3.0	$2.8x10^{-3}$
Blood	WFS1	4	0.083	rs17718958	4.5	rs4688982	-4.4	3.5	663	top1	-3.5	$5.5x10^{-4}$
Blood	MFSD4B	6	0.069	rs354527	-3.3	rs190246	5.6	-2.6	381	enet	-3.2	$1.5x10^{-3}$
Blood	MTUS1	8	0.33	rs17125822	4.4	rs17125481	11.9	3.7	870	enet	3.1	$2.1x10^{-3}$
Blood	PCM1	8	0.087	rs17125822	4.5	rs12718385	8.0	-3.7	868	enet	-3.7	$2.5x10^{-4}$
Blood	RFX3-AS1	9	0.071	rs10814233	3.1	rs7864107	4.1	3.1	532	top1	3.1	$1.8x10^{-3}$
Blood	C1QL3	10	0.42	rs7079565	2.9	rs7909832	-13.0	-2.7	589	enet	2.9	$3.8x10^{-3}$
Blood	LINC00958	11	0.50	rs11022588	-4.1	rs11022589	17.8	-4.1	546	lasso	-4.0	$6.9x10^{-5}$
Blood	RCE1	11	0.059	rs12419173	3.1	rs7122539	-5.5	-1.7	220	enet	2.9	$3.6x10^{-3}$
Blood	CD9	12	0.29	rs12814768	-3.8	rs10774398	11.5	2.8	489	enet	3.2	$1.5x10^{-3}$

Continuation of Table A14

Blood	LINC02446	12	0.12	rs7294858	-2.7	rs4076336	-4.6	2.0	460	enet	-3.2	$1.2x10^{-3}$
Blood	RP1-228P16.8	12	0.10	rs7485057	-3.1	rs17122920	-3.6	-1.9	525	susie	3.2	$1.6x10^{-3}$
Blood	NFE2	12	0.076	rs4759322	-2.5	rs10506328	-3.5	-0.12	430	enet	-2.9	$3.4x10^{-3}$
Blood	TXNRD1	12	0.045	rs4406890	4.6	rs7294778	6.0	3.1	826	top1	3.1	$2.2x10^{-3}$
Blood	PRMT5-AS1	14	0.040	rs4981454	-3.2	rs4981454	-4.5	-3.2	568	top1	3.2	$1.6x10^{-3}$
Blood	PRMT5	14	0.31	rs4981454	-3.2	rs4981454	-14.9	-3.2	568	susie	3.3	$1.0x10^{-3}$
Blood	PRMT5-DT	14	0.24	rs4981454	-3.2	rs4981454	-10.9	-3.2	568	susie	3.1	$2.1x10^{-3}$
Blood	Antisense to SERPINA9	14	0.086	rs11628686	-3.7	rs6575433	5.0	-3.6	805	susie	-3.5	$4.6x10^{-4}$
Blood	CTD-2313J17.1	15	0.17	rs7169046	-3.5	rs4274391	-6.7	-3.1	651	susie	3.0	$2.5x10^{-3}$
Blood	SEPTIN1	16	0.070	rs11862806	3.4	rs8050812	-5.2	2.6	202	lasso	-2.9	$3.9x10^{-3}$
Blood	PSME3IP1	16	0.10	rs158619	-3.3	rs12599485	-6.1	-1.5	525	enet	3.2	$1.5x10^{-3}$
Blood	ATP2C2	16	0.42	rs17739607	-3.4	rs4782936	-8.1	-2.3	865	enet	2.8	$4.7x10^{-3}$
Blood	TLCD3A	17	0.066	rs759974	-2.9	rs7813	4.0	2.1	425	susie	2.9	$3.7x10^{-3}$
Blood	ZNF780A	19	0.19	rs234355	-3.8	rs4577216	9.0	-2.9	362	susie	-2.8	$4.7x10^{-3}$
Blood	BAX	19	0.10	rs4021	3.4	rs7259013	-6.4	2.8	424	enet	-3.7	$2.4x10^{-4}$
Blood	ITPA	20	0.54	rs8362	-3.0	rs7270101	-14.0	2.3	429	lasso	-3.2	$1.6x10^{-3}$
Blood	LAMP5	20	0.094	rs2076392	-3.0	rs4816144	4.9	1.8	581	enet	3.0	$2.5x10^{-3}$
Blood	TST	22	0.078	rs3218318	3.8	rs2072861	3.9	3.5	690	top1	3.5	$5.4x10^{-4}$
Blood	ARHGAP8	22	0.13	rs3761481	-4.3	rs3761481	5.8	-4.3	705	top1	-4.3	$1.9x10^{-5}$
Muscle	ALG6	1	0.044	rs1391812	5.5	rs927019	-4.5	2.3	531	lasso	-2.9	$4.3x10^{-3}$

Continuation of Table A14

Muscle	MYOG	1	0.082	rs4950914	-3.4	rs4950914	-6.3	-3.4	505	top1	3.4	$7.1x10^{-4}$
Muscle	SERTAD4-AS1	1	0.069	rs654523	3.2	rs654523	5.9	3.2	548	top1	3.2	$1.5x10^{-3}$
Muscle	PNO1	2	0.093	rs12463718	-3.1	rs28694054	7.5	-3.1	520	susie	-2.9	$4.4x10^{-3}$
Muscle	ST3GAL5	2	0.099	rs4480982	-3.2	rs6547655	-7.6	-3.0	451	top1	3.0	$2.4x10^{-3}$
Muscle	RN7SL145P	3	0.086	rs2742395	3.0	rs2742395	-8.0	3.0	450	susie	-3.0	$2.9x10^{-3}$
Muscle	WDR6	3	0.17	rs35452137	-4.0	rs7643368	14.4	3.3	255	susie	3.0	$2.5x10^{-3}$
Muscle	NDUFAF3	3	0.090	rs35452137	-4.0	rs6806356	-5.5	2.6	257	lasso	-3.0	$3.2x10^{-3}$
Muscle	DALRD3	3	0.023	rs35452137	-4.0	rs3774800	-5.1	2.3	257	susie	-3.1	$1.9x10^{-3}$
Muscle	RBP1	3	0.26	rs3821546	3.4	rs11922772	9.1	3.0	490	top1	3.0	$3.0x10^{-3}$
Muscle	XXYLT1	3	0.11	rs7627043	3.6	rs6794037	5.8	3.1	377	enet	3.4	$8.0x10^{-4}$
Muscle	WFS1	4	0.17	rs17718958	4.5	rs13107806	-9.1	3.3	655	enet	-3.4	$6.2x10^{-4}$
Muscle	PHACTR1	6	0.032	rs1332845	3.6	rs1937774	5.0	2.9	495	top1	2.9	$3.5x10^{-3}$
Muscle	TRAPPC3L	6	0.17	rs7762318	3.1	rs7762318	-9.2	3.1	371	lasso	-3.1	$1.9x10^{-3}$
Muscle	OSBPL5	11	0.22	rs734458	3.3	rs734458	10.6	3.3	446	enet	3.2	$1.2x10^{-3}$
Muscle	CTD-2003C8.2	11	0.16	rs1533877	-3.4	rs2896567	-7.8	2.9	746	enet	-3.2	$1.6x10^{-3}$
Muscle	DDB2	11	0.058	rs4647709	-3.5	rs7940240	-6.3	-3.1	297	top1	3.1	$2.0x10^{-3}$
Muscle	Antisense to TM7SF3	12	0.65	rs4265668	3.2	rs6487582	-13.5	2.3	514	susie	-2.8	$4.7x10^{-3}$
Muscle	TM7SF3	12	0.12	rs4265668	3.2	rs1976205	6.2	2.9	521	top1	2.9	$4.1x10^{-3}$
Muscle	ATG101	12	0.11	rs12424271	-4.1	rs11521	-6.2	-3.2	615	susie	3.6	$3.8x10^{-4}$
Muscle	CTD-2292M16.8	14	0.15	rs11541061	3.0	rs1953550	-5.4	-2.2	575	lasso	2.8	$4.9x10^{-3}$

Continuation of Table A14

Muscle	DTD2	14	0.055	rs11156667	-3.1	rs17097892	-4.8	3.0	305	susie	-3.0	$2.7x10^{-3}$
Muscle	RYR3	15	0.36	rs10444855	3.1	rs4356445	9.5	0.13	818	enet	2.9	$3.4x10^{-3}$
Muscle	ZNF780A	19	0.19	rs4803313	3.4	rs24136	8.9	-2.5	353	enet	-3.2	$1.6x10^{-3}$
Muscle	RALGAPA2	20	0.057	rs6047273	-3.8	rs6137147	4.6	3.8	405	lasso	3.7	$2.7x10^{-4}$
Liver	RBM15-AS1	1	0.39	rs12760885	-3.1	rs12410178	4.2	-0.10	567	susie	-3.4	$5.8x10^{-4}$
Liver	ARIH2	3	0.13	rs35452137	-4.0	rs4279134	-5.2	2.6	261	susie	-3.1	$1.8x10^{-3}$
Liver	WDR6	3	0.25	rs35452137	-4.0	rs7643368	7.4	3.3	257	susie	3.2	$1.6x10^{-3}$
Liver	NDUFAF3	3	0.037	rs35452137	-4.0	rs7627404	-3.7	3.1	259	susie	-3.1	$1.7x10^{-3}$
Liver	DALRD3	3	0.11	rs35452137	-4.0	rs6446205	-5.0	3.3	259	lasso	-3.2	$1.3x10^{-3}$
Liver	NCBP2	3	0.20	rs548853	-2.7	rs4916567	4.0	-2.4	454	lasso	-3.4	$6.5x10^{-4}$
Liver	MFSD4B	6	0.18	rs354527	-3.3	rs240972	-4.6	2.3	385	enet	-2.8	$4.5x10^{-3}$
Liver	RFX3-AS1	9	0.39	rs10814233	3.1	rs10115088	5.6	3.1	538	lasso	2.9	$3.7x10^{-3}$
Liver	C1QL3	10	0.70	rs7079565	2.9	rs6602130	-10.1	-2.8	596	susie	2.8	$5.0x10^{-3}$
Liver	ARHGAP1	11	0.52	rs1352307	-3.4	rs10769205	-6.3	-2.4	238	enet	2.9	$3.5x10^{-3}$
Liver	ZNF408	11	0.14	rs1352307	-3.4	rs11039014	-5.4	-3.3	238	top1	3.3	$8.3x10^{-4}$
Liver	LRP4	11	0.12	rs4647709	-3.5	rs10734548	-5.6	-2.9	279	susie	2.9	$3.3x10^{-3}$
Liver	C11orf49	11	0.15	rs4647709	-3.5	rs4752816	-5.5	-2.5	281	susie	3.1	$2.0x10^{-3}$
Liver	NTN1	17	0.27	rs17673686	-4.0	rs9893768	-6.2	2.5	489	lasso	-2.9	$3.7x10^{-3}$
Liver	PLK5	19	0.26	rs8104249	-2.7	rs8104249	5.2	-2.7	387	lasso	-3.1	$1.7x10^{-3}$
Liver	FCGBP	19	0.3	rs4803313	3.6	rs2767607	6.9	-2.9	403	top1	-2.9	$3.9x10^{-3}$
Liver	ZNF780A	19	0.34	rs4803313	3.4	rs234346	7.4	-2.4	388	lasso	-2.9	$3.4x10^{-3}$
Testis	CFAP57	1	0.42	rs2225251	-3.0	rs603560	-8.1	-2.7	463	enet	2.9	$4.3x10^{-3}$
Testis	LINC02784	1	0.33	rs10888855	-3.0	rs10888855	8.7	-3.0	556	susie	-3.0	$3.0x10^{-3}$
Testis	RP5-943J3.1	1	0.15	rs1011702	3.8	rs4658321	-6.1	2.8	374	susie	-3.0	$2.9x10^{-3}$
Testis	TMEM167B-DT	1	0.098	rs12066164	3.3	rs616378	4.4	-2.9	409	top1	-2.9	$4.4x10^{-3}$

Continuation of Table A14

Testis	AC017002.1	2	0.71	rs3761705	-3.1	rs10171109	8.7	2.9	289	susie	2.9	$3.5x10^{-3}$
Testis	ARIH2	3	0.087	rs35452137	-4.0	rs6446205	-4.7	3.3	262	top1	-3.3	$1.0x10^{-3}$
Testis	WDR6	3	0.25	rs35452137	-4.0	rs6781790	10.9	3.3	258	top1	3.3	$1.1x10^{-3}$
Testis	QRICH1	3	0.28	rs7628719	3.4	rs7653408	9.1	2.9	250	enet	3.2	$1.5x10^{-3}$
Testis	USP19	3	0.047	rs7628719	3.4	rs7626445	-4.1	3.2	254	lasso	-3.1	$1.8x10^{-3}$
Testis	XXYLT1	3	0.22	rs7627043	3.6	rs6794037	5.1	3.1	382	susie	2.9	$3.6x10^{-3}$
Testis	WFS1	4	0.25	rs17718958	4.5	rs4688982	-7.9	3.5	668	top1	-3.5	$5.5x10^{-4}$
Testis	FAM114A1	4	0.53	rs4833079	-2.6	rs11730661	7.2	1.4	511	susie	3.0	$3.2x10^{-3}$
Testis	DEPDC1B	5	0.12	rs10077663	-4.1	rs7704338	5.3	3.4	320	top1	3.4	$7.7x10^{-4}$
Testis	RP11-557H15.5	6	0.31	rs13219414	-3.6	rs3966737	8.9	2.9	441	susie	2.9	$3.3x10^{-3}$
Testis	KIF25	6	0.43	rs4708702	3.3	rs4708627	7.0	1.3	470	susie	2.9	$3.3x10^{-3}$
Testis	RP1-182D15.2	6	0.17	rs9478048	-3.2	rs12196723	-4.2	-2.3	439	susie	3.5	$4.5x10^{-4}$
Testis	GUSBP6	7	0.68	rs1897815	-2.9	rs13241939	14.2	-2.8	242	lasso	-2.9	$3.8x10^{-3}$
Testis	FEZF1	7	0.73	rs1443753	3.1	rs1443753	-11.9	3.1	330	lasso	-2.9	$3.7x10^{-3}$
Testis	LINC00689	7	0.29	rs2602565	-3.2	rs4481540	5.1	1.2	334	enet	3.1	$2.2x10^{-3}$
Testis	PCM1	8	0.11	rs17125822	4.5	rs3850749	-4.8	3.2	875	top1	-3.2	$1.6x10^{-3}$
Testis	HIPK3	11	0.079	rs10768003	-3.4	rs10836046	-4.8	-3.1	370	susie	2.9	$3.4x10^{-3}$
Testis	LDLRAD3	11	0.11	rs16928390	-3.6	rs10768195	-3.7	-2.7	619	susie	3.1	$2.1x10^{-3}$
Testis	TM7SF3	12	0.13	rs4265668	3.2	rs10842871	4.6	2.7	526	enet	3.2	$1.6x10^{-3}$
Testis	CCDC38	12	0.60	rs3764036	2.6	rs3751264	-8.4	2.4	548	enet	-2.9	$3.3x10^{-3}$
Testis	LINC02385	12	0.13	rs4406890	4.6	rs4964288	4.1	4.0	793	top1	4.0	$7.2x10^{-5}$
Testis	RP11-497G19.2	12	0.11	rs748381	-2.8	rs748381	5.1	-2.8	430	top1	-2.8	$5.0x10^{-3}$
Testis	RP11-87C7.3	13	0.75	rs9319382	3.5	rs9319382	14.2	3.5	523	susie	3.2	$1.4x10^{-3}$
Testis	LINC00445	13	0.17	rs17053259	3.3	rs182152	5.4	3.0	536	enet	2.8	$4.8x10^{-3}$

Continuation of Table A14

Testis	TRAV8-5	14	0.27	rs12882371	-3.3	rs4982522	7.1	2.8	658	susie	2.9	$3.7x10^{-3}$
Testis	DTD2	14	0.21	rs11156667	-3.1	rs2274291	5.3	-2.7	318	enet	-3.1	$1.9x10^{-3}$
Testis	TCL1B	14	0.71	rs11160284	3.2	rs11160284	11.6	3.2	740	susie	3.2	$1.6x10^{-3}$
Testis	IGFALS	16	0.50	rs28364711	-2.7	rs2492883	-8.9	-2.6	475	enet	3.1	$2.1x10^{-3}$
Testis	CD2BP2	16	0.12	rs11862806	3.4	rs35480350	6.3	2.8	203	lasso	2.9	$3.7x10^{-3}$
Testis	Antisense to VPS53	17	0.40	rs6565733	-3.2	rs759974	-7.6	-2.9	376	susie	2.8	$4.7x10^{-3}$
Testis	SHPK	17	0.47	rs170313	3.0	rs17707155	6.9	2.1	526	susie	2.8	$4.8x10^{-3}$
Testis	CSNK1G2-AS1	19	0.42	rs8104249	-2.7	rs11881644	-8.8	-2.3	378	susie	3.4	$7.0x10^{-4}$
Testis	POU2F2	19	0.14	rs3826705	-3.0	rs10407506	5.5	-2.9	188	susie	-2.9	$3.8x10^{-3}$
Testis	RPS16P9	19	0.14	rs8105340	3.3	rs2287019	3.5	-0.36	369	susie	3.0	$3.0x10^{-3}$
Testis	ZNF667-AS1	19	0.44	rs9749084	-2.7	rs9749084	10.3	-2.7	506	enet	-3.2	$1.6x10^{-3}$

Abbreviations: eQTL, expression quantitative trait locus; CHR, chromosome, HSQ, mean heritability estimate; Best.GWAS.ID, most significantly associated variant in the locus; Best.GWAS.Z, z-score of most significantly associated variant in the locus; eQTL ID, best eQTL in the locus; eQTL.GWAS.Z, GWAS z-score for best eQTL; NSNP, number of SNPs in the locus; Model, best performing TWAS model; TWAS.Z, TWAS z-score; TWAS.P, TWAS p-value, enet, elastic-net regression (mixing parameter = 0.5); blup, best linear unbiased predictor from all variants; bslmm, Bayesian sparse linear model; lasso, least absolute shrinkage and selection operator; top1, single best eQTL, susie, sum of single effects regression, VO, visceral omentum; SC, subcutaneous.

Table A15. Genes associated with cisplatin-induced hearing loss by TWAS ($p < 0.05$)

Tissue	Gene	CHR	HSQ	BEST.GWAS.ID	BEST.GWAS.Z	EQTL.ID	EQTL.Z	EQTL.GWAS.Z	NSNP	MODEL	TWAS.Z	TWAS.P
Nerve	FGGY-DT	1	0.34	rs12739770	3.9	rs12758643	12.8	3.8	397	lasso	3.5	$4.6x10^{-4}$
Nerve	ATRIP	3	0.12	rs35452137	-4.0	rs3135941	-5.0	-2.6	244	enet	3.4	$7.8x10^{-4}$
Nerve	NCKIPSD	3	0.32	rs35452137	-4.0	rs12493578	-13.6	2.8	252	enet	-3.0	$3.1x10^{-3}$
Nerve	PRKAR2A	3	0.028	rs35452137	-4.0	rs7626445	4.9	3.2	262	susie	3.2	$1.3x10^{-3}$
Nerve	ARIH2	3	0.055	rs35452137	-4.0	rs3212	-6.5	2.6	254	susie	-3.1	$1.8x10^{-3}$
Nerve	P4HTM	3	0.14	rs35452137	-4.0	rs6772452	-9.5	2.8	250	lasso	-3.0	$2.4x10^{-3}$
Nerve	WDR6	3	0.37	rs35452137	-4.0	rs6446205	16.9	3.3	252	susie	3.1	$2.2x10^{-3}$
Nerve	DALRD3	3	0.083	rs35452137	-4.0	rs6781790	-7.9	3.3	254	lasso	-3.3	$8.9x10^{-4}$
Nerve	Antisense to IMPDH2 and QRICH1	3	0.037	rs35452137	-4.0	rs7429661	3.6	2.3	253	top1	2.3	$2.1x10^{-3}$
Nerve	QRICH1	3	0.18	rs7628719	3.4	rs4974081	10.1	2.9	252	lasso	2.8	$5.1x10^{-3}$
Nerve	LAMB2P1	3	0.051	rs7628719	3.4	rs4955416	-4.8	2.9	258	top1	-2.9	$4.3x10^{-2}$
Nerve	CCDC71	3	0.039	rs7628719	3.4	rs4974082	5.0	3.4	259	enet	3.2	$1.3x10^{-3}$
Nerve	KLHDC8B	3	0.071	rs7628719	3.4	rs10865954	6.2	2.7	262	top1	2.7	$7.6x10^{-3}$
Nerve	IHO1	3	0.33	rs7628719	3.4	rs4955418	-9.1	2.7	259	top1	-2.7	$8.0x10^{-3}$
Nerve	RP11-3B7.1	3	0.14	rs7628719	3.4	rs35174559	-8.0	2.7	271	susie	-2.7	$7.0x10^{-3}$
Nerve	RHOA	3	0.029	rs7628719	3.4	rs4241405	4.5	2.0	288	top1	2.0	$4.9x10^{-2}$
Nerve	AMT	3	0.36	rs7628719	3.4	rs3448	-16.5	2.1	288	enet	-2.2	$2.9x10^{-2}$
Nerve	APEH	3	0.18	rs12637576	2.7	rs9812791	6.5	-1.2	317	enet	-2.1	$3.8x10^{-2}$
Nerve	HYAL3	3	0.26	rs1076904	2.4	rs2236947	-9.5	2.0	306	susie	-2.1	$3.9x10^{-2}$

Continuation of Table A15

Nerve	WFS1	4	0.16	rs17718958	4.5	rs10010131	-8.2	3.8	662	susie	-3.8	$1.7x10^{-4}$
Nerve	CARMIL1	6	0.27	rs2690120	3.2	rs1883393	-7.2	1.3	636	susie	-3.1	$1.7x10^{-3}$
Nerve	BZW2	7	0.13	rs864212	-3.9	rs1167578	-7.2	-3.7	635	top1	3.7	$2.4x10^{-4}$
Nerve	AC087273.2	8	0.059	rs17125822	4.5	rs440182	-3.8	2.5	857	susie	-2.4	$1.6x10^{-2}$
Nerve	FGL1	8	0.068	rs17125822	4.5	rs3850746	4.8	-3.7	861	top1	-3.7	$2.5x10^{-4}$
Nerve	PCM1	8	0.35	rs17125822	4.5	rs12718385	9.0	-3.7	868	enet	-3.5	$5.4x10^{-4}$
Nerve	FOCAD	9	0.12	rs10125958	3.3	rs7874876	5.5	2.4	501	susie	2.4	$1.5x10^{-2}$
Nerve	HACD4	9	0.080	rs10125958	3.3	rs11789272	5.2	3.1	464	top1	3.1	$2.2x10^{-3}$
Nerve	CCDC169	13	0.38	rs1886856	-3.2	rs1170932	12.3	-2.9	527	enet	-2.3	$2.3x10^{-2}$
Nerve	SPART-AS1	13	0.062	rs1886856	-3.2	rs9547462	5.5	-3.0	512	enet	-3.1	$1.7x10^{-3}$
Nerve	SPART	13	0.17	rs1886856	-3.2	rs3736919	-8.5	2.5	520	enet	-3.0	$2.6x10^{-3}$
Nerve	CCNA1	13	0.10	rs1886856	-3.2	rs9547419	6.7	-2.4	485	susie	-2.4	$1.5x10^{-2}$
Nerve	HEATR5A	14	0.13	rs11156667	-3.1	rs12893465	-5.7	-2.4	288	top1	2.4	$1.7x10^{-2}$
Nerve	RP11-176H8.1	14	0.22	rs11156667	-3.1	rs1888576	9.3	-2.3	294	susie	-2.3	$2.0x10^{-2}$
Nerve	DTD2	14	0.24	rs11156667	-3.1	rs17097892	-7.9	3.0	307	enet	-3.3	$1.1x10^{-3}$
Nerve	NPIPB13	16	0.053	rs11862806	3.4	rs12929884	3.6	-1.0	211	lasso	-2.2	$3.2x10^{-2}$
Nerve	CA5A pseudogene	16	0.11	rs11862806	3.4	rs8051096	-8.1	3.4	209	top1	-3.4	$7.5x10^{-4}$
Nerve	CD2BP2	16	0.068	rs11862806	3.4	rs4787643	5.1	2.6	204	susie	2.7	$7.2x10^{-3}$
Nerve	SEPTIN1	16	0.25	rs11862806	3.4	rs4787643	-10.5	2.6	202	susie	-2.6	$9.1x10^{-3}$
Nerve	TXNL4B	16	0.80	rs8052152	-2.6	rs4788614	7.0	0.81	346	susie	3.1	$1.8x10^{-3}$
Nerve	ZFHX3	16	0.085	rs12373097	-3.2	rs2068360	4.8	-2.1	455	lasso	-2.1	$3.3x10^{-2}$
Nerve	ANKRD13B	17	0.055	rs2628165	-3.1	rs7222308	5.1	-2.0	315	enet	-3.3	$8.9x10^{-4}$

Continuation of Table A15

Nerve	RP11-68I3.10	17	0.037	rs2628165	-3.1	rs2628189	-4.7	2.6	307	susie	-2.6	$1.1x10^{-2}$
Nerve	SSH2	17	0.12	rs2628165	-3.1	rs2169810	-10.3	2.8	335	susie	-2.7	$7.1x10^{-3}$
Nerve	STX18 pseudogene	17	0.038	rs2628165	-3.1	rs3110494	5.3	-2.4	333	susie	-2.3	$2.1x10^{-2}$
Nerve	SLC6A4	17	0.11	rs2628165	-3.1	rs4356528	-4.7	-1.9	307	enet	2.2	$2.7x10^{-2}$
Nerve	TMEM91	19	0.34	rs12971430	3.0	rs3810174	5.1	-0.46	378	susie	-2.3	$2.4x10^{-2}$
Nerve	CEACAM21	19	0.11	rs10407506	-2.9	rs11882144	-5.6	-2.7	318	lasso	2.2	$2.7x10^{-2}$
Nerve	CEACAM4	19	0.21	rs16975663	-2.9	rs6508987	-6.4	-2.4	299	lasso	2.4	$1.6x10^{-2}$
Nerve	GRIK5	19	0.074	rs3826705	-3.0	rs8099939	4.9	-1.4	213	enet	-3.4	$6.0x10^{-4}$
Nerve	PAFAH1B3	19	0.060	rs3826705	-3.0	rs1206033	4.3	-1.6	152	enet	-2.6	$1.0x10^{-2}$
Nerve	CEACAM1	19	0.035	rs3826705	-3.0	rs10402401	-3.5	-2.5	119	top1	2.5	$1.3x10^{-2}$
Nerve	CD177P1	19	0.22	rs2239372	3.0	rs7257560	-6.9	-2.0	307	top1	2.0	$4.4x10^{-2}$
Nerve	IGFL2-AS1	19	0.084	rs12463382	-2.9	rs9676648	4.8	-2.1	411	enet	-2.0	$4.7x10^{-2}$
Nerve	CCDC9	19	0.20	rs2910996	2.7	rs2287689	-7.9	2.5	298	susie	-2.3	$2.5x10^{-2}$
Nerve	CARD8-AS1	19	0.088	rs4021	3.4	rs16981882	-4.5	-1.2	514	lasso	2.2	$2.9x10^{-2}$
Nerve	IZUMO1	19	0.33	rs4021	3.4	rs838143	8.7	3.0	424	enet	2.5	$1.3x10^{-2}$
Nerve	FUT1	19	0.11	rs4021	3.4	rs4021	5.7	3.4	419	top1	3.4	$7.0x10^{-4}$
Nerve	TRPM4	19	0.51	rs4021	3.4	rs11667393	-8.1	-1.7	384	enet	2.6	$8.9x10^{-3}$
Nerve	NAPSB	19	0.40	rs11666177	-3.2	rs1274514	-12.1	-2.3	400	top1	2.3	$2.2x10^{-2}$
Nerve	KLK5	19	0.14	rs2664155	-2.8	rs2569522	4.9	2.0	548	lasso	2.4	$1.6x10^{-2}$
Nerve	KLK10	19	0.29	rs2664155	-2.8	rs8104441	-5.9	1.8	580	susie	-2.0	$4.9x10^{-2}$
Cerebellum	ADORA1	1	0.30	rs4950914	-3.4	rs782803	-4.9	-1.8	511	enet	3.1	$2.3x10^{-3}$
Cerebellum	UCN2	3	0.13	rs35452137	-4.0	rs7633840	-4.2	2.8	248	top1	-2.8	$5.4x10^{-3}$
Cerebellum	NCKIPSD	3	0.29	rs35452137	-4.0	rs4858828	-8.9	2.8	262	susie	-2.9	$3.3x10^{-3}$

Continuation of Table A15

Cerebellum	P4HTM	3	0.11	rs35452137	-4.0	rs6769821	-6.3	2.3	260	susie	-2.3	$2.1x10^{-2}$
Cerebellum	WDR6	3	0.28	rs35452137	-4.0	rs7626445	9.4	3.2	261	top1	3.2	$1.2x10^{-3}$
Cerebellum	DALRD3	3	0.17	rs35452137	-4.0	rs9859473	-6.8	2.5	263	susie	-2.8	$5.3x10^{-3}$
Cerebellum	QRICH1	3	0.28	rs7628719	3.4	rs7100	7.5	3.0	253	top1	3.0	$3.2x10^{-3}$
Cerebellum	LAMB2P1	3	0.11	rs7628719	3.4	rs6769821	-4.8	2.3	258	susie	-2.5	$1.2x10^{-2}$
Cerebellum	CCDC71	3	0.28	rs7628719	3.4	rs12490393	8.2	2.7	259	enet	2.5	$1.4x10^{-2}$
Cerebellum	KLHDC8B	3	0.080	rs7628719	3.4	rs3774800	4.7	2.3	262	top1	2.3	$2.2x10^{-2}$
Cerebellum	USP4	3	0.047	rs7628719	3.4	rs6809851	4.3	2.3	278	top1	2.3	$2.1x10^{-2}$
Cerebellum	GPX1	3	0.16	rs7628719	3.4	rs11710434	5.8	2.0	277	enet	2.0	$4.7x10^{-2}$
Cerebellum	AMT	3	0.43	rs7628719	3.4	rs3448	-10.3	2.1	288	enet	-2.6	$1.1x10^{-2}$
Cerebellum	NICN1	3	0.10	rs7628719	3.4	rs7429661	-4.3	2.3	288	lasso	-2.4	$1.8x10^{-2}$
Cerebellum	MST1	3	0.39	rs12637576	2.7	rs9858542	5.5	-1.2	316	enet	-2.3	$1.9x10^{-2}$
Cerebellum	IFRD2	3	0.14	rs1076904	2.4	rs2236947	-4.5	2.0	328	top1	-2.0	$4.3x10^{-2}$
Cerebellum	NAA80	3	0.15	rs1076904	2.4	rs13100173	4.5	2.1	327	top1	2.1	$3.7x10^{-2}$
Cerebellum	HYAL3	3	0.51	rs1076904	2.4	rs2236947	-9.4	2.0	327	top1	-2.0	$4.3x10^{-2}$
Cerebellum	XXYLT1	3	0.22	rs7627043	3.6	rs6794037	5.5	3.1	381	susie	3.4	$7.8x10^{-4}$
Cerebellum	PPP4R2P6	3	0.45	rs12487782	-2.8	rs3749331	-7.6	2.1	290	lasso	-2.1	$3.6x10^{-2}$
Cerebellum	SDHAP2	3	0.52	rs12487782	-2.8	rs6773702	-6.5	2.3	287	susie	-2.2	$3.1x10^{-2}$
Cerebellum	WFS1	4	0.74	rs17718958	4.5	rs13107806	-10.0	3.3	672	susie	-3.4	$7.2x10^{-4}$
Cerebellum	PPP2R2C	4	0.39	rs17718958	4.5	rs13107806	-3.4	3.3	529	susie	-3.2	$1.3x10^{-3}$
Cerebellum	RPL10A	6	0.41	rs2076170	-3.0	rs2395626	5.2	-2.7	425	enet	-3.0	$2.9x10^{-3}$
Cerebellum	POU3F2	6	0.12	rs9493282	-3.6	rs2294405	5.6	3.1	427	top1	3.1	$1.8x10^{-3}$
Cerebellum	PPP1R9A	7	0.21	rs10085641	2.9	rs1830245	-3.5	2.6	355	susie	-3.3	$9.1x10^{-4}$
Cerebellum	RFX3-AS1	9	0.31	rs10814233	3.1	rs10814233	4.9	3.1	541	top1	3.1	$1.7x10^{-3}$
Cerebellum	CNTLN	9	0.16	rs16935340	-3.3	rs10962988	3.9	-2.5	546	lasso	-3.0	$2.9x10^{-3}$

Continuation of Table A15

Cerebellum	PARVA	11	0.55	rs11022381	-4.0	rs6485683	7.7	-2.0	665	susie	-2.0	$5.0x10^{-2}$
Cerebellum	LINC00958	11	0.27	rs11022588	-4.1	rs11022589	-5.8	-4.1	550	top1	4.1	$4.8x10^{-5}$
Cerebellum	EID3	12	0.11	rs4406890	4.6	rs4964788	-4.0	3.3	799	susie	-3.3	$8.9x10^{-4}$
Cerebellum	RP11-236L14.2	15	0.16	rs2589227	-3.3	rs2589227	-3.8	-3.3	540	susie	3.0	$3.2x10^{-3}$
Cerebellum	Antisense to WDR90	16	0.53	rs8063501	2.3	rs2301426	-7.4	-1.8	450	lasso	2.1	$3.4x10^{-2}$
Cerebellum	MSLN	16	0.61	rs2050114	2.5	rs7404985	6.5	0.92	458	enet	2.0	$4.2x10^{-2}$
Cerebellum	IGFALS	16	0.49	rs28364711	-2.7	rs2437744	-6.4	-2.3	473	enet	3.2	$1.2x10^{-3}$
Cerebellum	Antisense to PDPK1	16	0.32	rs886322	2.9	rs11642384	6.2	-1.6	294	lasso	-2.1	$3.8x10^{-2}$
Cerebellum	KCTD5 pseudogene	16	0.35	rs886322	2.9	rs11646366	6.2	-1.7	296	enet	-2.2	$2.9x10^{-2}$
Cerebellum	BICDL2	16	0.11	rs886322	2.9	rs1218762	3.5	1.7	365	susie	2.6	$1.0x10^{-2}$
Cerebellum	SLX4	16	0.51	rs7200737	-2.9	rs8061528	-7.7	-2.1	366	enet	2.4	$1.5x10^{-2}$
Cerebellum	Antisense to TRAP1	16	0.20	rs233634	3.2	rs710891	-4.6	-1.4	382	lasso	2.2	$2.5x10^{-2}$
Cerebellum	SMCHD1	18	0.40	rs7245003	-3.8	rs28377858	-7.7	-3.5	514	susie	2.8	$4.8x10^{-3}$
Cerebellum	DLGAP1-AS3	18	0.39	rs12954964	-4.3	rs9947561	4.3	2.9	566	top1	2.9	$4.3x10^{-3}$
Cerebellum	FAM98C	19	0.27	rs2302226	4.0	rs2286550	4.6	3.8	380	lasso	3.9	$9.1x10^{-5}$
Cerebellum	RINL	19	0.36	rs3136641	2.2	rs11879029	-5.2	-0.88	397	enet	2.4	$1.9x10^{-2}$
Cerebellum	FCGBP	19	0.16	rs4803313	3.6	rs34466648	6.2	-2.5	400	top1	-2.5	$1.2x10^{-2}$
Cerebellum	IZUMO1	19	0.38	rs4021	3.4	rs4021	6.3	3.4	429	susie	3.6	$3.9x10^{-4}$
Cerebellum	FCGRT	19	0.14	rs11670388	2.5	rs1132990	-3.7	1.1	366	susie	-2.0	$5.0x10^{-2}$
Brain	LRRC8C	1	0.079	rs1011702	3.8	rs473412	-6.4	3.4	410	top1	-3.4	$7.3x10^{-4}$
Brain	LOC151009	2	0.11	rs13426054	2.8	rs12474907	-5.3	2.5	144	blup	-3.5	$5.7x10^{-4}$
Brain	NCKIPSD	3	0.20	rs35452137	-4.0	rs4858831	-11.6	2.8	266	top1	-2.8	$5.7x10^{-3}$
Brain	P4HTM	3	0.13	rs35452137	-4.0	rs7432989	-8.3	3.3	264	blup	-3.2	$1.2x10^{-3}$
Brain	WDR6	3	0.17	rs35452137	-4.0	rs4513485	10.3	2.7	263	lasso	2.8	$5.7x10^{-3}$

Continuation of Table A15

Brain	DALRD3	3	0.045	rs35452137	-4.0	rs12493578	-5.2	2.8	265	lasso	-2.0	$4.7x10^{-2}$
Brain	GPX1	3	0.12	rs7628719	3.4	rs4955430	9.6	2.1	275	blup	2.7	$6.1x10^{-3}$
Brain	RHOA	3	0.025	rs7628719	3.4	rs4955430	4.1	2.1	294	blup	2.3	$2.1x10^{-2}$
Brain	NICN1	3	0.092	rs7628719	3.4	rs4955411	5.3	2.3	287	bslmm	2.2	$3.1x10^{-2}$
Brain	HYAL3	3	0.49	rs1076904	2.4	rs13100173	-13.2	2.1	275	lasso	-2.2	$2.7x10^{-2}$
Brain	NAT6	3	0.049	rs1076904	2.4	rs13100173	4.5	2.1	274	top1	2.1	$3.7x10^{-2}$
Brain	RBP1	3	0.13	rs3821546	3.4	rs6802598	6.5	2.7	500	lasso	3.2	$1.7x10^{-3}$
Brain	ZNF639	3	0.10	rs6443599	-3.5	rs1362650	5.7	-3.2	365	top1	-3.2	$1.4x10^{-3}$
Brain	WFS1	4	0.10	rs17718958	4.5	rs1046314	-4.7	3.8	671	top1	-3.8	$1.9x10^{-4}$
Brain	SEL1L3	4	0.19	rs316807	3.0	rs17627409	-5.3	-1.7	531	blup	3.1	$1.9x10^{-3}$
Brain	ELOVL7	5	0.037	rs10077663	-4.1	rs7722373	-4.8	3.1	355	top1	-3.1	$1.8x10^{-3}$
Brain	ERCC8	5	0.11	rs10077663	-4.1	rs162231	6.4	-3.0	327	lasso	-3.6	$2.7x10^{-4}$
Brain	PDLIM4	5	0.11	rs9791170	3.8	rs3900945	9.3	3.5	411	top1	3.5	$4.2x10^{-4}$
Brain	CADPS2	7	0.14	rs1443753	3.1	rs2402653	-5.1	2.6	565	enet	-2.5	$1.2x10^{-2}$
Brain	IQUB	7	0.13	rs7789409	3.3	rs12673749	-7.0	3.3	398	blup	-2.9	$3.7x10^{-3}$
Brain	LOC286186	8	0.29	rs10102473	-2.7	rs11992528	-12.4	-2.5	365	enet	2.9	$3.6x10^{-3}$
Brain	ANKRD30A	10	0.056	rs11011154	-3.1	rs12784034	-6.4	-3.1	371	top1	3.1	$2.0x10^{-3}$
Brain	ANKRD49	11	0.059	rs7950328	3.6	rs6483341	-5.2	-2.6	438	enet	3.6	$3.2x10^{-4}$
Brain	CWC15	11	0.19	rs13447623	3.1	rs1054532	-7.3	1.4	500	lasso	-2.2	$3.1x10^{-2}$
Brain	PRH1-PRR4	12	0.28	rs7294858	-2.7	rs7310849	-13.5	2.6	513	lasso	-2.9	$4.1x10^{-3}$
Brain	TAS2R13	12	0.054	rs7294858	-2.7	rs6488330	5.2	-2.4	368	blup	-3.1	$1.7x10^{-3}$
Brain	PRH2	12	0.10	rs7294858	-2.7	rs10772397	7.5	-2.2	373	lasso	-2.5	$1.3x10^{-2}$

Continuation of Table A15

Brain	TAS2R14	12	0.092	rs7294858	-2.7	rs10772397	7.1	-2.2	376	bslmm	-2.9	$3.4x10^{-3}$
Brain	TAS2R50	12	0.079	rs7294858	-2.7	rs6488334	6.7	-2.4	389	top1	-2.4	$1.8x10^{-2}$
Brain	TAS2R20	12	0.10	rs7294858	-2.7	rs4763611	8.4	-2.4	392	top1	-2.4	$1.6x10^{-2}$
Brain	TAS2R19	12	0.090	rs7294858	-2.7	rs7968647	7.9	-2.1	402	enet	-2.7	$7.2x10^{-3}$
Brain	TAS2R31	12	0.071	rs7294858	-2.7	rs7135018	6.5	-2.4	401	top1	-2.4	$1.6x10^{-2}$
Brain	TAS2R46	12	0.068	rs7294858	-2.7	rs1376250	5.0	-2.0	399	blup	-2.4	$1.7x10^{-2}$
Brain	TAS2R30	12	0.10	rs7294858	-2.7	rs7294858	7.4	-2.7	366	top1	-2.7	$6.7x10^{-3}$
Brain	LOC100129361	12	0.12	rs7294858	-2.7	rs1451772	7.6	-2.4	367	top1	-2.4	$1.9x10^{-2}$
Brain	SPTB	14	0.055	rs2987979	-2.7	rs2269292	-5.1	-2.3	528	top1	2.3	$2.0x10^{-2}$
Brain	EIF2AK4	15	0.32	rs566792	-3.0	rs8041057	-8.3	-1.3	485	bslmm	2.6	$1.1x10^{-2}$
Brain	NUP93	16	0.21	rs158619	-3.3	rs6499852	8.8	3.0	571	top1	3.0	$2.9x10^{-3}$
Brain	CIAPIN1	16	0.086	rs158619	-3.3	rs223839	4.2	-1.5	590	blup	-2.1	$3.4x10^{-2}$
Brain	ROCK1	18	0.028	rs394715	-2.8	rs11660183	3.6	-1.9	134	blup	-2.6	$8.2x10^{-3}$
Brain	ABHD3	18	0.085	rs16964670	-2.6	rs7343008	-4.5	-1.2	260	bslmm	2.0	$4.5x10^{-2}$
Brain	LOC100505812	19	0.10	rs4021	3.4	rs1421674	-3.8	-1.2	514	lasso	2.9	$4.1x10^{-3}$
Brain	FUT1	19	0.15	rs4021	3.4	rs4021	-8.7	3.4	433	lasso	-3.2	$1.3x10^{-3}$
Brain	RIN2	20	0.092	rs6046060	2.8	rs6046060	4.1	2.8	770	lasso	2.5	$1.4x10^{-2}$
Brain	PLK1S1	20	0.082	rs6047319	-4.0	rs6047267	5.3	-2.7	417	lasso	-3.0	$2.9x10^{-3}$
Brain	E2F1	20	0.063	rs2752901	2.7	rs7274811	-4.1	1.1	268	bslmm	-3.4	$6.6x10^{-4}$
Kidney	SLC1A7	1	0.80	rs34418279	3.2	rs12731800	4.1	2.2	475	lasso	3.6	$3.9x10^{-4}$

Continuation of Table A15

Kidney	RP5-943J3.1	1	0.41	rs1011702	3.8	rs7535521	3.9	-2.8	373	top1	-2.8	$5.0x10^{-3}$
Kidney	WDR6	3	0.24	rs35452137	-4.0	rs6446205	4.2	3.3	261	susie	3.1	$1.7x10^{-3}$
Kidney	AMT	3	0.22	rs7628719	3.4	rs12637576	-4.2	2.7	289	top1	-2.7	$6.6x10^{-3}$
Kidney	NICN1	3	0.15	rs7628719	3.4	rs6778080	-3.4	2.2	289	susie	-2.6	$1.0x10^{-2}$
Kidney	LINC02519	6	0.44	rs9478048	-3.2	rs3006184	-4.2	-2.7	604	enet	3.3	$1.0x10^{-3}$
Kidney	FAM85B	8	0.32	rs1986346	-3.8	rs4840913	-3.9	1.0	323	enet	-2.5	$1.2x10^{-2}$
Kidney	RPL10P19	8	0.73	rs1986346	-3.8	rs9693857	-4.3	-1.1	714	enet	2.2	$2.9x10^{-2}$
Kidney	C1QL3	10	0.66	rs7079565	2.9	rs7909832	-5.8	-2.7	597	top1	2.7	$6.1x10^{-3}$
Kidney	LINC00958	11	0.73	rs11022588	-4.1	rs11022588	-5.6	-4.1	553	top1	4.1	$4.4x10^{-5}$
Kidney	SUGT1P3	13	0.45	rs12865518	3.6	rs7320344	3.6	2.3	329	top1	2.3	$2.4x10^{-2}$
Kidney	CKAP2-DT	13	0.40	rs11618716	2.6	rs7333451	4.4	2.5	359	susie	2.3	$2.2x10^{-2}$
Kidney	MTHFD1	14	0.52	rs17093516	2.7	rs4365213	-3.6	-0.97	500	enet	2.5	$1.4x10^{-2}$
Kidney	LCTL	15	0.68	rs16949778	-3.3	rs1371781	-3.3	-2.2	590	lasso	2.3	$2.1x10^{-2}$
Kidney	OSCAR	19	0.62	rs4806674	3.1	rs2241790	-3.6	-1.1	453	enet	2.8	$5.6x10^{-3}$
Kidney	CTA-212A2.1	22	0.52	rs5755948	-2.6	rs6000005	-3.5	-1.5	500	lasso	2.1	$3.4x10^{-2}$
Adipose (SC)	FGGY-DT	1	0.28	rs12739770	3.9	rs12758288	12.3	3.1	396	enet	3.4	$5.8x10^{-4}$
Adipose (SC)	LRRC8C-DT	1	0.045	rs1011702	3.8	rs6684610	4.8	-2.6	364	top1	-2.6	$9.8x10^{-3}$
Adipose (SC)	RP5-943J3.1	1	0.31	rs1011702	3.8	rs473412	-15.1	3.4	373	susie	-3.4	$7.3x10^{-4}$
Adipose (SC)	ZNF639	3	0.25	rs6443599	-3.5	rs1362650	8.8	-3.2	365	enet	-3.4	$7.9x10^{-4}$
Adipose (SC)	WFS1	4	0.089	rs17718958	4.5	rs10010131	-6.7	3.8	657	susie	-3.8	$1.3x10^{-4}$
Adipose (SC)	CLASP2 pseudogene	5	0.023	rs9791170	3.8	rs17132288	-4.0	-3.0	392	enet	3.5	$5.3x10^{-4}$
Adipose (SC)	PDLIM4	5	0.12	rs9791170	3.8	rs10463891	8.8	3.2	391	lasso	3.3	$1.1x10^{-3}$
Adipose (SC)	SOBP	6	0.058	rs12194751	4.0	rs10457162	3.5	3.9	441	lasso	3.4	$6.0x10^{-4}$
Adipose (SC)	NSUN5P2	7	0.45	rs34014814	-2.7	rs34014814	8.4	-2.7	94	enet	-3.5	$5.1x10^{-4}$

Continuation of Table A15

Adipose (SC)	TRIM74	7	0.070	rs34014814	-2.7	rs34014814	3.3	-2.7	94	lasso	-2.1	$3.9x10^{-2}$
Adipose (SC)	PCM1	8	0.15	rs17125822	4.5	rs2301546	-6.6	3.1	868	susie	-4.2	$2.8x10^{-5}$
Adipose (SC)	RFX3-AS1	9	0.37	rs10814233	3.1	rs10814233	9.0	3.1	535	enet	3.1	$1.9x10^{-3}$
Adipose (SC)	ARHGAP1	11	0.11	rs1352307	-3.4	rs3816614	-7.7	-3.1	233	enet	3.4	$8.2x10^{-4}$
Adipose (SC)	C11orf49	11	0.12	rs4647709	-3.5	rs1352307	-6.9	-3.4	280	top1	3.4	$7.7x10^{-4}$
Adipose (SC)	DDB2	11	0.051	rs4647709	-3.5	rs4752969	-5.1	-2.8	297	susie	2.5	$1.2x10^{-2}$
Adipose (SC)	CCDC169	13	0.11	rs1886856	-3.2	rs9546762	-7.2	0.89	529	enet	-2.0	$4.8x10^{-2}$
Adipose (SC)	SPART-AS1	13	0.053	rs1886856	-3.2	rs1886856	5.3	-3.2	514	top1	-3.2	$1.4x10^{-2}$
Adipose (SC)	ATP5MC1P2	14	0.058	rs11156667	-3.1	rs11156673	5.1	-2.6	277	top1	-2.6	$9.7x10^{-3}$
Adipose (SC)	RP11-176H8.1	14	0.073	rs11156667	-3.1	rs1888576	7.0	-2.3	292	top1	-2.3	$2.0x10^{-2}$
Adipose (SC)	DTD2	14	0.18	rs11156667	-3.1	rs17097892	-8.2	3.0	305	enet	-3.5	$4.0x10^{-4}$
Adipose (SC)	SEZ6L2	16	0.085	rs11862806	3.4	rs7498372	5.5	1.3	174	enet	2.2	$3.0x10^{-2}$
Adipose (SC)	PPP4C	16	0.057	rs11862806	3.4	rs11862806	-4.5	3.4	220	susie	-2.7	$6.9x10^{-3}$
Adipose (SC)	CA5A pseudogene	16	0.11	rs11862806	3.4	rs11863150	-6.7	3.2	209	top1	-3.2	$1.5x10^{-3}$
Adipose (SC)	CD2BP2	16	0.085	rs11862806	3.4	rs4787643	6.1	2.6	204	susie	2.7	$6.7x10^{-3}$
Adipose (SC)	SEPTIN1	16	0.16	rs11862806	3.4	rs4787643	-10.2	2.6	202	top1	-2.6	$9.1x10^{-3}$
Adipose (SC)	ITGAM	16	0.056	rs3116150	-2.5	rs11150610	4.3	2.3	268	top1	2.3	$2.4x10^{-2}$
Adipose (SC)	RFLNB	17	0.085	rs6565733	-3.2	rs11869174	-4.3	-1.4	349	enet	3.2	$1.5x10^{-3}$
Adipose (SC)	YWHAE	17	0.092	rs16950948	-2.7	rs2131431	-5.2	0.77	447	enet	-2.0	$4.5x10^{-2}$
Adipose (SC)	IZUMO1	19	0.41	rs4021	3.4	rs838143	10.5	3.0	428	enet	3.6	$3.5x10^{-4}$

Continuation of Table A15

Adipose (SC)	C20orf141	20	0.068	rs8122680	3.1	rs6084189	5.2	2.0	538	susie	2.1	$3.8x10^{-2}$
Adipose (SC)	ITPA	20	0.39	rs8362	-3.0	rs7270101	-15.0	2.3	434	enet	-2.4	$1.5x10^{-2}$
Adipose (SC)	MAVS	20	0.12	rs12480318	2.9	rs6515831	6.1	-2.1	539	top1	-2.1	$3.3x10^{-2}$
Adipose (SC)	PANK2	20	0.092	rs12480318	2.9	rs12480318	5.4	2.9	556	enet	3.4	$5.9x10^{-4}$
Adipose (SC)	ARHGAP8	22	0.10	rs3761481	-4.3	rs3761481	4.9	-4.3	707	enet	-2.9	$3.5x10^{-3}$
Adipose (VO)	RP5-943J3.1	1	0.27	rs1011702	3.8	rs473412	-12.5	3.3	374	susie	-3.4	$8.0x10^{-4}$
Adipose (VO)	SERTAD4-AS1	1	0.18	rs654523	3.2	rs654523	6.1	3.2	547	lasso	3.4	$7.7x10^{-4}$
Adipose (VO)	ZNF532 pseudogene	2	0.16	rs7581640	2.7	rs6752335	-5.1	2.3	122	susie	-2.2	$3.0x10^{-2}$
Adipose (VO)	LINC01106	2	0.23	rs7581640	2.6	rs7609252	-6.1	2.6	140	enet	-2.6	$9.8x10^{-3}$
Adipose (VO)	GPAA1P2	2	0.17	rs7581640	2.6	rs7609252	-5.6	2.6	144	susie	-2.6	$1.0x10^{-2}$
Adipose (VO)	TPCN3 pseudogene	2	0.50	rs13388313	2.6	rs4443010	6.7	-1.6	158	enet	-3.3	$9.7x10^{-4}$
Adipose (VO)	SCAP	3	0.16	rs749512	-1.7	rs2306628	4.6	-1.7	146	enet	-2.4	$1.8x10^{-2}$
Adipose (VO)	ATRIP	3	0.35	rs35452137	-4.0	rs35452137	-7.5	-4.0	253	lasso	3.8	$1.8x10^{-4}$
Adipose (VO)	NCKIPSD	3	0.21	rs35452137	-4.0	rs4858828	-11.0	2.8	261	susie	-2.8	$5.1x10^{-3}$
Adipose (VO)	PRKAR2A	3	0.027	rs35452137	-4.0	rs990211	4.3	3.0	272	top1	3.0	$3.0x10^{-3}$
Adipose (VO)	ARIH2	3	0.089	rs35452137	-4.0	rs6446196	-4.8	3.3	264	top1	-3.3	$8.5x10^{-4}$
Adipose (VO)	P4HTM	3	0.088	rs35452137	-4.0	rs9311433	-6.1	3.1	260	susie	-3.1	$1.7x10^{-3}$
Adipose (VO)	WDR6	3	0.24	rs35452137	-4.0	rs9846123	13.3	3.3	262	enet	2.9	$3.3x10^{-3}$
Adipose (VO)	DALRD3	3	0.046	rs35452137	-4.0	rs9850134	-5.9	3.3	264	lasso	-3.2	$1.3x10^{-3}$
Adipose (VO)	QRICH1	3	0.10	rs7628719	3.4	rs9864243	6.4	2.9	254	susie	2.7	$6.1x10^{-3}$
Adipose (VO)	IHO1	3	0.14	rs7628719	3.4	rs4955418	-9.1	2.7	260	susie	-2.7	$7.6x10^{-3}$
Adipose (VO)	RP11-3B7.1	3	0.10	rs7628719	3.4	rs4955418	-8.0	2.7	272	susie	-2.9	$3.9x10^{-3}$

Continuation of Table A15

Adipose (VO)	C3orf62	3	0.084	rs7628719	3.4	rs12629759	-4.0	2.7	278	enet	-3.1	$2.0x10^{-3}$
Adipose (VO)	AMT	3	0.35	rs7628719	3.4	rs3448	-14.4	2.1	289	enet	-2.4	$1.7x10^{-2}$
Adipose (VO)	NICN1	3	0.20	rs7628719	3.4	rs9834003	-9.8	2.3	289	susie	-2.2	$2.5x10^{-2}$
Adipose (VO)	HYAL3	3	0.44	rs1076904	2.4	rs2236947	-10.3	2.0	310	enet	-2.0	$4.8x10^{-2}$
Adipose (VO)	ZNF639	3	0.12	rs6443599	-3.5	rs7610174	-5.9	2.7	365	enet	-3.4	$5.8x10^{-4}$
Adipose (VO)	XXYLT1	3	0.15	rs7627043	3.6	rs6794037	5.7	3.1	376	susie	3.4	$7.6x10^{-4}$
Adipose (VO)	TM4SF19-AS1	3	0.062	rs6809369	2.9	rs4459932	5.0	2.0	367	top1	2.0	$4.2x10^{-2}$
Adipose (VO)	NCBP2-AS1	3	0.075	rs548853	-2.7	rs548853	6.1	-2.7	456	top1	-2.7	$7.2x10^{-3}$
Adipose (VO)	NCBP2	3	0.10	rs548853	-2.7	rs548853	4.9	-2.7	455	top1	-2.7	$7.2x10^{-3}$
Adipose (VO)	WFS1	4	0.11	rs17718958	4.5	rs4689393	-5.8	4.2	665	top1	-4.2	$2.9x10^{-5}$
Adipose (VO)	CLASP2 pseudogene	5	0.045	rs9791170	3.8	rs2089855	-4.0	-3.2	396	top1	3.2	$1.3x10^{-3}$
Adipose (VO)	PDLIM4	5	0.069	rs9791170	3.8	rs6890009	5.8	3.5	396	lasso	3.6	$2.8x10^{-4}$
Adipose (VO)	KBTBD11	8	0.076	rs6983882	3.1	rs731869	-3.9	1.6	628	enet	-3.0	$2.7x10^{-3}$
Adipose (VO)	PCM1	8	0.17	rs17125822	4.5	rs2285306	-6.6	3.7	871	susie	-4.4	$1.1x10^{-5}$
Adipose (VO)	ASAH1-AS1	8	0.12	rs17125822	4.3	rs370429	-5.1	-2.6	869	susie	2.5	$1.3x10^{-2}$
Adipose (VO)	RFX3-AS1	9	0.31	rs10814233	3.1	rs10814233	8.1	3.1	536	susie	3.2	$1.5x10^{-3}$
Adipose (VO)	ARHGAP1	11	0.15	rs1352307	-3.4	rs10769205	-6.7	-2.4	237	enet	3.0	$2.5x10^{-3}$
Adipose (VO)	ZNF408	11	0.052	rs1352307	-3.4	rs4752927	-4.3	-2.7	237	enet	3.7	$2.4x10^{-4}$
Adipose (VO)	TAS2R10	12	0.055	rs7294858	-2.7	rs4763611	5.2	-2.4	385	top1	-2.4	$1.6x10^{-2}$
Adipose (VO)	TAS2R14	12	0.27	rs7294858	-2.7	rs10772397	11.2	-2.2	364	enet	-2.5	$1.2x10^{-2}$
Adipose (VO)	TAS2R20	12	0.20	rs7294858	-2.7	rs7132674	9.8	-2.6	377	enet	-2.3	$2.2x10^{-2}$
Adipose (VO)	TAS2R43	12	0.24	rs7294858	-2.7	rs2010481	12.1	2.3	378	susie	2.1	$3.9x10^{-2}$

Continuation of Table A15

Adipose (VO)	PRR4	12	0.30	rs7294858	-2.7	rs7132674	13.1	-2.6	358	enet	-2.5	$1.1x10^{-2}$
Adipose (VO)	LINC01252	12	0.67	rs16907647	-3.3	rs7132674	15.1	-2.6	438	enet	-2.7	$7.5x10^{-3}$
Adipose (VO)	LRP6	12	0.069	rs4763797	-3.4	rs4763797	-4.5	-3.4	550	top1	3.4	$8.1x10^{-4}$
Adipose (VO)	Antisense to TM7SF3	12	0.75	rs4265668	3.2	rs6487582	-12.1	2.3	514	lasso	-2.8	$4.9x10^{-3}$
Adipose (VO)	TM7SF3	12	0.28	rs4265668	3.2	rs11048950	7.6	3.0	522	enet	3.3	$8.7x10^{-4}$
Adipose (VO)	RP11-1060J15.4	12	0.33	rs4101552	3.2	rs2033024	8.9	-2.6	538	lasso	-2.0	$4.7x10^{-2}$
Adipose (VO)	CCDC169	13	0.14	rs1886856	-3.2	rs9547431	-5.6	-0.17	529	enet	-2.1	$4.1x10^{-2}$
Adipose (VO)	SPART-AS1	13	0.069	rs1886856	-3.2	rs11842927	4.2	-2.9	514	susie	-3.3	$8.3x10^{-4}$
Adipose (VO)	EXOSC8	13	0.078	rs9594184	3.5	rs9576206	4.8	2.0	526	top1	2.0	$4.7x10^{-2}$
Adipose (VO)	CTD-2292M16.8	14	0.22	rs11541061	3.0	rs1953550	-4.9	-2.2	575	lasso	3.4	$7.1x10^{-4}$
Adipose (VO)	HEATR5A	14	0.087	rs11156667	-3.1	rs10872851	4.1	-2.1	298	top1	-2.1	$3.9x10^{-2}$
Adipose (VO)	RP11-176H8.1	14	0.21	rs11156667	-3.1	rs1888576	8.5	-2.3	304	top1	-2.3	$2.0x10^{-2}$
Adipose (VO)	DTD2	14	0.20	rs11156667	-3.1	rs17097892	-7.3	3.0	317	enet	-3.4	$7.5x10^{-4}$
Adipose (VO)	GALNT16	14	0.11	rs2268966	-3.0	rs11623840	-4.1	-2.6	453	lasso	3.0	$3.1x10^{-3}$
Adipose (VO)	Sense Intronic to ZNF280D	15	0.047	rs1631079	-4.1	rs1963831	3.9	-2.8	340	susie	-3.3	$9.9x10^{-4}$
Adipose (VO)	ZNF280D	15	0.047	rs1631079	-4.1	rs28678122	4.6	-2.4	342	susie	-2.9	$3.9x10^{-3}$
Adipose (VO)	CD300C	17	0.17	rs11650024	-3.1	rs1171207	-6.1	-2.3	488	lasso	2.4	$1.8x10^{-2}$
Adipose (VO)	CDR2L	17	0.14	rs11650024	-3.1	rs902726	3.2	-2.7	395	lasso	-3.1	$1.7x10^{-3}$
Adipose (VO)	CBX3P2	18	0.080	rs7245003	-3.8	rs12608077	-3.3	0.89	507	susie	-2.9	$4.3x10^{-3}$
Adipose (VO)	MYL12A	18	0.18	rs12954964	-4.3	rs1662347	-5.4	-2.1	489	lasso	2.1	$3.2x10^{-2}$

Continuation of Table A15

Adipose (VO)	SRRM5	19	0.081	rs2239372	3.0	rs427115	4.0	0.85	395	enet	3.5	$5.3x10^{-4}$
Adipose (VO)	RALGAPA2	20	0.066	rs6047273	-3.8	rs6046818	-3.6	-2.5	410	top1	2.5	$1.4x10^{-2}$
Adipose (VO)	KIZ	20	0.13	rs6047319	-4.0	rs6082331	6.7	-2.9	394	top1	-2.9	$3.6x10^{-3}$
Blood	Antisense to NRD1	1	0.051	rs1770791	2.5	rs1770791	-4.6	2.5	191	enet	-3.3	$9.2x10^{-4}$
Blood	RP5-943J3.1	1	0.17	rs1011702	3.8	rs473412	-12.3	3.4	373	susie	-3.4	$7.8x10^{-4}$
Blood	LRRC8D	1	0.080	rs1011702	3.8	rs10922726	7.0	-2.1	381	susie	-2.1	$3.7x10^{-2}$
Blood	MFSD4B	6	0.069	rs354527	-3.3	rs190246	5.6	-2.6	381	enet	-3.2	$1.5x10^{-3}$
Blood	MTUS1	8	0.33	rs17125822	4.4	rs17125481	11.9	3.7	870	enet	3.1	$2.1x10^{-3}$
Blood	AC087273.2	8	0.083	rs17125822	4.5	rs440182	-6.0	2.5	857	lasso	-2.0	$4.2x10^{-2}$
Blood	PCM1	8	0.087	rs17125822	4.5	rs12718385	8.0	-3.7	868	enet	-3.7	$2.5x10^{-4}$
Blood	RFX3-AS1	9	0.071	rs10814233	3.1	rs7864107	4.1	3.1	532	top1	3.1	$1.8x10^{-3}$
Blood	LINC00958	11	0.50	rs11022588	-4.1	rs11022589	17.8	-4.1	546	lasso	-4.0	$6.9x10^{-5}$
Blood	PRMT5-AS1	14	0.040	rs4981454	-3.2	rs4981454	-4.5	-3.2	568	top1	3.2	$1.6x10^{-3}$
Blood	PRMT5	14	0.31	rs4981454	-3.2	rs4981454	-14.9	-3.2	568	susie	3.3	$1.0x10^{-3}$
Blood	PRMT5-DT	14	0.24	rs4981454	-3.2	rs4981454	-10.9	-3.2	568	susie	3.1	$2.1x10^{-3}$
Blood	HAUS4	14	0.47	rs4981454	-3.2	rs4981454	-12.9	-3.2	562	susie	2.4	$1.7x10^{-2}$
Blood	DHRS4L2	14	0.18	rs10151272	2.4	rs12891812	-6.1	-2.0	458	enet	2.2	$2.8x10^{-2}$
Blood	IFI27L2	14	0.21	rs11628686	-3.7	rs8011253	-5.1	-0.48	751	susie	2.1	$3.6x10^{-2}$
Blood	Antisense to SERPINA9	14	0.086	rs11628686	-3.7	rs6575433	5.0	-3.6	805	susie	-3.5	$4.6x10^{-4}$
Blood	CTD-2313J17.1	15	0.17	rs7169046	-3.5	rs4274391	-6.7	-3.1	651	susie	3.0	$2.5x10^{-3}$
Blood	PSME3IP1	16	0.10	rs158619	-3.3	rs12599485	-6.1	-1.5	525	enet	3.2	$1.5x10^{-3}$

Continuation of Table A15

Blood	DOK4	16	0.045	rs158619	-3.3	rs223895	4.8	-1.9	553	enet	-2.3	$1.9x10^{-2}$
Blood	ADGRG1	16	0.072	rs158619	-3.3	rs733464	4.3	2.0	507	susie	2.1	$3.9x10^{-2}$
Blood	DRC7	16	0.42	rs12448418	-2.8	rs8051301	15.6	2.0	503	top1	2.0	$4.8x10^{-2}$
Blood	BAX	19	0.10	rs4021	3.4	rs7259013	-6.4	2.8	424	enet	-3.7	$2.4x10^{-4}$
Blood	DDRGK1	20	0.18	rs8362	-3.0	rs11087571	-7.0	-2.9	427	susie	2.3	$1.9x10^{-2}$
Blood	ITPA	20	0.54	rs8362	-3.0	rs7270101	-14.0	2.3	429	lasso	-3.2	$1.6x10^{-3}$
Blood	LAMP5	20	0.094	rs2076392	-3.0	rs4816144	4.9	1.8	581	enet	3.0	$2.5x10^{-3}$
Blood	SLX4IP	20	0.092	rs6077783	3.0	rs4813935	6.2	2.2	578	top1	2.2	$2.7x10^{-2}$
Blood	TST	22	0.078	rs3218318	3.8	rs2072861	3.9	3.5	690	top1	3.5	$5.4x10^{-4}$
Blood	RTL6	22	0.13	rs3761481	-4.3	rs133754	8.8	2.3	758	lasso	2.4	$1.5x10^{-2}$
Blood	ARHGAP8	22	0.13	rs3761481	-4.3	rs3761481	5.8	-4.3	705	top1	-4.3	$1.9x10^{-5}$
Blood	UPK3A	22	0.25	rs12169108	2.6	rs2742624	-9.4	2.4	619	enet	-2.0	$4.1x10^{-2}$
Muscle	MYOG	1	0.082	rs4950914	-3.4	rs4950914	-6.3	-3.4	505	top1	3.4	$7.1x10^{-4}$
Muscle	SERTAD4-AS1	1	0.069	rs654523	3.2	rs654523	5.9	3.2	548	top1	3.2	$1.5x10^{-3}$
Muscle	XXYLT1	3	0.11	rs7627043	3.6	rs6794037	5.8	3.1	377	enet	3.4	$8.0x10^{-4}$
Muscle	SDHAP2	3	0.57	rs12487782	-2.8	rs6773702	-12.8	2.3	283	enet	-2.3	$2.0x10^{-2}$
Muscle	TNK2-AS1	3	0.069	rs12487782	-2.8	rs733119	4.3	2.0	288	top1	2.0	$4.8x10^{-2}$
Muscle	NCBP2	3	0.047	rs548853	-2.7	rs553783	5.0	2.1	454	top1	2.1	$3.5x10^{-2}$
Muscle	WFS1	4	0.17	rs17718958	4.5	rs13107806	-9.1	3.3	655	enet	-3.4	$6.2x10^{-4}$
Muscle	PDLIM4	5	0.045	rs9791170	3.8	rs1007602	5.9	3.2	388	enet	2.9	$4.4x10^{-3}$
Muscle	SLC22A4	5	0.066	rs9791170	3.8	rs2569265	7.4	2.5	387	enet	3.3	$1.0x10^{-3}$

Continuation of Table A15

Muscle	TSPYL1	6	0.20	rs7762318	3.1	rs7770769	6.7	0.61	373	enet	-2.1	$3.6x10^{-2}$
Muscle	CALHM4	6	0.14	rs7762318	3.1	rs7762318	-8.1	3.1	369	enet	-2.7	$7.1x10^{-3}$
Muscle	TRAPPC3L	6	0.17	rs7762318	3.1	rs7762318	-9.2	3.1	371	lasso	-3.1	$1.9x10^{-3}$
Muscle	RWDD1	6	0.19	rs7762318	3.1	rs12192126	10.0	-2.3	367	enet	-2.1	$3.2x10^{-2}$
Muscle	OSBPL5	11	0.22	rs734458	3.3	rs734458	10.6	3.3	446	enet	3.2	$1.2x10^{-3}$
Muscle	ATG101	12	0.11	rs12424271	-4.1	rs11521	-6.2	-3.2	615	susie	3.6	$3.8x10^{-4}$
Muscle	RP11-176H8.1	14	0.25	rs11156667	-3.1	rs1888576	12.3	-2.3	292	susie	-2.3	$2.0x10^{-2}$
Muscle	DTD2	14	0.055	rs11156667	-3.1	rs17097892	-4.8	3.0	305	susie	-3.0	$2.7x10^{-3}$
Muscle	RNMT	18	0.067	rs8097240	2.6	rs11659762	4.9	2.5	465	susie	2.6	$1.1x10^{-2}$
Muscle	ZNF780A	19	0.19	rs4803313	3.4	rs24136	8.9	-2.5	353	enet	-3.2	$1.6x10^{-3}$
Muscle	CYP2G1P	19	0.063	rs12971430	2.7	rs2644890	-3.7	1.4	418	enet	-2.0	$4.6x10^{-2}$
Muscle	RALGAPA2	20	0.057	rs6047273	-3.8	rs6137147	4.6	3.8	405	lasso	3.7	$2.7x10^{-4}$
Liver	AMIGO1	1	0.50	rs12066164	3.3	rs534135	8.6	2.1	422	susie	2.0	$4.1x10^{-2}$
Liver	RBM15-AS1	1	0.39	rs12760885	-3.1	rs12410178	4.2	-0.10	567	susie	-3.4	$5.8x10^{-4}$
Liver	NCKIPSD	3	0.28	rs35452137	-4.0	rs12493578	-8.0	2.8	260	susie	-2.8	$5.1x10^{-3}$
Liver	ARIH2	3	0.13	rs35452137	-4.0	rs4279134	-5.2	2.6	261	susie	-3.1	$1.8x10^{-3}$
Liver	P4HTM	3	0.071	rs35452137	-4.0	rs4955417	-3.7	2.3	256	susie	-2.7	$7.7x10^{-3}$
Liver	WDR6	3	0.25	rs35452137	-4.0	rs7643368	7.4	3.3	257	susie	3.2	$1.6x10^{-3}$
Liver	NDUFAF3	3	0.037	rs35452137	-4.0	rs7627404	-3.7	3.1	259	susie	-3.1	$1.7x10^{-3}$
Liver	DALRD3	3	0.11	rs35452137	-4.0	rs6446205	-5.0	3.3	259	lasso	-3.2	$1.3x10^{-3}$
Liver	QRICH1	3	0.20	rs7628719	3.4	rs9284885	4.9	2.4	250	top1	2.4	$1.5x10^{-2}$
Liver	AC127904.2	3	0.19	rs548853	-2.7	rs4916567	-4.6	-2.4	445	top1	2.4	$1.7x10^{-2}$
Liver	NCBP2	3	0.20	rs548853	-2.7	rs4916567	4.0	-2.4	454	lasso	-3.4	$6.5x10^{-4}$

Continuation of Table A15

Liver	MFSD4B	6	0.18	rs354527	-3.3	rs240972	-4.6	2.3	385	enet	-2.8	$4.5x10^{-3}$
Liver	RFX3-AS1	9	0.39	rs10814233	3.1	rs10115088	5.6	3.1	538	lasso	2.9	$3.7x10^{-3}$
Liver	C1QL3	10	0.70	rs7079565	2.9	rs6602130	-10.1	-2.8	596	susie	2.8	$5.0x10^{-3}$
Liver	APBB1IP	10	0.23	rs17668263	2.6	rs867354	4.6	-2.4	435	enet	-2.7	$8.0x10^{-3}$
Liver	ARHGAP1	11	0.52	rs1352307	-3.4	rs10769205	-6.3	-2.4	238	enet	2.9	$3.5x10^{-3}$
Liver	ZNF408	11	0.14	rs1352307	-3.4	rs11039014	-5.4	-3.3	238	top1	3.3	$8.3x10^{-4}$
Liver	LRP4	11	0.12	rs4647709	-3.5	rs10734548	-5.6	-2.9	279	susie	2.9	$3.3x10^{-3}$
Liver	C11orf49	11	0.15	rs4647709	-3.5	rs4752816	-5.5	-2.5	281	susie	3.1	$2.0x10^{-3}$
Liver	CKAP2	13	0.34	rs11618716	2.6	rs9568732	7.3	2.1	359	susie	2.1	$3.5x10^{-2}$
Liver	SERPINA11	14	0.26	rs11628686	-3.7	rs12891900	-4.9	2.9	803	lasso	-2.7	$7.4x10^{-3}$
Liver	LINC01169	15	0.33	rs16949778	-3.3	rs8027997	-6.9	-2.7	591	top1	2.7	$7.2x10^{-3}$
Liver	CD2BP2	16	0.20	rs11862806	3.4	rs8060853	6.1	2.5	204	top1	2.5	$1.3x10^{-2}$
Liver	PLK5	19	0.26	rs8104249	-2.7	rs8104249	5.2	-2.7	387	lasso	-3.1	$1.7x10^{-3}$
Liver	TMPRSS9	19	0.43	rs8107694	2.8	rs10407225	-7.6	-2.0	428	susie	2.0	$4.8x10^{-2}$
Liver	TIMM13	19	0.25	rs8107694	2.7	rs10407225	-5.9	-2.0	425	top1	2.0	$4.4x10^{-2}$
Liver	FCGBP	19	0.30	rs4803313	3.6	rs2767607	6.9	-2.9	403	top1	-2.9	$3.9x10^{-3}$
Liver	ZNF780A	19	0.34	rs4803313	3.4	rs234346	7.4	-2.4	388	lasso	-2.9	$3.4x10^{-3}$
Testis	NCKIPSD	3	0.27	rs35452137	-4.0	rs12493578	-10.1	2.8	261	top1	-2.8	$5.7x10^{-3}$
Testis	ARIH2	3	0.087	rs35452137	-4.0	rs6446205	-4.7	3.3	262	top1	-3.3	$1.0x10^{-3}$
Testis	WDR6	3	0.25	rs35452137	-4.0	rs6781790	10.9	3.3	258	top1	3.3	$1.1x10^{-3}$
Testis	QRICH1	3	0.28	rs7628719	3.4	rs7653408	9.1	2.9	250	enet	3.2	$1.5x10^{-3}$
Testis	USP19	3	0.047	rs7628719	3.4	rs7626445	-4.1	3.2	254	lasso	-3.1	$1.8x10^{-3}$
Testis	USP4	3	0.049	rs7628719	3.4	rs12637576	-4.6	2.7	275	enet	-2.6	$9.3x10^{-3}$
Testis	AMT	3	0.41	rs7628719	3.4	rs11710434	-11.6	2.0	285	enet	-2.5	$1.1x10^{-2}$
Testis	GMPPB	3	0.12	rs2117938	2.7	rs1491983	5.6	2.0	317	top1	2.0	$4.9x10^{-2}$

Continuation of Table A15

Testis	CDHR4	3	0.63	rs34364099	-2.8	rs1799843	13.9	-2.1	325	enet	-2.1	$3.6x10^{-2}$
Testis	INKA1	3	0.19	rs34364099	-2.8	rs2291542	7.0	-2.1	326	susie	-2.2	$2.7x10^{-2}$
Testis	TRAIP	3	0.12	rs34364099	-3.1	rs1799843	6.0	-2.1	336	top1	-2.1	$3.8x10^{-2}$
Testis	Antisense to MON1A	3	0.13	rs34364099	-3.2	rs12489386	-5.4	-2.2	337	top1	2.2	$2.9x10^{-2}$
Testis	NAA80	3	0.14	rs1076904	2.4	rs13100173	3.7	2.1	327	top1	2.1	$3.7x10^{-2}$
Testis	HYAL3	3	0.43	rs1076904	2.4	rs13100173	-7.9	2.1	327	top1	-2.1	$3.7x10^{-2}$
Testis	WFS1	4	0.25	rs17718958	4.5	rs4688982	-7.9	3.5	668	top1	-3.5	$5.5x10^{-4}$
Testis	DEPDC1B	5	0.12	rs10077663	-4.1	rs7704338	5.3	3.4	320	top1	3.4	$7.7x10^{-4}$
Testis	RP1-182D15.2	6	0.17	rs9478048	-3.2	rs12196723	-4.2	-2.3	439	susie	3.5	$4.5x10^{-4}$
Testis	PDCD2	6	0.24	rs9460208	-2.7	rs4428484	-7.1	-2.4	256	top1	2.4	$1.7x10^{-2}$
Testis	PCM1	8	0.11	rs17125822	4.5	rs3850749	-4.8	3.2	875	top1	-3.2	$1.6x10^{-3}$
Testis	SURF6 pseudogene	8	0.15	rs2299596	4.0	rs402227	-3.9	-2.1	863	top1	2.1	$3.8x10^{-2}$
Testis	NAT2	8	0.15	rs2299596	4.0	rs721398	5.5	-2.1	861	top1	-2.1	$3.6x10^{-2}$
Testis	LINC02385	12	0.13	rs4406890	4.6	rs4964288	4.1	4.0	793	top1	4.0	$7.2x10^{-5}$
Testis	RP11-87C7.3	13	0.75	rs9319382	3.5	rs9319382	14.3	3.5	523	susie	3.2	$1.4x10^{-3}$
Testis	TRAV8-5	14	0.27	rs12882371	-3.3	rs4982522	7.1	2.8	658	susie	2.9	$3.7x10^{-3}$
Testis	TRAV13-2	14	0.13	rs12882371	-3.3	rs12880366	-5.2	-2.2	663	lasso	2.3	$2.2x10^{-2}$
Testis	PRMT5-AS1	14	0.16	rs4981454	-3.2	rs1043209	-5.6	-2.5	573	top1	2.5	$1.2x10^{-2}$
Testis	CARMIL3	14	0.28	rs6573793	-2.5	rs11158525	-8.5	-2.0	491	top1	2.0	$4.8x10^{-2}$
Testis	LINC02286	14	0.69	rs17109940	-3.1	rs1241482	11.7	-2.0	552	enet	-2.1	$3.2x10^{-2}$
Testis	RP11-176H8.1	14	0.29	rs11156667	-3.1	rs12893465	8.8	-2.4	305	susie	-2.4	$1.7x10^{-2}$
Testis	DTD2	14	0.21	rs11156667	-3.1	rs2274291	5.3	-2.7	318	enet	-3.1	$1.9x10^{-3}$
Testis	TCL1B	14	0.71	rs11160284	3.2	rs11160284	11.6	3.2	740	susie	3.2	$1.6x10^{-3}$
Testis	CCDC40	17	0.60	rs715041	3.6	rs11650121	11.1	-2.4	402	susie	-3.3	$8.9x10^{-4}$

Continuation of Table A15

Testis	EIF4A3	17	0.13	rs715041	3.6	rs2361710	-4.4	3.0	463	top1	-3.0	$2.7x10^{-3}$
Testis	LLNLF-173C4.1	19	0.13	rs12151104	-2.7	rs6510799	3.6	1.5	227	susie	2.2	$2.6x10^{-2}$
Testis	ABCA7	19	0.28	rs8104249	-2.7	rs7247087	5.7	-1.6	467	enet	-2.2	$2.9x10^{-2}$
Testis	SCAMP4	19	0.29	rs8104249	-2.7	rs35684719	-7.3	-2.1	365	top1	2.1	$3.9x10^{-2}$
Testis	CSNK1G2-AS1	19	0.42	rs8104249	-2.7	rs11881644	-8.8	-2.3	378	susie	3.4	$7.0x10^{-4}$

Abbreviations: eQTL, expression quantitative trait locus; CHR, chromosome, HSQ, mean heritability estimate; Best.GWAS.ID, most significantly associated variant in the locus; Best.GWAS.Z, z-score of most significantly associated variant in the locus; eQTL ID, best eQTL in the locus; eQTL.GWAS.Z, GWAS z-score for best eQTL; NSNP, number of SNPs in the locus; Model, best performing TWAS model; TWAS.Z, TWAS z-score; TWAS.P, TWAS p-value, enet, elastic-net regression (mixing parameter = 0.5); blup, best linear unbiased predictor from all variants; bslmm, Bayesian sparse linear model; lasso, least absolute shrinkage and selection operator; top1, single best eQTL, susie, sum of single effects regression, VO, visceral omentum; SC, subcutaneous.

Table A16. Genes associated with multiple cisplatin-induced neurotoxicities by TWAS ($p < 0.005$)

Shared between PSN and tinnitus	**PSN GTEx Tissue**	**Tinnitus GTEx Tissue**	**PSN TWAS Z-score**	**Tinnitus TWAS Z-score**	**PSN TWAS p-value**	**Tinnitus TWAS p-value**
LINC01376	Nerve	Nerve	2.8	3.4	$4.5x10^{-3}$	$6.4x10^{-3}$
RAB27A	Adipose (SC)	Adipose (SC)	-2.8	-2.9	$4.7x10^{-3}$	$4.1x10^{-3}$
NICN1	Adipose (VO)	Adipose (VO)	-2.9	-2.8	$3.6x10^{-3}$	$4.6x10^{-3}$
	Nerve	-	-3.1	-	$2.0x10^{-3}$	-
	Adipose (SC)	-	-2.9	-	$3.4x10^{-3}$	-
DMAC2L	Adipose (VO)	Adipose (VO)	2.9	3.6	$4.0x10^{-3}$	$3.7x10^{-4}$
	Cerebellum	-	3.4	-	$7.9x10^{-4}$	-
	-	Kidney	-	3.2	-	$1.4x10^{-3}$
	-	Muscle	-	3.7	-	$2.4x10^{-4}$
	-	Testis	-	2.9	-	$4.3x10^{-3}$
ZFP30	Adipose (VO)	Adipose (VO)	-3.1	2.9	$1.7x10^{-3}$	$4.0x10^{-3}$
MMP11	Muscle	-	2.9	-	$3.8x10^{-3}$	-
	-	Blood	-	-2.9		$3.9x10^{-3}$
Shared between PSN and HL	**PSN GTEx Tissue**	**HL GTEX tissue**	**PSN TWAS Z-score**	**HL TWAS Z-score**	**PSN TWAS p-value**	**HL TWAS p-value**
LOC100505812	Brain	Brain	3.6	2.9	$3.9x10^{-4}$	$4.1x10^{-3}$
SOBP	Adipose (SC)	Adipose (SC)	3.2	3.4	1.3x10-3	$6.0x10^{-4}$
PRKAR2A	Adipose (VO)	Adipose (VO)	3.1	3.0	$1.9x10^{-3}$	$3.0x10^{-3}$
	-	Nerve	-	3.2	-	$1.3x10^{-3}$
	-	Adipose (SC)	-	2.9	-	$3.5x10^{-3}$
FDX1	Muscle	-	-2.9	-	$4.2x10^{-3}$	-
	-	Brain	-	-2.9	-	$3.4x10^{-3}$
FAM153C	Testis	-	-3.0	-	$2.5x10^{-3}$	-
	-	Nerve	-	-2.9	-	$4.3x10^{-3}$
Shared between tinnitus and HL	**Tinnitus GTEx Tissue**	**HL GTEx tissue**	**Tinnitus TWAS Z-score**	**HL TWAS Z-score**	**Tinnitus TWAS p-value**	**HL TWAS p-value**
SMYD2	Nerve	Nerve	2.9	3.1	$3.3x10^{-3}$	$1.7x10^{-3}$
TXNL4B	Nerve	Nerve	-3.6	3.1	$3.8x10^{-4}$	$1.8x10^{-3}$
P4HTM	Cerebellum	-	-2.8	-	$4.7x10^{-3}$	-
	-	Nerve	-	-3.0	-	$2.4x10^{-3}$
	-	Brain	-	-3.2	-	$1.2x10^{-3}$
	-	Adipose (SC)	-	-2.9	-	$3.4x10^{-3}$
	-	Adipose (VO)	-	-3.1	-	$1.7x10^{-3}$
ATP2C2	Brain	-	-3.2	-	$1.2x10^{-3}$	-
	-	Blood	-	2.8	-	$4.7x10^{-3}$
PANK2	Adipose (SC)	Adipose (SC)	3.1	3.4	$2.3x10^{-3}$	$5.9x10^{-4}$

Continuation of Table A16

ARHGAP8	Adipose (SC)	-	-3.1	-	$2.0x10^{-3}$	-
	-	Blood	-	-4.3	-	$1.9x10^{-5}$
TMEM45A	Adipose (VO)	Adipose (VO)	-3.1	-3.0	$1.7x10^{-3}$	$2.5x10^{-3}$
	Nerve	-	-3.5	-	$5.0x10^{-4}$	-
	Adipose (SC)	-	-3.6	-	$3.5x10^{-4}$	-
	Muscle	-	-3.0	-	$2.6x10^{-3}$	-
LINC02446	Blood	Blood	-3.2	-3.2	$1.2x10^{-3}$	$1.2x10^{-3}$
	Testis	-	3.0	-	$2.5x10^{-3}$	-

Abbreviations: SC, subcutaneous; VO, visceral omentum.

Table A17. Genes associated with multiple cisplatin-induced neurotoxicities by TWAS ($p < 0.05$)

Shared between PSN and tinnitus	**PSN GTEx Tissue**	**Tinnitus GTEx Tissue**	**PSN TWAS Z-score**	**Tinnitus TWAS Z-score**	**PSN TWAS p-value**	**Tinnitus TWAS p-value**
L2HGDH	-	Nerve	-	-2.7	-	$7.3x10^{-3}$
	Cerebellum	Cerebellum	-2.2	-3.7	$2.6x10^{-2}$	$1.8x10^{-4}$
	-	Muscle	-	3.8	-	$1.3x10^{-4}$
DMAC2L	Cerebellum	-	3.4	-	$7.9x10^{-4}$	-
	-	Adipose (VO)	2.9	3.6	$4.0x10^{-3}$	$3.7x10^{-4}$
	-	Kidney	-	3.2	-	$1.4x10^{-3}$
	-	Muscle	-	3.7	-	$2.4x10^{-4}$
TRIM9	Cerebellum	Cerebellum	2.3	2.0	$1.9x10^{-2}$	$4.9x10^{-2}$
PDGFB	Blood	Blood	3.3	2.3	$1.1x10^{-3}$	$1.9x10^{-2}$
NICN1	Cerebellum	-	-2.3	-	$2.1x10^{-2}$	-
	Adipose (VO)	-	-2.9	-	$3.6x10^{-3}$	-
	Muscle	-	-2.5	-	$1.3x10^{-2}$	-
	-	Kidney	-	-2.6	-	$9.2x10^{-3}$
GOLGA8N	Liver	-	3.5	-	$4.8x10^{-4}$	-
	-	Adipose (SC)	-	-2.0	-	$4.5x10^{-2}$
	-	Testis	-	-2.3	-	$2.4x10^{-2}$
AMT	Cerebellum	-	-2.1	-	$3.8x10^{-2}$	-
	Adipose (VO)	-	-2.5	-	$1.1x10^{-2}$	-
	Blood	-	-2.6	-	$1.0x10^{-2}$	-
	Muscle	-	-2.6	-	$8.5x10^{-3}$	-
	Testis	-	-2.1	-	$3.2x10^{-2}$	-
	-	Kidney	-	-2.5	-	$1.2x10^{-2}$
Shared between PSN and HL	**PSN GTEx Tissue**	**HL GTEX tissue**	**PSN TWAS Z-score**	**HL TWAS Z-score**	**PSN TWAS p-value**	**HL TWAS p-value**
CARD8-AS1	Nerve	Nerve	3.5	2.2	$5.2x10^{-4}$	$2.9x10^{-2}$
LAMB2P1	Cerebellum	Cerebellum	-2.4	-2.5	$1.8x10^{-2}$	$1.2x10^{-2}$
	-	Nerve	-	-2.9	-	$4.3x10^{-3}$
C3orf62	Cerebellum	-	2.0	-	$5.0x10^{-2}$	-
	-	Adipose (VO)	-	-3.1	-	$2.0x10^{-3}$
GPX1	Cerebellum	Cerebellum	2.6	2.0	$8.5x10^{-3}$	$4.7x10^{-2}$
	Brain	Brain	2.7	2.7	$8.1x10^{-3}$	$6.1x10^{-3}$
LOC100505812	Brain	Brain	3.6	2.9	$3.9x10^{-4}$	$4.1x10^{-3}$
CTA-212A2.1	Kidney	Kidney	2.4	2.1	$1.7x10^{-2}$	$3.4x10^{-2}$
SOBP	Adipose (SC)	Adipose (SC)	3.2	3.4	$1.3x10^{-3}$	$6.0x10^{-4}$
APEH	Adipose (VO)	-	-2.7	-	$6.5x10^{-3}$	-
	Blood	-	-2.7	-	$7.1x10^{-3}$	-
	-	Nerve	-	-2.1	-	$3.8x10^{-2}$
MST1	Cerebellum	Cerebellum	-3.0	-2.3	$3.1x10^{-3}$	$1.9x10^{-2}$
	Brain	-	-2.1	-	$3.3x10^{-2}$	-
	Blood	-	-2.0	-	$4.8x10^{-2}$	-

Continuation of Table A17

PRKAR2A	Adipose (VO)	Adipose (VO)	3.1	3.0	$1.9x10^{-3}$	$3.0x10^{-3}$
	Muscle	-	2.0	-	$4.9x10^{-2}$	-
	-	Nerve	-	3.2	-	$1.3x10^{-3}$
NDUFAF3	Muscle	-	-2.2	-	$3.1x10^{-2}$	-
	-	Liver	-	-3.1	-	$1.7x10^{-3}$
QRICH1	Muscle	-	2.0	-	$4.4x10^{-2}$	-
	-	Nerve	-	2.8	-	$5.1x10^{-3}$
	-	Cerebellum	-	3.0	-	$3.2x10^{-3}$
	-	Adipose (VO)	-	2.7	-	$6.1x10^{-3}$
	-	Liver	-	2.4	-	$1.5x10^{-2}$
	-	Testis	-	3.2	-	$1.5x10^{-3}$
KLHDC8B	Muscle	-	3.0	-	$2.8x10^{-3}$	-
	-	Nerve	-	2.7	-	$7.6x10^{-3}$
	-	Cerebellum	-	2.3	-	$2.2x10^{-3}$
USP4	Cerebellum	Cerebellum	2.5	2.3	$1.4x10^{-2}$	$2.1x10^{-2}$
	Muscle	-	2.1	-	$3.6x10^{-2}$	-
	-	Testis	-	-2.6	-	$9.3x10^{-3}$
RHOA	Muscle	-	2.6	-	$8.6x10^{-3}$	-
	-	Nerve	-	2.0	-	$4.9x10^{-2}$
	-	Brain	-	2.3	-	$2.1x10^{-2}$
NICN1	Cerebellum	Cerebellum	-2.3	-2.4	$2.1x10^{-2}$	$1.8x10^{-2}$
	Adipose (VO)	Adipose (VO)	-2.9	-2.2	$3.6x10^{-3}$	$2.5x10^{-2}$
	Muscle	-	-2.5	-	$1.3x10^{-2}$	-
	-	Brain	-	2.2	-	$3.1x10^{-2}$
	-	Kidney	-	-2.6	-	$1.0x10^{-2}$
INKA1	Cerebellum	-	2.2	-	$3.1x10^{-2}$	-
	Muscle	-	3.2	-	$1.6x10^{-3}$	-
	-	Testis	-	-2.2	-	$2.7x10^{-2}$
P4HTM	Cerebellum	Cerebellum	-2.4	-2.3	$1.6x10^{-2}$	$2.1x10^{-2}$
	Liver	Liver	-2.2	-2.7	$2.9x10^{-2}$	$7.7x10^{-3}$
	-	Nerve	-	-3.0	-	$2.4x10^{-3}$
	-	Brain	-	-3.2	-	$1.2x10^{-3}$
	-	Adipose (VO)	-	-3.1	-	$1.7x10^{-3}$
AMT	Cerebellum	Cerebellum	-2.1	-2.6	$3.8x10^{-2}$	$1.1x10^{-2}$
	Adipose (VO)	Adipose (VO)	-2.5	-2.4	$1.1x10^{-2}$	$1.7x10^{-2}$
	Blood	-	-2.6	-	$1.0x10^{-2}$	-
	Muscle	-	-2.6	-	$8.5x10^{-3}$	-
	Testis	Testis	-2.1	-2.5	$3.2x10^{-2}$	$1.1x10^{-2}$
	-	Nerve	-	-2.2	-	$2.9x10^{-2}$
	-	Kidney	-	-2.7	-	$6.6x10^{-3}$
GMPPB	Cerebellum	-	2.1	-	$3.3x10^{-2}$	-
	Adipose (VO)	-	2.3	-	$2.4x10^{-2}$	-
	Blood	-	2.6	-	$9.4x10^{-3}$	-
	Muscle	-	2.2	-	$3.2x10^{-2}$	-
	Liver	-	2.2	-	$3.1x10^{-2}$	-
	Testis	Testis	2.3	2.0	$2.0x10^{-2}$	$4.9x10^{-2}$

Continuation of Table A17

Shared between tinnitus and HL	Tinnitus GTEx Tissue	HL GTEx tissue	Tinnitus TWAS Z-score	HL TWAS Z-score	Tinnitus TWAS p-value	HL TWAS p-value
TXNL4B	Nerve	Nerve	-3.6	3.1	$3.8x10^{-4}$	$1.8x10^{-3}$
TIMM13	Brain	-	-2.4	-	$1.7x10^{-3}$	-
	-	Liver	-	2.0	-	$4.4x10^{-2}$
WDR6	Kidney	Kidney	2.2	3.1	$2.5x10^{-2}$	$1.7x10^{-3}$
	-	Nerve	-	3.1	-	$2.2x10^{-3}$
	-	Cerebellum	-	3.2	-	$1.2x10^{-3}$
	-	Brain	-	2.8	-	$5.7x10^{-3}$
	-	Adipose (VO)	-	2.9	-	$3.3x10^{-3}$
	-	Liver	-	3.2	-	$1.6x10^{-3}$
	-	Testis	-	3.3	-	$1.1x10^{-3}$
AMT	Kidney	Kidney	-2.5	-2.7	$1.2x10^{-2}$	$6.6x10^{-3}$
	-	Cerebellum	-	-2.6	-	$1.1x10^{-2}$
	-	Adipose (VO)	-	-2.4	-	$1.7x10^{-2}$
	-	Testis	-	-2.5	-	$1.1x10^{-2}$
	-	Nerve	-	-2.2	-	$2.9x10^{-2}$
NICN1	Kidney	Kidney	-2.6	-2.6	$9.2x10^{-3}$	$1.0x10^{-2}$
	-	Cerebellum	-	-2.4	-	$1.8x10^{-2}$
	-	Adipose (VO)	-	-2.2	-	$2.5x10^{-2}$
	-	Brain	-	2.2	-	$3.1x10^{-2}$
PANK2	Adipose (SC)	Adipose (SC)	3.1	3.4	$2.3x10^{-3}$	$5.9x10^{-4}$
ARHGAP8	Adipose (SC)	Adipose (SC)	-3.1	-2.9	$2.0x10^{-3}$	$3.5x10^{-3}$
	-	Blood	-	-4.3	-	$1.9x10^{-5}$
CD177P1	Blood	-	2.6	-	$9.4x10^{-3}$	-
	-	Nerve	-	2.0	-	$4.4x10^{-2}$

Abbreviations: SC, subcutaneous; VO, visceral omentum.

Table A18. Results for models predicting cisplatin-induced severe peripheral sensory neuropathy in the *Platinum Study* test set

Model	Inputs (Down-sampled training set)	AUROC (95% CI)	Sensitivity	Specificity
Random Forest	GWAS $1x10^{-4}$	0.54 (0.40-0.69)	0.36	0.73
Random Forest	GWAS $1x10^{-4}$ RFE	0.56 (0.41-0.71)	0.43	0.69
Random Forest	External PRS	0.61 (0.46-0.76)	0.57	0.65
Random Forest	**Clinical**	**0.71 (0.56-0.85)**	**0.64**	**0.77**
Random Forest	GWAS $1x10^{-4}$ + Clinical	0.69 (0.55-0.84)	0.57	0.81
Random Forest	GWAS $1x10^{-4}$ + Clinical RFE	0.71 (0.56-0.85)	0.64	0.77
Random Forest	GWAS $1x10^{-4}$ RFE + Clinical	0.69 (0.55-0.84)	0.57	0.81
Random Forest	**GWAS $1x10^{-4}$ RFE + Clinical RFE**	**0.75 (0.62-0.89)**	**0.71**	**0.79**
Random Forest	GWAS $1x10^{-4}$ RFE + External PRS	0.66 (0.51-0.81)	0.57	0.75
Random Forest	**External PRS + Clinical**	**0.76 (0.63-0.89)**	**0.79**	**0.73**
Random Forest	GWAS $1x10^{-4}$ RFE + Clinical + External PRS	0.69 (0.54-0.83)	0.64	0.73
SVM Radial	GWAS $1x10^{-4}$	0.57 (0.42-0.72)	0.43	0.71
SVM Radial	GWAS $1x10^{-4}$ RFE	0.58 (0.43-0.73)	0.43	0.73
SVM Radial	External PRS	0.49 (0.47-0.51)	0	0.98
SVM Radial	Clinical	0.62 (0.48-0.77)	0.43	0.81
SVM Radial	GWAS $1x10^{-4}$ + Clinical	0.61 (0.46-0.76)	0.43	0.79
SVM Radial	GWAS $1x10^{-4}$ + Clinical RFE	0.64 (0.49-0.78)	0.50	0.77
SVM Radial	GWAS $1x10^{-4}$ RFE + Clinical	0.59 (0.44-0.73)	0.36	0.81
SVM Radial	GWAS $1x10^{-4}$ RFE + Clinical RFE	0.67 (0.52-0.82)	0.57	0.77
SVM Radial	External PRS + Clinical	0.71 (0.56-0.85)	0.64	0.77
SVM Poly	GWAS $1x10^{-4}$	0.54 (0.40-0.69)	0.36	0.73
SVM Poly	GWAS $1x10^{-4}$ RFE	0.54 (0.40-0.69)	0.36	0.73
SVM Poly	External PRS	0.67 (0.52-0.81)	0.64	0.69
SVM Poly	Clinical	0.62 (0.47-0.77)	0.43	0.81
SVM Poly	GWAS $1x10^{-4}$ + Clinical	0.63 (0.49-0.78)	0.43	0.83
SVM Poly	GWAS $1x10^{-4}$ + Clinical RFE	0.63 (0.49-0.78)	0.43	0.83
SVM Poly	GWAS $1x10^{-4}$ RFE + Clinical	0.68 (0.53-0.82)	0.50	0.85

Continuation of Table A18

SVM Poly	GWAS $1x10^{-4}$ RFE + Clinical RFE	0.67 (0.52-0.81)	0.50	0.83
SVM Poly	GWAS $1x10^{-4}$ RFE + External PRS	0.54 (0.38-0.69)	0.43	0.65
SVM Poly	External PRS + Clinical	0.70 (0.56-0.85)	0.57	0.83
SVM Poly	GWAS $1x10^{-4}$ RFE + Clinical + External PRS	0.67 (0.52-0.81)	0.50	0.83
XGBoost	GWAS $1x10^{-4}$	0.56 (0.41-0.72)	0.50	0.63
XGBoost	GWAS $1x10^{-4}$ RFE	0.48 (0.33-0.63)	0.36	0.60
XGBoost	External PRS	0.55 (0.40-0.70)	0.43	0.67
XGBoost	**Clinical**	**0.74 (0.61-0.87)**	**0.79**	**0.69**
XGBoost	GWAS $1x10^{-4}$ + Clinical	0.69 (0.54-0.83)	0.64	0.73
XGBoost	GWAS $1x10^{-4}$ + Clinical RFE	0.68 (0.54-0.83)	0.57	0.79
XGBoost	GWAS $1x10^{-4}$ RFE + Clinical	0.71 (0.56-0.85)	0.64	0.77
XGBoost	GWAS $1x10^{-4}$ RFE + Clinical RFE	0.65 (0.50-0.78)	0.57	0.73
XGBoost	GWAS $1x10^{-4}$ RFE + External PRS	0.50 (0.34-0.65)	0.43	0.56
XGBoost	**External PRS + Clinical**	**0.80 (0.69-0.92)**	**0.86**	**0.75**
XGBoost	GWAS $1x10^{-4}$ RFE + Clinical + External PRS	0.69 (0.54-0.83)	0.64	0.73
LASSO	GWAS $1x10^{-4}$	0.55 (0.41-0.68)	0.29	0.81
LASSO	GWAS $1x10^{-4}$ RFE	0.50 (0.38-0.63)	0.21	0.79
LASSO	External PRS	0.50 (0.50-0.50)	0	1
LASSO	Clinical	0.64 (0.50-0.79)	0.43	0.85
LASSO	External PRS + Clinical	0.62 (0.48-0.75)	0.36	0.88
LASSO	GWAS $1x10^{-4}$ + Clinical	0.61 (0.47-0.75)	0.36	0.85
LASSO	GWAS $1x10^{-4}$ + Clinical RFE	0.62 (0.47-0.77)	0.43	0.81
LASSO	GWAS $1x10^{-4}$ RFE + Clinical	0.60 (0.45-0.74)	0.36	0.83
LASSO	GWAS $1x10^{-4}$ RFE + Clinical RFE	0.56 (0.43-0.69)	0.29	0.83
LASSO	GWAS $1x10^{-4}$ RFE + External PRS	0.53 (0.39-0.67)	0.29	0.77
LASSO	External PRS + Clinical	0.62 (0.48-0.75)	0.36	0.88
LASSO	GWAS $1x10^{-4}$ RFE + Clinical + External PRS	0.61 (0.47-0.74)	0.36	0.85

Continuation of Table A18

Ridge	GWAS $1x10^{-4}$	0.52 (0.40-0.65)	0.21	0.83
Ridge	GWAS $1x10^{-4}$ RFE	0.50 (0.38-0.63)	0.21	0.79
Ridge	External PRS	0.50 (0.50-0.50)	0	1
Ridge	Clinical	0.65 (0.51-0.79)	0.43	0.88
Ridge	External PRS + Clinical	0.66 (0.52-0.79)	0.36	0.96
Ridge	GWAS $1x10^{-4}$ + Clinical	0.57 (0.44-0.70)	0.29	0.85
Ridge	GWAS $1x10^{-4}$ + Clinical RFE	0.52 (0.40-0.65)	0.21	0.83
Ridge	GWAS $1x10^{-4}$ RFE + Clinical	0.56 (0.43-0.69)	0.29	0.83
Ridge	GWAS $1x10^{-4}$ RFE + Clinical RFE	0.56 (0.43-0.69)	0.29	0.83
Ridge	GWAS $1x10^{-4}$ RFE + External PRS	0.51 (0.37-0.65)	0.29	0.73
Ridge	GWAS $1x10^{-4}$ RFE + Clinical + External PRS	0.60 (0.45-0.74)	0.36	0.83

Abbreviations: RFE, recursive feature elimination.

Table A19. SNPs used as predictors in successful prediction models for cisplatin-induced peripheral sensory neuropathy (yes vs. no) and associated genes

SNP	GTEx	dbSNP	GWAS catalog
rs12987046	none	LOC107985792, LOC107985858	none
rs1593922	none	none	none
rs13012579	none	LOC107985792	none
rs7256305	RPL12P42, FBXW9	none	none
rs12749279	none	ST6GALNAC3	none
rs12703639	none	LOC107986854	none
rs75046595	none	LINC01173	none
rs55993388	N/A	PLPPR1	none
rs112348859	none	none	none
rs12650891	none	none	none
rs112913430	none	LINC01853	none
rs72891145	none	LINC01853	none
rs17018891	none	none	none
rs59466580	none	none	none
rs791315	C9orf153, TUT7, ISCA1, GOLM1	TUT7	none
rs844828	THBD, ENSG00000279164, ENSG00000279447	none	none
rs72705411	none	none	none
rs7572014	VAX2	none	none
rs2391713	MYO16-AS1	MYO16, LOC124903207	none
rs56062242	DLC1, ENSG00000253932	DLC1	none
rs10132283	FRMD-AS1	FRMD6	none
rs62265417	none	GBE1, LOC124906198	none
rs10139825	ENSG00000258526, ENSG00000285830 (antisense to TRAPPC6B), MIA2, TRAPPC6B	LOC105370460, LOC105370461	none
rs1628402	ENSG00000237612	LOC107984412	none
rs1711240	ZNF25, ZNF248, LINC00993, ENSG00000226578, ANKRD30A	none	none
rs11132186	N/A	none	none
rs8143191	ENSG00000287117	none	none
rs145937449	none	none	none
rs61880331	ANO5	LOC102723370	none
rs392275	none	none	none
rs1119882	none	none	none
rs4235233	SFRP2	LOC101927947	none

Continuation of Table A19

rs11647019	PKD1P3, NOMO1	MYH11	None
rs62010176	CSPG4P10, GOLGA2P10, UBE2Q2P2, GOLGA6L9, C15orf40, HOMER2, WHAMM, ENSG00000286872 (antisense to TM6SF1), ENSG00000260351 (antisense to BTBD1), ACTG1P17, ENSG00000228141	none	none
rs11156924	none	PAX9	none
rs12683367	BAAT	PLPPR1	none
rs1009983	none	none	none
rs56182369	CSNK1E, APOBEC3C, PLA2G6, C22orf23	CSNK1E, TPTEP2-CSNK1E	none
rs77008993	none	none	none
rs16960666	none	CPPED1	none
rs11212509	POGLUT3, ACAT1, EXPH5, ENSG00000285696 (antisense to ACAT1), ATM	CUL5	none
rs8085864	none	LAMA1	none
rs1957538	EEF1A1P2, LINC01467	none	none
rs4552520	none	LOC105377567	none
rs72658211	MYO16-AS1	MYO16, LOC124903207	none
rs6883364	FAM153CP	PROP1	none
rs10847427	none	LOC105370068	none
rs4772803	ARGLU1	none	none
rs8010499	MIA2, ENSG00000258526	LOC105370461	none
rs1956576	FRMD6-AS1	FRMD6	none
rs144930799	none	none	none
rs4904288	none	none	none
rs4852728	CLEC4F, CD207, LINC01143, FIGLA, ADD2	VAX2	none
rs512893	FHOD3, COSMOC, MOCOS	FHOD3	none
rs79337537	NDUFB2, ADCK2, TMEM178B	TMEM178B	none
rs7128440	ASS1P13, CWF19L2, ENSG00000261098, SLN	LOC105369477	none
rs62186945	ANKRD49P1, FAM124B	none	none
rs3110298	DPYS	none	none
rs13086980	none	IL12A-AS1	none
rs4133446	none	none	none
rs78480556	none	none	none
rs6083012	LINC00656, ENSG00000279164	LINC00656	none

Continuation of Table A19

rs61389544	SPINK2, SRP72	none	none
rs4532112	none	TP63	none
rs12884069	MIA2, ENSG00000258526	LOC105370461	none
rs4757366	none	none	none
rs2046571	none	none	none
rs2161249	RASA1	none	none
rs72658216	ENSG00000275216, MYO16-AS1	MYO16, LOC124903207	none
rs552231	MBOAT1	MBOAT1	none
rs1941473	none	none	none
rs7163690	none	none	none
rs906691	KIF2A, IPO11, DIMT1	LOC124900610	none
rs174579	FADS2, TMEM258, ENSG00000289268, FADS1, MYRF, DAGLA, FEN1, MYRF-AS1, STX5-DT, FADS3, RAB3IL1	FADS2	FADS2
rs79785345	SMARCA2	none	none
rs4783064	none	none	none
rs533408	none	none	none
rs2422052	CCDC93, DDX18, ENSG00000238207, ENSG00000279227	none	HTR5BP
rs28491826	SPINK2, HOPX	none	none
rs4839034	none	none	none
rs10897545	none	none	none
rs36053276	none	none	none

Table A20. SNPs with strongest association between genotype and cisplatin-induced peripheral sensory neuropathy (yes vs. no) ($p < 5.0x10^{-2}$)

SNP	chromosome	F_{ST}	Genotype	PSN Category Yes vs. No	
				OR	p-value
rs34904346	20	0.26	AA	ref.	ref.
			TT	1.9	$2.0x10^{-5}$
rs2063249	5	0.32	CC	ref.	ref.
			TT	2.0	$2.8x10^{-5}$
rs1778483	6	0.47	GG	ref.	ref.
			TT	2.1	$1.2x10^{-4}$
rs4236999	8	0.30	CC	ref.	ref.
			TT	1.9	$2.7x10^{-4}$
rs9494195	6	0.39	AA	ref.	ref.
			GG	2.5	$3.1x10^{-4}$
rs1150721	6	0.59	CC	ref.	ref.
			GG	1.8	$3.9x10^{-4}$
rs10213186	4	0.26	AA	ref.	ref.
			TT	2.3	$4.2x10^{-4}$
rs10085965	8	0.42	CC	ref.	ref.
			TT	0.59	$5.2x10^{-4}$
rs34015011	8	0.38	GG	ref.	ref.
			TT	0.55	$7.9x10^{-4}$
rs8182578	19	0.32	AA	ref.	ref.
			GG	0.58	$8.3x10^{-4}$
rs8059496	16	0.27	AA	ref.	ref.
			GG	2.4	$8.3x10^{-4}$
rs28481421	8	0.26	CC	ref.	ref.
			TT	1.7	$8.7x10^{-4}$
rs3777909	6	0.27	AA	ref.	ref.
			GG	0.36	$9.0x10^{-4}$
rs4736347	8	0.31	CC	ref.	ref.
			TT	1.7	$9.8x10^{-4}$
rs11024606	11	0.44	AA	ref.	ref.
			CC	1.7	$1.0x10^{-3}$
rs8131065	21	0.36	CC	ref.	ref.
			TT	6.1	$1.0x10^{-3}$
rs10957641	8	0.33	GG	ref.	ref.
			TT	1.7	$1.1x10^{-3}$
rs442439	6	0.54	AA	ref.	ref.
			GG	1.8	$1.3x10^{-3}$
rs4488948	4	0.54	CC	ref.	ref.
			TT	0.61	$1.4x10^{-3}$
rs4076424	8	0.41	CC	ref.	ref.
			TT	0.38	$1.4x10^{-3}$
rs4902768	14	0.28	CC	ref.	ref.
			TT	1.7	$1.4x10^{-3}$
rs7243210	18	0.26	CC	ref.	ref.
			TT	1.7	$1.5x10^{-3}$
rs2023509	20	0.36	CC	ref.	ref.
			TT	0.61	$1.57x10^{-3}$
rs4682783	3	0.40	AA	ref.	ref.
			GG	0.61	$1.6x10^{-3}$

Continuation of Table A20

rs7136124	12	0.34	AA	ref.	ref.
			GG	0.61	$1.6x10^{-3}$
rs900641	5	0.48	GG	ref.	ref.
			TT	4.2	$1.7x10^{-3}$
rs532543	9	0.29	AA	ref.	ref.
			GG	0.38	$1.8x10^{-3}$
rs11874776	18	0.57	CC	ref.	ref.
			TT	0.18	$1.8x10^{-3}$
rs7694450	4	0.39	AA	ref.	ref.
			GG	1.6	$1.8x10^{-3}$
rs28459852	8	0.37	AA	ref.	ref.
			TT	1.6	$1.8x10^{-3}$
rs303860	3	0.38	AA	ref.	ref.
			GG	0.42	$1.9x10^{-3}$
rs213228	6	0.29	AA	ref.	ref.
			CC	0.57	$2.0x10^{-3}$
rs4833705	4	0.40	CC	ref.	ref.
			TT	0.47	$2.0x10^{-3}$
rs11650955	17	0.27	AA	ref.	ref.
			GG	1.6	$2.1x10^{-3}$
rs3103583	5	0.38	CC	ref.	ref.
			TT	0.28	$2.1x10^{-3}$
rs558811	2	0.27	CC	ref.	ref.
			GG	1.7	$2.1x10^{-3}$
rs4683114	3	0.40	CC	ref.	ref.
			TT	1.6	$2.1x10^{-3}$
rs7897357	10	0.47	CC	ref.	ref.
			TT	1.7	$2.2x10^{-3}$
rs6717311	2	0.28	CC	ref.	ref.
			TT	0.59	$2.2x10^{-3}$
rs12611162	19	0.25	AA	ref.	ref.
			GG	1.8	$2.2x10^{-3}$
rs1592457	16	0.25	CC	ref.	ref.
			TT	0.55	$2.3x10^{-3}$
rs2869358	4	0.34	AA	ref.	ref.
			GG	1.7	$2.3x10^{-3}$
rs249834	12	0.32	CC	ref.	ref.
			TT	0.59	$2.3x10^{-3}$
rs9374263	6	0.28	CC	ref.	ref.
			GG	2.7	$2.3x10^{-3}$
rs10000663	4	0.42	CC	ref.	ref.
			TT	0.62	$2.3x10^{-3}$
rs10766514	11	0.32	AA	ref.	ref.
			GG	0.48	$2.3x10^{-3}$
rs34366795	3	0.33	AA	ref.	ref.
			GG	0.61	$2.4x10^{-3}$
rs2564117	2	0.31	AA	ref.	ref.
			TT	1.6	$2.4x10^{-3}$
rs12674115	7	0.31	CC	ref.	ref.
			GG	2.1	$2.5x10^{-3}$
rs6084530	20	0.26	AA	ref.	ref.
			CC	1.7	$2.5x10^{-3}$

Continuation of Table A20

rs726104	21	0.34	AA	ref.	ref.
			GG	1.6	$2.5x10^{-3}$
rs1582958	5	0.36	AA	ref.	ref.
			GG	0.50	$2.7x10^{-3}$
rs4739079	8	0.43	AA	ref.	ref.
			TT	0.63	$2.7x10^{-3}$
rs11644601	16	0.26	CC	ref.	ref.
			TT	1.8	$2.8x10^{-3}$
rs6769051	3	0.49	GG	ref.	ref.
			TT	1.7	$2.9x10^{-3}$
rs7809654	7	0.47	AA	ref.	ref.
			GG	2.3	$3.0x10^{-3}$
rs8104076	19	0.34	AA	ref.	ref.
			GG	2.4	$3.0x10^{-3}$
rs11719526	3	0.41	CC	ref.	ref.
			TT	1.6	$3.0x10^{-3}$
rs58018557	15	0.35	CC	ref.	ref.
			TT	2.3	$3.1x10^{-3}$
rs7529452	1	0.27	CC	ref.	ref.
			TT	0.57	$3.1x10^{-3}$
rs1514967	1	0.30	AA	ref.	ref.
			CC	1.6	$3.1x10^{-3}$
rs35558975	8	0.39	CC	ref.	ref.
			GG	0.58	$3.1x10^{-3}$
rs156737	6	0.56	AA	ref.	ref.
			GG	0.60	$3.3x10^{-3}$
rs11783227	8	0.31	GG	ref.	ref.
			TT	1.8	$3.4x10^{-3}$
rs2538046	7	0.29	AA	ref.	ref.
			GG	0.63	$3.4x10^{-3}$
rs61812714	1	0.31	AA	ref.	ref.
			CC	1.7	$3.5x10^{-3}$
rs1320893	7	0.30	AA	ref.	ref.
			GG	0.59	$3.5x10^{-3}$
rs3771605	2	0.37	AA	ref.	ref.
			GG	1.6	$3.6x10^{-3}$
rs5750911	22	0.33	AA	ref.	ref.
			GG	0.62	$3.6x10^{-3}$
rs6942249	6 (cisplatin)	0.39	AA	ref.	ref.
			GG	2.0	$3.7x10^{-3}$
rs1119229	19	0.30	CC	ref.	ref.
			TT	0.47	$3.8x10^{-3}$
rs11114340	12	0.30	CC	ref.	ref.
			TT	0.63	$3.9x10^{-3}$
rs174373	6	0.29	CC	ref.	ref.
			TT	2.3	$3.9x10^{-3}$
rs2422391	2	0.32	AA	ref.	ref.
			GG	2.0	$4.3x10^{-3}$
rs17423809	2	0.32	CC	ref.	ref.
			TT	1.7	$4.5x10^{-3}$
rs56039135	2	0.28	AA	ref.	ref.
			CC	0.42	$4.5x10^{-3}$

Continuation of Table A20

rs7798564	7	0.33	CC	ref.	ref.
			TT	2.1	$4.6x10^{-3}$
rs162556	2	0.43	AA	ref.	ref.
			GG	0.64	$4.6x10^{-3}$
rs12542796	8	0.30	CC	ref.	ref.
			TT	1.6	$4.7x10^{-3}$
rs4522527	19	0.32	AA	ref.	ref.
			GG	0.60	$4.7x10^{-3}$
rs11746505	5	0.31	CC	ref.	ref.
			TT	1.6	$4.8x10^{-3}$
rs653407	18	0.25	CC	ref.	ref.
			TT	1.7	$4.8x10^{-3}$
rs11024622	11	0.37	CC	ref.	ref.
			GG	0.64	$4.8x10^{-3}$
rs1626783	2	0.34	AA	ref.	ref.
			CC	1.6	$4.8x10^{-3}$
rs4314631	8	0.37	CC	ref.	ref.
			TT	0.62	$4.9x10^{-3}$
rs4862655	4	0.46	CC	ref.	ref.
			TT	0.65	$4.9x10^{-3}$
rs2852192	11	0.58	CC	ref.	ref.
			GG	0.59	$4.9x10^{-3}$
rs2301826	15	0.47	CC	ref.	ref.
			TT	0.51	$4.9x10^{-3}$
rs935613	2	0.49	CC	ref.	ref.
			TT	0.60	$4.9x10^{-3}$
rs4833906	4	0.32	AA	ref.	ref.
			TT	0.53	$4.9x10^{-3}$
rs4339575	7	0.27	AA	ref.	ref.
			GG	0.65	$4.9x10^{-3}$
rs2709956	7	0.38	CC	ref.	ref.
			TT	1.6	$5.0x10^{-3}$
rs1852492	10	0.46	CC	ref.	ref.
			TT	1.8	$5.0x10^{-2}$
rs1564582	11	0.28	AA	ref.	ref.
			GG	1.5	$5.0x10^{-3}$
rs10411647	19	0.47	AA	ref.	ref.
			GG	1.6	$5.0x10^{-3}$
rs10874472	13	0.30	AA	ref.	ref.
			TT	1.7	$5.1x10^{-3}$
rs10890805	11	0.27	AA	ref.	ref.
			GG	1.7	$5.1x10^{-3}$
rs12945908	17	0.44	CC	ref.	ref.
			TT	1.5	$5.1x10^{-3}$
rs819444	7	0.43	CC	ref.	ref.
			TT	0.65	$5.1x10^{-3}$
rs7097973	10	0.26	AA	ref.	ref.
			TT	1.6	$5.2x10^{-3}$
rs11167669	5	0.38	AA	ref.	ref.
			GG	1.5	$5.2x10^{-3}$
rs11758900	6	0.45	CC	ref.	ref.
			GG	1.5	$5.2x10^{-3}$

Continuation of Table A20

rs205431	16	0.40	AA	ref.	ref.
			GG	1.5	$5.3x10^{-3}$
rs4611652	2	0.38	CC	ref.	ref.
			TT	0.15	$5.3x10^{-3}$
rs6584195	10	0.28	AA	ref.	ref.
			GG	0.60	$5.3x10^{-3}$
rs12444479	16	0.53	AA	ref.	ref.
			GG	1.6	$5.4x10^{-3}$
rs10883082	10	0.39	CC	ref.	ref.
			TT	0.64	$5.4x10^{-3}$
rs28470223	17	0.30	AA	ref.	ref.
			GG	0.57	$5.5x10^{-3}$
rs12546178	8	0.47	AA	ref.	ref.
			CC	0.47	$5.5x10^{-2}$
rs12509116	4	0.39	CC	ref.	ref.
			TT	1.6	$5.6x10^{-3}$
rs11674947	2	0.43	AA	ref.	ref.
			GG	0.55	$5.6x10^{-3}$
rs2868148	19	0.42	AA	ref.	ref.
			GG	0.65	$5.7x10^{-3}$
rs4445206	8	0.44	AA	ref.	ref.
			CC	0.65	$5.7x10^{-3}$
rs7742724	6	0.38	AA	ref.	ref.
			GG	0.54	$5.7x10^{-3}$
rs1355281	9	0.48	CC	ref.	ref.
			GG	0.60	$5.8x10^{-3}$
rs12218	11	0.43	CC	ref.	ref.
			TT	1.5	$5.8x10^{-3}$
rs394912	8	0.27	CC	ref.	ref.
			GG	2.3	$5.8x10^{-3}$
rs1046611	11	0.44	GG	ref.	ref.
			TT	0.64	$5.9x10^{-3}$
rs2287497	17	0.46	AA	ref.	ref.
			GG	4.0	$5.9x10^{-3}$
rs78672939	18	0.26	AA	ref.	ref.
			GG	4.6	$5.9x10^{-3}$
rs8036979	15	0.25	AA	ref.	ref.
			TT	0.41	$5.9x10^{-3}$
rs9487668	6	0.49	AA	ref.	ref.
			GG	0.48	$5.9x10^{-3}$
rs10432659	2	0.31	AA	ref.	ref.
			GG	0.64	$5.9x10^{-3}$
rs1033102	4	0.32	CC	ref.	ref.
			GG	1.7	$6.0x10^{-3}$
rs203777	1	0.32	CC	ref.	ref.
			TT	1.7	$6.0x10^{-3}$
rs12906896	15	0.25	CC	ref.	ref.
			TT	1.5	$6.1x10^{-3}$
rs11070892	15	0.41	AA	ref.	ref.
			GG	0.31	$6.1x10^{-3}$
rs11943513	4	0.29	AA	ref.	ref.
			GG	1.6	$6.1x10^{-3}$

Continuation of Table A20

rs67050216	4	0.37	AA	ref.	ref.
			CC	1.6	$6.2x10^{-3}$
rs6757486	2	0.38	CC	ref.	ref.
			TT	0.66	$6.2x10^{-3}$
rs10749218	10	0.26	CC	ref.	ref.
			TT	2.0	$6.3x10^{-3}$
rs931708	4	0.37	AA	ref.	ref.
			GG	2.0	$6.3x10^{-3}$
rs4932163	15	0.33	AA	ref.	ref.
			GG	0.56	$6.3x10^{-3}$
rs2538038	7	0.43	GG	ref.	ref.
			TT	0.65	$6.3x10^{-3}$
rs584001	12	0.26	GG	ref.	ref.
			TT	0.62	$6.3x10^{-3}$
rs10817995	9	0.26	AA	ref.	ref.
			TT	0.59	$6.4x10^{-3}$
rs2709536	2	0.37	AA	ref.	ref.
			GG	1.5	$6.5x10^{-3}$
rs135757	22	0.27	AA	ref.	ref.
			GG	1.7	$6.6x10^{-3}$
rs680511	11	0.28	AA	ref.	ref.
			GG	1.6	$6.6x10^{-3}$
rs2287499	17	0.72	CC	ref.	ref.
			GG	0.31	$6.6x10^{-3}$
rs6985746	8	0.26	CC	ref.	ref.
			TT	0.63	$6.7x10^{-3}$
rs6870539	5	0.56	CC	ref.	ref.
			TT	1.6	$6.7x10^{-3}$
rs8111180	19	0.29	AA	ref.	ref.
			GG	1.5	$6.8x10^{-3}$
rs4715578	6	0.28	CC	ref.	ref.
			GG	1.5	$6.8x10^{-3}$
rs60965744	19	0.32	AA	ref.	ref.
			GG	0.65	$6.8x10^{-3}$
rs6007026	22	0.37	CC	ref.	ref.
			TT	1.6	$7.0x10^{-3}$
rs60075147	21	0.29	AA	ref.	ref.
			GG	2.6	$7.0x10^{-3}$
rs4665077	2	0.37	AA	ref.	ref.
			GG	1.6	$7.0x10^{-3}$
rs13028563	2	0.33	AA	ref.	ref.
			TT	1.5	$7.1x10^{-3}$
rs7086663	10	0.34	AA	ref.	ref.
			TT	0.63	$7.2x10^{-3}$
rs10068479	5	0.45	AA	ref.	ref.
			GG	1.6	$7.3x10^{-3}$
rs67387640	2	0.31	CC	ref.	ref.
			TT	0.61	$7.3x10^{-3}$
rs4665129	2	0.34	AA	ref.	ref.
			GG	0.64	$7.3x10^{-3}$
rs2195453	19	0.58	AA	ref.	ref.
			GG	3.2	$7.4x10^{-3}$

Continuation of Table A20

rs13072800	3	0.43	CC	ref.	ref.
			TT	3.5	$7.5x10^{-3}$
rs10876864	12	0.34	AA	ref.	ref.
			GG	0.65	$7.5x10^{-3}$
rs4785612	16	0.29	AA	ref.	ref.
			CC	0.50	$7.6x10^{-3}$
rs6557163	6	0.28	CC	ref.	ref.
			TT	0.31	$7.6x10^{-3}$
rs1550437	15	0.29	CC	ref.	ref.
			TT	2.2	$7.6x10^{-3}$
rs9900080	17	0.28	GG	ref.	ref.
			TT	1.7	$7.6x10^{-3}$
rs7630022	3	0.62	AA	ref.	ref.
			GG	0.46	$7.6x10^{-3}$
rs11690820	2	0.33	AA	ref.	ref.
			GG	1.5	$7.7x10^{-3}$
rs12617808	2	0.33	CC	ref.	ref.
			TT	0.66	$7.7x10^{-3}$
rs12150976	19	0.29	CC	ref.	ref.
			TT	0.65	$7.7x10^{-3}$
rs17768753	7	0.26	AA	ref.	ref.
			GG	2.0	$7.7x10^{-3}$
rs4645287	4	0.32	AA	ref.	ref.
			CC	1.5	$7.8x10^{-3}$
rs57119148	14	0.35	CC	ref.	ref.
			TT	1.8	$7.9x10^{-3}$
rs9845457	3	0.52	AA	ref.	ref.
			GG	1.5	$7.9x10^{-3}$
rs11749327	5	0.28	AA	ref.	ref.
			CC	0.54	$8.0x10^{-3}$
rs11599818	10	0.34	AA	ref.	ref.
			GG	0.67	$8.0x10^{-3}$
rs11610607	12	0.30	AA	ref.	ref.
			GG	0.64	$8.2x10^{-3}$
rs11631947	15	0.32	AA	ref.	ref.
			GG	0.65	$8.2x10^{-3}$
rs6704593	2	0.27	AA	ref.	ref.
			GG	0.64	$8.3x10^{-3}$
rs1979215	17	0.60	CC	ref.	ref.
			TT	0.64	$8.3x10^{-3}$
rs6084557	20	0.26	CC	ref.	ref.
			TT	1.5	$8.4x10^{-3}$
rs586053	11	0.30	AA	ref.	ref.
			GG	0.66	$8.5x10^{-3}$
rs28531895	8	0.27	AA	ref.	ref.
			GG	0.65	$8.5x10^{-3}$
rs149150396	20	0.26	CC	ref.	ref.
			TT	0.58	$8.5x10^{-3}$
rs2874900	17	0.41	CC	ref.	ref.
			TT	1.7	$8.6x10^{-3}$
rs8127467	21	0.34	GG	ref.	ref.
			TT	3.3	$8.6x10^{-3}$

Continuation of Table A20

rs8015958	14	0.50	GG	ref.	ref.
			TT	2.6	$8.7x10^{-3}$
rs2148532	2	0.29	CC	ref.	ref.
			TT	0.67	$9.2x10^{-3}$
rs2938388	3	0.26	AA	ref.	ref.
			GG	1.5	$9.3x10^{-3}$
rs4956451	4	0.51	AA	ref.	ref.
			GG	0.62	$9.3x10^{-3}$
rs9773022	8	0.35	CC	ref.	ref.
			TT	0.67	$9.3x10^{-3}$
rs1511216	2	0.32	AA	ref.	ref.
			GG	1.6	$9.3x10^{-3}$
rs11205808	1	0.42	AA	ref.	ref.
			TT	3.7	$9.4x10^{-3}$
rs4132142	8	0.27	AA	ref.	ref.
			GG	1.5	$9.5x10^{-3}$
rs7262503	20	0.51	AA	ref.	ref.
			CC	0.42	$9.7x10^{-3}$
rs17231993	2	0.46	CC	ref.	ref.
			TT	0.66	$9.7x10^{-3}$
rs2275824	1	0.31	AA	ref.	ref.
			TT	0.67	$9.7x10^{-3}$
rs9864328	3	0.26	CC	ref.	ref.
			TT	1.9	$9.7x10^{-3}$
rs2709534	2	0.27	CC	ref.	ref.
			TT	0.67	$9.8x10^{-3}$
rs414745	6	0.28	AA	ref.	ref.
			CC	0.60	$9.9x10^{-3}$
rs783541	15	0.26	CC	ref.	ref.
			TT	1.6	$1.0x10^{-2}$
rs7278621	21	0.26	AA	ref.	ref.
			CC	0.67	$1.0x10^{-2}$
rs2720900	3	0.36	CC	ref.	ref.
			TT	1.5	$1.0x10^{-2}$
rs257975	5	0.36	AA	ref.	ref.
			CC	0.67	$1.0x10^{-2}$
rs7957392	12	0.34	AA	ref.	ref.
			GG	0.24	$1.0x10^{-2}$
rs1425050	8	0.30	AA	ref.	ref.
			GG	0.62	$1.0x10^{-2}$
rs2887200	2	0.42	AA	ref.	ref.
			GG	0.67	$1.0x10^{-2}$
rs9772300	8	0.36	AA	ref.	ref.
			GG	1.5	$1.1x10^{-2}$
rs10173581	2	0.43	CC	ref.	ref.
			TT	0.50	$1.1x10^{-2}$
rs1277292	4	0.26	AA	ref.	ref.
			CC	0.67	$1.1x10^{-2}$
rs12362341	11	0.38	AA	ref.	ref.
			GG	0.51	$1.1x10^{-2}$
rs3773146	3	0.34	AA	ref.	ref.
			GG	0.67	$1.1x10^{-2}$

Continuation of Table A20

rs2057852	7	0.47	CC	ref.	ref.
			TT	1.5	$1.1x10^{-2}$
rs11101807	10	0.30	CC	ref.	ref.
			TT	5.1	$1.1x10^{-2}$
rs10771964	12	0.30	CC	ref.	ref.
			GG	0.67	$1.1x10^{-2}$
rs11557092	19	0.50	CC	ref.	ref.
			TT	1.7	$1.1x10^{-2}$
rs4964759	12	0.34	AA	ref.	ref.
			GG	0.67	$1.1x10^{-2}$
rs10206472	2	0.37	CC	ref.	ref.
			GG	1.5	$1.1x10^{-2}$
rs2168719	10	0.27	AA	ref.	ref.
			TT	1.8	$1.1x10^{-2}$
rs11065589	12	0.26	CC	ref.	ref.
			TT	0.68	$1.1x10^{-2}$
rs6467258	7	0.26	CC	ref.	ref.
			TT	1.5	$1.1x10^{-2}$
rs1605996	8	0.35	AA	ref.	ref.
			GG	0.67	$1.2x10^{-2}$
rs61823772	1	0.26	CC	ref.	ref.
			GG	0.67	$1.2x10^{-2}$
rs267930	5	0.26	AA	ref.	ref.
			GG	0.65	$1.2x10^{-2}$
rs6082455	20	0.38	AA	ref.	ref.
			GG	0.66	$1.2x10^{-2}$
rs4499344	19	0.37	AA	ref.	ref.
			GG	1.6	$1.2x10^{-2}$
rs11628647	14	0.30	AA	ref.	ref.
			TT	1.5	$1.2x10^{-2}$
rs3810253	19	0.34	AA	ref.	ref.
			CC	1.9	$1.2x10^{-2}$
rs10845304	12	0.30	CC	ref.	ref.
			TT	1.5	$1.2x10^{-2}$
rs2439701	8	0.25	CC	ref.	ref.
			TT	0.63	$1.2x10^{-2}$
rs213236	6	0.27	CC	ref.	ref.
			TT	1.5	$1.2x10^{-2}$
rs4733280	8	0.25	GG	ref.	ref.
			TT	1.8	$1.2x10^{-2}$
rs2795114	9	0.48	CC	ref.	ref.
			GG	0.44	$1.2x10^{-2}$
rs6878014	5	0.55	AA	ref.	ref.
			GG	1.7	$1.2x10^{-2}$
rs6671429	1	0.32	AA	ref.	ref.
			TT	1.6	$1.2x10^{-2}$
rs10415286	19	0.27	AA	ref.	ref.
			GG	0.67	$1.3x10^{-2}$
rs62510848	8	0.32	AA	ref.	ref.
			GG	1.5	$1.3x10^{-2}$
rs10829230	10	0.28	AA	ref.	ref.
			GG	0.67	$1.3x10^{-2}$

Continuation of Table A20

rs11214236	11	0.25	CC	ref.	ref.
			TT	0.63	$1.3x10^{-2}$
rs4484676	8	0.25	CC	ref.	ref.
			TT	0.68	$1.3x10^{-2}$
rs1295129	7	0.33	CC	ref.	ref.
			GG	1.5	$1.3x10^{-2}$
rs12938622	17	0.27	AA	ref.	ref.
			GG	1.5	$1.3x10^{-2}$
rs4802282	19	0.39	AA	ref.	ref.
			GG	0.68	$1.3x10^{-2}$
rs2852205	11	0.26	AA	ref.	ref.
			GG	0.68	$1.3x10^{-2}$
rs62190528	2	0.40	CC	ref.	ref.
			GG	1.5	$1.3x10^{-2}$
rs4761931	12	0.36	AA	ref.	ref.
			GG	0.67	$1.3x10^{-2}$
rs465782	6	0.56	AA	ref.	ref.
			GG	0.60	$1.3x10^{-2}$
rs11065549	12	0.31	CC	ref.	ref.
			TT	1.5	$1.3x10^{-2}$
rs7437355	4	0.32	CC	ref.	ref.
			GG	0.52	$1.3x10^{-2}$
rs4244480	11	0.31	CC	ref.	ref.
			TT	0.67	$1.3x10^{-2}$
rs1882163	2	0.27	CC	ref.	ref.
			TT	0.68	$1.3x10^{-2}$
rs10769985	11	0.30	AA	ref.	ref.
			GG	0.68	$1.4x10^{-2}$
rs3936747	2	0.30	CC	ref.	ref.
			TT	0.66	$1.4x10^{-2}$
rs7462877	8	0.26	CC	ref.	ref.
			GG	1.5	$1.4x10^{-2}$
rs2458284	8	0.40	AA	ref.	ref.
			CC	0.67	$1.4x10^{-2}$
rs4944885	11	0.29	CC	ref.	ref.
			TT	1.5	$1.4x10^{-2}$
rs6498140	16	0.42	CC	ref.	ref.
			GG	1.6	$1.4x10^{-2}$
rs1438307	2	0.41	GG	ref.	ref.
			TT	1.6	$1.4x10^{-2}$
rs12881376	14	0.34	CC	ref.	ref.
			TT	1.5	$1.4x10^{-2}$
rs1966476	5	0.36	CC	ref.	ref.
			TT	0.67	$1.4x10^{-2}$
rs2298632	1	0.35	CC	ref.	ref.
			TT	0.69	$1.4x10^{-2}$
rs12515329	5	0.49	AA	ref.	ref.
			CC	1.9	$1.4x10^{-2}$
rs4367974	11	0.50	CC	ref.	ref.
			TT	3.1	$1.4x10^{-2}$
rs740495	19	0.26	AA	ref.	ref.
			GG	1.7	$1.4x10^{-2}$

Continuation of Table A20

rs2288271	15	0.51	AA	ref.	ref.
			GG	1.6	$1.4x10^{-2}$
rs2038281	14	0.36	AA	ref.	ref.
			GG	0.68	$1.4x10^{-2}$
rs7759398	6	0.28	AA	ref.	ref.
			CC	4.2	$1.4x10^{-2}$
rs4547578	2	0.28	CC	ref.	ref.
			TT	1.4	$1.4x10^{-2}$
rs3736174	5	0.64	CC	ref.	ref.
			GG	1.6	$1.4x10^{-2}$
rs1902585	15	0.36	CC	ref.	ref.
			GG	1.5	$1.4x10^{-2}$
rs13053013	21	0.28	AA	ref.	ref.
			GG	0.68	$1.4x10^{-2}$
rs4757644	11	0.31	AA	ref.	ref.
			CC	1.5	$1.4x10^{-2}$
rs6496742	15	0.36	CC	ref.	ref.
			TT	0.60	$1.4x10^{-2}$
rs4868665	5	0.27	CC	ref.	ref.
			TT	0.67	$1.4x10^{-2}$
rs8033620	15	0.40	AA	ref.	ref.
			GG	1.7	$1.5x10^{-2}$
rs147724030	11	0.25	CC	ref.	ref.
			TT	0.61	$1.5x10^{-2}$
rs72697775	9	0.32	AA	ref.	ref.
			GG	0.67	$1.5x10^{-2}$
rs10052497	5	0.38	AA	ref.	ref.
			GG	4.8	$1.5x10^{-2}$
rs9295778	6	0.25	GG	ref.	ref.
			TT	0.43	$1.5x10^{-2}$
rs5763221	22	0.29	AA	ref.	ref.
			GG	3.0	$1.5x10^{-2}$
rs10766929	11	0.36	GG	ref.	ref.
			TT	0.65	$1.5x10^{-2}$
rs11851556	14	0.35	CC	ref.	ref.
			GG	0.68	$1.5x10^{-2}$
rs11649	4	0.38	CC	ref.	ref.
			GG	0.25	$1.5x10^{-2}$
rs4851000	2	0.34	CC	ref.	ref.
			TT	0.66	$1.5x10^{-2}$
rs6533427	4	0.37	CC	ref.	ref.
			GG	0.21	$1.5x10^{-2}$
rs10402672	19	0.27	AA	ref.	ref.
			GG	1.5	$1.5x10^{-2}$
rs1547166	13	0.43	CC	ref.	ref.
			TT	1.9	$1.5x10^{-2}$
rs2295313	14	0.34	GG	ref.	ref.
			TT	0.68	$1.5x10^{-2}$
rs6601374	8	0.34	AA	ref.	ref.
			GG	2.0	$1.5x10^{-2}$
rs790103	3	0.32	AA	ref.	ref.
			CC	1.4	$1.5x10^{-2}$

Continuation of Table A20

rs2243620	7	0.39	AA	ref.	ref.
			GG	1.5	$1.5x10^{-2}$
rs11723482	4	0.51	AA	ref.	ref.
			TT	0.60	$1.5x10^{-2}$
rs13267843	8	0.27	CC	ref.	ref.
			TT	1.6	$1.5x10^{-2}$
rs7997328	13	0.40	AA	ref.	ref.
			GG	0.61	$1.6x10^{-2}$
rs1793157	11	0.36	AA	ref.	ref.
			CC	1.5	$1.6x10^{-2}$
rs4726132	7	0.31	CC	ref.	ref.
			TT	1.5	$1.6x10^{-2}$
rs1967313	2	0.31	GG	ref.	ref.
			TT	1.5	$1.6x10^{-2}$
rs1397643	4	0.32	AA	ref.	ref.
			CC	0.68	$1.6x10^{-2}$
rs9409797	9	0.43	AA	ref.	ref.
			CC	0.62	$1.6x10^{-2}$
rs709142	3	0.29	CC	ref.	ref.
			TT	0.69	$1.6x10^{-2}$
rs7141840	14	0.29	AA	ref.	ref.
			GG	1.5	$1.6x10^{-2}$
rs10987708	9	0.52	AA	ref.	ref.
			GG	6.6	$1.6x10^{-2}$
rs10998681	10	0.35	CC	ref.	ref.
			TT	0.69	$1.6x10^{-2}$
rs1150705	6	0.43	GG	ref.	ref.
			TT	1.5	$1.6x10^{-2}$
rs10890860	11	0.28	CC	ref.	ref.
			TT	1.5	$1.6x10^{-2}$
rs62175484	2	0.42	AA	ref.	ref.
			CC	0.69	$1.6x10^{-2}$
rs2091329	1	0.38	AA	ref.	ref.
			GG	0.62	$1.6x10^{-2}$
rs11088978	21	0.42	AA	ref.	ref.
			GG	2.4	$1.6x10^{-2}$
rs12142154	1	0.26	AA	ref.	ref.
			CC	0.66	$1.6x10^{-2}$
rs823069	1	0.56	AA	ref.	ref.
			GG	0.53	$1.6x10^{-2}$
rs1892252	6	0.55	CC	ref.	ref.
			GG	0.39	$1.6x10^{-2}$
rs3807957	7	0.37	AA	ref.	ref.
			GG	0.69	$1.6x10^{-2}$
rs9935205	16	0.30	AA	ref.	ref.
			TT	0.41	$1.7x10^{-2}$
rs2824401	21	0.33	AA	ref.	ref.
			GG	0.68	$1.7x10^{-2}$
rs7707671	5	0.32	CC	ref.	ref.
			TT	1.6	$1.7x10^{-2}$
rs11177655	12	0.40	CC	ref.	ref.
			TT	0.69	$1.7x10^{-2}$

Continuation of Table A20

rs7014896	8	0.45	AA	ref.	ref.
			CC	1.5	$1.7x10^{-2}$
rs3898068	12	0.28	CC	ref.	ref.
			TT	1.7	$1.7x10^{-2}$
rs77491076	2	0.36	CC	ref.	ref.
			TT	0.69	$1.7x10^{-2}$
rs6449593	5	0.32	AA	ref.	ref.
			GG	1.5	$1.7x10^{-2}$
rs9916525	17	0.70	CC	ref.	ref.
			TT	0.58	$1.7x10^{-2}$
rs13136593	4	0.39	AA	ref.	ref.
			GG	1.5	$1.7x10^{-2}$
rs2698193	2	0.42	CC	ref.	ref.
			TT	0.69	$1.7x10^{-2}$
rs4075613	19	0.60	AA	ref.	ref.
			GG	2.5	$1.7x10^{-2}$
rs1898671	5	0.26	CC	ref.	ref.
			TT	0.65	$1.7x10^{-2}$
rs11733307	4	0.45	CC	ref.	ref.
			TT	0.70	$1.7x10^{-2}$
rs7713314	5	0.29	AA	ref.	ref.
			GG	2.2	$1.7x10^{-2}$
rs156425	7	0.27	CC	ref.	ref.
			TT	0.67	$1.7x10^{-2}$
rs28617425	4	0.31	CC	ref.	ref.
			GG	0.61	$1.7x10^{-2}$
rs3807041	6	0.28	CC	ref.	ref.
			TT	1.5	$1.7x10^{-2}$
rs12000	6	0.38	AA	ref.	ref.
			GG	0.57	$1.8x10^{-2}$
rs6662706	1	0.30	GG	ref.	ref.
			TT	1.4	$1.8x10^{-2}$
rs782883	7	0.30	AA	ref.	ref.
			CC	1.5	$1.8x10^{-2}$
rs9567117	13	0.26	AA	ref.	ref.
			GG	1.5	$1.8x10^{-2}$
rs13023868	2	0.63	AA	ref.	ref.
			GG	0.24	$1.8x10^{-2}$
rs3771707	2	0.26	AA	ref.	ref.
			TT	0.51	$1.8x10^{-2}$
rs953074	8	0.29	AA	ref.	ref.
			GG	1.4	$1.8x10^{-2}$
rs9752697	2	0.32	AA	ref.	ref.
			GG	0.68	$1.8x10^{-2}$
rs2570923	15	0.62	CC	ref.	ref.
			TT	1.6	$1.8x10^{-2}$
rs9993113	4	0.28	CC	ref.	ref.
			GG	1.5	$1.8x10^{-2}$
rs6676287	1	0.47	AA	ref.	ref.
			GG	1.5	$1.8x10^{-2}$
rs2513374	8	0.28	CC	ref.	ref.
			TT	1.4	$1.8x10^{-2}$

Continuation of Table A20

rs1860122	17	0.35	CC	ref.	ref.
			TT	0.68	$1.8x10^{-2}$
rs10183838	2	0.65	CC	ref.	ref.
			TT	2.5	$1.9x10^{-2}$
rs146797903	2	0.36	AA	ref.	ref.
			CC	1.4	$1.9x10^{-2}$
rs2382365	9	0.57	CC	ref.	ref.
			TT	0.62	$1.9x10^{-2}$
rs613686	11	0.51	CC	ref.	ref.
			TT	0.50	$1.9x10^{-2}$
rs79490227	5	0.31	AA	ref.	ref.
			GG	1.5	$1.9x10^{-2}$
rs2105955	1	0.44	CC	ref.	ref.
			TT	0.48	$1.9x10^{-2}$
rs238419	19	0.25	CC	ref.	ref.
			TT	0.67	$1.9x10^{-2}$
rs1778478	6	0.30	AA	ref.	ref.
			TT	0.51	$1.9x10^{-2}$
rs2986741	1	0.42	AA	ref.	ref.
			GG	0.23	$1.9x10^{-2}$
rs1416920	6	0.42	AA	ref.	ref.
			GG	0.62	$1.9x10^{-2}$
rs11079645	17 (cisplatin)	0.25	GG	ref.	ref.
			TT	0.69	$1.9x10^{-2}$
rs8081176	17	0.38	CC	ref.	ref.
			TT	0.65	$1.9x10^{-2}$
rs2069245	8	0.44	CC	ref.	ref.
			GG	1.4	$1.9x10^{-2}$
rs7521302	1	0.52	GG	ref.	ref.
			TT	1.6	$2.0x10^{-2}$
rs1108956	13	0.26	CC	ref.	ref.
			TT	1.5	$2.0x10^{-2}$
rs72955755	2	0.38	CC	ref.	ref.
			GG	0.67	$2.0x10^{-2}$
rs17516457	5	0.29	CC	ref.	ref.
			TT	0.68	$2.0x10^{-2}$
rs10741741	11	0.25	CC	ref.	ref.
			TT	1.5	$2.0x10^{-2}$
rs8131541	21	0.28	AA	ref.	ref.
			TT	0.33	$2.0x10^{-2}$
rs1545473	5	0.27	AA	ref.	ref.
			GG	1.4	$2.0x10^{-2}$
rs1341868	1	0.32	AA	ref.	ref.
			GG	1.4	$2.0x10^{-2}$
rs7621308	3	0.37	AA	ref.	ref.
			GG	1.4	$2.0x10^{-2}$
rs380092	2	0.31	AA	ref.	ref.
			TT	0.64	$2.0x10^{-2}$
rs6996702	8	0.27	CC	ref.	ref.
			GG	1.5	$2.0x10^{-2}$
rs7785317	7	0.26	GG	ref.	ref.
			TT	2.1	$2.0x10^{-2}$

Continuation of Table A20

rs6731545	2	0.28	AA	ref.	ref.
			GG	0.70	$2.0x10^{-2}$
rs240977	6	0.29	AA	ref.	ref.
			GG	0.50	$2.0x10^{-2}$
rs201380018	4	0.26	CC	ref.	ref.
			GG	0.70	$2.0x10^{-2}$
rs6986573	8	0.29	AA	ref.	ref.
			GG	1.8	$2.0x10^{-2}$
rs7077436	10	0.26	AA	ref.	ref.
			CC	1.4	$2.0x10^{-2}$
rs818495	7	0.33	CC	ref.	ref.
			GG	1.5	$2.1x10^{-2}$
rs1580278	4	0.39	AA	ref.	ref.
			CC	1.4	$2.1x10^{-2}$
rs7868696	9	0.40	CC	ref.	ref.
			TT	4.1	$2.1x10^{-2}$
rs2303547	2	0.47	CC	ref.	ref.
			TT	0.68	$2.1x10^{-2}$
rs7036499	9	0.30	CC	ref.	ref.
			TT	0.46	$2.1x10^{-2}$
rs11653029	17	0.25	AA	ref.	ref.
			GG	1.4	$2.1x10^{-2}$
rs2190600	5	0.28	AA	ref.	ref.
			CC	1.5	$2.1x10^{-2}$
rs171821	5	0.46	CC	ref.	ref.
			TT	0.23	$2.1x10^{-2}$
rs2729708	2	0.30	AA	ref.	ref.
			GG	0.66	$2.1x10^{-2}$
rs6846997	4	0.35	AA	ref.	ref.
			GG	1.7	$2.1x10^{-2}$
rs4783045	16	0.36	CC	ref.	ref.
			TT	0.69	$2.1x10^{-2}$
rs2162500	2	0.25	CC	ref.	ref.
			GG	0.69	$2.1x10^{-2}$
rs737146	2	0.40	CC	ref.	ref.
			GG	1.8	$2.1x10^{-2}$
rs12774262	10	0.32	AA	ref.	ref.
			CC	0.66	$2.1x10^{-2}$
rs1790998	7	0.38	AA	ref.	ref.
			CC	0.70	$2.1x10^{-2}$
rs39749	7	0.35	CC	ref.	ref.
			TT	0.69	$2.1x10^{-2}$
rs500391	6	0.29	AA	ref.	ref.
			GG	0.65	$2.1x10^{-2}$
rs353410	19	0.52	AA	ref.	ref.
			GG	1.8	$2.1x10^{-2}$
rs12471607	2	0.32	CC	ref.	ref.
			TT	0.68	$2.2x10^{-2}$
rs4862652	4	0.26	AA	ref.	ref.
			GG	0.66	$2.2x10^{-2}$
rs9400505	6	0.55	CC	ref.	ref.
			TT	0.46	$2.2x10^{-2}$

Continuation of Table A20

rs41399344	9	0.28	AA	ref.	ref.
			GG	0.68	$2.2x10^{-2}$
rs4712879	6	0.30	CC	ref.	ref.
			TT	0.70	$2.2x10^{-2}$
rs591579	9	0.28	AA	ref.	ref.
			CC	1.5	$2.2x10^{-2}$
rs1438673	5	0.28	CC	ref.	ref.
			TT	1.4	$2.2x10^{-2}$
rs6909448	6	0.38	AA	ref.	ref.
			GG	0.16	$2.2x10^{-2}$
rs10205435	2	0.43	CC	ref.	ref.
			TT	0.66	$2.2x10^{-2}$
rs7176482	15	0.43	AA	ref.	ref.
			GG	0.70	$2.2x10^{-2}$
rs12731328	1	0.38	AA	ref.	ref.
			GG	1.4	$2.2x10^{-2}$
rs2302970	19	0.45	CC	ref.	ref.
			GG	0.70	$2.2x10^{-2}$
rs7221792	17	0.44	GG	ref.	ref.
			TT	0.67	$2.2x10^{-2}$
rs607423	11	0.34	CC	ref.	ref.
			TT	2.1	$2.2x10^{-2}$
rs9677383	2	0.28	CC	ref.	ref.
			TT	1.4	$2.2x10^{-2}$
rs3905112	1	0.31	CC	ref.	ref.
			TT	1.4	$2.2x10^{-2}$
rs869778	2	0.30	AA	ref.	ref.
			GG	0.32	$2.2x10^{-2}$
rs882930	4	0.31	GG	ref.	ref.
			TT	0.65	$2.2x10^{-2}$
rs4984913	16	0.51	AA	ref.	ref.
			GG	1.6	$2.2x10^{-2}$
rs213238	6	0.43	CC	ref.	ref.
			TT	1.5	$2.2x10^{-2}$
rs7648531	3	0.29	AA	ref.	ref.
			TT	0.69	$2.2x10^{-2}$
rs112770581	21	0.37	AA	ref.	ref.
			GG	2.0	$2.2x10^{-2}$
rs10900251	10	0.30	CC	ref.	ref.
			TT	3.3	$2.2x10^{-2}$
rs7638848	3	0.29	AA	ref.	ref.
			GG	0.56	$2.2x10^{-2}$
rs17035272	2	0.26	AA	ref.	ref.
			CC	5.7	$2.2x10^{-2}$
rs2925681	5	0.37	AA	ref.	ref.
			GG	0.54	$2.2x10^{-2}$
rs1719968	18	0.27	CC	ref.	ref.
			TT	2.2	$2.2x10^{-2}$
rs943824	13	0.34	CC	ref.	ref.
			TT	1.4	$2.2x10^{-2}$
rs7152189	14	0.26	AA	ref.	ref.
			CC	0.65	$2.3x10^{-2}$

Continuation of Table A20

rs7654682	4	0.32	CC	ref.	ref.
			TT	3.2	$2.3x10^{-2}$
rs11661685	18	0.61	AA	ref.	ref.
			GG	0.66	$2.3x10^{-2}$
rs7145551	14	0.54	CC	ref.	ref.
			TT	1.6	$2.3x10^{-2}$
rs7579428	2	0.50	CC	ref.	ref.
			TT	0.70	$2.3x10^{-2}$
rs11648491	16	0.39	CC	ref.	ref.
			GG	1.4	$2.3x10^{-2}$
rs7703394	5	0.31	AA	ref.	ref.
			GG	1.8	$2.3x10^{-2}$
rs603315	9	0.32	CC	ref.	ref.
			TT	2.1	$2.3x10^{-2}$
rs4722063	7	0.41	CC	ref.	ref.
			TT	0.69	$2.3x10^{-2}$
rs3103584	5	0.41	AA	ref.	ref.
			GG	2.5	$2.3x10^{-2}$
rs10077929	5	0.54	CC	ref.	ref.
			TT	0.49	$2.3x10^{-2}$
rs6892681	5	0.29	GG	ref.	ref.
			TT	0.70	$2.3x10^{-2}$
rs109894	5	0.39	CC	ref.	ref.
			TT	1.5	$2.3x10^{-2}$
rs6089809	20	0.45	AA	ref.	ref.
			GG	1.4	$2.3x10^{-2}$
rs2748244	5	0.41	AA	ref.	ref.
			TT	1.5	$2.3x10^{-2}$
rs2241474	4	0.28	CC	ref.	ref.
			TT	1.4	$2.3x10^{-2}$
rs6939562	6	0.38	AA	ref.	ref.
			TT	0.53	$2.3x10^{-2}$
rs10429035	7	0.34	AA	ref.	ref.
			GG	0.61	$2.3x10^{-2}$
rs7144355	14	0.55	AA	ref.	ref.
			CC	1.5	$2.3x10^{-2}$
rs118202	6	0.31	GG	ref.	ref.
			TT	0.53	$2.3x10^{-2}$
rs1221430	5	0.36	CC	ref.	ref.
			TT	0.70	$2.4x10^{-2}$
rs2378607	1	0.35	GG	ref.	ref.
			TT	1.5	$2.4x10^{-2}$
rs1970568	1	0.39	AA	ref.	ref.
			GG	0.54	$2.4x10^{-2}$
rs712572	5	0.28	AA	ref.	ref.
			GG	0.60	$2.4x10^{-2}$
rs35103294	17	0.37	CC	ref.	ref.
			TT	0.70	$2.4x10^{-2}$
rs10401713	19	0.26	AA	ref.	ref.
			GG	2.3	$2.4x10^{-2}$
rs7248005	19	0.40	GG	ref.	ref.
			TT	0.70	$2.4x10^{-2}$

Continuation of Table A20

rs12352811	9	0.25	CC	ref.	ref.
			GG	9.1	$2.4x10^{-2}$
rs1474117	15	0.41	CC	ref.	ref.
			GG	0.70	$2.4x10^{-2}$
rs6791150	3	0.39	CC	ref.	ref.
			TT	0.70	$2.4x10^{-2}$
rs35877082	1	0.26	CC	ref.	ref.
			TT	0.38	$2.4x10^{-2}$
rs7091709	10	0.33	AA	ref.	ref.
			GG	0.63	$2.4x10^{-2}$
rs186064	3	0.25	AA	ref.	ref.
			GG	0.71	$2.4x10^{-2}$
rs332842	19	0.33	AA	ref.	ref.
			GG	0.70	$2.4x10^{-2}$
rs13207467	6	0.47	CC	ref.	ref.
			TT	1.4	$2.4x10^{-2}$
rs2252226	1	0.31	CC	ref.	ref.
			TT	1.4	$2.4x10^{-2}$
rs4074641	8	0.42	AA	ref.	ref.
			GG	1.7	$2.4x10^{-2}$
rs818505	7	0.33	AA	ref.	ref.
			GG	0.63	$2.5x10^{-2}$
rs27471	5	0.43	AA	ref.	ref.
			GG	0.70	$2.5x10^{-2}$
rs11853517	15	0.62	AA	ref.	ref.
			GG	4.1	$2.5x10^{-2}$
rs12055718	6	0.27	CC	ref.	ref.
			TT	1.5	$2.5x10^{-2}$
rs4745642	9	0.39	GG	ref.	ref.
			TT	0.59	$2.5x10^{-2}$
rs13280182	8	0.30	CC	ref.	ref.
			TT	1.4	$2.5x10^{-2}$
rs11653314	17	0.33	CC	ref.	ref.
			GG	0.70	$2.5x10^{-2}$
rs4619740	3	0.35	AA	ref.	ref.
			GG	1.4	$2.5x10^{-2}$
rs10840161	11	0.40	AA	ref.	ref.
			GG	0.71	$2.5x10^{-2}$
rs829563	2	0.25	AA	ref.	ref.
			TT	2.0	$2.5x10^{-2}$
rs1079242	10	0.27	AA	ref.	ref.
			GG	1.4	$2.5x10^{-2}$
rs7874518	9	0.27	CC	ref.	ref.
			TT	1.4	$2.5x10^{-2}$
rs2672777	5	0.28	CC	ref.	ref.
			TT	1.6	$2.5x10^{-2}$
rs4485890	5	0.44	CC	ref.	ref.
			TT	1.6	$2.6x10^{-2}$
rs6429772	1	0.41	CC	ref.	ref.
			TT	1.7	$2.6x10^{-2}$
rs1320571	1	0.25	AA	ref.	ref.
			GG	4.9	$2.6x10^{-2}$

Continuation of Table A20

rs8095694	18	0.30	GG	ref.	ref.
			TT	0.48	$2.6x10^{-2}$
rs1871750	1	0.45	CC	ref.	ref.
			TT	0.31	$2.6x10^{-2}$
rs9986918	7	0.29	GG	ref.	ref.
			TT	10.8	$2.6x10^{-2}$
rs4438438	2	0.37	AA	ref.	ref.
			GG	0.71	$2.6x10^{-2}$
rs897201	2	0.26	CC	ref.	ref.
			GG	0.68	$2.6x10^{-2}$
rs11097236	4	0.56	AA	ref.	ref.
			GG	1.6	$2.6x10^{-2}$
rs357972	2	0.31	CC	ref.	ref.
			TT	1.4	$2.6x10^{-2}$
rs925411	2	0.37	GG	ref.	ref.
			TT	0.71	$2.6x10^{-2}$
rs56193008	2	0.30	AA	ref.	ref.
			GG	0.63	$2.6x10^{-2}$
rs6511183	19	0.38	AA	ref.	ref.
			GG	0.19	$2.7x10^{-2}$
rs359542	3	0.68	AA	ref.	ref.
			TT	1.8	$2.7x10^{-2}$
rs276504	6	0.39	CC	ref.	ref.
			TT	1.4	$2.7x10^{-2}$
rs35028620	1	0.25	AA	ref.	ref.
			GG	0.7	$2.7x10^{-2}$
rs10871590	18	0.44	AA	ref.	ref.
			GG	1.5	$2.7x10^{-2}$
rs4745451	9	0.48	AA	ref.	ref.
			CC	1.9	$2.7x10^{-2}$
rs7706772	5	0.27	CC	ref.	ref.
			TT	1.6	$2.7x10^{-2}$
rs1679181	3	0.28	AA	ref.	ref.
			CC	0.087	$2.7x10^{-2}$
rs1329778	9	0.30	AA	ref.	ref.
			GG	2.0	$2.7x10^{-2}$
rs2408803	12	0.32	GG	ref.	ref.
			TT	0.68	$2.7x10^{-2}$
rs35288880	2	0.42	CC	ref.	ref.
			TT	1.8	$2.7x10^{-2}$
rs1866896	6	0.33	AA	ref.	ref.
			GG	1.4	$2.7x10^{-2}$
rs34847696	19	0.43	GG	ref.	ref.
			TT	0.71	$2.7x10^{-2}$
rs402886	8	0.27	CC	ref.	ref.
			TT	0.70	$2.7x10^{-2}$
rs73626678	11	0.33	CC	ref.	ref.
			TT	0.54	$2.7x10^{-2}$
rs9876919	3	0.30	CC	ref.	ref.
			TT	0.70	$2.7x10^{-2}$
rs256733	19	0.35	CC	ref.	ref.
			TT	0.71	$2.7x10^{-2}$

Continuation of Table A20

rs3011714	10	0.25	CC	ref.	ref.
			TT	0.63	$2.7x10^{-2}$
rs603424	10	0.49	AA	ref.	ref.
			GG	1.7	$2.7x10^{-2}$
rs7809670	7	0.28	AA	ref.	ref.
			GG	0.40	$2.7x10^{-2}$
rs12186767	5	0.28	AA	ref.	ref.
			GG	0.68	$2.7x10^{-2}$
rs2018393	22	0.44	GG	ref.	ref.
			TT	1.4	$2.7x10^{-2}$
rs1016364	11	0.31	AA	ref.	ref.
			GG	2.1	$2.8x10^{-2}$
rs7000552	8	0.26	AA	ref.	ref.
			GG	0.69	$2.8x10^{-2}$
rs9612334	22	0.40	AA	ref.	ref.
			GG	0.69	$2.8x10^{-2}$
rs12221081	10	0.27	AA	ref.	ref.
			GG	1.8	$2.8x10^{-2}$
rs11007117	10	0.27	CC	ref.	ref.
			TT	0.70	$2.8x10^{-2}$
rs10788235	10	0.42	AA	ref.	ref.
			GG	0.64	$2.8x10^{-2}$
rs10783458	12	0.26	AA	ref.	ref.
			GG	0.70	$2.8x10^{-2}$
rs7289126	22	0.34	AA	ref.	ref.
			CC	1.4	$2.8x10^{-2}$
rs11157721	14	0.32	CC	ref.	ref.
			TT	1.4	$2.8x10^{-2}$
rs276370	6	0.37	CC	ref.	ref.
			TT	0.57	$2.8x10^{-2}$
rs8051029	16	0.46	AA	ref.	ref.
			GG	1.9	$2.8x10^{-2}$
rs8031580	15	0.29	AA	ref.	ref.
			GG	0.71	$2.8x10^{-2}$
rs1657162	16	0.29	AA	ref.	ref.
			CC	1.4	$2.8x10^{-2}$
rs688402	12	0.25	CC	ref.	ref.
			TT	0.65	$2.8x10^{-2}$
rs646320	21	0.31	AA	ref.	ref.
			GG	0.69	$2.8x10^{-2}$
rs4366742	17 (cisplatin)	0.27	CC	ref.	ref.
			TT	1.4	$2.8x10^{-2}$
rs35025581	16	0.30	CC	ref.	ref.
			TT	0.69	$2.8x10^{-2}$
rs7792863	7	0.54	AA	ref.	ref.
			GG	1.53	$2.8x10^{-2}$
rs4657741	1	0.45	AA	ref.	ref.
			GG	0.67	$2.8x10^{-2}$
rs4528685	19	0.27	CC	ref.	ref.
			TT	1.5	$2.8x10^{-2}$
rs9847068	3	0.47	AA	ref.	ref.
			GG	0.64	$2.8x10^{-2}$

Continuation of Table A20

rs2022051	11	0.33	AA	ref.	ref.
			GG	0.53	$2.8x10^{-2}$
rs56270098	5	0.26	CC	ref.	ref.
			GG	0.29	$2.8x10^{-2}$
rs4511131	1	0.26	CC	ref.	ref.
			TT	2.3	$2.8x10^{-2}$
rs477445	18	0.27	CC	ref.	ref.
			TT	1.5	$2.9x10^{-2}$
rs2271277	17	0.51	AA	ref.	ref.
			GG	1.5	$2.9x10^{-2}$
rs749282	3	0.39	AA	ref.	ref.
			GG	0.5	$2.9x10^{-2}$
rs7591933	2	0.30	AA	ref.	ref.
			GG	0.41	$2.9x10^{-2}$
rs1497681	1	0.27	CC	ref.	ref.
			TT	1.5	$2.9x10^{-2}$
rs2531805	6	0.42	CC	ref.	ref.
			TT	0.71	$2.9x10^{-2}$
rs10201851	2	0.27	CC	ref.	ref.
			TT	2.6	$2.9x10^{-2}$
rs498193	8	0.37	CC	ref.	ref.
			TT	1.5	$2.9x10^{-2}$
rs10007472	4	0.27	CC	ref.	ref.
			TT	1.9	$2.9x10^{-2}$
rs922504	8	0.37	CC	ref.	ref.
			TT	0.71	$2.9x10^{-2}$
rs12944462	17	0.31	AA	ref.	ref.
			CC	0.65	$2.9x10^{-2}$
rs2070379	21	0.32	CC	ref.	ref.
			TT	2.9	$2.9x10^{-2}$
rs6465515	7	0.52	CC	ref.	ref.
			TT	1.5	$2.9x10^{-2}$
rs2562510	19	0.31	CC	ref.	ref.
			TT	0.63	$2.9x10^{-2}$
rs73456903	22	0.35	AA	ref.	ref.
			GG	2.2	$2.9x10^{-2}$
rs8057310	16	0.46	CC	ref.	ref.
			TT	1.5	$2.9x10^{-2}$
rs67798148	2	0.35	CC	ref.	ref.
			TT	1.5	$2.9x10^{-2}$
rs296759	12	0.36	CC	ref.	ref.
			TT	0.69	$3.0x10^{-2}$
rs3744549	17	0.29	CC	ref.	ref.
			TT	1.9	$3.0x10^{-2}$
rs10888603	1	0.47	AA	ref.	ref.
			CC	0.59	$3.0x10^{-2}$
rs1925237	9	0.49	CC	ref.	ref.
			TT	0.70	$3.0x10^{-2}$
rs3748976	16	0.53	GG	ref.	ref.
			TT	0.52	$3.0x10^{-2}$
rs589907	11	0.47	AA	ref.	ref.
			GG	0.69	$3.0x10^{-2}$

Continuation of Table A20

rs112369387	7	0.30	CC	ref.	ref.
			GG	0.10	$3.0x10^{-2}$
rs7994748	13	0.68	AA	ref.	ref.
			GG	0.60	$3.0x10^{-2}$
rs1783079	21	0.26	AA	ref.	ref.
			GG	1.7	$3.0x10^{-2}$
rs12609950	19	0.28	GG	ref.	ref.
			TT	1.5	$3.0x10^{-2}$
rs3749114	2	0.45	AA	ref.	ref.
			TT	0.71	$3.0x10^{-2}$
rs10766775	11	0.39	CC	ref.	ref.
			TT	0.67	$3.0x10^{-2}$
rs11761199	7	0.26	AA	ref.	ref.
			GG	1.4	$3.0x10^{-2}$
rs78239101	12	0.31	AA	ref.	ref.
			CC	0.41	$3.0x10^{-2}$
rs622833	11	0.31	AA	ref.	ref.
			GG	0.36	$3.0x10^{-2}$
rs9993426	4	0.56	AA	ref.	ref.
			CC	1.6	$3.0x10^{-2}$
rs1932366	1	0.47	AA	ref.	ref.
			CC	1.8	$3.0x10^{-2}$
rs1760904	14	0.46	AA	ref.	ref.
			GG	0.72	$3.0x10^{-2}$
rs4958339	5	0.25	CC	ref.	ref.
			GG	0.69	$3.0x10^{-2}$
rs7715378	5	0.30	CC	ref.	ref.
			TT	0.71	$3.0x10^{-2}$
rs12504694	4	0.35	CC	ref.	ref.
			TT	1.4	$3.0x10^{-2}$
rs564913	17	0.44	AA	ref.	ref.
			CC	1.4	$3.0x10^{-2}$
rs6803880	3	0.28	CC	ref.	ref.
			TT	0.39	$3.0x10^{-2}$
rs10890817	11	0.25	AA	ref.	ref.
			CC	0.70	$3.0x10^{-2}$
rs61998493	14	0.26	AA	ref.	ref.
			GG	0.70	$3.0x10^{-2}$
rs11195948	10	0.29	CC	ref.	ref.
			TT	0.68	$3.0x10^{-2}$
rs10092601	8	0.25	AA	ref.	ref.
			CC	1.9	$3.1x10^{-2}$
rs28393495	16	0.29	CC	ref.	ref.
			TT	0.62	$3.1x10^{-2}$
rs7094347	10	0.31	AA	ref.	ref.
			GG	0.29	$3.1x10^{-2}$
rs7244902	18	0.27	AA	ref.	ref.
			GG	0.56	$3.1x10^{-2}$
rs2833859	21	0.39	CC	ref.	ref.
			TT	0.72	$3.1x10^{-2}$
rs6758574	2	0.45	CC	ref.	ref.
			TT	2.1	$3.1x10^{-2}$

Continuation of Table A20

rs10404025	19	0.34	CC	ref.	ref.
			TT	0.65	$3.1x10^{-2}$
rs2727525	4	0.38	AA	ref.	ref.
			CC	0.72	$3.1x10^{-2}$
rs12490614	3	0.36	CC	ref.	ref.
			TT	0.71	$3.1x10^{-2}$
rs635674	20	0.27	CC	ref.	ref.
			TT	0.47	$3.1x10^{-2}$
rs12694349	2	0.30	CC	ref.	ref.
			TT	0.71	$3.1x10^{-2}$
rs4671936	2	0.32	AA	ref.	ref.
			GG	0.72	$3.1x10^{-2}$
rs3198697	16	0.35	CC	ref.	ref.
			TT	0.71	$3.1x10^{-2}$
rs10925262	1	0.39	AA	ref.	ref.
			GG	1.7	$3.1x10^{-2}$
rs1644512	5	0.26	GG	ref.	ref.
			TT	0.68	$3.1x10^{-2}$
rs174466	11	0.50	AA	ref.	ref.
			GG	1.5	$3.1x10^{-2}$
rs1259310	3	0.47	AA	ref.	ref.
			GG	1.6	$3.1x10^{-2}$
rs12442313	15	0.38	AA	ref.	ref.
			GG	1.4	$3.1x10^{-2}$
rs2835522	21	0.47	AA	ref.	ref.
			TT	1.6	$3.1x10^{-2}$
rs4071641	17	0.36	CC	ref.	ref.
			TT	1.4	$3.1x10^{-2}$
rs6602910	13	0.45	CC	ref.	ref.
			TT	1.4	$3.1x10^{-2}$
rs3924985	10	0.33	AA	ref.	ref.
			GG	0.35	$3.1x10^{-2}$
rs1561398	5	0.44	CC	ref.	ref.
			TT	1.6	$3.1x10^{-2}$
rs4455607	5	0.26	AA	ref.	ref.
			GG	1.4	$3.2x10^{-2}$
rs55889708	9	0.26	AA	ref.	ref.
			GG	1.5	$3.2x10^{-2}$
rs1106123	13	0.30	CC	ref.	ref.
			TT	1.9	$3.2x10^{-2}$
rs472473	1	0.36	AA	ref.	ref.
			GG	7.6	$3.2x10^{-2}$
rs12567108	1	0.47	AA	ref.	ref.
			GG	1.4	$3.2x10^{-2}$
rs6499107	16	0.62	CC	ref.	ref.
			TT	0.45	$3.2x10^{-2}$
rs4240935	1	0.32	GG	ref.	ref.
			TT	0.72	$3.2x10^{-2}$
rs56994118	17	0.56	CC	ref.	ref.
			TT	0.47	$3.2x10^{-2}$
rs7007264	8	0.35	CC	ref.	ref.
			TT	1.4	$3.2x10^{-2}$

Continuation of Table A20

rs12773600	10	0.26	CC	ref.	ref.
			GG	1.6	$3.2x10^{-2}$
rs10950696	7	0.45	CC	ref.	ref.
			TT	1.4	$3.2x10^{-2}$
rs622330	21	0.33	AA	ref.	ref.
			GG	1.4	$3.2x10^{-2}$
rs112214228	1	0.28	AA	ref.	ref.
			GG	0.72	$3.2x10^{-2}$
rs6858245	4	0.30	CC	ref.	ref.
			TT	1.7	$3.2x10^{-2}$
rs2300773	3	0.25	AA	ref.	ref.
			GG	0.71	$3.2x10^{-2}$
rs13169759	5	0.31	CC	ref.	ref.
			TT	0.70	$3.2x10^{-2}$
rs506645	13	0.26	CC	ref.	ref.
			TT	0.66	$3.3x10^{-2}$
rs11160715	14	0.34	CC	ref.	ref.
			TT	0.52	$3.3x10^{-2}$
rs7608738	2	0.28	AA	ref.	ref.
			GG	1.4	$3.3x10^{-2}$
rs6583810	10	0.69	AA	ref.	ref.
			GG	2.1	$3.3x10^{-2}$
rs71337725	2	0.27	AA	ref.	ref.
			GG	0.71	$3.3x10^{-2}$
rs13025070	2	0.34	AA	ref.	ref.
			GG	1.4	$3.3x10^{-2}$
rs7630226	3	0.31	AA	ref.	ref.
			TT	1.5	$3.3x10^{-2}$
rs56071959	7	0.37	CC	ref.	ref.
			TT	0.62	$3.3x10^{-2}$
rs13106276	4	0.47	AA	ref.	ref.
			GG	1.6	$3.3x10^{-2}$
rs13136146	4	0.26	AA	ref.	ref.
			CC	0.72	$3.3x10^{-2}$
rs10750171	11	0.28	GG	ref.	ref.
			TT	1.4	$3.3x10^{-2}$
rs7309178	12	0.30	CC	ref.	ref.
			TT	1.8	$3.3x10^{-2}$
rs6945372	7	0.38	AA	ref.	ref.
			GG	0.59	$3.3x10^{-2}$
rs706037	7	0.50	AA	ref.	ref.
			GG	1.8	$3.3x10^{-2}$
rs4831751	8	0.43	CC	ref.	ref.
			GG	1.4	$3.3x10^{-2}$
rs7534064	1	0.30	AA	ref.	ref.
			GG	0.66	$3.3x10^{-2}$
rs11191385	10	0.25	GG	ref.	ref.
			TT	1.5	$3.3x10^{-2}$
rs17124984	14	0.29	GG	ref.	ref.
			TT	0.53	$3.3x10^{-2}$
rs838086	2	0.45	AA	ref.	ref.
			CC	1.5	$3.3x10^{-2}$

Continuation of Table A20

rs7865593	9	0.34	AA	ref.	ref.
			GG	0.67	$3.3x10^{-2}$
rs11121046	1	0.33	GG	ref.	ref.
			TT	1.4	$3.3x10^{-2}$
rs34432998	1	0.39	AA	ref.	ref.
			GG	1.4	$3.3x10^{-2}$
rs7660832	4	0.52	AA	ref.	ref.
			GG	0.57	$3.4x10^{-2}$
rs4749924	10	0.29	AA	ref.	ref.
			CC	1.5	$3.4x10^{-2}$
rs6716937	2	0.31	AA	ref.	ref.
			GG	0.71	$3.4x10^{-2}$
rs17813538	2	0.27	AA	ref.	ref.
			GG	0.65	$3.4x10^{-2}$
rs2237306	7	0.27	AA	ref.	ref.
			CC	2.2	$3.4x10^{-2}$
rs11633933	15	0.44	CC	ref.	ref.
			TT	0.62	$3.4x10^{-2}$
rs12472193	2	0.67	AA	ref.	ref.
			CC	1.6	$3.4x10^{-2}$
rs2478348	6 (cisplatin)	0.32	AA	ref.	ref.
			GG	1.5	$3.4x10^{-2}$
rs34408426	11	0.34	AA	ref.	ref.
			GG	0.70	$3.4x10^{-2}$
rs1608984	2	0.71	GG	ref.	ref.
			TT	0.50	$3.4x10^{-2}$
rs9300090	11	0.37	AA	ref.	ref.
			GG	1.4	$3.4x10^{-2}$
rs1622800	6	0.33	AA	ref.	ref.
			CC	1.5	$3.4x10^{-2}$
rs6494466	15	0.71	AA	ref.	ref.
			GG	1.5	$3.4x10^{-2}$
rs640655	11	0.29	CC	ref.	ref.
			TT	0.090	$3.4x10^{-2}$
rs12196289	6	0.26	AA	ref.	ref.
			GG	0.72	$3.4x10^{-2}$
rs13301970	9	0.55	AA	ref.	ref.
			CC	0.68	$3.4x10^{-2}$
rs6439154	3	0.35	AA	ref.	ref.
			GG	1.4	$3.4x10^{-2}$
rs4676448	2	0.29	AA	ref.	ref.
			CC	0.71	$3.4x10^{-2}$
rs2568044	11	0.48	CC	ref.	ref.
			TT	0.64	$3.4x10^{-2}$
rs28758996	12	0.33	AA	ref.	ref.
			GG	0.72	$3.4x10^{-2}$
rs2040978	7	0.34	GG	ref.	ref.
			TT	1.8	$3.4x10^{-2}$
rs8052595	16	0.33	CC	ref.	ref.
			TT	0.68	$3.4x10^{-2}$
rs548987	6	0.26	CC	ref.	ref.
			GG	2.9	$3.5x10^{-2}$

Continuation of Table A20

rs1023115	1	0.27	AA	ref.	ref.
			GG	0.72	$3.5x10^{-2}$
rs1058600	5	0.37	CC	ref.	ref.
			TT	0.62	$3.5x10^{-2}$
rs2375475	1	0.41	CC	ref.	ref.
			TT	0.68	$3.5x10^{-2}$
rs8053240	16	0.26	AA	ref.	ref.
			CC	0.68	$3.5x10^{-2}$
rs7257406	19	0.32	CC	ref.	ref.
			TT	1.4	$3.5x10^{-2}$
rs10819341	9	0.37	CC	ref.	ref.
			TT	1.8	$3.5x10^{-2}$
rs55748512	3	0.34	CC	ref.	ref.
			GG	1.4	$3.5x10^{-2}$
rs2216721	5	0.28	AA	ref.	ref.
			GG	1.5	$3.5x10^{-2}$
rs11049881	12	0.27	AA	ref.	ref.
			TT	0.69	$3.5x10^{-2}$
rs1119396	21	0.40	CC	ref.	ref.
			TT	2.9	$3.5x10^{-2}$
rs930921	15	0.37	AA	ref.	ref.
			GG	1.4	$3.5x10^{-2}$
rs1652728	10	0.33	CC	ref.	ref.
			TT	1.4	$3.5x10^{-2}$
rs1836837	6	0.35	GG	ref.	ref.
			TT	0.69	$3.5x10^{-3}$
rs12463449	2	0.27	CC	ref.	ref.
			TT	0.72	$3.5x10^{-2}$
rs2009836	7	0.26	CC	ref.	ref.
			TT	1.5	$3.5x10^{-2}$
rs1390964	14	0.27	CC	ref.	ref.
			TT	2.3	$3.5x10^{-2}$
rs7862716	9	0.31	CC	ref.	ref.
			TT	1.7	$3.5x10^{-2}$
rs1793399	11	0.32	CC	ref.	ref.
			TT	0.46	$3.5x10^{-2}$
rs12948905	17	0.28	AA	ref.	ref.
			CC	0.72	$3.5x10^{-2}$
rs6978163	7	0.33	AA	ref.	ref.
			GG	1.4	$3.6x10^{-2}$
rs3814206	10	0.34	AA	ref.	ref.
			GG	0.72	$3.6x10^{-2}$
rs398329	8	0.35	CC	ref.	ref.
			TT	1.8	$3.6x10^{-2}$
rs884973	17	0.62	GG	ref.	ref.
			TT	2.5	$3.6x10^{-2}$
rs7794226	7	0.39	CC	ref.	ref.
			GG	2.1	$3.6x10^{-2}$
rs882175	15	0.48	CC	ref.	ref.
			TT	1.4	$3.6x10^{-2}$
rs11205417	1	0.53	AA	ref.	ref.
			GG	2.2	$3.6x10^{-2}$

Continuation of Table A20

rs7776156	6	0.43	AA	ref.	ref.
			GG	0.72	$3.6x10^{-2}$
rs72959469	2	0.26	AA	ref.	ref.
			GG	0.65	$3.6x10^{-2}$
rs10149217	14	0.32	CC	ref.	ref.
			TT	0.68	$3.6x10^{-2}$
rs11038107	11	0.42	CC	ref.	ref.
			GG	0.72	$3.6x10^{-2}$
rs9550683	13	0.29	CC	ref.	ref.
			TT	0.58	$3.6x10^{-2}$
rs438384	11	0.28	CC	ref.	ref.
			TT	1.4	$3.6x10^{-2}$
rs57743958	19	0.69	CC	ref.	ref.
			TT	2.9	$3.6x10^{-2}$
rs4384764	2	0.43	AA	ref.	ref.
			GG	1.6	$3.6x10^{-2}$
rs7968967	12	0.26	AA	ref.	ref.
			GG	1.5	$3.6x10^{-2}$
rs1049951	10	0.43	AA	ref.	ref.
			GG	5.2	$3.6x10^{-2}$
rs17057769	4	0.43	AA	ref.	ref.
			GG	1.4	$3.6x10^{-2}$
rs7110845	11	0.38	AA	ref.	ref.
			GG	0.71	$3.6x10^{-2}$
rs59431377	8	0.37	CC	ref.	ref.
			TT	0.49	$3.6x10^{-2}$
rs2295251	22	0.29	AA	ref.	ref.
			GG	0.63	$3.6x10^{-2}$
rs2065482	9	0.28	GG	ref.	ref.
			TT	0.70	$3.6x10^{-2}$
rs7404524	16	0.36	AA	ref.	ref.
			GG	0.66	$3.6x10^{-2}$
rs1564760	3	0.32	AA	ref.	ref.
			CC	1.5	$3.6x10^{-2}$
rs11065857	12	0.51	AA	ref.	ref.
			GG	0.65	$3.7x10^{-2}$
rs9903200	17	0.33	AA	ref.	ref.
			GG	0.67	$3.7x10^{-2}$
rs6588196	1	0.32	CC	ref.	ref.
			TT	1.4	$3.7x10^{-2}$
rs28661866	8	0.28	AA	ref.	ref.
			GG	1.8	$3.7x10^{-2}$
rs33221	12	0.30	CC	ref.	ref.
			TT	1.5	$3.7x10^{-2}$
rs72710517	4	0.28	GG	ref.	ref.
			TT	0.68	$3.7x10^{-2}$
rs6995156	8	0.27	AA	ref.	ref.
			GG	1.5	$3.7x10^{-2}$
rs7292297	22	0.35	GG	ref.	ref.
			TT	1.39	$3.7x10^{-2}$
rs249833	12	0.28	CC	ref.	ref.
			TT	1.4	$3.7x10^{-2}$

Continuation of Table A20

rs2375473	1	0.35	AA	ref.	ref.
			GG	1.7	$3.7x10^{-2}$
rs1101154	20	0.33	CC	ref.	ref.
			TT	1.4	$3.7x10^{-2}$
rs494078	18	0.30	CC	ref.	ref.
			GG	1.5	$3.7x10^{-2}$
rs551890	11	0.37	CC	ref.	ref.
			TT	2.2	$3.7x10^{-2}$
rs10927791	1	0.56	CC	ref.	ref.
			TT	0.72	$3.8x10^{-2}$
rs4738679	8	0.28	AA	ref.	ref.
			GG	1.5	$3.8x10^{-2}$
rs4275717	12	0.28	AA	ref.	ref.
			GG	1.4	$3.8x10^{-2}$
rs10251964	7	0.50	CC	ref.	ref.
			TT	0.61	$3.8x10^{-2}$
rs8082024	17	0.49	CC	ref.	ref.
			TT	1.7	$3.8x10^{-2}$
rs9349180	6	0.53	AA	ref.	ref.
			GG	0.58	$3.8x10^{-2}$
rs7990216	13	0.75	CC	ref.	ref.
			TT	2.3	$3.8x10^{-2}$
rs11101269	10	0.32	CC	ref.	ref.
			GG	2.0	$3.8x10^{-2}$
rs62313888	4	0.29	CC	ref.	ref.
			TT	0.7	$3.8x10^{-2}$
rs7147201	14	0.29	AA	ref.	ref.
			GG	1.9	$3.8x10^{-2}$
rs9640029	7	0.47	CC	ref.	ref.
			TT	1.4	$3.8x10^{-2}$
rs3754824	2	0.28	AA	ref.	ref.
			GG	1.4	$3.8x10^{-2}$
rs73276994	14	0.36	CC	ref.	ref.
			TT	3.5	$3.8x10^{-2}$
rs268165	2	0.33	GG	ref.	ref.
			TT	0.55	$3.8x10^{-2}$
rs4320747	1	0.33	AA	ref.	ref.
			GG	0.71	$3.8x10^{-2}$
rs6578259	11	0.43	AA	ref.	ref.
			TT	0.72	$3.8x10^{-2}$
rs4291387	9	0.31	AA	ref.	ref.
			GG	1.4	$3.8x10^{-2}$
rs12448510	16	0.27	AA	ref.	ref.
			CC	0.72	$3.8x10^{-2}$
rs6532181	4	0.32	AA	ref.	ref.
			GG	0.72	$3.9x10^{-2}$
rs12086362	1	0.25	AA	ref.	ref.
			GG	0.69	$3.9x10^{-2}$
rs11994	5	0.26	AA	ref.	ref.
			GG	0.71	$3.9x10^{-2}$
rs2235775	22	0.25	AA	ref.	ref.
			CC	1.5	$3.9x10^{-2}$

Continuation of Table A20

rs2773298	6	0.27	CC	ref.	ref.
			TT	0.54	$3.9x10^{-2}$
rs7960669	12	0.39	AA	ref.	ref.
			GG	1.4	$3.9x10^{-2}$
rs6545430	2	0.40	CC	ref.	ref.
			TT	0.51	$3.9x10^{-2}$
rs12594507	15	0.42	CC	ref.	ref.
			TT	0.72	$3.9x10^{-2}$
rs6447135	4	0.37	CC	ref.	ref.
			GG	1.63	$3.9x10^{-2}$
rs2370413	12	0.45	CC	ref.	ref.
			TT	0.73	$3.9x10^{-2}$
rs13085411	3	0.31	AA	ref.	ref.
			CC	0.72	$3.9x10^{-2}$
rs11669059	19	0.26	AA	ref.	ref.
			GG	1.4	$3.9x10^{-2}$
rs4908377	1	0.28	AA	ref.	ref.
			GG	0.64	$3.9x10^{-2}$
rs12203413	6	0.26	CC	ref.	ref.
			TT	1.4	$3.9x10^{-2}$
rs9824840	3	0.30	GG	ref.	ref.
			TT	2.5	$3.9x10^{-2}$
rs9364226	6	0.30	GG	ref.	ref.
			TT	0.68	$3.9x10^{-2}$
rs7564165	2	0.37	CC	ref.	ref.
			TT	0.72	$3.9x10^{-2}$
rs4611172	11	0.36	GG	ref.	ref.
			TT	0.72	$3.9x10^{-2}$
rs2476227	13	0.47	CC	ref.	ref.
			TT	1.4	$4.0x10^{-2}$
rs2112593	5	0.38	CC	ref.	ref.
			TT	1.9	$4.0x10^{-2}$
rs10249786	7	0.27	AA	ref.	ref.
			TT	8.9	$4.0x10^{-2}$
rs12461550	19	0.26	AA	ref.	ref.
			CC	1.4	$4.0x10^{-2}$
rs2762463	9	0.36	AA	ref.	ref.
			TT	0.70	$4.0x10^{-2}$
rs629112	1	0.44	AA	ref.	ref.
			GG	1.5	$4.0x10^{-2}$
rs12828225	12	0.35	AA	ref.	ref.
			TT	1.4	$4.0x10^{-2}$
rs1424148	16	0.32	CC	ref.	ref.
			GG	1.7	$4.0x10^{-2}$
rs6458052	6	0.29	AA	ref.	ref.
			GG	1.4	$4.0x10^{-2}$
rs1254415	6	0.31	CC	ref.	ref.
			GG	0.72	$4.0x10^{-2}$
rs17248895	14	0.57	AA	ref.	ref.
			CC	2.4	$4.0x10^{-2}$
rs7760535	6	0.41	CC	ref.	ref.
			GG	1.4	$4.0x10^{-2}$

Continuation of Table A20

rs253296	5	0.25	AA	ref.	ref.
			GG	0.69	$4.0x10^{-2}$
rs4805858	19	0.29	CC	ref.	ref.
			TT	1.6	$4.0x10^{-2}$
rs28628836	4	0.34	CC	ref.	ref.
			GG	0.73	$4.1x10^{-2}$
rs11631685	15	0.33	CC	ref.	ref.
			TT	0.61	$4.1x10^{-2}$
rs12700312	7	0.28	CC	ref.	ref.
			GG	1.4	$4.1x10^{-2}$
rs2494262	1	0.46	AA	ref.	ref.
			CC	0.73	$4.1x10^{-2}$
rs10495760	2	0.31	AA	ref.	ref.
			GG	0.73	$4.1x10^{-2}$
rs1703452	14	0.26	GG	ref.	ref.
			TT	1.4	$4.1x10^{-2}$
rs35828065	20	0.25	CC	ref.	ref.
			TT	1.7	$4.1x10^{-2}$
rs11708617	3	0.37	AA	ref.	ref.
			GG	1.4	$4.1x10^{-2}$
rs28999107	12	0.40	GG	ref.	ref.
			TT	0.71	$4.1x10^{-2}$
rs67306087	15	0.44	CC	ref.	ref.
			TT	1.4	$4.1x10^{-2}$
rs285729	15	0.42	CC	ref.	ref.
			TT	0.59	$4.1x10^{-2}$
rs9549757	13	0.27	AA	ref.	ref.
			GG	0.72	$4.1x10^{-2}$
rs7961366	12	0.32	CC	ref.	ref.
			TT	0.73	$4.1x10^{-2}$
rs56727143	5	0.27	GG	ref.	ref.
			TT	2.0	$4.1x10^{-2}$
rs3766298	1	0.28	AA	ref.	ref.
			TT	1.4	$4.1x10^{-2}$
rs7660927	4	0.37	CC	ref.	ref.
			TT	0.54	$4.1x10^{-2}$
rs1614887	6	0.26	AA	ref.	ref.
			GG	1.4	$4.1x10^{-2}$
rs137705	22	0.29	CC	ref.	ref.
			TT	0.69	$4.1x10^{-2}$
rs6456814	6	0.28	AA	ref.	ref.
			CC	1.6	$4.1x10^{-2}$
rs17232243	16	0.41	AA	ref.	ref.
			GG	1.4	$4.1x10^{-2}$
rs5030411	11	0.39	AA	ref.	ref.
			GG	1.4	$4.2x10^{-2}$
rs1595804	7	0.39	AA	ref.	ref.
			GG	1.4	$4.2x10^{-2}$
rs13303065	1	0.46	CC	ref.	ref.
			TT	1.4	$4.2x10^{-2}$
rs4147332	8	0.26	CC	ref.	ref.
			GG	1.4	$4.2x10^{-2}$

Continuation of Table A20

rs2568194	2	0.27	CC	ref.	ref.
			GG	1.6	$4.2x10^{-2}$
rs12411515	10	0.25	CC	ref.	ref.
			TT	1.5	$4.2x10^{-2}$
rs940234	3	0.33	CC	ref.	ref.
			GG	4.2	$4.2x10^{-2}$
rs4400971	14	0.40	AA	ref.	ref.
			CC	0.74	$4.2x10^{-2}$
rs11007172	10	0.41	AA	ref.	ref.
			GG	0.73	$4.2x10^{-2}$
rs4129668	7	0.26	CC	ref.	ref.
			GG	0.73	$4.2x10^{-2}$
rs1785333	18	0.33	CC	ref.	ref.
			TT	1.5	$4.2x10^{-2}$
rs545787	6	0.26	AA	ref.	ref.
			GG	1.5	$4.2x10^{-2}$
rs11807791	1	0.26	CC	ref.	ref.
			TT	4.5	$4.2x10^{-2}$
rs8131205	21	0.29	GG	ref.	ref.
			TT	1.8	$4.2x10^{-2}$
rs448714	5	0.32	AA	ref.	ref.
			GG	0.56	$4.2x10^{-2}$
rs9321476	6	0.36	AA	ref.	ref.
			CC	1.5	$4.2x10^{-2}$
rs7703057	5	0.26	AA	ref.	ref.
			GG	0.38	$4.2x10^{-2}$
rs6439655	3	0.36	AA	ref.	ref.
			GG	1.4	$4.2x10^{-2}$
rs11236448	11	0.32	AA	ref.	ref.
			GG	0.42	$4.2x10^{-2}$
rs145787392	6	0.45	GG	ref.	ref.
			TT	1.5	$4.2x10^{-2}$
rs7948009	11	0.27	AA	ref.	ref.
			GG	0.70	$4.2x10^{-2}$
rs12468735	2	0.31	AA	ref.	ref.
			GG	1.4	$4.2x10^{-2}$
rs12746615	1	0.27	AA	ref.	ref.
			GG	1.4	$4.2x10^{-2}$
rs9535188	13	0.25	CC	ref.	ref.
			TT	0.73	$4.3x10^{-2}$
rs2098205	7	0.36	AA	ref.	ref.
			GG	1.4	$4.3x10^{-2}$
rs11611855	12	0.32	CC	ref.	ref.
			TT	0.71	$4.3x10^{-2}$
rs2755998	10	0.25	AA	ref.	ref.
			TT	0.63	$4.3x10^{-2}$
rs12496482	3	0.41	AA	ref.	ref.
			CC	0.60	$4.3x10^{-2}$
rs9582483	13	0.44	AA	ref.	ref.
			CC	0.31	$4.3x10^{-2}$
rs10000436	4	0.35	AA	ref.	ref.
			TT	1.5	$4.3x10^{-2}$

Continuation of Table A20

rs6602909	13	0.25	CC	ref.	ref.
			TT	1.5	$4.3x10^{-2}$
rs67977616	3	0.25	AA	ref.	ref.
			GG	2.8	$4.3x10^{-2}$
rs9386581	6	0.28	AA	ref.	ref.
			GG	1.4	$4.3x10^{-2}$
rs6499106	16	0.33	AA	ref.	ref.
			GG	2.2	$4.3x10^{-2}$
rs1538669	9	0.31	CC	ref.	ref.
			GG	0.64	$4.3x10^{-2}$
rs495562	1	0.40	CC	ref.	ref.
			GG	1.5	$4.3x10^{-2}$
rs4850680	2	0.30	AA	ref.	ref.
			GG	0.72	$4.3x10^{-2}$
rs55639815	2	0.28	AA	ref.	ref.
			GG	1.5	$4.3x10^{-2}$
rs11125859	2	0.25	GG	ref.	ref.
			TT	0.72	$4.3x10^{-2}$
rs11666686	19	0.27	CC	ref.	ref.
			TT	0.71	$4.3x10^{-2}$
rs3755552	2	0.44	CC	ref.	ref.
			TT	1.4	$4.3x10^{-2}$
rs176482	7	0.25	AA	ref.	ref.
			GG	1.6	$4.3x10^{-2}$
rs7580141	2	0.32	AA	ref.	ref.
			GG	1.4	$4.3x10^{-2}$
rs7753551	6	0.28	AA	ref.	ref.
			GG	1.4	$4.3x10^{-2}$
rs9295772	6	0.50	AA	ref.	ref.
			GG	0.73	$4.3x10^{-2}$
rs257758	5	0.46	AA	ref.	ref.
			GG	0.71	$4.3x10^{-2}$
rs187923046	19	0.26	AA	ref.	ref.
			GG	0.41	$4.4x10^{-2}$
rs35078732	11	0.31	AA	ref.	ref.
			GG	0.71	$4.4x10^{-2}$
rs13020822	2	0.29	CC	ref.	ref.
			TT	0.70	$4.4x10^{-2}$
rs10750027	11	0.30	AA	ref.	ref.
			GG	0.73	$4.4x10^{-2}$
rs597403	6	0.39	AA	ref.	ref.
			GG	0.54	$4.4x10^{-2}$
rs2673623	12	0.31	AA	ref.	ref.
			GG	1.4	$4.4x10^{-2}$
rs4660934	1	0.31	CC	ref.	ref.
			TT	1.4	$4.4x10^{-2}$
rs11676277	2	0.47	CC	ref.	ref.
			TT	1.4	$4.4x10^{-2}$
rs6005757	22	0.39	CC	ref.	ref.
			TT	2.7	$4.4x10^{-2}$
rs10147905	14	0.63	CC	ref.	ref.
			TT	3.2	$4.4x10^{-2}$

Continuation of Table A20

rs11042883	11	0.35	CC	ref.	ref.
			TT	0.72	$4.4x10^{-2}$
rs10887266	10	0.32	AA	ref.	ref.
			GG	0.60	$4.4x10^{-2}$
rs874546	3	0.43	AA	ref.	ref.
			GG	1.9	$4.4x10^{-2}$
rs4134058	1	0.32	CC	ref.	ref.
			TT	0.73	$4.4x10^{-2}$
rs4282745	1	0.26	AA	ref.	ref.
			CC	1.5	$4.4x10^{-2}$
rs11150715	16	0.26	AA	ref.	ref.
			CC	0.48	$4.4x10^{-2}$
rs10249357	7	0.27	CC	ref.	ref.
			TT	0.72	$4.4x10^{-2}$
rs3809767	17	0.30	AA	ref.	ref.
			GG	0.48	$4.4x10^{-2}$
rs10926995	1	0.25	AA	ref.	ref.
			GG	1.4	$4.4x10^{-2}$
rs4800541	18	0.38	CC	ref.	ref.
			TT	0.73	$4.4x10^{-2}$
rs11891859	2	0.48	AA	ref.	ref.
			CC	2.4	$4.4x10^{-2}$
rs5764733	22	0.33	CC	ref.	ref.
			GG	1.5	$4.4x10^{-2}$
rs4320563	8	0.28	AA	ref.	ref.
			GG	1.4	$4.5x10^{-2}$
rs7196453	16	0.41	AA	ref.	ref.
			GG	0.53	$4.5x10^{-2}$
rs7523764	1	0.28	CC	ref.	ref.
			TT	0.35	$4.5x10^{-2}$
rs739442	9	0.52	AA	ref.	ref.
			GG	1.4	$4.5x10^{-2}$
rs1855080	1	0.25	AA	ref.	ref.
			TT	0.71	$4.5x10^{-2}$
rs7853254	9	0.30	CC	ref.	ref.
			TT	0.66	$4.5x10^{-2}$
rs2836173	21	0.28	AA	ref.	ref.
			GG	0.72	$4.5x10^{-2}$
rs11601870	11	0.34	CC	ref.	ref.
			TT	1.4	$4.5x10^{-2}$
rs6685599	1	0.41	AA	ref.	ref.
			GG	1.4	$4.5x10^{-2}$
rs7691652	4	0.58	AA	ref.	ref.
			CC	0.45	$4.5x10^{-2}$
rs3814609	10	0.26	AA	ref.	ref.
			GG	1.5	$4.5x10^{-2}$
rs4796791	17	0.57	CC	ref.	ref.
			TT	0.71	$4.5x10^{-2}$
rs56060134	13	0.42	AA	ref.	ref.
			GG	0.73	$4.5x10^{-2}$
rs3010273	5	0.40	AA	ref.	ref.
			GG	1.6	$4.5x10^{-2}$

Continuation of Table A20

rs4836555	9	0.26	AA	ref.	ref.
			GG	1.7	$4.5x10^{-2}$
rs5758660	22	0.33	AA	ref.	ref.
			CC	0.73	$4.5x10^{-2}$
rs10852509	16	0.26	AA	ref.	ref.
			GG	1.4	$4.5x10^{-2}$
rs10405133	19	0.39	CC	ref.	ref.
			TT	1.6	$4.5x10^{-2}$
rs2278238	19	0.40	CC	ref.	ref.
			TT	0.68	$4.5x10^{-2}$
rs10841114	12	0.33	AA	ref.	ref.
			TT	1.4	$4.5x10^{-2}$
rs59623988	13	0.25	AA	ref.	ref.
			GG	1.9	$4.5x10^{-2}$
rs3904193	10	0.58	GG	ref.	ref.
			TT	0.19	$4.5x10^{-2}$
rs12187973	5	0.26	GG	ref.	ref.
			TT	1.4	$4.6x10^{-2}$
rs10078121	5	0.32	AA	ref.	ref.
			GG	0.67	$4.6x10^{-2}$
rs9840975	3	0.39	AA	ref.	ref.
			CC	0.50	$4.6x10^{-2}$
rs10890807	11	0.32	AA	ref.	ref.
			TT	1.4	$4.6x10^{-2}$
rs10840103	11	0.26	CC	ref.	ref.
			TT	0.72	$4.6x10^{-2}$
rs72979934	4	0.26	CC	ref.	ref.
			TT	0.58	$4.6x10^{-2}$
rs1599762	3	0.43	AA	ref.	ref.
			TT	0.73	$4.6x10^{-2}$
rs1998355	14	0.26	AA	ref.	ref.
			GG	1.4	$4.6x10^{-2}$
rs62367685	5	0.30	CC	ref.	ref.
			GG	0.74	$4.6x10^{-2}$
rs35467921	16	0.34	CC	ref.	ref.
			TT	1.4	$4.6x10^{-2}$
rs7016661	8	0.36	CC	ref.	ref.
			TT	1.5	$4.6x10^{-2}$
rs7858659	9	0.44	AA	ref.	ref.
			CC	0.47	$4.6x10^{-2}$
rs10489550	1	0.28	CC	ref.	ref.
			GG	1.4	$4.6x10^{-2}$
rs4985147	16	0.29	CC	ref.	ref.
			TT	1.4	$4.6x10^{-2}$
rs2727788	11	0.25	AA	ref.	ref.
			CC	0.66	$4.6x10^{-2}$
rs12129486	1	0.49	AA	ref.	ref.
			GG	0.73	$4.6x10^{-2}$
rs9839994	3	0.30	CC	ref.	ref.
			TT	0.72	$4.6x10^{-2}$
rs6713572	2	0.26	AA	ref.	ref.
			CC	0.73	$4.6x10^{-2}$

Continuation of Table A20

rs7731297	5	0.25	AA	ref.	ref.
			GG	2.7	$4.6x10^{-2}$
rs7873398	9	0.30	CC	ref.	ref.
			TT	1.4	$4.6x10^{-2}$
rs11169270	12	0.28	AA	ref.	ref.
			GG	1.5	$4.6x10^{-2}$
rs6603811	1	0.42	CC	ref.	ref.
			TT	3.7	$4.6x10^{-2}$
rs839237	3	0.27	CC	ref.	ref.
			TT	1.5	$4.7x10^{-2}$
rs2304509	3	0.28	CC	ref.	ref.
			GG	1.8	$4.7x10^{-2}$
rs7211643	17	0.55	CC	ref.	ref.
			TT	4.6	$4.7x10^{-2}$
rs58869119	7	0.39	CC	ref.	ref.
			TT	0.52	$4.7x10^{-2}$
rs12733277	1	0.38	AA	ref.	ref.
			CC	0.74	$4.7x10^{-2}$
rs10769872	11	0.30	GG	ref.	ref.
			TT	0.69	$4.7x10^{-2}$
rs9931992	16	0.41	CC	ref.	ref.
			TT	0.71	$4.7x10^{-2}$
rs6573082	14	0.27	AA	ref.	ref.
			CC	3.1	$4.7x10^{-2}$
rs62391554	5	0.26	AA	ref.	ref.
			TT	1.8	$4.7x10^{-2}$
rs4935734	10	0.27	AA	ref.	ref.
			GG	1.4	$4.7x10^{-2}$
rs38859	7	0.39	CC	ref.	ref.
			TT	0.74	$4.7x10^{-2}$
rs2268256	21	0.27	AA	ref.	ref.
			GG	0.62	$4.7x10^{-2}$
rs5998317	22	0.38	AA	ref.	ref.
			GG	1.4	$4.7x10^{-2}$
rs62477268	7	0.32	AA	ref.	ref.
			GG	0.67	$4.7x10^{-2}$
rs3094097	6	0.27	AA	ref.	ref.
			GG	3.7	$4.7x10^{-2}$
rs14067	13	0.43	AA	ref.	ref.
			GG	1.4	$4.7x10^{-2}$
rs60612724	7	0.73	AA	ref.	ref.
			GG	0.26	$4.7x10^{-2}$
rs6438575	3	0.36	CC	ref.	ref.
			TT	1.4	$4.7x10^{-2}$
rs13040791	20	0.37	CC	ref.	ref.
			TT	1.4	$4.7x10^{-2}$
rs4442855	17	0.33	CC	ref.	ref.
			TT	0.44	$4.8x10^{-2}$
rs10250563	7	0.61	CC	ref.	ref.
			TT	1.5	$4.8x10^{-2}$
rs4791220	17	0.55	CC	ref.	ref.
			TT	1.6	$4.8x10^{-2}$

Continuation of Table A20

rs16964254	15	0.47	GG	ref.	ref.
			TT	3.2	$4.8x10^{-2}$
rs12578547	12	0.35	CC	ref.	ref.
			TT	1.6	$4.8x10^{-2}$
rs17693106	19	0.47	AA	ref.	ref.
			GG	1.4	$4.8x10^{-2}$
rs228277	17	0.29	CC	ref.	ref.
			GG	0.58	$4.8x10^{-2}$
rs1610216	16	0.32	AA	ref.	ref.
			GG	0.60	$4.8x10^{-2}$
rs4490220	2	0.29	AA	ref.	ref.
			GG	1.4	$4.8x10^{-2}$
rs6577049	13	0.27	CC	ref.	ref.
			TT	0.69	$4.8x10^{-2}$
rs10992639	9	0.44	CC	ref.	ref.
			TT	1.4	$4.8x10^{-2}$
rs10448090	8	0.45	AA	ref.	ref.
			TT	1.6	$4.8x10^{-2}$
rs3108809	13	0.31	AA	ref.	ref.
			GG	1.5	$4.8x10^{-2}$
rs2837503	21	0.32	CC	ref.	ref.
			GG	0.74	$4.8x10^{-2}$
rs7722687	5	0.39	GG	ref.	ref.
			TT	8.5	$4.8x10^{-2}$
rs2360737	17	0.27	CC	ref.	ref.
			TT	1.4	$4.8x10^{-2}$
rs11514809	7	0.48	AA	ref.	ref.
			GG	2.1	$4.8x10^{-2}$
rs12891732	14	0.43	CC	ref.	ref.
			TT	1.4	$4.8x10^{-2}$
rs12467859	2	0.27	AA	ref.	ref.
			TT	0.69	$4.8x10^{-2}$
rs4577309	2	0.32	AA	ref.	ref.
			GG	1.4	$4.8x10^{-2}$
rs10260959	7	0.58	GG	ref.	ref.
			TT	0.53	$4.8x10^{-2}$
rs2480	6	0.41	CC	ref.	ref.
			TT	1.4	$4.8x10^{-2}$
rs4236039	6	0.32	AA	ref.	ref.
			CC	0.66	$4.8x10^{-2}$
rs3990965	1	0.30	AA	ref.	ref.
			GG	0.58	$4.8x10^{-2}$
rs2877590	14	0.37	CC	ref.	ref.
			TT	1.4	$4.8x10^{-2}$
rs11577090	1	0.30	CC	ref.	ref.
			TT	0.72	$4.8x10^{-2}$
rs10819302	9	0.26	CC	ref.	ref.
			TT	0.12	$4.8x10^{-2}$
rs7599243	2	0.48	AA	ref.	ref.
			GG	0.48	$4.8x10^{-2}$
rs28504650	9	0.25	CC	ref.	ref.
			TT	1.4	$4.9x10^{-2}$

Continuation of Table A20

rs132721	22	0.50	AA	ref.	ref.
			GG	0.73	$4.9x10^{-2}$
rs1476679	7	0.26	CC	ref.	ref.
			TT	1.5	$4.9x10^{-2}$
rs7008955	8	0.35	GG	ref.	ref.
			TT	1.4	$4.9x10^{-2}$
rs2717068	2	0.34	AA	ref.	ref.
			CC	1.4	$4.9x10^{-2}$
rs1120330	7	0.39	CC	ref.	ref.
			TT	1.7	$4.9x10^{-2}$
rs6665129	1	0.26	AA	ref.	ref.
			GG	0.43	$4.9x10^{-2}$
rs2456512	15	0.45	CC	ref.	ref.
			TT	1.5	$4.9x10^{-2}$
rs1233666	6	0.30	AA	ref.	ref.
			CC	0.55	$4.9x10^{-2}$
rs12879393	14	0.27	CC	ref.	ref.
			TT	1.4	$4.9x10^{-2}$
rs72967450	2	0.30	AA	ref.	ref.
			GG	1.5	$4.9x10^{-2}$
rs6959056	7	0.28	AA	ref.	ref.
			GG	1.4	$4.9x10^{-2}$
rs6760458	2	0.25	CC	ref.	ref.
			GG	1.5	$4.9x10^{-2}$
rs7913156	10	0.34	AA	ref.	ref.
			GG	0.22	$4.9x10^{-2}$
rs6488075	12	0.30	AA	ref.	ref.
			GG	1.5	$4.9x10^{-2}$
rs10504127	8	0.30	AA	ref.	ref.
			GG	10.4	$4.9x10^{-2}$
rs7523530	1	0.41	AA	ref.	ref.
			GG	1.4	$4.9x10^{-2}$
rs7593448	2	0.57	CC	ref.	ref.
			GG	0.68	$4.9x10^{-2}$
rs4517889	19	0.45	CC	ref.	ref.
			TT	1.5	$4.9x10^{-2}$
rs12043212	1	0.37	AA	ref.	ref.
			GG	1.4	$4.9x10^{-2}$
rs28403936	12	0.25	AA	ref.	ref.
			GG	0.65	$4.9x10^{-2}$
rs7157201	14	0.39	CC	ref.	ref.
			TT	0.38	$4.9x10^{-2}$
rs35818720	19	0.35	AA	ref.	ref.
			GG	1.4	$4.9x10^{-2}$
rs2888892	12	0.28	CC	ref.	ref.
			TT	0.24	$4.9x10^{-2}$
rs137699	22	0.36	AA	ref.	ref.
			GG	1.4	$5.0x10^{-2}$
rs7620040	3	0.46	AA	ref.	ref.
			CC	1.4	$5.0x10^{-2}$
rs666796	18	0.27	CC	ref.	ref.
			TT	0.73	$5.0x10^{-2}$

Continuation of Table A20

rs1833459	17	0.27	AA	ref.	ref.
			GG	0.73	$5.0x10^{-2}$
rs418464	19	0.26	CC	ref.	ref.
			TT	0.73	$5.0x10^{-2}$
rs4074076	4	0.26	AA	ref.	ref.
			GG	1.5	$5.0x10^{-2}$
rs1890651	1	0.42	CC	ref.	ref.
			GG	0.74	$5.0x10^{-2}$
rs1000156	8	0.33	AA	ref.	ref.
			GG	0.59	$5.0x10^{-2}$
rs11114824	12	0.25	AA	ref.	ref.
			CC	0.19	$5.0x10^{-2}$

Abbreviations: F_{ST}, fixation index.

Table A21. SNPs with strongest association between genotype and cisplatin-induced vertigo phenotype ($p < 5.0x10^{-2}$)

SNP	chromosome	F_{ST}	Genotype	Vertigo Yes vs. No	
				OR	p-value
rs2297771	9	0.38	AA	ref.	ref.
			GG	0.098	$3.0x10^{-5}$
rs3777909	6	0.27	AA	ref.	ref.
			GG	0.21	$3.1x10^{-5}$
rs28516482	5	0.26	AA	ref.	ref.
			GG	0.091	$5.0x10^{-5}$
rs56819906	11	0.34	AA	ref.	ref.
			GG	0.14	$7.6x10^{-5}$
rs663398	1	0.26	AA	ref.	ref.
			GG	7.5	$1.2x10^{-4}$
rs73626678	11	0.33	CC	ref.	ref.
			TT	0.21	$1.8x10^{-4}$
rs308442	4	0.57	AA	ref.	ref.
			TT	0.27	$2.0x10^{-4}$
rs28405640	14	0.37	CC	ref.	ref.
			GG	4.0	$2.6x10^{-4}$
rs7704574	5	0.58	AA	ref.	ref.
			CC	0.24	$3.4x10^{-4}$
rs167428	4	0.53	CC	ref.	ref.
			TT	0.26	$4.2x10^{-4}$
rs9469327	6	0.47	CC	ref.	ref.
			TT	4.1	$5.4x10^{-4}$
rs7987832	13	0.41	AA	ref.	ref.
			GG	0.29	$5.5x10^{-4}$
rs1561398	5	0.44	CC	ref.	ref.
			TT	3.4	$5.9x10^{-4}$
rs289802	15	0.62	AA	ref.	ref.
			GG	0.091	$6.0x10^{-4}$
rs12890652	14	0.29	CC	ref.	ref.
			TT	0.32	$6.0x10^{-4}$
rs3924985	10	0.33	AA	ref.	ref.
			GG	0.16	$6.4x10^{-4}$
rs2716578	16	0.41	CC	ref.	ref.
			GG	0.19	$7.4x10^{-4}$
rs6789962	3	0.42	CC	ref.	ref.
			TT	0.14	$7.5x10^{-4}$
rs8108374	19	0.32	AA	ref.	ref.
			CC	0.28	$9.2x10^{-4}$
rs2603749	12	0.50	CC	ref.	ref.
			TT	0.14	$9.4x10^{-4}$
rs6871601	5	0.28	CC	ref.	ref.
			GG	0.29	$9.5x10^{-4}$
rs7297582	12	0.26	CC	ref.	ref.
			TT	3.3	$9.8x10^{-4}$
rs2976230	17	0.29	AA	ref.	ref.
			GG	3.7	$1.0x10^{-3}$
rs73870865	3	0.33	AA	ref.	ref.
			GG	0.068	$1.0x10^{-3}$

Continuation of Table A21

rs7560799	2	0.28	CC	ref.	ref.
			TT	0.29	$1.1x10^{-3}$
rs1076743	6	0.26	CC	ref.	ref.
			GG	3.6	$1.1x10^{-3}$
rs6704593	2	0.27	AA	ref.	ref.
			GG	0.34	$1.1x10^{-3}$
rs56218597	16	0.42	CC	ref.	ref.
			TT	0.23	$1.2x10^{-3}$
rs11757702	6	0.47	AA	ref.	ref.
			GG	5.7	$1.2x10^{-3}$
rs6767856	3	0.36	AA	ref.	ref.
			GG	5.6	$1.2x10^{-3}$
rs112192561	6	0.29	AA	ref.	ref.
			GG	0.21	$1.4x10^{-3}$
rs932917	10	0.29	AA	ref.	ref.
			CC	0.23	$1.4x10^{-3}$
rs2004197	6	0.28	AA	ref.	ref.
			CC	0.26	$1.5x10^{-3}$
rs4851000	2	0.34	CC	ref.	ref.
			TT	0.36	$1.6x10^{-3}$
rs4440991	11	0.53	AA	ref.	ref.
			TT	0.28	$1.6x10^{-3}$
rs58824895	2	0.33	CC	ref.	ref.
			TT	6.4	$1.7x10^{-3}$
rs9467046	6	0.32	AA	ref.	ref.
			GG	0.29	$1.8x10^{-3}$
rs4529254	5	0.30	GG	ref.	ref.
			TT	3.5	$1.8x10^{-3}$
rs1067399	2	0.31	AA	ref.	ref.
			GG	0.34	$2.3x10^{-3}$
rs948421	8	0.52	CC	ref.	ref.
			TT	0.31	$2.3x10^{-3}$
rs7129085	11	0.31	GG	ref.	ref.
			TT	6.2	$2.5x10^{-3}$
rs564913	17	0.44	AA	ref.	ref.
			CC	0.30	$2.6x10^{-3}$
rs2289500	3	0.41	CC	ref.	ref.
			GG	2.8	$2.7x10^{-3}$
rs6578259	11	0.43	AA	ref.	ref.
			TT	0.32	$2.8x10^{-3}$
rs7432556	3	0.29	CC	ref.	ref.
			TT	3.0	$2.9x10^{-3}$
rs9913445	17	0.54	CC	ref.	ref.
			TT	0.28	$2.9x10^{-3}$
rs1374795	3	0.33	AA	ref.	ref.
			GG	0.25	$3.1x10^{-3}$
rs11788775	9	0.25	AA	ref.	ref.
			GG	0.35	$3.2x10^{-3}$
rs7561569	2	0.40	AA	ref.	ref.
			CC	3.1	$3.2x10^{-3}$
rs7897357	10	0.47	CC	ref.	ref.
			TT	2.9	$3.4x10^{-3}$

Continuation of Table A21

rs7191766	16	0.41	AA	ref.	ref.
			GG	0.33	$3.5x10^{-3}$
rs8028552	15	0.28	CC	ref.	ref.
			TT	0.28	$3.5x10^{-3}$
rs2346747	3	0.40	AA	ref.	ref.
			GG	0.33	$3.6x10^{-3}$
rs2945905	8	0.29	GG	ref.	ref.
			TT	0.24	$3.8x10^{-3}$
rs12423277	12	0.42	AA	ref.	ref.
			CC	3.1	$3.9x10^{-3}$
rs673253	1	0.29	CC	ref.	ref.
			TT	2.9	$4.0x10^{-3}$
rs10786134	10	0.32	AA	ref.	ref.
			CC	0.20	$4.0x10^{-3}$
rs7048572	9	0.45	CC	ref.	ref.
			TT	0.30	$4.1x10^{-3}$
rs4888325	16	0.25	AA	ref.	ref.
			CC	0.34	$4.1x10^{-3}$
rs454182	6	0.37	CC	ref.	ref.
			GG	58	$4.1x10^{-3}$
rs9471070	6	0.54	CC	ref.	ref.
			TT	0.17	$4.2x10^{-3}$
rs4131218	2	0.60	AA	ref.	ref.
			GG	0.36	$4.2x10^{-3}$
rs10206472	2	0.37	CC	ref.	ref.
			GG	2.9	$4.2x10^{-3}$
rs7990359	13	0.28	AA	ref.	ref.
			GG	7.1	$4.3x10^{-3}$
rs62168405	2	0.27	CC	ref.	ref.
			TT	0.35	$4.3x10^{-3}$
rs1085495	2	0.29	AA	ref.	ref.
			GG	0.35	$4.4x10^{-3}$
rs11834161	12	0.25	AA	ref.	ref.
			CC	0.16	$4.4x10^{-3}$
rs9378357	6	0.36	GG	ref.	ref.
			TT	6.1	$4.5x10^{-3}$
rs4464929	8	0.35	CC	ref.	ref.
			GG	0.23	$4.6x10^{-3}$
rs34382810	12	0.28	AA	ref.	ref.
			CC	2.7	$4.6x10^{-3}$
rs9487668	6	0.49	AA	ref.	ref.
			GG	0.32	$4.7x10^{-3}$
rs2028554	8	0.32	GG	ref.	ref.
			TT	0.32	$4.7x10^{-3}$
rs11604893	11	0.46	CC	ref.	ref.
			TT	0.34	$4.7x10^{-3}$
rs4953598	2	0.27	CC	ref.	ref.
			TT	3.1	$4.7x10^{-3}$
rs7742724	6	0.39	AA	ref.	ref.
			GG	0.35	$4.8x10^{-3}$
rs11720410	3	0.28	CC	ref.	ref.
			TT	0.33	$5.0x10^{-3}$

Continuation of Table A21

rs4809718	20	0.39	AA	ref.	ref.
			TT	0.31	$5.1x10^{-3}$
rs11871088	17	0.27	AA	ref.	ref.
			GG	0.31	$5.1x10^{-3}$
rs60075147	21	0.29	AA	ref.	ref.
			GG	0.26	$5.3x10^{-3}$
rs7635650	3	0.34	AA	ref.	ref.
			TT	0.27	$5.4x10^{-3}$
rs12802652	11	0.27	GG	ref.	ref.
			TT	2.8	$5.4x10^{-3}$
rs8046826	16	0.52	AA	ref.	ref.
			GG	2.9	$5.5x10^{-3}$
rs7587670	2	0.28	AA	ref.	ref.
			GG	0.35	$5.6x10^{-3}$
rs943284	13	0.53	AA	ref.	ref.
			GG	2.9	$5.7x10^{-3}$
rs73187868	7	0.26	AA	ref.	ref.
			GG	0.35	$5.8x10^{-3}$
rs2842193	1	0.25	CC	ref.	ref.
			TT	0.34	$5.9x10^{-3}$
rs4275402	1	0.29	CC	ref.	ref.
			TT	0.37	$6.0x10^{-3}$
rs7005674	8	0.32	AA	ref.	ref.
			GG	0.12	$6.1x10^{-3}$
rs28469605	9	0.28	CC	ref.	ref.
			TT	2.8	$6.2x10^{-3}$
rs174373	6	0.29	CC	ref.	ref.
			TT	3.1	$6.2x10^{-3}$
rs200854587	6	0.30	GG	ref.	ref.
			TT	5.5	$6.2x10^{-3}$
rs6903242	6	0.26	AA	ref.	ref.
			GG	0.14	$6.2x10^{-3}$
rs62526680	8	0.25	AA	ref.	ref.
			GG	3.5	$6.2x10^{-3}$
rs4660446	1	0.36	CC	ref.	ref.
			TT	2.7	$6.2x10^{-3}$
rs4147332	8	0.26	CC	ref.	ref.
			GG	2.5	$6.4x10^{-3}$
rs1109866	2	0.42	CC	ref.	ref.
			TT	0.20	$6.4x10^{-3}$
rs12550773	8	0.46	CC	ref.	ref.
			TT	3.1	$6.8x10^{-3}$
rs9357291	6	0.27	AA	ref.	ref.
			GG	0.39	$6.9x10^{-3}$
rs11242110	5	0.34	GG	ref.	ref.
			TT	3.2	$6.9x10^{-3}$
rs2370414	12	0.30	AA	ref.	ref.
			GG	2.6	$7.0x10^{-3}$
rs17622656	5	0.26	AA	ref.	ref.
			GG	0.37	$7.2x10^{-3}$
rs9633995	11	0.25	AA	ref.	ref.
			CC	2.8	$7.2x10^{-3}$

Continuation of Table A21

rs786618	2	0.31	CC	ref.	ref.
			TT	0.39	$7.2x10^{-3}$
rs28841991	1	0.28	AA	ref.	ref.
			GG	0.19	$7.2x10^{-3}$
rs1806790	10	0.26	CC	ref.	ref.
			TT	2.6	$7.4x10^{-3}$
rs11161750	1	0.35	AA	ref.	ref.
			GG	0.35	$7.4x10^{-3}$
rs6026445	20	0.26	AA	ref.	ref.
			GG	0.23	$8.1x10^{-3}$
rs1955026	8	0.36	CC	ref.	ref.
			TT	10.0	$8.1x10^{-3}$
rs258099	16	0.48	CC	ref.	ref.
			TT	0.36	$8.2x10^{-3}$
rs2634675	12	0.43	AA	ref.	ref.
			GG	0.35	$8.3x10^{-3}$
rs7566508	2	0.32	AA	ref.	ref.
			CC	0.27	$8.3x10^{-3}$
rs6790517	3	0.30	CC	ref.	ref.
			TT	3.7	$8.5x10^{-3}$
rs10950696	7	0.45	CC	ref.	ref.
			TT	5.6	$8.8x10^{-3}$
rs2007044	12	0.36	AA	ref.	ref.
			GG	2.6	$8.9x10^{-3}$
rs2531361	5	0.26	AA	ref.	ref.
			GG	3.1	$8.9x10^{-3}$
rs10857438	10	0.39	CC	ref.	ref.
			TT	0.42	$8.9x10^{-3}$
rs17158441	15	0.35	GG	ref.	ref.
			TT	0.040	$9.0x10^{-3}$
rs56007435	4	0.54	AA	ref.	ref.
			GG	2.6	$9.2x10^{-3}$
rs1016364	11	0.31	AA	ref.	ref.
			GG	3.4	$9.3x10^{-3}$
rs1580278	4	0.39	AA	ref.	ref.
			CC	0.33	$9.4x10^{-3}$
rs4849727	2	0.25	AA	ref.	ref.
			GG	0.30	$9.5x10^{-3}$
rs6663581	1	0.26	AA	ref.	ref.
			GG	0.27	$9.6x10^{-3}$
rs1854156	9	0.33	CC	ref.	ref.
			GG	0.21	$9.6x10^{-3}$
rs2900177	9	0.37	CC	ref.	ref.
			TT	0.38	$9.6x10^{-3}$
rs242596	4	0.27	CC	ref.	ref.
			TT	0.20	$9.6x10^{-3}$
rs13202545	6	0.29	AA	ref.	ref.
			GG	22	$9.7x10^{-3}$
rs7956181	12	0.27	CC	ref.	ref.
			TT	0.17	$9.7x10^{-3}$
rs3810232	19	0.26	AA	ref.	ref.
			CC	2.7	$9.8x10^{-3}$

Continuation of Table A21

rs7638848	3	0.29	AA	ref.	ref.
			GG	0.34	$1.0x10^{-2}$
rs9311268	3	0.26	AA	ref.	ref.
			GG	3.2	$1.0x10^{-2}$
rs2292404	3	0.25	AA	ref.	ref.
			GG	0.25	$1.0x10^{-2}$
rs17467210	8	0.39	AA	ref.	ref.
			GG	0.41	$1.0x10^{-2}$
rs55693289	18	0.34	AA	ref.	ref.
			GG	0.46	$1.0x10^{-2}$
rs1594968	8	0.49	CC	ref.	ref.
			GG	4.9	$1.0x10^{-2}$
rs3764912	9	0.27	AA	ref.	ref.
			GG	0.38	$1.1x10^{-2}$
rs769246	4	0.41	AA	ref.	ref.
			GG	2.6	$1.1x10^{-2}$
rs12610863	19	0.25	AA	ref.	ref.
			GG	0.39	$1.1x10^{-2}$
rs2232935	11	0.28	GG	ref.	ref.
			TT	5.3	$1.1x10^{-2}$
rs2098728	16	0.31	AA	ref.	ref.
			GG	2.5	$1.1x10^{-2}$
rs10231090	7	0.30	AA	ref.	ref.
			TT	2.6	$1.1x10^{-2}$
rs6455712	6	0.28	AA	ref.	ref.
			GG	0.37	$1.1x10^{-2}$
rs6803404	3	0.31	AA	ref.	ref.
			GG	5.1	$1.1x10^{-2}$
rs7207255	17	0.31	AA	ref.	ref.
			GG	2.6	$1.1x10^{-2}$
rs28436997	18	0.25	CC	ref.	ref.
			TT	0.29	$1.1x10^{-2}$
rs4438438	2	0.37	AA	ref.	ref.
			GG	0.37	$1.1x10^{-2}$
rs37470	1	0.26	CC	ref.	ref.
			GG	0.39	$1.1x10^{-2}$
rs10238028	7	0.76	AA	ref.	ref.
			GG	6.5	$1.1x10^{-2}$
rs4635011	10	0.35	CC	ref.	ref.
			TT	0.26	$1.1x10^{-2}$
rs6801800	3	0.55	AA	ref.	ref.
			GG	6.5	$1.1x10^{-2}$
rs6753723	2	0.37	CC	ref.	ref.
			TT	2.5	$1.2x10^{-2}$
rs9831488	3	0.53	AA	ref.	ref.
			GG	2.5	$1.2x10^{-2}$
rs7328253	13	0.34	AA	ref.	ref.
			CC	0.37	$1.2x10^{-2}$
rs11161497	1	0.45	AA	ref.	ref.
			GG	2.7	$1.2x10^{-2}$
rs7722687	5	0.39	GG	ref.	ref.
			TT	7.2	$1.2x10^{-2}$

Continuation of Table A21

rs6855458	4	0.52	AA	ref.	ref.
			GG	2.6	$1.2x10^{-2}$
rs11050147	12	0.36	GG	ref.	ref.
			TT	2.8	$1.2x10^{-2}$
rs924201	1	0.35	AA	ref.	ref.
			GG	0.19	$1.2x10^{-2}$
rs10925182	1	0.42	CC	ref.	ref.
			TT	0.44	$1.2x10^{-2}$
rs3765581	10	0.45	CC	ref.	ref.
			TT	3.6	$1.2x10^{-2}$
rs4234597	3	0.33	AA	ref.	ref.
			TT	2.9	$1.2x10^{-2}$
rs13136171	4	0.25	AA	ref.	ref.
			TT	0.40	$1.2x10^{-2}$
rs66500441	1	0.26	AA	ref.	ref.
			GG	0.43	$1.2x10^{-2}$
rs6584190	10	0.60	CC	ref.	ref.
			TT	0.25	$1.3x10^{-2}$
rs12600113	16	0.27	CC	ref.	ref.
			TT	2.5	$1.3x10^{-2}$
rs6090435	20	0.29	AA	ref.	ref.
			GG	4.0	$1.3x10^{-2}$
rs893220	15	0.28	CC	ref.	ref.
			TT	0.43	$1.3x10^{-2}$
rs9371533	6	0.31	AA	ref.	ref.
			GG	3.8	$1.3x10^{-2}$
rs9468628	6	0.26	CC	ref.	ref.
			TT	5.7	$1.3x10^{-2}$
rs7009759	8	0.44	CC	ref.	ref.
			GG	0.36	$1.3x10^{-2}$
rs2117341	21	0.33	AA	ref.	ref.
			GG	0.16	$1.3x10^{-2}$
rs422646	11	0.26	AA	ref.	ref.
			CC	0.42	$1.3x10^{-2}$
rs7544839	1	0.25	AA	ref.	ref.
			CC	0.36	$1.3x10^{-2}$
rs10495760	2	0.31	AA	ref.	ref.
			GG	0.38	$1.3x10^{-2}$
rs690467	15	0.58	AA	ref.	ref.
			GG	0.35	$1.3x10^{-2}$
rs12466957	2	0.28	AA	ref.	ref.
			GG	0.39	$1.3x10^{-2}$
rs878422	8	0.36	AA	ref.	ref.
			GG	3.1	$1.3x10^{-2}$
rs4953082	2	0.37	AA	ref.	ref.
			GG	2.4	$1.3x10^{-2}$
rs1882119	12	0.36	CC	ref.	ref.
			TT	0.26	$1.3x10^{-2}$
rs2780816	1	0.34	AA	ref.	ref.
			CC	0.37	$1.4x10^{-2}$
rs3828044	1	0.30	CC	ref.	ref.
			GG	0.27	$1.4x10^{-2}$

Continuation of Table A21

rs2341354	1	0.26	AA	ref.	ref.
			GG	0.41	$1.4x10^{-2}$
rs7417106	1	0.26	AA	ref.	ref.
			GG	0.34	$1.4x10^{-2}$
rs1317945	2	0.34	AA	ref.	ref.
			GG	0.28	$1.4x10^{-2}$
rs11781637	8	0.25	AA	ref.	ref.
			GG	3.7	$1.4x10^{-2}$
rs12322561	12	0.41	AA	ref.	ref.
			GG	5.2	$1.4x10^{-2}$
rs62206951	20	0.31	CC	ref.	ref.
			TT	3.2	$1.4x10^{-2}$
rs2921755	8	0.30	AA	ref.	ref.
			GG	0.27	$1.4x10^{-2}$
rs462581	5	0.28	CC	ref.	ref.
			GG	2.8	$1.4x10^{-2}$
rs10781539	9	0.26	AA	ref.	ref.
			GG	3.4	$1.4x10^{-2}$
rs9509447	13	0.43	CC	ref.	ref.
			TT	2.9	$1.4x10^{-2}$
rs2370413	12	0.45	CC	ref.	ref.
			TT	0.43	$1.4x10^{-2}$
rs2425637	20	0.26	GG	ref.	ref.
			TT	0.37	$1.4x10^{-2}$
rs4958849	5	0.29	AA	ref.	ref.
			GG	3.4	$1.4x10^{-2}$
rs10162914	15	0.39	CC	ref.	ref.
			TT	0.28	$1.4x10^{-2}$
rs3808862	9	0.27	AA	ref.	ref.
			GG	0.36	$1.4x10^{-2}$
rs35442897	12	0.27	CC	ref.	ref.
			TT	3.0	$1.4x10^{-2}$
rs2185490	14	0.35	AA	ref.	ref.
			CC	0.39	$1.5x10^{-2}$
rs146301201	3	0.31	CC	ref.	ref.
			TT	2.9	$1.5x10^{-2}$
rs2517261	8	0.35	CC	ref.	ref.
			TT	0.40	$1.5x10^{-2}$
rs61828523	1	0.27	AA	ref.	ref.
			GG	2.6	$1.5x10^{-2}$
rs1468603	12	0.26	CC	ref.	ref.
			TT	0.43	$1.5x10^{-2}$
rs13014512	2	0.27	AA	ref.	ref.
			TT	3.2	$1.5x10^{-2}$
rs2263511	8	0.31	AA	ref.	ref.
			CC	0.28	$1.5x10^{-2}$
rs1071664	17	0.25	AA	ref.	ref.
			GG	0.25	$1.5x10^{-2}$
rs2488553	9	0.39	AA	ref.	ref.
			GG	2.8	$1.5x10^{-2}$
rs2929395	3	0.36	AA	ref.	ref.
			GG	3.2	$1.5x10^{-2}$

Continuation of Table A21

rs5764733	22	0.33	CC	ref.	ref.
			GG	2.5	$1.6x10^{-2}$
rs7200013	16 (cisplatin)	0.31	AA	ref.	ref.
			GG	0.41	$1.6x10^{-2}$
rs12702528	7	0.38	CC	ref.	ref.
			TT	0.33	$1.6x10^{-2}$
rs762953	22	0.37	AA	ref.	ref.
			GG	0.42	$1.6x10^{-2}$
rs281382	19	0.29	AA	ref.	ref.
			GG	3.8	$1.6x10^{-2}$
rs1920659	3	0.26	AA	ref.	ref.
			TT	0.30	$1.6x10^{-2}$
rs10008069	4	0.29	AA	ref.	ref.
			GG	0.40	$1.6x10^{-2}$
rs6669160	1	0.32	AA	ref.	ref.
			GG	14.6	$1.6x10^{-2}$
rs9180	22	0.49	CC	ref.	ref.
			TT	0.39	$1.6x10^{-2}$
rs4716408	6	0.32	CC	ref.	ref.
			TT	0.40	$1.6x10^{-2}$
rs162430	17	0.30	AA	ref.	ref.
			GG	0.25	$1.6x10^{-2}$
rs2641526	12	0.37	AA	ref.	ref.
			GG	6.8	$1.6x10^{-2}$
rs12644	10	0.64	CC	ref.	ref.
			TT	0.030	$1.6x10^{-2}$
rs55649245	2	0.34	AA	ref.	ref.
			GG	0.39	$1.6x10^{-2}$
rs7350746	14	0.34	CC	ref.	ref.
			TT	3.0	$1.6x10^{-2}$
rs740495	19	0.26	AA	ref.	ref.
			GG	2.4	$1.6x10^{-2}$
rs2815376	1	0.32	AA	ref.	ref.
			GG	2.5	$1.6x10^{-2}$
rs7082507	10	0.35	GG	ref.	ref.
			TT	0.40	$1.6x10^{-2}$
rs5746439	22	0.32	AA	ref.	ref.
			GG	2.9	$1.7x10^{-2}$
rs214086	11	0.29	CC	ref.	ref.
			GG	3.3	$1.7x10^{-2}$
rs2086655	5	0.31	AA	ref.	ref.
			CC	2.5	$1.7x10^{-2}$
rs2924	1	0.38	AA	ref.	ref.
			GG	2.6	$1.7x10^{-2}$
rs62302275	4	0.26	AA	ref.	ref.
			GG	2.4	$1.7x10^{-2}$
rs2805906	10	0.30	CC	ref.	ref.
			GG	0.40	$1.7x10^{-2}$
rs7523508	1	0.53	AA	ref.	ref.
			GG	2.5	$1.7x10^{-2}$
rs11687195	2	0.37	AA	ref.	ref.
			GG	0.39	$1.7x10^{-2}$

Continuation of Table A21

rs28374262	2	0.46	AA	ref.	ref.
			GG	0.35	$1.7x10^{-2}$
rs10282706	7	0.59	AA	ref.	ref.
			GG	0.20	$1.7x10^{-2}$
rs80141110	4	0.26	CC	ref.	ref.
			TT	2.2	$1.7x10^{-2}$
rs2031006	16	0.74	CC	ref.	ref.
			GG	6.3	$1.7x10^{-2}$
rs304653	4	0.58	CC	ref.	ref.
			TT	0.39	$1.8x10^{-2}$
rs9840622	3	0.52	CC	ref.	ref.
			TT	3.6	$1.8x10^{-2}$
rs8019864	14	0.29	CC	ref.	ref.
			GG	0.062	$1.8x10^{-2}$
rs11667051	19	0.27	AA	ref.	ref.
			GG	2.3	$1.8x10^{-2}$
rs2991690	9	0.31	CC	ref.	ref.
			GG	2.2	$1.8x10^{-2}$
rs2003532	7	0.38	CC	ref.	ref.
			TT	2.8	$1.8x10^{-2}$
rs652348	18	0.31	CC	ref.	ref.
			TT	0.31	$1.8x10^{-2}$
rs1429146	6	0.27	CC	ref.	ref.
			TT	2.7	$1.8x10^{-2}$
rs6459465	6	0.41	CC	ref.	ref.
			GG	0.38	$1.8x10^{-2}$
rs751946	10	0.28	AA	ref.	ref.
			GG	4.5	$1.8x10^{-2}$
rs10264122	7	0.26	CC	ref.	ref.
			TT	0.27	$1.8x10^{-2}$
rs9449841	6	0.47	GG	ref.	ref.
			TT	0.16	$1.8x10^{-2}$
rs7185839	16	0.50	GG	ref.	ref.
			TT	0.17	$1.8x10^{-2}$
rs519834	11	0.40	CC	ref.	ref.
			TT	0.38	$1.8x10^{-2}$
rs10987708	9	0.52	AA	ref.	ref.
			GG	5.1	$1.9x10^{-2}$
rs67426328	15	0.33	CC	ref.	ref.
			GG	0.28	$1.9x10^{-2}$
rs11780158	8	0.33	CC	ref.	ref.
			TT	2.4	$1.9x10^{-2}$
rs2733617	15	0.35	CC	ref.	ref.
			TT	0.39	$1.9x10^{-2}$
rs1338624	1	0.51	AA	ref.	ref.
			GG	0.26	$1.9x10^{-2}$
rs3176336	6	0.40	AA	ref.	ref.
			TT	0.43	$1.9x10^{-2}$
rs6584195	10	0.28	AA	ref.	ref.
			GG	0.44	$1.9x10^{-2}$
rs10030922	4	0.28	CC	ref.	ref.
			TT	0.42	$1.9x10^{-2}$

Continuation of Table A21

rs59305313	16	0.39	CC	ref.	ref.
			GG	2.5	$1.9x10^{-2}$
rs1722845	3	0.26	CC	ref.	ref.
			TT	2.6	$1.9x10^{-2}$
rs10906912	10	0.28	AA	ref.	ref.
			GG	0.47	$1.9x10^{-2}$
rs11634351	15	0.34	AA	ref.	ref.
			GG	3.2	$1.9x10^{-2}$
rs10900836	5	0.40	CC	ref.	ref.
			TT	2.7	$1.9x10^{-2}$
rs2395307	6	0.27	GG	ref.	ref.
			TT	0.34	$1.9x10^{-2}$
rs2157104	4	0.44	AA	ref.	ref.
			TT	2.5	$1.9x10^{-2}$
rs6696888	1	0.61	AA	ref.	ref.
			GG	0.19	$1.9x10^{-2}$
rs11101383	10	0.26	CC	ref.	ref.
			TT	0.44	$1.9x10^{-2}$
rs3757960	8	0.28	CC	ref.	ref.
			GG	2.5	$1.9x10^{-2}$
rs3917263	2	0.27	CC	ref.	ref.
			GG	0.44	$1.9x10^{-2}$
rs12416994	11	0.38	CC	ref.	ref.
			TT	0.42	$1.9x10^{-2}$
rs2409807	8	0.47	AA	ref.	ref.
			GG	0.38	$1.9x10^{-2}$
rs56177149	8	0.25	AA	ref.	ref.
			GG	0.22	$2.0x10^{-2}$
rs10161020	12	0.30	CC	ref.	ref.
			TT	0.19	$2.0x10^{-2}$
rs7164838	15	0.26	AA	ref.	ref.
			GG	0.41	$2.0x10^{-2}$
rs4244480	11	0.31	CC	ref.	ref.
			TT	0.41	$2.0x10^{-2}$
rs11236350	11	0.28	CC	ref.	ref.
			TT	0.35	$2.0x10^{-2}$
rs8037089	15	0.25	AA	ref.	ref.
			GG	0.43	$2.0x10^{-2}$
rs158761	1	0.28	AA	ref.	ref.
			CC	3.2	$2.0x10^{-2}$
rs10169414	2	0.26	CC	ref.	ref.
			TT	0.38	$2.0x10^{-2}$
rs8032781	15	0.27	CC	ref.	ref.
			GG	0.39	$2.0x10^{-2}$
rs752446	8	0.25	AA	ref.	ref.
			GG	4.1	$2.0x10^{-2}$
rs11230914	11	0.36	CC	ref.	ref.
			GG	0.35	$2.0x10^{-2}$
rs9857908	3	0.39	CC	ref.	ref.
			TT	2.3	$2.0x10^{-2}$
rs2048459	3	0.54	AA	ref.	ref.
			GG	0.28	$2.1x10^{-2}$

Continuation of Table A21

rs111990	1	0.31	AA	ref.	ref.
			CC	0.45	$2.1x10^{-2}$
rs729022	1	0.45	CC	ref.	ref.
			TT	6.0	$2.1x10^{-2}$
rs7946916	11	0.50	CC	ref.	ref.
			TT	2.8	$2.1x10^{-2}$
rs56320525	19	0.31	CC	ref.	ref.
			TT	0.41	$2.1x10^{-2}$
rs3856810	3	0.40	CC	ref.	ref.
			TT	5.6	$2.1x10^{-2}$
rs57103278	16	0.30	CC	ref.	ref.
			GG	0.11	$2.1x10^{-2}$
rs55746797	17	0.30	AA	ref.	ref.
			GG	0.41	$2.1x10^{-2}$
rs10104421	8	0.26	AA	ref.	ref.
			GG	0.41	$2.1x10^{-2}$
rs7216019	17 (cisplatin)	0.49	AA	ref.	ref.
			GG	0.41	$2.1x10^{-2}$
rs10023020	4	0.29	AA	ref.	ref.
			GG	4.1	$2.2x10^{-2}$
rs8065158	17	0.36	AA	ref.	ref.
			GG	2.3	$2.2x10^{-2}$
rs647423	15	0.37	AA	ref.	ref.
			GG	0.39	$2.2x10^{-2}$
rs13266003	8	0.52	AA	ref.	ref.
			GG	0.42	$2.2x10^{-2}$
rs1474927	1	0.51	AA	ref.	ref.
			GG	0.25	$2.2x10^{-2}$
rs2528585	2	0.27	AA	ref.	ref.
			GG	0.36	$2.2x10^{-2}$
rs7004998	8	0.25	GG	ref.	ref.
			TT	0.21	$2.2x10^{-2}$
rs76919723	15	0.28	CC	ref.	ref.
			TT	3.1	$2.2x10^{-2}$
rs1110002	2	0.25	CC	ref.	ref.
			GG	2.4	$2.2x10^{-2}$
rs11724635	4	0.38	AA	ref.	ref.
			CC	2.1	$2.2x10^{-2}$
rs4326897	13	0.39	AA	ref.	ref.
			GG	0.42	$2.2x10^{-2}$
rs10104438	8	0.59	AA	ref.	ref.
			GG	2.4	$2.3x10^{-2}$
rs10118790	9	0.51	AA	ref.	ref.
			GG	0.26	$2.3x10^{-2}$
rs9934217	16	0.46	AA	ref.	ref.
			CC	3.2	$2.3x10^{-2}$
rs62389864	5	0.34	AA	ref.	ref.
			GG	3.1	$2.3x10^{-2}$
rs342511	3	0.25	AA	ref.	ref.
			GG	2.3	$2.3x10^{-2}$
rs55648810	11	0.25	CC	ref.	ref.
			TT	0.25	$2.3x10^{-2}$

Continuation of Table A21

rs2586205	18	0.66	GG	ref.	ref.
			TT	2.8	$2.3x10^{-2}$
rs4075641	15	0.52	AA	ref.	ref.
			GG	0.23	$2.3x10^{-2}$
rs7731564	5	0.39	CC	ref.	ref.
			TT	3.2	$2.3x10^{-2}$
rs4774979	15	0.30	AA	ref.	ref.
			GG	0.41	$2.3x10^{-2}$
rs55639815	2	0.28	AA	ref.	ref.
			GG	10.2	$2.3x10^{-2}$
rs2121941	16	0.26	AA	ref.	ref.
			GG	2.3	$2.3x10^{-2}$
rs4349188	17	0.41	CC	ref.	ref.
			TT	2.6	$2.3x10^{-2}$
rs62262502	3	0.36	CC	ref.	ref.
			TT	2.4	$2.3x10^{-2}$
rs28877870	16	0.37	CC	ref.	ref.
			GG	0.078	$2.3x10^{-2}$
rs6809724	3	0.31	AA	ref.	ref.
			GG	2.9	$2.3x10^{-2}$
rs6779422	3	0.32	AA	ref.	ref.
			GG	0.25	$2.3x10^{-2}$
rs2707755	12	0.37	GG	ref.	ref.
			TT	3.4	$2.3x10^{-2}$
rs659805	8	0.37	CC	ref.	ref.
			TT	0.39	$2.3x10^{-2}$
rs1368393	5	0.25	AA	ref.	ref.
			GG	2.4	$2.3x10^{-2}$
rs61749301	18	0.27	CC	ref.	ref.
			TT	3.1	$2.4x10^{-2}$
rs4071641	17	0.36	CC	ref.	ref.
			TT	2.3	$2.4x10^{-2}$
rs10887943	10	0.44	AA	ref.	ref.
			GG	0.45	$2.4x10^{-2}$
rs1532401	6	0.40	CC	ref.	ref.
			TT	0.18	$2.4x10^{-2}$
rs7837545	8	0.35	CC	ref.	ref.
			TT	0.42	$2.4x10^{-2}$
rs3791878	2	0.28	GG	ref.	ref.
			TT	2.4	$2.4x10^{-2}$
rs2182220	13	0.53	AA	ref.	ref.
			GG	0.44	$2.4x10^{-2}$
rs4467387	3	0.34	CC	ref.	ref.
			TT	2.7	$2.4x10^{-2}$
rs10785127	12	0.42	CC	ref.	ref.
			TT	0.40	$2.4x10^{-2}$
rs55952639	2	0.29	CC	ref.	ref.
			TT	0.18	$2.4x10^{-2}$
rs4725972	7	0.26	AA	ref.	ref.
			GG	0.43	$2.4x10^{-2}$
rs9526573	13	0.50	CC	ref.	ref.
			TT	6.8	$2.4x10^{-2}$

Continuation of Table A21

rs4570414	1	0.50	GG	ref.	ref.
			TT	0.47	$2.4x10^{-2}$
rs2863234	10	0.27	CC	ref.	ref.
			TT	3.6	$2.4x10^{-2}$
rs1553850	10	0.36	AA	ref.	ref.
			TT	2.3	$2.4x10^{-3}$
rs4339575	7	0.26	AA	ref.	ref.
			GG	0.37	$2.4x10^{-2}$
rs1288852	15	0.45	CC	ref.	ref.
			TT	4.7	$2.4x10^{-2}$
rs6436978	2	0.26	CC	ref.	ref.
			TT	3.9	$2.4x10^{-2}$
rs61115773	8	0.31	AA	ref.	ref.
			CC	0.41	$2.4x10^{-2}$
rs4683180	3	0.31	CC	ref.	ref.
			TT	2.5	$2.4x10^{-2}$
rs11693314	2	0.27	CC	ref.	ref.
			TT	2.4	$2.4x10^{-2}$
rs835592	12	0.26	CC	ref.	ref.
			TT	2.9	$2.5x10^{-2}$
rs12893484	14	0.27	AA	ref.	ref.
			GG	2.5	$2.5x10^{-2}$
rs11794029	9	0.27	CC	ref.	ref.
			GG	0.44	$2.5x10^{-2}$
rs9353335	6	0.33	AA	ref.	ref.
			GG	2.3	$2.5x10^{-2}$
rs595413	6	0.54	CC	ref.	ref.
			TT	6.0	$2.5x10^{-2}$
rs3787137	20	0.43	AA	ref.	ref.
			GG	2.2	$2.5x10^{-2}$
rs55862027	12	0.28	AA	ref.	ref.
			CC	4.7	$2.5x10^{-2}$
rs72794414	5	0.25	AA	ref.	ref.
			GG	0.25	$2.5x10^{-2}$
rs186348799	7	0.31	CC	ref.	ref.
			TT	2.5	$2.5x10^{-2}$
rs822490	1	0.36	CC	ref.	ref.
			TT	5.5	$2.5x10^{-2}$
rs66559745	1	0.33	AA	ref.	ref.
			GG	0.42	$2.5x10^{-2}$
rs13253543	8	0.25	AA	ref.	ref.
			GG	2.2	$2.5x10^{-2}$
rs4635556	2	0.26	CC	ref.	ref.
			GG	2.3	$2.5x10^{-2}$
rs7318195	13	0.33	CC	ref.	ref.
			GG	0.41	$2.5x10^{-2}$
rs6907381	6	0.27	AA	ref.	ref.
			GG	0.30	$2.5x10^{-2}$
rs34213675	8	0.44	CC	ref.	ref.
			TT	3.0	$2.5x10^{-2}$
rs7144975	14	0.45	GG	ref.	ref.
			TT	2.1	$2.5x10^{-2}$

Continuation of Table A21

rs1582958	5	0.36	AA	ref.	ref.
			GG	0.41	$2.5x10^{-2}$
rs7498934	16	0.29	AA	ref.	ref.
			GG	2.3	$2.5x10^{-2}$
rs13267976	8	0.33	AA	ref.	ref.
			CC	4.0	$2.5x10^{-2}$
rs4314513	6	0.27	AA	ref.	ref.
			GG	2.8	$2.5x10^{-2}$
rs16896398	6	0.26	AA	ref.	ref.
			TT	2.2	$2.5x10^{-2}$
rs1085447	2	0.28	AA	ref.	ref.
			GG	0.42	$2.5x10^{-2}$
rs4458029	17	0.42	AA	ref.	ref.
			GG	0.41	$2.5x10^{-2}$
rs3820610	1	0.39	CC	ref.	ref.
			TT	3.9	$2.5x10^{-2}$
rs27129	5	0.40	CC	ref.	ref.
			GG	0.26	$2.5x10^{-2}$
rs2488098	6	0.27	CC	ref.	ref.
			TT	0.45	$2.6x10^{-2}$
rs911043	20	0.52	GG	ref.	ref.
			TT	0.45	$2.6x10^{-2}$
rs927565	20	0.26	GG	ref.	ref.
			TT	0.27	$2.6x10^{-2}$
rs35193178	17	0.26	AA	ref.	ref.
			GG	2.9	$2.6x10^{-2}$
rs2844477	6	0.32	CC	ref.	ref.
			TT	0.45	$2.6x10^{-2}$
rs3768725	2	0.29	CC	ref.	ref.
			GG	0.24	$2.6x10^{-2}$
rs6946598	7	0.32	CC	ref.	ref.
			TT	0.28	$2.6x10^{-2}$
rs10945597	6	0.43	CC	ref.	ref.
			TT	4.0	$2.6x10^{-2}$
rs10458162	6	0.27	CC	ref.	ref.
			TT	2.2	$2.6x10^{-2}$
rs10953289	7	0.41	CC	ref.	ref.
			GG	0.13	$2.6x10^{-2}$
rs3611	8	0.26	CC	ref.	ref.
			TT	2.3	$2.7x10^{-2}$
rs11853076	15	0.51	AA	ref.	ref.
			TT	0.33	$2.7x10^{-2}$
rs10043238	5	0.47	CC	ref.	ref.
			GG	0.46	$2.7x10^{-2}$
rs7324901	13	0.33	CC	ref.	ref.
			GG	2.2	$2.7x10^{-2}$
rs17232243	16	0.41	AA	ref.	ref.
			GG	2.6	$2.7x10^{-2}$
rs1171086	13	0.31	AA	ref.	ref.
			GG	0.41	$2.7x10^{-2}$
rs41377249	13	0.34	AA	ref.	ref.
			GG	0.47	$2.7x10^{-2}$

Continuation of Table A21

rs11673515	19	0.37	CC	ref.	ref.
			GG	0.11	$2.7x10^{-2}$
rs1811328	4	0.26	AA	ref.	ref.
			CC	0.44	$2.7x10^{-2}$
rs11690820	2	0.33	AA	ref.	ref.
			GG	2.4	$2.7x10^{-2}$
rs3764855	17	0.39	CC	ref.	ref.
			TT	0.33	$2.7x10^{-2}$
rs748193	8	0.31	CC	ref.	ref.
			TT	0.37	$2.7x10^{-2}$
rs299218	5	0.26	CC	ref.	ref.
			TT	0.24	$2.7x10^{-2}$
rs10751753	10	0.63	AA	ref.	ref.
			GG	0.28	$2.8x10^{-2}$
rs16978956	20	0.34	AA	ref.	ref.
			GG	2.4	$2.8x10^{-2}$
rs3117227	6	0.27	AA	ref.	ref.
			GG	5.1	$2.8x10^{-2}$
rs4653750	1	0.34	AA	ref.	ref.
			TT	3.0	$2.8x10^{-2}$
rs11580264	1	0.26	AA	ref.	ref.
			CC	0.46	$2.8x10^{-2}$
rs2967774	19	0.45	AA	ref.	ref.
			GG	3.1	$2.8x10^{-2}$
rs11176078	12	0.25	CC	ref.	ref.
			TT	0.41	$2.8x10^{-2}$
rs858526	17	0.28	AA	ref.	ref.
			GG	0.45	$2.8x10^{-2}$
rs10117830	9	0.59	CC	ref.	ref.
			TT	0.043	$2.8x10^{-2}$
rs1333759	13	0.26	AA	ref.	ref.
			GG	0.41	$2.8x10^{-2}$
rs10868791	9	0.81	AA	ref.	ref.
			GG	3.6	$2.8x10^{-2}$
rs34185023	3	0.33	AA	ref.	ref.
			GG	2.3	$2.8x10^{-2}$
rs1700801	16	0.28	AA	ref.	ref.
			CC	2.6	$2.8x10^{-2}$
rs4978050	9	0.48	CC	ref.	ref.
			TT	0.27	$2.8x10^{-2}$
rs10760133	9	0.40	CC	ref.	ref.
			TT	0.43	$2.8x10^{-2}$
rs6573516	14	0.45	CC	ref.	ref.
			TT	0.28	$2.8x10^{-2}$
rs13336816	16	0.38	CC	ref.	ref.
			GG	2.3	$2.8x10^{-2}$
rs9374263	6	0.28	CC	ref.	ref.
			GG	2.8	$2.8x10^{-2}$
rs11948306	5	0.29	AA	ref.	ref.
			GG	2.9	$2.9x10^{-2}$
rs13263799	8	0.25	AA	ref.	ref.
			TT	0.43	$2.9x10^{-2}$

Continuation of Table A21

rs7179456	15	0.41	GG	ref.	ref.
			TT	4.0	$2.9x10^{-2}$
rs2708318	3	0.42	GG	ref.	ref.
			TT	0.29	$2.9x10^{-2}$
rs6901866	6 (cisplatin)	0.25	CC	ref.	ref.
			TT	0.46	$2.9x10^{-2}$
rs13218344	6	0.33	AA	ref.	ref.
			CC	2.48	$2.9x10^{-2}$
rs12947658	17	0.62	AA	ref.	ref.
			GG	0.45	$2.9x10^{-2}$
rs1800759	4	0.32	GG	ref.	ref.
			TT	0.37	$2.9x10^{-2}$
rs7297538	12	0.28	CC	ref.	ref.
			TT	0.46	$2.9x10^{-2}$
rs4063936	13	0.28	AA	ref.	ref.
			TT	2.1	$2.9x10^{-2}$
rs465782	6	0.56	AA	ref.	ref.
			GG	0.45	$2.9x10^{-2}$
rs11194834	10	0.26	CC	ref.	ref.
			GG	0.44	$2.9x10^{-2}$
rs7624084	3	0.36	CC	ref.	ref.
			TT	2.6	$2.9x10^{-2}$
rs56193008	2	0.30	AA	ref.	ref.
			GG	0.44	$2.9x10^{-2}$
rs3024239	8	0.25	CC	ref.	ref.
			TT	2.4	$2.9x10^{-2}$
rs155934	16	0.44	AA	ref.	ref.
			GG	0.45	$2.9x10^{-2}$
rs9383476	6	0.35	AA	ref.	ref.
			GG	2.3	$2.9x10^{-2}$
rs1424145	16	0.27	AA	ref.	ref.
			GG	0.46	$2.9x10^{-2}$
rs670644	8	0.41	CC	ref.	ref.
			TT	2.3	$2.9x10^{-2}$
rs1263732	11	0.26	AA	ref.	ref.
			GG	2.6	$2.9x10^{-2}$
rs2302350	12	0.39	AA	ref.	ref.
			GG	2.5	$2.9x10^{-2}$
rs12679861	8	0.26	AA	ref.	ref.
			GG	0.34	$2.9x10^{-2}$
rs4705950	5	0.30	CC	ref.	ref.
			TT	2.2	$2.9x10^{-2}$
rs1032226	8	0.30	AA	ref.	ref.
			GG	2.5	$2.9x10^{-2}$
rs7091709	10	0.33	AA	ref.	ref.
			GG	0.40	$2.9x10^{-2}$
rs10765655	11	0.27	AA	ref.	ref.
			GG	2.1	$2.9x10^{-2}$
rs9635707	17	0.27	AA	ref.	ref.
			GG	0.45	$3.0x10^{-2}$
rs4903927	14	0.27	CC	ref.	ref.
			GG	2.0	$3.0x10^{-2}$

Continuation of Table A21

rs35480968	9	0.26	AA	ref.	ref.
			GG	2.3	$3.0x10^{-2}$
rs4236175	6	0.30	CC	ref.	ref.
			TT	0.44	$3.0x10^{-2}$
rs9999033	4	0.38	AA	ref.	ref.
			GG	0.36	$3.0x10^{-2}$
rs12165542	22	0.28	AA	ref.	ref.
			GG	2.2	$3.0x10^{-2}$
rs2279926	15	0.56	AA	ref.	ref.
			GG	0.092	$3.0x10^{-2}$
rs13082582	3	0.41	CC	ref.	ref.
			GG	0.48	$3.0x10^{-2}$
rs1057451	16	0.28	GG	ref.	ref.
			TT	3.2	$3.0x10^{-2}$
rs1155507	7	0.34	AA	ref.	ref.
			CC	0.20	$3.0x10^{-2}$
rs4655674	1	0.26	AA	ref.	ref.
			TT	0.43	$3.0x10^{-2}$
rs4900714	14	0.28	GG	ref.	ref.
			TT	2.6	$3.0x10^{-2}$
rs329655	11	0.28	AA	ref.	ref.
			CC	0.45	$3.0x10^{-2}$
rs659288	11	0.29	AA	ref.	ref.
			GG	0.46	$3.0x10^{-2}$
rs10240738	7	0.37	CC	ref.	ref.
			TT	2.4	$3.0x10^{-2}$
rs112826171	2	0.36	AA	ref.	ref.
			GG	2.9	$3.0x10^{-2}$
rs6772869	3	0.32	AA	ref.	ref.
			CC	2.3	$3.0x10^{-2}$
rs2968481	16	0.25	AA	ref.	ref.
			GG	0.47	$3.0x10^{-2}$
rs2355571	2	0.40	CC	ref.	ref.
			TT	0.37	$3.0x10^{-2}$
rs2899264	22	0.29	AA	ref.	ref.
			GG	2.3	$3.0x10^{-2}$
rs4320563	8	0.28	AA	ref.	ref.
			GG	2.3	$3.0x10^{-2}$
rs10659441	15	0.45	AA	ref.	ref.
			CC	0.13	$3.1x10^{-2}$
rs12613325	2	0.34	AA	ref.	ref.
			GG	2.6	$3.1x10^{-2}$
rs17777974	2	0.30	AA	ref.	ref.
			GG	0.44	$3.1x10^{-2}$
rs6966129	7	0.31	CC	ref.	ref.
			TT	4.2	$3.1x10^{-2}$
rs7773552	6	0.46	AA	ref.	ref.
			GG	2.3	$3.1x10^{-2}$
rs7176011	15	0.33	AA	ref.	ref.
			GG	6.8	$3.1x10^{-2}$
rs8069639	17	0.45	AA	ref.	ref.
			GG	2.4	$3.1x10^{-2}$

Continuation of Table A21

rs12481743	21	0.29	AA	ref.	ref.
			GG	2.4	$3.1x10^{-2}$
rs11771785	7	0.27	AA	ref.	ref.
			GG	3.8	$3.1x10^{-2}$
rs7694450	4	0.39	AA	ref.	ref.
			GG	2.7	$3.1x10^{-2}$
rs10153802	2	0.30	AA	ref.	ref.
			CC	2.3	$3.1x10^{-2}$
rs7185367	16	0.28	AA	ref.	ref.
			GG	2.3	$3.1x10^{-2}$
rs6683352	1	0.35	CC	ref.	ref.
			TT	3.5	$3.1x10^{-2}$
rs1455167	2	0.31	GG	ref.	ref.
			TT	2.6	$3.1x10^{-2}$
rs6795995	3	0.44	AA	ref.	ref.
			GG	3.4	$3.1x10^{-2}$
rs28767869	1	0.30	CC	ref.	ref.
			TT	0.44	$3.1x10^{-2}$
rs668708	15	0.61	CC	ref.	ref.
			TT	0.43	$3.1x10^{-2}$
rs11690161	2	0.43	CC	ref.	ref.
			TT	2.4	$3.2x10^{-2}$
rs1859143	4	0.38	CC	ref.	ref.
			TT	0.31	$3.2x10^{-2}$
rs9551199	13	0.41	CC	ref.	ref.
			TT	0.48	$3.2x10^{-2}$
rs35350746	2	0.38	CC	ref.	ref.
			GG	0.44	$3.2x10^{-2}$
rs12143987	1	0.35	CC	ref.	ref.
			GG	0.40	$3.2x10^{-2}$
rs934262	2	0.27	AA	ref.	ref.
			GG	0.35	$3.2x10^{-2}$
rs2241474	4	0.28	CC	ref.	ref.
			TT	0.44	$3.2x10^{-2}$
rs2005827	17	0.53	AA	ref.	ref.
			CC	2.3	$3.2x10^{-2}$
rs8094488	18	0.51	AA	ref.	ref.
			CC	0.46	$3.2x10^{-2}$
rs8054784	16	0.30	CC	ref.	ref.
			TT	0.35	$3.2x10^{-2}$
rs79609284	15	0.30	AA	ref.	ref.
			AG	0.68	0.29
rs6770412	3	0.26	AA	ref.	ref.
			TT	4.7	$3.2x10^{-2}$
rs12714251	2	0.41	AA	ref.	ref.
			GG	0.37	$3.2x10^{-2}$
rs3766117	1	0.54	CC	ref.	ref.
			TT	11.9	$3.2x10^{-2}$
rs3806251	1	0.40	AA	ref.	ref.
			TT	3.2	$3.2x10^{-2}$
rs4968213	17	0.26	CC	ref.	ref.
			TT	0.19	$3.2x10^{-2}$

Continuation of Table A21

rs882195	12	0.27	CC	ref.	ref.
			GG	0.46	$3.2x10^{-2}$
rs9392668	6	0.43	AA	ref.	ref.
			GG	0.41	$3.2x10^{-2}$
rs8140025	22	0.40	AA	ref.	ref.
			GG	2.0	$3.2x10^{-2}$
rs6901118	6	0.53	CC	ref.	ref.
			TT	0.047	$3.2x10^{-2}$
rs4646437	7	0.70	AA	ref.	ref.
			GG	0.28	$3.3x10^{-2}$
rs7090847	10	0.29	AA	ref.	ref.
			GG	0.34	$3.3x10^{-2}$
rs457487	12	0.38	AA	ref.	ref.
			CC	2.2	$3.3x10^{-2}$
rs6125596	20	0.25	AA	ref.	ref.
			CC	0.39	$3.3x10^{-2}$
rs4903565	14	0.30	AA	ref.	ref.
			GG	2.3	$3.3x10^{-2}$
rs9899846	17	0.28	CC	ref.	ref.
			TT	2.8	$3.3x10^{-2}$
rs7699519	4	0.41	CC	ref.	ref.
			TT	0.44	$3.3x10^{-2}$
rs4075401	1	0.48	GG	ref.	ref.
			TT	0.19	$3.3x10^{-2}$
rs2472384	9	0.36	CC	ref.	ref.
			TT	4.4	$3.3x10^{-2}$
rs6709870	2	0.27	AA	ref.	ref.
			GG	0.27	$3.3x10^{-2}$
rs1553013	13	0.44	CC	ref.	ref.
			TT	0.45	$3.3x10^{-2}$
rs4350671	19	0.30	CC	ref.	ref.
			TT	2.1	$3.3x10^{-2}$
rs7100642	10	0.34	CC	ref.	ref.
			TT	0.48	$3.3x10^{-2}$
rs2294481	6	0.29	AA	ref.	ref.
			TT	11.3	$3.3x10^{-2}$
rs9915042	17	0.28	CC	ref.	ref.
			TT	0.22	$3.3x10^{-2}$
rs1132659	11	0.31	CC	ref.	ref.
			TT	0.46	$3.3x10^{-2}$
rs2267994	14	0.25	AA	ref.	ref.
			GG	0.27	$3.3x10^{-2}$
rs4758621	11	0.25	AA	ref.	ref.
			GG	2.3	$3.3x10^{-2}$
rs597403	6	0.39	AA	ref.	ref.
			GG	0.37	$3.3x10^{-2}$
rs886771	2	0.35	AA	ref.	ref.
			GG	0.41	$3.3x10^{-2}$
rs4926300	19	0.34	CC	ref.	ref.
			TT	0.45	$3.3x10^{-2}$
rs6996702	8	0.27	CC	ref.	ref.
			GG	3.7	$3.3x10^{-2}$

Continuation of Table A21

rs6893456	5	0.30	AA	ref.	ref.
			CC	0.43	$3.3x10^{-2}$
rs251295	5	0.30	AA	ref.	ref.
			GG	0.26	$3.3x10^{-2}$
rs6844099	4	0.56	CC	ref.	ref.
			TT	0.070	$3.4x10^{-2}$
rs920036	16	0.47	AA	ref.	ref.
			GG	2.0	$3.4x10^{-2}$
rs4660435	1	0.27	CC	ref.	ref.
			TT	2.2	$3.4x10^{-2}$
rs4855720	3	0.27	CC	ref.	ref.
			GG	2.3	$3.4x10^{-2}$
rs7213900	17	0.30	AA	ref.	ref.
			GG	2.4	$3.4x10^{-2}$
rs9483497	6	0.27	AA	ref.	ref.
			GG	0.33	$3.4x10^{-2}$
rs8025445	15	0.32	AA	ref.	ref.
			CC	11	$3.4x10^{-2}$
rs9856245	3	0.41	CC	ref.	ref.
			TT	4.3	$3.4x10^{-2}$
rs33765	3	0.31	AA	ref.	ref.
			GG	3.2	$3.4x10^{-2}$
rs17856697	17	0.32	AA	ref.	ref.
			GG	2.1	$3.4x10^{-2}$
rs1425050	8	0.30	AA	ref.	ref.
			GG	0.20	$3.4x10^{-2}$
rs8105482	19	0.32	AA	ref.	ref.
			GG	2.2	$3.4x10^{-2}$
rs2173114	8	0.35	CC	ref.	ref.
			GG	0.43	$3.4x10^{-2}$
rs9651889	12	0.25	CC	ref.	ref.
			TT	0.43	$3.4x10^{-2}$
rs281284	15	0.44	AA	ref.	ref.
			CC	2.9	$3.5x10^{-2}$
rs7763210	6	0.41	CC	ref.	ref.
			TT	2.2	$3.5x10^{-2}$
rs7608738	2	0.28	AA	ref.	ref.
			GG	2.3	$3.5x10^{-2}$
rs3772132	3	0.26	CC	ref.	ref.
			TT	0.43	$3.5x10^{-2}$
rs2887200	2	0.42	AA	ref.	ref.
			GG	0.41	$3.5x10^{-2}$
rs4980855	12	0.29	CC	ref.	ref.
			GG	2.4	$3.5x10^{-2}$
rs1507278	1	0.25	AA	ref.	ref.
			GG	2.7	$3.5x10^{-2}$
rs2497115	6	0.43	GG	ref.	ref.
			TT	2.4	$3.5x10^{-2}$
rs878775	1	0.49	CC	ref.	ref.
			GG	0.41	$3.5x10^{-2}$
rs4659695	1	0.50	CC	ref.	ref.
			TT	2.2	$3.5x10^{-2}$

Continuation of Table A21

rs7327579	13	0.28	AA	ref.	ref.
			GG	2.3	$3.5x10^{-2}$
rs4243391	2	0.25	AA	ref.	ref.
			TT	0.31	$3.5x10^{-2}$
rs34545402	5	0.35	AA	ref.	ref.
			CC	0.45	$3.5x10^{-2}$
rs10978293	9	0.31	CC	ref.	ref.
			TT	4.8	$3.5x10^{-2}$
rs12103	1	0.69	CC	ref.	ref.
			TT	0.15	$3.5x10^{-2}$
rs9509354	13	0.30	CC	ref.	ref.
			TT	0.48	$3.5x10^{-2}$
rs7259535	19	0.46	CC	ref.	ref.
			TT	0.41	$3.5x10^{-2}$
rs1568400	17	0.39	CC	ref.	ref.
			TT	0.43	$3.5x10^{-2}$
rs6508435	18	0.28	AA	ref.	ref.
			GG	0.37	$3.5x10^{-2}$
rs773561	1	0.29	CC	ref.	ref.
			TT	0.12	$3.6x10^{-2}$
rs4935046	10	0.25	CC	ref.	ref.
			TT	0.43	$3.6x10^{-2}$
rs12570505	10	0.26	GG	ref.	ref.
			TT	0.28	$3.6x10^{-2}$
rs1015887	6	0.26	CC	ref.	ref.
			TT	0.42	$3.6x10^{-2}$
rs2306459	1	0.28	AA	ref.	ref.
			GG	0.22	$3.6x10^{-2}$
rs2340596	1	0.27	AA	ref.	ref.
			GG	2.1	$3.6x10^{-2}$
rs3104554	9	0.47	CC	ref.	ref.
			TT	2.2	$3.6x10^{-2}$
rs3771313	2	0.25	CC	ref.	ref.
			TT	2.1	$3.6x10^{-2}$
rs3910104	4	0.34	CC	ref.	ref.
			TT	2.3	$3.7x10^{-2}$
rs2267995	14	0.29	CC	ref.	ref.
			GG	0.50	$3.7x10^{-2}$
rs1882396	2	0.31	GG	ref.	ref.
			TT	0.49	$3.7x10^{-2}$
rs62476177	7	0.36	AA	ref.	ref.
			GG	2.1	$3.7x10^{-2}$
rs62248376	3	0.53	AA	ref.	ref.
			GG	0.22	$3.7x10^{-2}$
rs4970414	1	0.33	GG	ref.	ref.
			TT	0.46	$3.7x10^{-2}$
rs4683603	3	0.36	GG	ref.	ref.
			TT	0.38	$3.7x10^{-2}$
rs1965484	3	0.37	GG	ref.	ref.
			TT	0.36	$3.7x10^{-2}$
rs35958394	19	0.32	CC	ref.	ref.
			GG	0.46	$3.7x10^{-2}$

Continuation of Table A21

rs10405300	19	0.25	AA	ref.	ref.
			CC	0.32	$3.7x10^{-2}$
rs4880432	10	0.27	AA	ref.	ref.
			GG	2.1	$3.7x10^{-2}$
rs10034650	4	0.30	AA	ref.	ref.
			GG	4.1	$3.7x10^{-2}$
rs690435	15	0.34	CC	ref.	ref.
			TT	0.45	$3.7x10^{-2}$
rs11759127	6	0.40	AA	ref.	ref.
			TT	0.41	$3.7x10^{-3}$
rs11070654	15	0.36	CC	ref.	ref.
			TT	2.0	$3.7x10^{-2}$
rs7540556	1	0.29	CC	ref.	ref.
			TT	2.1	$3.7x10^{-2}$
rs7248898	19	0.30	AA	ref.	ref.
			GG	0.46	$3.8x10^{-2}$
rs6685508	1	0.42	AA	ref.	ref.
			GG	0.36	$3.8x10^{-2}$
rs9971544	11	0.25	CC	ref.	ref.
			TT	0.50	$3.8x10^{-2}$
rs17135121	7	0.45	CC	ref.	ref.
			TT	3.8	$3.8x10^{-2}$
rs7167513	15	0.29	CC	ref.	ref.
			GG	2.1	$3.8x10^{-2}$
rs13418478	2	0.27	AA	ref.	ref.
			GG	0.19	$3.8x10^{-2}$
rs133856	22	0.47	AA	ref.	ref.
			CC	2.2	$3.8x10^{-2}$
rs7616140	3	0.35	AA	ref.	ref.
			GG	3.3	$3.8x10^{-2}$
rs10888603	1	0.47	AA	ref.	ref.
			CC	2.7	$3.8x10^{-2}$
rs652046	3	0.35	AA	ref.	ref.
			GG	0.45	$3.8x10^{-2}$
rs675265	1	0.27	AA	ref.	ref.
			GG	0.39	$3.8x10^{-2}$
rs11615137	12	0.34	AA	ref.	ref.
			TT	0.33	$3.8x10^{-2}$
rs67621798	5	0.48	CC	ref.	ref.
			TT	2.4	$3.9x10^{-2}$
rs13379492	15	0.29	AA	ref.	ref.
			TT	3.6	$3.9x10^{-2}$
rs2071442	20	0.41	CC	ref.	ref.
			GG	0.45	$3.9x10^{-2}$
rs11111088	12	0.36	CC	ref.	ref.
			TT	0.50	$3.9x10^{-2}$
rs723720	11	0.33	CC	ref.	ref.
			TT	2.6	$3.9x10^{-2}$
rs12650569	4	0.48	AA	ref.	ref.
			GG	3.3	$3.9x10^{-2}$
rs1860385	12	0.42	CC	ref.	ref.
			TT	2.2	$3.9x10^{-2}$

Continuation of Table A21

rs6011489	20	0.27	CC	ref.	ref.
			TT	2.3	$3.9x10^{-2}$
rs2443775	8	0.40	AA	ref.	ref.
			GG	0.44	$3.9x10^{-2}$
rs739677	11	0.59	AA	ref.	ref.
			GG	0.22	$3.9x10^{-2}$
rs7226265	17	0.26	AA	ref.	ref.
			GG	2.7	$3.9x10^{-2}$
rs1967313	2	0.31	GG	ref.	ref.
			TT	3.0	$3.9x10^{-2}$
rs207633	13	0.30	CC	ref.	ref.
			TT	0.43	$3.9x10^{-2}$
rs11980329	7	0.40	AA	ref.	ref.
			TT	13.3	$3.9x10^{-2}$
rs1960476	5	0.27	AA	ref.	ref.
			CC	2.7	$3.9x10^{-2}$
rs1186196	11	0.31	CC	ref.	ref.
			TT	2.6	$3.9x10^{-2}$
rs829311	9	0.26	CC	ref.	ref.
			TT	2.1	$3.9x10^{-2}$
rs9506574	13	0.36	CC	ref.	ref.
			TT	2.1	$3.9x10^{-2}$
rs7758778	6	0.26	CC	ref.	ref.
			TT	0.37	$3.9x10^{-2}$
rs7921146	10	0.31	AA	ref.	ref.
			GG	0.42	$3.9x10^{-2}$
rs12154073	6	0.27	CC	ref.	ref.
			TT	0.48	$3.9x10^{-2}$
rs7545094	1	0.41	AA	ref.	ref.
			TT	3.0	$3.9x10^{-2}$
rs17140401	7	0.63	CC	ref.	ref.
			TT	3.2	$3.9x10^{-2}$
rs12904145	15	0.46	AA	ref.	ref.
			GG	2.1	$3.9x10^{-2}$
rs11072794	15	0.52	CC	ref.	ref.
			TT	2.2	$3.9x10^{-2}$
rs61731321	7	0.27	GG	ref.	ref.
			TT	6.7	$3.9x10^{-2}$
rs6909448	6	0.38	AA	ref.	ref.
			GG	0.24	$4.0x10^{-2}$
rs1888967	10	0.27	AA	ref.	ref.
			TT	0.48	$4.0x10^{-2}$
rs13252887	8	0.42	CC	ref.	ref.
			TT	0.44	$4.0x10^{-2}$
rs3782181	12	0.51	AA	ref.	ref.
			CC	4.1	$4.0x10^{-2}$
rs1048015	22	0.40	CC	ref.	ref.
			TT	5.9	$4.0x10^{-2}$
rs33763	3	0.37	AA	ref.	ref.
			TT	3.1	$4.0x10^{-2}$
rs13266997	8	0.26	GG	ref.	ref.
			TT	2.3	$4.0x10^{-2}$

Continuation of Table A21

rs1075790	11	0.25	AA	ref.	ref.
			CC	0.47	$4.0x10^{-2}$
rs11670287	19	0.45	GG	ref.	ref.
			TT	0.49	$4.0x10^{-2}$
rs12547114	8	0.40	AA	ref.	ref.
			GG	0.35	$4.0x10^{-2}$
rs11623972	14	0.44	AA	ref.	ref.
			GG	2.5	$4.0x10^{-2}$
rs10465810	1	0.58	AA	ref.	ref.
			TT	0.37	$4.0x10^{-2}$
rs11259474	10	0.42	CC	ref.	ref.
			TT	0.28	$4.0x10^{-2}$
rs2436042	8	0.35	AA	ref.	ref.
			GG	0.25	$4.0x10^{-2}$
rs976560	15	0.25	AA	ref.	ref.
			CC	2.2	$4.1x10^{-2}$
rs2075678	20	0.31	AA	ref.	ref.
			GG	2.1	$4.1x10^{-2}$
rs4431825	1	0.45	AA	ref.	ref.
			GG	0.47	$4.1x10^{-2}$
rs11994	5	0.26	AA	ref.	ref.
			GG	0.46	$4.1x10^{-2}$
rs6572953	14	0.32	AA	ref.	ref.
			GG	0.46	$4.1x10^{-2}$
rs9900080	17	0.28	GG	ref.	ref.
			TT	2.1	$4.1x10^{-2}$
rs1286332	14	0.29	AA	ref.	ref.
			CC	2.3	$4.1x10^{-2}$
rs3783627	14	0.28	AA	ref.	ref.
			CC	0.44	$4.1x10^{-2}$
rs928603	10	0.28	CC	ref.	ref.
			TT	0.44	$4.1x10^{-2}$
rs2461134	7	0.42	CC	ref.	ref.
			TT	0.43	$4.1x10^{-2}$
rs6440994	3	0.48	CC	ref.	ref.
			TT	0.11	$4.1x10^{-2}$
rs7529274	1	0.65	AA	ref.	ref.
			GG	2.9	$4.1x10^{-2}$
rs1913820	12	0.48	AA	ref.	ref.
			GG	0.083	$4.1x10^{-2}$
rs11203899	8	0.33	AA	ref.	ref.
			GG	2.2	$4.1x10^{-2}$
rs59690870	3	0.32	CC	ref.	ref.
			TT	3.2	$4.1x10^{-2}$
rs7569646	2	0.33	AA	ref.	ref.
			GG	0.28	$4.1x10^{-2}$
rs12516924	5	0.28	AA	ref.	ref.
			GG	2.1	$4.1x10^{-2}$
rs12691883	2	0.47	CC	ref.	ref.
			TT	3.6	$4.1x10^{-2}$
rs1325596	1	0.26	AA	ref.	ref.
			GG	0.43	$4.1x10^{-2}$

Continuation of Table A21

rs7918733	10	0.31	CC	ref.	ref.
			TT	2.2	$4.1x10^{-2}$
rs10150121	14	0.33	CC	ref.	ref.
			TT	2.8	$4.2x10^{-2}$
rs73265918	7	0.28	AA	ref.	ref.
			CC	0.22	$4.2x10^{-2}$
rs12540177	7	0.28	AA	ref.	ref.
			GG	0.41	$4.2x10^{-2}$
rs10946744	6	0.26	AA	ref.	ref.
			CC	3.0	$4.2x10^{-2}$
rs1258192	10	0.29	CC	ref.	ref.
			TT	2.7	$4.2x10^{-2}$
rs10937106	3	0.63	AA	ref.	ref.
			GG	0.19	$4.2x10^{-2}$
rs6588126	1	0.63	AA	ref.	ref.
			TT	0.34	$4.2x10^{-2}$
rs3776078	5	0.29	CC	ref.	ref.
			GG	2.1	$4.2x10^{-2}$
rs4868603	5	0.32	CC	ref.	ref.
			TT	2.3	$4.2x10^{-2}$
rs8089369	18	0.25	CC	ref.	ref.
			TT	0.28	$4.2x10^{-2}$
rs4763697	12	0.44	CC	ref.	ref.
			TT	0.49	$4.2x10^{-2}$
rs7562879	2	0.36	AA	ref.	ref.
			GG	0.29	$4.2x10^{-2}$
rs13243421	7	0.34	AA	ref.	ref.
			GG	0.47	$4.2x10^{-2}$
rs4981013	12	0.37	AA	ref.	ref.
			GG	2.2	$4.2x10^{-2}$
rs34552497	12	0.36	CC	ref.	ref.
			TT	0.46	$4.2x10^{-2}$
rs2298632	1	0.35	CC	ref.	ref.
			TT	0.44	$4.2x10^{-2}$
rs3765204	8	0.27	CC	ref.	ref.
			TT	0.45	$4.2x10^{-2}$
rs2307097	12	0.34	CC	ref.	ref.
			TT	0.44	$4.2x10^{-2}$
rs11172665	12	0.26	CC	ref.	ref.
			TT	2.3	$4.3x10^{-2}$
rs9464401	6	0.27	AA	ref.	ref.
			GG	0.37	$4.3x10^{-2}$
rs1434575	19	0.26	CC	ref.	ref.
			TT	2.4	$4.3x10^{-2}$
rs6936397	6	0.32	CC	ref.	ref.
			GG	4.4	$4.3x10^{-2}$
rs9469775	6	0.44	CC	ref.	ref.
			TT	0.18	$4.3x10^{-2}$
rs2273814	14	0.34	AA	ref.	ref.
			GG	0.37	$4.3x10^{-2}$
rs7795892	7	0.34	CC	ref.	ref.
			TT	0.45	$4.3x10^{-2}$

Continuation of Table A21

rs72697725	9	0.30	AA	ref.	ref.
			GG	4.5	$4.3x10^{-2}$
rs10866722	5	0.29	GG	ref.	ref.
			TT	2.2	$4.3x10^{-2}$
rs2296527	20	0.42	AA	ref.	ref.
			CC	0.33	$4.3x10^{-2}$
rs13336442	16	0.41	AA	ref.	ref.
			GG	0.32	$4.3x10^{-2}$
rs553305	17	0.44	AA	ref.	ref.
			GG	2.3	$4.3x10^{-2}$
rs7979600	12	0.42	AA	ref.	ref.
			GG	0.41	$4.3x10^{-2}$
rs6962006	7	0.26	AA	ref.	ref.
			GG	0.40	$4.3x10^{-2}$
rs11643752	16	0.32	AA	ref.	ref.
			GG	3.0	$4.3x10^{-2}$
rs9788522	14	0.27	AA	ref.	ref.
			CC	0.19	$4.3x10^{-2}$
rs13004643	2	0.37	AA	ref.	ref.
			GG	2.1	$4.3x10^{-2}$
rs9299457	10	0.31	CC	ref.	ref.
			GG	4.8	$4.3x10^{-2}$
rs4939146	11	0.39	AA	ref.	ref.
			GG	3.9	$4.3x10^{-2}$
rs13126350	4	0.25	AA	ref.	ref.
			GG	2.2	$4.3x10^{-2}$
rs2403565	11	0.31	CC	ref.	ref.
			GG	0.51	$4.4x10^{-2}$
rs4722409	7	0.31	CC	ref.	ref.
			TT	0.48	$4.4x10^{-2}$
rs10403969	19	0.52	AA	ref.	ref.
			CC	0.38	$4.4x10^{-2}$
rs4927168	1	0.27	AA	ref.	ref.
			CC	0.17	$4.4x10^{-2}$
rs1343630	1	0.44	AA	ref.	ref.
			GG	0.18	$4.4x10^{-2}$
rs2075663	9	0.27	AA	ref.	ref.
			GG	2.2	$4.4x10^{-2}$
rs12401987	1	0.32	AA	ref.	ref.
			GG	0.38	$4.4x10^{-2}$
rs12639564	3	0.36	AA	ref.	ref.
			GG	3.0	$4.4x10^{-2}$
rs4387616	16	0.27	AA	ref.	ref.
			CC	0.37	$4.4x10^{-2}$
rs1725214	7	0.29	AA	ref.	ref.
			CC	3.9	$4.4x10^{-2}$
rs3803578	16	0.32	AA	ref.	ref.
			GG	0.50	$4.4x10^{-2}$
rs7192882	16	0.34	AA	ref.	ref.
			GG	0.29	$4.4x10^{-2}$
rs11065589	12	0.26	CC	ref.	ref.
			TT	0.47	$4.4x10^{-2}$

Continuation of Table A21

rs8347	6	0.26	CC	ref.	ref.
			TT	0.38	$4.4x10^{-2}$
rs1204682	1	0.33	AA	ref.	ref.
			GG	2.4	$4.5x10^{-2}$
rs1341022	20	0.31	CC	ref.	ref.
			GG	2.1	$4.5x10^{-2}$
rs11668398	19	0.45	CC	ref.	ref.
			TT	0.42	$4.5x10^{-2}$
rs2335338	12	0.37	AA	ref.	ref.
			GG	0.50	$4.5x10^{-2}$
rs149500958	7	0.25	AA	ref.	ref.
			CC	3.6	$4.5x10^{-2}$
rs12755846	1	0.60	CC	ref.	ref.
			GG	4.3	$4.5x10^{-2}$
rs7157482	14	0.42	CC	ref.	ref.
			TT	0.37	$4.5x10^{-2}$
rs12028158	1	0.30	AA	ref.	ref.
			GG	0.13	$4.5x10^{-2}$
rs12809767	12	0.28	AA	ref.	ref.
			CC	2.3	$4.5x10^{-2}$
rs4949447	1	0.51	AA	ref.	ref.
			GG	3.2	$4.5x10^{-2}$
rs6878763	5	0.29	AA	ref.	ref.
			GG	0.46	$4.5x10^{-2}$
rs4745451	9	0.48	AA	ref.	ref.
			CC	2.5	$4.5x10^{-2}$
rs2490485	10	0.31	CC	ref.	ref.
			TT	0.41	$4.5x10^{-2}$
rs7611385	3	0.45	CC	ref.	ref.
			TT	2.0	$4.5x10^{-2}$
rs12486843	3	0.42	AA	ref.	ref.
			GG	0.38	$4.5x10^{-2}$
rs17071932	18	0.49	AA	ref.	ref.
			GG	0.10	$4.5x10^{-2}$
rs5759676	22	0.30	GG	ref.	ref.
			TT	0.17	$4.5x10^{-2}$
rs66696244	4	0.33	AA	ref.	ref.
			GG	0.47	$4.5x10^{-2}$
rs2322604	8	0.34	CC	ref.	ref.
			TT	0.47	$4.6x10^{-2}$
rs12746615	1	0.27	AA	ref.	ref.
			GG	2.9	$4.6x10^{-2}$
rs10430783	10	0.26	CC	ref.	ref.
			TT	0.29	$4.6x10^{-2}$
rs7329320	13	0.26	CC	ref.	ref.
			TT	0.47	$4.6x10^{-2}$
rs35176895	5	0.38	CC	ref.	ref.
			TT	0.47	$4.6x10^{-2}$
rs1346408	3	0.52	CC	ref.	ref.
			TT	0.38	$4.6x10^{-2}$
rs2564733	1	0.47	CC	ref.	ref.
			TT	2.1	$4.6x10^{-2}$

Continuation of Table A21

rs4738438	8	0.32	CC	ref.	ref.
			TT	0.12	$4.6x10^{-2}$
rs12940684	17	0.29	CC	ref.	ref.
			TT	0.48	$4.6x10^{-2}$
rs10458360	1	0.46	CC	ref.	ref.
			GG	2.4	$4.6x10^{-2}$
rs12212480	6	0.26	GG	ref.	ref.
			TT	0.42	$4.6x10^{-2}$
rs7278357	21	0.39	CC	ref.	ref.
			TT	2.8	$4.6x10^{-2}$
rs9296115	6	0.32	AA	ref.	ref.
			CC	0.10	$4.6x10^{-2}$
rs6024876	20	0.33	AA	ref.	ref.
			GG	2.2	$4.6x10^{-2}$
rs8069671	17	0.37	GG	ref.	ref.
			TT	0.37	$4.6x10^{-2}$
rs56398807	2	0.25	AA	ref.	ref.
			GG	2.6	$4.6x10^{-2}$
rs1040436	6	0.29	AA	ref.	ref.
			GG	6.0	$4.6x10^{-2}$
rs139283	22	0.38	CC	ref.	ref.
			GG	0.40	$4.6x10^{-2}$
rs1838192	18	0.27	GG	ref.	ref.
			TT	0.46	$4.6x10^{-2}$
rs11868441	17	0.70	AA	ref.	ref.
			GG	0.40	$4.6x10^{-2}$
rs12800570	11	0.30	CC	ref.	ref.
			TT	0.11	$4.6x10^{-2}$
rs9895272	17	0.39	CC	ref.	ref.
			TT	2.2	$4.7x10^{-2}$
rs7500197	16	0.30	AA	ref.	ref.
			GG	2.2	$4.7x10^{-2}$
rs1875957	5	0.31	AA	ref.	ref.
			GG	2.4	$4.7x10^{-2}$
rs2005460	6	0.53	AA	ref.	ref.
			GG	2.3	$4.7x10^{-2}$
rs10070231	5	0.36	CC	ref.	ref.
			TT	2.1	$4.7x10^{-2}$
rs4348477	8	0.43	CC	ref.	ref.
			TT	2.3	$4.7x10^{-2}$
rs270848	1	0.27	CC	ref.	ref.
			TT	2.1	$4.7x10^{-2}$
rs2038219	20	0.26	AA	ref.	ref.
			GG	0.42	$4.7x10^{-2}$
rs2745452	6	0.30	AA	ref.	ref.
			GG	0.34	$4.7x10^{-2}$
rs5994328	22	0.28	CC	ref.	ref.
			TT	0.37	$4.7x10^{-2}$
rs10802624	1	0.29	AA	ref.	ref.
			GG	2.2	$4.7x10^{-2}$
rs6587616	1	0.26	CC	ref.	ref.
			TT	2.2	$4.7x10^{-2}$

Continuation of Table A21

rs1475520	14	0.42	AA	ref.	ref.
			GG	0.43	$4.7x10^{-2}$
rs4853562	2	0.57	AA	ref.	ref.
			GG	0.48	$4.7x10^{-2}$
rs670666	1	0.27	AA	ref.	ref.
			GG	2.0	$4.8x10^{-2}$
rs61823772	1	0.26	CC	ref.	ref.
			GG	0.49	$4.8x10^{-2}$
rs2490479	10	0.44	CC	ref.	ref.
			TT	2.1	$4.8x10^{-2}$
rs10807026	6	0.29	AA	ref.	ref.
			CC	3.5	$4.8x10^{-2}$
rs11780153	8	0.42	AA	ref.	ref.
			GG	0.41	$4.8x10^{-2}$
rs9726786	1	0.26	CC	ref.	ref.
			TT	4.7	$4.8x10^{-2}$
rs13248595	8	0.25	AA	ref.	ref.
			GG	0.11	$4.8x10^{-2}$
rs139406379	12	0.28	CC	ref.	ref.
			TT	0.29	$4.8x10^{-2}$
rs11129896	3	0.29	CC	ref.	ref.
			TT	2.5	$4.8x10^{-2}$
rs6820509	4	0.50	AA	ref.	ref.
			GG	0.43	$4.8x10^{-2}$
rs13238033	7	0.48	AA	ref.	ref.
			GG	0.45	$4.8x10^{-2}$
rs12902139	15	0.25	AA	ref.	ref.
			GG	2.2	$4.9x10^{-2}$
rs11650119	17	0.29	AA	ref.	ref.
			CC	0.45	$4.9x10^{-2}$
rs224102	10	0.43	AA	ref.	ref.
			CC	3.8	$4.9x10^{-2}$
rs13147253	4	0.43	AA	ref.	ref.
			GG	0.46	$4.9x10^{-2}$
rs2794589	1	0.42	AA	ref.	ref.
			GG	0.41	$4.9x10^{-2}$
rs4927910	3	0.47	CC	ref.	ref.
			TT	0.28	$4.9x10^{-2}$
rs12488642	3	0.33	CC	ref.	ref.
			TT	2.9	$4.9x10^{-2}$
rs11045812	12	0.39	CC	ref.	ref.
			TT	2.0	$4.9x10^{-2}$
rs7605521	2	0.42	AA	ref.	ref.
			CC	2.1	$4.9x10^{-2}$
rs11198817	10	0.34	AA	ref.	ref.
			GG	0.48	$4.9x10^{-2}$
rs281253	15	0.31	CC	ref.	ref.
			TT	0.47	$4.9x10^{-2}$
rs55880431	16	0.39	CC	ref.	ref.
			GG	2.0	$4.9x10^{-2}$
rs751198	11	0.26	AA	ref.	ref.
			GG	2.1	$5.0x10^{-2}$

Continuation of Table A21

rs10853027	17	0.59	CC	ref.	ref.
			TT	0.44	$5.0x10^{-2}$
rs3912117	12	0.26	AA	ref.	ref.
			GG	2.1	$5.0x10^{-2}$
rs4757644	11	0.31	AA	ref.	ref.
			CC	2.0	$5.0x10^{-2}$
rs7565518	2	0.54	CC	ref.	ref.
			GG	3.1	$5.0x10^{-2}$
rs3736956	1	0.45	CC	ref.	ref.
			TT	2.2	$5.0x10^{-2}$
rs6664664	1	0.41	AA	ref.	ref.
			GG	2.8	$5.0x10^{-2}$
rs10843344	12	0.29	CC	ref.	ref.
			TT	2.1	$5.0x10^{-2}$
rs7616492	3	0.32	AA	ref.	ref.
			GG	0.48	$5.0x10^{-2}$

Abbreviations: F_{ST}, fixation index.

7. References

1. Siegel, R. L., Miller, K. D., Wagle, N. S. & Jemal, A. Cancer statistics, 2023. *CA Cancer J Clin* **73**, 17–48 (2023).

2. Ries, LAG *et al.* SEER Cancer Statistics Review, 1973-1994. (1997).

3. Howland, N. *et al.* SEER Cancer Statistics Review, 1975-2017. (2021).

4. Bhatia, S., Tonorezos, E. S. & Landier, W. Clinical Care for People Who Survive Childhood Cancer: A Review. *JAMA* **330**, 1175–1186 (2023).

5. Miller, K. D. *et al.* Cancer treatment and survivorship statistics, 2022. *CA Cancer J Clin* **72**, 409–436 (2022).

6. Nurgali, K., Jagoe, R. T. & Abalo, R. Editorial: Adverse Effects of Cancer Chemotherapy: Anything New to Improve Tolerance and Reduce Sequelae? *Front Pharmacol* **9**, 245 (2018).

7. Wang, K. & Tepper, J. E. Radiation therapy-associated toxicity: Etiology, management, and prevention. *CA Cancer J Clin* **71**, 437–454 (2021).

8. Gumusay, O., Callan, J. & Rugo, H. S. Immunotherapy toxicity: identification and management. *Breast Cancer Res Treat* **192**, 1–17 (2022).

9. Lu Lee, E. & Westcarth, L. Neurotoxicity associated with cancer therapy. *J Adv Pract Oncol* **3**, 11–21 (2012).

10. Das, A. *et al.* An Overview on Chemotherapy-induced Cognitive Impairment and Potential Role of Antidepressants. *Curr Neuropharmacol* **18**, 838–851 (2020).

11. Trendowski, M. R., El Charif, O., Dinh, P. C., Travis, L. B. & Dolan, M. E. Genetic and Modifiable Risk Factors Contributing to Cisplatin-induced Toxicities. *Clin Cancer Res* **25**, 1147–1155 (2019).

12. Armstrong, T., Almadrones, L. & Gilbert, M. R. Chemotherapy-induced peripheral neuropathy. *Oncol Nurs Forum* **32**, 305–311 (2005).

13. Zajączkowska, R. *et al.* Mechanisms of Chemotherapy-Induced Peripheral Neuropathy. *Int J Mol Sci* **20**, 1451 (2019).

14. Schultz, C., Goffi-Gomez, M. V. S., Pecora Liberman, P. H., Pellizzon, A. C. de A. & Carvalho, A. L. Hearing loss and complaint in patients with head and neck cancer treated with radiotherapy. *Arch Otolaryngol Head Neck Surg* **136**, 1065–1069 (2010).

15. Prayuenyong, P. *et al.* Imbalance Associated With Cisplatin Chemotherapy in Adult Cancer Survivors: A Clinical Study. *Otol Neurotol* **42**, e730–e734 (2021).

16. Breglio, A. M. *et al.* Cisplatin is retained in the cochlea indefinitely following chemotherapy. *Nat Commun* **8**, 1654 (2017).

17. Chattaraj, A., Syed, M. P., Low, C. A. & Owonikoko, T. K. Cisplatin-Induced Ototoxicity: A Concise Review of the Burden, Prevention, and Interception Strategies. *JCO Oncol Pract* **19**, 278–283 (2023).

18. Kaltenbach, J. A. *et al.* Cisplatin-induced hyperactivity in the dorsal cochlear nucleus and its relation to outer hair cell loss: relevance to tinnitus. *J Neurophysiol* **88**, 699–714 (2002).

19. Fleihan, T., Nader, M. E. & Dickman, J. D. Cisplatin vestibulotoxicity: a current review. *Front Surg* **11**, 1437468 (2024).

20. Fries, J. F., Bruce, B. & Cella, D. The promise of PROMIS: using item response theory to improve assessment of patient-reported outcomes. *Clin Exp Rheumatol* **23**, S53-57 (2005).

21. Dinh, P. C. *et al.* Impact of pain and adverse health outcomes on long-term US testicular cancer survivors. *J Natl Cancer Inst* **116**, 455–467 (2024).

22. van Sloten, T. T. *et al.* Peripheral neuropathy, decreased muscle strength and obesity are strongly associated with walking in persons with type 2 diabetes without manifest mobility limitations. *Diabetes Res Clin Pract* **91**, 32–39 (2011).

23. Hicks, C. W., Wang, D., Matsushita, K., Windham, B. G. & Selvin, E. Peripheral Neuropathy and All-Cause and Cardiovascular Mortality in U.S. Adults : A Prospective Cohort Study. *Ann Intern Med* **174**, 167–174 (2021).

24. Henry, J. A., Dennis, K. C. & Schechter, M. A. General review of tinnitus: prevalence, mechanisms, effects, and management. *J Speech Lang Hear Res* **48**, 1204–1235 (2005).

25. Deal, J. A. *et al.* Hearing Impairment and Incident Dementia and Cognitive Decline in Older Adults: The Health ABC Study. *J Gerontol A Biol Sci Med Sci* **72**, 703–709 (2017).

26. Dalton, D. S. *et al.* The impact of hearing loss on quality of life in older adults. *Gerontologist* **43**, 661–668 (2003).

27. Kerns, S. L. *et al.* Factors associated with longitudinal progression of the cumulative burden of morbidity and overall mortality after cisplatin-based chemotherapy for testicular cancer. *J Natl Cancer Inst* djaf014 (2025) doi:10.1093/jnci/djaf014.

28. Dinh, P. C. *et al.* Cognitive function in long-term testicular cancer survivors: impact of modifiable factors. *JNCI Cancer Spectr* **8**, pkae068 (2024).

29. Newman, C. W., Weinstein, B. E., Jacobson, G. P. & Hug, G. A. The Hearing Handicap Inventory for Adults: psychometric adequacy and audiometric correlates. *Ear Hear* **11**, 430–433 (1990).

30. Tyler, R. *et al.* Development and validation of the tinnitus primary function questionnaire. *Am J Audiol* **23**, 260–272 (2014).

31. Sanchez, V. A. *et al.* Patient-Reported Functional Impairment Due to Hearing Loss and Tinnitus After Cisplatin-Based Chemotherapy. *J Clin Oncol* **41**, 2211–2226 (2023).

32. ArdeshirRouhaniFard, S. *et al.* Use of Medications for Treating Anxiety or Depression among Testicular Cancer Survivors: A Multi-Institutional Study. *Cancer Epidemiol Biomarkers Prev* **30**, 1129–1138 (2021).

33. Loprinzi, C. L. *et al.* Prevention and Management of Chemotherapy-Induced Peripheral Neuropathy in Survivors of Adult Cancers: ASCO Guideline Update. *J Clin Oncol* **38**, 3325–3348 (2020).

34. Pfeiffer, P. *et al.* Calmangafodipir for Prevention of Oxaliplatin-Induced Peripheral Neuropathy: Two Placebo-Controlled, Randomized Phase 3 Studies (POLAR-A/POLAR-M). *JNCI Cancer Spectr* **6**, pkac075 (2022).

35. Farshchian, N., Alavi, A., Heydarheydari, S. & Moradian, N. Comparative study of the effects of venlafaxine and duloxetine on chemotherapy-induced peripheral neuropathy. *Cancer Chemother Pharmacol* **82**, 787–793 (2018).

36. Radkhah, H. *et al.* Comparative Study of the Effects of Duloxetine and Venlafaxine on Acute Symptomatic Taxane-induced Neuropathy in Breast Cancer Patients: A Randomized Clinical Trial. *J Community Hosp Intern Med Perspect* **14**, 18–24 (2024).

37. Bae, E. H., Greenwald, M. K. & Schwartz, A. G. Chemotherapy-Induced Peripheral Neuropathy: Mechanisms and Therapeutic Avenues. *Neurotherapeutics* **18**, 2384–2396 (2021).

38. Desforges, A. D. *et al.* Treatment and diagnosis of chemotherapy-induced peripheral neuropathy: An update. *Biomed Pharmacother* **147**, 112671 (2022).

39. Dhillon, S. Sodium Thiosulfate: Pediatric First Approval. *Paediatr Drugs* **25**, 239–244 (2023).

40. Brock, P. R. *et al.* Sodium Thiosulfate for Protection from Cisplatin-Induced Hearing Loss. *N Engl J Med* **378**, 2376–2385 (2018).

41. Choi, J. *et al.* Protective effects of apocynin on cisplatin-induced ototoxicity in an auditory cell line and in zebrafish. *J Appl Toxicol* **33**, 125–133 (2013).

42. Kim, K.-H. *et al.* Evaluating protective and therapeutic effects of alpha-lipoic acid on cisplatin-induced ototoxicity. *Cell Death Dis* **9**, 827 (2018).
43. Yu, D. *et al.* Current Strategies to Combat Cisplatin-Induced Ototoxicity. *Front Pharmacol* **11**, 999 (2020).

44. Paken, J., Govender, C. D., Pillay, M. & Sewram, V. Cisplatin-Associated Ototoxicity: A Review for the Health Professional. *J Toxicol* **2016**, 1809394 (2016).

45. Molassiotis, A. *et al.* Risk factors for chemotherapy-induced peripheral neuropathy in patients receiving taxane- and platinum-based chemotherapy. *Brain Behav* **9**, e01312 (2019).

46. Mizrahi, D. *et al.* Hemoglobin, Body Mass Index, and Age as Risk Factors for Paclitaxel- and Oxaliplatin-Induced Peripheral Neuropathy. *JAMA Netw Open* **4**, e2036695 (2021).

47. Zhang, X. *et al.* Pharmacogenomics of cisplatin-induced neurotoxicities: Hearing loss, tinnitus, and peripheral sensory neuropathy. *Cancer Med* **11**, 2801–2816 (2022).

48. Dolan, M. E. *et al.* Clinical and Genome-Wide Analysis of Cisplatin-Induced Peripheral Neuropathy in Survivors of Adult-Onset Cancer. *Clin Cancer Res* **23**, 5757–5768 (2017).

49. Wheeler, H. E. *et al.* Variants in WFS1 and Other Mendelian Deafness Genes Are Associated with Cisplatin-Associated Ototoxicity. *Clin Cancer Res* **23**, 3325–3333 (2017).

50. El Charif, O. *et al.* Clinical and Genome-wide Analysis of Cisplatin-induced Tinnitus Implicates Novel Ototoxic Mechanisms. *Clin Cancer Res* **25**, 4104–4116 (2019).

51. Trendowski, M. R. *et al.* Clinical and Genome-Wide Analysis of Multiple Severe Cisplatin-Induced Neurotoxicities in Adult-Onset Cancer Survivors. *Clin Cancer Res* **26**, 6550–6558 (2020).

52. He, Y.-Q. *et al.* Clinical and genome-wide association analysis of chemoradiation-induced hearing loss in nasopharyngeal carcinoma. *Hum Genet* **142**, 759–772 (2023).

53. Vos, H. I. *et al.* Replication of a genetic variant in ACYP2 associated with cisplatin-induced hearing loss in patients with osteosarcoma. *Pharmacogenet Genomics* **26**, 243–247 (2016).

54. Baldwin, R. M. *et al.* A genome-wide association study identifies novel loci for paclitaxel-induced sensory peripheral neuropathy in CALGB 40101. *Clin Cancer Res* **18**, 5099–5109 (2012).

55. Schneider, B. P. *et al.* Genome-Wide Association Studies for Taxane-Induced Peripheral Neuropathy in ECOG-5103 and ECOG-1199. *Clin Cancer Res* **21**, 5082–5091 (2015).

56. Hertz, D. L. *et al.* Genetic heterogeneity beyond CYP2C8*3 does not explain differential sensitivity to paclitaxel-induced neuropathy. *Breast Cancer Res Treat* **145**, 245–254 (2014).

57. Leandro-García, L. J. *et al.* Regulatory polymorphisms in β-tubulin IIa are associated with paclitaxel-induced peripheral neuropathy. *Clin Cancer Res* **18**, 4441–4448 (2012).

58. Beutler, A. S. *et al.* Sequencing of Charcot-Marie-Tooth disease genes in a toxic polyneuropathy. *Ann Neurol* **76**, 727–737 (2014).

59. Schneider, B. P. *et al.* Charcot-Marie-Tooth gene, SBF2, associated with taxane-induced peripheral neuropathy in African Americans. *Oncotarget* **7**, 82244–82253 (2016).

60. Nakamura, T. *et al.* Vincristine exacerbates asymptomatic Charcot-Marie-tooth disease with a novel EGR2 mutation. *Neurogenetics* **13**, 77–82 (2012).

61. Egbelakin, A. *et al.* Increased risk of vincristine neurotoxicity associated with low CYP3A5 expression genotype in children with acute lymphoblastic leukemia. *Pediatr Blood Cancer* **56**, 361–367 (2011).

62. Nagappa, M., Sharma, S. & Taly, A. B. Charcot-Marie-Tooth Disease. in *StatPearls* (StatPearls Publishing, Treasure Island (FL), 2025).

63. Hansson, P. *et al.* Pharmacogenomics in pediatric oncology patients with solid tumors related to chemotherapy-induced toxicity: A systematic review. *Crit Rev Oncol Hematol* **211**, 104720 (2025).

64. Trendowski, M. R. *et al.* Clinical and Genome-Wide Analysis of Serum Platinum Levels after Cisplatin-Based Chemotherapy. *Clin Cancer Res* **25**, 5913–5924 (2019).

65. Xu, H. *et al.* Common variants in ACYP2 influence susceptibility to cisplatin-induced hearing loss. *Nat Genet* **47**, 263–266 (2015).

66. Thiesen, S. *et al.* TPMT, COMT and ACYP2 genetic variants in paediatric cancer patients with cisplatin-induced ototoxicity. *Pharmacogenet Genomics* **27**, 213–222 (2017).

67. Ghosh, S. Cisplatin: The first metal based anticancer drug. *Bioorg Chem* **88**, 102925 (2019).

68. Rocha, C. R. R., Silva, M. M., Quinet, A., Cabral-Neto, J. B. & Menck, C. F. M. DNA repair pathways and cisplatin resistance: an intimate relationship. *Clinics (Sao Paulo)* **73**, e478s (2018).

69. Travis, L. B. *et al.* Adolescent and Young Adult Germ Cell Tumors: Epidemiology, Genomics, Treatment, and Survivorship. *J Clin Oncol* **42**, 696–706 (2024).

70. Rossen, P. B., Pedersen, A. F., Zachariae, R. & von der Maase, H. Health-related quality of life in long-term survivors of testicular cancer. *J Clin Oncol* **27**, 5993–5999 (2009).

71. Fleer, J. *et al.* Quality of life of testicular cancer survivors and the relationship with sociodemographics, cancer-related variables, and life events. *Support Care Cancer* **14**, 251–259 (2006).

72. Mykletun, A. *et al.* Side effects and cancer-related stress determine quality of life in long-term survivors of testicular cancer. *J Clin Oncol* **23**, 3061–3068 (2005).

73. Dahl, C. F. *et al.* A controlled study of risk factors for disease and current problems in long-term testicular cancer survivors. *J Cancer Surviv* **4**, 256–265 (2010).

74. Hartung, T. J. *et al.* Age-related variation and predictors of long-term quality of life in germ cell tumor survivors. *Urol Oncol* **34**, 60.e1–6 (2016).

75. Hooshmand, K. *et al.* Polygenic risk of paclitaxel-induced peripheral neuropathy: a genome-wide association study. *J Transl Med* **20**, 564 (2022).

76. Yamada, H. *et al.* A machine learning model using SNPs obtained from a genome-wide association study predicts the onset of vincristine-induced peripheral neuropathy. *Pharmacogenomics J* **22**, 241–246 (2022).

77. Cao, C. & Moult, J. GWAS and drug targets. *BMC Genomics* **15 Suppl 4**, S5 (2014).

78. Kooperberg, C., LeBlanc, M. & Obenchain, V. Risk prediction using genome-wide association studies. *Genet Epidemiol* **34**, 643–652 (2010).

79. Abdellaoui, A., Yengo, L., Verweij, K. J. H. & Visscher, P. M. 15 years of GWAS discovery: Realizing the promise. *Am J Hum Genet* **110**, 179–194 (2023).

80. Kumuthini, J. *et al.* The clinical utility of polygenic risk scores in genomic medicine practices: a systematic review. *Hum Genet* **141**, 1697–1704 (2022).

81. Haug, C. J. & Drazen, J. M. Artificial Intelligence and Machine Learning in Clinical Medicine, 2023. *N Engl J Med* **388**, 1201–1208 (2023).

82. Grapov, D., Fahrmann, J., Wanichthanarak, K. & Khoomrung, S. Rise of Deep Learning for Genomic, Proteomic, and Metabolomic Data Integration in Precision Medicine. *OMICS* **22**, 630–636 (2018).

83. Sidey-Gibbons, J. A. M. & Sidey-Gibbons, C. J. Machine learning in medicine: a practical introduction. *BMC Med Res Methodol* **19**, 64 (2019).

84. Sharma, A., Lysenko, A., Jia, S., Boroevich, K. A. & Tsunoda, T. Advances in AI and machine learning for predictive medicine. *J Hum Genet* **69**, 487–497 (2024).

85. Zhang, B., Shi, H. & Wang, H. Machine Learning and AI in Cancer Prognosis, Prediction, and Treatment Selection: A Critical Approach. *J Multidiscip Healthc* **16**, 1779–1791 (2023).

86. Howard, F. M., Kochanny, S., Koshy, M., Spiotto, M. & Pearson, A. T. Machine Learning-Guided Adjuvant Treatment of Head and Neck Cancer. *JAMA Netw Open* **3**, e2025881 (2020).

87. Fang, F. *et al.* Ultrasound-based deep learning radiomics nomogram for risk stratification of testicular masses: a two-center study. *J Cancer Res Clin Oncol* **150**, 18 (2024).

88. Chang, W.-T. *et al.* An artificial intelligence approach for predicting cardiotoxicity in breast cancer patients receiving anthracycline. *Arch Toxicol* **96**, 2731–2737 (2022).

89. Huang, S.-H. *et al.* How platinum-induced nephrotoxicity occurs? Machine learning prediction in non-small cell lung cancer patients. *Comput Methods Programs Biomed* **221**, 106839 (2022).

90. Garcia, S. L. *et al.* Predicting Hearing Loss in Testicular Cancer Patients after Cisplatin-Based Chemotherapy. *Cancers (Basel)* **15**, 3923 (2023).

91. Mapes, B., El Charif, O., Al-Sawwaf, S. & Dolan, M. E. Genome-Wide Association Studies of Chemotherapeutic Toxicities: Genomics of Inequality. *Clin Cancer Res* **23**, 4010–4019 (2017).

92. Sirugo, G., Williams, S. M. & Tishkoff, S. A. The Missing Diversity in Human Genetic Studies. *Cell* **177**, 26–31 (2019).

93. Mills, M. C. & Rahal, C. The GWAS Diversity Monitor tracks diversity by disease in real time. *Nat Genet* **52**, 242–243 (2020).

94. Bentley, A. R., Callier, S. & Rotimi, C. N. Diversity and inclusion in genomic research: why the uneven progress? *J Community Genet* **8**, 255–266 (2017).

95. Komatsu, M. *et al.* Pharmacoethnicity in Paclitaxel-Induced Sensory Peripheral Neuropathy. *Clin Cancer Res* **21**, 4337–4346 (2015).

96. Rotimi, C. N. & Jorde, L. B. Ancestry and disease in the age of genomic medicine. *N Engl J Med* **363**, 1551–1558 (2010).

97. Nkhoma, E. T., Poole, C., Vannappagari, V., Hall, S. A. & Beutler, E. The global prevalence of glucose-6-phosphate dehydrogenase deficiency: a systematic review and meta-analysis. *Blood Cells Mol Dis* **42**, 267–278 (2009).

98. Shord, S. S., Thompson, D. M., Krempl, G. A. & Hanigan, M. H. Effect of concurrent medications on cisplatin-induced nephrotoxicity in patients with head and neck cancer. *Anticancer Drugs* **17**, 207–215 (2006).

99. Faig, J. *et al.* Retrospective Analysis of Cisplatin Nephrotoxicity in Patients With Head and Neck Cancer Receiving Outpatient Treatment With Concurrent High-dose Cisplatin and Radiotherapy. *Am J Clin Oncol* **41**, 432–440 (2018).

100. Mersha, T. B. & Abebe, T. Self-reported race/ethnicity in the age of genomic research: its potential impact on understanding health disparities. *Hum Genomics* **9**, 1 (2015).

101. Chen, Z. *et al.* Specific Safety Profile of Bevacizumab in Asian Patients With Advanced NSCLC: A Meta-Analysis. *Medicine (Baltimore)* **94**, e975 (2015).

102. Schneider, B. P. *et al.* Impact of Genetic Ancestry on Outcomes in ECOG-ACRIN-E5103. *JCO Precis Oncol* **2017**, PO.17.00059 (2017).

103. Schneider, B. P. *et al.* Genetic variant predicts bevacizumab-induced hypertension in ECOG-5103 and ECOG-2100. *Br J Cancer* **111**, 1241–1248 (2014).

104. Polite, B. N. *et al.* Exploring racial differences in outcome and treatment for metastatic colorectal cancer: results from a large prospective observational cohort study (BRiTE). *Cancer* **118**, 1083–1090 (2012).

105. Nyrop, K. A. *et al.* Patient-reported treatment toxicity and adverse events in Black and White women receiving chemotherapy for early breast cancer. *Breast Cancer Res Treat* **191**, 409–422 (2022).

106. Simon, N. B., Danso, M. A., Alberico, T. A., Basch, E. & Bennett, A. V. The prevalence and pattern of chemotherapy-induced peripheral neuropathy among women with breast cancer receiving care in a large community oncology practice. *Qual Life Res* **26**, 2763–2772 (2017).

107. Adjei, A. A. *et al.* Genetic Predictors of Chemotherapy-Induced Peripheral Neuropathy from Paclitaxel, Carboplatin and Oxaliplatin: NCCTG/Alliance N08C1, N08CA and N08CB Study. *Cancers (Basel)* **13**, 1084 (2021).

108. Sucheston-Campbell, L. E. *et al.* Genome-wide meta-analyses identifies novel taxane-induced peripheral neuropathy-associated loci. *Pharmacogenet Genomics* **28**, 49–55 (2018).

109. Renbarger, J. L., McCammack, K. C., Rouse, C. E. & Hall, S. D. Effect of race on vincristine-associated neurotoxicity in pediatric acute lymphoblastic leukemia patients. *Pediatr Blood Cancer* **50**, 769–771 (2008).

110. Dennison, J. B. *et al.* Selective metabolism of vincristine in vitro by CYP3A5. *Drug Metab Dispos* **34**, 1317–1327 (2006).

111. Li, Y., Lu, Q., Wang, Y. & Ma, S. Racial differences in testicular cancer in the United States: descriptive epidemiology. *BMC Cancer* **20**, 284 (2020).

112. Livingston, G. *et al.* Dementia prevention, intervention, and care: 2020 report of the Lancet Commission. *Lancet* **396**, 413–446 (2020).

113. Travis, L. B. *et al.* Chemotherapy-induced peripheral neurotoxicity and ototoxicity: new paradigms for translational genomics. *J Natl Cancer Inst* **106**, dju044 (2014).

114. Uddin, S., Khan, A., Hossain, M. E. & Moni, M. A. Comparing different supervised machine learning algorithms for disease prediction. *BMC Med Inform Decis Mak* **19**, 281 (2019).

115. Dhungana, A. *et al.* Development and validation of a clinical breast cancer tool for accurate prediction of recurrence. *NPJ Breast Cancer* **10**, 46 (2024).

116. Prelaj, A. *et al.* Artificial intelligence for predictive biomarker discovery in immuno-oncology: a systematic review. *Ann Oncol* **35**, 29–65 (2024).

117. Agius, R. *et al.* Machine learning can identify newly diagnosed patients with CLL at high risk of infection. *Nat Commun* **11**, 363 (2020).

118. Cole, K. M. *et al.* Using machine learning to predict individual patient toxicities from cancer treatments. *Support Care Cancer* **30**, 7397–7406 (2022).

119. Araújo, A. L. D. *et al.* Machine learning for the prediction of toxicities from head and neck cancer treatment: A systematic review with meta-analysis. *Oral Oncol* **140**, 106386 (2023).

120. Millstein, J. *et al.* Development and Validation of a Novel Prediction Model for Hearing Loss From Cisplatin Chemotherapy. *J Clin Oncol* **43**, 2173–2183 (2025).

121. Postma, T. J. *et al.* The development of an EORTC quality of life questionnaire to assess chemotherapy-induced peripheral neuropathy: the QLQ-CIPN20. *Eur J Cancer* **41**, 1135–1139 (2005).

122. Oldenburg, J., Fosså, S. D. & Dahl, A. A. Scale for chemotherapy-induced long-term neurotoxicity (SCIN): psychometrics, validation, and findings in a large sample of testicular cancer survivors. *Qual Life Res* **15**, 791–800 (2006).

123. Mosteller, R. D. Simplified calculation of body-surface area. *N Engl J Med* **317**, 1098 (1987).

124. Das, S. *et al.* Next-generation genotype imputation service and methods. *Nat Genet* **48**, 1284–1287 (2016).

125. McCarthy, S. *et al.* A reference panel of 64,976 haplotypes for genotype imputation. *Nat Genet* **48**, 1279–1283 (2016).

126. Machiela, M. J. & Chanock, S. J. LDlink: a web-based application for exploring population-specific haplotype structure and linking correlated alleles of possible functional variants. *Bioinformatics* **31**, 3555–3557 (2015).

127. 1000 Genomes Project Consortium *et al.* A global reference for human genetic variation. *Nature* **526**, 68–74 (2015).

128. Sherry, S. T. *et al.* dbSNP: the NCBI database of genetic variation. *Nucleic Acids Res* **29**, 308–311 (2001).

129. Martin, F. J. *et al.* Ensembl 2023. *Nucleic Acids Res* **51**, D933–D941 (2023).

130. Gusev, A. *et al.* Integrative approaches for large-scale transcriptome-wide association studies. *Nat Genet* **48**, 245–252 (2016).

131. GTEx Consortium. The Genotype-Tissue Expression (GTEx) project. *Nat Genet* **45**, 580–585 (2013).

132. Hoffman, G. E. *et al.* CommonMind Consortium provides transcriptomic and epigenomic data for Schizophrenia and Bipolar Disorder. *Sci Data* **6**, 180 (2019).

133. Szklarczyk, D. *et al.* The STRING database in 2021: customizable protein-protein networks, and functional characterization of user-uploaded gene/measurement sets. *Nucleic Acids Res* **49**, D605–D612 (2021).

134. Sudlow, C. *et al.* UK biobank: an open access resource for identifying the causes of a wide range of complex diseases of middle and old age. *PLoS Med* **12**, e1001779 (2015).

135. Privé, F. *et al.* Portability of 245 polygenic scores when derived from the UK Biobank and applied to 9 ancestry groups from the same cohort. *Am J Hum Genet* **109**, 12–23 (2022).

136. Sinnott-Armstrong, N. *et al.* Genetics of 35 blood and urine biomarkers in the UK Biobank. *Nat Genet* **53**, 185–194 (2021).

137. Euesden, J., Lewis, C. M. & O'Reilly, P. F. PRSice: Polygenic Risk Score software. *Bioinformatics* **31**, 1466–1468 (2015).

138. Rose, M. C., Kostyanovskaya, E. & Huang, R. S. Pharmacogenomics of cisplatin sensitivity in non-small cell lung cancer. *Genomics Proteomics Bioinformatics* **12**, 198–209 (2014).

139. Mucaki, E. J., Zhao, J. Z. L., Lizotte, D. J. & Rogan, P. K. Predicting responses to platin chemotherapy agents with biochemically-inspired machine learning. *Signal Transduct Target Ther* **4**, 1 (2019).

140. Wang, L., Zhao, X., Fu, J., Xu, W. & Yuan, J. The Role of Tumour Metabolism in Cisplatin Resistance. *Front Mol Biosci* **8**, 691795 (2021).

141. Stekhoven, D. J. & Bühlmann, P. MissForest—non-parametric missing value imputation for mixed-type data. *Bioinformatics* **28**, 112–118 (2012).

142. Doerken, S., Avalos, M., Lagarde, E. & Schumacher, M. Penalized logistic regression with low prevalence exposures beyond high dimensional settings. *PLoS One* **14**, e0217057 (2019).

143. Black, J. E., Kueper, J. K. & Williamson, T. S. An introduction to machine learning for classification and prediction. *Family Practice* **40**, 200–204 (2023).

144. Chen, T. & Guestrin, C. XGBoost: A Scalable Tree Boosting System. in *Proceedings of the 22nd ACM SIGKDD International Conference on Knowledge Discovery and Data Mining* 785–794 (ACM, San Francisco California USA, 2016). doi:10.1145/2939672.2939785.

145. Guyon, I., Weston, J., Barnhill, S. & Vapnik, V. Gene Selection for Cancer Classification using Support Vector Machines. *Machine Learning* **46**, 389–422 (2002).

146. Radovic, M., Ghalwash, M., Filipovic, N. & Obradovic, Z. Minimum redundancy maximum relevance feature selection approach for temporal gene expression data. *BMC Bioinformatics* **18**, 9 (2017).

147. De Jay, N. *et al.* mRMRe: an R package for parallelized mRMR ensemble feature selection. *Bioinformatics* **29**, 2365–2368 (2013).

148. Sollis, E. *et al.* The NHGRI-EBI GWAS Catalog: knowledgebase and deposition resource. *Nucleic Acids Res* **51**, D977–D985 (2023).

149. Sun, M., Sun, X., Wang, F. & Liu, L. Machine learning-based prediction of diabetic peripheral neuropathy: model development and clinical validation. *Front Endocrinol (Lausanne)* **16**, 1614657 (2025).

150. Lian, X. *et al.* Study on risk factors of diabetic peripheral neuropathy and establishment of a prediction model by machine learning. *BMC Med Inform Decis Mak* **23**, 146 (2023).

151. Baskozos, G. *et al.* Classification of painful or painless diabetic peripheral neuropathy and identification of the most powerful predictors using machine learning models in large cross-sectional cohorts. *BMC Med Inform Decis Mak* **22**, 144 (2022).

152. King, K. A. & Brewer, C. C. Clinical trials, ototoxicity grading scales and the audiologist's role in therapeutic decision making. *Int J Audiol* **57**, S89–S98 (2018).

153. Hornemann, T. Mini review: Lipids in Peripheral Nerve Disorders. *Neurosci Lett* **740**, 135455 (2021).

154. Tesfaye, S. *et al.* Vascular risk factors and diabetic neuropathy. *N Engl J Med* **352**, 341–350 (2005).

155. Avraham, O. *et al.* Satellite glial cells promote regenerative growth in sensory neurons. *Nat Commun* **11**, 4891 (2020).

156. Yeung, N. *et al.* Plasma Lipidomic Profiling Identifies Elevated Triglycerides as Potential Risk Factor in Chemotherapy-Induced Peripheral Neuropathy. *JCO Precis Oncol* **8**, e2300690 (2024).

157. Boyd, J. T. *et al.* Elevated dietary ω-6 polyunsaturated fatty acids induce reversible peripheral nerve dysfunction that exacerbates comorbid pain conditions. *Nat Metab* **3**, 762–773 (2021).

158. Fernando, S. & Polkinghorne, K. R. Cystatin C: not just a marker of kidney function. *J Bras Nefrol* **42**, 6–7 (2020).

159. Miller, R. P., Tadagavadi, R. K., Ramesh, G. & Reeves, W. B. Mechanisms of Cisplatin nephrotoxicity. *Toxins (Basel)* **2**, 2490–2518 (2010).

160. Visacri, M. B. *et al.* Adverse drug reactions and kinetics of cisplatin excretion in urine of patients undergoing cisplatin chemotherapy and radiotherapy for head and neck cancer: a prospective study. *Daru* **25**, 12 (2017).

161. Drögemöller, B. I. *et al.* Further Investigation of the Role of ACYP2 and WFS1 Pharmacogenomic Variants in the Development of Cisplatin-Induced Ototoxicity in Testicular Cancer Patients. *Clin Cancer Res* **24**, 1866–1871 (2018).

162. Cryns, K. *et al.* The WFS1 gene, responsible for low frequency sensorineural hearing loss and Wolfram syndrome, is expressed in a variety of inner ear cells. *Histochem Cell Biol* **119**, 247–256 (2003).

163. Liiv, M. *et al.* ER calcium depletion as a key driver for impaired ER-to-mitochondria calcium transfer and mitochondrial dysfunction in Wolfram syndrome. *Nat Commun* **15**, 6143 (2024).

164. Tserga, E. *et al.* The genetic vulnerability to cisplatin ototoxicity: a systematic review. *Sci Rep* **9**, 3455 (2019).

165. Kim, H.-J. *et al.* Analysis of the prevalence and associated risk factors of tinnitus in adults. *PLoS One* **10**, e0127578 (2015).

166. Shahbazi, M. *et al.* Comparison of GWAS results between de novo tinnitus and cancer treatment-related tinnitus suggests distinctive roles for genetic risk factors. *Sci Rep* **14**, 27952 (2024).

167. Ramos, E. *et al.* Pharmacogenomics, ancestry and clinical decision making for global populations. *Pharmacogenomics J* **14**, 217–222 (2014).

168. Yang, H.-C., Chen, C.-W., Lin, Y.-T. & Chu, S.-K. Genetic ancestry plays a central role in population pharmacogenomics. *Commun Biol* **4**, 171 (2021).

169. Clasen, S. C. *et al.* Cisplatin, environmental metals, and cardiovascular disease: an urgent need to understand underlying mechanisms. *Cardiooncology* **7**, 34 (2021).

170. Joneidi, Z. *et al.* The impact of genetic variation on metabolism of heavy metals: Genetic predisposition? *Biomed Pharmacother* **113**, 108642 (2019).

171. Weir, B. S. & Cockerham, C. C. ESTIMATING F-STATISTICS FOR THE ANALYSIS OF POPULATION STRUCTURE. *Evolution* **38**, 1358–1370 (1984).

172. DepMap, B. DepMap 24Q2 Public. 25031191226 Bytes Figshare+ https://doi.org/10.25452/FIGSHARE.PLUS.25880521.V1 (2024).

173. Yang, W. *et al.* Genomics of Drug Sensitivity in Cancer (GDSC): a resource for therapeutic biomarker discovery in cancer cells. *Nucleic Acids Res* **41**, D955-961 (2013).

174. Bhat, Z. Y. *et al.* Understanding the Risk Factors and Long-Term Consequences of Cisplatin-Associated Acute Kidney Injury: An Observational Cohort Study. *PLoS One* **10**, e0142225 (2015).

175. Zhou, Y. & Lauschke, V. M. Population pharmacogenomics: an update on ethnogeographic differences and opportunities for precision public health. *Hum Genet* **141**, 1113–1136 (2022).

176. Eom, S.-Y. *et al.* Allele Frequencies of the Single Nucleotide Polymorphisms Related to the Body Burden of Heavy Metals in the Korean Population and Their Ethnic Differences. *Toxicol Res* **32**, 195–205 (2016).

177. Hancock, A. M., Alkorta-Aranburu, G., Witonsky, D. B. & Di Rienzo, A. Adaptations to new environments in humans: the role of subtle allele frequency shifts. *Philos Trans R Soc Lond B Biol Sci* **365**, 2459–2468 (2010).

178. Hayward, L. K. & Sella, G. Polygenic adaptation after a sudden change in environment. *Elife* **11**, e66697 (2022).

179. Lussier, M. P., Lepage, P. K., Bousquet, S. M. & Boulay, G. RNF24, a new TRPC interacting protein, causes the intracellular retention of TRPC. *Cell Calcium* **43**, 432–443 (2008).

180. Selvaraj, S., Sun, Y. & Singh, B. B. TRPC channels and their implication in neurological diseases. *CNS Neurol Disord Drug Targets* **9**, 94–104 (2010).

181. Huang, J., Du, W., Yao, H. & Wang, Y. TRPC Channels in Neuronal Survival. in *TRP Channels* (ed. Zhu, M. X.) (CRC Press/Taylor & Francis, Boca Raton (FL), 2011).

182. Lussier, M. P., Lepage, P. K. & Boulay, G. TRPCs interact with RNF24 at the level of the Golgi apparatus. *FASEB j.* **21**, (2007).

183. Gualdani, R., de Clippele, M., Ratbi, I., Gailly, P. & Tajeddine, N. Store-Operated Calcium Entry Contributes to Cisplatin-Induced Cell Death in Non-Small Cell Lung Carcinoma. *Cancers (Basel)* **11**, 430 (2019).

184. Shen, L. *et al.* Calcium efflux from the endoplasmic reticulum regulates cisplatin-induced apoptosis in human cervical cancer HeLa cells. *Oncol Lett* **11**, 2411–2419 (2016).

185. Perland, E. *et al.* Structural prediction of two novel human atypical SLC transporters, MFSD4A and MFSD9, and their neuroanatomical distribution in mice. *PLoS One* **12**, e0186325 (2017).

186. Ayka, A. & Şehirli, A. Ö. The Role of the SLC Transporters Protein in the Neurodegenerative Disorders. *Clin Psychopharmacol Neurosci* **18**, 174–187 (2020).

187. Li, H. *et al.* Neurons require glucose uptake and glycolysis in vivo. *Cell Rep* **42**, 112335 (2023).

188. Drögemöller, B. I. *et al.* Association Between SLC16A5 Genetic Variation and Cisplatin-Induced Ototoxic Effects in Adult Patients With Testicular Cancer. *JAMA Oncol* **3**, 1558–1562 (2017).

189. Martin, S. K. & Wood, R. D. DNA polymerase ζ in DNA replication and repair. *Nucleic Acids Res* **47**, 8348–8361 (2019).

190. Lehmann, H. C., Staff, N. P. & Hoke, A. Modeling chemotherapy induced peripheral neuropathy (CIPN) in vitro: Prospects and limitations. *Exp Neurol* **326**, 113140 (2020).

191. Diouf, B. *et al.* Association of an inherited genetic variant with vincristine-related peripheral neuropathy in children with acute lymphoblastic leukemia. *JAMA* **313**, 815–823 (2015).

192. Wheeler, H. E., Wing, C., Delaney, S. M., Komatsu, M. & Dolan, M. E. Modeling chemotherapeutic neurotoxicity with human induced pluripotent stem cell-derived neuronal cells. *PLoS One* **10**, e0118020 (2015).

193. Hertz, D. L. *et al.* Pharmacogenetic Discovery in CALGB (Alliance) 90401 and Mechanistic Validation of a VAC14 Polymorphism that Increases Risk of Docetaxel-Induced Neuropathy. *Clin Cancer Res* **22**, 4890–4900 (2016).

194. Yin, K., Baillie, G. J. & Vetter, I. Neuronal cell lines as model dorsal root ganglion neurons: A transcriptomic comparison. *Mol Pain* **12**, 1744806916646111 (2016).

195. Vetter, I. *et al.* Characterisation of Na(v) types endogenously expressed in human SH-SY5Y neuroblastoma cells. *Biochem Pharmacol* **83**, 1562–1571 (2012).

196. Lopez-Suarez, L., Awabdh, S. A., Coumoul, X. & Chauvet, C. The SH-SY5Y human neuroblastoma cell line, a relevant in vitro cell model for investigating neurotoxicology in human: Focus on organic pollutants. *Neurotoxicology* **92**, 131–155 (2022).

197. Sogos, V. *et al.* Human Neuronal Cell Lines as An In Vitro Toxicological Tool for the Evaluation of Novel Psychoactive Substances. *Int J Mol Sci* **22**, 6785 (2021).

198. Vencappa, S., Donaldson, L. F. & Hulse, R. P. Cisplatin induced sensory neuropathy is prevented by vascular endothelial growth factor-A. *Am J Transl Res* **7**, 1032–1044 (2015).

199. Zhu, J. *et al.* Ethoxyquin prevents chemotherapy-induced neurotoxicity via Hsp90 modulation. *Ann Neurol* **74**, 893–904 (2013).

200. Donzelli, E. *et al.* Neurotoxicity of platinum compounds: comparison of the effects of cisplatin and oxaliplatin on the human neuroblastoma cell line SH-SY5Y. *J Neurooncol* **67**, 65–73 (2004).

201. Rathinam, R., Ghosh, S., Neumann, W. L. & Jamesdaniel, S. Cisplatin-induced apoptosis in auditory, renal, and neuronal cells is associated with nitration and downregulation of LMO4. *Cell Death Discov* **1**, 15052- (2015).

202. Ghazarian, A. A. & McGlynn, K. A. Increasing Incidence of Testicular Germ Cell Tumors among Racial/Ethnic Minorities in the United States. *Cancer Epidemiol Biomarkers Prev* **29**, 1237–1245 (2020).

203. Williams, P. A., Zaidi, S. K., Ramian, H. & Sengupta, R. AACR Cancer Disparities Progress Report 2024: Achieving the Bold Vision of Health Equity. *Cancer Epidemiol Biomarkers Prev* **33**, 870–873 (2024).

204. Wang, T., Larcher, L. M., Ma, L. & Veedu, R. N. Systematic Screening of Commonly Used Commercial Transfection Reagents towards Efficient Transfection of Single-Stranded Oligonucleotides. *Molecules* **23**, 2564 (2018).

205. Benati, D. *et al.* Induced Pluripotent Stem Cells and Genome-Editing Tools in Determining Gene Function and Therapy for Inherited Retinal Disorders. *Int J Mol Sci* **23**, 15276 (2022).

206. Liao, H., Wu, J., VanDusen, N. J., Li, Y. & Zheng, Y. CRISPR-Cas9-mediated homology-directed repair for precise gene editing. *Mol Ther Nucleic Acids* **35**, 102344 (2024).

207. Husain, M. *et al.* An overview of the unique challenges facing African-American breast cancer survivors. *Support Care Cancer* **27**, 729–743 (2019).

208. Won, H.-H. *et al.* Polymorphic markers associated with severe oxaliplatin-induced, chronic peripheral neuropathy in colon cancer patients. *Cancer* **118**, 2828–2836 (2012).

209. Oguri, T. *et al.* Genetic polymorphisms associated with oxaliplatin-induced peripheral neurotoxicity in Japanese patients with colorectal cancer. *Int J Clin Pharmacol Ther* **51**, 475–481 (2013).

210. Cecchi, C. *et al.* Interaction between acylphosphatase and SERCA in SH-SY5Y cells. *Mol Cell Biochem* **211**, 95–102 (2000).

211. Thomas, A. J. *et al.* Functional mechanotransduction is required for cisplatin-induced hair cell death in the zebrafish lateral line. *J Neurosci* **33**, 4405–4414 (2013).

212. Starobova, H. & Vetter, I. Pathophysiology of Chemotherapy-Induced Peripheral Neuropathy. *Front Mol Neurosci* **10**, 174 (2017).

213. Yamazaki, Y., Ogihara, S., Harada, S. & Tokuyama, S. Activation of cerebral sodium-glucose transporter type 1 function mediated by post-ischemic hyperglycemia exacerbates the development of cerebral ischemia. *Neuroscience* **310**, 674–685 (2015).

214. Yang, C.-F. & Tsai, W.-C. Calmodulin: The switch button of calcium signaling. *Tzu Chi Med J* **34**, 15–22 (2022).

215. Arduino, D. M. & Perocchi, F. Pharmacological modulation of mitochondrial calcium homeostasis. *J Physiol* **596**, 2717–2733 (2018).

216. Woods, J. J. & Wilson, J. J. Inhibitors of the mitochondrial calcium uniporter for the treatment of disease. *Curr Opin Chem Biol* **55**, 9–18 (2020).

217. Xie, N. *et al.* Inhibition of the mitochondrial calcium uniporter inhibits Aβ-induced apoptosis by reducing reactive oxygen species-mediated endoplasmic reticulum stress in cultured microglia. *Brain Res* **1676**, 100–106 (2017).

218. Abramov, A. Y. & Duchen, M. R. Mechanisms underlying the loss of mitochondrial membrane potential in glutamate excitotoxicity. *Biochim Biophys Acta* **1777**, 953–964 (2008).

219. Kleckner, I. R. *et al.* Effects of exercise during chemotherapy on chemotherapy-induced peripheral neuropathy: a multicenter, randomized controlled trial. *Support Care Cancer* **26**, 1019–1028 (2018).

220. Zimmer, P. *et al.* Eight-week, multimodal exercise counteracts a progress of chemotherapy-induced peripheral neuropathy and improves balance and strength in metastasized colorectal cancer patients: a randomized controlled trial. *Support Care Cancer* **26**, 615–624 (2018).

221. Okuda, Y. *et al.* Long-term effects of eicosapentaenoic acid on diabetic peripheral neuropathy and serum lipids in patients with type II diabetes mellitus. *J Diabetes Complications* **10**, 280–287 (1996).

222. Coste, T. C., Gerbi, A., Vague, P., Pieroni, G. & Raccah, D. Neuroprotective effect of docosahexaenoic acid-enriched phospholipids in experimental diabetic neuropathy. *Diabetes* **52**, 2578–2585 (2003).

223. Stubblefield, M. D. *et al.* NCCN task force report: management of neuropathy in cancer. *J Natl Compr Canc Netw* **7 Suppl 5**, S1–S26; quiz S27-28 (2009).

224. Zhang, H., De, T., Zhong, Y. & Perera, M. A. The Advantages and Challenges of Diversity in Pharmacogenomics: Can Minority Populations Bring Us Closer to Implementation? *Clin Pharmacol Ther* **106**, 338–349 (2019).

225. Hernandez, W. *et al.* Ethnicity-specific pharmacogenetics: the case of warfarin in African Americans. *Pharmacogenomics J* **14**, 223–228 (2014).

226. Cavaletti, G. *et al.* Self-Reported Assessment of the Socio-Economic Impact of Anticancer Chemotherapy-Related Neurotoxicity. *Toxics* **11**, 104 (2023).

227. Pike, C. T., Birnbaum, H. G., Muehlenbein, C. E., Pohl, G. M. & Natale, R. B. Healthcare costs and workloss burden of patients with chemotherapy-associated peripheral neuropathy in breast, ovarian, head and neck, and nonsmall cell lung cancer. *Chemother Res Pract* **2012**, 913848 (2012).

228. Bhuta, R. *et al.* Children's Oncology Group's 2023 blueprint for research: Germ cell tumors. *Pediatr Blood Cancer* **70 Suppl 6**, e30562 (2023).

229. Calhoun, E. A. *et al.* Psychometric evaluation of the Functional Assessment of Cancer Therapy/Gynecologic Oncology Group-Neurotoxicity (Fact/GOG-Ntx) questionnaire for patients receiving systemic chemotherapy. *Int J Gynecol Cancer* **13**, 741–748 (2003).

230. Whelan, J. S. *et al.* EURAMOS-1, an international randomised study for osteosarcoma: results from pre-randomisation treatment. *Ann Oncol* **26**, 407–414 (2015).

231. Freites-Martinez, A., Santana, N., Arias-Santiago, S. & Viera, A. Using the Common Terminology Criteria for Adverse Events (CTCAE - Version 5.0) to Evaluate the Severity of Adverse Events of Anticancer Therapies. *Actas Dermosifiliogr (Engl Ed)* **112**, 90–92 (2021).

232. de Jong, C., Herder, G. J. M. & Deneer, V. H. M. Genetic variants as predictors of toxicity and response in patients with non-small cell lung cancer undergoing first-line platinum-based chemotherapy: Design of the multicenter PGxLUNG study. *Thorac Cancer* **11**, 3634–3640 (2020).

233. de Jong, C. *et al.* Association between Genetic Variants and Peripheral Neuropathy in Patients with NSCLC Treated with First-Line Platinum-Based Therapy. *Genes (Basel)* **14**, 170 (2023).

234. Cristina Oliveira, R., Gama, A. C. C. & Magalhães, M. D. C. Fundamental Voice Frequency: Acoustic, Electroglottographic, and Accelerometer Measurement in Individuals With and Without Vocal Alteration. *J Voice* **35**, 174–180 (2021).

235. Shahbazi, M. *et al.* Comprehensive association analysis of speech recognition thresholds after cisplatin-based chemotherapy in survivors of adult-onset cancer. *Cancer Med* **12**, 2999–3012 (2023).

236. Bhatt, I. S., Wilson, N., Dias, R. & Torkamani, A. A genome-wide association study of tinnitus reveals shared genetic links to neuropsychiatric disorders. *Sci Rep* **12**, 22511 (2022).

237. Gui, Y. *et al.* Sex-specific genetic association between psychiatric disorders and cognition, behavior and brain imaging in children and adults. *Transl Psychiatry* **12**, 347 (2022).

238. Sarink, D. *et al.* Racial/Ethnic Differences in Ovarian Cancer Risk: Results from the Multiethnic Cohort Study. *Cancer Epidemiol Biomarkers Prev* **29**, 2019–2025 (2020).

239. Mazul, A. L., Chidambaram, S., Zevallos, J. P. & Massa, S. T. Disparities in head and neck cancer incidence and trends by race/ethnicity and sex. *Head Neck* **45**, 75–84 (2023).

240. de Boer, S. M. *et al.* Toxicity and quality of life after adjuvant chemoradiotherapy versus radiotherapy alone for women with high-risk endometrial cancer (PORTEC-3): an open-label, multicentre, randomised, phase 3 trial. *Lancet Oncol* **17**, 1114–1126 (2016).

241. Kaasa, S. *et al.* The EORTC core quality of life questionnaire (QLQ-C30): validity and reliability when analysed with patients treated with palliative radiotherapy. *Eur J Cancer* **31A**, 2260–2263 (1995).

242. Zazuli, Z. *et al.* Association between Genetic Variants and Cisplatin-Induced Nephrotoxicity: A Genome-Wide Approach and Validation Study. *J Pers Med* **11**, 1233 (2021).

243. Khrunin, A. V., Moisseev, A., Gorbunova, V. & Limborska, S. Genetic polymorphisms and the efficacy and toxicity of cisplatin-based chemotherapy in ovarian cancer patients. *Pharmacogenomics J* **10**, 54–61 (2010).